UNIVERSIDADE ESTADUAL DE CAMPINAS

FACULDADE DE ENGENHARIA ELÉTRICA

DEPARTAMENTO DE COMUNICAÇÕES

FUNDAMENTOS DE ENGENHARIA DE RÁDIO MÓVEL

(RESUMO)

Prof. Dr. Michel Daoud Yacoub

Tese apresentada à Faculdade de Engenharia Elétrica da Unicamp como parte dos requisitos exigidos para a obtenção do título de Prof. Livre-Docente na área de Sistemas de Comunicações.

- 1992 -

À minha querida Nídia

Aos meus queridos Alexandre, Helena e Carolina

Aos gêmeos, tão carinhosamente esperados

AGRADECIMENTOS

Ao Professor Attílio José Giarola pelo paciente trabalho de revisão dos originais do meu livro, pelo acompanhamento de todo o processo que culminou com a aceitação do mesmo por várias editoras, pelo incentivo nas horas de dificuldade, pela orientação segura no processo de negociação com as editoras e por muito mais do que consigo exprimir em palavras. Ao Prof. Giarola o meu muito obrigado.

Aos professores do Departamento de Comunicações pelas valiosas sugestões e esclarecimentos de inúmeros tópicos inclusos no livro.

Aos meus alunos do curso *Comunicações Móveis* e orientados pelas ricas discussões. Em particular, agradeço a J. C. Espinal Mencia, O. C. Branquinho, J. L. A. D'Annibale, E. J. Leonardo, N. F. Keffer, A. A. Shinoda, A. F. Victória e E. Nisembaum cujos resultados de pesquisa foram incorporados ao livro.

Aos diretores da Faculdade de Engenharia Elétrica, Professores Mauro S. Miskulim e Wagner C. do Amaral, pelo apoio na utilização dos recursos da faculdade.

Ao Centro de Pesquisa e Desenvolvimento - CPqD - TELEBRÁS pelo patrocínio na confecção das ilustrações do livro.

À SERIFA Editoração e Informática S/C Ltda. pela feitura das ilustrações.

Às editoras CRC Press, Kluwer Academic Press, Oxford University Press e Prentice Hall pela aceitação do meu trabalho e pela oportunidade oferecida para a publicação de meu livro.

À Srta. Janete Sayoko Toma pelo árduo, paciente e longo trabalho de datilografia das várias versões do meu manuscrito.

À minha querida família por ter vivido comigo esta difícil e longa fase de escrita do livro, quando sofremos juntos as incertezas, derrotas e tristezas; por ter me dado forças e coragem para persistir e não esmorecer diante das muitas dificuldades; por ter me ensinado a virtude da paciência e perseverança. À minha querida família o meu profundo amor.

RESUMO

Este trabalho mostra de maneira resumida a proposta do livro *Foundations of Mobile Radio Engineering*, do mesmo autor, a ser publicado pela CRC Press, Boca Raton, FL, USA. O corpo da tese apresenta a mesma estrutura do livro onde acrescentam-se Prefácio e Conclusões. O Prefácio introduz a motivação da escrita e o apelo do livro, enquanto o capítulo Conclusões delinea os principais resultados dos temas abordados. O corpo da tese é constituido de doze capítulos agrupados em seis partes onde tratam-se dos seguintes temas : Sistema Rádio Móvel, Rádio Móvel Celular, Modelo de Propagação de Rádio Móvel, Efeitos de Propagação de Multipercurso, Combate ao Desvanecimento, Transmissão de Dados e Sinalização, Ruído e Interferência, Modulação Analógica para Rádio Móvel, Técnicas Digitais para Rádio Móvel, Arquitetura de Múltiplo Acesso, Protocolos de Acesso e Aspectos de Tráfego em Sistemas de Rádio Móvel.

ÍNDICE

PARTE IV RUÍDO, INTERFERÊNCIA E MODULAÇÃO

PARTE V MÚLTIPLO ACESSO

PARTE VI TRÁFEGO

PREFÁCIO

MOTIVAÇÃO

Durante todos estes anos de envolvimento com a área de comunicações móveis, sendo através da pesquisa, do ensino ou mesmo de alguns projetos específicos para a indústria, senti a necessidade de um livro texto que abordasse os vários tópicos relacionados com este campo tão abrangente. Contudo, a engenharia de rádio móvel envolve virtualmente todas as áreas de telecomunicações, e um livro cobrindo toda a matéria de uma forma ampla requereria vários volumes e diversos autores.

Muitos fenômenos de comunicação rádio móvel já foram explorados em diversos livros ou textos clássicos mas geralmente abordados como tópicos avançados. Além disso, muitas das técnicas, inicialmente usadas para outras aplicações, acabaram adaptando-se perfeitamente às necessidades de rádio móvel. Assim, escrever um livro especializado nesta área requereria apenas uma compilação das várias matérias disponíveis na literatura. Isto é apenas parcialmente verdade. Desde o surgimento dos primeiros sistemas celulares, a pesquisa na área foi intensificada e uma grande quantidade de novos e interessantes resultados obtidos. O que inicialmente constituiu uma pequena área de pesquisa, hoje tornou-se parte fundamental da maioria dos trabalhos em telecomunicações.

Compilar material básico e avançado num único livro de um único autor é literalmente impossível. Neste livro procurei explorar o que, de uma certa forma, constitui um subconjunto bastante significativo deste vasto campo. O livro visa ambos, os iniciantes na área e os já familiares com sistemas de rádio móvel.

Os capítulos são ordenados de forma a que o leitor encontre uma introdução à matéria, descrição e análise dos fenômenos básicos, soluções práticas aos problemas e material mais avançado. Cada capítulo começa com Preâmbulo, onde resumem-se os tópicos a serem tratados no mesmo, e termina com Sumário e Conclusões, onde os principais resultados e comentários gerais são incluídos. Além disso, uma vez que não se espera que os leitores tenham a mesma bagagem matemática, as passagens são minuciosas e

sempre que necessário, informações adicionais são colocadas em forma de apêndices no final do capítulo correspondente. Neste sentido o livro do ponto de vista didático é, de certa forma, auto suficiente.

Devido à escassa literatura nesta área e com este tipo de abordagem, o livro foi escrito em inglês para uma possível maior penetração no mercado mundial. O nome proposto é *Foundations of Mobile Radio Engineering.* Os livros disponíveis ou são bastante superficiais ou então objetivam uma classe de leitores com experiência profissional na área e/ou com uma bagagem matemática considerável.

O livro proposto é dividido em seis partes :

PARTE I - INTRODUÇÃO

Contém os Capítulos 1 e 2.

O Capítulo 1 introduz os vários sistemas de rádio móvel.

O Capítulo 2 descreve a arquitetura celular e os tópicos relacionados.

PARTE II - O CANAL DE RÁDIO MÓVEL

Contém os Capítulos 3 e 4.

O Capítulo 3 analisa os métodos de cálculo de perdas de percurso, sombreamento, propagação de multipercurso e suas estatísticas básicas.

O Capítulo 4 é inteiramente dedicado aos vários tópicos relacionados com os fenômenos de multipercurso.

PARTE III - MÉTODOS DE DIVERSIDADE-COMBINAÇÃO

Contém os Capítulos 5 e 6.

O Capítulo 5 analisa os diversos esquemas de diversidade e combinação para combater o desvanecimento.

O Capítulo 6 investiga os métodos de combater o desvanecimento especificamente num ambiente digital.

PARTE IV - RUÍDO, INTERFERÊNCIA E MUDULAÇÃO

Contém os Capítulos 7, 8 e 9.

O Capítulo 7 estuda os problemas relativos a ruído, interferências de canal adjacente e de cocanal.

O Capítulo 8 examina os vários esquemas de modulação analógica num ambiente móvel.

O Capítulo 9 analisa alguns esquemas específicos de modulação digital de maior ordem e também algumas técnicas de codificação de voz, aplicados no ambiente móvel.

PARTE V - MÚLTIPLO ACESSO

Contém os Capítulos 10 e 11.

O Capítulo 10 descreve as arquiteturas de múltiplo acesso tais como FDMA, TDMA e CDMA.

O Capítulo 11 aborda os vários protocolos de múltiplo acesso e investiga o desempenho do *Slotted ALOHA* no ambiente de rádio móvel.

PARTE VI - TRÁFEGO

Contém o Capítulo 12.

Este capítulo mostra o desempenho de algumas técnicas de melhoria de tráfego. Mais especificamente, ele analisa um algorítmo de abordagem global e outro local por meio de simulação e análise numérica.

O livro pode ser usado como texto para um curso de pós graduação de um semestre (60 horas).

MERCADO

Depois da indústria petrolífera as telecomunicações constituem o mercado mais rentável no mundo. Juntamente com a informática este mercado representará aproximadamente 40% do Produto Nacional Bruto da maioria dos países no futuro bem próximo. Dentro das telecomunicações a *Comunicação Móvel* apresenta o maior potencial de expansão. Estima-se que o mercado atual na Europa triplicará por volta do ano 2001. Os sistemas analógicos ainda constituem um mercado bastante rentável registrando um aumento de 25% de equipamentos e serviços em 1991 em relação a 1990. Estima-se ainda que os serviços da Rede de Comunicação Pessoal (PCN - Personal Communication Network) atrairá mais que 60000 assinantes em 1995, subindo para 2.5 milhões ao final da década.

Uma tendência mercadológica semelhante é prevista para a América do Norte e Ásia. Quanto ao restante do mundo os serviços de rádio móvel já são uma realidade, embora a grande maioria dos assinantes é constituída por empresários. No entanto acredita-se que, como tem acontecido nos países do primeiro mundo, o consumidor comum deverá constituir a maior porção do mercado dos assinantes móveis no futuro bem próximo.

Assim, existe um interesse crescente dos vários setores da comunidade em conhecer um pouco melhor este importante meio de comunicação. As pesquisas na área tem se intensificado, caracterizando a necessidade de livros textos.

OBJETIVO DA TESE

Este trabalho tem como objetivo apresentar de forma bastante resumida os principais assuntos tratados no livro *Foundations of Mobile Radio Communications Engineering*, do mesmo autor. Para um detalhamento maior do assunto o leitor deve se referir ao manuscrito em anexo. O livro foi aceito para publicação pelas editoras (i) CRC Press, Boca Raton, Fl, USA, (ii) Kluwer Academic Press, Norwell, MA, USA, (iii) Oxford University Press, Oxford, England e (iv) Prentice Hall, Hemel Hempstead,

England. O mesmo encontra-se em fase de produção pela primeira editora.

ESTRUTURA DA TESE

A tese segue exatamente a mesma estrutura do livro, como aquela exposta acima, sendo acrescida de um capítulo de conclusões onde são ressaltados os principais resultados de cada capítulo.

PARTE I

INTRODUÇÃO

CAPÍTULO 1

SISTEMA RÁDIO MÓVEL

INTRODUÇÃO

O primeiro uso de rádio móvel data do século XIX quando M. G. Marconi estabeleceu uma conexão via rádio entre uma estação base terrena e um barco de reboque distante 18 milhas. A partir de então os sistemas de rádio móvel se desenvolveram ràpidamente espalhando-se de uma maneira considerável. A utilidade dos Serviços de Rádio Móvel foi inicialmente reconhecida pelos serviços de segurança pública, tais como os departamentos de polícia e bombeiros, conservação de florestas, manutenção de rodovias e serviços públicos locais. Em seguida os setores privados, tais como os de geração e distribuição de eletricidade, petróleo, cinema, manutenção do sistema telefônico, serviços de transporte, frotas de táxis e caminhões passaram a fazer uso do rádio móvel. A taxa de crescimento destes serviços nos Estados Unidos na década de 50 já era superior a 20% ao ano, quando o número de assinantes era de apenas alguns milhares. Conseqüentemente, por volta de 1963 o número de usuários móveis excedia a casa dos 1,3 milhões, muito embora apenas alguns poucos canais (em torno de 12) eram disponíveis.

Estes primeiros sistemas, também conhecidos como Sistemas Móveis Convencionais, consistiam de uma estação base com o seu transmissor e receptor instalados num topo de uma colina. A área de cobertura era intencionalmente grande como à dos serviços de rádio difusão (rádio e televisão). O transmissor operava geralmente com uma alta potência (200 a 300 watts) garantindo uma significativa área de cobertura (rálo de 25 milhas ou mais).

Os Sistemas Móveis Convencionais são, em geral, isolados uns dos outros, tendo apenas alguns deles acesso à rede telefônica pública. Os sistemas providos deste tipo de conexão são chamados Sistemas Telfônicos Móveis, onde a unidade de comunicação é atribuída ao assinante e não a uma localização física.

CONTEÚDO

Este capítulo traça um breve histórico dos sistemas de rádio móvel, trazendo à tona os principais eventos que contribuíram para o desenvolvimento deste eficiente meio de comunicação. Destaca-se nestes eventos a evolução tecnológica sofrida pelos esquemas de modulação, empacotamento do equipamento e aspectos de arquitetura de sistema. Além disso delineam-se os vários problemas de alocação de espectro de freqüência e da disponibilidade de canais de rádio para os serviços.

Alguns dos principais serviços de rádio móvel (*Radio Paging, Packet Radio, Future Public Telecommunications Systems, Cordless Telephone, Personal Communications* e *Mobile Satellite Communications*) são brevemente descritos e considerações de projeto de sistemas são examinadas. Mostra-se ainda que, dado que rádio-propagação não leva em conta as fronteiras geopolíticas, o uso eficiente do espectro de freqüência só é possível se forem estabelecidos acordos de âmbito internacional. Sob estas premissas o ITU (*International Telecommunication Union*) surgiu para prover esta "harmonia mundial". A alocação internacional de freqüências para alguns serviços de rádio é então apresentada sob forma de tabela.

CAPÍTULO 2

RÁDIO MÓVEL CELULAR

INTRODUÇÃO

Os sistemas móveis convencionais consistiam de uma estação base com o seu transmissor e seu receptor montados num topo de uma colina. A área de cobertura era, em geral, grande e apenas um pequeno número de canais era disponível. Como inicialmente estes sistemas eram de controle manual, cada chamada tinha que ser estabelecida com a intervenção de uma operadora. Os sistemas automáticos surgiram em meados dos anos 60, mas ainda com poucas facilidades. Por exemplo, se um assinante tivesse uma chamada estabelecida em uma área geográfica, esta chamada deveria ser reiniciada caso este assinante se movesse para uma outra área.

Apesar das limitações destes sistemas e do alto custo dos serviços, o crescimento da demanda pelos serviços móveis era considerável. Tais sistemas, providos de um pequeno número de canais de rádio e com limitada capacidade de crescimento modular, não podiam suportar esta demanda. Novas idéias para o desenvolvimento de um sistema versátil, onde os assinantes pudessem "perambular" com o seu telefone móvel numa rede globalmente integrada, começaram a se materializar. A pedra fundamental deste sonho é a idéia CELULAR como descrito neste capítulo.

A expansão de um sistema móvel convencional depende principalmente da disponibilidade de espectro. O planejamento de rádio freqüência é um tópico extremamente intrincado, uma vez que o espectro de freqüência deve ser compartilhado por outros tipos de serviços. Existe uma considerável disponibilidade de espectro nas faixas mais altas, onde os problemas de propagação são extremamente complicados, dificultando a implementação de equipamentos para operar nestas bandas.

Contudo, se por um lado o espectro de freqüência, um recurso escasso e estritamente controlado pelos órgãos regulamentadores, dificulta a expansão dos sistemas, por outro lado a pressão da demanda por serviços móveis é de fato relevante.

A saída é obviamente a concepção de novas idéias básicas (conceituais). A implementação destas novas idéias pode requerer uma nova tecnologia, com o que é então possível implementar-se um sistema capaz não só de satisfazer a demanda inicial, mas também de oferecer novos serviços. Estes novos serviços podem gerar nova demanda e precisam ser regulamentados. Um novo ciclo então se inicia.

CONTEÚDO

Este capítulo estabelece os princípios básicos dos sistemas celulares de rádio móvel dando uma visão geral dos pontos principais a serem considerados no projeto de sistema. Destacam-se as diferenças relevantes entre as redes convencionais e as celulares, introduzindo-se os jargões comumente usados nestes últimos. Descreve-se brevemente cada componente celular e mostra-se como eles podem ser interligados para as diferentes arquiteturas. Introduz-se a teoria dos padrões e simetria de forma que alguns dos conceitos bem aceitos da geometria celular, hoje tidos como postulados, possam ser melhor entendidos.

O conceito celular tem embutido em si uma arquitetura modular que, em teoria, pode ser expandida indefinidamente. Existem, no entanto, restrições práticas que limitam este crescimento a tal ponto acima do que algumas técnicas alternativas são recomendadas. Estas técnicas são examinadas neste capítulo. Considera-se também a questão do desempenho do sistema, quando três medidas de eficiência (espectral, de troncalização e de custo) são descritas. O próximo tópico considerado neste capítulo relaciona-se com a transmissão de dados e controle de sinalização nos canais de rádio. Neste mesmo tópico ilustra-se de forma pictorial uma chamada bem sucedida do assinante móvel para o assinante fixo e vice-versa. Além disso ilustram-se também as seqüências de *handoff*.

Ainda dentro do intuito de se dar uma visão geral sistêmica, as especificações básicas de projeto de sistema seguidas pelos passos principais no projeto celular são abordados. Para finalizar o capítulo, algumas das técnicas não convencionais de

melhoria de desempenho de tráfego são mostradas. Novamente a abordagem dada aqui é superficial, mas um estudo mais detalhado é levado a cabo no Capítulo 12.

PARTE II

O CANAL DE RÁDIO MÓVEL

CAPÍTULO 3

MODELO DE PROPAGAÇÃO DE RÁDIO MÓVEL

INTRODUÇÃO

A comunicação com ou entre pontos móveis constitui uma tarefa bastante complicada e, com a tecnologia de hoje, é feita por meio de ondas de rádio. Este meio de transmissão tem uma grande dependência do ambiente onde a comunicação se processa. Desta forma ela pode ser influenciada por uma infinidade de parâmetros que caracterizam este ambiente.

Os sistemas de rádio móvel tem seguido uma tendência comum de utilizar altas freqüências devido ao congestionamento dos serviços que usam a parte baixa do espectro. Entretanto, trabalhar com altas freqüências geralmente leva a problemas intrincados e de difícil solução. A análise teórica dos fenômenos envolvidos é, na sua grande maioria, extremamente complexa devido ao número de variáveis a serem levadas em consideração. Muitas destas variáveis são simplesmente desprezadas para a maioria das aplicações de baixa freqüência. Considere, por exemplo, uma transmissão de rádio a 60 MHz, o que corresponde a um comprimento de onda de 5 m. Caso as obstruções encontradas por esta onda forem da ordem de alguns comprimentos de onda, estas poderão funcionar como espalhadores. De fato, se agora imaginarmos uma transmissão de rádio a 900 MHz (faixa geralmente utilizada para rádio móvel), obstruções de apenas algumas dezenas de centímetros podem espalhar o sinal.

Devido à propagação de multipercurso o sinal de rádio sofre desvanecimentos rápidos, com os mínimos chegando a 40 dB abaixo do nível médio do sinal. Os desvanecimentos também ocorrem devido ao sombreamento provocado por colinas, túneis e outras obstruções. A perda de percurso, sombreamento e desvanecimento rápido podem deteriorar o sinal propagado de tal forma que, se o sistema não for muito bem dimensionado, as perdas de comunicação podem tornar-se bastante freqüentes.

Além de tudo isto, a comunicação móvel também pode ser afetada pela interferência

de cocanal e de canal adjacente juntamente com os vários tipos de ruído gerados dentro do equipamento de rádio e pelo ambiente. O movimento do veículo impõe ainda algumas variações aleatórias no sinal, deteriorando bastante a comunicação.

Nota-se, pelo que foi brevemente exposto, que uma solução determinística para a variabilidade da potência do sinal de rádio móvel é de fato impossível. Parte-se então para o tratamento estatístico do sinal estudando-se os vários fenômenos envolvidos de maneira probabilística.

CONTEÚDO

Este capítulo descreve com um certo detalhe os vários modelos referentes aos fenômenos de propagação no ambiente de rádio móvel. Inicia-se por uma breve revisão de alguns tópicos relativos aos fundamentos de antenas, com o objetivo de chegar-se à fórmula de Friis para transmissão em espaço livre. Esta fórmula constitui a base para os modelos de perdas de propagação apresentados em seguida.

Os modelos de propagação podem ser divididos em dois grupos, a saber, os modelos teóricos e os empíricos. Os modelos teóricos são geralmente descritos através de expressões matemáticas fechadas, enquanto que os empíricos baseiam-se em tabelas e curvas obtidas em medidas de campo nas mais diversas condições. No primeiro caso muitas aproximações são feitas, de forma que os modelos não são diretamente aplicáveis às situações práticas. No segundo caso muitos parâmetros são levados em consideração, tornando os modelos bastante complexos. Uma combinação de ambos os grupos de modelos dá origem a um modelo de predição simplificado com excelentes resultados. Os vários parâmetros que afetam a propagação de rádio móvel são também discutidos e analisados.

Descreve-se então o comportamento estocástico do sinal de rádio móvel por meio das várias distribuições estatísticas de interesse (distribuição lognormal, de Rayleigh, de Rice e de Suzuki). Combinando-se convenientemente estas distribuições e alguns dos resultados mais importantes obtidos dos modelos de predição de perda de percurso, determina-se a área de cobertura da célula. Da mesma forma determinam-se as

fronteiras entre as células com o principal objetivo de obter-se o quanto as áreas de cobertura de células vizinhas se sobrepõe. Esta informação é de especial interesse quando técnicas de encaminhamento de tráfego alternativo podem ser aplicadas para melhorar o desempenho de tráfego do sistema de rádio móvel.

CAPÍTULO 4

EFEITOS DE PROPAGAÇÃO DE MULTIPERCURSO

INTRODUÇÃO

Um sinal de rádio transmitido de uma estação base chega à estação móvel como um conjunto de ondas espalhadas. O espalhamento pode ser provocado por múltiplas reflexões devido às irregularidades dos terrenos, presença de um grande número de obstruções, variação das constantes dielétricas dos meios, etc. Devido à aleatoriedade destes fenômenos, o sinal de rádio móvel é geralmente tratado numa base estatística. O envelope, a fase e a freqüência do sinal recebido variam aleatóriamente de acordo com algumas distribuições de probabilidade bem conhecidas. Em particular, o envelope do sinal recebido segue a distribuição de Rayleigh, enquanto a fase é uniformemente distribuida de 0 a 2π rad..

Outras estatísticas de relevância devem ser determinadas de forma a melhor caracterizar o sinal com desvanecimento Rayleigh. Uma destas estatísticas relaciona-se com a variação no tempo do envelope recebido. De maneira semelhante, a distribuição conjunta de dois sinais com desvanecimento de Rayleigh é de particular interesse. Com estas duas estatísticas é possível descrever e caracterizar alguns dos vários efeitos de propagação de multipercurso tais como *largura de banda coerente, taxa de cruzamento de nível, duração média do desvanecimento, FM aleatório* e outros. Assim, o capítulo dedica algumas de suas sessões para o detalhamento e obtenção destas distribuições.

Outros tópicos também tratados neste capítulo incluem o *efeito Doppler, delay spread, espectro de potência do sinal, medidas de campo* e *simulação de desvanecimento.*

CONTEÚDO

Neste capítulo selecionam-se para análise alguns dos aspectos mais relevantes a serem considerados no ambiente de propagação de multipercurso. Inicia-se com o conceito básico de velocidade de onda para, em seguida, derivar-se uma relação descrevendo o desvio de freqüência do sinal propagado devido à movimentação do veículo. A fórmula obtida é, na realidade, uma aproximação de uma mais complexa dada pela Teoria da Relatividade.

Estuda-se então o comportamento estatístico do *time delay* e *delay spread* do sinal propagado. O efeito deste *delay* é analisado de forma a determinar-se o fator de correlação de dois sinais recebidos, dados o *time delay* e/ou a separação em freqüência entre eles. A separação em freqüência entre dois sinais para um dado fator de correlação é conhecida como largura de banda coerente. Uma vez que no meio de multipercurso lida-se com desvanecimento rápido, torna-se interessante determinar-se a freqüência de ocorrência do desvanecimento dado um nível de tensão de limiar: isto é conhecido como taxa de cruzamento de nível. A duração do desvanecimento é também de interesse.

O próximo tópico de relevância concerne o estudo da aleatoriedade da variação da freqüência (fase) e seus efeitos na qualidade do sinal recebido. Mostra-se que este fenômeno, conhecido como modulação em freqüência aleatória, introduz um ruído cuja potência varia com o quadrado da velocidade do veículo. Determinam-se também os espectros de potência do sinal e suas dependências com o ganho da antena. Todos estes fenômenos podem ser observados por medidas de campo. Salientam-se ainda os pontos principais a serem considerados na aquisição e análise de dados em campo. Finalmente mostram-se as várias maneiras de implentarem-se simuladores de desvanecimento, incluindo uma abordagem analógica e outra com técnicas de processamento digital de sinais.

PARTE III

MÉTODOS DE DIVERSIDADE-COMBINAÇÃO

CAPÍTULO 5

COMBATE AO DESVANECIMENTO

INTRODUÇÃO

A demanda crescente por serviços de rádio móvel obriga a que os projetistas de sistema e operadoras encontrem meios não só de satisfazer tal demanda mas também de melhorar o desempenho do sistema. Uma das maiores causas de degradação do desempenho dos sistemas de rádio móvel é a ocorrência de desvanecimento. O sinal recebido por um veículo movimentando-se em um ambiente urbano típico pode sofrer variações extremas, e 40 dB abaixo da média do sinal não é tão incomum. O envelope do sinal desvanece-se de acordo com a distribuição de Rayleigh com sucessivos mínimos ocorrendo a cada meio comprimento de onda da portadora, aproximadamente.

No que concerne à transmissão de voz, os efeitos da propagação de multipercurso, embora não agradáveis, podem não ser essencialmente críticos. O maior problema ocorre quando dados ou sinalização estão envolvidos: uma perda de comunicação em instantes cruciais pode ser extremamente prejudicial (imagine, por exemplo, o sistema perdendo o controle de uma longa chamada internacinal exatamente no instante de bilhetagem...). Existe um consenso geral no sentido de prover o sistema com melhores serviços onde a transmissão de voz e dados alcance os padrões de grau de serviço estabelecidos.

Contudo, superar os efeitos do multipercurso (o desvanecimento) não é uma tarefa simples, e, de fato, contitui um dos problemas mais difíceis a ser solucionado no projeto do sistema de rádio móvel.

O desvanecimento é em geral combatido através de métodos de diversidade. Os princípios de diversidade baseiam-se no fato que desvanecimentos ocorrendo em canais independentes constituem eventos independentes. Portanto, se uma dada informação estiver redundantemente disponível em dois ou mais canais (conhecidos como "ramos de diversidade"), a probabilidade que esta informação seja afetada por um desvanecimento profundo, ocorrendo simultaneamente em todos os ramos, é muito pequena. Assim, com um

algorítmo conveniente (conhecido como "método de combinação") é possível obter-se um sinal resultante tal que os efeitos do desvanecimento sejam minimizados.

O uso de algumas técnicas de diversidade em sistemas de comunicação data dos anos 20. Desde aquela época os esquemas de diversidade sofreram algumas melhorias. Embora não tão largamente conhecido como tal, o *handoff* de uma estação base para outra constitui uma forma de diversidade. Neste capítulo enfatizam-se os métodos alternativos, que não o *handoff*. Inicialmente descrevem-se os métodos usados para a obtenção dos ramos independentes, isto é, como a informação pode ser repetida e propagada através de diferentes percursos. Em seguida examinam-se os métodos de combinação (processamento) do sinal recebido de forma a obter-se a melhor saída (*output*).

Existem bàsicamente dois tipos de desvanecimento no ambiente móvel: o de longo prazo (*long term*) e o de curto prazo (*short term*). Os métodos de combater os seus efeitos são òbviamente diferentes e serão considerados separadamente.

CONTEÚDO

O objetivo deste capítulo é descrever os princípios, funcionamento, desempenho, vantagens e desvantagens das várias técnicas de combate aos efeitos do desvanecimento. O problema é inicialmente abordado pelo lado macroscópico, quando será visto que apenas um método é efetivo para combater o desvanecimento lento (lognormal): diversidade espacial. No lado microscópico, seis técnicas para combater o desvanecimento rápido (Rayleigh) são descritas: diversidade espacial, de polarização, de ângulo, de freqüência, de tempo e *hopping*. Equalização adaptativa e codificação também constituem meios eficientes de combater o desvanecimento. Contudo, como estas técnicas são essencialmente aplicáveis às comunicações digitais, elas serão exploradas no Capítulo 6.

Quatro métodos de combinação tais como seleção pura, seleção por limiar, razão máxima e ganho unitário são investigados. O desempenho de cada técnica de combinação é

medido pela razão sinal-ruído obtido na saída do combinador. Assim, as distribuições destas várias razões sinal-ruído como funções do número de ramos de diversidade são determinadas e analisadas.

É mostrado que, levando-se em conta o fator custo-benefício, o esquema de diversidade de dois ramos constitui a melhor opção para o combate ao desvanecimento.

CAPÍTULO 6

TRANSMISSÃO DE DADOS E SINALIZAÇÃO

INTRODUÇÃO

No sistema de rádio móvel dados e sinalização podem ser transmitidos em canais de voz ou em canais especiais de sinalização, dependendo da tarefa de controle a ser implementada. Exemplos de tarefas de controle incluem as diversas fases do estabelecimento de uma chamada, *handoff* entre estações bases, desconexão da chamada, etc. A troca de mensagens entre a estação móvel e a estação base é feita via rádio, enquanto que mensagens entre a estação base e a central de comutação móvel geralmente seguem via fios.

Existem dois tipos de mensagens transmitidas sobre os canais de rádio: (i) aquelas enviadas como um fluxo contínuo de bits e (ii) aquelas enviadas em surtos. As primeiras incluem a rádio chamada (*paging*) da estação móvel, relatórios do *status* do sistema e mensagens de *overhead*, e são transmitidas em canais especiais de sinalização. As últimas compreedem: (a) liberação de chamadas e *handoff*, que fazem uso dos canais de voz, e também (b) requisições de serviços da estação móvel à estação base, e fazem uso de canais especiais de sinalização.

Nos sistemas analógicos uma atenção especial deve ser dada aos problemas que surgem da associação de voz, usando transmissão analógica, e dados, usando transmissão digital. Nos sistemas digitais dados e voz digitalizada podem fazer uso das mesmas técnicas de modulação digital.

Uma questão de especial importância na transmissão digital é a sincronização. *Jitter* de tempo e desvio de freqüência do relógio podem provocar um aumento da taxa de erro de bit ou palavra degradando o desempenho do sistema. Torna-se importante o uso de técnicas que minimizem os efeitos destes fenômenos. Uma seqüência de 1s e 0s alternados pode ser usada para obter-se sincronização de bit. Da mesma forma, a inclusão de padrões conhecidos no início e/ou fim do quadro pode ser usada para obter-

se sincronização de quadro.

Apesar da sincronização erros de bits ou palavras ainda podem ocorrer devido a muitos outros fatores, incluindo principalmente o desvanecimento. Este capítulo objetiva examinar a ocorrência de erros na transmissão de dados em sistemas de rádio móvel e também investigar os métodos usuais empregados para minimizar a ocorrência de erros. Presta-se especial atenção aos sistemas de modulação binária devido à sua simplicidade e aplicabilidade universal. Além disso, estes são os esquemas de modulação utilizados pelos sistemas analógicos. É sabido, no entanto, que os sistemas móveis digitais usam modulação de maior ordem. O objetivo do capítulo, entretanto, não é comparar esquemas de modulação mas investigar os efeitos qualitativos das técnicas utilizadas para melhorar o desempenho da taxa de erro de bits. Além disso, todos os procedimentos aqui descritos podem ser diretamente aplicados aos esquemas de modulação de maior ordem.

CONTEÚDO

Este capítulo examina o desempenho da transmissão digital em um ambiente com desvanecimento. A medida de desempenho é a taxa de erro de bit (ou, equivalentemente, a probabilidade de erro de bit) para uma dada razão sinal-ruído por bit.

Procede-se inicialmente a uma revisão da taxa de erro de bit para algumas modulações binárias, tais como FSK e PSK, para em seguida examinar-se como os seus desempenhos podem ser melhorados. O objetivo é obter-se uma idéia qualitativa da melhora alcançada quando diversidade, codificação ou transmissão múltipla são empregados. Desta forma, as técnicas de modulação binária foram escolhidas para facilitar a análise. Contudo, os princípios básicos aqui descritos podem ser diretamente aplicados aos esquemas de modulação mais elaborados como aqueles estudados no Capítulo 9. Algumas outras técnicas tais como interpolação, ARQ e equalização adaptativa são também brevemente investigadas. Um apêndice sobre codificação de canal é incluído com o objetivo de introduzir os conceitos básicos e os principais códigos.

PARTE IV

RUÍDO, INTERFERÊNCIA E MODULAÇÃO

CAPÍTULO 7

RUÍDO E INTERFERÊNCIA

INTRODUÇÃO

Ruído e interferência são dois fenômenos que limitam a operação dos equipamentos de comunicação. O ruído é uma perturbação indesejada presente dentro da faixa de freqüência de operação tendo origem em várias fontes com diferentes características. A interferência de rádio é gerada dentro dos próprios sistemas de comunicações. Isto tem se tornado um dos maiores problemas a serem atacados, uma vez que o crescimento de tais sistemas ocorre de maneira rápida e de certa forma caótica. Torna-se, portanto, essencial caracterizar os diferentes tipos de ruído e interferência para que os sistemas possam ser projetados de forma a garantir um sinal convenientemente acima do ruído e interferência. A caracterização destes fatores limitantes é importante no desenvolvimento de métodos de predição do desempenho dos sistemas de comunicação. Como conseqüência, sistemas projetados para operar adequadamente sob circunstâncias desfavoráveis podem ser atingidos.

Uma importante medida de desempenho na avaliação da qualidade de transmissão é a razão portadora-ruído que será examinada para o caso do sistema de rádio móvel. Outra medida, agora concernente à interferência, é a razão portadora-interferência, calculada diferentemente para os casos de canal adjacente e cocanal, uma vez que suas características são, de fato, diferentes. Será visto que o desempenho para uma dada razão portadora-ruído é dependente do esquema de modulação utilizado, enquanto que o desempenho para uma dada razão portadora-interferência depende predominantemente do padrão celular. Serão discutidos os diferentes métodos de melhoria do desempenho do sistema onde os novos padrões celulares são de fundamental interesse. Estes padrões são obtidos de maneira não convencional através do uso de antenas direcionais.

CONTEÚDO

Este capítulo aborda as questões relativas a Ruído e Interferência. Uma vez que ruído constitui um assunto já bastante explorado nos estudos dos sistemas de comunicação em geral, o tratamento dado aqui será breve e apenas descritivo. Os dois tipos de ruído, aditivo e multiplicativo, são estudados mas uma atenção especial será dada ao do tipo aditivo uma vez que o multiplicativo é o próprio desvanecimento, já extensivamente explorado nos capítulos anteriores.

O principal objetivo deste capítulo é, portanto, o estudo da interferência que pode ser classificada em quatro categorias: intermodulação, intersimbólica, de canal adjacente e de cocanal. Os problemas de intermodulação e interferência intersimbólica são examinados, mas o foco principal será sobre interferências de canal adjacente e cocanal.

A interferência de canal adjacente é tratada aqui de uma maneira diferente daquela feita por outros autores. Aqui a ênfase será sobre a influência da distribuição de tráfego na probabilidade de ocorrência de interferência de canal adjacente. Mais especificamante, será estudada como esta probabilidade é afetada pela presença de estações móveis nas proximidades da fronteira entre as células.

Os problemas de interferência de cocanal serão atacados com o interesse inicial de obter-se uma solução analítica. Isto é feito para o caso do ambiente Rayleigh, embora casos mais complexos podem ser tratados por meio de análise numérica. Estes casos incluem múltiplos sinais interferentes com o desvanecimento puramente lognormal ou puramente Rayleigh ou ambos combinados. Uma abordagem alternativa pode ser dada através do uso de simulação de Monte Carlo, descrita no final do capítulo. Mostra-se que esta abordagem oferece uma maior flexibilidade e que o problema pode ser tratado de uma maneira mais realística. O uso de antena direcional como meio de minimizar a interferência de cocanal é também discutido e a descoberta de novos padrões celulares é facilitado pelo uso de simulação.

CAPÍTULO 8

MODULAÇÃO ANALÓGICA PARA RÁDIO MÓVEL

INTRODUÇÃO

Modulação é o processo pelo qual um ou mais parâmetros (amplitude, ângulo) de uma portadora são variados de acordo um sinal mensagem (onda moduladora). Como resultado do processo de modulação a faixa de freqüência do sinal mensagem é deslocada para uma região do espectro de forma a tornar a comunicação pelo canal viável. À recepção o receptor reverte o processo de modulação implementando a demodulação ou detecção, de forma a recuperar o sinal mensagem transmitido.

Os sistemas de rádio móvel da primeira geração usam modulação analógica para a transmissão de voz. Os primeiros sistemas móveis (sistemas convencionais) usavam Modulação em Amplitude (AM), uma vez que este era o esquema disponível na época. O esquema foi mudado ràpidamente para Modulação em Freqüência tão logo ficou demonstrada a sua viabilidade prática. A técnica SSB (Single SideBand) também teve sua vez em alguns serviços móveis. Contudo, FM acabou predominando e hoje todos os sistemas celulares analógicos adotam este esquema para modulação de voz. Algumas formas mais avançadas de SSB tais como o *Transparent Tone In Band* (TTIB), *Feed Forward Signal Regeneration* (FFSR) e *Amplitude Companded Single Sideband* (ACSSB) tem sido propostas e intensivamente investigadas, com uma boa chance de virem a ser utilizadas por alguns serviços de rádio móvel.

CONTEÚDO

Este capítulo objetiva o estudo do desempenho de algumas técnicas de modulação analógica, tais como AM, SSB e FM no ambiente de rádio móvel. Inicia-se o capítulo com a definição dos parâmetros de desempenho, consistindo bàsicamente da razão sinal-ruído e suas variações.

Analisa-se em seguida cada técnica de modulação separadamente revendo-se os seus princípios básicos, a largura de banda para transmissão e os meios de geração e detecção dos sinais modulados. Formula-se então um modelo geral do sinal recebido e analisa-se o desempenho da técnica de modulação na presença de ruído aditivo e multiplicativo. Mostra-se que o ruído multiplicativo (desvanecimento) tem um efeito desastroso nos sistemas AM e SSB e que o efeito de captura dos sistemas FM não é tão acentuado na presença de desvanecimento.

Consideram-se ainda algumas formas alternativas que melhoram o desempenho dos sistemas SSB e os tornam bons candidatos para aplicações em rádio móvel.

CAPÍTULO 9

TÉCNICAS DIGITAIS PARA RÁDIO MÓVEL

INTRODUÇÃO

Um sinal analógico em um sistema de comunicações digitais passa por dois processos básicos antes da transmissão: Conversão A/D e Modulação. A conversão Analógica-Digital (A/D) reduz a complexa forma de onda analógica a uma conveniente configuração digital. A Modulação então processa a forma de onda digital obtida de modo a torná-la apta à transmissão.

Conversão A/D

A Conversão A/D compreende três passos básicos, quais sejam, Amostragem, Quantização e Codificação. A amostragem é um processo de detecção do valor instantâneo da forma de onda, geralmente feita a intervalos regulares de tempo. O teorema da amostragem requer que o sinal seja amostrado a uma freqüência maior ou igual a duas vezes a máxima freqüência presente neste sinal. Para sinais telefônicos, com faixa de 3,4 kHz adicionada a uma faixa de guarda de 600 Hz, a freqüência de amostragem deve ser no mínimo de 8 kHz (correspondendo a um intervalo máximo de 125 μs entre amostras). Depois da amostragem obtem-se uma seqüência de pulsos. Estes pulsos tem suas amplitudes iguais (ou proporcionais) à amplitude do sinal analógico nos instantes da amostragem. A forma de onda resultante é conhecida como sinal Modulado por Amplitude de Pulso (PAM).

O próximo passo no processo de digitalização é a Quantização. Quantização consiste em atribuir um novo valor de amplitude a cada pulso dentro do domínio de níveis de amplitudes discretas especialmente criadas para este fim. Este passo introduz um ruído no processo, o Ruído de Quantização, devido às possíveis diferenças entre a verdadeira amplitude e aquela atribuída. Quanto maior o número de níveis de quantização menor o ruído de quantização. Sabe-se que para sinais telefônicos uma razão sinal-ruído de quantização entre 30 a 40 dB é bastante razoável e pode ser

obtida com 256 níveis.

Codificação é o próximo passo no processo de digitalização. Uma das técnicas mais antigas e conceitualmente mais simples usada para sinais de voz e vídeo é o PCM (*Pulse Code Modulation*). Em PCM o sinal PAM é convertido em uma seqüência de bits e multiplexado para transmissão serial. Os 256 níveis de quantização podem ser representados (codificados) por um mínimo de 8 bits, resultando numa taxa de transmissão de 8000 amostras/segundo x 8 bits/amostra = 64 kbits/s. Desta forma um sinal analógico de 3,4 kHz de faixa usando PCM requer uma faixa muito grande para transmissão (algumas dezenas de kHz), o que constitui uma dos principais restrições ao uso de sinais digitais para sistemas de rádio móvel.

No sistema PCM convencional de 64 kbits/s cada amostra é quantizada e codificada independentemente uma da outra. Sabe-se que amostras sucessivas apresentam uma correlação de mais de 0,85. Se a correlação entre amostras for levada em consideração, menos bits podem ser utilizados para representar o sinal de voz. Os algorítmos modernos de codificação de voz exploram este fato para reduzir a taxa de transmissão. Existe um número "incontável" de algorítmos de codificação de voz. Um estudo completo destas técnicas está muito acima do escopo deste livro. Serão mostrados os fundamentos das técnicas de codificação de voz, explorando os algorítmos escolhidos para serem utilizados nos sistemas celulares digitais europeu e americano.

Modulação

Modulação pode ser considerada como um segundo estágio de codificação. Muitos aspectos devem ser considerados na escolha de um esquema de modulação, incluindo (i) a largura da faixa requerida, (ii) interferência intersimbólica, (iii) interferência de canal adjacente e (iv) taxa de erro de bit (BER).

As modulações binárias, tais como ASK, FSK e PSK, são deveras simples, robustas mas ineficientes em termos de utilização do espectro. Neste sentido, técnicas de modulação multinível são preferidas, apesar de apresentarem um desempenho pior em BER. Para se ter uma idéia do problema, considere um canal de largura de B kHz. Grosseiramente falando, um modulador binário pode transmitir B kbits/s por este canal.

Suponha agora que cada par de um símbolo binário seja codificado em apenas um símbolo. Por exemplo, em ASK isto poderia ser feito atribuindo os símbolos 0, 1, 2 e 3 aos pares 00, 01, 10 e 11, respectivamente. Assim a taxa de símbolo é dividida por 2 com uma correspondente diminuição da banda ocupada. Por outro lado, a taxa de erro é aumentada devido ao número de níveis que deve ser reconhecido na recepção.

Da mesma forma que a codificação de voz, também existe um número muito grande de técnicas de modulação digital. Portanto, uma investigação completa destas técnicas está acima do escopo deste livro. O capítulo deverá enfocar as técnicas utilizadas pelos sistemas celulares digitais europeu e americano.

CONTEÚDO

Este capítulo examina duas técnicas básicas usadas em sistemas de rádio móvel digitais, quais sejam, codificação de voz e modulação. Uma vez que existe um número "incontável" de esquemas de codificação de voz e modulação, serão analisadas apenas aquelas selecionadas para serem utilizadas nos sistemas celulares digitais europeu e americano, além das técnicas mais próximas destas (ou que deram origem às mesmas).

Inicialmente introduzem-se os princípios de Codificação por Predição Linear e Quantização Vetorial. Em Codificação por Predição Linear os princípios básicos de Predição Linear são brevemente examinados. Descrevem-se em seguida algumas técnicas LPC tais como RELP, RPE-LPC, MPE-LPC, RPE-LTP, MPE-LTP, CELP e VSELP. Como as técnicas RPE-LTP e VSELP foram as selecionadas para serem utilizadas nos sistemas europeu e americano, respectivamente, elas serão melhor exploradas.

Examinam-se então alguns esquemas de modulação de maior ordem, tais como QPSK, DQPSK, MSK e GMSK. Seus princípios básicos são estudados juntamente com os métodos usados para geração, detecção, além de serem determinados os seus espectros de potência e taxa de erro de bit. Nos estudos de taxa de erro de bit o desempenho das técnicas é examinado levando-se em consideração o canal Gaussiano e também o canal de desvanecimento de Rayleigh. Neste último consideram-se os casos de devanecimento lento

e rápido apenas para as técnicas DQPSK e GMSK , uma vez que estas são as selecionadas para serem usadas nos sistemas europeu e americano, respectivamente.

PARTE V

MÚLTIPLO ACESSO

CAPÍTULO 10

ARQUITETURA DE MÚLTIPLO ACESSO

INTRODUÇÃO

O compartilhamento de recursos em redes de comunicações constitui uma maneira eficiente de atingir-se alta capacidade . Relativamente aos sistemas de rádio móvel os recursos são os canais de rádio, ou mais genèricamente, a faixa de freqüência disponível. Para maior eficiência o método de acesso deve permitir que qualquer terminal (as estações bases) esteja apto a usar os recursos num sistema totalmente troncalizado. Quando os canais são alocados sob demanda, o procedimento é conhecido como DAMA (*Demand-Assigned Multiple Access*).

Dependendo de como o espectro disponível é utilizado o sistema pode ser classificado como de Faixa Estreita ou de Faixa Larga. Na arquitetura de faixa estreita a banda de freqüência disponível é dividida em canais de faixa estreita, enquanto que na arquitetura de faixa larga todo o espectro ou uma parte significativa deste é compartilhado por todos os usuários.

Existem bàsicamente três métodos de acesso de acordo com os meios (freqüência, tempo ou código) utilizados para sua implementação:

- Múltiplo Acesso por Divisão de Freqüência (FDMA)
- Múltiplo Acesso por Divisão de Tempo (TDMA)
- Múltiplo Acesso por Divisão de Código (CDMA)

FDMA é intrinsecamente uma arquitetura de faixa estreita enquanto que CDMA é uma arquitetura de faixa larga. TDMA, por outro lado, pode ser implementado como de faixa estreita ou de faixa larga.

No caso de comunicações do tipo *two way* (ping pong) , a conexão pode ser feita por meio de divisão de freqüência ou por divisão de tempo. No primeiro caso o sistema é conhecido como *Frequency Division Duplex* (FDD) e no segundo caso tem-se o *Time Division Duplex* (TDD).

CONTEÚDO

Este capítulo examina as várias tecnologias de transmissão que podem ser utilizadas em sistemas de rádio móvel. As diferentes abordagens podem ser classificadas em basicamente duas categorias: transmissão de faixa estreita ou de faixa larga.

Os sistemas de faixa estreita e de faixa larga são examinados e suas características e limitações discutidas. O capítulo investiga os esquemas de acesso FDMA, TDMA e CDMA. Estes métodos de acesso são examinados independentemente uns dos outros de acordo com suas próprias características. Os princípios básicos destes três tipos de esquema de acesso com suas vantagens/desvantagens são também considerados.

Em particular, para o caso de FDMA discutem-se os efeitos das não linearidades dos circuitos dos equipamentos de rádio. Nos sistemas TDMA as principais questões são hierarquia, sincronização e medidas de eficiência. Os sistemas CDMA são então analisados à luz da tecnologia de *spread spectrum*. Assim, uma parte significativa da sessão correspondente é dedicada aos fundamentos de *spread spectrum*. Finalmente, discutem-se as maneiras como uma comunicação do tipo ping pong pode ser implementada. As técnicas correspondentes, *Frequency Division Duplex* e *Time Division Duplex*, são brevemente descritas.

CAPÍTULO 11

PROTOCOLOS DE ACESSO

INTRODUÇÃO

O sistema de rádio móvel contitui um típico exemplo de uma rede de comunicação de múltiplo acesso onde os terminais, representados pelas estações móveis, compartilham os canais de rádio como recursos comuns. Os canais de rádio são divididos em canais de voz e de controle, o modo de acesso aos últimos sendo o objeto de estudo deste capítulo.

O compartilhamento de recursos pode aumentar de maneira considerável a eficiência do sistema. Assim, é desejável que se otimize o uso dos canais, mantendo-os ocupados com informação útil a maior parte de seu tempo. Contudo, devido ao compartilhamento, podem ocorrer colisões no caso de mais que um terminal tentar transmitir simultaneamente no mesmo canal. Desta forma estabelece-se uma certa disciplina de acesso, para que os conflitos entre os terminais sejam mantidos a um mínimo mas com a máxima utilização dos canais.

CONTEÚDO

Este capítulo introduz os protocolos de múltiplo acesso mais comumente utilizados em redes de comunicação com múltiplo acesso. O objetivo é prover os princípios básicos para a análise de um protocolo em particular no ambiente de rádio móvel.

O sistema de rádio móvel constitui um exemplo típico de uma rede de comunicação com múltiplo acesso, onde os canais de controle são compartilhados pelas estações móveis. O desempenho dos protocolos é avaliado pela vazão (*throughput*) e uma atenção especial é dada ao *Slotted ALOHA*, escolhido para ser analisado no ambiente de rádio móvel. O canal de rádio é caracterizado pela perda de percurso (efeito *near/far*) e desvanecimento Rayleigh. Além disso cosidera-se o receptor operando com o efeito de

captura. Ao contrário do que inicialmente é esperado, a combinação destes fenômenos melhora de maneira considerável o desempenho do protocolo escolhido.

PARTE VI

TRÁFEGO

CAPÍTULO 12

ASPECTOS DE TRÁFEGO EM SISTEMAS DE RÁDIO MÓVEL

INTRODUÇÃO

Embora as características de tráfego do sistema de rádio móvel sejam bastante distintas daquelas da rede telefônica fixa, o planejamento e o projeto de sistema são ainda feitos usando-se as mesmas técnicas da teoria de tráfego convencional. De acordo com o perfil de tráfego esperado e dados os requisitos de interferência de cocanal, a região geográfica é dividida em células. Dado o tráfego por célula e a probabilidade de bloqueio admissível, usa-se a fórmula Erlang-B para determinar-se o número de canais por célula, assumindo-se a não ocorrência de *handoff* ou *roaming*. O projeto é posteriormente ajustado para levar estes fatores em consideração.

É possível projetarem-se as células de forma que elas tenham a mesma área mas diferentes números de canais, de acordo com os requisitos de probabilidade de bloqueio e com o tráfego oferecido. Alternativamente, as células podem apresentar o mesmo número de canais mas áreas diferentes, também de acordo com o grau de serviço desejado.

A distribuição de tráfego varia no tempo e no espaço, mas é em geral do tipo "formato de sino" (*bell shape*). Uma alta concentração de tráfego é encontrada no centro da cidade e durante a hora do *rush*, decrescendo em direção à periferia. Após a hora do *rush* e mais para o final do dia, esta concentração de tráfego muda, uma vez que os assinantes deslocam-se do local do trabalho (centro da cidade) para suas casas.

Note que, por causa da mobilidade dos assinantes *handoff* e *roaming* estão sempre ocorrendo, reduzindo assim o tempo de retenção das chamadas nas células onde estas chamadas são originadas. Conseqüentemente, o tráfego da célula para onde os usuários se deslocam aumenta. Desta forma a fórmula Erlang-B não mais se aplica. Uma investigação completa do desempenho do tráfego do sistema de rádio móvel onde todos os fenômenos são levados em consideração é deveras complicada. É possível, no entanto,

introduzirem-se algumas simplificações a fim de obter-se um resultado qualitativo e não quantitativo para um melhor entendimento dos fenômenos principais.

CONTEÚDO

Este capítulo examina algumas das principais técnicas de alocação de canal que podem ser utilizadas em sistemas de rádio móvel. Inicia-se por uma revisão dos princípios básicos das teorias de tráfego e filas, comumente utilizadas na análise de problemas de teletráfego. As técnicas de alocação de canais são divididas em dois grupos, a saber, Globais e Locais. As técnicas globais geralmente implicam uma mudança substancial no padrão de uso dos canais, envolvendo o controle central do sistema. Nas técnicas locais, embora alguma mudança deste padrão possa ocorrer, os canais são usados dentro da ou adjacente à área de serviço inicialmente planejada. Neste caso as decisões são tomadas localmente por envolverem apenas células vizinhas.

As técnicas globais de alocação são investigadas por meio de simulação, onde os principais fenômenos, tais como *handoff*, interferência de cocanal, interferência de canal adjacente e outros, são levados em consideração. Uma atenção especial é dada à técnica de alocação Híbrida onde mostra-se que com apenas uma pequena proporção de canais dinâmicos é possível obter um ganho considerável na capacidade de tráfego.

As técnicas locais são investigadas por meio do processo de Markov num sistema de duas células. O objetivo é obter uma idéia dos principais fenômenos envolvidos e não uma medida quantitativa de desempenho. Em particular, examina-se a técnica Variação de Limiar de Bloqueio usando-se análise numérica. Mostra-se que o uso de uma pequena quantidade de canais para encaminhamento alternativo proporciona um ganho significativo na capacidade de tráfego. Uma expressão aproximada para o bloqueio médio do sistema é encontrada fornecendo resultados bastante próximos da solução exata.

CONCLUSÕES

O objetivo desta sessão é salientar as principais conclusões de cada uma das partes que compreedem o livro *Foundations of Mobile Radio Engineering*, do mesmo autor.

INTRODUÇÃO

Os serviços de rádio móvel iniciaram-se logo após a invenção do rádio passando por uma série de estágios de regulamentação e evolução tecnológica. Ainda hoje, devido à grande demanda por serviços móveis, tanto a regulamentação quanto a implementação de novas tecnologias passam por um processo de conturbados debates, onde os grandes interesses estão em jogo.

O conceito celular já é bastante antigo mas só recentemente pode ser colocado em prática, e hoje ao se falar em comunicações móveis o modelo celular está implícito. Com este novo conceito novas medidas de avaliação da eficiência de sistema apareceram, destacando-se entre elas a eficiência espectral que combina tráfego por área e largura da banda disponível.

O CANAL DE RÁDIO MÓVEL

Os modelos de predição da potência do sinal de rádio móvel podem ser divididos em (I) teóricos, (II) empíricos e (III) estatísticos. Os teóricos tem aplicabilidade bastante restrita e servem apenas de base para entender os principais fenômenos de propagação. Os empíricos são em grande número, variando de modelos muito simples até bastante sofisticados, estes últimos requerendo o uso de um elevado número de dados referentes à topografia do terreno. Os modelos empíricos foram obtidos através de medidas de campo tomadas em diversas localidades e em diferentes ocasiões. A utilização destes modelos requer o uso de curvas e parâmetros de ajustes às diversas aplicações. Os modelos estatísticos combinam alguns resultados principais dos modelos empíricos e as distribuições estatísticas do envelope do sinal.

De uma maneira geral, em relação ao canal de rádio móvel pode-se dizer que:

(I) A potência do sinal decresce com a distância d como $d^{-\alpha}$, onde α é um parâmetro dependente do ambiente variando entre 3 e 4;

(II) O desvanecimento lento devido ao sombreamento segue uma distribuição lognormal com desvio padrão entre 4 e 12 dB;

(III) O desvanecimento devido ao multipercurso tem uma distribuição de Rayleigh. Dentro de edifícios e para microcélulas, onde existe linha de visada, o sinal segue a distribuição de Rice.

Os fenômenos de propagação de multipercurso tais como o *delay spread*, *time delay* e *Doppler Shift* são importantes na determinação da largura de banda coerente, a partir do que os sistemas podem ser definidos como de faixa estreita ou de faixa larga. Em particular os sistemas analógicos são do primeiro tipo enquanto que os digitais tendem à arquitetura faixa larga.

MÉTODOS DE DIVERSIDADE-COMBINAÇÃO

O combate ao desvanecimento lento só pode ser feito através de diversidade espacial (macroscópica) de forma a se evitar o sombreamento. Por outro lado, o desvanecimento rápido pode ser combatido através da diversidade microscópica que inclui a espacial, de polarização, de ângulo, de tempo, de freqüência e *hopping*. Os métodos de combinação podem ser do tipo razão máxima, ganho unitário, seleção pura e seleção por limiar. O desempenho destes métodos de combinação segue esta ordem, do melhor para o pior. Mostra-se que quanto maior o número de ramos utilizados melhor a relação sinal-ruído à saída do combinador. Contudo, na prática, o uso de mais que dois ramos é inviável devido ao encarecimento do equipamento, e de fato desnecessário já que o benefício conseguido não é significativo.

Relativamente à transmissão digital os métodos acima citados também podem ser utilizados para combater os efeitos do desvanecimento. Acrescentam-se a estes a codificação, a múltipla transmissão, interpolação, *automatic repeat request* e

equalização adaptativa. A diversidade espacial continua sendo uma técnica bastante poderosa melhorando a relação sinal-ruído em mais de 12 dB para uma taxa de erro de bit de 10^{-3}. Os códigos de detecção e correção de erros só são efetivos se combinados com interpolação. A transmissão múltipla também é uma boa opção mas requer uma largura de banda maior. A transmissão de dados pode, em geral, suportar algum atraso enquanto que a sinalização requer resposta rápida e com baixa taxa de erro. Assim codificação é uma técnica apropriada para dados e sinalização. A transmissão múltipla é mais apropriada para sinalização enquanto que ARQ é mais conveniente para dados.

RUÍDO, INTERFERÊNCIA E MODULAÇÃO

Dos tipos de ruídos aditivos o de maior influência no desempenho dos sistemas de comunicações móveis são aqueles provocados pelo homem (*man-made noise*). Estes ruídos ocupam uma faixa muito grande do espectro sendo difícil caracterizá-los ou modelá-los convenientemente. Os ruídos multiplicativos são os próprios desvanecimentos.

A interferência de canal adjacente depende substancialmente do esquema de modulação utilizado. Além disto a distribução geográfica dos assinantes e o perfil de tráfego do sistema podem afetar este tipo de interferência. Em particular, se técnicas de encaminhamento de tráfego alternativo forem utilizadas a qualidade de transmissão pode ficar comprometida.

A interferência de cocanal é um parâmetro de grande importância no projeto de sistema e que depende substancialmente do padrão celular utilizado. Na verdade este constitui um dos parâmetros mais difíceis de ser determinado devido ao grande número de variáveis envolvido na estimação do mesmo. Uma abordagem bastante conveniente para este fim é a simulação de Monte Carlo devido à flexibilidade de inclusão e manipulação das variáveis envolvidas.

Os efeitos do desvanecimento nos sistemas AM e SSB são desastrosos. Assim, apesar de requerer mais faixa, os sistemas FM são preferidos e de fato FM é o tipo de modulação utilizado nos sistemas celulares analógicos. Algumas formas alternativas de

modulação SSB usando um tom piloto dentro da faixa juntamente com compansão de amplitude tem sido propostas e investigadas, com grande chance de virem a ser utilizadas nos serviços móveis via satélite.

Um dos maiores desafios no uso de comunicação rádio digital no ambiente móvel é a redução da faixa requerida. De fato, redução de faixa de frequência está intimamente relacionada com redução de taxa de bit. O uso apropriado de algorítmos de codificação de voz pode reduzir drásticamente o número de bits necessários na codificação. Além disso, o uso de modulações de maior ordem também pode colaborar neste sentido. No ambiente móvel é conveniente que o envelope do sinal seja aproximadamente constante para robustecimento contra o desvanecimento. Além disso a modulação deve ser insensível à amplificação não linear. O grande desafio,, no entanto, é conciliar eficiência espectral e eficiência de potência. As técnicas que proporcionam eficiência de potência apresentam baixa taxa de erro de bit, obtida às custas de uma maior faixa de freqüência. Técnicas com eficiência espectral, por outro lado, apresentam um baixo desempenho em termos da taxa de erro de bit. Uma abordagem bastante promissora é aquela que combina modulação e codificação simultaneamente como, por exemplo, *Trellis Coded Modulation*.

MÚLTIPLO ACESSO

A escolha de um esquema de múltiplo acesso para sistema de rádio móvel envolve diversos aspectos além da simples questão de capacidade sistêmica. Em particular, para os sistemas digitais os três métodos de acesso, FDMA, TDMA e CDMA, podem ser usados, ao contrário dos sistemas analógicos onde apenas FDMA é viável. De fato, existe uma disputa acirrada entre as grandes companhias, umas apostando no esquema TDMA e outras investindo largamente em CDMA. Ambos os lados "provam" que, levando-se em conta o fator custo-benefício, o esquema apoiado por cada um dos contendores é o melhor.

Os esquemas de faixa estreita (FDMA e TDMA de faixa estreita) são mais simples de serem implementados mas tem pouco a oferecer com relação a proteção contra

interferência, ruído, probabilidade de bloqueio, etc. Os sistemas de faixa larga (CDMA e TDMA de faixa larga) são potencialmente mais atrativos, mas exigem um considerável avanço na tecnologia antes que eles possam ser totalmente explorados.

No que concerne aos protocolos de acesso aos canais de sinalização o *Slotted ALOHA* é um dos mais utilizados tanto nos sistemas analógicos quanto nos digitais. O desempenho do protocolo é afetado pelas perdas de percurso (efeito *near/far*), desvanecimento de Rayleigh e sombreamento. Mostra-se que tanto a perda de pacotes quanto a instabilidade são bastante atenuadas no ambiente de rádio móvel quando comparadas com estes mesmos parâmetros das redes locais convencionais usando o *Slotted ALOHA*. De fato, estes fenômenos de rádio móvel agem diretamente nos usuários, dividindo-os em diferentes classes de potência para o acesso. Uma vez que os assinantes estão em movimento, a aleatoriedade da potência do sinal e o tempo para iniciar uma retransmissão provê uma priorização natural.

TRÁFEGO

Embora o processo de tráfego em sistemas de rádio móvel seja bastante diferente daquele em redes telefônicas fixas, as considerações de projeto de sistemas utilizam os mesmos recursos utilizados nestas últimas. Por exemplo, a medida de desempenho de tráfego continua sendo a probabilidade de bloqueio, tomando-se os assinantes como fixos e não móveis. Os requisitos de bloqueio são os mesmos (2% na hora de maior movimento) embora, devido à demanda, eles raramente são cumpridos e o assinante pode experimentar bloqueio até dez vezes maior que o especificado.

Devido às características próprias do sistema celular (gerenciamento centralizado dos canais, áreas de serviço com sobreposição) é possível utilizar alguns algorítmos de alocação de canais para a melhoria do desempenho de tráfego do sistema. Estas técnicas podem ser do tipo global ou local, dependendo se elas exigem o envolvimento de um processamento centralizado ou local, respectivamente. A implementação dos algoritmos do primeiro tipo é, óbviamente, bem mais complicada que as do segundo. De

fato recomendam-se as do tipo global quando o perfil de tráfego for bastante variável com o tempo. As do segundo tipo, por outro lado, podem ser usadas para corrigir desbalanceamentos locais de tráfego.

ANEXO A

VOLUME I

FOUNDATIONS OF MOBILE RADIO ENGINEERING

MICHEL DAOUD YACOUB

PART I

INTRODUCTION

CHAPTER 1

MOBILE RADIO SYSTEM

PREAMBLE

This chapter traces a brief history of mobile radio communications, bringing up the main events that have contributed to the development of such an efficient and successful means of communications. Spectrum allocation problems and technological evolution, the latter addressing equipment packaging, modulation schemes and system architecture aspects, are outlined. Some mobile radio services are then briefly described and system design considerations are examined. It is also shown that, since radio propagation does not recognize geopolitical boundaries, effective use of the spectrum is possible only if international agreement is achieved. Under such circumstances the ITU has emerged to provide the "worldwide harmony". The international frequency allocation for some radio services is then presented in table form.

1.1 INTRODUCTION

The first successful use of mobile radio dates from the late 1800's, when M.G. Marconi established a radio link between a land-based station and a tug boat, over an 18-mile path. Since then the mobile systems have developed and spread considerably. The usefulness of the Mobile Radio Services was first recognized by the public safety services (police and fire departments, forestry conservation, highway maintenance and local government services), followed by private sectors (power, oil, motion picture,

telephone maintenance and transportation services, as well as taxis and lorry fleets). The growth rate of these services in the United States by the 1950's was greater than 20% a year [1], when the number of subscribers was just a few thousands. Consequently, by 1963 the number of users exceeded the figure of 1.3 million although only a few channels (about 12) were available.

These early systems (conventional mobile systems – CMS) consisted of a base station whose transmitter and receiver were assembled on a hilltop. The coverage area was chosen to be large, in a way similar to the radio or television broadcast services. The transmitter usually operated with high power (200 or 250 watts [3]), assuring a large coverage area (25-mile radius).

Conventional mobile systems are usually isolated from each other, with only a few of them accessing the public switched telephone network. Those having connection with the telephone network are named Mobile Telephone Systems where the communication unit is assigned to the subscriber and not to a physical location.

1.2 CONVENTIONAL MOBILE SYSTEMS

By the end of the nineteenth century H.G. Hertz, a german scientist, demonstrated that radio waves could propagate in a wireless medium, in fact, over a few yards path between transmitter and receiver. Still before the twentieth century, Marconi showed the first wireless communication "on the move" between a land-based station and a tug boat. Thereafter, many maritime mobile services were established and operated successfully.

On land, the Detroit Police Department started its experiments with mobile radio in 1921, first operating as a dispatching system. Initially, only the base station could transmit. Later on the mobile unit was also able to communicate to the base station. The frequency used was around 2 MHz. Soon, other police departments installed their own systems. As a consequence, the available frequency spectrum became congested. By the middle of the 1930's the Federal Communications Commission (FCC)

authorized four more channels between 30 MHz and 40 MHz. In 1946 six channels near 150 MHz were available for use. In fact, due to technological restraint, out of those six channels only three could be utilized because of adjacent channel interference problems. These radio frequencies were first used by the mobile telephone services. Starting in St. Louis this system quickly spread throughout the USA. Shortly after, frequencies around 40 MHz were available for use in highways. Again the highway mobile services grew rapidly, although this did not seem to have worked out well due to radio interference. By the middle of the 1950's, due to the reduction of the channel spacing from 60 kHz to 30 kHz, a total of 11 channels could be used at 150 MHz Almost at the same time the FCC released 12 channels at 450 MHz. Up to that time the mobile telephone systems were manually operated with each call having to be handled through an operator. It was only in the 1960's that the automatic systems appeared, allowing the subscribers themselves to do the direct dialling. Automatic mobile telephone systems operated initially with frequencies around 150 MHz, moving later on to 450MHz.

Already in 1975, after a long period of negotiations involving the mobile industries and the FCC, a 40 MHz band between 800 MHz and 900 MHz was released. The year of 1978 was marked by the beginning of a new era in the mobile communications history, when the first cellular system was sent to the field test [22].

1.3 TECHNOLOGICAL EVOLUTION

Before the second world war mobile radio systems were largely dominated by the military (and paramilitary) users. Consequently, the evolution and the development of such systems were supported by and closely linked to the military needs, requirements and standards.

Recently, however, this tendency is being reversed, as more and more mobile services are steering towards civil applications. Consequently, as far as system design and technology are concerned commercial mobile systems have taken the lead [4].

a) Equipment Packages Evolution

The early mobile radio systems were equipped with vacuum tube equipment requiring powerful batteries. In fact, before 1930 [2] only the receivers were mobile, implying an one-way communication. Mobile transmitters soon appeared, but they were still bulky and heavy, requiring special power supplies. The total apparatus could occupy most of the vehicle's boot room.

By the 1950's equipment was already small enough to be man-transportable, although the volume was still quite considerable and the main application was for military purposes.

Transistorization of the mobile radio products started in 1957 with the power supplies. Soon after, the receivers and part of the transmitters had their vacuum tubes replaced by transistors, contributing to a 50% reduction of the volume, lower power consumption and higher reliability. The packages could then be mounted in the car's dashboard or even in motorcycles. Maintenance costs diminished because of the reduction of the required spare parts and also because of the very rapid decrease of the transistors' price. By the 1960's the mobile products were all built with solid-state components. The design of the equipment introduced some new components such as printed circuit boards, sockets and heat sinks.

The first hand-held portable radios appeared in the 1960's, initially for the commercial and later for military systems. At this point mobile civil applications started to take the lead.

The changing from transistors into integrated circuits was an obvious and natural step occurring by the middle of the 1970's. By this time cordless telephones were already available. Today the equipment includes LSI and VLSI circuits rendering the products smaller, lighter and less costly.

b) Modulation Scheme Evolution

Analog Systems

Similar to any other early systems using voice transmission by radio, mobile

radio systems also employed Amplitude Modulation (AM), initially in the HF band and later in the VHF band.

The introduction of Frequency Modulation (FM) into mobile radio services started soon after its invention in 1935. In the 1940's most of the military and some commercial equipment was already operating in VHF FM. However, if on the one hand FM systems had a remarkably better signal-to-noise ratio performance in the presence of fading as compared to AM systems, on the other hand they required a much wider frequency band. While for voice transmission AM occupied around 6 KHz in the spectrum, the early FM channel needed 120 KHz. The 120 KHz bandwidth used in the 1940's was then reduced to 60 kHz in the 1950's, 30 kHz in the 1960's and 25 kHz in the 1970's. It is believed that a further reduction to 12 kHz would not substantially deteriorate the speech quality.

Except for (i) the cordless telephones and the citizen's band radio, where in the 1970's AM was used, and (ii) the military mobile systems of 1960's, using single sideband, FM is the modulation scheme widely used in analog mobile systems.

Nevertheless, because the radio spectrum is a scarce resource, a great deal of research has been steered towards the "old" Single SideBand (SSB) modulation. Like the AM systems, one of the biggest problems of SSB is its disastrous signal-to-noise ratio performance in the presence of fading. On the other hand, it requires five to six times less spectrum than FM, rendering this scheme very attractive for mobile applications. Accordingly, many enhanced forms of SSB, such as "Transparent Tone in Band", "Feed Forward Signal Regeneration", etc. have been investigated.

The reader is referred to Chapter 8 for a deeper study of the analog modulation schemes.

Digital Systems

Digital is always seen as the natural evolution of the analog approach. This is quite true for most of the applications where there is physical connection or bandwidth is not a limiting factor [4]. In the mobile radio environment, however, spectrum efficiency is probably one of the strongest aspects to be taken into account

if a change of technology is to be considered. Digital techniques appeared before the analog ones, but only became feasible with the advent of the transistor and later the integrated circuits. As far as mobile radio is concerned, the word "digital" is essentially related to voice digitization and to digital transmission.

The main problem with digital transmission is spectrum utilization. The standard (conventional PAM) 64 kbit/s, used for voice communication in the fixed telephone network, if transmitted by radio, would occupy 100 kHz of the spectrum, four times the 25 kHz FM currently in use. This, by itself, is such a constraint that it makes any digital mobile radio unthinkable. Efforts have then been concentrated in diminishing the transmission rate to 16 kbit/s (as adopted by the pan-European GSM system) or even less (8 kbit/s as proposed by the American digital system [5]). On the other hand, digital techniques provide robustness against interference and flexibility for integration into the emerging digital network, with capability of transmitting data, voice, etc.

Another clear advantage of the digital system is to allow other options for channel access. In analog systems only Frequency Division Multiple Access (FDMA) can be used. In digital systems, besides FDMA, other access schemes such as TDMA and CDMA can be used.

The reader is referred to Chapter 9 for the studies of digital techniques and to Chapter 10 for the various access schemes.

c) System Evolution

As far as access methods and operational aspects of mobile radio are concerned, there have been several stages of evolution as follows.

1) *Simplex System - SS*

It operates with one frequency, and only the base station can transmit. The mobile unit is just a single receiver (Figure 1.1a).

2) *(Single) Half-Duplex System - (S)HDS*

In this system both the mobile and the base station use only one frequency. It operates on a push-to-talk basis, where the base station competes with the mobile

(Figure 1.1b).

3) *Double Half-Duplex System - DHDS*

In this case the transmitter of the mobile and the receiver of the base station operate with one frequency, whereas the receiver of the mobile and the transmitter of the base station operate with another frequency. Here again, the push-to-talk scheme is used, but the base station does not compete with the mobiles (Figure 1.1c).

4) *Duplex Base Double Half-Duplex System - DBDHDS*

This system operates with two frequencies where only the base station can transmit and receive simultaneously. The mobiles make use of the push-to-talk scheme (Figure 1.1d).

5) *(Full) Duplex System - (F)DS*

Both base station and mobile operate duplex. They are able to transmit on one frequency while receiving on another frequency. Two antennas in each end (mobile and base) must be provided so that transmitter and receiver work independently with different frequencies. It is possible, however, to include filters between transmitters and receivers in order to avoid interference, and use only one antenna at each end. Here the push-to-talk procedure is no longer used (Figure 1.1e).

6) *Mobile Telephone System - MTS*

In general terms, mobile services can be classified in two categories, namely, Non-Trunked Mobile System (NTMS) and Trunked Mobile System (TMS).

The first category - NTMS - comprises the systems where only one or just a small number of channels is available for use and the channels are allocated for special services. Non trunked systems are characterized by absence of privacy, where all the users can take part in the communication. Examples of such systems include the Private Mobile Radio (PMR) network such as the radio taxis, lorry fleet radio, citizens' band (CB) radio, etc. These systems are intended to serve a very limited number of users for a particular application.

The early mobile systems were limited by the available technology. The radios could only operate with one or a small sub-set of the already scarce set of channels,

since each frequency was obtained by means of a quartz crystal. With the advent of solid-state technology and the use of frequency synthesizer, the subscribers themselves were able to select a free channel for conversation. This improvement, however, was not enough to enable the system to cope with the traffic demand.

Consider a NTMS operating with only one channel (Figure 1.2a). Suppose also that this channel is on the average 30% of the time busy (i.e, the carried traffic is 0.3 erl. which, in an one-channel system, corresponds to a blocking probability of 30%). Thus, the total traffic offered is $0.3/(1 - 0.3) \simeq 0.43$ erl.. If each mobile can generate 0.01 erl., then the maximum number of users this system can support is 43 (43 subscribers will experience 30% blocking probability !). In order to maintain this grade of service and increase the number of subscribers, another channel must be provided and allocated to the other group of users as shown in Figure 1.2b (now 86 subscribers will experience 30% blocking probability !)

Suppose now that this system has been doubled in size, but with all the subscribers being able to share all the channels (86 users and 2 channels), as in Figure 1.2c. The total amount of traffic is also doubled but the blocking probability will go down to approximately 16% . If this (unacceptable) figure of 30% is to be maintained, then the number a subscribers could go up to 145 ! This is the principle of a Trunked Mobile System (refer to Chapter 12 for studies of traffic).

Both the NTMS and TMS used in a private network require the subscribers to have some sort of discipline so that the channels can be efficiently used. In the case of the TMS, if there are many channels available, usually one channel is reserved for control (e.g., the conversation will always start on a specific channel and move to another channel).

Although in TMS the channel usage is substantially increased, there still remains a serious concern with respect to the bounds imposed to the subscriber's mobility. The users can only communicate among themselves within the restricted area covered by the radio transmitter.

A higher degree of flexibility can be achieved when the mobile system is

integrated into the fixed telephone network, resulting in the Mobile Telephone System - MTS. On the other hand, the subscribers of the fixed telephone network will experience some unusual degradation in the voice signal due to fading and man-made noise.

The MTS's have gone through several stages of evolution as follows:

(i) Initially the MTS's were NTMS, operating in half-duplex and push-to-talk mode with the calls being handled by a special mobile operator.

(ii) Then, with the availability of more channels, the MTS went through a TMS phase, but the channels were selected manually. The mobiles operated on a push-to-talk basis and the land-line subscribers could already dial directly, without the need of the operator.

(iii) The next step was to operate in a duplex mode with both sides (mobile and land-line users) making direct dialling. Channel selection was still manual.

(iv) The only change at this stage was towards the automatic channel selection.

A schematic representation of a Mobile Telephone System is shown in Figure 1.3.

The MTS's reached their final stage of evolution by the middle of 1960's. One decade later there were more than one thousand of those systems already in operation in the United States, most of them at their limit of capacity. Just to have an idea of how overloaded the systems were [6], the New York Telephone Company operated two MTS's with 6 channels each in 1976 serving a total of 543 subscribers (a concentration of approximately 46 subscribers per channel) in a 50-mile area. The number of applicants wait-listed was about 3700.

7) *Cellular Mobile Radio System*

In a cellular system the service area is divided into regions (the cells) each containing a sub-set of the total number of available channels. Channels used in a given cell can be reused in another cell sufficiently far away that interference is minimized. The cells can be placed in a modular way and, in theory, the system can grow indefinitely. The structure of a cellular system is shown in Figure 1.4.

A proper treatment of the cellular concept will be given in Chapter 2. In terms

of revolutionary ideas the cellular architecture is a cornerstone of this revolution. The systems now can be considered as before or after cellular. There has been some progress as far as the size of the cells are concerned, but still the architecture remains cellular.

1.4 MOBILE RADIO SERVICES

In the previous section we showed how the mobile systems evolved to the configuration of the present day's systems. It must be emphasized, however, that the advent of a better network, in general, did not make the earlier systems unviable. New and old systems can coexist for a long time until the gradual replacement of the latter is finally accomplished.

Mobile radio systems do vary according to the specific application for which they are designed. The most flexible network using the latest technology will be able to meet the requirements of a simpler system, but will also be much more expensive. In this sense there are many different types of radio systems, some of them using solutions considered to be obsolete for certain types of mobile services.

1) *Radio Paging*

Paging systems provide only one-way communication between base station and mobile users. In the simplest systems the base station operator selects the wanted user and sends him or her an alert tone. The user is then required to report by telephone to a fixed location for further information [15]. More advanced systems allow voice or alphanumeric messages to be transmitted. Initially, the paging systems covered small areas (2 – 5 Km radius), requiring small and low consumption receivers.

In large cities, however, users of the paging services experienced the need for a wider range operation. Accordingly, some wide-area paging systems appeared in various countries, each of which with its own standards. Later on a paging code and signalling format were proposed gaining international recognition by the CCIR. The POCSAG code [16], as it was known, "has the capacity to cope with eight million

pagers, provides the facility for alphanumeric messages and can operate in 12.5 or 25 kHz channels". [2].

2) *Packet Radio*

"Packet radio networks (PR nets) represent the extension of packet switching technology into the environment of mobile radio. They are intended to provide data communications to users located over a broad geographic region where connection between the source and destination users is not practical or cost effective" [17]. The network is composed by a number of packet radio units, consisting of transmitter, receiver, antenna and controller. Usually, full connectivity among all the radio units in the network is not provided, because not all nodes are within line-of-sight of one another. Accordingly, a packet may reach its destination after being received by and relayed to as many radio units in its path as required. Therefore, all nodes must provide for store-and-forward operation. Note that, due to the limited range of transmission and the mobility of the nodes, the connectivity (network topology) changes dynamically.

3) *Future Public Land Mobile Telecommunication Systems (FPLMTS)*

FPLMTS is a new concept, arising from the CCIR study groups, where cellular mobile technology is used for fixed services purposes. The initial application of FPLMTS aimed at the developing countries where the lack of service in rural and remote areas or lack of capacity to offer a good grade of service in urban areas are critical. Providing rural wireline networks is usually extremely costly due to the long distances, difficult terrain and climatic conditions. Moreover, planning network expansion in urban areas is not easy because of the high and unpredictable demand. Accordingly, FPLMTS may become an attractive alternative to the wireline systems because of its (i) flexibility, (ii) modular design, (iii) capability for covering wide geographical areas and (iv) cost reductions resulting from technology improvements. Industrialized countries with large territories, rough terrain and thinly populated areas may also profit from FPLMTS. Besides voice, other services such as point to multipoint, short messages, paging, facsimile, text and data are also

planned to be offered by these systems [19].

4) *Cordless Telephone*

a) CT1 - The First Generation

Cordless Telephone (CT) has been in the market for a long time, but with analog technology. It is, in fact, a wireless extension of the wireline telephone with a very limited transmission range (50 - 200 m). Moreover, since a small number of channels is available and the apparatus uses only one fixed channel, interference (or lack of privacy) is quite common.

b) CT2 - The Second Generation

The second generation of cordless telephone uses digital technology, providing "high speech quality, higher degree of security and the possibility of introducing new services" [20]. It has three main applications, as follows:

- Domestic Use, replacing its analog counterpart with the advantage of automatic channel selection and other advantages provided by the digital technology.

- Cordless PABX, where a linked network of base stations allows staff to move with their handset in the building, being able to receive and make calls.

- Telepoint, where base stations are connected to the public switched telephone network. These base stations are usually located at shops, bus stations, train stations, airports, etc, and the users within their coverage areas are able to make calls (but not receive).

The CT2 systems use FDMA architecture*, 4 MHz - bandwidth, 1 channel per carrier and a total of 40 carriers.

c) CT3 - The Third Generation

This system uses TDMA architecture*, 8 MHz - bandwidth, 8 channels per carrier and a total of 8 carriers. The great difference between CT2 and CT3 is that in the former "the cordless handset is sending or receiving radio transmissions all the time while a call is in progress" [20]. In the latter the handset operates for one-eighth of the time. Accordingly, the rest of the time can be used for other applications.

* Refer to Chapter 10

d) DECT – The Third Generation

The Digital European Cordless Telephone (DECT) is also a third generation cordless telephone, specified to be used throughout Europe. It is very similar to CT3 using TDMA architecture, 20 MHz bandwidth, 12 channels per cell and a total of 12 channels per carriers.

5) *Personal Communications*

Personal Communications Networks (PCN) aim at providing a "go-anywhere telephone that can be used at any time with a guarantee of a quality service" [21]. The idea is to provide low-cost and high-quality mobile communications for the mass market. The cellular architecture is kept but the cells are much smaller with a consequent reduction of the handset power. On the other hand, the number of base stations required for this service increases drastically. Cells size may vary from 1 km radius in city centres to 6 km in the country. The spectrum space planned to be allotted to PCN is at 1.8 GHz, where the spectrum is fairly clean.

6) *Mobile Satellite Communications*

"Mobile-Satellite Service provides communication between earth stations and one or more space stations, or between mobile earth station via one or more space stations" [23]. The earth stations can be located on-board ships, on-board aircrafts or on-board terrestrial vehicles characterizing the Maritime, Aeronautical or Land Mobile-Satellite Services, respectively. In addition, "this service can be used to detect and locate distress signals from survival craft stations and emergency position-indicating radio beacon stations." [23].

Among the various international systems providing telecommunications (in general) by satellite we quote the INTELSAT (International Telecommunications Satellite Organization), the EUTELSAT (European Telecommunications Satellite Organization) and the INMARSAT (International Maritime Satellite Organization). These organizations are financed by their members (countries) to whom the given services are hired out.

In particular, the INMARSAT's primary mission is to provide data, voice and

emergency communications to ships and platforms. More recently INMARSAT is aiming at offering its services to be used for air traffic and control worldwide. A global integration of the mobile services is likely to occur in the near future and will certainly make use of satellites. Motorola has given a step forward proposing the Iridium System, where 77 low-orbit satellites in connection with 37 cells would cover the entire globe. The advantage of having low-orbit satellites is the use of low power handset.

1.5 SYSTEM DESIGN CONSIDERATIONS

While the use of electromagnetic waves would restrict the mobile communication to some specific types of services, the connection with the fixed telephone network gives the flexibility which makes the mobile network able to give support to all sorts of communications services. On the other hand, the design of such a system is complicated for it may involve most of the areas in telecommunications as well as other related areas.

Let us mention some of these areas.

- Radio system design and propagation, where, for instance, the topography of the terrain is carefully studied. The results of this study constitute input data for the radio coverage planning. At this point it may be detected the need for the use of Repeaters*, a very common method for range extension in most mobile radio networks.

- Frequency regulation and planning. Each radio service utilizes its own portion of frequency spectrum. Given that only a limited amount of the spectrum is available, the frequency allocation plan has to be carefully done so that interferences are minimized and the traffic demand is satisfied.

---

* A repeater is an electronic assembly which processes a receiving signal for retransmission. Basically, the processing may consist of a pure amplification of the signal either keeping or changing its frequency. In the first case it is important to obtain a high isolation between receive and retransmit antennas to avoid oscillation.

- Modulation. As far as voice in an analog system is concerned, very few services still use AM, while the majority uses narrowband FM. With the advent of digital systems, there is a variety of possibilities and the choice is not so straightforward.

- Antenna design. In the early systems only omnidirectional antennas were used. With the increase in traffic demand the cells were then split into sectors for which directional antennas are required. Today new cellular patterns [7] are being suggested for which more complex antennas are required (sectorization and the use of directional antennas are covered in Chapters 2 and 7).

- Transmission planning. There are many aspects to be considered here, such as: a) the structures of the channels used for signalling and voice; b) the characteristics of the message/voice transmitted; c) the performance of the components of the transmission systems (power capacity, noise, bandwidth, stability, etc). We can also include the design of the transmitters and the receivers whose main features include robustness and portability.

- Switching system design. In most of the cases this consists in adapting the existing switching network for mobile purposes.

- Teletraffic. One of the ways of assessing the performance of the system is to estimate the overall blocking probability. Consequently, the concepts of traffic engineering are required. For a given grade of service and number of channels available, how many subscribers can be served ? What routing strategy should be able to enhance the traffic performance ? How many channels should be used for voice and how many for signalling ?

- Software design. With the use of microprocessors throughout the system there is software application in the mobile, base station and in the exchange adapted for that service.

Other aspects such as human factors, economics, etc, will also influence the design of a mobile radio system.

1.6 FREQUENCY PLANNING AND SPECTRUM ALLOCATION

Mobile radio is just one among tens of radio communication services. Like all the other systems involving radio transmission, the allocation of radio frequencies for this service is subject to a series of administrative and technical factors.

The electromagnetic spectrum is a renewable resource which, in theory, can be used indiscriminately. In practice, however, the chaotic manipulation of the radio frequencies would only lead to, at least, an inefficient use of this limited resource, restricting the advent of new services and the growth of those already established. Since radio propagation does not recognize geopolitical boundaries and the political, economic and social aspirations may vary from country to country, there is a need for international cooperation and participation, so that an orderly worldwide use of the radio spectrum can be agreed. Many other factors such as historical developments, regional policy and extent of current usage do also influence the selection of frequencies.

In order to accomplish effective use of the radio spectrum, the frequencies are allocated to specific services with similarity in terms of radiated power and interference features. This has been agreed under a global organization - the International Telecommunication Union (ITU).

1.6.1 The Worldwide Harmony

The International Telecommunication Union (ITU) was founded in 1932 as a result of the fusion between the International Telegraph Union, founded in 1865, and the Radio Telegraph Union, founded in 1903, and today constitutes a specialized agency of the United Nations. Its main objective is to harmonize and care for telecommunications around the world, including the efficient utilization of the radio spectrum.

The ITU is backed by an international treaty - the ITU Convention - where its structure, responsibilities, rights and obligations are defined. Its general structure is shown in Figure 1.5.

The Plenipotentiary Conference re-examines the Convention in periodic meetings (usually every five years), determines the general policies, budget, salaries, elects the Secretary General, the Deputy Secretary General and the members of the Administrative Council.

The Administrative Council is composed of 36 members responsible for directing the work of the Union in the period between the Plenipotentiary Conference. It usually meets every year.

The next four blocks shown in Figure 1.5 constitute the permanent organs of the ITU.

- The General Secretariat is in charge of executive management and technical cooperation. It translates, interprets and publishes the documents of the Union.

- The International Frequency Registration Board (IFRB) is in charge of the analysis and records of the frequency assignments made by the countries which may potentially cause interference to the services of other administrations. Should an interference problem be found, a solution is suggested and returned to the originating administration.

- The International Radio Consultative Committee (Comité Consultatif International de Radio - CCIR) has the task of studying the technical and operating issues related to radio communications.

- The International Telegraph and Telephone Consultative Committee (Comité Consultatif International des Téléphonique et Télégraphique - CCITT) has the task of studying the technical, operational and tariff questions concerning the telegraphy and telephony.

The studies by CCIR and CCITT result in decisions, resolutions, recommendations and reports. Study Groups are then set up in order to carry on the analysis of the recommendations.

Besides those four permanent organs the ITU is also composed by the Administrative Conferences where the technical regulations are agreed. These conferences, called for by the Administrative Council, are held if a sufficient number

of ITU member nations agree to participate. Their aim is to revise the technical regulations whenever such procedure is required. Accordingly, there are the Administrative Radio Conference and the Administrative Telegraph and Telephone Conference.

The Administrative Conferences may be Worldwide or just Regional ones. The World Administrative Conference care for the regulations worldwide. The Regional Administrative Conferences deal with the telecommunication matters of a regional nature. For this the ITU has divided the world into three regions:

- Region 1: Europe, including all former USSR territory outside Europe, Mongolian People's Republic, Asia Minor and Africa.
- Region 2: Western Hemisphere including Hawaii
- Region 3: Australia, New Zealand, Oceania and Asia excluding former USSR territory and Asia Minor.

All the decisions taken by these conferences must be in conformity with the ITU Convention and, moreover, the outcomes of the Regional Conferences have to be in accordance with the World Conference.

The World Conference, responsible for the radio communication questions, is the WARC - World Administrative Radio Conference. There have been eight general WARC's: 1906 in Berlin, 1912 in London, 1927 in Washington D.C., 1932 in Madrid, 1938 in Cairo, in 1947 in Atlantic City, 1959 in Geneva and 1979 again in Geneva. Several other small conferences have been held in order to deal with specific matters, such as, for example, Mobile Services.

1.6.2 Frequency Assignment and National Control

Several regions of the frequency spectrum are allocated to more than one radio service. There are however, other regions for the exclusive use of a particular service. Again, for the sake of efficient and orderly usage of the spectrum, in one or the other case, there must be a centralized organization regulating the assignment and

use of the radio frequencies.

In most of the countries this central administration is performed by a government entity such as Ministry or Secretary or Department of Communications, or similar. A well-known exception for that is the United States where the nongovernment radio services are administered by the Federal Communications Commission (FCC). The government services are controlled by the Interdepartment Radio Advisory Committee (IRAC), which in fact acts under a government agency.

The concession for the radio service operation is a rather complicated matter since all sorts of factors, such as historical, economic, political, social, etc may be involved. Another very important issue is the congestion, which may occur in many portions of the spectrum already occupied by other services. In this case there may occur a frequency reassignment procedure when the concerned service is shifted to another region of the spectrum. Again this is an extremely difficult issue where many interests are at play.

Table 1.1, shows some radio services, namely Broadcasting (BRC), Fixed (FIX) and Mobile (MOB), allocated on a primary basis to the various regions (1,2,3 or combinations of them). The mobile services may include land, maritime and/or aeronautical mobile communications.

1.7 SUMMARY AND CONCLUSIONS

Mobile radio services started soon after the invention of radio. Since then they have undergone several stages of regulatory and technological evolution starting with the bulky and extremely heavy equipment and evolving to pocket size portable telephones.

As in the majority of communication systems, the evolution of the various services occurred independently with each system using its own solution. Today, there has been a move towards global standardization and, perhaps, a worldwide integration of the mobile radio services. As far as frequency planning and spectrum allocation are

concerned, the chaotic manipulation of the radio frequencies has been avoided by the creation of the ITU, a global organization where this matter is carefully discussed and controlled.

REFERENCES

[1] Neal H. Shepherd, "Mobile Radio Services" in *Communications System Engineering Handbook*, edited by Donald H. Hamsher, McGraw Hill Book Company, New York, 1967.

[2] George Calhoun, *Digital Cellular Radio*, Artech House, Inc., New Jersey, 1988.

[3] W.R. Young, "Advanced Mobile Phone Service: Introduction, Background and Objectives", *ESTJ*, vol. 58, Nº 1, January 1979.

[4] G.J. Lomer, "Telephoning on the Move - Dick Tracy to Captain Kirk", *IEE Proceedings*, Vol. 134, Past F, Nº 1, February 1987.

[5] G. Zysman, "AT&T Proposed Digital Cellular System", *2nd International Seminar on Cellular Ratio Telephony* (in portuguese), São Paulo, S.P., Brazil 1988.

[6] W.C.Y. Lee, *Mobile Communications Engineering*, McGraw-Hill, Inc, New York, 1976

[7] S. Heeralall, *The Applications of Directional Antennas in Cellular Mobile* Radio *Systems*, Ph. D. Thesis, University of Essex, England, July 1988.

[8] R. Steile, V.K. Prabru, "High-User - Density Digital Cellular Mobile Radio Systems", *IEE Proceedings*, Vol. 132, p. 396, August 1985.

[9] C.J. Hughes, *Notes on Mobile Radio Systems Course*, University of Essex, 1987.

[10] J. Hoff, "Mobile Telephony in the Next Decade", *2nd Nordic Seminar on Digital Land Mobile Radio Communication*, Stockholm, October 1986.

[11] Donald H. Hamsher, Ed, *Communication System Engineering Handbook*, McGraw-Hill Book Company, 1967.

[12] Dennis Bodson, Richard G. Gould, George H. Hagn, Willian F. Utlaut, "Spectrum Management and the 1979 World Administrative Radio Conference", *IEEE Trans. on Communications*, Vol. Com-29, Nº 8, August 1981.

[13] Richard E Shrum, "A Nontechnical Overview of 1979 WARC", *IEEE Trans. on Communications*, Vol. Com-29, Nº 8, August 1981.

[14] *Final Acts of the World Administrative Radio Conference for the Mobile Services* (MOB-87), Geneva, 1987

[15] J.D. Parsons, J.G. Gardiner, *Mobile Communication Systems*, Blackie & Son Ltd., 1989.

[16] British Telecom. A Standard Code for Radio Paging. Report of the Post Office Code Standardization Advisory Group (POCSAG), June 1978 and Nov. 1980.

[17] B.M. Leiner, D.L. Nielsen and F.A.Tobagi, "Scanning the Issue", *Special Issue on Packet Radio Networks, Proc. IEEE*, Vol. 75, Nº 1, Jan. 1987.

[18] N. Shacham and J. Westcott, "Future Directions in Packet Radio Architectures and Protocols", *Special Issue on Packet Radio Networks, Proc. IEEE*, Vol. 75, Nº 1, Jan. 1987.

[19] CCIR Study Groups (1986-1990), Interim Working Party 8/13, (Question 77/8), "Adaptation of Mobile Radiocommunication Technology to the Needs of Developing Country".

[20] R. Caldwell, "Towards a European Standard with a Common Air Interface", *Telecommunications*, Int. Edition, Vol. 24, Nº 9, Sept. 1990.

[21] R. Potter, "Personal Communications for the Mass Market", *Telecommunications*, Int Edition, Vol. 24, Nº 9, Sept. 1990.

[22] D.L. Huff, "Advanced Mobile Phone Service: The Developmental System", *BSTJ*, Vol. 58, January 1978.

[23] G. Maral and M. Bousquet, "Satellite Communications Systems", John Wiley & Sons, 1986.

TABLE 1.1 - Allocation of Frequencies to Some Radio Services

Bandwidth (KHz)	BRC	FIX	MOB	Bandwidth(MHz)	BRC	FIX	MOB	Bandwidth(MHz)	BRC	FIX	MOB
130 - 160		23	23	18.168 - 18.780		123		610 - 890	3	3	3
130 - 148.5		1	1	87 - 100	3	3	3	614 - 806	2		
148.5 - 255	1			87.5 - 100	1			790 - 862	1	1	
160 - 190		23		88 - 100	2			806 - 890	2	2	2
255 - 283.5	1			100 - 108	123			862 - 890	1	1	1
415 - 435			1	136 - 137			123	890 - 902		2	2
415 - 495			23	150.05 - 153		1	1	890 - 942	13	13	13
435 - 495			1	150.05 - 156.7625		23	23	902 - 942		2	
505 - 510			2	153 - 154		1	1	942 - 960	13	13	13
505 - 526.5			13	156.7625 - 156.8365			123	1530 - 1660.5	Dedicated to Mobile		
510 - 525			2	156.8375 - 174		123	123		Satellite Communica-		
525 - 535	2			174 - 216	2				tions (Land-mobile,		
526.5 - 535	3			174 - 223	13	3	3		maritime-mobile or		
526.5 - 1605.5	1			216 - 225		2	2		aeronautical-mobile)		
535 - 1605	23			223 - 230	13	3	3	1700 - 2450		123	23
1605 - 1625	2			225 - 235		2	2	2450 - 2500		123	123
1605.5 - 1800		3	3	230 - 235		13	13	2500 - 2535		3	3
1606.5 - 1625		1	1	406 - 406.1			123*	2500 - 2655	123*	123	123
1625 - 1705	2	2	2	470 - 512	2						
1635 - 1800		1	1	470 - 585	3	3	3				
1705 - 1800		2	2	470 - 790	1						
1800 - 2000		3	3	512 - 608	2						
1850 - 2000		12	12	585 - 610	3	3	3				

where BRC: Broadcasting
FIX: Fixed
MOB: Mobile

* Using satellite

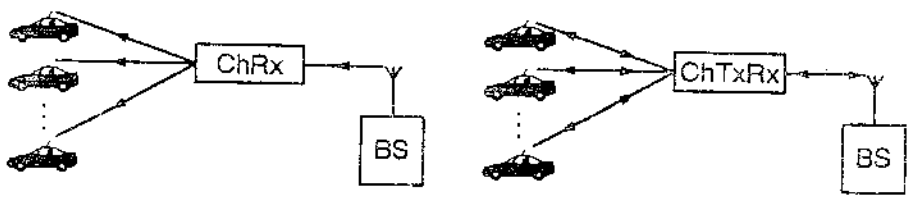

(a) SS

(b) (S) HDS

Fig 1-1(a,b) ISDN

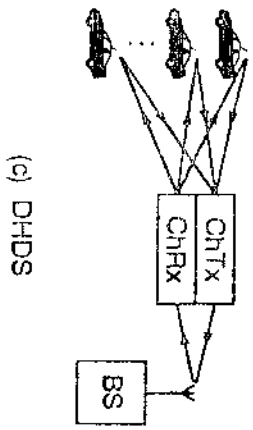

(c) DHDS

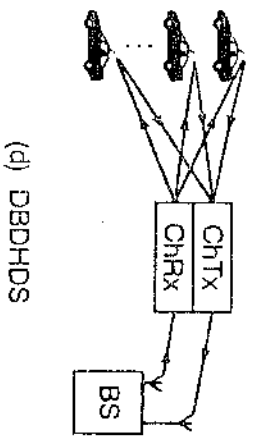

(d) DBDHDS

fig1-1c.gif 1.0cm

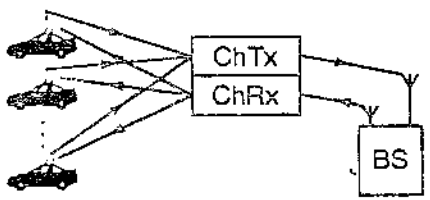

(e) (F) DS

where: ChTx = Transmission Channel
ChRx = Reception Channel
ChTxRx = Transmission and Reception Channel
BS = Base Station

Fig 1(e) 150

(a) One-channel - NTMS

(b) Two-channel - NTMS

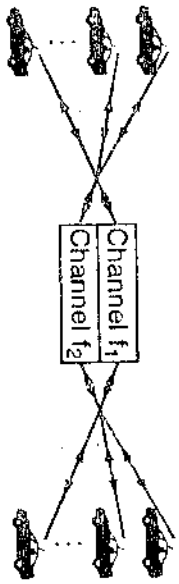

(c) Two-channel - TMS

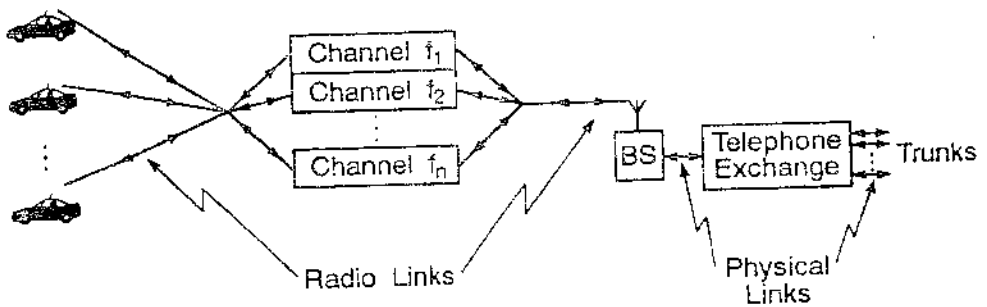

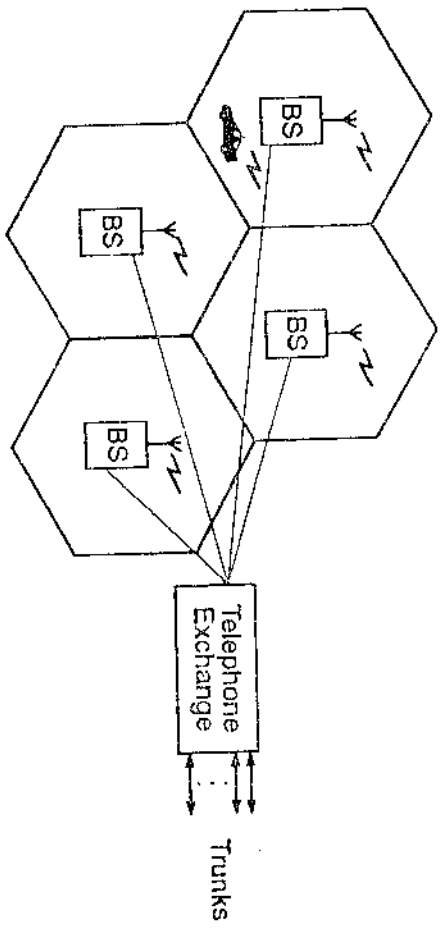

fig1.wmf

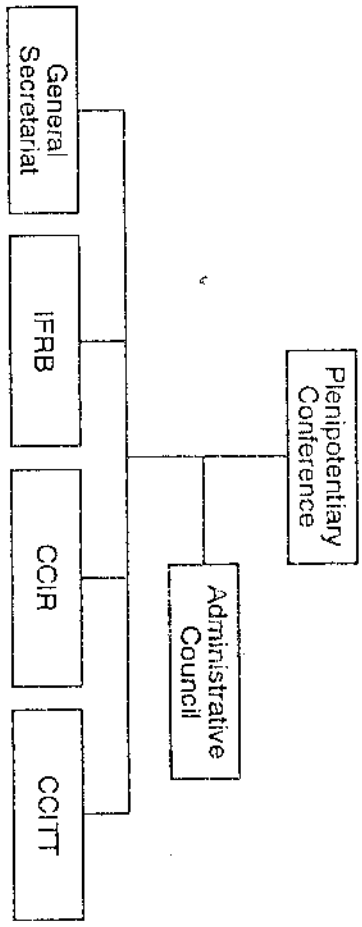

CHAPTER 2

CELLULAR MOBILE RADIO

PREAMBLE

This chapter addresses the basic principles of cellular mobile radio systems giving an overview of the main points to be considered in a system design. It traces the outstanding differences between conventional and cellular networks introducing the jargons commonly used in the latter. There is a brief functional description of each cellular component and of how they can be interconnected to give different architectures. A theory of patterns and symmetry is introduced so that some of the well accepted cell geometry assumptions, today taken for granted, can be better understood.

The cellular system has, from its inception, a modular architecture which, in theory, can be expanded indefinitely, as required. There are, however, several practical constraints that limit this modular growth, to a certain extent, above which some alternative techniques are recommended. These techniques are examined in this chapter. The issue of system performance is also considered, where three different types of efficiency measures are described. The next topic considered in the chapter is related with the data and signalling control over the radio channels. In this same topic, a successful mobile-to-fixed and fixed-to-mobile call sequence and also the handoff process are illustrated in pictorial form.

Finally, still within this overview approach, the basic system design specifications followed by the main steps in a cellular design are given. To end the chapter, some non-conventional traffic performance enhancement techniques are shown. Again the approach given here is superficial, but a deeper study will be carried out in Chapter 12.

2.1 INTRODUCTION

The early conventional mobile systems consisted of a base station with its transmitter and receiver assembled on a hilltop. The coverage area was chosen to be large and, generally, a very small number of channels was available. As initially those systems were manually controlled, each call had to be conducted through a special mobile operator. The automatic systems appeared by the middle of the 1960's but they were still very limited as, for example, if a customer had a call already established in one area, that call would drop as he moved into another area, and a new call process would have to be initiated.

Notwithstanding the limitations of the systems and the high cost of the services, the growth of the demand for mobile telephones was indeed remarkable. Such systems, having a small number of channels, poor signalling protocols and limited capacity for modular growth, could not cope with such demand. New conceptual ideas for the development of a versatile system, where the subscribers could roam with his telephone in a worldwide integrated network, started to materialize. The cornerstone of this dream is the cellular idea as described in this chapter.

The expansion of a conventional mobile system relies heavily upon spectrum availability. Radio frequency planning is a complicated matter since the frequency spectrum has to be shared by several other different types of services. There is plenty of spectrum available at higher frequency bands, but technology has not as yet been able to overcome the difficulties of operating in those frequency bands.

However, if on the one hand there is scarcity of frequency spectrum, strictly controlled by the regulatory agencies, on the other hand there is the pressure of the demand for mobile services. The way out is the conception of new ideas. The implementation of these new ideas may require a new technology, giving rise to a new system capable, not only of meeting the initial demand, but also of offering new services. These new services can generate new demand and need to be regulated. A new cycle starts as illustrated in Figure 2.1.

In the analysis that follows we will be considering an analog system. Digital systems will be continuously mentioned and analyzed throughout the following chapters at convenient instants.

2.2 THE CELLULAR JARGON

The "new" conceptual ideas implemented today in mobile systems were proposed by the Bell Telephone Laboratories during the middle of this century. The implementation of such ideas would require, among others, complicated means for administering the system, which was feasible with the advent of electronic switching technology [21].

The basic concept is the FREQUENCY REUSE: if a channel of a certain frequency covers an area of radius R, then the same frequency can be reused to cover another area. Each one of the areas constitutes a CELL. The cells using the same carrier frequency are called COCELLS. They are positioned sufficiently apart from each other, so that COCHANNEL-INTERFERENCE can be within tolerable limits. With this new concept, a region initially served by one base station in a conventional mobile system is split into several cells, each of which with its own base station, served by its own set of channels.

"The main purpose of defining cells in a mobile radio system is to delineate areas in which either specific channels or a specific base station will be used at least preferentially, if not exclusively" [2]. If omnidirectional transmitting antennas are used, ideally, the coverage area would be circular. Therefore, if for modelling purposes a cell shape is required, a circle would be the straightforward choice. However, a plane filled up with circles can exhibit overlapped areas or gaps, adding difficulties to the frequency planning. Regular polygons such as equilateral triangles, squares and hexagons do not present these constraints. The REGULAR HEXAGON is the most convenient format, since it most closely resembles the circle.

To understand this in a quantitative way, consider three different cellular systems, the first with the triangular, the second with the square and the third with

the hexagonal array of cells. Suppose that the base station is situated at the centre of the cells, i.e., equidistantly from the vertices. Let R be this distance. Therefore, the coverage areas, corresponding to the area of the triangle, square and hexagon are $3\sqrt{3}\ R^2/4$, $2R^2$ and $3\sqrt{3}\ R^2/2$, respectively. Note, for a given R, that the hexagon (then square followed by the triangle) can cover a larger area. Accordingly, a hexagonal array requires fewer cells (and consequently fewer base stations) to cover the same region [2].

The set of channels available in the system is assigned to a group of cells constituting the CLUSTER. The same set can be reused only in different clusters. The number of cells per cluster determines the REPEAT PATTERN. Due to geometrical constraints (see section 2.6) only certain repeat patterns can tessellate, the most common having 4, 7 and 12 cells per cluster. The smaller the repeat pattern the higher the number of channels per cell, corresponding to a higher traffic capacity system. On the other hand, the smaller the repeat pattern the smaller the distance between cocells, leading to a higher cochannel interference.

Channel allocation strategies play an important role as far as ADJACENT CHANNEL INTERFERENCE is concerned. Although the radio equipment is designed to select only the wanted channels, cutting off adjacent frequencies, there may be situations when adjacent channels can cause interference. For instance, this may happen when two mobiles using adjacent channels transmit to the base station from a short and from a long distance, respectively. The interference problem is worsened in the presence of fading.

The sizes of the cells vary according to the network planning, made to meet a certain traffic demand. The cells are considered to be very small when compared with the conventional systems. Recent studies [1] suggest the use of microcells (90 m radius) with the frequencies allocated at a 60 GHz band.

Although the mobile can travel from cell to cell, it is required that the call already established (or in progress) must not be interrupted. Therefore, changes of channels may occur without the need of the intervention of the subscriber. This action

of changing channels is known as HANDOVER or HANDOFF. Handoff occurs whenever the signal strength measured at the base station falls below a threshold value. The process of monitoring the quality of the signal, recommending the change of channels, if necessary, is called LOCATING. The process of determining a mobile's availability to receive a given incoming call is named PAGING. The function of beginning a call, performed by the mobile unit, is termed ACCESS.

2.3 ESSENTIAL CHARACTERISTICS OF THE CELLULAR SYSTEMS

The main difference between conventional and cellular systems is that the first is a Noise Limited System (NLS) and the second is an Interference Limited System (ILS). Let us describe some of main features of each one of them.

- *Conventional (Noise Limited) Systems:*
  1) serve low subscriber densities;
  2) rely heavily upon spectrum availability;
  3) do not take advantage of the frequency reuse;
  4) require high power transmitters mounted on a hill top;
  5) have a large coverage service area;
  6) do not allow modular expansion;
  7) do not allow handoff

- *Cellular (Interference Limited) Systems:*
  1) serve high subscriber densities;
  2) consider the spectrum availability as a limiting factor;
  3) take advantage of the frequency reuse;
  4) require low power transmitters located at low elevation;
  5) divide the whole service area into small coverage cells;
  6) allow (theoretically) an endless modular expansion;
  7) allow handoff.

In terms of figures, the typical characteristics of the cellular systems are:

1) around 650 channels are available;
2) transmitters provide output power ranging from 10 to 45 watts;
3) transmitters are mounted at elevations typically 30 to 100 m above the service area;
4) the coverage area varies from 2 to 16 km radius;
5) generally each cell is served by 25 to 75 channels.

2.4 BASIC COMPONENTS OF A CELLULAR MOBILE SYSTEM

A general overview of a cellular mobile network is illustrated in Figure 2.2. There are four main elements, as follows:

1) Mobile Station
2) Base Station
3) Mobile Switching Centre
4) Public Switched Telephone Network

We shall briefly describe each component.

- *Mobile Station*

The mobile station (MS) constitutes the interface between the mobile subscriber and the base station. Besides voice communication the MS also provides control and signalling functions, usually performed by a microprocessor. The mobile unit is able to tune, under the system command, to any channel in the frequency spectrum allocated to the system. Each channel comprises a pair of frequencies for a two-way conversation. The control messages are transmitted in a digital form and can be sent through voice or signalling channels, depending on the task to be performed, as shall be seen in section 2.10. The power levels of the transmitter can also be controlled by the system.

Every call from a mobile yields the subscriber's identification and the dialled

digits. In order to provide a more efficient use of the channels, the digits are first held in a memory in the telephone and, when the called party number is complete, they are sent, initiating the communications with the base station.

The Mobile Station consists of two elements: the telephone set and the radio set.

The telephone set provides the contact between the subscriber and the system. It is mounted near the car front seat, where the driver may have a comfortable and safe access to it. It includes a handset, keypad, display and some kind of alert signal (lamp or tone). It is also possible to have some sort of loud-speaker so that the driver does not need to use the handset while driving.

The radio set comprises two distinct pieces of equipment: the radio itself and the control. The radio deals with all the frequencies available in the system in a full duplex mode. The transmitter provides up to (approximately) 10W output power and has its level controlled by the system. It transmits both voice and data which, in the analog systems, experience different types of modulation. The receiver demodulates voice and data. The control is a logic unit with a microprocessor with the role of managing the control tasks within the mobile. Some examples of control messages include:

1) origination request from the mobile in order to access a channel;

2) registration of the mobile in the current service area;

3) channel assignment message from the base station to the mobile;

4) handoff message for a retuning to another channel from the base station, etc.

- *Base Station*

The base stations are responsible for serving the calls to or from the mobile units located in their respective cells. They are connected to the Mobile Switching Centre via land links. Base Stations consist of two elements: the radio and the control. The radio comprises the transmitters, receivers, towers and antennas. The control is a microprocessor unit responsible for the control, monitoring and supervision of the calls. The assignment and reassignment of channels to the mobile units can be carried out by the base station. In addition, the base station monitors

the signal levels to recommend the handoff.

- *Mobile Switching Centre*

The Mobile Switching Centre (MSC) is a telephone exchange specially assembled for cellular radio services. It works as a central controller, interfacing the mobile units and the fixed telephone network. The MSC uses standard telephone signalling and is equivalent to a class 5 local exchange.

The number of cells connected to (controlled by) a MSC varies according to the needs. One MSC can be responsible for a large metropolitan area or for a small number of small neighbouring cities. The area served by one MSC is known as a Service Area. The mobile subscriber within his service area is a Home subscriber. It is possible, however, for the subscriber to move out from his area into another area in which case he is called a Roamer. The main tasks performed by a MSC include paging, locating and handoff. Moreover, it performs functions of an ordinary digital switching exchange such as signalling, switching, A/D conversion of the audio circuits (in the analog systems), detection of on-hook-off-hook status, line scanning for dial pulse signalling, etc.

The communications between the base stations and the MSC are usually carried out through land lines providing speech and data paths. The MSC is also connected to the fixed network by means of land links.

- *Public Switched Telephone Network*

The Public Switched Telephone Network (PSTN) treats the MSC's as ordinary fixed telephone exchanges.

It has not been shown in Figure 2.2, but the cellular systems have a Control Centre where some operations and information are centralized. This control centre can be located at one of the Mobile Switching Centres. It contains the main data base for the whole system and performs the following: call record administration, traffic analysis, network management, maintenance, equipment configurations, etc.

2.5 SYSTEM ARCHITECTURE

A cellular mobile radio system can be built according to a centralized or decentralized architecture. In a centralized architecture the Mobile Switching Centre is usually very large and controls many base stations. In this case the MSC includes clusters situated near and in remote areas as well. In a decentralized system the MSC's are smaller, controlling smaller number of clusters.

Small systems are generally centralized and large systems tend to the decentralized approach. In fact, there are different degrees of decentralization in that there may or may not be interconnection between the MSC's. In the first case a call from a mobile will go through the PSTN only when the called party is a fixed subscriber. In the second case, even if the called party is a mobile, but from a different service area, this call will have to pass through the PSTN (calls within the same service area are handled by the corresponding MSC without the need of a PSTN involvement). The different architectures are shown in Figure 2.3.

When a mobile moves outwards its service area (roams into another area) the first task to be done is to inform the corresponding MSC that this mobile is within that new zone. The visited MSC informs the home MSC of the presence of its user. When this particular mobile is called, his (her) original MSC will direct that call to the MSC within which he (she) is registered.

2.6 THE THEORY OF CELLULAR PATTERNS

The applications of the theory of symmetry and patterns have usually had as main target the studies of crystallography, and only recently (by the 1970's [6]) this has been used in engineering, mainly in cellular mobile radio (a good reference for that can be found in [7]). In this section we should first recall the main concepts for our particular purposes.

a) Any plane repetitive pattern can always be decomposed into fundamental regions

also known as areas or cells, with a general shape of a parallelogram. In fact, the sides of the cells can be of any shape, but opposite sides must have the same shape.

b) A whole pattern can be obtained by translating the fundamental region in a regular way. In a plane this means placing each cell in a position X^mY^n, where X^m represents m steps of X along the OX direction and Y^n represents n steps of Y along the OY direction, where m and n are integers and O is the origin. This is done until the whole area is filled up.

c) A tessellation is defined as a pattern having a polygon as a fundamental region. Regular polygons generate regular tessellation. Equilateral triangles, squares and hexagons are the only regular polygons that can tessellate [3].

d) Colour Symmetry is a feature presented by figures or patterns having symmetrical parts with a choice of colours. In cellular radio terms this corresponds to a set of channels (i.e., each set of channels is a colour). It will be seen that such system exhibits a polychromatic pattern.

Although the theory of symmetry and patterns is well established, the creation of a pattern is still an art and, in this respect, it is open to the imagination. Some patterns, however, due to their symmetry or regularity may be easily tessellated in a logical and sequential manner. The creation of a pattern can be carried out by different manners. A few of them (extracted from [4]) are listed below:

- by breaking down a fundamental area into sub-areas and placing an identical design into each sub-area ;
- by making a design across several sub-areas;
- by distorting the boundaries of sub-areas to form similar interlocking shapes;
- by using a basic pattern as a grid and by colouring only certain areas between the lines of the grid.
- by replacing the straight lines of a basic pattern with curved ones;
- by using mirrors, as in the kaleidoscope;
- by using a computer to replicate a motif with any combination of symmetry operations.

The regular patterns

In this section we shall consider the patterns formed by the regular polygons, namely, regular triangles, squares and hexagons. Special attention will be given to the hexagons.

Consider initially the equilateral triangle. For this figure it is convenient to choose the set of coordinates as shown in Figure 2.4. The positive portions of the two axes form a 60° angle, and the unit distance along the axes is R (where R is the cell radius). The distance between two points (u_1, v_1) and (u_2, v_2) is given by:

$$D^2 = i^2 + ij + j^2 \tag{2.1}$$

where $i = u_2 - u_1$ and $j = v_2 - v_1$

Now consider the square. The set of coordinates lies obviously at the orthogonal axes (Figure 2.5) and the distance D is given by

$$D^2 = i^2 + j^2 \tag{2.2}$$

and the unit distance is $\sqrt{2}$ R

For the hexagonal array the (u,v) axes are chosen to have their positive portions crossing at 60° angle (Figure 2.6), and the unit distance being $\sqrt{3}$ R. Then

$$D^2 = i^2 + ij + j^2 \tag{2.3}$$

We shall concentrate our studies on the hexagonal array of cells. Nevertheless, the subject discussed below can be easily adapted to the triangular or square arrays.

In order to determine the cell pattern, i.e., the cluster, the fundamental procedure is to place the cocells at equidistant points from a reference cocell. The next step is to label another cell as a reference and proceed in the same way as before. It is possible, and in fact more plausible, to simplify this procedure by just determining the first set of cocells. Then, by translation without rotation, the first pattern (first set of cocells) can be replicated around the initial reference.

Now we need to find the loci of points where the equidistant cocells are located.

If we impose that the reuse distance must be isotropic, there are six hexagons equidistant from the reference hexagons. Using (2.3) it can be seen that, if we position the hexagons at the set of coordinates (p,q), (p+q,-p), (-q,p+q), (-p,-q), (-p-q,p) and (q,-p-q) their distances to the reference hexagon (centred at (0,0)) are equally given by $p^2 + pq + q^2$. Therefore, these are the required cocell positions. An equivalent procedure is to use a system of axes as that shown in Figure 2.6 and then position the coordinates (p,q) using all six possible pairs of consecutive axes, i.e., axes ij, jk, kl, lm, mn, no (Note that i = -l, j = -m, and k = -n). As an illustration consider (p,q) equal to (1,2). The corresponding cocells represented as cell 1 are as shown in Figure 2.7. Now by translating without rotating the set of cocells, we obtain another set of cocells (named cell 2). This can be done until the whole pattern is filled up. This is shown in Figure 2.8.

The theory of cellular pattern is based on the concept that a pattern is set up by replicating the fundamental area known as a cluster. It is assumed that a cluster is a contiguous group of cells. Consequently, all of the clusters must be identical. The shape of the clusters is also of a regular hexagonal form and this is intuitively deduced. The explanation given here is taken from McDonald [2], but a more rigorous approach can be found in Heeralall [7] .

The intuitive idea is based on three facts:

a) each cell has six equidistant nearest cochannel cells;

b) each adjacent pair of the six axes connecting the centre of the reference cell to the centres of the six surrounding cochannel cells has an angle separation of 60°;

c) the above observations are valid for any arbitrary cell.

In short, the main constraints forcing the clusters to have an hexagonal shape are:

a) reuse distances must be isotropic;

b) a cluster must be a contiguous group of cells.

This can be seen in Figure 2.8 where the dotted hexagons represent the clusters.

Assuming that a cluster has a hexagonal shape, we want to determine the number N of hexagonal cells per cluster. Let a and A be the areas of the cell and of the cluster, respectively. The area a is then

$$a = 3\sqrt{3}\, R^2/2 = \sqrt{3}/2 \quad * \tag{2.4}$$

The distance between the centres of two cocells is D. Let us choose these cells to be the centres of the corresponding hexagonal clusters. Hence the area A is

$$A = 3\sqrt{3}\left(\frac{D/2}{\cos 30^\circ}\right)^2/2 = \sqrt{3}\, D^2/2 \tag{2.5}$$

The number of cells per cluster is obviously

$$N = A/a = D^2 \tag{2.6}$$

or equivalently, using (2.3)

$$N = I^2 + IJ + J^2 \tag{2.7}$$

Since I and J are integers, the clusters will accommodate only certain numbers of cells such as 1, 3, 4, 7, 9, 12, 13, 16, 19, 21, ...

The patterns 7 and 12 are the most common configurations of the cellular systems. Figure 2.9 shows these patterns and the hypothetical hexagonal shape of the corresponding clusters.

An important parameter of a cellular layout is the D/R ratio, known as cochannel reuse ratio. This ratio gives an indication of both the transmission quality and also traffic capacity. On the transmission side, the D/R ratio gives an indication of the cochannel interference statistics: the higher the ratio the lower the interference potential. As far as traffic capacity is concerned the D/R ratio can also give a measure of performance evaluation. This is promptly seen if we express the ratio as a

---

* Note that $\sqrt{3}\, R$ has been assumed to be the distance unit.

function of the number of cells per clusters. Using the above equations

$$D/R = \sqrt{N} / (1/\sqrt{3}) = \sqrt{3N} \tag{2.8}$$

The fewer cells per cluster (or equivalently, the smaller D/R ratio) the larger the number of channels per cell, i.e., a higher density of channels corresponding to a higher traffic carrying capacity.

It can be seen that transmission quality and traffic capacity work in opposite directions (see Figure 2.10). Moreover the smaller the cluster size the lower the cost of the system. The determination of the D/R ratio is then a trade off between these factors and, obviously, an intermediate point can be found so that a reasonable grade of service can be accomplished.

Assume, for example, that the total amount of channels in the system is 360. Then Table 2.1 depicts a comparison between the traffic capacity and the transmission quality.

Table 2.1 - Traffic Capacity and Cochannel Interference

Cluster Size	D/R	Channels/Cell	Traffic Capacity	Transmission Quality
1	1.73	360	Highest	Lowest
3	3.00	120	↑	↓
4	3.46	90	↑	↓
7	4.58	51	↑	↓
12	6.00	30	Lowest	Highest

2.7 SYSTEM EXPANSION TECHNIQUES

One of the many advantages of the cellular architecture is its modular growth capability. A start-up system is usually constituted of hexagonal cells of the largest possible radii. As the demand for service grows, the system will tend to absorb the

new users up to a limit where it can still offer a good grade of service. If the quality of the service is initially high, it may be possible to accept an increase of the traffic load and allow a system performance degradation, but still within acceptable levels. This in fact, constitutes a very convenient way of allowing the system to adapt to a sudden growth of the traffic demand. However, this adaptation is only efficient on a short term basis, since any additional growth can cause a disastrous degradation. The network will be able to accommodate more subscribers if there is a change in the system itself. We shall examine some of the techniques that may be used.

a) *Adding New Channels*

This can be done only if there are channels available. Initially, when a system is set up not all the channels need be used, and growth and expansion can be planned in an orderly manner. However, once all the channels have already been used, new expansion methods have to be found.

b) *Frequency Borrowing*

The channels are allocated to the cells according to the geographic distribution of the traffic. If the traffic demand shows a greater concentration in certain regions, i.e., if some cells become more overloaded than others, it may be possible to reallocate channels by transferring frequencies from the less loaded to the more loaded cells. This works on an interim basis as further growth will require that those borrowed frequencies return to their original cell. The advantage of this technique is that it does not require a big change in the hardware of the system.

c) *Change of Cell Pattern*

It has been previously seen that a smaller number of cells per cluster represents a higher traffic capacity. However, it has also been seen that this corresponds to a degradation of the transmission quality (higher cochannel interference). This technique, nevertheless, is rather costly and seldom applied.

d) *Cell Splitting*

Cell splitting is a technique aimed at diminishing the size of larger cells by dividing them into a number of smaller cells. By reducing the size of the cells, more cells per area will be available with a consequent increase of channels in such area and an increase in traffic capacity.

Radius reduction by a factor of K reduces the coverage area and increases the number of base stations both by a factor of K^2. It is advisable to choose K so that mixed cell sizes can co-exist taking also advantage of using the old base stations. Figure 2.11 depicts two stages of cell splitting.

Cell splitting usually takes place at the midpoint of the congested area. Further splitting may occur until the minimum size of the cell radius is reached. This minimum size is determined taking into account (i) the minimum cochannel reuse distance that can be achieved while maintaining voice quality objectives, (ii) the problem of siting the base stations and, obviously, (iii) the economic aspects.

e) *Overlaid / Underlaid Cells*

When cell splitting occurs, there may be cells with different sizes in the system. The start-up system is conceived so that a D/R ratio is maintained throughout the network. With different cell sizes, special attention must be given to cochannel interference problems. Consider the example of Figure 2.12 where a 7-cell cluster is the pattern. The distance between bigger cocells is 4.6R, where R is the bigger cell radius. The distance between smaller cocells is 4.6r where $r = R/2$ is the smaller cell radius. Cochannel interference between the bigger cells must be within tolerable limits as designed at the conception of the system. The same applies to the smaller cells since the cochannel reuse ratio is maintained. The calls within smaller cocells will not cause undue interference on the channels of the bigger cells, because if the cochannel ratio requirement is satisfied for the smaller cells, it is also satisfied for the bigger ones. The opposite situation, however, is not true. Calls being served by the smaller cells will suffer interference from the cochannels of the bigger cells since the distance between them will be 2.3R (half of the initial value 4.6R).

A possible solution for this is to visualize the bigger cell as if it were composed by two tiers (layers) as shown in Figure 2.13. The coverage area of the cell is still the same. The difference now is that the inner layer and the outer layer operate with distinct set of channels. The main restriction is that the outer tier cannot be served by any of the frequencies used in the smaller cocells. Suppose that the bigger cell has a set of channels C divided into subsets A and B (C = A + B). Suppose also that the smaller cocell will use the subset A. Consequently the outer layer can only be served by the subset B.

The inner cells coverage area is controlled by transmission power reduction and handoff control parameters. If a mobile moves out from its layer a handoff procedure must take place. Handoff occurring when the mobile moves from the inner to the outer layer is called handout. The converse is named handin. Note that the cell is still served by the same amount of frequencies and that the outer voice channels are also available for the mobiles within the inner radius.

f) *Sectorization*

In theory, the cell splitting process may be carried out indefinitely. In practice, however, there are some very obvious constraints, such as:

(i) as the distance between cells reduces the cochannel interference increases, although the same repeat pattern is kept;

(ii) finding a suitable location for the base station may become a difficult task, since the siting tolerance is contracted as well.

(iii) the total cost of the system is increased because the number of required base stations is increased.

An alternative to cell splitting is SECTORIZATION. This technique consists of dividing the cell into a number of sectors, each of which is served by a different set of channels and illuminated by a directional antenna. The sector, therefore, can be considered as a new cell. The most common arrangements are 3 and 6 sectors/cell.

The base stations can be located either at the centre or at the corner of the cell. The first case is referred to as centre-excited cells and the second as corner-

excited cells. In fact, there is no difference between the system conceived in one or another way. These two approaches are illustrated in Figure 2.14 where the dotted lines sketch the main lobe of a hypothetical directional antenna.

It will be shown later that the use of directional antennas substantially cuts down the cochannel interference, thus allowing the cocells to be more closely spaced. Closer spaced cells imply smaller D/R ratio, corresponding to smaller numbers of cells per cluster (see equation (2.8)). In other words, more channels per cell can be used, corresponding to a higher capacity, since the total amount of available channels in the system is constant. Sectorization is then very attractive since it allows the system to grow with a reduced investment when compared with the cell splitting technique.

The question that may arise is "Why not start up the system with directional antennas already?" At the inception of a cellular mobile system, the aim is to have as few base stations as possible to cover the required geographical region, since base stations constitute a high investment. Since the use of directional antennas reduces the covered area, not only more antennas but also more transmitters are needed. When the system expands, the aim is to maintain the same cell sites, but still reducing the cell area to increase capacity. This is achieved by means of sectorization with the use of directional antennas.

2.8 PERFORMANCE MEASURES AND EFFICIENCY

The systems are usually designed to meet certain specifications. These specifications include some performance parameters directly influencing the network efficiency. The ultimate requirement of any communication network is the CAPACITY. Particularly, in mobile radio system this is related to traffic capacity. Hence two main parameters are of interest:

(i) Carrier to Cochannel Interference ratio (C/I_c) and

(ii) Blocking Probability (E) or Grade of Service (GOS)

The C/I_c ratio, as previously mentioned, varies according to the cellular pattern. It can be easily calculated if the mobiles are assumed to be fixed and positioned for the worst case performance. In fact, C/I_c is a random variable affected by random phenomena such as location of mobiles, fading (Rayleigh and Gaussian), antenna characteristics and base station locations. It is indeed a complex parameter to be estimated if all the variables are to be taken into account. The connection between the performance parameter C/I_c and the traffic capacity is that variations in C/I_c can be directly translated into reuse distance (D/R ratio) giving a measure of the compactness of the cellular layout. The larger the C/I_c ratio (less interference), the larger the D/R ratio, leading to a larger cell pattern. On the other hand, the larger the cell pattern the smaller number of channels per cell, leading to a smaller traffic capacity. Design specifications require that a minimum C/I_c (usually 18 dB, 17 dB or sometimes even less) must be achieved over a large percentage of the coverage area (usually 90%).

Blocking probability or Grade of Service is a performance parameter easily associated with traffic capacity. Several formulas for blocking probability calculations are available and they are used according to specific applications. Among them, the most widely used is the Erlang-B given by

$$GOS = E(A,N) = \frac{A^N/N!}{\sum_{I=0}^{N} A^I/I!} \qquad (2.9)$$

where A is the offered traffic in Erlang (erl.) and N is the number of channels. Note, however, that this is a general purpose formula used only for a quick traffic performance assessment. It does not take into account the various phenomena of the mobile radio system, mainly characterized by the mobility of the subscriber (handoff, etc). For the purposes of this section the use of this formula will be sufficient.*

The start-up system usually begins with a grade of service of P.02 (2% of blocking probability), rising up to P.05 as this system grows. If more subscribers are

* Refer to Chapter 12 for studies of traffic in mobile radio systems.

allowed in the system the blocking probability may reach unacceptable values. Accordingly, some system expansion techniques must be used.

It can be seen that both the C/I_c and the GOS constitute isolated parameters not clearly expressing the overall system performance. Particularly, the GOS can be associated with one specific cell while the C/I_c ratio can be determined for a specific region or situation. For instance, C/I_c is high in a large cluster where the blocking probability (GOS) can be very small. At first sight, high C/I_c and low GOS is the ideal situation. But note that in this case a cluster may not be using the channels efficiently. Therefore, an overall measure of efficiency, taking into account all the relevant parameters in a mobile radio system, is required.

There are three main efficiency measures: (i) *spectrum efficiency*, (ii) *trunking efficiency* and (iii) *economic efficiency*.

(i) The *spectrum efficiency*, η_S, is a measure of how efficiently space, frequency and time are used. These three variables are combined into a product form as

$$\eta_S = \frac{\text{number of reuses}}{\text{coverage area}} \times \frac{\text{number of channels}}{\text{bandwidth available}} \times \frac{\text{time the channel is busy}}{\text{total time of the channel}}$$

Hence η_S is expressed in units of Erlangs m^{-2} Hz^{-1}. Several techniques can be implemented to improve the spectrum efficiency. We shall examine some of them

1) Given that the available bandwidth is fixed, the only way to increase the number of channels is to reduce the channel bandwidth. This can be accomplished by means of improving the modulation techniques, filters response, etc.

2) The cell area can be reduced by the cell splitting technique or sectorization.

3) The channel usage can be optimized if the messages are compressed or interleaved, taking advantage of the fact that the carried information (speech or data) is not continuously present. Additionally, channel usage can be increased with the application of some dynamic channel assignment or alternative routing strategies.

(ii) The *trunking efficiency* measures the number of subscribers that each channel in each cell can accommodate. This, of course, intrinsically depends on the grade of service that the system is prepared to offer. Given a grade of service GOS

and number of channels, the total traffic can be calculated using the Erlang-B formula. If on average, each subscriber generates a certain amount of traffic, then the total number of subscribers is estimated. In the graphs of the Figure 2.15 the curves are given for three different grades of service (2%, 5% and 10%) and it is assumed a traffic of 0.02 Erlang/subscriber.

It can be seen that the trunking efficiency decreases rapidly when the number of channels per cell falls bellow twenty.

(III) The *economic efficiency* depends on many factors and a simple assessment is not available. It aims at measuring how affordable to people and cellular operator the mobile service is. In other words, this is directly related with the costs of service per customer.

2.9 TRAFFIC ENGINEERING

The starting point to engineer the traffic is the knowledge of the required grade of service. This is usually specified to be around 2% during the busy hour. The definition of the busy hour may vary according to the license administrator's point of view. There are usually three options:

- busy hour at the busiest cell;
- system busy hour;
- system average over all hours.

The estimate of the subscriber usage rates is usually made on a demographic basis since this can vary according to the region. The traffic distribution is then worked out and the cell areas identified. The calculations are generally simplified if the traffic is assumed to be evenly distributed. However, in practice, even traffic distribution is quite rare. In urban areas there is a high concentration of traffic at the town centre during the rush hour, decreasing smoothly towards its outskirts. This distribution is known as "bell shaped". In the start up system, however, the traffic

distribution is not well known. The calculations are carried out based on the best available traffic estimates. The final system capacity is obtained by grossly exaggerating the calculated figures.

2.10 DATA AND CONTROL SIGNALLING

Similar to any other communication network, the mobile radio channels need to handle data transmission, at least for signalling purposes. There are two ways of transmitting data: (i) using the speech channels or (ii) using dedicated channels. In the first method, when the channel is not busy with voice transmission, then an idle tone is inserted in order to indicate its availability for data transmission. In the second method, a percentage of the total amount of radio channels is exclusively used for signalling transmission. The first method was initially used by the early mobile radio systems. However, for the cellular purposes, the idle tone speech channel method is not appropriate. This is due to the amount of signalling required to handle the enormous quantity of voice channels, cells and subscribers present in the cellular systems.

2.10.1 Control over the Signalling Channels

The proportion of signalling channels may vary with the system capacity. A start-up system requires a small number of these dedicated channels, with this number increasing as the system expands. The allocation of the channels to their functions also varies with the network. In the AMPS system [22] these signalling channels are divided into three groups: (i) *dedicated control channels (CC)*, (ii) *paging channels (PC)* and *access channels (AC)*.

The dedicated control channels are common to all the mobiles throughout the system. Every mobile is programmed to tune to one of the CC's, in fact, to the strongest one. The CC's carry overhead messages giving specific information about the

system. The messages include the service area identification, the number of the paging channels available, etc. The paging channels are mainly used for seeking a called mobile. The PC's transmit the identification number of the called subscriber, over the whole service area (the mobile is "paged"). The PC's also carry the number of the access channels in that region. These channels are used when a mobile wants to initiate a call. Each AC has a busy/idle bit indicating its availability for use. Now we shall briefly describe a successful simplified call sequence [22]. We first present the initialization process.

Once the mobile unit is switched on, it scans over all the dedicated control channels and it tunes to the strongest one. The mobile is then informed about the available paging channels in that area. It scans these channels and it tunes to the strongest one.

(i) Call from mobile to fixed subscriber.

a) The mobile receives on the PC the number of the AC available in its area;

b) It scans the AC's and tunes to the strongest one. The selected AC should, most likely, belong to the closest base station;

c) The mobile then sends the dialled digits and its own identification. The base station receives and routes these digits to the mobile switching centre (MSC);

d) The MSC determines and transmits the voice channel number to be allocated to the mobile, and the mobile tunes to it;

e) The MSC sends the dialled digits to the Public Switched Telephone Network (PSTN);

f) The PSTN completes the voice path.

(ii) Call from fixed to mobile subscriber

a) The PSTN routes the call to the MSC, having the called mobile registered within;

b) The MSC impels (causes) all its base stations to transmit, on their PC's, the identification number of the called mobile;

c) The mobile identifies its number, tunes to the strongest AC and acknowledges the paging. The base station relays this acknowledgment to the MSC;

d) The MSC selects an idle voice channel of that base station and the mobile tunes to it;

e) An alerting tone is sent through the voice channel to the mobile and a ring tone is sent to the calling subscriber;

f) The voice path will be completed as soon as the called user answers (the alerting and ringing tone are, obviously, removed).

These two sequences are depicted in the Figures 2.16 and 2.17, respectively. In these figures the arrowed lines indicate the direction of the action. The dotted lines indicate signalling and the solid lines represent voice.

2.10.2 Control over Speech Channels

The speech channels must also carry some sort of signalling information, so that the established conversation be under control. Suppose, for instance, a mobile moving from one cell into another. How does the handoff take place? How is the signal strength monitoring carried out? How is the on-hook-off-hook status detected? These control tasks are provided by means of supervision tones, inserted somewhere above the voice band in the speech channels. The AMPS system [2] uses the (i) *signalling tone* and (ii) *supervisory audio tone*, having their functions briefly described below.

(i) The *signalling tone (ST)* is an one-way (from mobile to base station) 10 kHz tone used in bursts for disconnection, alerting, handoff and flashing.

(ii) The *supervisory audio tone (SAT)* comprises a set of three continuous tones (6 kHz and 6 kHz ± 30 Hz). Only one frequency, however, is used by the base station of a given cluster. Neighbouring clusters employ one of the remaining two audio tones.

This allocation scheme assures a more reliable supervision control because interference is greatly reduced. Cochannels using the same supervisory tone are spaced farther apart from each other. In effective terms, as far as supervision is concerned, the size of the cluster is multiplied by three, and, consequently, the reuse D/R ratio is increased by $\sqrt{3}$. The supervisory audio tone is continuously sent by the base station to the mobile that loops it back to the base station. If the received tone differs from the tone that has been sent, some sort of interference may have occurred. If no tone is returned, either the mobile is in fading or its transmitter is off.

The speech channels can also transmit data messages while the mobile is in conversation, this occurring, for instance, in the handoff process. We shall briefly describe the handoff procedure:

a) The serving and the surrounding base stations monitor the transmission quality of the channel in use. The mobile switching centre receives this information over the data link. An analysis is then carried out and the MSC decides to which base station the call must be handed off.

b) The MSC informs the new base station that a call is to be handed off to a specified channel. This base station switches on its transmitter and the supervisory audio tone is sent over the channel.

c) The MSC informs the serving base station that such call is to be handed off to a new channel having a given supervisory audio tone. This information is passed over to the mobile in the speech channel in use.

d) The mobile sends a burst of the signalling tone, turns its transmitter on, tunes to the new channel and loops back the audio tone.

e) The former base station clears the call and the new base station, by recognizing the looped back audio tone, activates the call.

These steps are depicted in the Figure 2.18

The algorithms used for handoff can vary according to the system. The simplest criterion is based only on the signal strength measurement. The supervisory audio tone may also be involved to determine the distance from the mobile to the base stations.

2.11 CELLULAR SYSTEM REQUIREMENTS AND ENGINEERING

The basic objective of the cellular mobile radio is to provide flexibility to the subscriber, initially familiar with the fixed telephone network. Therefore, the basic specifications require the services to be offered with telephone quality. As far as traffic is concerned, the blocking probability during the busy hour should be kept below 2%. In fact, the 5% figure is quite acceptable, but there are systems already working with 10% or more. On the transmission aspect the aim is to provide most of the customers with a good transmission quality for at least 90% of the time. This "good quality" is something rather subjective, and many tests are carried out so that different opinions are gathered among people volunteered to be submitted to those tests [10,12].

The transmission quality in cellular systems depends mainly on the (i) signal to cochannel interference (S/I_c) ratio and (ii) adjacent channel selectivity (ACS). The S/I_c is a subjective measure, usually taken around 17 dB [2]. The ACS is a specification of the CCIR having a minimum of 70 dB. The cochannel-to-interference C/I_c ratio depends on the modulation scheme. For a 25 kHz FM the C/I_c is around 8 dB and for a 12.5 kHz FM this is 12 dB [10]. The minimum signal-to-interference ($S/I = S/(noise+I_c)$) requirement is 18 dB. An improvement of this figure does not result in a significant voice quality enhancement. Below this figure there would probably be a "crosstalk" and further below, the call is cutoff [13].

Engineering a cellular system to meet the above mentioned goals is not a straightforward task. It requires a great deal of information such as (i) market demographics, (ii) area to be served, (iii) traffic offered, etc., not usually available in the earlier stages of the system design. If some data are available, they are usually not enough to achieve an optimized planning. Anyhow, the data available at the time of the system inception are always the best (only) input and must be used. As the network evolves, additional statistics will help the system performance assessment and replanning. The main steps in a cellular system design are shown in the flow chart

form of Figure 2.19.

2.12 ALTERNATIVE TRAFFIC PERFORMANCE ENHANCEMENT TECHNIQUES

In section 2.6 we mentioned some system expansion techniques . In this section we shall describe some traffic oriented procedures that can be explored. The aim is just to highlight the main points and leave a deeper discussion to be done in Chapter 12.

2.12.1 Channel Assignment Algorithms

The efficient use of channels determines the good performance of the system and can be obtained by different channel assignment techniques. A great deal of studies and computations have shown that there is a noticeable increase in channel occupancy as some dynamic assignment algorithms are applied. The main techniques for allocating channels are briefly described below.

(i) *Fixed Channel Allocation*: In this technique a sub-set of the channels available in the system is assigned to each cell. The same sub-set is reassigned to the cell with the required reuse distance (to avoid cochannel interference). If all the channels are busy in one cell the call is blocked. When the traffic profile is well known, the allocation of the channels can be optimized to give the best performance. However, any sudden traffic variation can cause disturbance.

(ii) *Dynamic Channel Allocation*: this algorithm, in fact, comprises a number of strategies with the common characteristics that all the channels in the system are available to all the cells. The assignment is carried out according to the dynamic traffic demand of the subscribers. This algorithm can cope with the varying non-uniform spatial traffic distribution but gives poor results at high load [15,16].

(iii) *Hybrid Channel Allocation*: this technique is a combination of the two previous ones. Each cell has a fixed percentage of pre-allocated channels, while the rest of the channels are assigned dynamically. The performance then depends on both

the traffic distribution as well as on the proportion of fixed-to-dynamic channels.

(iv) *Borrowed Channel Allocation*: In this approach a cell having all of its channels busy looks for a free channel in the neighbouring cell. If there are no channels available, then the call is blocked. It is possible to improve this by "forcing" the borrowing from the adjacent cell even if that cell is blocked. This blocked cell will, by its turn, force a borrowing from another cell and so on [17].

A full performance analysis of those techniques and their variations is carried out by Sanchez [18], where realistic models and conditions are applied.

2.12.2 Fuzzy Cell Boundaries

The implementation of any of the above channel assignment techniques (except for the fixed one) implies a complete involvement of the central processing control unit with any call having to be handled through it. It may be possible to consider a more local approach, with the decision needing to be taken not so far away (i.e., centrally) perhaps within the local MSC itself. If there is traffic available for alternative routing between adjacent cells, then its management can lie within the concerned traffic area. It is just a question of determining the cell and the amount of traffic that this cell must be offered so that, by sharing the load among neighbouring cells, the system can be led to a traffic balance condition.

Many aspects of cellular radio design and performance are studied on the assumption of fixed cell boundaries. Practically, the cell boundaries are uncertain and shifting because radio propagation is variable both in space and time. Handoff procedures take some account of this, normally being based on the relative signal levels of two paths from a mobile to two base stations. However, in general, planning and design have not been optimized for the practical situation in which boundaries are Fuzzy and base station service areas overlap.

If a mobile is near a cell boundary it may well have adequate communication with more than one base station. It should then be possible to use this property as the basis for alternative routing techniques, in the light of information such as the

current channel occupancy in each cell, and the mean or forecast traffic in each cell, so as to maximize the joint traffic capacity of a set of contiguous cells.

The first step in evaluation of alternative routing strategies is to estimate the proportion of traffic that might reasonably be treated as available for alternative routing. This will be done in Chapter 3, but it is still possible to have a rough idea, just by using a very simple geometrical approach as follows.

Mobiles with more than one path - A rough estimate

The hexagonal shape of the cells in a mobile radio system is just considered as an ideal model. It cannot be obtained in a real world. With the use of omnidirectional antennas, the coverage area can ideally be approximated by a circle. In a hexagonal cell array, if each cell is superseded by circles (Figure 2.20) there will be overlapped areas representing regions being served by two base stations. Note that this is just a simplistic model since in a real system the mobile can be served by several base stations. Usually, the best relative signal strength is chosen for communication. What we will show here is the potential benefits of choosing the channel not only based on the relative signal strength criteria, but also on the traffic load of the system. Chapters 3 and 12 treat this subject in more detail.

Define γ as the proportion of overlapped area with seven base stations taken two at a time, i.e.,

$$\gamma = \frac{\text{overlapped area}}{\text{total hexagonal area}}$$

By simple area calculations, from Figure 2.20, γ is obtained as approximately 21% . Assuming that the mobiles are uniformly distributed within the cell it can be concluded that 21% of the subscribers are within the Fuzzy area, i.e. can be served by two base stations.

Even if it were physically possible, there is no interest or advantage, for the sake of the system performance, in making the boundaries between cells completely rigid. That is, there is no interest or advantage in having the coverage area of one

base station starting exactly at the point where the area served by an adjacent base station ends. An overlapping region has to be allowed so that handoff can take place safely. There should be a certain *flexibility* for the continuity of the calls from mobiles crossing the border between cells. Such flexible area assures the system a practical *adaptability* to conditions when calls cannot be handed-off immediately (e.g., when there are no free channels in the other cell, or when any other higher priority task is being processed at the moment of the request, etc.). Accordingly, if the cell coverage area is expanded to allow for more flexibility, there will be overlapped areas common to three cells. Therefore, the traffic at this region may have access to three base stations. Let δ be the proportion of the overlapped area common to the three neighbouring cells. It is obvious that δ is a function of γ. Moreover, a linear variation in γ implies a quadratic variation in δ, because this is reflected into area variation. Hence $\delta \propto \gamma^2$. For the purposes of this section we can use

$$\delta \propto \gamma^2 \tag{2.10}$$

It will be shown in Chapter 3 that (2.10) is in fact an underestimate of δ.

Potential benefits from alternative routing for three contiguous cell

In order to have an insight into the improvement in traffic performance that can be achieved with the use of the fuzzy traffic, consider a 3-cell system with a traffic distribution as follows: cell 1 with 0.75 erl., cell 2 with 4.25 erl. and cell 3 with 2.5 erl. If γ is the proportion of mobiles with two or more paths, δ is the proportion of mobiles with three or more paths, then the proportion of mobiles with only two paths is $\gamma - \delta$. Assuming the approximation given by (2.10), with $\gamma = 45\%$, then the distribution of the fixed and flexible traffics is as shown in Figure 2.21. The streams of traffic have been calculated as follows.

Flexible traffic between cell 1 and cell 2 = $(0.75 + 4.25)\left(\frac{\delta - \gamma}{2}\right)$

Flexible traffic between cell 2 and cell 3 = $(4.25 + 2.5)\left(\frac{\delta - \gamma}{2}\right)$

Flexible traffic between cell 3 and cell 1 = $(2.5 + 0.75)\left(\frac{\delta - \gamma}{2}\right)$

Flexible traffic between cell 1 and cell 2 and cell 3 = $(0.75 + 4.25 + 2.5)\delta$

We have assumed the flexible traffic of each cell to be equally distributed between its boundaries. This is the reason for the factor 1/2 in the above calculations. Note that if the traffic in Figure 2.21 is conveniently redistributed between the cells, the system can restore the balance with each cell being offered 2.5 erl.. If each cell has 5 channels, the initial mean blocking probability of the system (when no fuzzy traffic is used) is 16% whereas this blocking falls to 7% after the traffic redistribution.

2.13 SUMMARY AND CONCLUSIONS

Mobile communications have been in use since the early days of the invention of the radio, and the cellular concept is rather old. However, only more recently the cellular systems appeared as a consequence of the high demand for mobile services, radio frequency spectrum limitation and availability of technological resources.

Radio is a rather complex communication medium, and there is no universally accepted propagation model applicable to all the situations. A considerable amount of parameters have to be taken into account and usually not all the necessary input data are easily available. The cellular architecture imposes additional complexity when interferences are to be considered. Hence special attention in assigning the frequencies has to be paid so that interference may be kept within acceptable limits.

There are many ways of assessing the system performance. The main efficiency measure, however, combines the amount of traffic per area and bandwidth. The aim, then, is to include as many channels as possible in an as-small-cell-as-possible, and make efficient use of the channels. This is not a straightforward task since system capacity and interference work in opposite directions. The question then is to achieve a more efficient use of the available channels, keeping the interference within

acceptable tolerances. The tolerance limits are subjective measures, requiring tests involving people. This has already been done in some pioneer systems and those figures are generally accepted as standards. In terms of blocking probability the objective is to maintain the same requirements as for the fixed network. Nevertheless, due to the increasing demand, this is seldom achieved and the subscriber may experience blocking up to 10 times as high as that of the initial requirement.

In order to increase the channel occupancy in the cellular system, traffic enhancement techniques have been proposed. They all aim at improving the performance and may be a very good option for a near future application.

REFERENCES

[1] R. Steele, V.K. Prabru, "High-User-Density Digital Cellular Mobile Radio Systems", *IEEE Proceedings*, Part F, vol 132, p. 396, August 1985.

[2] V.H. MacDonald, "Advanced Mobile Phone Service: The Cellular Concept", *BSTJ*, Vol. 58, January 1979.

[3] W.B Coxeter, Introduction to Geometry, John Wiley & Sons Inc., *2nd edition*, New York, 1969.

[4] E.H. Lockwood and R.H. Macmillan, Geometric Symmetry, Cambridge University Press, Cambridge, 1978.

[5] A.V. Shubnikov, N.V. Belov and others, *Colored Symmetry*, Pergamon Press, Oxford 1964.

[6] D.C. Cox, "Cochannel Interference Considerations in Frequency Reuse Small-Coverage Area Radio Systems", *IEEE Transactions on Vehicular Technology*, Vol. VT-32, Nº 3, pp. 217-224, August 1983.

[7] S. Heeralall, "The Applications of Directional Antennas in Cellular Mobile Radio Systems", Ph. D. Thesis, University of Essex, England, 1988.

[8] Dennis Paschke, "RF Engineering Considerations for Cellular Systems", (a presentation for TELEBRAS), Novatel, Canada, October 1988.

[9] D.R. Cown and R. Maciczko, "User Density for 800 MHz Microwave Mobile Radiotelephone Communications", 1980, *International Zurich Seminar on Digital* Communications, pp. C2.1-3, March 1980.

[10] R.C. French, "The Effect of Fading and Shadowing on Channel Reuse in Mobile Radio", *IEEE Transactions on Vehicular Technology*, pp. 171-181, August 1979.

[11] J. Hoff, "Mobile Telephony in The Next Decade", 2nd *Nordic Seminar on Digital Land Mobile Radio Communication*, Stockholm, October 1986.

[12] P.J.Garner, "Co-channel and Quasi- Synchronous Characteristics of SSB Relative to FM in Mobile Radio Communication Systems", *IEE Communications 80*, pp. 16-18, April 1980, *Communications Equipment and Systems*, Conference Publication Nº 184, pp. 174-7.

[13] K. Sowell and J. Kolano, "Factor in the Cellular System Capacity Formula", U.S. West presentation in the 2nd *International Seminar on Cellular Mobile Telephony* (in Portuguese), pp. 28-29, November 88, RNT, Sao Paulo, SP., Brazil.

[14] V. Johansson, "The Best in Yet to Come", *Communications Systems Worldwide*, October 1987.

[15] D.C. Cox, D.O. Reudinik, "A Comparison of Channel Assignment Strategies in Large-Scale Mobile Communications Systems", *IEEE Transactions on Communications*, Vol. Com-20, Nº 2, April 1972.

[16] D.C. Cox, D.O.Reudinik, "Increasing Channel Occupancy in Large-Scale Mobile Radio Systems:"Dynamic Channel Reassignment", *IEEE Transactions on Communications*, Vol. Com-21, Nº 11, November 1973.

[17] Antennas Specialists, "Dynamic Frequency Allocations Increases Cellular Efficiency", *Communications Engineering International*, November 1986.

[18] J.H. Sanchez V., "Traffic Performance of Cellular Mobile Radio Systems", Ph. D. Thesis, University of Essex, 1988.

[19] D. Gross, C.M. Harris, *Fundamental of Queueing Theory*, John Wiley & Sons, 1974.

[20] M.D. Yacoub, "Mobile Radio with Fuzzy Cell Boundaries", Ph. D. Thesis, University of Essex, 1988.

[21] W.R. Young, "Advanced Mobile Phone Service: Introduction, Background and Objectives", *BSTJ*, Vol. 58, January 1979.

[22] Z.C. Fluhr and P.. Porter, "Advanced Mobile Phone Service: Control Architecture", *BSTJ*, Vol. 58, January 1979.

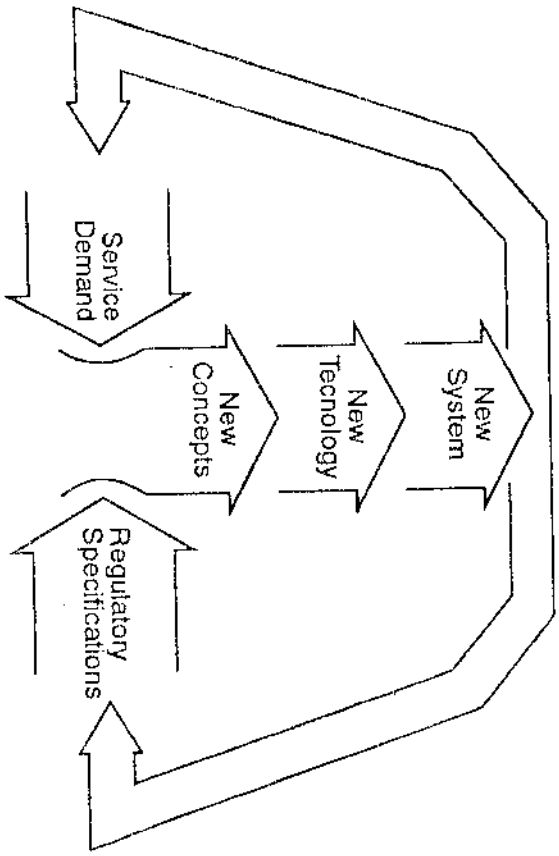

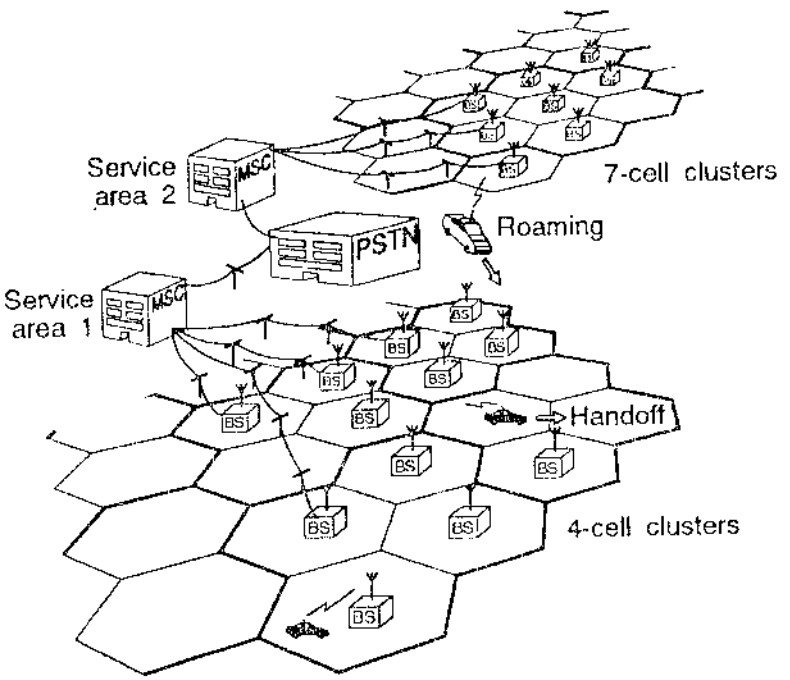
Service
area 2
MSC
7-cell clusters
PSTN
Roaming
Service
area 1
MSC
BS
Handoff
4-cell clusters

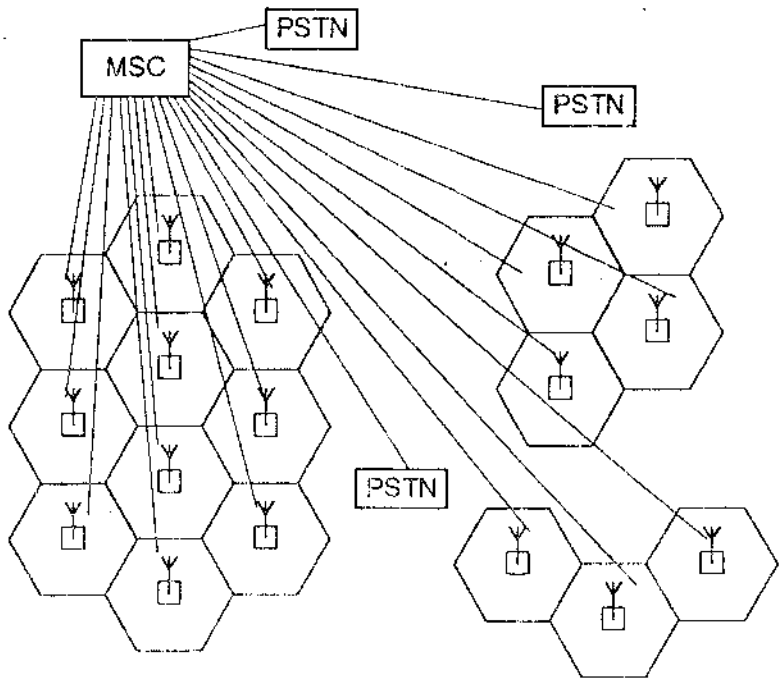

(a)

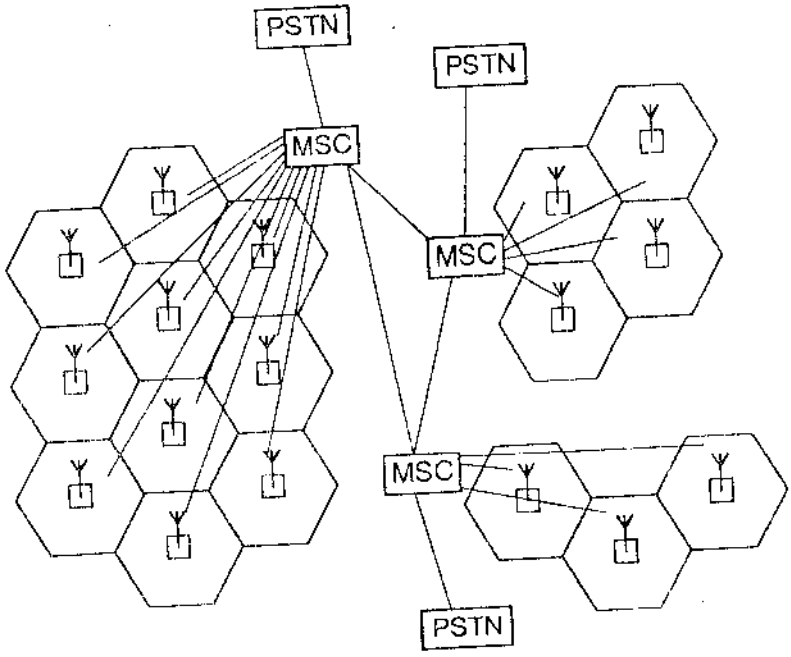

(b)

FIG. 1(b)

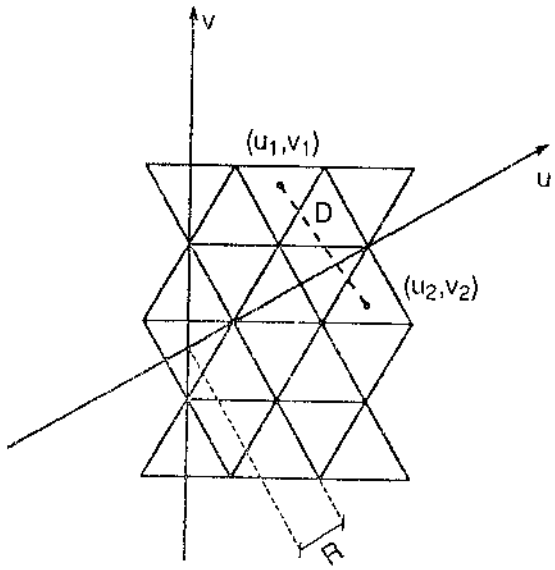
v
u
(u_1,v_1)
(u_2,v_2)
D
R

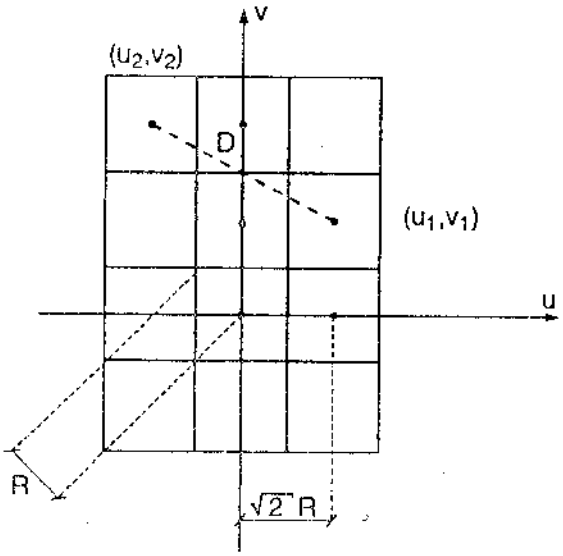
v
(u_2,v_2)
D
(u_1,v_1)
u
R
$\sqrt{2}$ R

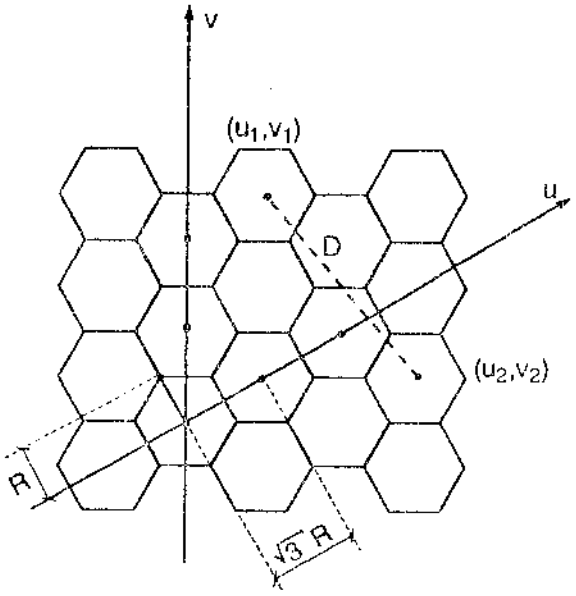
v
(u1,v1)
u
D
(u2,v2)
R
√3 R

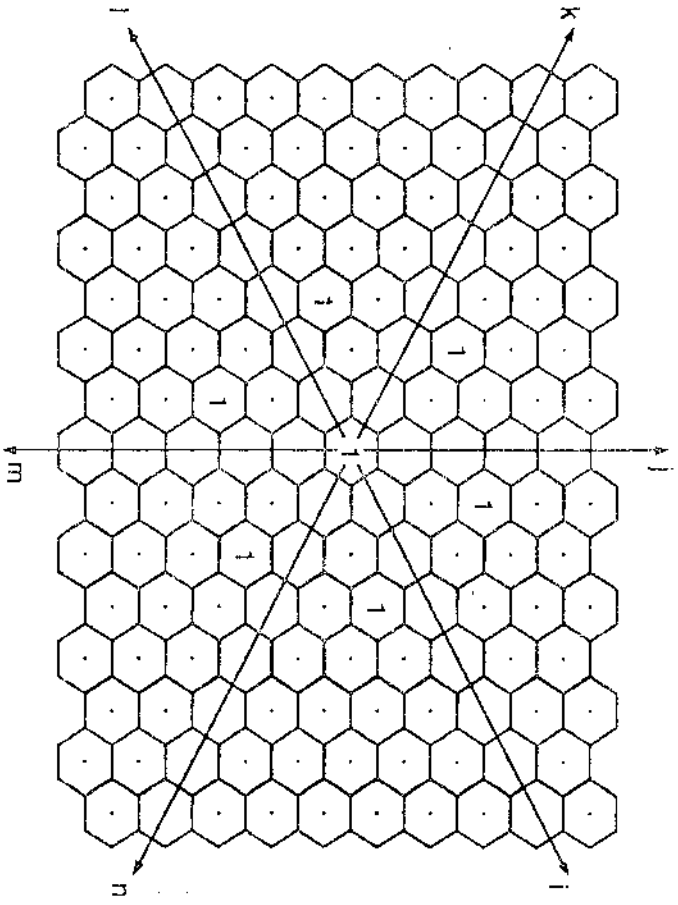

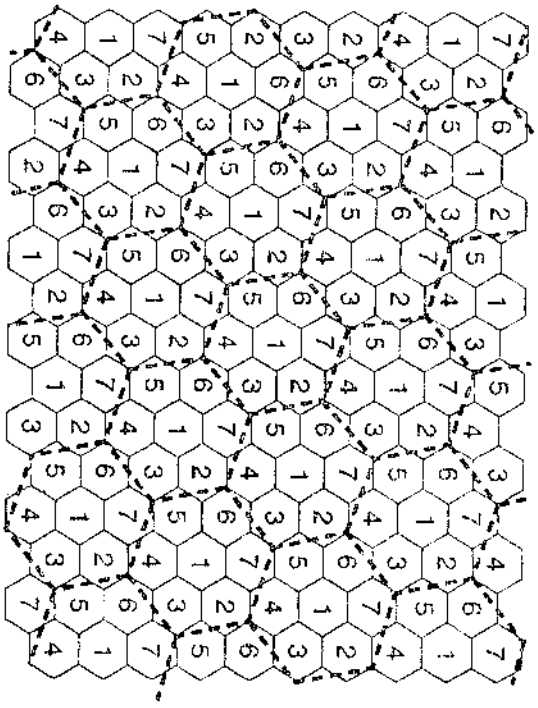

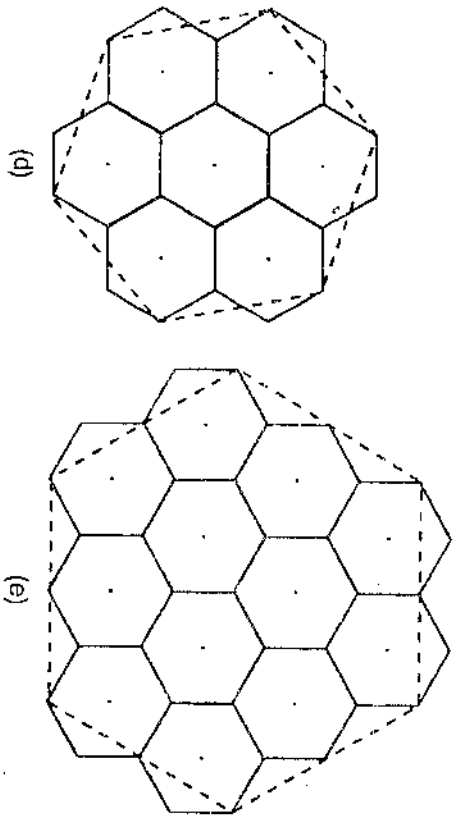

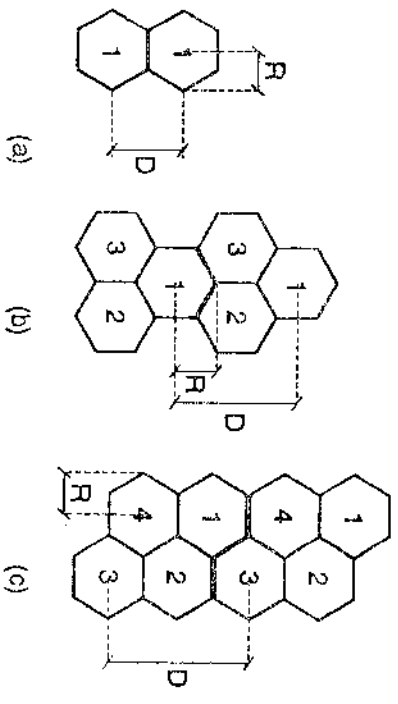

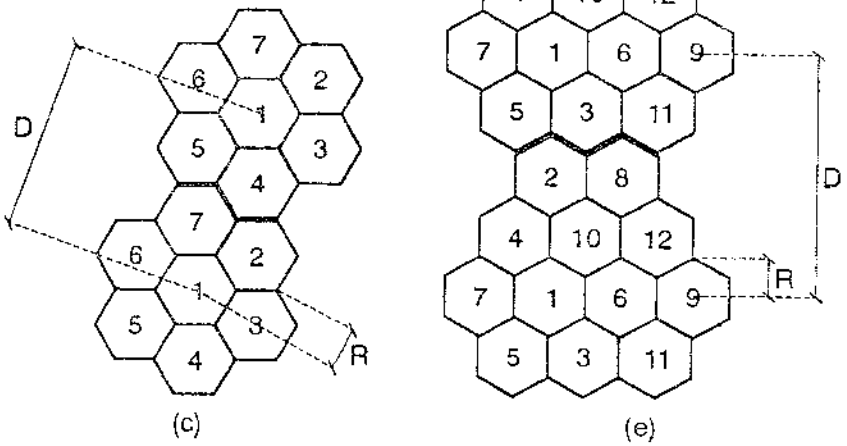

(c) (e)

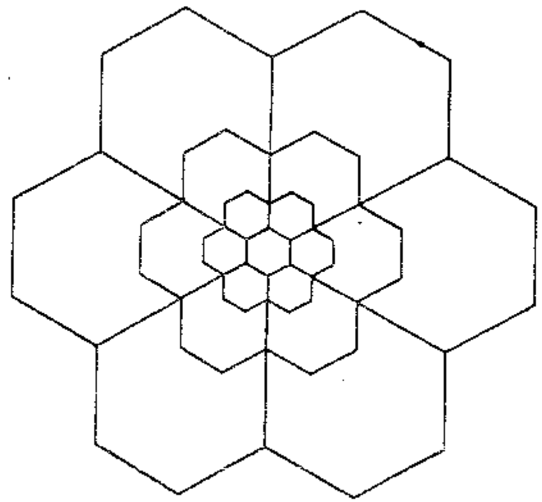

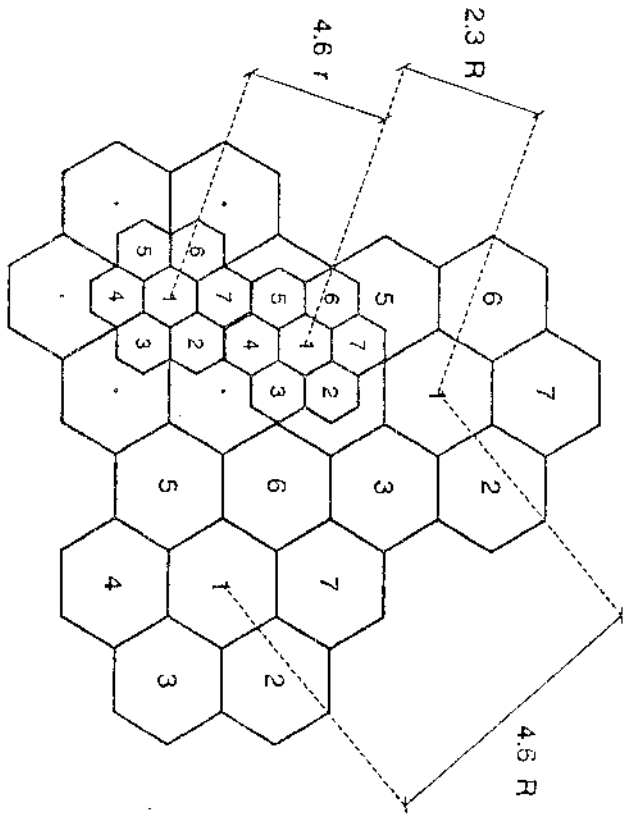

Fig 2-13 2005

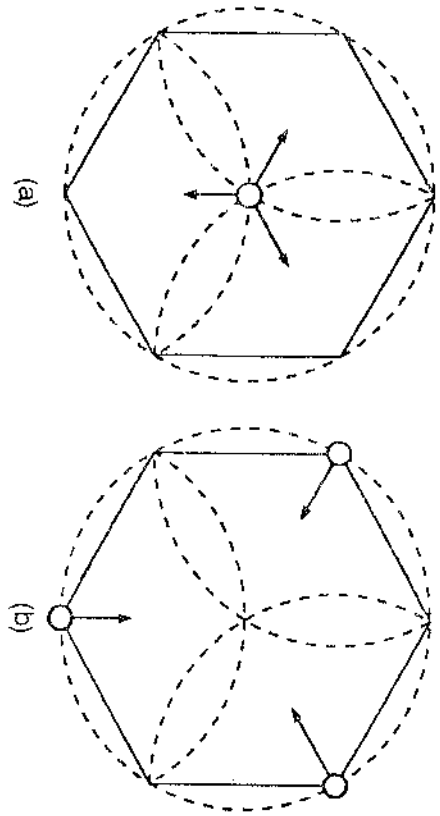

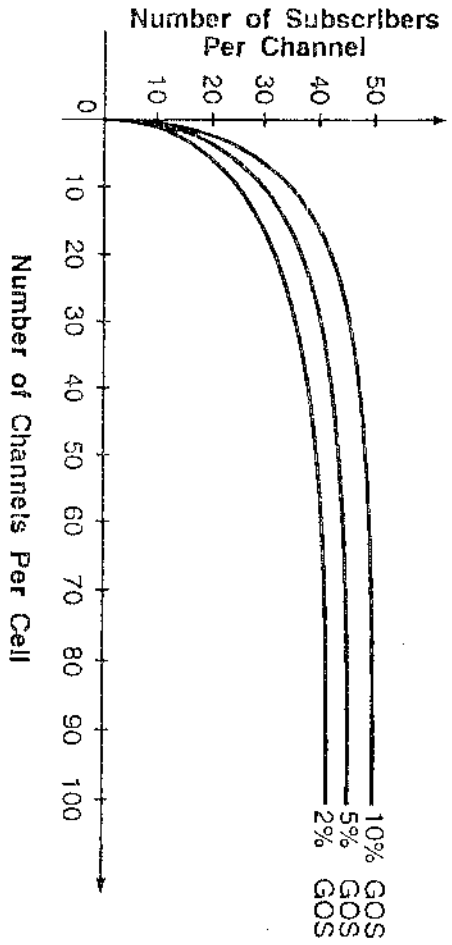

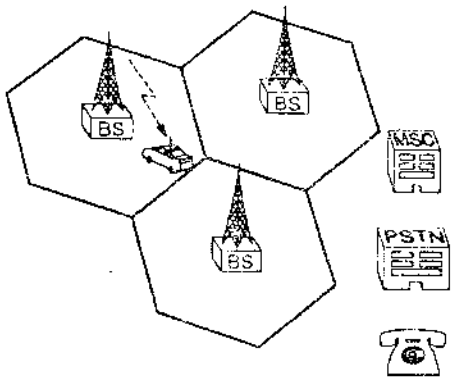

(a) Mobile wants to make a call

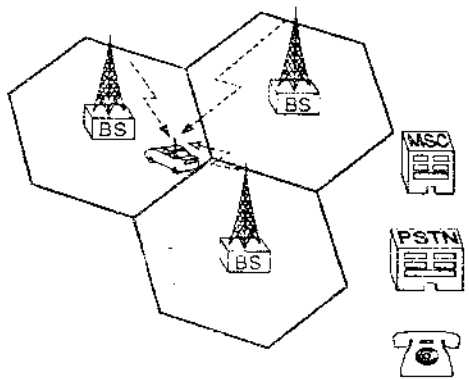

(b) Mobile selects base station

(c) MSC receives dialled digits

(d) MSC designates a voice channel

(e) PSTN receives dialled digits

(f) Conversation

(a) MSC receives dialled digits (b) Mobile is paged

(c) Mobile acknowledges paging

(d) MSC designates a voice channel

(e) Mobile receives alerting tone
Fixed receives ringing tone

(f) Conversation

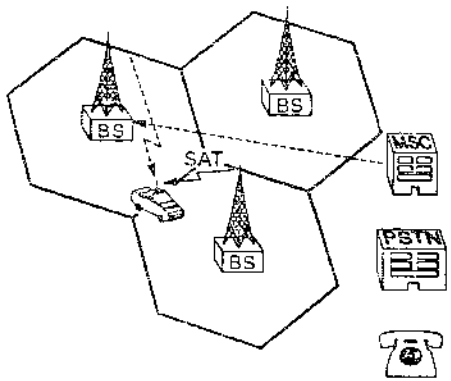

(c) Mobile is informed of the new channel

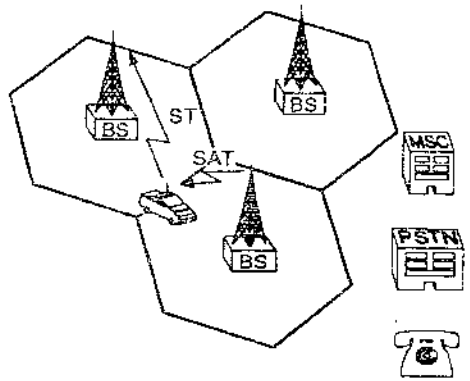

(d) Mobile releases former channel

(a) Transmission quality monitoring

(b) New channel on the air

(e) Conversation over new channel

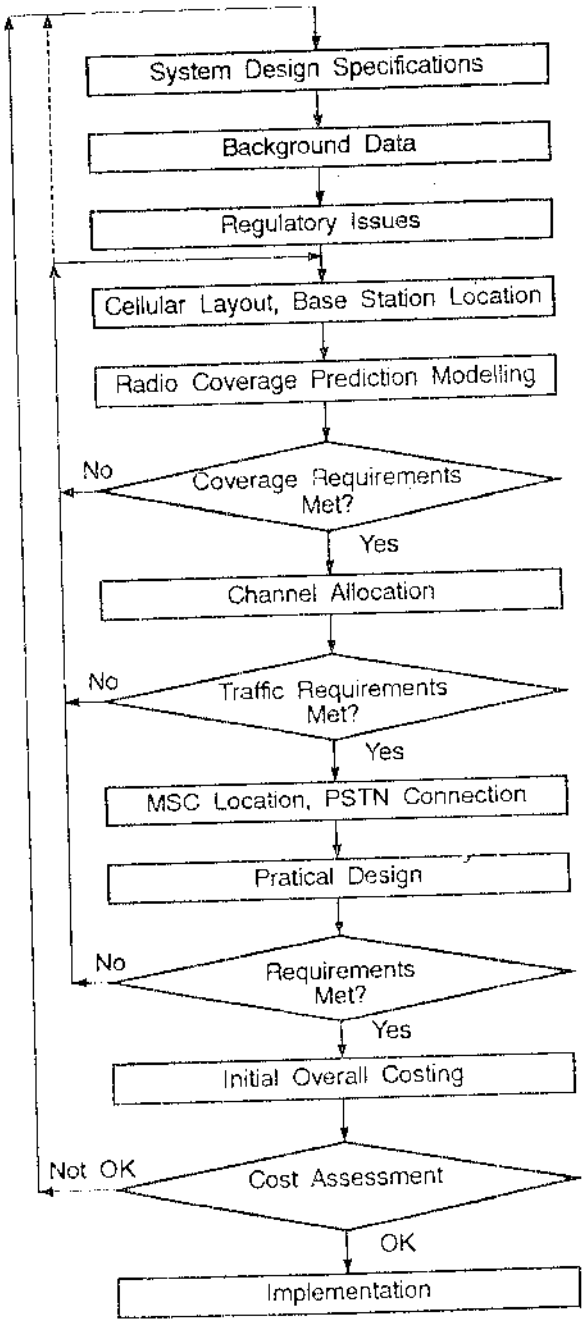

fig2-19 1508

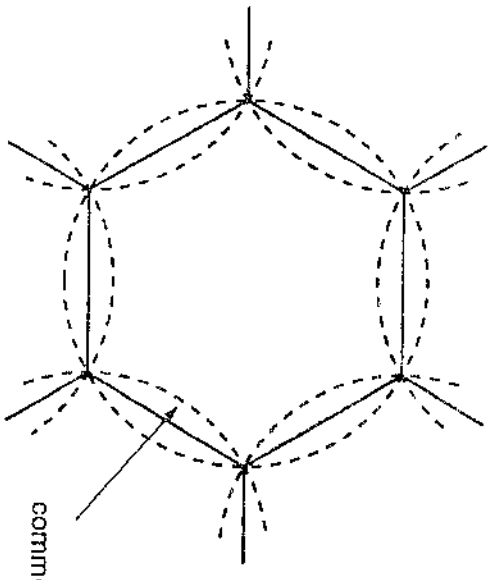

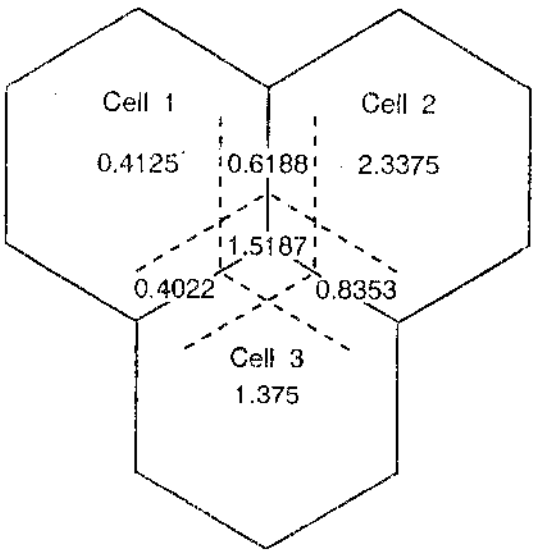
Cell 1
Cell 2
0.4125
0.6188
2.3375
1.5187
0.4022
0.8353
Cell 3
1.375

PART II

MOBILE RADIO CHANNEL

CHAPTER 3

MOBILE RADIO PROPAGATION MODEL

PREAMBLE

This chapter is concerned with the description of the models used to characterize the propagation phenomena in a mobile radio environment. It starts by reviewing some topics on the antenna's fundamentals with the aim at obtaining the Friis free space transmission formula. This formula constitutes the basis for the propagation path loss models presented next.

The propagation models can be divided into two groups, namely, theoretical models and empirical models. The theoretical models are usually described by means of closed form expressions, whereas the empirical ones are derived from field measurements, taken at different conditions. In the first case, many approximations are carried out, so that the models are not directly applicable to real situations. In the second case many parameters are taken into account, so that the models are usually very complex. A combination of these groups of models gives rise to a simplified prediction model with excellent results, if high accuracy is not required. The various parameters affecting the mobile radio propagation are also discussed and analyzed.

We then describe the stochastic behaviour of the mobile radio signal by means of its statistical distributions. By combining these statistics with some of the main results of the propagation path loss models, we determine the signal coverage area (base station service area). In the same way we determine the fuzzy boundaries between cells. It is shown that the proportion of overlapped areas between pair of cells or group of three cells is rather substantial.

3.1 INTRODUCTION

Communication with mobile points is a rather difficult task, and with today's technology, can only be achieved by means of radio waves. This transmission medium is greatly dependent on the environment. Accordingly, it can be affected by an "infinitude" of parameters describing such environment.

The mobile radio systems have been driven to use high radio frequencies due to the frequency congestion at the low part of the spectrum. Nevertheless, dealing with high frequencies usually leads to intricate problems. The theoretical analysis of the involved phenomena are, in general, very complex due to the number of variables that has to be taken into consideration. Many of these variables are simply neglected for low frequency applications. As an example, consider a radio transmission at 60 MHz, corresponding to a wavelength of 5m. If the sizes of the obstructions encountered by this radio frequency are equivalent over many wavelengths, these obstructions may work as scatterers. If we imagine a radio transmission at 900 MHz, obstructions with a size of only tens of centimetres can work as scatterers.

Due to multipath propagation the radio signal fades rapidly, with minima reaching more than 40 dB below the mean signal level. Fading also occurs due to shadowing provoked by hills, tunnels and other obstructions. Path loss, shadowing and rapid fading may deteriorate the propagated signal in such a way that, if the system is not carefully engineered, loss of communication may become quite often.

In addition to this, the mobile communication may also experience cochannel and adjacent channel interferences together with the various types of noise generated within to radio equipment and by the environment. The motion of the vehicle also imposes random variations in the signal, deteriorating even more the communication.

It can be seen that a deterministic solution for the variability and prediction of the mobile radio signal strength is rather impracticable. Instead, a statistical treatment of the signal can be used to describe the various phenomena.

3.2 ANTENNAS FUNDAMENTALS

In this section we shall briefly recall some of the basic concepts and formulas of the antenna theory. Our aim is to use this to arrive at the Friis free space transmission formula. For a thorough and rigorous approach refer to Kraus [7].

Basic Concepts

1) *Isotropic Source* : is a source radiating energy in all directions

2) *Poyting Vector (P) or Power Density* : is the electromagnetic power flow per unit area (watts/m^2).

3) *Radiated Power Crossing a Surface S (W)* : is defined by

$$W = \iint P \cdot ds = \iint Pds \tag{3.1}$$

where P is the radial component of $\mathbf{P}$ and ds is an infinitesimal area in S. An isotropic source radiates uniformly through a spherical surface. Consequently, W = $P4\pi d^2$, where d is the sphere's radius.

4) *Free Space Transmission Formula* : From the above definition we see that, in a lossless medium, the received power density P, at a distance d, is

$$P = \frac{W}{4\pi d^2} \tag{3.2}$$

5) *Radiation Intensity (U)*: is the power per unit solid angle. At a distance d

$$U = d^2P \tag{3.3}$$

For an isotropic source $U_o = d^2P = W/4\pi$.

6) *Radiation Pattern*: is the geographical distribution of the power radiated by the source. It is usually shown on both azimuthal (horizontal) and elevation (vertical) planes. An isotropic source's radiation pattern is a circle in both planes.

a real antenna, however, will more intensely illuminate one region (the target) than another. In the corresponding power pattern this is shown as the main lobe (for the target) and side lobes (otherwise). Antennas having a nearly circular azimuthal radiation pattern are known as omnidirectional. Antennas with directional properties are referred to as directional.

7) *Directivity* (D): is the ratio between the maximum radiation intensity (U_M) from the source under consideration and the radiation intensity from an isotropic source (U_o) radiating the same power

$$D = U_M/U_o \tag{3.4}$$

Accordingly, the directivity of an isotropic source is equal to 1. In the same way, a source with a hemisphere power pattern has directivity 2. The directivity can also be expressed as

$$D = \frac{\text{maximum radiation intensity}}{\text{average radiation intensity}} \tag{3.5}$$

The average radiation intensity is the total power averaged over the total solid angle 4π steel

$$D = \frac{U_M}{W/4\pi} = \frac{4\pi}{B} \tag{3.6}$$

where

$$B \triangleq W/U_M \tag{3.7}$$

is the beam area. Rigorously speaking, B is dimensionless, but it corresponds to the solid angle of the considered region. Consequently, it may be expressed without any unit or accompanied by square radian. Using (3.3) in (3.1) and then (3.1) in (3.7) we obtain

$$B = \frac{\iint \frac{U}{d^2}\, da}{U_M} \tag{3.8}$$

In spherical coordinates the infinitesimal area ds is found to be (see Figure 3.1)

$$ds = d^2 \sin\theta d\theta d\phi \tag{3.9}$$

Consequently, the beam area B is given by

$$B = \frac{\iint U d\Omega}{U_M} \tag{3.10}$$

where

$$d\Omega \triangleq \sin\theta d\theta d\phi \tag{3.11}$$

is the infinitesimal element of the solid angle Ω.

Suppose, as an example, that we want to calculate the directivity of a source having a conical radiation pattern as sketched in the Figure 3.2.

The total power W within the conical region is given by

$$W = \int_0^{2\pi} \int_0^{\theta} U_M \sin\theta' d\theta' d\phi = 2\pi(1 - \cos\theta)U_M$$

Consequently

$$D = \frac{4\pi}{2\pi(1 - \cos\theta)}$$

For a hemisphere $\theta = \pi/2$, such that $D = 2$. For a complete sphere (isotropic source) $\theta = \pi$, such that $D = 1$. For more complex geometries an approximate formula for the beam area can be used as follows [7]

$$B \simeq \Delta\theta\Delta\phi \tag{3.12}$$

where $\Delta\theta$ and $\Delta\phi$ are half power beamwidths, in radians.

As an example, consider an unidirectional cosine power pattern source U, such that $U = U_M \cos\theta$ (see Figure 3.3).

The total power W is given by

$$W = \int_0^{2\pi}\int_0^{\pi/2} U_M \cos\theta \sin\theta d\theta d\phi = \pi U_M$$

The directivity is, then $D = 4$. Using the approximate method, the half power is obtained when $\theta = \phi = \pi/3$. Consequently, $\Delta\theta = \Delta\phi = \pi/3 - (-\pi/3) = 2\pi/3$, and the approximate directivity is $D \approx 4\pi/(2\pi/3)^2 = 2.87$.

8) *Gain (G)*: gives a measure of the antenna's efficiency. Its is expressed in relation to a reference source. Usually the gain is referred to an isotropic source, such that

$$G \triangleq \frac{\text{maximum radiation intensity}}{\text{radiation Intensity from an isotropic source}} \qquad (3.13)$$

Let U_M' be the maximum radiation intensity of a real (lossy) antenna and U_M be this intensity for an ideal (lossless) 100% efficient antenna. Then $U_M' = \eta U_M$, where $0 \le \eta \le 1$ is the efficiency. Accordingly, using (3.13) and (3.4) we have

$$G = \frac{U_M'}{U_0} = \eta \frac{U_M}{U_0} = \eta D \qquad (3.14)$$

For a lossless isotropic source $G = D = 1$. In general, gain and directivity are given in dB, i.e., $10\log G$ and $10\log D$, respectively.

9) *Antenna Aperture* : A receiving antenna can be modelled as having a terminating and an intrinsic impedance. The terminating impedance corresponds to the load receiving the power delivered to the antenna. The intrinsic impedance is responsible for the losses, corresponding to the power dissipated by heat or reradiated by the antenna. The antenna aperture (given in m^2) is defined as the ratio between the power loss (watts) and the power density (watts/m^2) of the wave. The aperture may be interpreted as the virtual area of the antenna immersed in a electromagnetic field. Depending on the loss to be considered we may have different types of antenna's aperture as follows.

- *Effective Aperture*: is the ratio between the power delivered to the terminating impedance and the power density. The maximum effective aperture is known as Effective Area.

- *Loss Aperture*: is the ratio between the power dissipated as heat and the power density.
- *Scattering Aperture*: is the ratio between the power reflected back by the antenna and the power density.
- *Collecting Aperture*: is the sum of the above apertures.
- *Physical Aperture*: is the physical size of the antenna.

10) *Gain, Directivity and Aperture* : Gain, directivity and aperture are intrinsically related to each other. The relation between gain and directivity is expressed by (3.14). The common parameter between directivity and aperture is the power. In a receiving antenna the power extracted from the electromagnetic field increases with the increase of both directivity and effective area. Therefore,

$$D = KA \tag{3.15}$$

where K is a constant and A is the antenna's effective area. Accordingly, for two antennas having directivities D_i and D_j and effective areas A_i and A_j

$$\frac{D_i}{D_j} = \frac{A_i}{A_j} \tag{3.16}$$

Using (3.14) and (3.16) we have

$$\frac{\eta_j G_i}{\eta_i G_j} = \frac{D_i}{D_j} = \frac{A_i}{A_j} \tag{3.17}$$

where η_i, η_j and G_i, G_j are the efficiencies and gains of the antennas i and j, respectively.

These parameters have been determined for some antennas of interest and they are shown below [7].

- Isotropic antenna, $A = \lambda^2/4\pi$, $D = 1$
- Short dipole antenna, $A = 3\lambda^2/8\pi$, $D = 3/2$
- Dipole (linear half-wavelength), $A = 30/73\pi$, $D = 1.64$

Using (3.16) and any pair of A and D of the above antennas it is

straightforward to show that, for any antenna i,

$$A_i = \frac{\lambda^2}{4\pi} D_i \tag{3.18}$$

11) *Friis Free Space Transmission Formula* : Let W_t be the input power of a transmitting antenna having a gain G_t. The radiated power is $G_t W_t$ and the power density P at a distance d is

$$P = G_t W_t / 4\pi d^2 \tag{3.19}$$

The total power W_r received by the load at d is

$$W_r = A_r P = A_r G_t W_t / 4\pi d^2 \tag{3.20}$$

where A_r is the antenna's aperture. With (3.18) in (3.20) we obtain

$$\frac{W_r}{W_t} = G_t D_r \left(\frac{\lambda}{4\pi d}\right)^2$$

If the gain is equal to the directivity ($\eta = 1$) at the receiver, then

$$\frac{W_r}{W_t} = G_t G_r \left(\frac{\lambda}{4\pi d}\right)^2 \tag{3.21}$$

Equation (3.21) is known as the Friis free space transmission formula.

3.3 PROPAGATION PATH LOSS

A measure of great interest in the radio propagation studies is the Path Loss (l). This is defined as the ratio between the received power (W_r) and the transmitted power, such that

$$l \triangleq W_r / W_t \tag{3.22}$$

In dB it is given as

$$L = -10\log l = -10\log W_r + 10\log W_t$$

An exact estimate of the path loss in a mobile radio environment is not available. In the next sub-sections we shall consider some theoretical models applicable to very special cases. Then we modify these models to give an approximate measure of the path loss in the mobile environment. Finally, we describe the various empirical methods and their applicability.

3.3.1 Free-Space Path Loss

The ratio between the received and transmitted powers in a free-space propagation condition is given by the Friis free-space transmission formula. Hence

$$\frac{W_r}{W_t} = G_t G_r \left(\frac{\lambda}{4\pi d}\right)^2 \tag{3.23}$$

Accordingly, the path loss (in dB) is

$$L = -10\log G_t - 10\log G_r - 20\log\lambda + 20\log d + 21.98$$

Using lossless and isotropic antennas ($G_t = G_r = 1$), with the frequency in MHz and the distance in km we have

$$L = 20\log f + 20\log d + 32.44 \text{ dB} \tag{3.24}$$

3.3.2 Plane Earth Path Loss

Consider the propagation of a radiowave in a flat terrain environment. The transmitted signal may reach the receiving antenna by several ways:

- through a direct path;
- through an indirect path, consisting of the radiowave reflected by the ground;
- through an indirect path, consisting of surface wave;
- through other secondary means.

The received signal is a combination of all of the above described waves with a resultant power equal to the sum of their individual powers. The signal power due to the direct path is given by the Friis free-space formula. The reflected wave will

have a power given by the Friis formula but attenuated by a factor equal to the ground reflection coefficient ρ. Moreover, the reflected signal will be shifted by a phase $\Delta\varphi$ due to the indirect path. The ground wave is provoked by the signal that has been absorbed by the ground. The proportion of the absorbed signal is given by $(1 - \rho)$, corresponding to the non-reflected signal times an attenuation factor A. Therefore, the ratio between the received and transmitted powers in a flat terrain environment is

$$\frac{W_r}{W_t} = G_t G_r \left(\frac{\lambda}{4\pi d}\right)^2 \left|1 + \rho e^{j\Delta\varphi} + (1 - \rho)Ae^{j\Delta\varphi} + \ldots\right|^2 \qquad (3.25)$$

Both ρ and A depend on various factors such as incidence angle, polarization, earth constants and frequency. In particular

$$\rho = \frac{\sin\theta - K}{\sin\theta + K} \qquad (3.26)$$

where θ is the incidence angle and K varies with all of the parameters above mentioned . For a grazing angle $\theta \approx 0^\circ$ (corresponding to the case where the distance between base station and mobile is much greater than the antenna height) then $\rho \approx -1$ (see (3.26)). Moreover, ρ tends to -1 for frequencies above 100 MHz and incidence angles less than 10° [2]. The effects of the ground waves are sensed only a few wavelengths above the ground. Therefore, they can be neglected for the case of mobile radio using microwave frequencies. Consequently, (3.25) is reduced to

$$\frac{W_r}{W_t} \approx G_t G_r \left(\frac{\lambda}{4\pi d}\right)^2 \left|1 - e^{j\Delta\varphi}\right|^2 \qquad (3.27)$$

Consider transmitting and receiving antennas of heights h_t and h_r, respectively, separated by a distance d, as shown in Figure 3.4.

If the time delay between the direct and indirect waves is Δt, then the phase shift $\Delta\varphi$ is given by $\Delta\varphi = 2\pi f\Delta t$, where f is the signal frequency. Therefore,

$$\Delta\varphi = 2\pi\frac{\Delta d}{\lambda} \qquad (3.28)$$

where

$$\Delta d = (l_1 + l_2) - (d_1 + d_2) \tag{3.29}$$

is the difference between the indirect and direct paths. The distance difference Δd can be easily written as a function of h_t, h_r and d. Then

$$\Delta\varphi = \frac{2\pi d}{\lambda}\left\{\left[\left(\frac{h_t + h_r}{d}\right)^2 + 1\right]^{1/2} - \left[\left(\frac{h_t - h_r}{d}\right)^2 + 1\right]^{1/2}\right\} \tag{3.30}$$

Using the approximation $(1 + x)^{1/2} \simeq 1 + x/2$, for small x, from (3.30) we obtain

$$\Delta\varphi \simeq 4\pi\frac{h_t h_r}{\lambda d} \tag{3.31}$$

The squared modulus in (3.27) can be expanded as

$$\left|1 - e^{j\Delta\varphi}\right|^2 = 2(1 - \cos\Delta\varphi) = 4\sin^2\frac{\Delta\varphi}{2} \tag{3.32}$$

For small $\Delta\varphi$, $\sin\frac{\Delta\varphi}{2} \simeq \frac{\Delta\varphi}{2}$. Then

$$\sin^2\frac{\Delta\varphi}{2} \simeq \left(\frac{\Delta\varphi}{2}\right)^2 \tag{3.33}$$

With the appropriate use of equations (3.33), (3.32), (3.31) and (3.27) we finally obtain

$$\frac{W_r}{W_t} = G_t G_r\left(\frac{h_t h_r}{d^2}\right)^2 \tag{3.34}$$

This is the inverse fourth power loss formula. The corresponding path loss in dB is

$$L = -10\log G_t - 10\log G_r - 20\log(h_t h_r) + 40\log d \tag{3.35}$$

Note that there is a loss of 12 dB when the distance is doubled. On the other hand, there is a gain of 6 dB when the antenna height is doubled.*

* Field measurement have shown that this is only true for the base station's antenna. For the mobile's antenna the gain is only 3dB, if $h_r < 3$ m or 6 dB if $3\text{m} \leq h_r \leq 10\text{m}$ (refer to section 3.3.6 for the Okumura Model)

The flat terrain model can be applied to an environment considered to be smooth. The measure of the terrain smoothness, S, depends on various parameters, including the frequency. One of such measure is given by the Rayleigh criterion as follows [2]

$$S = \frac{4\pi\sigma\theta}{\lambda} \tag{3.36}$$

where σ is the standard deviation of the irregularities' mean heights, θ is the incidence angle and λ is the wavelength. A surface with $S < 0.1$ is considered to be smooth, while with $S > 10$ is considered as rough.

3.3.3 Knife Edge Diffraction Loss

A radio wave radiated from a transmitting antenna can be intercepted by obstructions such as hills, buildings, trees and others. In this case the signal reaching the receiving antenna will arrive as a diffracted ray as shown in Figure 3.5. If the radiated electric field strength is E_0, the diffracted field E is [2]

$$E = E_0 F e^{j\Delta\varphi} \tag{3.37}$$

where F is the diffraction coefficient and $\Delta\varphi$ is the phase difference between the indirect and direct paths. These parameters are given by [2,3]

$$F = \frac{S(x) + 0.5}{\sqrt{2}\,\sin(\Delta\varphi + \pi/4)} \tag{3.38}$$

and

$$\Delta\varphi = \tan^{-1}\left[\frac{S(x) + 0.5}{C(x) + 0.5}\right] - \frac{\pi}{4} \tag{3.39}$$

where C(x) and S(x) are respectively the Fresnel cosine and sine integrals

$$C(x) = \int_0^x \cos\left(\frac{\pi}{2}u^2\right) du \tag{3.40}$$

$$S(x) = \int_0^x \sin\left(\frac{\pi}{2}u^2\right)du \tag{3.41}$$

and

$$x = -h\sqrt{\frac{2}{\lambda}\left(\frac{d_1 + d_2}{d_1 d_2}\right)} \tag{3.42}$$

Note that the height h can also be negative as shown in Figure 3.6. In such case there will be a direct path between the two antennas. From (3.37) the loss due to the diffraction is

$$L = 10\log|E/E_0|^2 = 20\log F \tag{3.43}$$

The Fresnel integrals can be evaluated by means of series expansion as follows

$$S(x) = \sqrt{\frac{2}{\pi}} \sum_{n=0}^{\infty} (-1)^{n+2} \frac{\left(\sqrt{\pi/2}\ x\right)^{3+4n}}{(1 + 2n)!\ (3 + 4n)} \tag{3.44}$$

$$C(x) = \sqrt{\frac{2}{\pi}} \sum_{n=0}^{\infty} (-1)^{n+2} \frac{\left(\sqrt{\pi/2}\ x\right)^{1+4n}}{(2n)!\ (1 + 4n)} \tag{3.45}$$

It is interesting to note that $S(-x) = -S(x)$ and $C(-x) = -C(x)$. Moreover, $S(\infty) = C(\infty) = 0.5$ and $S(0) = C(0) = 0$. Consequently,

$$\lim_{x\to\infty} F = 1, \quad \lim_{x\to-\infty} F = 0 \text{ and } F = 0.5 \text{ when } x = 0$$

A sketch of diffraction loss is shown in Figure 3.7.

Equation (3.42) can be written as $x = -hK$, where K is a non-negative constant. A positive height (+h) implies a negative x corresponding to the situation as in Figure 3.5. In this case the receiving antenna is in a shadowed region and the loss curve is that of the left semi-plane of the Figure 3.7. The greater the height the larger the loss. On the other hand, a negative height implies a positive x corresponding to the situation as in Figure 3.6. In this case the receiving antenna is in the illuminated region. If the obstruction is just "touching" the direct path

(x = h = 0), the received electric field will have half of the magnitude of the transmitted field. In other words, the received power is one fourth (0.5^2) of the transmitted power.

3.3.4 Multiple Knife Edge Diffraction Loss

In a real situation a radiated wave may be diffracted not only by one obstruction but by several ones. A mathematical approach to deal with this situation is rather complicated and no simple solution is available. There are some approximate methods as we shall examine next.

a) *Bullington's Model*

This model was primarily developed to tackle the two-obstruction path loss case. Consequently, the results are better for this situation. As the number of obstructions increases the model gives a poorer performance due to the over simplification. The aim of the model is to reduce an n-dimensional problem to one dimension by replacing the n obstructions by one equivalent knife edge. This corresponds to find an equivalent height producing the same effects as those produced by all of the other knife edges together. This method is illustrated in Figure 3.8. Note that some obstructions are ignored.

b) *Epstein - Peterson's Model*

This model considers each knife edge individually and approximates the total loss as the sum of the individual losses, as shown in Figure 3.9.

The first loss is calculated by considering the path "transmitter, first obstruction, second obstruction". The other loss considers the subsequent path constituted by "first obstruction, second obstruction, receiver". If the obstructions are very close to each other some of the heights (at least one) will not be correctly determined. In this case this method gives poor results.

c) *Deygout's Model*

This model initially estimates a path loss by considering the dominant

obstruction in the environment. The other losses due to the remaining knife edges are determined with respect to this dominant edge, as shown in the Figure 3.10.

3.3.5 Path Clearance Conditions

As we have seen, the path loss depends on several parameters including antennas' heights, distances between the antennas, frequency and others. For a given set of these parameters we may estimate the proportion of the path loss caused by the diffracted waves as well as by the reflected waves. Consider the situation depicted in Figure 3.11.

If the height h is sufficiently large, the received wave will not be affected by the diffracted waves. However, the indirect path may be long enough to provoke a phase difference between the direct and indirect signals so that the resultant signal can be substantially deteriorated. In this case the path loss is dominated by the reflected signal. On the other hand, if the height h is sufficiently small, there will not be much difference between the direct and indirect paths. Accordingly, the phase shift in the indirect wave will be small. However, the effects of the knife edge can be significant. In this case the path loss is dominated by the diffracted waves. We shall investigate these two situations.

Loss Due to Reflection/Refraction

From Figure 3.7 we understand that the condition $x > 0$ corresponds to have the receiving antenna in the illuminated region. Moreover, a careful look at this figure (or equivalently, at the equations (3.38) and (3.39)) shows that, for $x > \sqrt{2}$ the diffraction coefficient F (diffraction loss) tends to unity. In other words, for $x > \sqrt{2}$ the diffraction loss tends to be negligible. Therefore, using (3.42) and the constraint $x > \sqrt{2}$ we have*

$$h \sqrt{\frac{2}{\lambda}\left(\frac{d_1 + d_2}{d_1 d_2}\right)} > \sqrt{2}$$

* Note that in Figure 3.11 the height h corresponds to -h in Figure 3.6.

Therefore,

$$h > \sqrt{\lambda\left(\frac{d_1 d_2}{d_1 + d_2}\right)} \tag{3.46}$$

The condition $x > \sqrt{2}$ corresponds to $\Delta\varphi > \pi/2$. Accordingly, we can say that when $\Delta\varphi > \pi/2$ the indirect wave is not substantially affected by diffraction. We may express (3.46) in terms of d, h_t and h_r by using the simple geometric relations obtained from Figure 3.11. Then,

$$d < 4\, h_t h_r/\lambda \tag{3.47}$$

Hence, if (3.46) (or equivalently (3.47)) is satisfied, then the loss is mainly due to the reflected wave. Otherwise, the loss is due to the diffracted wave.

Avoiding Nulls at the Reception

At the receiver a null will occur if the direct and indirect waves arrive with equal amplitudes and opposite phases. Both the power of the resultant signal as well as the phase shift of the reflected wave have been determined in section 3.3.2. From (3.27) we see that a null will occur if $\left|1 - e^{j\Delta\varphi}\right|^2 = 0$. Equivalently, using (3.32) the null will occur if $4\sin^2(\Delta\varphi/2) = 0$, resulting in $\Delta\varphi = 2n\pi$ where n is an integer. Accordingly, with $\Delta\varphi = 2n\pi$ in (3.31) we obtain,

$$d = \frac{2h_t h_r}{n\lambda}$$

Note that in the above equation the distance d decreases with the increase of n (maximum obtained when n = 1). Therefore, we conclude that for distances

$$d > \frac{2h_t h_r}{\lambda} \tag{3.48}$$

nulls will not occur any longer. Expressing (3.48) in terms of h, d_1 and d_2 (refer to Figure 3.4) we obtain

$$h < \sqrt{2\lambda\left(\frac{d_1 d_2}{d_1 + d_2}\right)} \tag{3.49}$$

3.3.6 Prediction Models

The field strength prediction models are usually based on some of the above described path loss models, modified by parameters obtained in the field measurements. The models take into account the information about the topography of the terrain including the orography (description of the hills) and the category of the land usage (built-up area, forest, open area or water). The degree of the terrain undulation is given by the parameter known as "interdecile range" (Δh), measured at a distance of 10 km, as illustrated in Figure 3.12.

Some estimates of Δh according to the terrain topography are shown in the diagram of Figure 3.13 [2].

The prediction algorithms usually deal with a significant amount of data, requiring a computer to process these data. The choice of the model will mainly depend on what is required: a rough estimate or a precise prediction. Moreover, the availability of data plays an important role in this. Accordingly, the algorithms can be chosen within the range from a trivial equation to a very sophisticated (and expensive) software. After the prediction estimates, field measurements must be carried out in order to validate the model. This step will probably require the parameters to be readjusted. In this section we chose to describe some of the main prediction models. A thorough survey on these models would probably require a separate book .

1) *Egli Method*

This method is mainly based on the fourth power loss (plane earth path loss). It uses some perturbation factors such as frequency, antenna height and polarization to improve the results. It predicts the field strength at distances up to 60 km with a frequency range of 40-900 MHz. The median transmission loss for a 1.5 m high mobile antenna is estimated as

$$L = 139.1 - 20 \log h_t + 40 \log d \qquad (3.50)$$

In (3.50) d is the distance between transmitting and receiving antennas and h_t is

the base station antenna height, given in m and km respectively.

2) *Blomquist - Ladell Method*

This method considers the free space loss (L_0), plane earth loss (L_p) and knife edge loss (L_k) combined to give the total loss (L) as follows

$$L = L_0 + \text{Max}(L_p, L_k) \tag{3.51a}$$

or

$$L = L_0 + \sqrt{L_p^2 + L_k^2} \tag{3.51b}$$

Equation (3.51b) seems to give better results, but lacks theoretical justification. The model applies to frequencies within the range 30-900 MHz and distances between 5-22 km.

3) *Longley - Rice Method*

This method predicts the attenuation relative to the free space loss. It requires parameters such as frequency, heights of the transmitting and receiving antennas, distance between antennas, mean surface refractivity, earth's conductivity, earth's dielectric constant, polarization and description of the terrain. This is a computer based algorithm working in the following ranges

20 MHz≤ Frequency ≤ 40 GHz

0.5 m ≤ Antenna height ≤ 3 km

1 km ≤ Distance ≤ 2000 km

One of the interesting outcomes of the Longley-Rice's work is that the degree of the terrain undulation was found as a function of the distance as follows

$$\Delta h' = \Delta h\left[1 - \exp(-0.02\ d)\right] \tag{3.52}$$

where $\Delta h'$ and Δh are given in metres and d in km. Note that $\Delta h' = \Delta h$ for $d = 0$. Hence, if the profile of the terrain is known, the interdecile range can be more accurately estimated.

4) *Okumura Method*

This model is based on field measurements taken in the Tokyo area. It provides an initial path loss estimate for a quasi-smooth terrain ($\Delta h \approx 20$ m). Then some correction factors must be used to adapt these results to other conditions. This initial estimate comprises a set of curves "Attenuation, A(f,d), versus Frequency, f," for a base station antenna height h_t of 200 m and a mobile station antenna height of 3 m having the distance d as a parameter, as shown in Figure 3.14. These prediction curves are relative to the free space loss. The correction factor G_{area} (gain) for the type of terrain is also given as a function of the frequency, as depicted in Figure 3.15. For different antenna heights the correction factors (gain) are as follows

Gain $G(h_t)$ of 6 dB per octave for base station antenna height, i.e., of

$$G(h_t) = 20\log(h_t/200), \qquad h_t > 10 \text{ m}.$$

Gain $G(h_r)$ of 3 dB or 6 dB per octave for mobile station antenna height depending on the range, i.e.,

$$G(h_r) = 10\log(h_r/3), \qquad h_r < 3\text{m}$$

$$G(h) = 20\log(h_r/3), \qquad 3\text{m} \le h_r \le 10 \text{ m}$$

The procedure to estimate the resultant path loss is the following:

a) Given the distance d and frequency f find the attenuation A(f,d) using the curves of Figure 3.14.

b) According to the type of the terrain, for the same frequency, find the correction factor G_{area} subtracting it from A(f,d) obtained in (a).

c) Determine the correction factors $G(h_t)$ and $G(h_r)$ according to the antennas' heights h_t and h_r, subtracting them from the result in (b).

d) The loss obtained in (c) is added to the free space path loss (L_0) to obtain the overall loss.

Therefore, the overall loss is given by

$$L = L_0 + A(f,d) - G_{area} - G(h_t) - G(h_r) \qquad (3.53)$$

5) *Hata's Formula*

The Okumura method cannot be easily automated, since it involves various curves. An empirical formula based on Okumura's results has been developed by Hata [32]. It gives predictions almost indistinguishable from those given by Okumura's method over the limited range for which it applies. The loss L is

$$L = 69.55 + 26.16\log f - 13.82\log h_t - A(h_r) + (44.9 - 6.55\log h_t)\log d \text{ dB} \quad (3.54a)$$

where $150 \text{ MHz} \le f \le 1500 \text{ MHz}$

$30 \text{ m} \le h_t \le 300 \text{ m}$

$1 \text{ km} \le d \le 20 \text{ km}$

The correction factor $A(h_r)$ is computed as follows.

For small or medium size city

$$A(h_r) = (1.1\log f - 0.7)h_r - (1.56\log f - 0.8) \text{ dB} \quad (3.54b)$$

where $1\text{m} \le h_r \le 10 \text{ m}$

For a large city

$$A(h_r) = 8.29\log^2(1.54h_r) - 1.1 \text{ dB} \qquad (f \le 200 \text{ MHz}) \quad (3.54c)$$

and

$$A(h_r) = 3.2\log^2(11.75h_r) - 4.97 \text{ dB} \qquad (f \le 400 \text{ MHz}) \quad (3.54d)$$

6) *Ibrahim - Parsons Method*

This method was designed for path loss in the city of London. It proposes an empirical model based on the data collected by measurements and also a semi-empirical model based on the plane earth equation. In the first case an equation is developed to fit the collected data. In the second case the fourth power path loss equation is multiplied by a clutter factor varying with the land usage [8, 15,16].

3.3.7 A Simplified Path Loss Model

Field measurements have shown that, with appropriate correction factors, the

plane earth path loss formula can be used to predict the field strength. In this section we shall use some of the results obtained from the prediction models to modify the plane earth loss formula in order to introduce a simplified path loss model. For convenience we rewrite (3.34) as follows.

$$\frac{W_r}{W_t} = G_t G_r \left(\frac{h_t h_r}{d^2} \right)^2 \tag{3.55}$$

The Okumura's method showed that there is a gain of 6 dB per octave for the base station antenna height. In order words the factor h_t^2 in (3.55) is correct. As far as the mobile station antenna is concerned this gain varies from 3 dB to 6 dB. Accordingly, the loss is proportional to h_r^x, where $x = 1$ or $x = 2$, as follows

$$\frac{W_r}{W_t} \approx h_r^x \quad , \quad \begin{array}{lll} x = 1 & \text{for} & h_r < 3\text{m} \\ x = 2 & \text{for} & 3\text{m} \le h_r \le 10\ \text{m} \end{array}$$

The loss with the distance d varies with $d^{-\alpha}$, where $3 \le \alpha \le 4$. The parameter α depends on the topography of the terrain. Then

$$\frac{W_r}{W_t} \approx \frac{1}{d^\alpha} \quad , \quad 2 \le \alpha \le 4$$

The main limitation of (3.55) is that it suggests an independence between path loss and frequency. From the Okumura's method it was shown that

$$\frac{W_r}{W_t} \approx \frac{1}{f^y} \quad , \quad 2 \le y \le 3$$

The parameter y depends on both the environment and the frequency itself. It was found to be equal to 2 by Young [17] and equal to 3 by Okumura, but in different conditions.

With all of the above considerations we may rewrite (3.55) as

$$\frac{W_r}{W_t} = K \frac{G_t G_r h_t^2 h_r^x}{d^\alpha f^y} \tag{3.56}$$

where K is a constant for a given environment, and

$3 \leq \alpha \leq 4$

$2 \leq y \leq 3$

$x = 1$ for $h_r < 3m$

$x = 2$ for $3m \leq h_r \leq 10\ m$

In particular $y \propto 2$ both in a suburban area and in an open area with $f < 450$ MHz, and $y \propto 3$ in urban area with $f > 450$ MHz. For any given environment (3.56) can be used to predict the path loss if a high accuracy is not required. However, it is mainly used for comparative purposes as we shall see. Consider, that, for a given situation, the parameters in (3.56) assume the values G_{tI}, G_{rI}, h_{tI}, h_{rI}, d_I and f_I. Therefore, the received power W_{rI}, given that the power W_{tI} has been transmitted, is

$$W_{rI} = K \frac{W_{tI} G_{tI} G_{rI} h_t^2 h_{rI}^x}{d_I^\alpha f_I^y} \tag{3.57}$$

If, for the same environment, these parameters are G_{tJ}, G_{rJ}, h_{tJ}, h_{rJ}, d_{rJ} and f_J, then the ratio between the received powers W_{rJ} and W_{rI} is

$$\frac{W_{rJ}}{W_{rI}} = \left(\frac{d_J}{d_I}\right)^{-\alpha} \beta_J \tag{3.58}$$

where

$$\beta_J = \frac{W_{tJ} G_{tJ} G_{rJ}}{W_{tI} G_{tI} G_{rI}} \left(\frac{h_{tJ}}{h_{tI}}\right)^2 \left(\frac{h_{rJ}}{h_{rI}}\right)^x \left(\frac{f_J}{f_I}\right)^{-y} \tag{3.59}$$

Suppose that the transmitted power, antenna gains, antenna's heights and frequencies are kept in both situations. In this case $\beta_J = 1$ and the ratio between the received powers is given by

$$\frac{W_{rJ}}{W_{rI}} = \left(\frac{d_J}{d_I}\right)^{-\alpha} \tag{3.60a}$$

Expressed in dB

$$10\log\left(\frac{W_{rj}}{W_{ri}}\right) = -\alpha 10\log\left(\frac{d_j}{d_i}\right) \tag{3.60b}$$

Note that the curve $10\log(W_{rj}/W_{ri})$ versus $10\log(d_j/d_i)$ is a straight line with slope $-\alpha$. Accordingly, the parameter α is known as path loss slope. For free space condition the path loss slope is $\alpha = 2$ and for conductive terrain this is $\alpha = 4$. A graph sketching the path loss curve is shown in Figure 3.16.

Consider that the mobile travels through regions with different path loss slopes as shown in Figure 3.17. It is easily seen that

$$\frac{W_{r1}}{W_{r0}} = \left(\frac{d_1}{d_0}\right)^{-\alpha_1}$$

$$\frac{W_{r2}}{W_{r1}} = \left(\frac{d_2}{d_1}\right)^{-\alpha_2}$$

$$\vdots$$

$$\frac{W_{rn}}{W_{rn-1}} = \left(\frac{d_n}{d_{n-1}}\right)^{-\alpha_n}$$

Then

$$\frac{W_{rn}}{W_{r0}} = \prod_{i=1}^{n}\left(\frac{d_i}{d_{i-1}}\right)^{-\alpha_i} \tag{3.61a}$$

Equation (3.61a) can be rewritten as

$$\frac{W_{rn}}{W_{r0}} = \left(\frac{d_n}{d_0}\right)^{-\alpha_1} C_1 \tag{3.61b}$$

where

$$C_1 = d_1^{-\alpha_1} d_n^{\alpha_1} \prod_{i=2}^{n}\left(\frac{d_i}{d_{i-1}}\right)^{-\alpha_i}$$

The constant C_1 may be seen as a correction factor due to the various parameters affecting the radio propagation (foliage, street orientation, sloping terrain and others). If the mobile remains within the same environment where the path

loss is equal to α_1, then $C_1 = 1$.

3.3.8 Considerations on Other Effects

Several other factors affect the radio propagation conditions. We shall comment on some of these factors.

1) *Atmospheric Conditions*

The moisture in the atmosphere attenuates the radio signal, depending on the radio frequency. Above 10 GHz the loss due to the rain is already considerable. There is a peak of absorption due to water vapour at 24 GHz and due to oxygen at 60 GHz [2].

2) *Foliage*

Trees work as obstructions diffracting, reflecting and absorbing the radio signal. In urban areas, where there is a small concentration of trees, the effects are negligible. The estimates of the attenuation due to trees is rather complex since there is a considerable amount of involved variables. Attenuation may vary with height, shape, density, season, humidity, etc. The loss is negligible at low frequencies (low VHF) but substantial at higher frequencies (UHF). Moreover, the loss varies with the field polarization as shown by (3.61), for vertical polarization, and (3.62) for horizontal polarization [33].

$$L = 1637\sigma + \frac{\exp(-90/f)\log(1 + f/10)}{2.99} \text{ dB/m} \qquad (3.62a)$$

and

$$L = 1637\sigma + \frac{\exp(-210/f)\log(1 + f/200)}{2.34} \text{ dB/m} \qquad (3.62b)$$

where σ is the conductivity (Siemens/m) and f is the frequency (MHz). Some values of σ are given in Table 3.1 [33].

Table 3.1 - Conductivity of various types of foliages (after Camwell [33]).

Foliage	σ (x 10^{-5}) Dry	σ (x 10^{-5}) Wet
Bare tree, branches	0.5 - 1	2 - 10
Deciduous, full leaf	1	5 - 20
Evergreen forest	2 - 5	5 - 20
Thin jungle scrub	1 - 10	3 - 20
Dense rain forest	10 - 50	50

The tree's tops may be considered as knife edge at distances bigger than the mean tree height above the transmitting antenna. As far as radio coverage planning is concerned a 10 dB tolerance is usually allowed when the service area contains trees varying from bare in the winter to full leaf in the summer.

3) *Street Orientation*

The lined buildings of the streets work as "wave guides" affecting the propagation direction of the radio wave. Mobiles on streets running radially from the base station, or on the streets parallel to these, may receive a signal 10-20 dB higher than that received when they run on the perpendicular streets. This effect is more significant in the vicinities of the base station (up to 2 km away), becoming negligible at distances above 10 km [2].

4) *Tunnel*

Microwave frequencies are substantially attenuated by the structure of the tunnels. This attenuation can reach 20 dB or more, greatly affecting the radio communication. On the other hand, tunnels may work as "wave guides" channelling the radio signal. Reudink [18] carried out an investigation where he placed a transmitter at approximately 300 m inside the tunnel, taking the measurements at a distance of 600 m inside the tunnel in a line-of-sight path. Some of his results are shown in Figure 3.18.

3.4 STATISTICAL DISTRIBUTIONS OF THE MOBILE RADIO SIGNAL

In the previous sections we described some of the parameters affecting the mobile radio signals. From our limited survey on the subject it is not difficult to infer that, in fact, a countless number of factors may influence the radio signal. Accordingly, a single deterministic treatment of this signal will certainly be reducing the problem to an over simplified model. Therefore, we may treat the signal in a statistical basis and interpret the results as random events occurring with a given probability.

Three distributions are closely related to the mobile radio statistics: Log-normal, Rayleigh and Ricean. The log-normal distribution describes the envelope of the received signal shadowed by the obstructions such as hills, buildings and others. The Rayleigh distribution describes the envelope of the received signal resulting from the multipath propagation. The Ricean distribution considers the envelope of the received signal with the multipath propagation plus a line-of-sight component. We may also combine the log-normal and the Rayleigh distributions to obtain an overall distribution, known as Suzuki distribution.

In this section we shall obtain, describe and analyze these probability distributions. The way of obtaining these statistics, by means of field measurements, is described in Chapter 4.

3.4.1 Log-Normal Distribution

Wave Equations

The wave equations for the electromagnetic fields in a dispersive medium with electric permittivity ε, magnetic permeability μ and conductivity σ are obtained from the Maxwell's equations as

$$\nabla^2 \mathbf{e} - \mu\varepsilon\frac{\partial^2 \mathbf{e}}{\partial t^2} - \mu\sigma\frac{\partial \mathbf{e}}{\partial t} = 0 \qquad (3.63a)$$

and

$$\nabla^2 \mathbf{h} - \mu\varepsilon \frac{\partial^2 \mathbf{h}}{\partial t^2} - \mu\sigma \frac{\partial \mathbf{h}}{\partial t} = 0 \qquad (3.63b)$$

If the field has a harmonic time dependence, then the derivative $\partial/\partial t$ is replaced by* $j\omega$. Hence, for electric field

$$\nabla^2 \mathbf{E} + \omega^2 \mu\varepsilon \left(1 + \frac{\sigma}{j\omega\varepsilon}\right) \mathbf{E} = 0 \qquad (3.64)$$

(for the magnetic field the results are analogous).

It is not difficult to prove that the solution

$$\mathbf{E} = \mathbf{E}_0 e^{\pm \gamma . \mathbf{r}} \qquad (3.65)$$

satisfies (3.64). In (3.65) $\mathbf{E}_0$ is the amplitude of the electric field in the propagation medium (free space), $\mathbf{r}$ is the direction of the propagation and γ is the vector propagation constant. Substituting (3.65) in (3.64) we conclude that

$$\gamma = \sqrt{(\sigma + j\omega\varepsilon) j\omega\mu} = \alpha + j\beta \qquad (3.66)$$

where

$$\alpha^2 = \omega^2 \frac{\mu\varepsilon}{2} \left(\sqrt{1 + \left(\frac{\sigma}{\omega\varepsilon}\right)^2} - 1 \right)$$

$$\beta^2 = \omega^2 \frac{\mu\varepsilon}{2} \left(\sqrt{1 + \left(\frac{\sigma}{\omega\varepsilon}\right)^2} + 1 \right)$$

The parameters α and β are the attenuation constant (neper/metre or dB/m) and the phase constant (rad/metre), respectively.

If we consider that the field propagates at the direction of $\mathbf{r}$, then, from (3.65), the magnitude of $\mathbf{E}$ is

$$E_M = E_0 \exp\left[- (\alpha + j\beta) r \right] \qquad (3.67)$$

From (3.67) the modulus of E_M is

---

* For a harmonic time dependence electric field, $e \triangleq \mathbf{E} = \mathbf{E}_0 e^{j(\omega t + \theta)}$, and $\frac{\partial e}{\partial t} = j\omega \mathbf{E}$.

$$E = E_0 \exp(-\alpha r) \tag{3.68}$$

Log-Normal Distribution

Consider a radio wave propagating in a mobile radio environment. When reaching the mobile station the radio wave will have travelled through different obstructions such as buildings, tunnels, hills, trees, etc. Each obstruction presents its own attenuation constant as well as thickness. Suppose that the $i^{\underline{th}}$ obstruction has an attenuation constant α_i and thickness Δr_i. If the amplitude of the wave entering this obstruction is E_{i-1}, and E_i is this amplitude after the obstruction, then

$$E_i = E_{i-1} \exp(-\alpha_i \Delta r_i) \tag{3.69}$$

Using recursivity, it follows that the signal leaving the $n^{\underline{th}}$ obstruction is given by

$$E_n = E_0 \exp\left(- \sum_{i=1}^{n} \alpha_i \Delta r_i \right) \tag{3.70}$$

It is reasonable to admit that α_i and Δr_i vary randomly from obstruction to obstruction. Define x as

$$x \triangleq - \sum_{i=1}^{n} \alpha_i \Delta r_i \tag{3.71}$$

Then

$$E_n = E_0 \exp(x) \tag{3.72}$$

If the number of obstructions is large enough ($n \to \infty$ in (3.71)) we can use the central limit theorem* to state that the random variable x has a normal distribution $p(x)$ such that

---

* "The probability distribution function of a sum of independent random variables approaches that of a Gaussian random variable as the number of independent random variables increases without limit" [20]. In our case we are also assuming the obstructions to be independent.

$$p(x) = \frac{1}{\sqrt{2\pi}\,\sigma_x} \exp\left[-\frac{1}{2}\left(\frac{x - m_x}{\sigma_x}\right)^2\right] \tag{3.73}$$

where m_x is the mean value of x and σ_x^2 is its variance. Now let us find the distribution of the ratio y of the fields E_n/E_0 as expressed in (3.72)

$$y = \frac{E_n}{E_0} = \exp(x)$$

Then, define Y as

$$Y \triangleq \log y = x\log e \tag{3.74a}$$

The mean and the variance of Y are M_Y and σ_Y^2, respectively, and are defined as

$$M_Y \triangleq \log m_Y = m_x \log e \tag{3.74b}$$

$$\sigma_Y \triangleq \log \sigma_Y = \sigma_x \log e \tag{3.74c}$$

In order to find the probability density $p(Y)$ of Y we equate the areas under the densities $p(Y)$ and $p(x)$, such that

$$p(Y)|dY| = p(x)|dx| \tag{3.75}$$

From (3.74a)

$$|dY| = \log e\,|dx| \tag{3.76}$$

Then, using (3.76) in (3.75) and taking $p(x)$ from (3.73) we obtain

$$p(Y) = \frac{1}{\log e}\, p(x) = \frac{1}{\sqrt{2\pi}\,\sigma_x \log e} \exp\left[-\frac{1}{2}\left(\frac{x - m_x}{\sigma_x}\right)^2\right]$$

Therefore,

$$p(Y) = \frac{1}{\sqrt{2\pi}\,\sigma_Y} \exp\left[-\frac{1}{2}\left(\frac{Y - M_Y}{\sigma_Y}\right)^2\right] \tag{3.77a}$$

It can be seen that Y also has a normal distribution but, since Y, M and σ_Y are given in a logarithmic form, this function is known as Log-Normal Probability Density Function. We then conclude that the excess path loss, i.e. the difference in dB between the received signal and the free space signal, $20\log(E_R/E_0)$, has a log-normal distribution. It is obvious that the received signal R, when measured in decibel, also has a log-normal distribution (the proof follows the same steps) given by

$$p(R) = \frac{1}{\sqrt{2\pi}\,\sigma_R} \exp\left[-\frac{1}{2}\left(\frac{R - M_R}{\sigma_R}\right)^2\right] \qquad (3.77b)$$

where M_R and σ_R^2 are respectively the mean and variance of R given in dB. Measurements [2] have shown that the standard deviation σ_R is in the range of 4-10 dB. Note that the same reasoning may be used to obtain

$$p(y) = \frac{1}{\sqrt{2\pi}\,y\sigma_x} \exp\left[-\frac{1}{2}\left(\frac{\ln y - m_x}{\sigma_x}\right)^2\right] \qquad (3.78a)$$

In the same way, if $R = \log r$ then

$$p(r) = \frac{1}{\sqrt{2\pi}\,r\sigma_x} \exp\left[-\frac{\ln^2(r/m_r)}{2\sigma_x^2}\right] \qquad (3.78b)$$

The cumulative distribution is

$$P(Y_0) = \text{prob}(Y \le Y_0) = \int_{-\infty}^{Y_0} p(Y)\, dY \qquad (3.79)$$

Both functions are sketched in Figure 3.19.

3.4.2 Rayleigh Distribution

The received signal at a mobile will rarely have a direct line-of-sight to a transmitter. It is the sum of the signals formed by the transmitted signal scattered by randomly placed obstructions imposing different attenuations and phases to the

resultant signals. This is known as multipath propagation. It is plausible to suppose that the phases of the scattered waves are uniformly distributed from 0 to 2π rad. and that amplitudes and phases are statistically independent from each other. Consequently, we may expect that, at a certain instant the waves will be in phase, producing a large amplitude (constructive interference), while at another instant they will be out of phase, producing a small amplitude (destructive interference). In this section we shall determine the statistics of this fading signal.

Consider a carrier signal s at a frequency ω_0 and with an amplitude a written in its exponential form

$$s = a\exp(j\omega_0 t) \tag{3.80}$$

(The actual signal is given by either the real part or imaginary part of s)

Let a_i and θ_i be the amplitude and the phase of the i^{th} scattered wave, respectively. The resultant signal s_r at the mobile is the sum of the n scattered waves as follows

$$s_r = \sum_{i=1}^{n} a_i \exp\left[j(\omega_0 t + \theta_i)\right] \tag{3.81a}$$

Equivalently,

$$s_r = r\exp\left[j(\omega_0 t + \theta)\right] \tag{3.81b}$$

where

$$r\exp(j\theta) = \sum_{i=1}^{n} a_i \exp(j\theta_i)$$

But

$$r\exp(j\theta) = \sum_{i=1}^{n} a_i\cos\theta_i + j\sum_{i=1}^{n} a_i\sin\theta_i \triangleq x + jy \tag{3.82a}$$

Then

$$x \triangleq \sum_{i=1}^{n} a_i\cos\theta_i \qquad \text{and} \qquad y \triangleq \sum_{i=1}^{n} a_i\sin\theta_i$$

where

$$r^2 = x^2 + y^2 \tag{3.82b}$$

$$x = r\cos\theta \tag{3.82c}$$

$$y = r\sin\theta \tag{3.82d}$$

Since (i) n is usually very large, (ii) the individual amplitudes a_i are random and (iii) the phases θ_i have an uniform distribution, it can be assumed that (calling for the central limit theorem again) x and y are both Gaussian variates with means equal to zero and variances $\sigma_x^2 = \sigma_y^2 \triangleq \sigma_r^2$. Consequently, their distributions are

$$p(z) = \frac{1}{\sqrt{2\pi}\,\sigma_z} \exp\left(-\frac{z^2}{2\sigma_z^2}\right) \tag{8.83}$$

where $z = x$ or $z = y$ as required.

It is shown in section 4.5 that x and y are independent random variables, despite being Gaussian with the same standard deviation. Then the joint distribution p(x,y) is

$$p(x,y) = p(x)p(y) = \frac{1}{2\pi\sigma_r^2} \exp\left(-\frac{x^2 + y^2}{2\sigma_r^2}\right) \tag{3.84}$$

The distribution $p(r,\theta)$ can be written as a function of p(x,y) as follows

$$p(r,\theta) = |J|\,p(x,y) \tag{3.85a}$$

where

$$J \triangleq \begin{vmatrix} \partial x/\partial r & \partial x/\partial\theta \\ \partial y/\partial r & \partial y/\partial\theta \end{vmatrix} \tag{3.85b}$$

is the Jacobian of the transformation of the random variables x,y into r,θ. Using (3.82c) and (3.82d) in (3.85b) we obtain $J = r$. Therefore, with (3.84) in (3.85a) we have

$$p(r,\theta) = \frac{r}{2\pi\sigma_r} \exp\left(-\frac{r^2}{2\sigma_r^2}\right) \tag{3.86}$$

The density $p(r)$ is obtained by averaging $p(r,\theta)$ over the range of variation of θ. Hence

$$p(r) = \int_0^{2\pi} p(r,\theta)d\theta$$

$$= \begin{cases} \dfrac{r}{\sigma_r^2}\exp\left(-\dfrac{r^2}{2\sigma_r^2}\right) & , r \geq 0 \\ 0 & , \text{otherwise} \end{cases} \qquad (3.87)$$

Equation (3.87) is the Rayleigh probability density function. Its distribution $P(r_0)$ is

$$P(r_0) = \text{prob}(r \leq r_0) = \int_0^{r_0} p(r)dr = 1 - \exp\left(-\frac{r_0^2}{2\sigma_r^2}\right) \qquad (3.88)$$

Both functions (3.87) and (3.88) are shown in Figure 3.20

Some important points of this distribution are

- Mean value = $E[r] = \int_0^{\infty} rp(r)dr = \sqrt{\pi/2}\,\sigma_r$
- Most likely value = $\text{Max}\{p(r)\} = \sigma_r$
- Second moment (mean squared value) = $E[r^2] = \int_0^{\infty} r^2 p(r)dr = 2\sigma_r^2$

  Then its rms value is $\sqrt{2}\,\sigma_r$
- Variance = $E[r^2] - E^2[r] = (2 - \pi/2)\sigma_r^2$
- Median, defined as the value r_0 obtained when $\int_{r_0}^{\infty} p(r)dr = 0.5$. Then, $r = 1.18\,\sigma_r$

3.4.3 Ricean Distribution

The Rayleigh fading model holds only in the case where there is a large number of indirect paths and they greatly predominate over the direct path. However, in some circumstances, when there is a line-of-sight propagation, the direct path predominates over the indirect ones. This may happen, for instance, within a building: most of the

buildings have a reinforced central core, curtain walls and ceilings/floors containing a large amount of metal. It is plausible to expect that, if a transmitting antenna is placed on a floor, some ducting of waves will occur, added to multipath scattering of the waves. Consequently, the received signal is a sum of the scattered and direct signals. We want to investigate how the statistics of the received envelope will vary according to the proportion of direct waves to scattered waves.

Using (3.81b) and (3.80), the received signal s_r is

$$s_r = \overbrace{re^{x(j\omega_0 t + \theta)}}^{\text{scattered waves}} + \overbrace{ae^{x(j\omega_0 t)}}^{\text{direct waves}} \qquad (3.89a)$$

or, equivalently

$$s_r = \Big[(x + a) + jy\Big]\exp(j\omega_0 t) \qquad (3.89b)$$

Note that, in this case,

$$r^2 = (x + a)^2 + y^2 \qquad (3.89c)$$

$$x + a = r\cos\theta \qquad (3.89d)$$

$$y = r\sin\theta \qquad (3.89e)$$

By following the same steps described in section 3.4.2 we obtain

$$p(r) = \frac{r}{\sigma_r^2}\exp\left(-\frac{r^2 + a^2}{2\sigma_r^2}\right) I_0\left(\frac{ar}{\sigma_r^2}\right) \qquad (3.90a)$$

where

$$I_0\left(\frac{ar}{\sigma_r^2}\right) = \frac{1}{2\pi}\int_0^{2\pi}\exp\left(\frac{ar\cos\theta}{\sigma_r^2}\right)d\theta \qquad (3.90b)$$

is the modified zeroth order Bessel function. This function can be found in tabulated form (e.g.,see Abramowitz and Stegun [31]) or evaluated numerically by [31]

$$I_0(x) = \sum_{i=0}^{\infty}\left(\frac{x^i}{i!\,2^i}\right) \qquad (3.90c)$$

Equation (3.90a) corresponds to the Ricean distribution. Note that if $a = 0$ we obtain the Rayleigh distribution. If the ratio a/σ is large enough, the in-phase component $(x + a)$ will predominate over the quadrature component y of the signal. Therefore, the distribution $p(r)$, of $r = x + a$, is equal to that of $p(x)$, but with a mean value equal to a. Accordingly, the Ricean distribution is the link between the Rayleigh and the Gaussian distributions as shown in Figure 3.21.

3.4.4 Suzuki Distribution

As we have seen, the long-term fading signal has a log-normal distribution, while the short-term fading signal has a Rayleigh distribution*. It is reasonable to expect the overall distribution of the received signal to be a mixture of Rayleigh and log-normal. In this section we shall obtain such distribution.

Let R be the local mean value of the received signal r, and M_R its area mean value. The distribution of R is log-normal as shown in (3.77b). The distribution of r conditional on the mean value R is the Rayleigh distribution, i.e.,

$$p(r|R) = \frac{r}{\sigma_r^2} \exp\left(-\frac{r^2}{2\sigma_r^2}\right) \tag{3.91}$$

The mean of the above distribution, as shown in section 3.4.2, is $E\left[r|R\right] = \sqrt{\pi/2}\ \sigma_r$. Such mean equals R when expressed in logarithmic form. Therefore

$$20\log\left(E\left[r|R\right]\right) = 20\log\left(\sqrt{\pi/2}\ \sigma_r\right) = R \tag{3.92}$$

or, equivalently

$$\sigma_r = \sqrt{2/\pi}\ 10^{R/20} \tag{3.93}$$

Using (3.93) in (3.91) we obtain

---

* We are assuming outdoor propagation. Short-term fading signal has a Ricean distribution for indoor propagation.

$$p(r|R) = \frac{\pi r}{2\ 10^{R/10}} \exp\left(-\frac{\pi r^2}{4\ 10^{R/10}}\right) \tag{3.94}$$

The unconditional probability $p(r)$ is obtained by averaging the conditional probability $p(r|R)$ over all possible values of R. Hence

$$p(r) = \int_{-\infty}^{\infty} p(r|R)p(R)dR$$

Finally, using (3.94) and (3.77b) in the above equation, we obtain

$$p(r) = \sqrt{\frac{\pi}{8\sigma_R^2}} \int_{-\infty}^{\infty} \frac{r}{10^{R/10}} \exp\left(-\frac{\pi r^2}{4\ 10^{R/10}}\right) \exp\left[-\frac{1}{2}\left(\frac{R - M_R}{\sigma_R}\right)^2\right] dR \tag{3.95}$$

Equation (3.95) is known as Suzuki distribution [33].

3.5 SIGNAL COVERAGE AREA (CELL AREA)

Let w_l be the mean power received by the mobile at a distance l from the base station. Let w_L be the mean power received by the mobile positioned at the cell's border (radius L). If at l the environment is not exactly the same as that at L then, from (3.61b), the ratio between these two powers is

$$\frac{w_l}{w_L} = \left(\frac{l}{L}\right)^{-\alpha} c \tag{3.96}$$

where α is the path loss slope at l and c is a correction factor, due to the change of environment. Define $m_w \triangleq$ as the mean signal power such that

$$m_w \triangleq k(l/L)^{-\alpha} \tag{3.97a}$$

where $k = cw_L$. Expressed in dB.

$$M_w \triangleq 10\log m_w = K - 10\alpha\log(l/L) \tag{3.97b}$$

where $K = 10\log k$.

The problem of estimating the cell area, or equivalently the signal coverage area, can be approached by two different ways. In the first approach we may wish to determine the proportion of the locations at L (circumference defined by L) where the received signal power w is above a power threshold w_0. In the second approach we may determine the proportion of the circular area defined by L where the received signal is above w_0. Note that in the first case this proportion is averaged over the perimeter of the circumference, whereas in the second case the average is over the entire circular area.

In both cases it is assumed that the probability density p(w) of w and the mean signal strength m_w at a given distance I are known. The mean signal strength can be determined by one of the prediction models or by field measurements. As for the distribution of w, any of the statistics described in section 3.4 can be used, as appropriate. In the analyses that follow we shall consider separately the fading signal to follow (i) a log-normal or (ii) a Rayleigh distribution.

Proportion of Locations at Distance L

The proportion β of locations at this distance where a mobile would experience a received signal above the threshold w_0 (or equivalently, the probability β that the received signal at L is greater than w_0) is

$$\beta \triangleq \text{prob}(w \geq w_0) = \int_{w_0}^{\infty} p(w)dw \tag{3.98a}$$

or

$$\beta \triangleq \text{prob}(W \geq W_0) = \int_{W_0}^{\infty} p(W)dW \tag{3.98b}$$

where $W = 10\log w$ and $W_0 = 10\log w_0$.

Proportion of Locations Within the Area Defined by L

If we assume that the mobiles are uniformly distributed within the cell area, then the proportion of locations within the circle defined by L, receiving a signal

above the threshold w_0, also corresponds to the proportion of mobiles receiving such signal. Equivalently, this proportion gives the probability that a mobile within the defined area receive a signal above the threshold w_0. Let μ be such proportion and prob($w \geq w_0$) be the probability that w exceeds w_0 within an infinitesimal area dA. Therefore, the wanted proportion μ is the probability prob($w \geq w_0$) averaged over the entire circular area. Thus

$$\mu = \frac{1}{A} \int_A \text{prob}(w \geq w_0) dA \tag{3.99}$$

where $A = \pi L^2$ and $dA = l dl d\theta$. Therefore

$$\mu = \frac{1}{\pi L^2} \int_0^L \int_0^{2\pi} \text{prob}(w \geq w_0) l dl d\theta$$

$$= \frac{1}{L^2} \int_0^L \text{prob}(w \geq w_0) l dl \tag{3.100a}$$

If W and W_0 are expressed in dB

$$\mu = \frac{1}{L^2} \int_0^L \text{prob}(W \geq W_0) l dl \tag{3.100b}$$

3.5.1 Log-Normal Fading Case

Consider a pure log-normal fading environment. The envelope R of the received signal follows a normal distribution as that given by (3.77b). Since R is given in dB, then W = R and the distribution p(W) of W is

$$p(W) = \frac{1}{\sqrt{2\pi}\,\sigma_w} \exp\left[-\frac{1}{2} \left(\frac{W - M_w}{\sigma_w} \right)^2 \right] \tag{3.101}$$

With (3.101) in (3.98b) we obtain

$$\beta = \text{prob}(W \geq W_0) = \frac{1}{2}\left[1 - \text{erf}\left(\frac{W_0 - M_w}{\sqrt{2}\,\sigma_w}\right)\right] \tag{3.102}$$

where erf(·) is the error function.

Using (3.97b) and (3.102) in (3.100b) yields

$$\mu = \frac{2}{L^2}\int_0^L \int_{u_0}^{\infty} \frac{1}{\sqrt{\pi}} \exp(-u^2)\,du\,dl \tag{3.103}$$

where

$$u = \frac{W - K + 10\alpha \log(l/L)}{\sqrt{2}\,\sigma_W}$$

and

$$u_0 = \frac{W_0 - K + 10\alpha \log(l/L)}{\sqrt{2}\,\sigma_W} \tag{3.104}$$

We may express (3.103) in terms of the error function $\text{erf}(u_0)$

$$\text{erf}(u_0) \triangleq 2\int_0^{u_0} \frac{1}{\sqrt{\pi}} \exp(-v^2)\,dv$$

such that

$$\mu = \frac{2}{L^2}\int_0^L \left[\frac{1}{2} - \frac{1}{2}\,\text{erf}(u_0)\right] l\,dl = \frac{1}{2} - \frac{1}{L^2}\int_0^L \text{erf}(u_0)\,l\,dl \tag{3.105}$$

From (3.104)

$$l\,dl = \frac{\sqrt{2}\,\sigma_W}{10\alpha \log e}\, l^2\,du_0 \tag{3.106}$$

With (3.104) and (3.106) in (3.105) we get

$$\mu = \frac{1}{2} - \frac{\sqrt{2}\,\sigma_W}{10\alpha \log e} \exp\left(-2 \frac{W_0 - K}{10\alpha \log e}\right) \int_{-\infty}^{\frac{W_0 - K}{\sqrt{2}\,\sigma_W}} \exp\left(\frac{2\sqrt{2}\,u_0}{10\alpha \log e}\right) \operatorname{erf}(u_0)\,du_0 \quad (3.107)$$

This integral is then rearranged to be found in integral tables. Finally

$$\mu = \frac{1}{2}\left\{1 + \operatorname{erf}\left(\frac{K - W_0}{\sqrt{2}\,\sigma_W}\right) + \exp\left[\frac{2(K - W_0)10\alpha \log e + 2\sigma_W^2}{100\alpha^2 \log^2 e}\right]\right.$$

$$\left.\left[1 - \operatorname{erf}\left(\frac{(K - W_0)10\alpha \log e + 2\sigma_W^2}{(10\alpha \log e)\sqrt{2}\,\sigma_W}\right)\right]\right\} \quad (3.108)$$

The proportion μ given by (3.108) is plotted versus $(W_0 - K)/\sigma_w$ in Figure 3.22 for some values of α and σ_w.

3.5.2 Rayleigh Fading Case

In a pure Rayleigh fading environment the envelope, r, of the received signal has a probability density p(r) as given by (3.87). Accordingly, the density p(w) of $w = r^2/2$ is such that

$$p(w)|dw| = p(r)|dr|$$

Since $dw = rdr$, then

$$p(w) = \frac{1}{m_w} \exp\left(-\frac{w}{m_w}\right) \quad (3.109)$$

Note that both the mean and the standard deviation of w are equal to m_w.

With (3.109) in (3.98a) we obtain

$$\beta = \text{prob}(w \geq w_0) = \exp\left(-\frac{w_0}{m_w}\right) \quad (3.110)$$

Now, using (3.97a) and (3.110) in (3.100a) we obtain

$$\mu = \frac{2}{\alpha}\left(\frac{k}{w_0}\right)^{2/\alpha} \Gamma_c\left(\frac{2}{\alpha}, \frac{w_0}{k}\right) \qquad (3.111)$$

where

$$\Gamma_c(x,y) = \int_0^y t^{x-1}\exp(-t)dt$$

is the complementary incomplete gamma function. The proportion μ given by (3.111) is plotted versus $W_0 - K$ in Figure 3.23 for some values of α.

3.5.3 Some Examples

1) Let the mean signal strength at l = L be $M_w = K = -100$ dBm* in an environment where $\alpha = 3.5$. We want to estimate the probability that the received signal exceed a threshold $W_0 = -105$ dBm a) within the circular area delimited by L and b) at the perimeter of the corresponding circumference.

Log-Normal Fading Case

Assume that $\sigma_w = 5$ dB. Hence $(W_0 - K)/\sigma_w = (W_0 - M_w)/\sigma_w = -1$.

a) From Figure 3.22 $\mu = 96\%$

b) From (3.102) $\beta = 84.13\%$

Rayleigh Fading Case

Since $W_0 - K = -5$ dBm

a) From Figure 3.23 $\mu = 90\%$

b) From (3.110) $\beta = 73\%$

2) Let the mean signal strength at l = 10 Km be $M_w = -100$ dBm in an environment where $\alpha = 3.5$. We want to estimate the cell radius L such that the mobile stations receive a signal power above $W_0 = -110$ dBm 90% of the time a) within the circular area delimited by L and b) at the perimeter of the corresponding circumference.

---

* If P is a power given in watts and p is the same power expressed in milliwatts, then $10\log p = 10\log\frac{P}{10^3}$ is given in dBm.

Log-Normal Fading Case

Assume that σ_w = 5 dB.

a) From Figure 4.22 with μ = 90% we find $(W_0 - K)/\sigma_w = -0.47$, yielding K = -107.65 dBm. Since $M_w - K = -10\alpha\log(1/L)$, then L = 16.5 Km.

b) From (3.102) with β = 90% we find $(W_0 - K)/\sigma_w = -1.28$, yielding K = - 103.6 dBm. Then L = 12.7 Km.

Rayleigh Fading Case

a) From Figure 4.23 with μ = 90% we find $W_0 - K = -5.2$ dBm, yielding K = -104.8 dBm. Then L = 13.7 Km.

b) From (3.110) with β = 90% we find $W_0 - K \approx -100$ dBm. Then L = 10 Km.

3.6 BOUNDARIES BETWEEN CELLS

The cells of the mobile radio systems are not clearly defined but have fuzzy boundaries because of the statistical fluctuation in radio path losses. If the mobiles are near the cell border they may well have adequate communication with more than one base station. The proportion of the cell area within which mobiles are considered to have more than one radio path depends on the fading distribution, on the permissible tolerance in path loss for satisfactory communication and on the geographical distribution of cells and mobiles. This section examines the joint statistics of paths to two and three base stations and estimates such proportion. We impose that the path losses shall differ by not more than A dB, while neither is more than C dB below the long term mean of these paths. That is, by choice of parameters it may be stipulated that the paths are sufficiently similar and also neither of them is in deep fade.

3.6.1 Joint Rayleigh Fading

Consider two Rayleigh-fading signals with instantaneous amplitude r_i, mean amplitude $\sqrt{\frac{\pi}{2}}\, m_i$ and probability density

$$p(r_i) = \frac{r_i}{m_i^2} \exp\left[\frac{-r_i^2}{2m_i^2}\right] \qquad i = 1, 2 \tag{3.113}$$

If the fadings are independent, the joint density is simply

$$p(r_1,r_2) = p(r_1)p(r_2) \tag{3.114}$$

An important parameter of the joint distribution is the difference in mean levels, denoted by

$$b = \frac{m_2}{m_1}$$

$$B = 20\log b$$

It is intended to estimate the probability P(a,b) that the two signals differ in instantaneous level by not more than A dB, where

$$A = 20\log a$$

It is perhaps desirable to require that neither of the two signals be below a threshold level c. The required probability can be determined by integrating (3.114) over the region shown in Figure 3.24. The parameter c is defined by

$$C = -10\log(c^2/m_1m_2)$$

By successive applications of the integral

$$\int r\exp(kr^2)dr = -\frac{\exp(-kr^2)}{2k}$$

it can be shown that

$$P(a,b,c) = \frac{\exp\left[-\frac{c^2}{2m_2^2}\left(1+\frac{b^2}{a^2}\right)\right]}{1+\frac{b^2}{a^2}} + \frac{\exp\left[-\frac{c^2}{2m_1^2}\left(1+\frac{1}{a^2b^2}\right)\right]}{1+\frac{1}{a^2b^2}} - \exp\left[-\frac{c^2}{2}\left(\frac{1}{m_1^2}+\frac{1}{m_2^2}\right)\right] \tag{3.115}$$

By expansion of the exponential function in P(a,b,c) it may be shown that

$$P(a,b,c) - P(a,b,0) = \frac{c^4}{4m_1^2 m_2^2}\left(1 - \frac{1}{a^2}\right) + 0\,(c^6)$$

which is small for likely values of c. Moreover, exact calculation shows that the term in c^4 exceeds the true probability. For example, with A = C = 6 dB the approximation gives 0.0118, while the exact expression gives 0.0103 for B = 0, falling to 0.0089 for B = 12 dB. The overall effect on the results is small, and the simpler expression, P(a,b,0) gives a good guide. Then

$$P(a,b,0) = \frac{a^2 - \frac{1}{a^2}}{\left(a^2 + \frac{1}{a^2}\right) + \left(b^2 + \frac{1}{b^2}\right)} \qquad (3.115b)$$

3.6.2 Joint Log-Normal Fading

With this distribution is simpler to use the logarithmic variables, each of which having a Gaussian (normal) distribution. Consider two signals with instantaneous levels R_i, and mean levels M_i, expressed in decibels. Their probability densities are

$$p(R_i) = \varphi\left(\frac{R_i - M_i}{\sigma_i}\right) \qquad (3.116)$$

where the notation $\varphi(\cdot)$ signifies the Gaussian distribution

$$\varphi(u) = \frac{1}{(2\pi)^{1/2}} \exp\left(-\frac{u^2}{2}\right) \qquad (3.117)$$

$$\phi(u) = \int_{-\infty}^{u} \varphi(x)dx \qquad (3.118)$$

The main concern is the ratio of the instantaneous amplitudes, which, when expressed in logarithmic measure, is the difference

$$R = R_2 - R_1$$

Similarly, the parameter B is the difference in mean levels

$$B = M_2 - M_1$$

Now, the difference between two Gaussian random variables is another Gaussian random variable. In particular, R has the density $\varphi[R - M)/\sigma]$ where

$$M = M_2 - M_1 = B$$

and

$$\sigma^2 = \sigma_1^2 + \sigma_2^2 - 2\rho_R\sigma_1\sigma_2$$

In the above equation ρ_R is the correlation coefficient of the two variables. If these variables are independent, $\rho_R = 0$. This is the case explored in this section.

In estimating the probability that the two signals have a level difference not exceeding A dB, it is not necessary to distinguish between the cases $R_1 > R_2$ and $R_2 > R_1$. Thus the distribution of A is effectively that of the modulus $|R|$. Its density is

$$p(A) = \varphi\left(\frac{A - B}{\sigma}\right) + \varphi\left(\frac{A + B}{\sigma}\right) \qquad (3.119)$$

and the cumulative distribution is

$$P(A) = \phi\left(\frac{B + A}{\sigma}\right) - \phi\left(\frac{B - A}{\sigma}\right) \qquad (3.120)$$

where always $A \geq 0$.

3.6.3 The Geographical Distribution of the Mean Power Ratio

Suppose that the mean signal power diminishes with distance x as $x^{-\alpha}$, where α is the path loss slope. Consider a mobile at distances x_1, x_2 from two base stations of equal power. Recalling from section 3.3.7 (equation (3.60a)) the ratio m_2^2/m_1^2 of the received powers is

$$b^2 = \left(\frac{m_2}{m_1}\right)^2 = \left(\frac{x_1}{x_2}\right)^{\alpha} \qquad (3.121a)$$

The locus of points with a given b is, therefore, that of points with a given distance ratio

$$h = \frac{x_1}{x_2} = b^{2/\alpha} \tag{3.121b}$$

The locus may be found by simple algebra. Expressing (3.121b) in Cartesian coordinates with origin midway between the base stations (Figure 3.25) and rearranging as a quadratic equation we obtain

$$y^2 + \left(x - \frac{h^2 + 1}{h^2 - 1}\right)^2 = \left(\frac{2h}{h^2 - 1}\right)^2 \tag{3.122}$$

Equation (3.122) defines a circle as sketched in Figure 3.25

Now it is intended to estimate the proportion of cell area where the difference in mean path loss to seven base stations, taken two at a time, is within some assigned tolerance B dB. Consider two adjacent base stations as in Figure 3.26a. By symmetry, it is necessary to consider only a triangular sector (triangle OAB as shown in Figure 3.26b) comprising 1/12 of a cell. For the given tolerance, the power ratio b can be calculated and thence the distance ratio h. This defines a circular locus with centre C, of which DE is an arc. Within the area OBED, the ratio of the mean powers will be within the tolerance. Averaged over the whole array, the proportion of area with such power ratio will be

$$\gamma = \frac{\text{area OBED}}{\text{area OBA}} \tag{3.123}$$

Clearly (3.123) is a function of the tolerance B. With the scale used here OBA = $1/2\sqrt{3}$. By simple geometry we have

$$\gamma = 1 + \frac{2\sqrt{3}\, Y_E}{h^2 - 1} - 4\sqrt{3}\left(\frac{h}{h^2 - 1}\right)^2 \sin^{-1}\left(\frac{Y_E(h^2 - 1)}{2h}\right) \tag{3.124a}$$

where

$$2\sqrt{3}\, Y_E = -3\left(\frac{1}{h^2 - 1}\right) + \sqrt{\left(\frac{2h^2 + 1}{h^2 + 1}\right)^2 - 4} \tag{3.124b}$$

As a check and convenient approximation, it can be seen that the area OBED is approximated from below by OBFD, where FD is a tangent to the circle. Consequently

$$\gamma > \gamma_u = 1 - \left(\frac{2}{h+1}\right)^2$$

In the same way, the area OBED can be approximated from above if the arc DE is approximated by a straight line. Then

$$\gamma < \gamma_0 = 1 - \frac{2\sqrt{3}\ Y_E}{h+1}$$

The parameters γ, γ_0 and γ_u are plotted in Figure 3.28 where α is assumed to be equal to 3.5. If mobiles are considered to be evenly distributed over the cell, on the average, then these areas give directly the proportion of mobiles with access to two paths whose mean losses differ by only a small amount. It is not difficult to make similar calculations for uneven distribution of mobiles, for example a gradient in density causing adjacent cells to have traffic imbalance. Unless very extreme, this leads to minor changes in the proportions.

3.6.4 The Geographical Distribution of Instantaneous Power Ratio

The occurrence of fading will modify the distribution of the signal strength ratio, as compared with simple distribution of the section 3.7.3. Not all mobiles within the border zone will have paths within the assigned tolerance, because one or both path losses may depart from the mean value. On the other hand, some mobiles outside the border zone will have such pairs of paths. It is possible to estimate the overall proportion of mobiles with satisfactory path-pairs on an instantaneous rather than a mean criterion, by combining some of the methods of section 3.7.3 with those of 3.7.2 and 3.7.1.

Refer to Figure 3.25, where x is a position variable. Let the density of mobiles in the vicinity of x be $d(x)$. In a hexagonal cell array $d(x) = 2(1 - x)$ gives a good approximation to the distribution of an uniform cell. This density would

be obtained by using OBFD as an approximation to the border zone OBED (as it has been seen, it gives a small underestimate of the proportion of mobiles in the border zone). The mean signal strength ratio b is given in (3.121b), and conditional on the value of b, the probability P(a,b) that the path losses differ by not more than A dB can be calculated using equations (3.115b) or (3.120), as desired. It is noteworthy saying that both joint probability functions ((3.115b) and (3.120)) give approximately the same results if we use σ = 5 dB in (3.120). Then the probability P(a,x)* can be obtained conditional on the variable x. This is the probability that a mobile, having a location described by the position variable x, has a path-pair within the tolerance A dB. The unconditional probability

$$\gamma = \int_0^1 d(x)P(a,x)dx \qquad (3.125)$$

is the mean proportion of mobiles within a cell having a path-pair within tolerance allowing for fading. The conditional probability P(a,x) is shown as a function of x in Figure 3.27.

The integral of (3.125) does not appear to lend itself to a closed-form evaluation, but has been evaluated numerically and is shown in Figure 3.28.

3.6.5 Proportion of the Cell Area With Three Alternative Paths

It is intended in the following sections to extend this model in order to consider the joint statistics to three base stations and then estimate the proportion of the cell area with three alternative radio paths. It may be possible to find an approximate function relating the proportion of the cell area with three paths with that with two paths. The theory has been worked out for (i) no fading and (ii) log-normal fading with standard deviation σ = 5 dB.

---

* Note that $b^2 = \left(\frac{x_1}{x_2}\right)^{\alpha} \simeq \left(\frac{1+x}{1-x}\right)^{\alpha}$, if we consider that geometry for underestimated approximation of γ.

3.6.6 The Geographical Distribution of Mean Power Ratio

Consider a mobile at distances x_1, x_2, x_3 from three base stations of equal power as shown in Figure 3.29. The ratios of received powers are

$$b_1^2 = \left(\frac{m_2}{m_1}\right)^2 = \left(\frac{x_1}{x_2}\right)^{\alpha} \tag{3.126a}$$

$$b_2^2 = \left(\frac{m_2}{m_3}\right)^2 = \left(\frac{x_3}{x_2}\right)^{\alpha} \tag{3.126b}$$

The locus of points with a given b_1 is, therefore, that of points with the distance ratio

$$h_1 = \frac{x_1}{x_2} = b_1^{2/\alpha} \tag{3.127a}$$

Similarly,

$$h_2 = \frac{x_3}{x_2} = b_2^{2/\alpha} \tag{3.127b}$$

Expressing the distance in Cartesian coordinates and rearranging the expressions in a quadratic form we obtain

$$y^2 + \left(x - \frac{h_1^2 + 1}{h_1^2 - 1}\right)^2 = \left(\frac{2h_1^2}{h_1^2 - 1}\right)^2 \tag{3.128a}$$

$$\left(y + \frac{\sqrt{3}}{h_2^2 - 1}\right)^2 + \left(x - \frac{h_2^2}{h_2^2 - 1}\right)^2 = \left(\frac{2h_2^2}{h_2^2 - 1}\right)^2 \tag{3.128b}$$

which define the circles as plotted in Figure 3.29.

Consider three adjacent base stations in a hexagonal array of cells. It is desired to estimate the proportion of cell area where the difference in mean path losses to three adjacent stations is within some assigned tolerance $B = 20\log b$. By symmetry it is necessary to consider only a triangular sector OBA as shown in Figure

3.30. For the given tolerance, the power ratio b and hence the distance ratio h can be calculated. This defines two circular loci with centres at C and C' respectively. Within the area OBEG the ratios of mean powers will be within tolerance. Averaged over the whole cell the proportion of area with such power ratio is

$$\delta = \frac{\text{area OBEG}}{\text{area OBA}}$$

With simple geometry (but not straightforward expressions)

$$\delta = 1 + \frac{2\sqrt{3}\, Y'_G}{h^2 - 1} - \sqrt{3}\, CD^2 \left[\sin^{-1}\left(\frac{Y'_G}{CD} \right) - \sin^{-1}\left(\frac{Y_E}{CD} \right) \right]$$

$$- \frac{4 \tan(\phi) \left[\sqrt{3}\, Y_E (h^2 - 1) - 3 \right]}{(h^2 - 1)^2 (\sqrt{3} - \tan(\phi))} \qquad (3.129a)$$

where Y'_G and Y_E are the ordinates of the points G' and E respectively and

$$Y_E = \frac{-\sqrt{3} + \sqrt{4h^2 - 1}}{2(h^2 - 1)} \qquad (3.129b)$$

$$Y'_G = \frac{\sqrt{3} \left(-1 + \sqrt{4h^2 - 3} \right)}{2(h^2 - 1)} \qquad (3.129c)$$

$$CD = \frac{2h}{h^2 - 1} \qquad (3.129d)$$

$$\tan(\phi) = \frac{Y_E}{\sqrt{CD^2 - Y_E^2}} \qquad (3.129e)$$

Equation (3.129a) applies within the range AG ≤ 1. i.e.,

$$AG = AG' = \frac{Y'_G}{\cos(30^\circ)} \leq 1$$

Thus this geometry is valid for $h \geq \sqrt{3}$.

Now consider the case where $1 \le h \le \sqrt{3}$. The overlapped area is shown in Figure 3.31.

In a similar way

$$\delta = \frac{\text{area BEG}}{\text{area OBA}} \tag{3.130}$$

With simple geometry (but again not straightforward expressions)

$$\delta = 1 + \frac{12\tan(\theta)}{(\sqrt{3} - \tan(\theta))(h^2 - 1)^2} - \sqrt{3}\,CD^2\left[\sin^{-1}\left(\frac{Y'_G}{CD}\right) - \sin^{-1}\left(\frac{Y_E}{CD}\right)\right] \tag{3.131a}$$

$$- \frac{4\tan(\phi)\left[\sqrt{3}\,Y_E(h^2 - 1) - 3\right]}{(h^2 - 1)^2(\sqrt{3} - \tan(\phi))} - (3 - 2\sqrt{3}\,Y'_G)\left[1 - \frac{4\tan(\theta)}{(h^2 - 1)(\sqrt{3} - \tan(\theta))}\right]$$

where Y_E, CD and $\tan(\phi)$ are given by (3.129b), (3.129d) and (3.129e) respectively, and

$$Y'_G = \frac{h\left(\sqrt{3}\,h - \sqrt{4 - h^2}\right)}{2(h^2 - 1)} \tag{3.131b}$$

$$\tan(\theta) = \frac{Y'_G}{\sqrt{CD^2 - Y'^2_G}} \tag{3.131c}$$

The expressions for δ given by equations (131a) ($1 \le h \le \sqrt{3}$) and (3.129a) ($\sqrt{3} \le h$) are rather complex. It is convenient to determine simpler equations which, although approximated, may yield quicker means of evaluation and checking. This is carried out as follows.

Underestimated δ

Refer to Figure 3.30 for $h \ge \sqrt{3}$. The area OBEG is approximated from below by OBFG, where FG is tangent to the circle of which GE is an arc. Hence

$$\delta > \delta_u = 1 - \frac{2\left(-1 + \sqrt{4h^2 - 3}\right)}{(h + 1)(h^2 - 1)} \tag{3.132a}$$

Now refer to Figure 3.31 for $1 \le h \le \sqrt{3}$. In the same way the area BEG is approximated from below by BFG. Then

$$\delta > \delta_u = 2\sqrt{3}\left(\frac{h-1}{h+1}\right)\left(Y'_G - \frac{1}{\sqrt{3}}\right) \tag{3.132b}$$

where Y'_G is given by (3.131b)

Overestimated δ

Refer to Figure 3.30 ($h \ge \sqrt{3}$). If the area OBEG is delimited by straight lines then the approximation is from above. Thus

$$\delta < \delta_0 = 1 - 2Y_E Y'_G \tag{3.133a}$$

where Y_E and Y'_G are given by equations (3.129b) and (3.129c) respectively.

The same approach can be used for $1 \le h \le \sqrt{3}$ (Figure 3.30), i.e., with BEG approximated by straight lines. Then

$$\delta < \delta_0 = 6\left(Y'_G - \frac{1}{\sqrt{3}}\right)\left(Y_E - \frac{1}{\sqrt{3}}\right) \tag{3.133b}$$

where Y_E and Y'_G are given by equations (3.129b) and (3.131b) respectively.

Equations (3.131a) and (3.129a) for the exact δ, (3.132b) and (3.132a) for the underestimated δ and (3.133b) and (3.133a) for the overestimated δ are plotted as function of B in Figure 3.33.

3.6.7 Joint Log-Normal Fading

This section aims at determining the joint probability density of three log-normal fading signals and calculating its cumulative distribution. As we shall see, such distribution can be put in a form of a bivariate normal distribution. The bivariate normal distribution function is well established in the form of tables. The use of these tables requires specific procedures varying according to the application. The application used here is detailed in Yacoub [23].

Consider three log-normal fading signals with instantaneous level R_i and mean

levels M_i expressed in decibels. Their probability densities are as given by (3.116), for $i = 1,2,3$. Assuming independent fading signals with the same standard deviation σ, the joint density is given by

$$p(R_1,R_2,R_3) = \frac{1}{\left(\sqrt{2\pi}\ \sigma\right)^3} \exp\left\{\frac{-1}{2\sigma^2}\left[\left(R_1 - M_1\right)^2 + \left(R_2 - M_2\right)^2 + \left(R_3 - M_3\right)^2\right]\right\} \quad (3.134)$$

The next step is to determine the probability that each pair of signals has an instantaneous level difference not exceeding A dB, that is

$$P(R_1,R_2,R_3) = \iiint_S p(R_1,R_2,R_3)dR_1dR_2dR_3 \quad (3.135)$$

where S is the solid determined by

$$\begin{aligned} |R_1 - R_2| &\le A \\ |R_2 - R_3| &\le A \\ |R_3 - R_1| &\le A \end{aligned} \quad (3.136)$$

Such solid is a hexagonal cylinder centred along the axis $R_1 = R_2 = R_3$.

By means of linear transformation (rotation of axes) it is possible to make one of the Gaussians coincide with one of the axes of the new system of coordinates, so that (3.135) is reduced to an integration of a 2-D Gaussian over a hexagon. Let (x,y,z) be the new system of coordinates with the axis of the hexagonal cylinder centred along z. Then

$$P(R_1,R_2,R_3) = \int_{-\infty}^{\infty}\iint_H p'(x,y,z)|J|dxdydz \quad (3.137)$$

where

(i) $$p'(x,y,z) = \frac{1}{\left(\sqrt{2\pi}\ \sigma\right)^3} \exp\left\{\frac{-1}{2\sigma^2}\left[(x - \mu_x) + (y - \mu_y)^2 + (z - \mu_z)^2\right]\right\} \quad (3.138)$$

(ii) μ_x,μ_y,μ_z are the means in the new system;

(iii) J is the Jacobian of the transformation;

(iv) H is the hexagon of integration.

From (3.137)

$$P(R_1,R_2,R_3) = \frac{1}{2\pi\sigma^2} \iint_H \exp\left\{\frac{-1}{2\sigma^2}\left[(x-\mu_x)^2 + (y-\mu_y)^2\right]\right\} |J|\,dxdy \qquad (3.139)$$

With the proposed rotation of axes

$$\begin{bmatrix} R_1 \\ R_2 \\ R_3 \end{bmatrix} = \begin{bmatrix} -2/\sqrt{6} & 0 & 1/\sqrt{3} \\ 1/\sqrt{6} & 1/\sqrt{2} & 1/\sqrt{3} \\ 1/\sqrt{6} & -1/\sqrt{2} & 1/\sqrt{3} \end{bmatrix} \begin{bmatrix} x \\ y \\ z \end{bmatrix} \qquad (3.140)$$

Consequently, the Jacobian of the transformation is given by determinant of the matrix shown in (3.140). Thus $|J| = 1$. The means M1,M2,M3 relate to μ_x,μ_y,μ_z as in (3.140). The region delimited by (3.136) in the new coordinates defines a hexagonal area as follows

$$\begin{aligned} |-3/\sqrt{6}\ x - 1/\sqrt{2}\ y| &\le A \\ |\ 3/\sqrt{6}\ x - 1/\sqrt{2}\ y| &\le A \\ |\sqrt{2}\ y| &\le A \end{aligned} \qquad (3.141)$$

Due to the symmetry we shall explore only one triangular sector of such integration hexagon. Let $x = 0$ and $y = \sqrt{3}x$ define this sector. Equation (3.139) can be evaluated by taking the means μ_x and μ_y from the lines $x = 0$ and $y = \sqrt{3}x$. The probabilities $P(R_1,R_2,R_3)$ are shown as functions of μ_{xy} in Figure 3.32 [23], where

$$\mu_{xy}^2 \triangleq \mu_x^2 + \mu_y^2 \qquad (3.142)$$

Note that the probabilities with the means taken from the line $x = 0$ and $y = \sqrt{3}x$ do not significantly differ from each other. Accordingly, we may use μ_{xy} as an overall mean to estimate $P(R_1,R_2,R_3)$.

3.6.8 The Geographical Distribution of the Instantaneous Power Ratio

In this section we shall estimate the overall proportion of the cell area with satisfactory paths to three base stations on an instantaneous rather than on a mean criterion, by combining some of the methods described in sections 3.7.6 and 3.7.7. The mean signal strength is a function of the position of the mobile in the cell

$$\mu_{xy} = f(x,y) \tag{3.143}$$

Conditional on the value of μ_{xy}, the probability $P(R_1,R_2,R_3,\mu_{xy})$ that each pair of signals has an instantaneous level difference not exceeding A dB can be estimated by using the curves of Figure 3.32. Hence $P(R_1,R_2,R_3,x,y)$ conditional on the position (x,y) can be estimated. The unconditional probability

$$\delta = \frac{1}{T}\int\int_{T} P(R_1,R_2,R_3,x,y)dxdy \tag{3.144}$$

(where T is triangular sector) is the mean proportion of the cell area with a signal strength within a tolerance allowing for fading. Again by symmetry only 1/12 of the hexagon needs to be considered. Rewriting (3.142) as a function of the means M_1,M_2 and M_3, yields

$$\mu_{xy}^2 = \frac{1}{6}\left(2M_1 - M_2 - M_3\right)^2 + \frac{1}{2}\left(M_2 - M_3\right)^2 \tag{3.145}$$

Define differences of means as

$$\begin{aligned} D_1 &= M_1 - M_2 \\ D_2 &= M_2 - M_3 \\ D_3 &= M_3 - M_1 \end{aligned} \tag{3.146}$$

Thus

$$\mu_{xy}^2 = \frac{2}{3}\left(D_1^2 + D_2^2 + D_1D_2\right) \tag{3.147}$$

3.6.8 The Geographical Distribution of the Instantaneous Power Ratio

In this section we shall estimate the overall proportion of the cell area with satisfactory paths to three base stations on an instantaneous rather than on a mean criterion, by combining some of the methods described in sections 3.7.6 and 3.7.7. The mean signal strength is a function of the position of the mobile in the cell

$$\mu_{xy} = f(x,y) \tag{3.143}$$

Conditional on the value of μ_{xy}, the probability $P(R_1,R_2,R_3,\mu_{xy})$ that each pair of signals has an instantaneous level difference not exceeding [illegible] can be estimated by using the curves of [illegible]. Hence $P(R_1,R_2,R_3,x,y)$ conditional on the position (x,y) can be estimated [illegible]

[illegible]

is shown in Figure 3.33.

Consider a mobile in the position (-x,y) (this is the mirror image of the situation of Figure 3.29). The mobiles in this triangular sector of the hexagon will have $M_1 \geq M_2 \geq M_3$ (the other five possible combinations correspond to the respective five other triangular sectors around the common corner of the three hexagons). The ratios of the received powers are

$$h_1^\alpha = \left(\frac{x_2}{x_1}\right)^\alpha = \left(\frac{m_1}{m_2}\right)^2 = d_1 = \left(\frac{y^2 + (x-1)^2}{y^2 + (x+1)^2}\right)^{\alpha/2}$$

$$h_2^\alpha = \left(\frac{x_3}{x_2}\right)^\alpha = \left(\frac{m_2}{m_3}\right)^2 = d_2 = \left(\frac{(y-\sqrt{3})^2 + x^2}{y^2 + (x-1)^2}\right)^{\alpha/2} \qquad (3.148)$$

$$h_3^\alpha = \left(\frac{x_3}{x_1}\right)^\alpha = \left(\frac{m_1}{m_3}\right)^2 = d_3 = \left(\frac{(y-\sqrt{3})^2 + x^2}{y^2 + (x+1)^2}\right)^{\alpha/2}$$

with $D_i = 20\log d_i = 10\alpha\log h_i$. From (3.148) and (3.147)

$$\mu_{xy}^2 = \frac{200\alpha^2\left[\log^2(h_3) - \log(h_2)\log(h_1)\right]}{3} \qquad (3.149)$$

In order to calculate the mean μ_{xy} in that sector, each one of the two sides composing the right angle of the triangle was divide into 20 equal distances and for each point (-x,y) (3.149) was applied (a total of 231 points). For each calculated μ_{xy}, the probability distribution of the signals within tolerance in that sector is determined. Equation (3.144) is evaluated by numerical methods from

$$\delta \simeq \frac{\Delta x \Delta y}{T} \sum_{i=0}^{\frac{1}{\Delta x}} \sum_{j=0}^{\frac{1}{\Delta x} - i} W\left(-i\Delta x, j\frac{\Delta x}{\sqrt{3}}\right) P\left(-i\Delta x, j\frac{\Delta x}{\sqrt{3}}\right) \qquad (3.150)$$

where $W(i,j)$ are the weights of $P(i,j)$ and Δx and Δy are the incremental distances into which the sector has been split, in x and y directions respectively. The result is shown in Figure 3.33.

3.6.9. δ as Function of γ

There are two distinct situations to be considered, namely $\delta = f(\gamma)$ without fading and $\delta = f(\gamma)$ with fading.

$\delta = f(\gamma)$ without fading

Refer to sections 3.7.3 and 3.7.6 where the functions $\gamma = f(h)$ and $\delta = f(h)$ are respectively determined for the case of no fading. It is obvious that $\delta = f(\gamma)$ can be found , but not necessarily in a closed form. If the exact functions are considered then neither $h = f^{-1}(\gamma)$ nor $h = f^{-1}(\delta)$ can be put in closed form. Nevertheless this is straightforward for the approximate formulas (underestimate and overestimate approximations). The exact curve is plotted in Figure 3.34 (the underestimate and overestimate curves are almost coincident with the exact one).

$\delta = f(\gamma)$ with log-normal fading

Refer to section 3.7.4 and 3.7.8 where $\gamma = f(A)$ and $\delta = f(A)$ are determined. Here definitely $\delta = f(\gamma)$ cannot be expressed in a closed form, but can be plotted with the help of the respective graphs having the tolerance A dB as a common variable. Figure 3.34 shows $\delta = f(\gamma)$ with and without fading, and suggests that $\delta = 1.25\ \gamma^2$ is a good approximation in the range of $0 \leq \gamma \leq 0.8$.

3.7 SUMMARY AND CONCLUSIONS

The mobile radio propagation phenomena are very complex and cannot be entirely described by one single model. Many signal strength prediction algorithms are available but a good prediction is only accomplished with a reasonable amount of input data. Some of these algorithms are applicable to very specific situations while others can be used in a wider range of conditions when correction factors must be employed. A simplified model is also available and can be used mainly for comparative purposes.

The prediction models yield the mean signal strength at a given distance from the

base station. However, due to the statistical fluctuations of the various phenomena involving the mobile radio propagation, the mobile radio signal cannot be treated only by deterministic methods. Accordingly, we may establish a 3-part model to better describe the various phenomena. This model has proved to be very efficient and is in very good agreement with the field measurements, as follows:

(i) Mean signal decreases with distance d as $d^{-\alpha}$, where α is a parameter typically in the range 3-4, depending on the environment;

(ii) Slow fading due to shadowing has an approximately log-normal distribution with standard deviation in the range 4-10 dB;

(iii) Fast fading due to multipath propagation has a Rayleigh distribution. Within buildings, where both multipath and line-of-sight waves can be found, the fast fading follows a Riccan distribution.

The resultant (received) signal is a combination of all of these phenomena, as sketched in Figure 3.35.

As far as boundaries between cells are concerned we have calculated two statistics

(i) The probability that a mobile user in some definite set of locations has two or more paths whose mean losses differ only within a given tolerance. The averaging is implicitly over both time (long-term) and space (within the set of locations);

(ii) The probability that a mobile user, at a randomly chosen point within some definite set of locations , has at a randomly chosen time two or more paths whose losses differ only within a given tolerance. At first sight it might appear that this differs form (i) in that it is averaged over space but not over time. However, the matter is more complex, since the loss fluctuations occur both in time and in space, and those are coupled by the movement of the user.

Those two statistics are not very dissimilar from one another in quantitative terms. Hence we may argue that a true evaluation of the proportion of the cell area,

where mobiles may have two or more alternative paths, lies somewhere between these statistics.

It can be seen from the graphs of Figure 3.28 that, if it is accepted that paths within 6 dB of each other are valid alternatives, the proportion of the cell area where mobiles may have access to at least two base stations, is somewhere in the range 30–40%. For the same tolerance the proportion with possible access to three base stations is 12–20%.

In fact, it is usually accepted [27] that, in order to avoid unnecessary handoff, the signal strength has to be set as high as 10–15 dB, implying that the proportion of overlapped area is even larger.

REFERENCES

[1] J.D. Parsons, "Editorial–Land Mobile Radio", *IEE Proceedings,* Vol. 132 Part F, No. 5, August 1985.

[2] W.C. Jakes, *Microwave Mobile Communications*, John Wiley & Sons, 1974.

[3] W.C.Y. Lee, *Mobile Communications Engineering*, McGraw–Hill Inc., 1982

[4] W.C.Y. Lee, *Mobile Communications Design Fundamentals*, Howard W. Sams & Co., 1986.

[5] P.L. Camwell and J.G. McRory, "Experimental Results of In–Building Anisotropic Propagation at 835 MHz Using Leaky Feeders and Dipole Antennas", Montech, 1987.

[6] R.E. Collins, *Antennas and Radiowave Propagation*, McGraw–Hill, Inc., 1985.

[7] J.D. Kraus, *Antennas*, McGraw–Hill, 1950.

[8] J.D. Parsons, *Land Mobile Radio Systems*, ed. R.J.Holbeche, Peter Peregrinus, 1985.

[9] S. Ramo, J.R.Whinnery and V. Duzer, *Fields and Waves in Communication Electronics*, John Wiley & Sons, 1965.

[10] Y. Okumura, E. Ohmori, T. Kawano and K. Fukuda, "Field Strength and Its Variability in VHF and UHF Land Mobile Service", *Rev. Elec. Comm. Lab.*, vol. 16, pp. 825–873, September–October, 1968.

[11] P.L. Rice, A.G. Longley, K.A. Norton and A.P. Barsis, "Transmission Loss Prediction for Tropospheric Communication Circuits", *NBS Tech.*, Note No. 101, Vols. 1, 2, 1967.

[12] K. Bullington, "Radio Propagation Fundamentals", *B.S.T.J. 36*, May 1957.

[13] A.G. Longley and P.E. Rice, "Prediction of Tropospheric Radio Transmission Loss Over Irregular Terrain", *A Computer Method – 1968, ESSA Research Laboratories ERL79-ITS67, U.S. Government Printing Office*, Washington, D.C., 1968.

[14] R.W. Lorenz, "Frequency Planning of Cellular Radio by the Use of Topographical Data Base", *35th IEEE Vehicular Technology Conference*, 1985.

[15] M.F. Ibrahim and J.D. Parsons, "Urban Mobile Radio Propagation at 900 MHz", *Electronics Letters*, pp. 113–115, 1982, 18, (3).

[16] M.F. Ibrahim, J.A. Edwards and J.D. Parsons, "Automated Logging and Analysis System for VHF and UHF Signal Strength Measurements", *Conf. on Radio Receivers and Associated Systems, Leeds, IERE Conference Proceedings No. 50*, July 1981.

[17] W.R. Young, "Mobile Radio Transmission Compared at 150 to 3700 MC" *BSTJ 31*, pp. 1068–1085, November 1952.

[18] D.O. Reudink, "Mobile Radio Propagation in Tunnels", *IEEE Vehicular Technology Group Conference*, San Francisco, Ca., December 2–4, 1968

[19] J.F. Aurand and R.E. Post, "A Comparison of Prediction Methods for 800 MHz Mobile Radio Propagation", *IEEE Trans. Veh. Technology*, Vol. VT-34, No. 4, November 1985.

[20] W.B. Davenport Jr., *Probability and Random Processes*, McGraw-Hill KogaKusha, LTD, International Student Edition, 1970.

[21] M. Schwartz, *Information Transmission, Modulation and Noise*, McGraw-Hill, Inc., 1959.

[22] Edward W.Ng., Murray Geller, "A Table of Integral of the Error Functions", *J. Res. of NBS-B, 73B*, Jan-March 1969.

[23] M.D. Yacoub, "Mobile Radio with Fuzzy Cell Boundaries," *Ph.D Thesis*, University of Essex, England, April 1988.

[24] M.D.Yacoub, D.M. Rodriguez and K.W. Cattermole, "Alternative Routing in Cellular Mobile Radio", *3rd Teletraffic Symposium*, Colchester, England, June 1986.

[25] M.D.Yacoub and K.W. Cattermole, "Cellular Mobile Radio with Fuzzy Cell Boundaries", *4th Teletraffic Symposium*, Bristol, England, May 1987.

[26] "Tables of Bivariate Normal Distribution Function", U.S.A. National Bureau of Standards, 1959.

[27] C.F. Garcia-Hernandez and C.J. Hughes, "Simulation of Handovers Conditions for Cellular Radio Systems", *Electronics Letters*, Vol. 22, No. 17, pp. 904-905 14th August 1986.

[28] K. Loew, "Boundaries Between Radio Cells - Influence of Buildings and Vegetation", *IEE Proceedings*, Vol. 132, Pat F, No. 5, August 1985.

[29] B.R. Davis and R.E. Bogner, "Propagation at 500 MHz for Mobile Radio", *IEE Proceedings*, Vol. 132, Part F, No. 5, August 1985.

[30] I.S. Gradshteym and I.W. Ryahik, Table of Integrals, Series and Products, Academic, New York, 1965.

[31] M. Abramowitz and I.A. Stegun (ed), *Handbook of Mathematical Functions with Formulas, Graphs and Mathematical Tables*, National Bureau of Standards, Applied Mathematical series 55, June 1964.

[32] M. Hata, "Empirical Formula for Propagation Loss in Land-Mobile Radio Services, *IEEE Trans.*, VT-29, pp. 317-325, 1980.

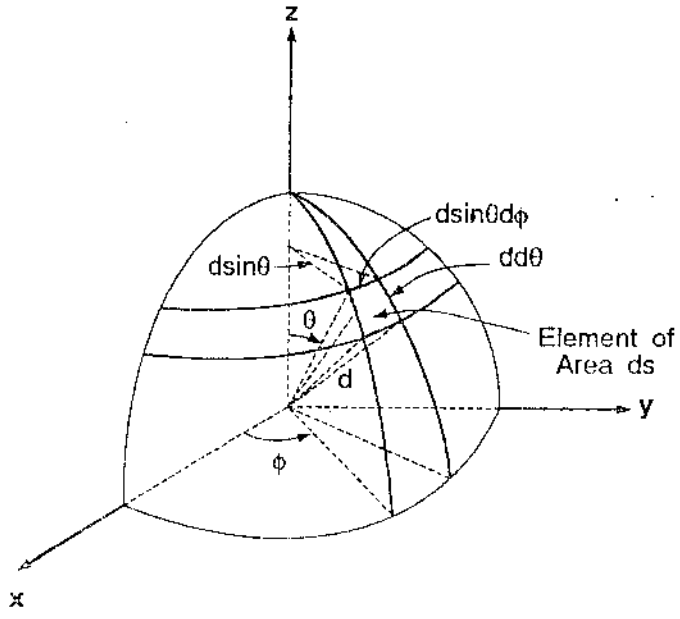
z
dsinθdϕ
dsinθ
ddθ
θ
Element of
Area ds
d
y
ϕ
x

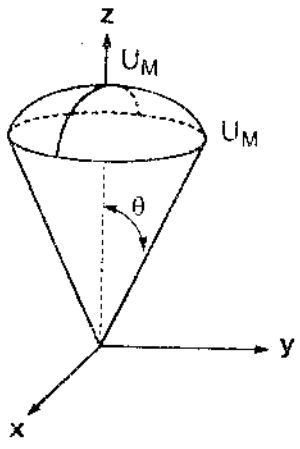
z
U_M
U_M
θ
y
x

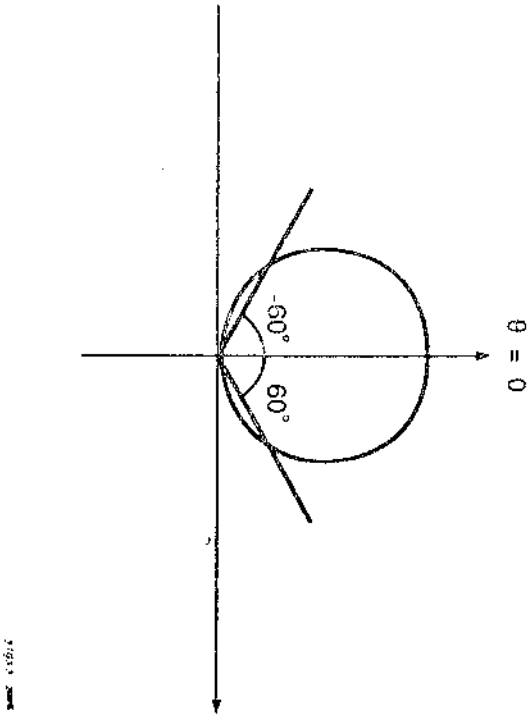

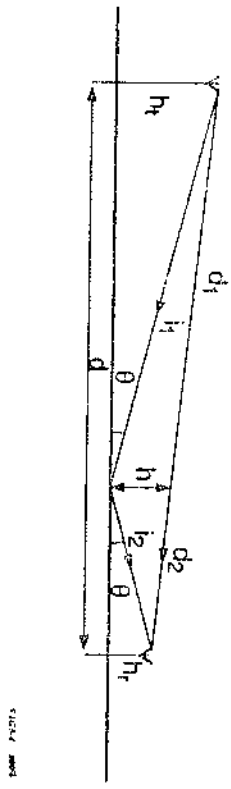

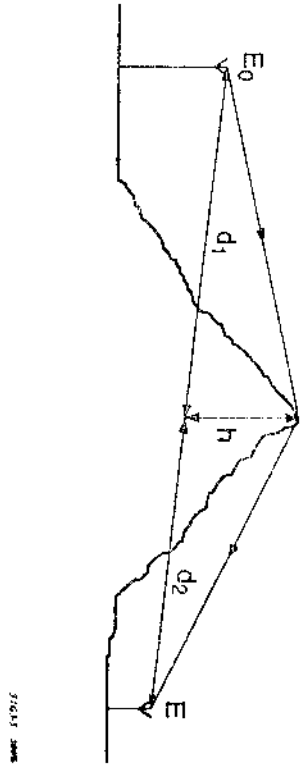

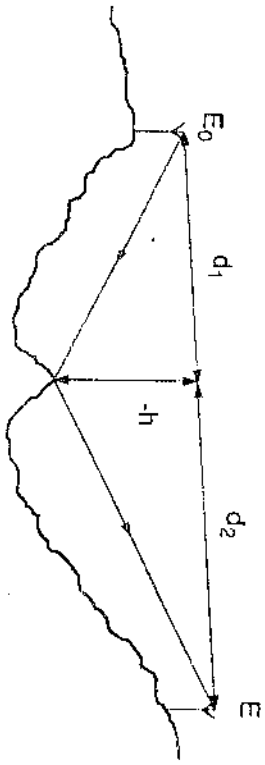

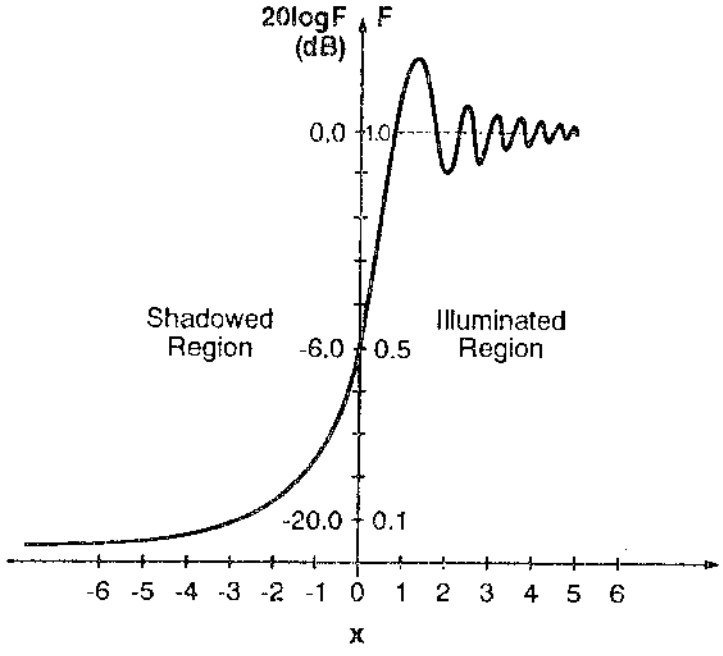
20logF
(dB)
F
0.0
1.0
Shadowed
Region
-6.0
0.5
Illuminated
Region
-20.0
0.1
-6 -5 -4 -3 -2 -1 0 1 2 3 4 5 6
x

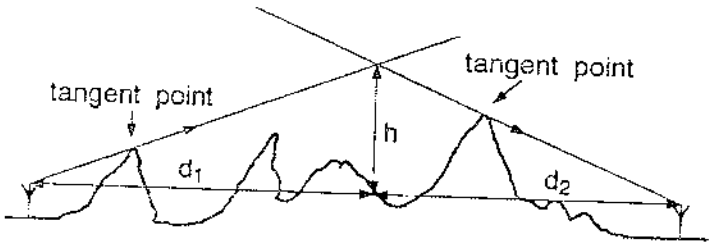

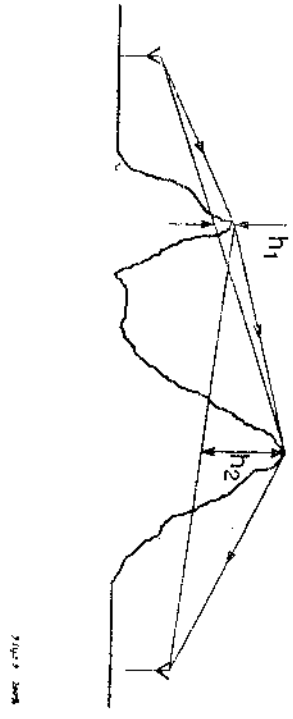

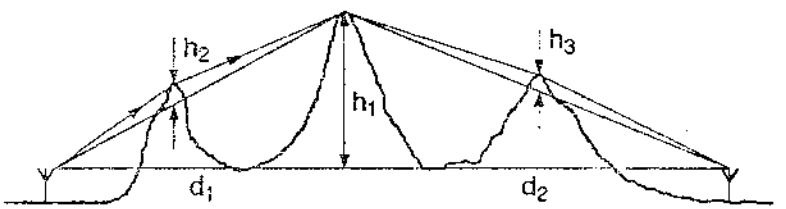

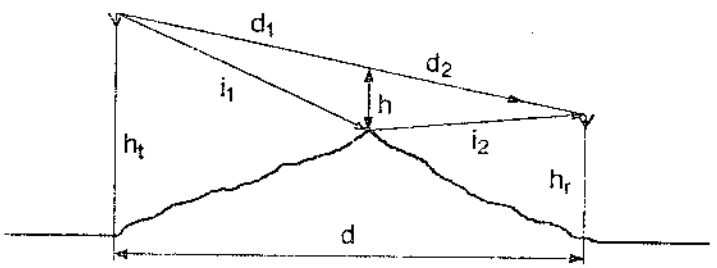

Fig 3-11 2006

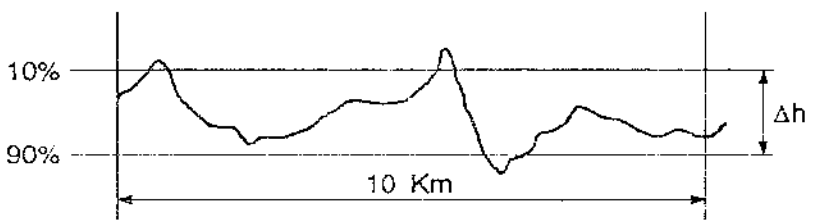

Fig 3-12 2006

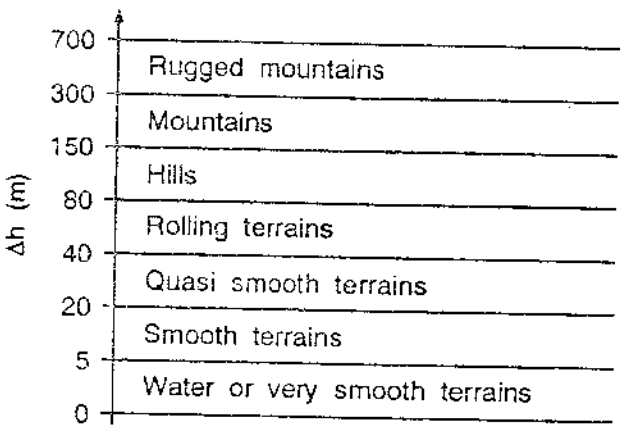

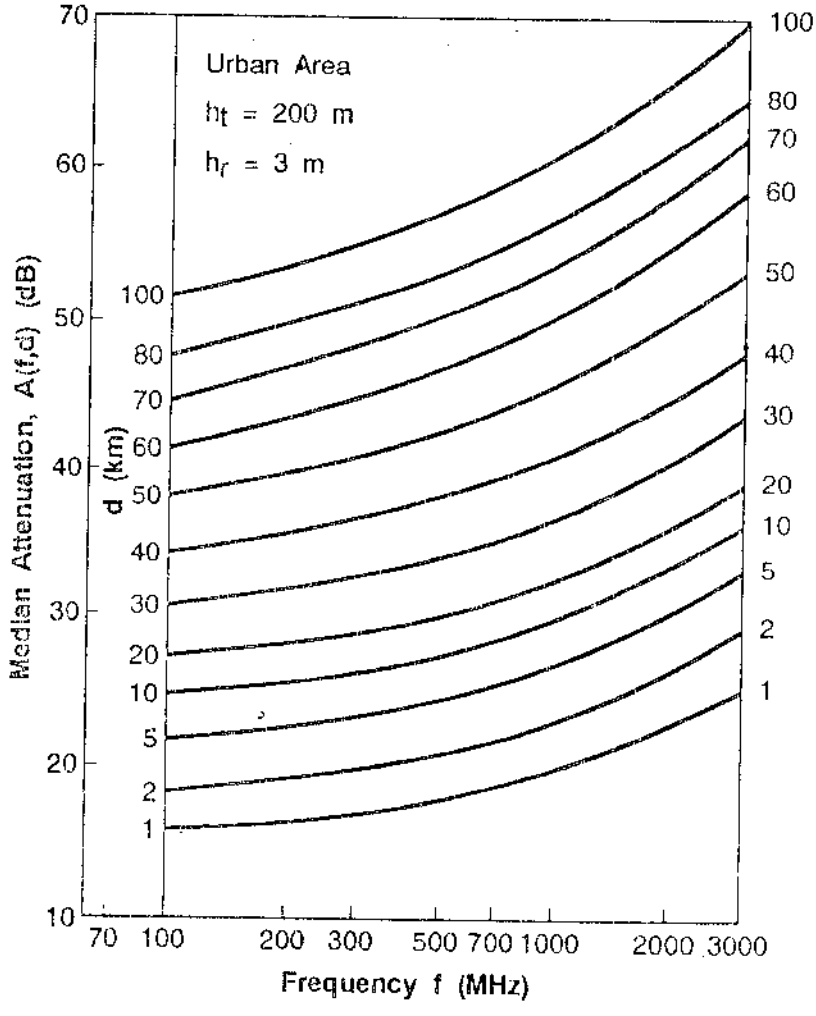

Fig3-14 1906

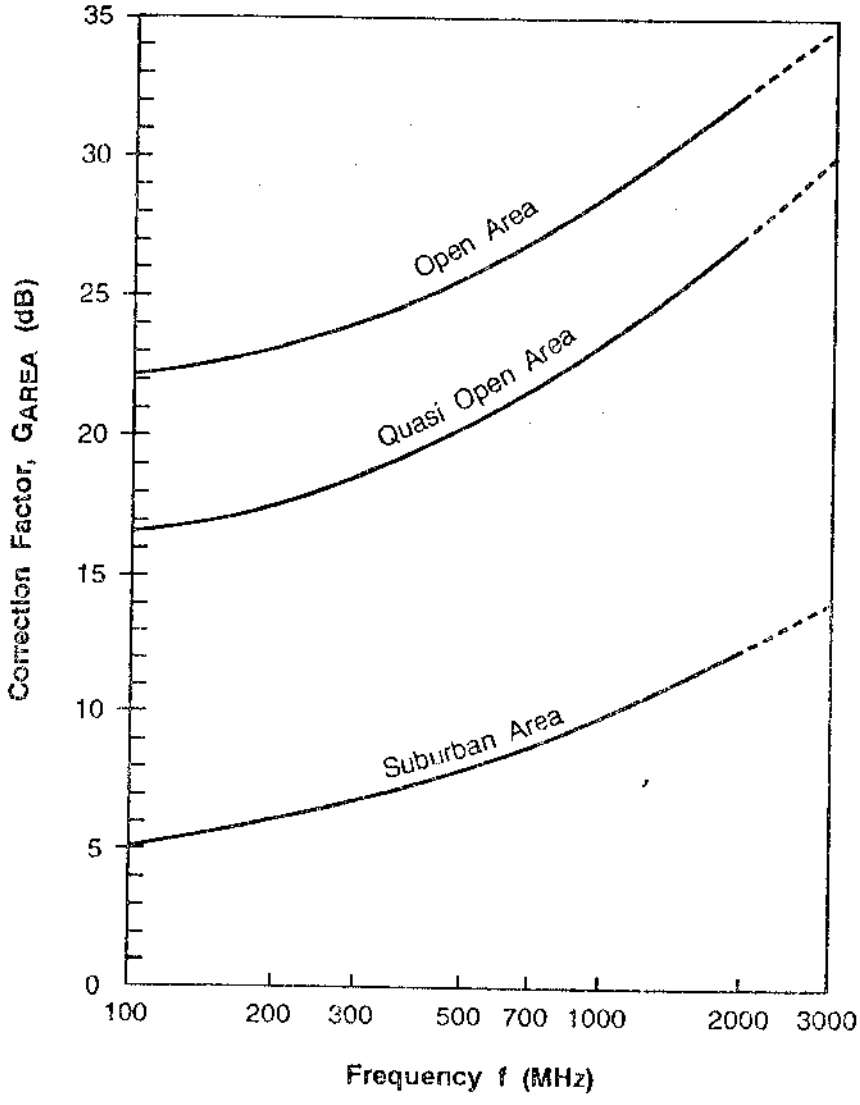

FIG3-15 1509

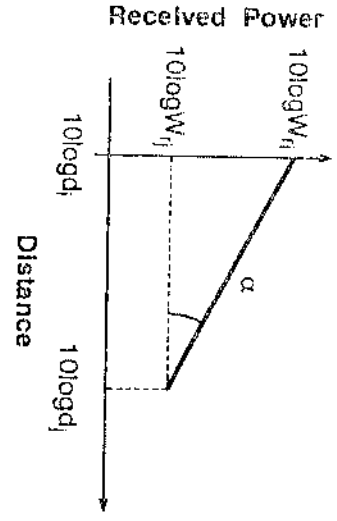

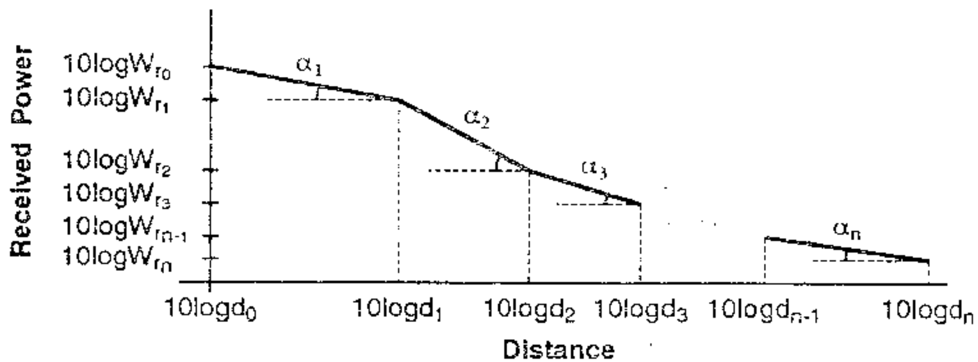

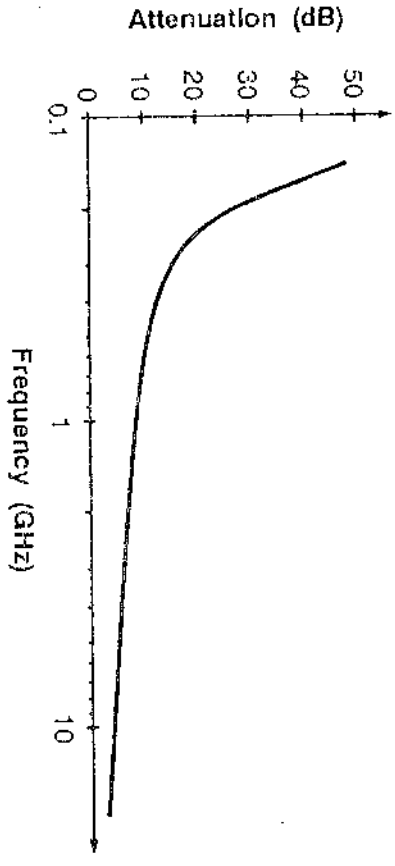

(a)
p(M)
$\frac{\sqrt{2\pi}}{2\pi\sigma_Y}$
1
0
M_Y
Y
(b)
P(Y₀)
1.0
0.5
0
M_Y
Y_0

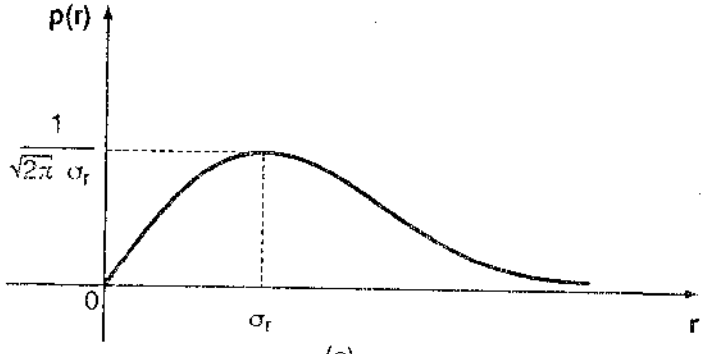

(a)

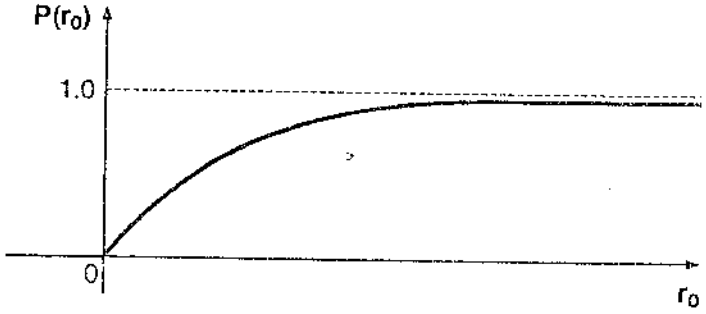

(b)

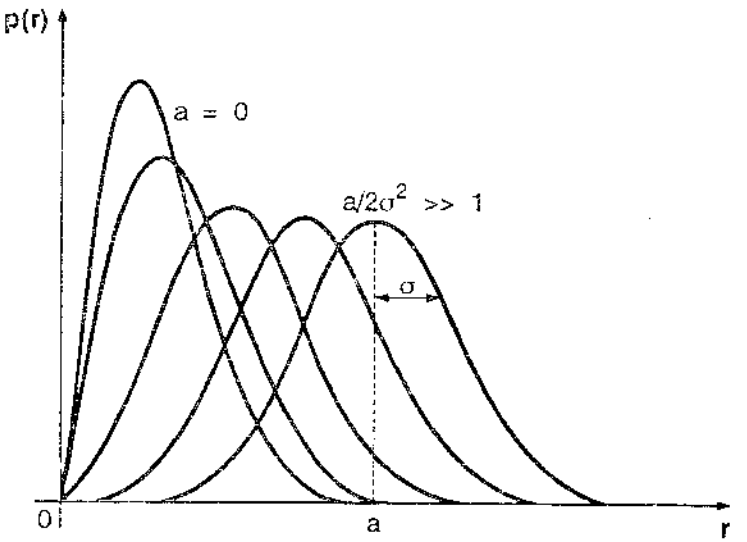

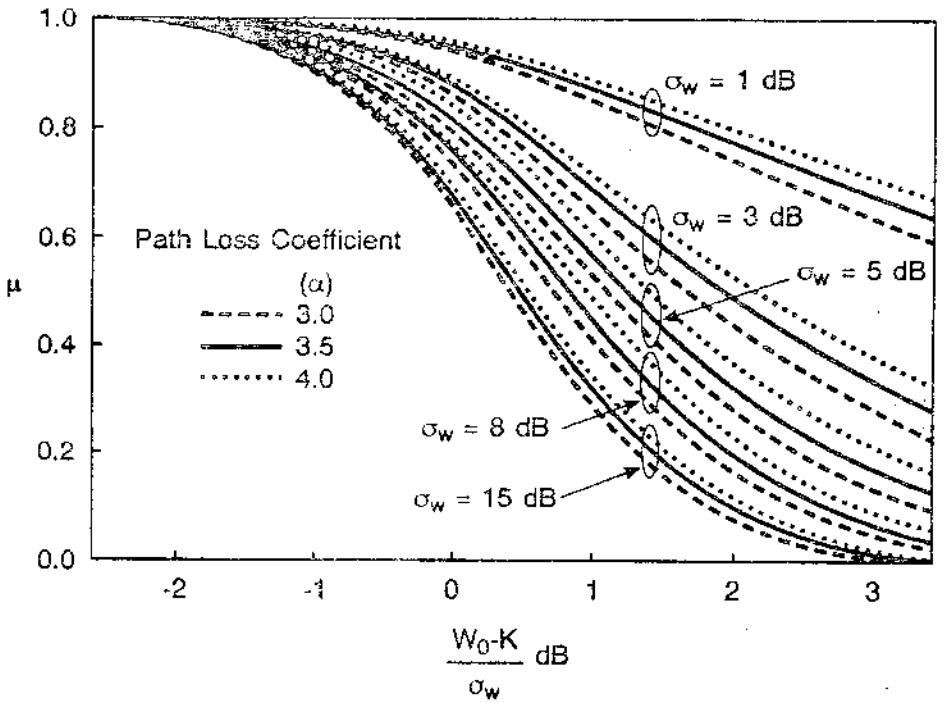
1.0
0.8
0.6
0.4
0.2
0.0
μ
Path Loss Coefficient
(α)
3.0
3.5
4.0
σw = 1 dB
σw = 3 dB
σw = 5 dB
σw = 8 dB
σw = 15 dB
-2
-1
0
1
2
3
W0-K / σw dB

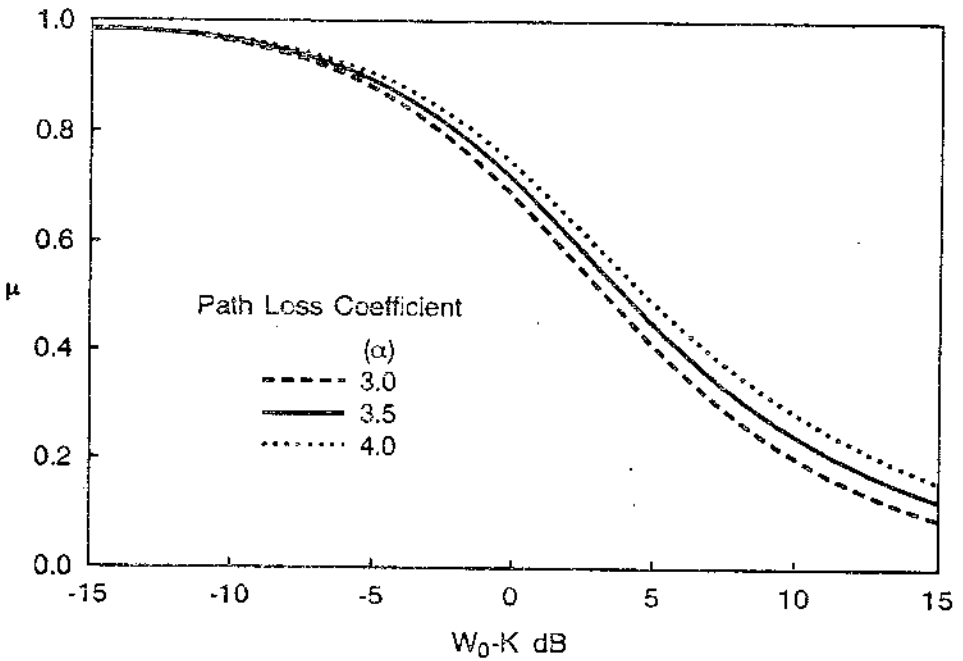
1.0
0.8
0.6
0.4
0.2
0.0
μ
Path Loss Coefficient
(α)
3.0
3.5
4.0
-15
-10
-5
0
5
10
15
W0-K dB

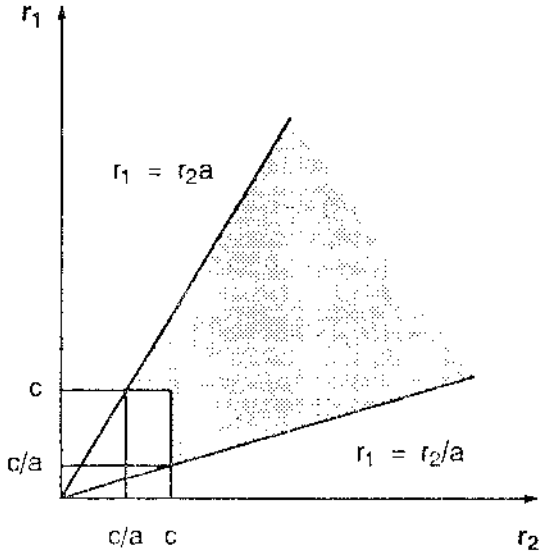
r_1
$r_1 = r_2 a$
c
c/a
$r_1 = r_2/a$
c/a
c
r_2

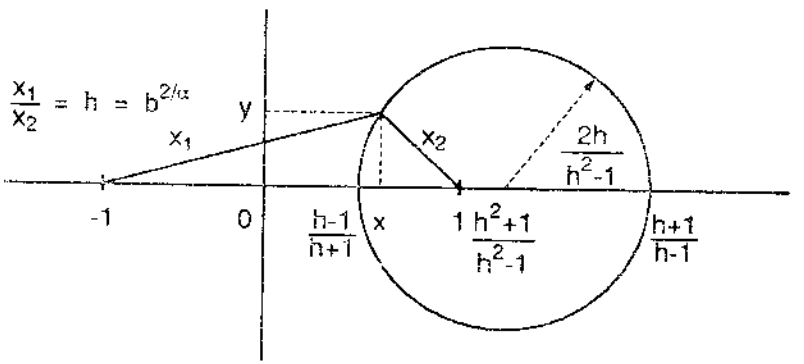
$\frac{x_1}{x_2} = h = b^{2/\alpha}$
y
x_1
x_2
$\frac{2h}{h^2-1}$
-1
0
$\frac{h-1}{h+1}$
x
1
$\frac{h^2+1}{h^2-1}$
$\frac{h+1}{h-1}$

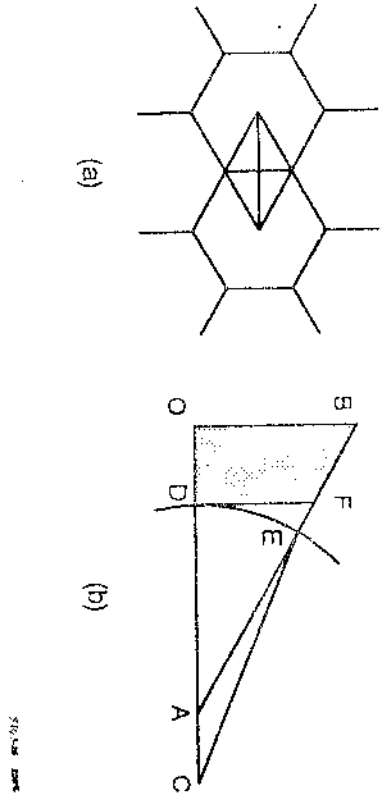

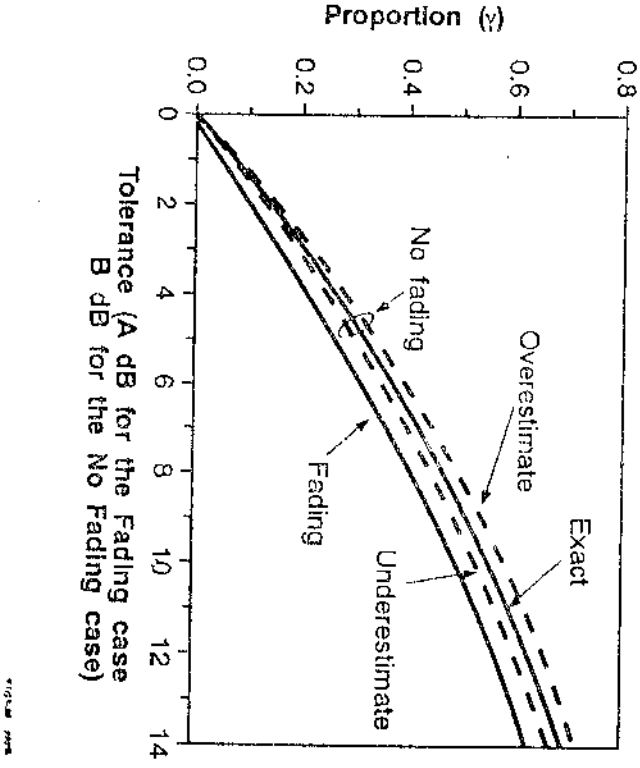

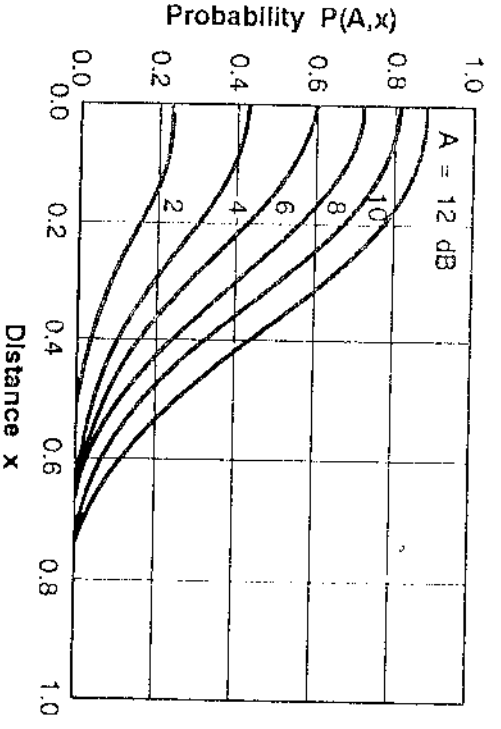

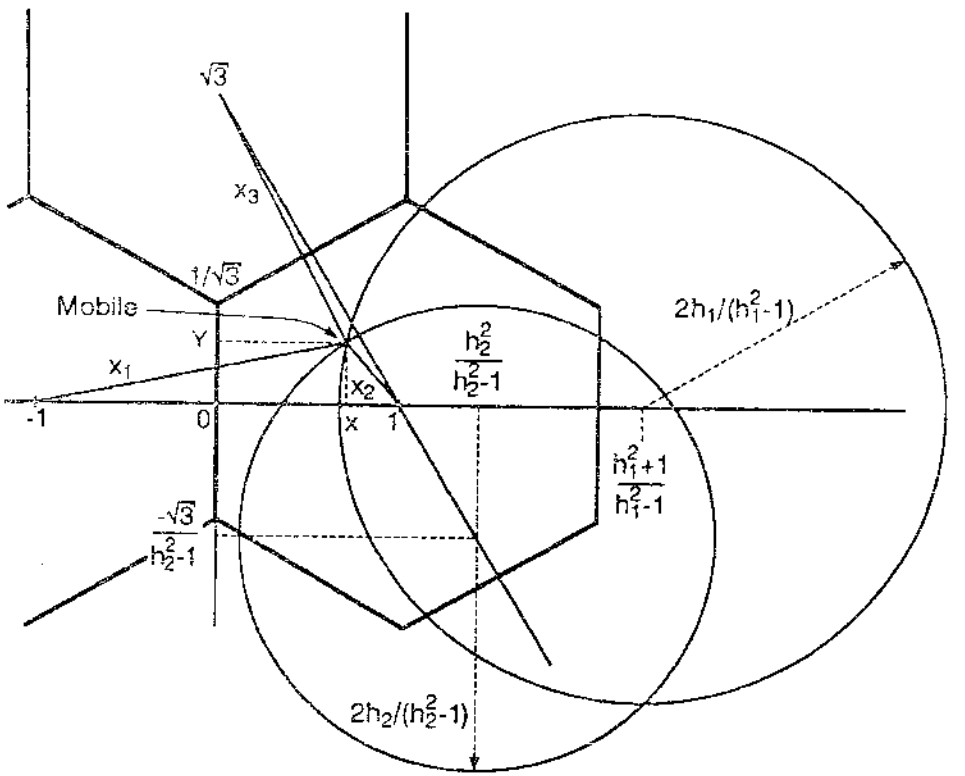

fig3-29 150%

FILE: fig3-30.cdr COLOR: Composite SCREEN: Device's default TIME: Wed Nov 20 14:48:19 1991

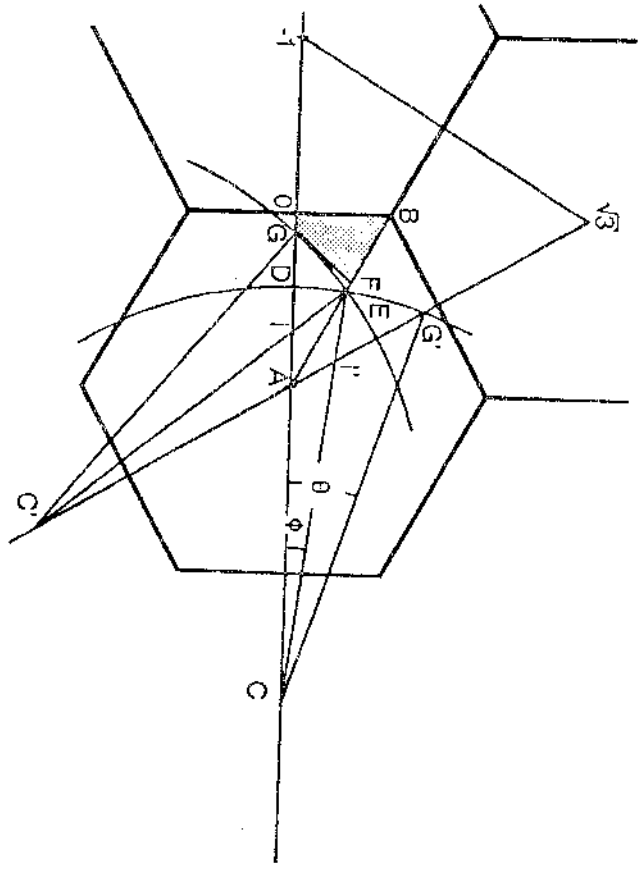

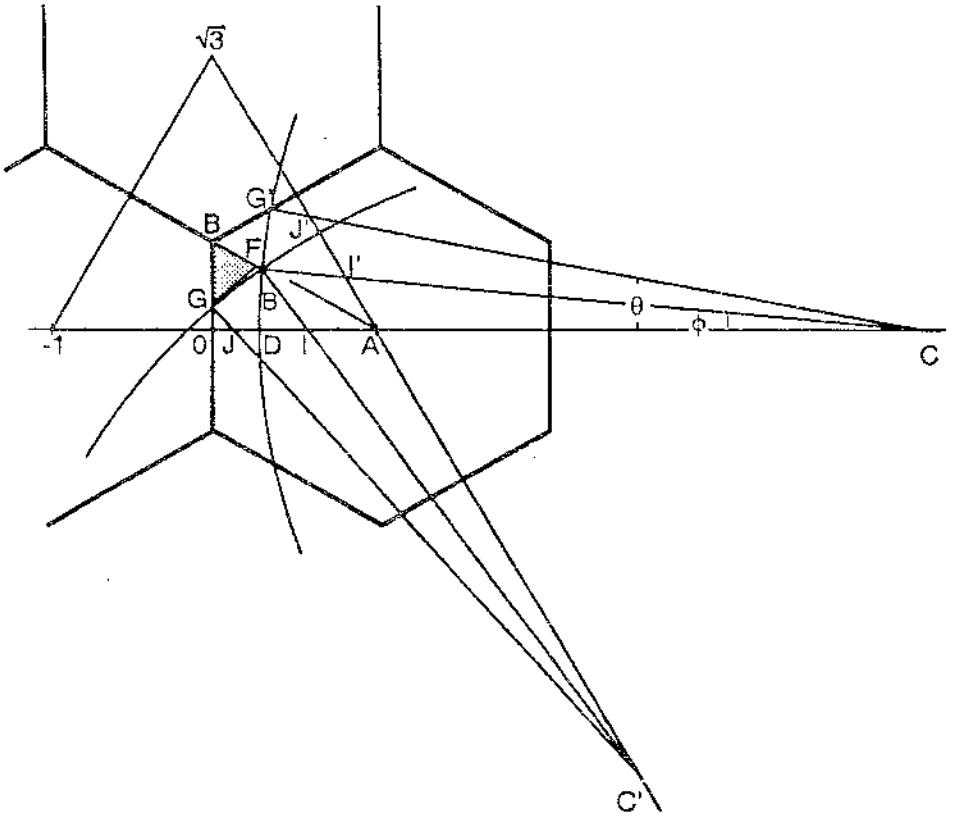

FIG 3-31 150%

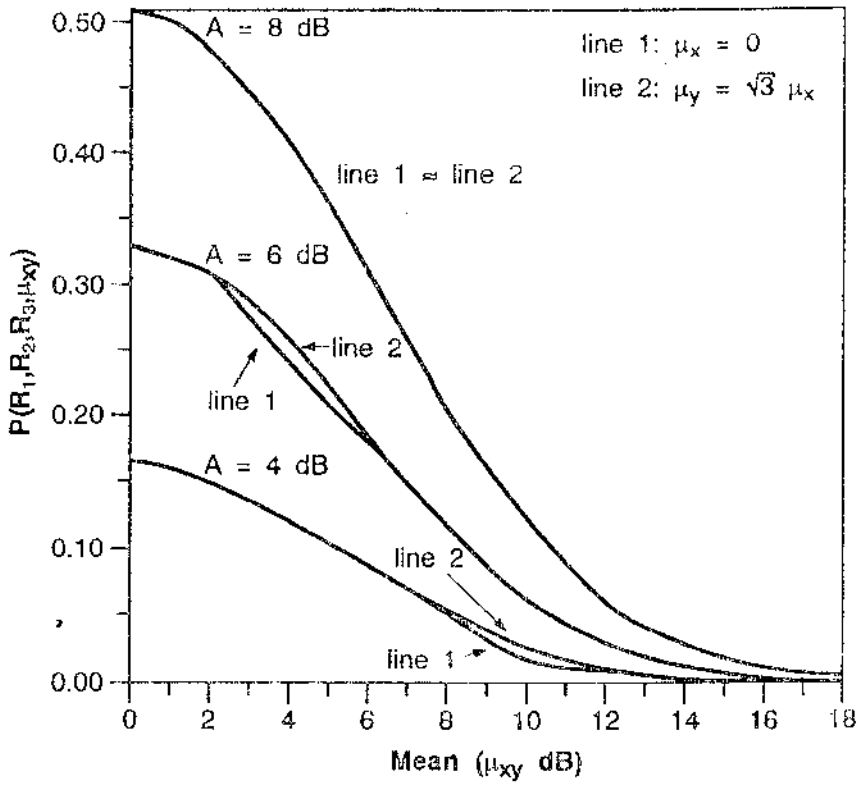

Fig. 4. (98)

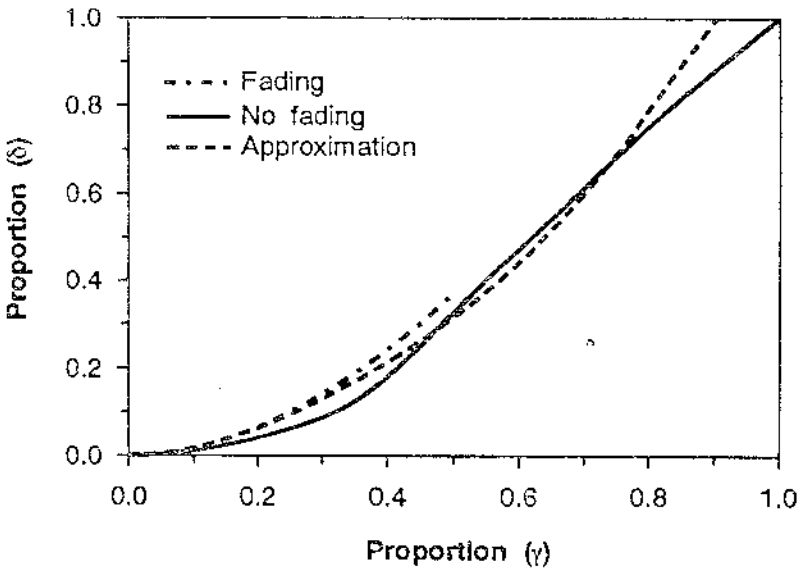

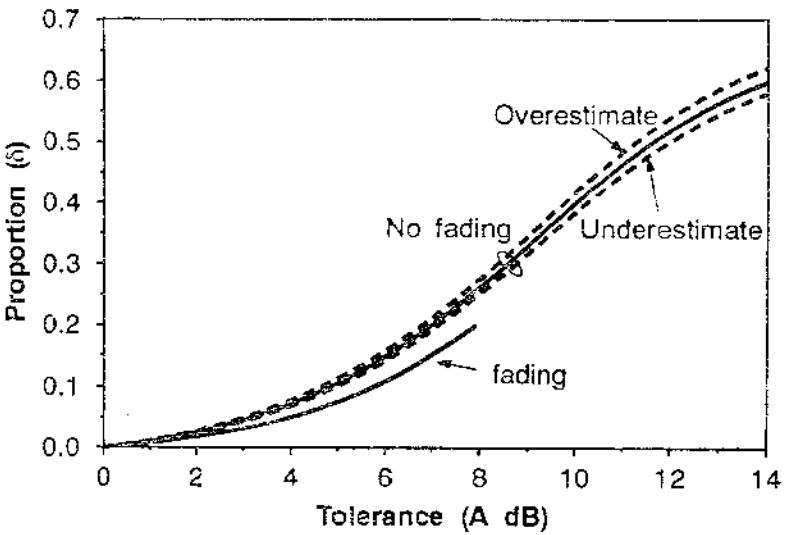

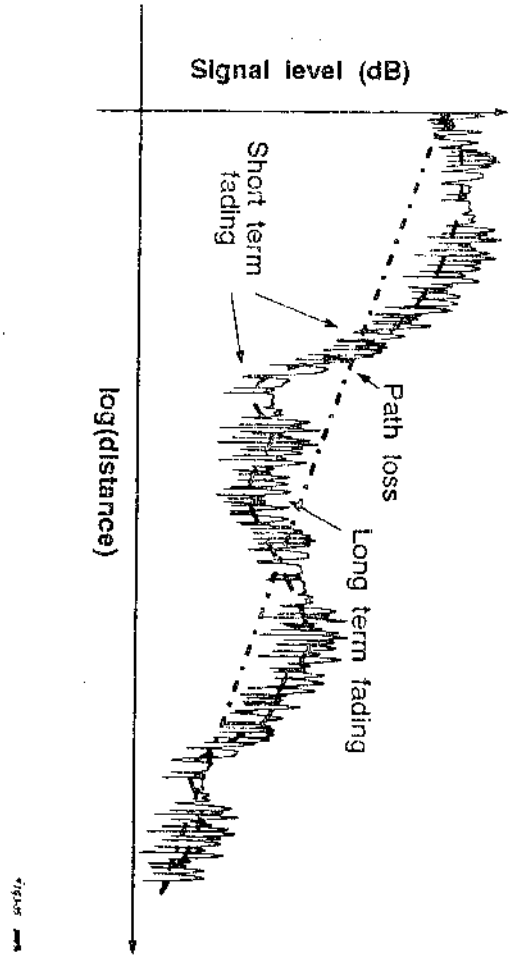

CHAPTER 4

MULTIPATH PROPAGATION EFFECTS

PREAMBLE

In this chapter we select to analyze some of the most relevant aspects to be considered in a multipath propagation environment. We start with the basic concept of wave velocity to, thereafter, derive a relationship describing the frequency deviation of the propagated signal due to the motion of the vehicle. The simple formula is, in fact, an approximation of a more complex one given by the Theory of Relativity. We then study the statistical behaviour of the time delay and the delay spread of the propagated signal. The effect of such delay is analyzed in order to determine how strongly correlated two received signals are, given a time delay or frequency separation between them. The frequency separation for a given correlation factor is named coherence bandwidth. Since in a multipath medium we deal with fast fading, it is interesting to determine how often the fades occur given a threshold voltage level: this is known as level crossing rate. The duration of the fades is also of interest. The next relevant topic is concerned with the study of the randomness of the signal's frequency (phase) variation and its effect on the quality of the received signal. It is shown that this phenomenon, known as random frequency modulation, introduces a noise having a power varying with a quadratic function of the vehicle's speed. We also determine the power spectra of the signal and their dependence on the antenna gain. All of these phenomena can then be observed by means of field measurements. We outline the main points to be considered in the acquisition and analysis of data. We finally show the various manners of implementing fading simulators, including the analog and digital approaches.

4.1 INTRODUCTION

A radio signal transmitted from the base station reaches the mobile station as a large number of scattered waves. The scattering can be provoked by multiple reflections over irregular terrains, presence of a great number of obstructions, variations of the medium's dielectric constant, etc. Due to the randomness of these phenomena, the mobile radio signal is usually treated in a statistical basis. The envelope, phase and frequency of the received signal vary randomly according to some well-known probability distributions. In particular, the envelope follows the Rayleigh distribution, while the phase is uniformly distributed in the range $0-2\pi$ rad..

Other statistics must be determined in order to better characterize the Rayleigh fading signal. One of such statistics is related with the variation of the received envelope. In the same way, a joint distribution of two Rayleigh fading signals is also of interest. With these two statistics it is possible to describe and characterize some of the various multipath propagation effects such as coherence bandwidth, level crossing rate, average duration of fades, random FM and others. Accordingly, we shall dedicate some sections of this chapter to obtain these distributions.

Other related topics treated in this chapter include the Doppler effect, delay spread, signal's power spectra, field measurement and fading simulation.

4.2 VELOCITIES OF WAVE PROPAGATION

Let e be the instantaneous value of the electric field propagating in a dispersive medium. From section 3.4.1 ((equation (3.67))

$$e = E_M \exp(j\omega t) = E_0 \exp(-\alpha r)\, \exp\left[j(\omega t - \beta r)\right] \tag{4.1}$$

where E_0 is the electric field in the free space, r is the distance, ω is the frequency, α is the attenuation constant and β is the phase constant.

Phase Velocity

Phase Velocity (v_p) corresponds to the velocity the wave must travel in order keep its instantaneous phase constant. Hence, for a single-frequency electric field we must have

$$\omega t - \beta r = \text{constant}$$

Therefore,

$$v_p = \frac{dr}{dt} = \frac{\omega}{\beta} \tag{4.2}$$

In a lossless medium the conductivity σ equals 0. Hence from (3.66) $\alpha = 0$ and $\beta = \omega\sqrt{\mu\varepsilon}$ where μ is the magnetic permeability and ε is the electric permittivity. Thus

$$v_p = 1/\sqrt{\mu\varepsilon} \tag{4.3}$$

Since the wavelength λ is defined as the distance the wave propagates within one period ($T = 1/f$), then

$$\lambda = v_p \frac{1}{f} = \frac{\omega}{\beta} \frac{1}{f} = \frac{2\pi}{\beta} \tag{4.4}$$

Group Velocity

In a dispersive medium the spectral components of an arbitrary wave may travel with different speeds, characterizing the phenomenon known as dispersion. In such case the use of the group velocity v_g, as defined in (4.5), is more appropriate

$$v_g = d\omega/d\beta \tag{4.5}$$

The group velocity approximately represents the velocity of the wave and is often referred to as the "velocity of energy travel". From (4.5) and (4.4) it can be shown that

$$v_g = \frac{v_p}{1 - \frac{\omega}{v_p}\frac{dv_p}{d\omega}} \tag{4.6}$$

4.3 DOPPLER FREQUENCY

The Doppler frequency refers to the apparent shift in frequency of the carrier as experienced by a vehicle moving under free space conditions [1].

Insight into the Problem

Consider a vehicle moving at speed v and a carrier with phase velocity v_p arriving at an angle θ as shown in Figure 4.1. The speed of the vehicle will impose an apparent phase velocity v_p' to the wave such that

$$v_p' = v_p - v\cos\theta \tag{4.7}$$

From (4.4) $v_p' = \lambda f'$ and $v_p = \lambda f$ where f' is the apparent frequency and f is the propagated frequency. Using this in (4.7) we have

$$f' = f - f_D \tag{4.8}$$

where

$$f_D = \frac{v}{\lambda}\cos\theta \tag{4.9a}$$

is the Doppler shift. Writing (4.9a) in terms of the angular frequency we obtain

$$\omega_D = \omega_m \cos\theta \tag{4.9b}$$

where $\omega_m \triangleq \beta v$ is the maximum Doppler shift

Relativity Theory

The above approach is very simplistic and does not give the exact solution to the problem. This question is much more intricate and the exact solution is given by the Relativity Theory. The predicted Doppler frequency f' for $\theta = 0^\circ$ is [2].

$$f' = f\,\frac{1 \pm v/c}{\sqrt{1 - (v/c)^2}}$$

where c is the speed of light, v is the speed of the observer and f is the propagated

frequency. The plus sign in the numerator applies to the case when either the observer or the source is moving away from each other. The minus sign refers to the opposite situation. Using Newton's binomial expansion in (4.10), for the plus sign case we have

$$f' = f\left[1 - \frac{v}{c} + \frac{1}{2}\left(\frac{v}{c}\right)^2 - \ldots.\right] \tag{4.11}$$

Since the ratio v/c is usually very small we may neglect the higher order terms. Therefore,

$$f' \simeq f - fv/c$$

Given that $c = \lambda f$, then

$$f' \simeq f - v/\lambda \tag{4.12}$$

as would be obtained by the "simplistic" solution given by (4.8) and (4.9) when $\theta = 0$.

As an example consider a vehicle moving at 72 Km/h (20 m/s) and frequency of 1000 MHz ($\lambda = 0.3$ m). Then the maximum Doppler shift is $20/0.3 \simeq 66.7$ Hz.

4.4 DELAY SPREAD

Due to the multipath propagation, a transmitted signal arrives at the receiver at different time instants and with different amplitudes. If an impulse $a\delta(t)$, having "amplitude" a is propagated at time instant $t = 0$, the received signal will be h(t), such that

$$h(t) = \sum_{i=1}^{n} a_i \, \delta(t - T_i) \tag{4.13}$$

where n is the number of scatterers, a_i is the "amplitude" of the received impulse due to the $i^{\underline{th}}$ path and T_i is the time delay of the $i^{\underline{th}}$ arrived impulse. The longer the path, the smaller the received amplitude, the longer the time delay. Accordingly, we may expect the received signals to have a profile as sketched in Figure 4.2.

The impulse arrival time T is usually characterized by a probability density function. Accordingly, the *mean time delay* $\overline{T}$ is the mean of this density function and the *delay spread* σ_T corresponds to its standard deviation. Let p(T) be the probability density function of T. Its $k^{\underline{th}}$ moment is

$$E\left[T^k\right] \triangleq \int_0^\infty T^k p(T)\, dT$$

Therefore, the mean time delay is

$$\overline{T} = E\,[T] \tag{4.14}$$

and the delay spread is

$$\sigma_T = \left\{E\,[T^2] - E^2[T]\right\}^{1/2} \tag{4.15}$$

An exact characterization of the impulse arrival time is not available. In general, a negative exponential distribution is used to describe its density function. Accordingly,

$$p(T) = \frac{1}{\overline{T}} \exp\left(-\frac{T}{\overline{T}}\right) \tag{4.16}$$

With such distribution both the mean time delay and the delay spread are equal to $\overline{T}$.

In practice, the delay spreads vary from fractions of microseconds to many microseconds. In urban areas the delays are usually longer (greater than 3 μs) while in suburban areas and in open areas they are shorter (0.5 μs and less than 0.2 μs, respectively). The characterization of the delay spread is very important for digital mobile radio applications where intersymbol interference may occur (refer to Chapter 6 and Chapter 10).

4.5 COHERENCE BANDWIDTH

Consider an arbitrary radio signal with a given bandwidth, propagating in a mobile radio environment. Due to the multipath effect, each frequency component of this signal may reach the destination (the mobile station) with different time delays. It is, therefore, essential to determine the maximum frequency separation for which the signals are still considered to be correlated. This frequency separation is named *Coherence Bandwidth.*

Systems operating with channels substantially narrower than the coherence bandwidth are known as *narrowband systems. Wideband systems* are those operating with channels wider than the coherence bandwidth. In the narrowband systems all of the components of the signal are equally influenced by the multipath propagation. Accordingly, although with different amplitudes and affected by noise and interference, the received signal is essentially "the same" as the transmitted signal. In other words, the radio signal experiences non-selective fading. In the wideband systems the various frequency components of the signal may be differently affected by the fading, characterizing the phenomenon known as selective fading.

In order to estimate the coherence bandwidth, the first step is to determine the envelope and phase correlations between two signals arriving at two different time instants. This can only be carried out if the joint probability density function of these signals is known. Accordingly, in the next sections we shall (i) model the received signal, (ii) determine their joint density function, (iii) calculate the envelope and (iv) phase correlations and finally (v) the coherence bandwidth.

4.5.1 Received Signal

Let $e_0 = E_0 \exp(j\omega t)$ be a transmitted wave, propagating in the mobile radio environment. If we consider only one radio path, the received wave is that given by (4.1). However, due to the multipath propagation, each path of length r_i will impose a phase shift equal to $\beta r_i = (\omega/v) r_i = \omega T_i$, where T_i is the time delay of the i^{th}

path. Moreover, each delayed wave i, arriving at an angle θ_i, will contribute to a Doppler shift equal to $\omega_i = \beta v \cos\theta_i$. Therefore, the i^{th} received wave e_i can be written as

$$e_i = E_0 \exp(-\alpha_i r_i) \exp\left[j(\omega t + \omega_i t - \omega T_i)\right] \tag{4.17}$$

where α_i is the attenuation constant of the i^{th} path.

If we consider that the propagated wave has been reflected by n scatterers, then within an infinitesimal time delay dT and arrival angle dθ, the resultant signal received by an omnidirectional antenna, is*

$$e = E_0 \sum_{i=1}^{n} a_i \exp\left[j(\omega t + \omega_i t - \omega T_i)\right] \tag{4.18a}$$

where $a_i^2 = \exp^2(-\alpha_i r_i) p(\theta_i) d\theta p(T_i) dT$

In the above equation the term $p(\theta_i)d\theta p(T_i)dT$ represents the fraction of the incoming power within $d\theta$ of the angle θ and within dT of the time T in the limit with i very large.

Since we are only interested in the effects of the multipath propagation (and not in the effects of the shadowing) we shall assume $\exp(\alpha_i r_i) = 1$. We further assume an uniform distribution in angle of the incident power. Hence, $p(\theta) = 1/2\pi$ for

---

* Rigorously speaking, for each scatterer i causing the reflected wave to arrive at an angle θ_i and with a time delay T_i, there are m other scatterers causing m other waves to arrive at m different angles but with the same time delay. Consequently, the received wave is

$$e = E_0 \sum_{i=1}^{n} \sum_{j=1}^{m} a_{ij} \exp\left[j(\omega t + \omega_{ij} t + \omega T_i)\right]$$

where $a_{ij}^2 = \exp^2(-\alpha_i r_1) p(\theta_{ij}) d\theta p(T_i) dT$

and $\omega_{ij} = \beta v \cos\theta_{ij}$

The only implication of having a double-sum in the expression for the received wave is that in our calculations with $n \to \infty$ and $m \to \infty$, the double sum becomes double integrals. We obviously take this into account, as shall be seen in the following paragraphs. We decided, however, to keep (4.18a) with a single sum just for simplification.

$0 \le \theta \le 2\pi$ rad. and $p(\theta) = 0$, otherwise. Using (4.16) for the density of T, it follows that

$$\lim_{I \to \infty} a_I^2 = \frac{1}{2\pi\bar{T}} \exp\left(-\frac{T}{\bar{T}}\right) d\theta \, dT \tag{4.18b}$$

Taking the real part of the signal e given by (4.18a), we obtain

$$s(t) \triangleq Re(e) = X \cos\omega t - Y \sin\omega t \tag{4.19a}$$

where

$$\begin{aligned} X &= E_0 \sum_{I=1}^{n} a_I \cos(\omega_I t - \omega T_I) \triangleq r \cos\varphi \\ Y &= E_0 \sum_{I=1}^{n} a_I \sin(\omega_I t - \omega T_I) \triangleq r \sin\varphi \end{aligned} \tag{4.19b}$$

Note that $r^2 = X^2 + Y^2$ is the envelope of the signal and $\varphi = \tan^{-1}(Y/X)$ is its phase. As shown in section 3.4.2, r is Rayleigh distributed, while φ is uniformly distributed in the range $0-2\pi$ rad.. The random variables X and Y have a Gaussian distribution.

4.5.2 Joint Probability Density Function

Consider two signals $s_J(t)$, $J = 1, 2$, propagated at frequencies ω_J, $J = 1, 2$. Assume that $s_1(t)$ arrives at an instant t and $s_2(t)$ at $t + \tau$, where τ is a time delay. The four corresponding Gaussian random variables are

$$\begin{aligned} X_1 &= E_0 \sum_{I=1}^{n} a_I \cos(\omega_I t - \omega_1 T_I) \triangleq r_1 \cos\varphi_1 \\ Y_1 &= E_0 \sum_{I=1}^{n} a_I \sin(\omega_I t - \omega_1 T_I) \triangleq r_1 \sin\varphi_1 \\ X_2 &= E_0 \sum_{I=1}^{n} a_I \cos(\omega_I t + \omega_I \tau - \omega_2 T_I) \triangleq r_2 \cos\varphi_2 \\ Y_2 &= E_0 \sum_{I=1}^{n} a_I \sin(\omega_I t + \omega_I \tau - \omega_2 T_I) \triangleq r_2 \cos\varphi_2 \end{aligned} \tag{4.20}$$

We want to determine the joint distribution of X_1, Y_1, X_2 and Y_2.

An n-dimensional Gaussian probability density function is written as follows [4].

$$p(R_1,R_2,\ ...,R_n) = \frac{\exp\left[-\frac{1}{2|\Lambda|}\sum_{j=1}^{n}\sum_{k=1}^{n}|\Lambda|_{jk}(R_j-M_j)(R_k-M_k)\right]}{(2\pi)^{n/2}\ |\Lambda|^{1/2}} \tag{4.21}$$

where R_j, $j = 1, \ldots, n$ are the random variables

$M_j = E\left[R_j\right]$ are their mean values

and $|\Lambda|_{jk}$ is the cofactor of the element λ_{jk} of the determinant $|\Lambda|$. The matrix Λ is called *Covariance Matrix* and its elements λ_{jk} are the covariances, defined as follows.

$$\begin{aligned}\lambda_{jk} \triangleq \text{Cov}\ (R_j,R_k) &= E\left[(R_j-M_j)(R_k-M_k)\right] \\ &= E\left[R_jR_k\right] - M_kE\left[R_j\right] - M_jE\left[R_k\right] + M_jM_k = \\ &= E\left[R_jR_k\right] - E\left[R_j\right]\ E\left[R_k\right]\end{aligned} \tag{4.22}$$

For the random variables X_1, Y_1, X_2 and Y_2 we assume the following covariance matrix

$$\Lambda = \begin{bmatrix} \text{Cov}(X_1,X_1) & \text{Cov}(X_1,Y_1) & \text{Cov}(X_1,X_2) & \text{Cov}(X_1,Y_2) \\ \text{Cov}(Y_1,X_1) & \text{Cov}(Y_1,Y_1) & \text{Cov}(Y_1,X_2) & \text{Cov}(Y_1,Y_2) \\ \text{Cov}(X_2,X_1) & \text{Cov}(X_2,Y_1) & \text{Cov}(X_2,X_2) & \text{Cov}(X_2,Y_2) \\ \text{Cov}(Y_2,X_1) & \text{Cov}(Y_2,Y_1) & \text{Cov}(Y_2,X_2) & \text{Cov}(Y_2,Y_2) \end{bmatrix} \tag{4.23}$$

In order to compose the covariance matrix we must determine the various moments $E\left[R_jR_k\right]$, $E\left[R_j\right]$ and $E\left[R_k\right]$. In particular

$$E\left[X_1\right] = \langle X_1 \rangle = E_\theta \sum_{i=1}^{n} \langle a_i\cos(\omega_i t - \omega_i T_i)\rangle = 0 \tag{4.24}$$

where

$$\langle x(t) \rangle = \lim_{T\to\infty} \frac{1}{2T} \int_{-T}^{T} x(t)\ dt$$

is the time average of x(t) over the period 2T. In the same way $E\left[X_1\right] = E\left[Y_1\right] = E\left[X_2\right] = E\left[Y_2\right] = 0$. Therefore, in this case $\mathrm{Cov}\left[R_j R_k\right] = E\left[R_j R_k\right]$. Then

$$\mathrm{Cov}\left[X_1,X_1\right] = E\left[X_1^2\right] = \langle X_1^2 \rangle = E_0^2 \sum_{i,j} \langle a_i a_j \cos(\omega_i t - \omega_1 T_i)\cos(\omega_j t - \omega_1 T_i)\rangle$$

It is clear that the above average will vanish unless i = j. In this case $\langle a_i^2\cos^2(\omega_i t - \omega_1 T_i)\rangle = a_i^2/2$. Therefore,

$$\mathrm{Cov}\left[X_1,X_1\right] = \sigma^2 \sum_i a_i^2$$

where $\sigma^2 = E_0^2/2$ (refer to section 3.4.2).

In the limit with $i\to\infty$, the above equation takes the integral form. Then

$$\mathrm{Cov}\left[X_1,X_1\right] = \sigma^2 \int_0^{2\pi}\int_0^{\infty} \frac{1}{2\pi\overline{T}} \exp\left(-\frac{T}{\overline{T}}\right) d\theta\, dT = \sigma^2 \tag{4.25}$$

Similarly,

$$\mathrm{Cov}\left[X_i,X_i\right] = \mathrm{Cov}\left[Y_i,Y_i\right] = \sigma^2, \quad i = 1, 2 \tag{4.26}$$

$$\mathrm{Cov}\left[X_1,Y_1\right] = \mathrm{Cov}\left[Y_1,X_1\right] = \mathrm{Cov}\left[X_2,Y_2\right] = \mathrm{Cov}\left[Y_2,X_2\right] = 0 \tag{4.27}$$

$$\mathrm{Cov}\left[X_1,X_2\right] = \mathrm{Cov}\left[X_2,X_1\right] = \mathrm{Cov}\left[Y_1,Y_2\right] = \mathrm{Cov}\left[Y_2,Y_1\right] \triangleq \mu_1, \quad \text{to be determined}$$

$$\mathrm{Cov}\left[X_1,Y_2\right] = \mathrm{Cov}\left[Y_2,X_1\right] = -\mathrm{Cov}\left[Y_1,X_2\right] = -\mathrm{Cov}\left[X_2,Y_1\right] \triangleq \mu_2, \text{to be determined}$$

Using the same procedure

$$\mu_1 = E\left[X_1X_2\right] = \langle X_1X_2 \rangle = E_0^2 \sum_{i,j} \langle a_i a_j \cos(\omega_i t - \omega_1 T_i)\cos(\omega_j t + \omega_j \tau - \omega_2 T_j)\rangle$$

The average will vanish unless i = j. For this case, using a well known trigonometric identity, we have

$$\mu_1 = E\left[X_1\, X_2\right] = \sigma^2 \sum_i a_i^2 \cos(\omega_i \tau - \Delta\omega T_i)$$

where $\Delta\omega = \omega_2 - \omega_1$ and $\sigma^2 = E_0^2/2$

In the limit, with $1 \to \infty$

$$\mu_1 = \sigma^2 \int_0^{2\pi}\int_0^{\infty} \frac{1}{2\pi\overline{T}} \exp\left(-\frac{T}{\overline{T}}\right)\cos(\beta v\tau\cos\theta - \Delta\omega T)\, d\theta\, dT$$

Then

$$\mu_1 = \frac{\sigma^2 J_0(\omega_m \tau)}{1 + (\Delta\omega\overline{T})^2} \tag{4.28}$$

where $\omega_m = \beta v$ is the maximum Doppler shift and

$$J_n(z) = \frac{1}{\pi}\int_0^{\pi} \cos(z\sin x - nx)dx, \quad n \text{ integer}$$

is the Bessel function of the first kind of order n

In a similar way,

$$\mu_2 = \frac{-\sigma^2\Delta\omega\overline{T}J_0(\omega_m\tau)}{1 + (\Delta\omega\overline{T})^2} \tag{4.29}$$

Therefore, the covariance matrix is

$$\Lambda = \begin{bmatrix} \sigma^2 & 0 & \mu_1 & \mu_2 \\ 0 & \sigma^2 & -\mu_2 & \mu_1 \\ \mu_1 & -\mu_2 & \sigma^2 & 0 \\ \mu_2 & \mu_1 & 0 & \sigma^2 \end{bmatrix}$$

Its determinant is given by

$$|\Lambda| = \sigma^8 (1 - \rho^2)^2 \tag{4.30}$$

where

$$\rho^2 = \frac{\mu_1^2 + \mu_2^2}{\sigma^4} \tag{4.31a}$$

Using (4.28) and (4.29) in (4.31a) we obtain

$$\rho^2 = \frac{J_0^2(\omega_m \tau)}{1 + (\Delta\omega\bar{T})^2} \tag{4.31b}$$

After a tedious procedure to determine the cofactors $|\Lambda|_{jk}$ we arrive at the following joint distribution

$$p(X_1,Y_1,X_2,Y_2) = \frac{1}{4\pi^2\sigma^4(1-\rho^2)} \exp\left\{-\frac{1}{2\sigma^8(1-\rho^2)^2}\left[\sigma^2(X_1^2 + Y_1^2 + X_2^2 + Y_2^2)\right.\right.$$

$$\left.\left. - 2\mu_1(X_1X_2 + Y_1Y_2) - 2\mu_2(X_1Y_2 - X_2Y_1)\right]\right\} \tag{4.32}$$

The above density can be expressed in terms of the random variables r_1, φ_1, r_2 and φ_2. Hence

$$p(r_1,r_2,\varphi_1,\varphi_2) = |J|p(X_1,Y_1,X_2,Y_2) \tag{4.33}$$

where $|J|$ is the Jacobian of the transformation, given by

$$J = \begin{bmatrix} \frac{\partial X_1}{\partial r_1} & \frac{\partial X_1}{\partial \varphi_1} & \frac{\partial X_1}{\partial r_2} & \frac{\partial X_1}{\partial \varphi_2} \\ \frac{\partial Y_1}{\partial r_1} & \frac{\partial Y_1}{\partial \varphi_1} & \frac{\partial Y_1}{\partial r_2} & \frac{\partial Y_1}{\partial \varphi_2} \\ \frac{\partial X_2}{\partial r_1} & \frac{\partial X_2}{\partial \varphi_1} & \frac{\partial X_2}{\partial r_2} & \frac{\partial X_2}{\partial \varphi_2} \\ \frac{\partial Y_2}{\partial r_1} & \frac{\partial Y_2}{\partial \varphi_1} & \frac{\partial Y_2}{\partial r_2} & \frac{\partial Y_2}{\partial \varphi_2} \end{bmatrix} \tag{4.34}$$

After determining the required derivatives of (4.20) and substituting them in (4.34) we obtain (unbelievable!).

$$|J| = r_1 r_2 \tag{4.35}$$

Therefore,

$$p(r_1,r_2,\varphi_1,\varphi_2) = \frac{r_1 r_2}{4\pi^2\sigma^4(1-\rho^2)} \exp\left\{-\frac{1}{2\sigma^8(1-\rho^2)^2}\left[\sigma^2(r_1^2 + r_2^2)\right.\right.$$

$$\left.\left. - 2r_1r_2\mu_1\cos(\varphi_2-\varphi_1) - 2r_1r_2\mu_2\sin(\varphi_2-\varphi_1)\right]\right\} \qquad (4.36)$$

The joint density of the envelope is

$$p(r_1,r_2) = \int_0^{2\pi}\int_0^{2\pi} p(r_1,r_2,\varphi_1,\varphi_2)\, d\varphi_1\, d\varphi_2$$

Then

$$p(r_1,r_2) = \frac{r_1 r_2}{\sigma^4(1-\rho^2)} \exp\left[-\frac{r_1^2 + r_2^2}{2\sigma^2(1-\rho^2)}\right] I_0\left(\frac{r_1 r_2 \rho}{\sigma^2(1-\rho^2)}\right) \qquad (4.37)$$

where $I_0(x)$ is the modified Bessel function of zero order (refer to equation (3.90b)).

In a similar way, the joint density of the phases is

$$p(\varphi_1,\varphi_2) = \int_0^{\infty}\int_0^{\infty} p(r_1,r_2,\varphi_1,\varphi_2)\, dr_1\, dr_2$$

Then

$$p(\varphi_1,\varphi_2) = \left(\frac{1-\rho^2}{4\pi^2}\right) \frac{\left(1-U^2\right)^{1/2} + U\cos^{-1}(-U)}{\left(1-U^2\right)^{3/2}} \qquad (4.38)$$

where

$$U = \rho\cos\left[\varphi_2 - \varphi_1 + \tan^{-1}(\Delta\omega\bar{T})\right]$$

Note that if both signals are independent then $\mu_1 = \mu_2 = \rho = 0$ and $I_0(0) = 1$. Therefore,

$$p(r_1,r_2) = p(r_1)\, p(r_2) = \frac{r_1 r_2}{\sigma^4} \exp\left[-\frac{r_1^2 + r_2^2}{2\sigma^2}\right]$$

In the same way, $U = 0$ and

$$p(\varphi_1,\varphi_2) = p(\varphi_1,\varphi_2) = \frac{1}{4\pi^2}$$

as expected.

4.5.3 Envelope Correlation

The normalized envelope covariance, also known as envelope correlation coefficient, is given by [4]

$$\rho_r = \frac{\mathrm{Cov}(r_1,r_2)}{\sqrt{\mathrm{Var}(r_1)}\sqrt{\mathrm{Var}(r_2)}} = \frac{E\left[r_1 r_2\right] - E\left[r_1\right]\,E\left[r_2\right]}{\sqrt{E\left[r_1^2\right] - E^2\left[r_1\right]}\;\sqrt{E\left[r_2^2\right] - E^2\left[r_2\right]}} \tag{4.39}$$

From section (3.4.2)

$$E\left[r_1\right] = E\left[r_2\right] = \sqrt{\pi/2}\,\sigma$$
$$\mathrm{Var}(r_1) = \mathrm{Var}(r_2) = (2 - \pi/2)\sigma^2 \tag{4.40}$$

The joint moment of the envelope is

$$E\left[r_1\, r_2\right] = \int_0^\infty \int_0^\infty r_1 r_2\; p(r_1,r_2)\; dr_1\; dr_2 \tag{4.41}$$

where $p(r_1,r_2)$ is given by (4.37). Using tables of integrals [5] we obtain

$$E\left[r_1\, r_2\right] = \frac{\pi}{2}\,\sigma^2\; F(-1/2,\; -1/2;\; 1;\; \rho^2) \tag{4.42}$$

where F(a, b; c; z) is the hypergeometric function. This function can be evaluated by [6].

$$F(a,\; b;\; c;\; z) = \sum_{n=0}^{\infty} \frac{(a)_n\,(b)_n}{(c)_n}\,\frac{z^n}{n!}$$
$$= 1 + \frac{ab}{c}\,z + \frac{a(a+1)\;b(b+1)}{c(c+1)}\,\frac{z^2}{2!} + \cdots \tag{4.43}$$

Expanding (4.42) as in (4.43) we obtain

$$E\left[r_1\, r_2\right] = \frac{\pi}{2}\,\sigma^2\left[1 + \left(\frac{1}{2}\right)^2\rho^2 + \left(\frac{1}{2}\right)^6\rho^4 + \left(\frac{1}{2}\right)^9\rho^6 + \cdots\right]$$

If the higher order terms are neglected,

$$E\left[r_1\, r_2\right] \approx \frac{\pi}{2}\,\sigma^2\left[1 + \left(\frac{\rho}{2}\right)^2\right] \tag{4.44}$$

With (4.40) and (4.44) in (4.39) we have

$$\rho_r = \frac{\pi}{4(4-\pi)}\,\rho^2 \approx \rho^2 \tag{4.45}$$

Therefore, from (4.31b)

$$\rho_r = \frac{J_0^2(\omega_m \tau)}{1 + (\Delta\omega\bar{T})^2} \tag{4.46}$$

Note that, from (4.46) the larger the frequency separation $\Delta\omega$ and/or the larger the delay spread $\bar{T}$, the smaller the correlation coefficient. Moreover, the correlation coefficient is a quadratic function of $J_0(\omega_m\tau)$. Figure 4.3 shows some plots of the correlation coefficient.

4.5.4 Phase Correlation

In a way similar to the envelope correlation, the phase correlation is given by

$$\rho_\varphi = \frac{E\left[\varphi_1\varphi_2\right] - E\left[\varphi_1\right]\,E\left[\varphi_2\right]}{\sqrt{E\left[\varphi_1^2\right] - E^2\left[\varphi_1\right]}\;\sqrt{E\left[\varphi_2^2\right] - E^2\left[\varphi_2\right]}} \tag{4.47}$$

Both phases φ_1 and φ_2 are random variables uniformly distributed in the range 0-2π rad.. In other words

$$p(\varphi_i) = \begin{cases} 1/2\pi & ,\ 0 \le \varphi_i \le 2\pi \qquad i = 1,\ 2 \\ 0 & ,\ \text{otherwise} \end{cases}$$

Therefore,

$$E\left[\varphi_1\right] = E\left[\varphi_2\right] = \frac{1}{2\pi} \int_0^{2\pi} \varphi \, d\varphi = \pi$$

$$E\left[\varphi_1^2\right] = E\left[\varphi_2^2\right] = \frac{1}{2\pi} \int_0^{2\pi} \varphi^2 \, d\varphi = \frac{4}{3} \pi^2 \tag{4.48}$$

Hence

$$\rho_\varphi = \frac{3}{\pi^2} \left(E\left[\varphi_1 \varphi_2\right] - \pi^2 \right) \tag{4.49}$$

The expectation $E\left[\varphi_1 \, \varphi_2\right]$ is given by

$$E\left[\varphi_1 \, \varphi_2\right] = \int_0^{2\pi} \int_0^{2\pi} \varphi_1 \varphi_2 \, p(\varphi_1, \varphi_2) \, d\varphi_1 \, d\varphi_2 \tag{4.50}$$

where $p(\varphi_1, \varphi_2)$ is given by (4.38)

The integral (4.50) does not lend itself to a closed form evaluation. A good approximation to this integral is given by Jakes [7] as follows

$$E\left[\varphi_1 \, \varphi_2\right] = \pi^2 \left[1 + \Gamma(\rho,\phi) + 2\Gamma^2(\rho,\phi) - \frac{1}{4\pi^2} \sum_{n=1}^{\infty} \frac{\rho^{2n}}{n^2} \right] \tag{4.51}$$

where

$$\Gamma(\rho,\phi) = \frac{1}{2\pi} \sin^{-1}(\rho \cos\phi)$$

$$\phi = - \tan^{-1}(\Delta\omega \overline{T})$$

and

$$\rho^2 = \frac{J_0^2(\omega_m \tau)}{1 + (\Delta\omega \overline{T})^2}$$

Finally, the phase correlation is

$$\rho_\varphi = 3 \, \Gamma(\rho,\phi) \left[1 + 2\Gamma(\rho,\phi) \right] - \frac{3}{4\pi^2} \sum_{n=1}^{\infty} \frac{\rho^{2n}}{n^2} \tag{4.52}$$

For a time delay $\tau = 0$ we have the plot of the phase correlation as shown in

Figure 4.4.

4.5.5 Coherence Bandwidth

There is not a rigid rule used to determine the coherence bandwidth. One well-accepted criterion establishes that the coherence bandwidth corresponds to the frequency separation for which the envelope correlation equals 0.5.

Let B_c be the coherence bandwidth. As far as envelope correlation is concerned, for a time delay $\tau = 0$, it follows that, from (4.46)

$$\rho_r = \frac{J_0^2(\omega_m 0)}{1 + (\Delta\omega\overline{T})^2} = 0.5$$

Then,

$$B_c \triangleq \frac{\Delta\omega}{2\pi} = \frac{1}{2\pi\overline{T}} \tag{4.53}$$

As for the phase correlation, the coherence bandwidth is extracted from the Figure 4.4. Hence

$$B_c = \frac{1}{4\pi\overline{T}} \tag{4.54}$$

Note that the coherence bandwidth given by (4.53) is always greater than that given by (4.54). Therefore, to be on the safe side (4.53) should preferably be used. Thus, for a delay spread $\overline{T} = 2\ \mu s$, the corresponding B_c is 80 kHz. Values of delay spread exceeding $10\mu s$ are comparatively rare [1]. Consider $\overline{T} = 5\mu s$, such that $B_c = 32$ kHz. Consequently, a narrowband FM system of up to 30 kHz bandwidth would essentially experience non-selective fading. However, wideband systems will obviously experience selective fading.

4.6 LEVEL CROSSING RATE

Level crossing rate is defined as the average number of times a fading signal crosses a given signal level within a certain period. Let the time variation of the

received envelope r be $\dot{r}$ ($\dot{r} \triangleq dr/dt$) and the crossing signal level be R. Hence, the level crossing rate R_c is the mean value of $\dot{r}$ at $r = R$, i.e.,

$$R_c = E\left[\dot{r} \mid r=R\right] = \int_0^\infty \dot{r}\, p(R,\dot{r})\, d\dot{r} \tag{4.55}$$

where $p(R,\dot{r})$ is the joint probability density function of r and $\dot{r}$ at $r = R$.

Joint Probability Density Function

Consider the fading signal as described by (4.19b). Their derivatives are

$$\dot{X} = E_0 \beta v \sum_{i=1}^{n} -a_i \sin(\omega_i t - \omega T_i)\cos\theta_i$$

$$\dot{Y} = E_0 \beta v \sum_{i=1}^{n} a_i \cos(\omega_i t - \omega T_i)\cos\theta_i \tag{4.56}$$

By following the same steps as in section 4.5.2 we arrive at

$$E\left[\dot{X}\right] = E\left[\dot{Y}\right] = E\left[XY\right] = E\left[X\dot{X}\right] = E\left[X\dot{Y}\right] = E\left[Y\dot{X}\right] = E\left[Y\dot{Y}\right] = E\left[\dot{X}\dot{Y}\right] = 0$$

$$E\left[X^2\right] = E\left[Y^2\right] = E_0^2/2 = \sigma^2 \tag{4.57}$$

$$E\left[\dot{X}^2\right] = E\left[\dot{Y}^2\right] = (E_0 \beta v/2)^2 \triangleq \dot{\sigma}^2$$

(note that $\dot{\sigma}$ is not the derivative of σ, but just a notation).

The above results are then used to compose the covariance matrix Λ. Note that, from (4.57) Λ is a diagonal matrix with the diagonal elements equal to σ^2, σ^2, $\dot{\sigma}^2$ and $\dot{\sigma}^2$.

Accordingly, its determinant is $|\Lambda| = \sigma^4\, \dot{\sigma}^4$. Using these results in (4.21) we obtain

$$p(X,Y,\dot{X},\dot{Y}) = \frac{1}{4\pi^2\sigma^2\dot{\sigma}^2} \exp\left[-\frac{1}{2}\left(\frac{X^2+Y^2}{\sigma^2} + \frac{\dot{X}^2+\dot{Y}^2}{\dot{\sigma}^2}\right)\right] \tag{4.58}$$

With the transformation of variables we have

$$p(r,\dot{r},\varphi,\dot{\varphi}) = |J|\; p(X,Y,\dot{X},\dot{Y}) \tag{4.59}$$

where J is the Jacobian of the transformation. From (4.19b)

$$X = r\cos\varphi$$

$$Y = r\sin\varphi$$

Therefore

$$\dot{X} = \dot{r}\cos\varphi - r\dot{\varphi}\sin\varphi$$

$$\dot{Y} = \dot{r}\sin\varphi + r\dot{\varphi}\cos\varphi \qquad (4.60)$$

The Jacobian is easily found to be* $|J| = r^2$. Thus

$$p(r,\dot{r},\varphi,\dot{\varphi}) = \frac{r^2}{4\pi^2\sigma^2\dot{\sigma}^2}\exp\left[-\frac{1}{2}\left(\frac{r^2}{\sigma^2} + \frac{\dot{r}^2 + r^2\dot{\varphi}^2}{\dot{\sigma}^2}\right)\right] \qquad (4.61)$$

The distribution $p(r,\dot{r})$ can be obtained by integrating (4.61) over φ from 0 to 2π and over $\dot{\varphi}$ from $-\infty$ to ∞. Hence

$$p(r,\dot{r}) = \frac{r}{\sigma^2\sqrt{2\pi\dot{\sigma}^2}}\exp\left[-\frac{1}{2}\left(\frac{r^2}{\sigma^2} + \frac{\dot{r}^2}{\dot{\sigma}^2}\right)\right] \qquad (4.62)$$

Using (4.62) in (4.55) we have

$$R_c = \frac{1}{\sqrt{2\pi}}\frac{\dot{\sigma}}{\sigma^2}R\exp\left[-\left(\frac{R}{\sqrt{2}\,\sigma}\right)^2\right] \qquad (4.63)$$

With σ and $\dot{\sigma}$ given by (4.57)

$$R_c = \sqrt{2\pi}\,f_m\frac{R}{\sqrt{2}\,\sigma}\exp\left[-\left(\frac{R}{\sqrt{2}\,\sigma}\right)^2\right] \qquad (4.64)$$

where $f_m = \omega_m/2\pi = \beta v/2\pi = v/\lambda$ is the maximum Doppler shift. The curve $R_c/\sqrt{2\pi}\,f_m$ versus $R/\sqrt{2}\,\sigma$ is plotted in Figures 4.5 and 4.6.

Note that the maximum rate occurs at $R = \sigma$ (obtained from

---

* Equation (4.34) may be used with the following adaptations

X,Y	in place of	X_1,Y_1
$\dot{X},\dot{Y}$	in place of	X_2,Y_2
r,φ	in place of	r_1,φ_1
$\dot{r},\dot{\varphi}$	in place of	r_2,φ_2

$dR_c/d(R/\sqrt{2}\,\sigma) = 0$). In other words, since the rms value of the envelope* is $\sqrt{2}\,\sigma$, the maximum rate occurs at a level 3 dB below this value. In this case $R_c = 1.08\ f_m$. As an example, consider a mobile travelling at 72 km/h and a frequency of 900 MHz. Then $f_m = v/\lambda = 60$ Hz and $R_c = 65$ crossings/s at the rms value of the received envelope.

Let N_c be the mean number of crossings within a period of time T. Then $N_c = R_c T$, and at the maximum R_c

$$N_c = 1.08\ vT/\lambda = 1.08\ d/\lambda$$

where d is the distance travelled by the vehicle in T. Therefore, the mean distance between crossings at the maximum rate is $d/N_c = 0.93\ \lambda$. It is shown in Appendix 5A that the overall mean distance between crossings is approximately equal to $\lambda/2$.

4.7 AVERAGE DURATION OF FADES

Given a signal level R, the average duration of fades is the ratio between the total time the received signal is below R and the total number of fades, both measured during a time interval T. Let τ be the average duration of fades and τ_i the duration of each fade, then

$$\tau = \frac{\sum \tau_i}{R_c T} \tag{4.65}$$

The ratio $\sum \tau_i/T$ in (4.65) corresponds to the probability that the signal is below R. Hence

$$\tau = \frac{1}{R_c}\ \text{prob}\,[r \le R] = \frac{1}{R_c} \int_0^R p(r)\ dr \tag{4.66}$$

Using (3.88) in the above equation we obtain

---

* Refer to section 3.4.2

$$\tau = \frac{1}{\sqrt{2\pi}\, f_m\, (R/\sqrt{2}\,\sigma)} \left[\exp\left(\frac{R}{\sqrt{2}\,\sigma} \right)^2 - 1 \right] \tag{4.67}$$

Figures 4.5 and 4.6 show a plot of the normalized average fade duration. Note that, at the maximum crossing rate ($R = \tau$), the average duration of fade is $0.33/f_m$. For the example of the previous section where $f_m = 60$ Hz, the fade duration is 5.5 ms.

4.8 RANDOM FREQUENCY MODULATION

The random nature of the time-varying phase of the fading signal causes a phenomenon known as Random Frequency Modulation (random FM). As we shall see, the random FM adds an extra noise component to the already deteriorated signal, having a power proportional to the square of the vehicle's speed.

4.8.1 Probability Distribution

Since the random variable φ describes the fading signal's phase, its derivative $\dot{\varphi}$ characterizes the random FM. Its probability density function $p(\dot{\varphi})$ is obtained from (4.61) as follows

$$p(\dot{\varphi}) = \int_0^{\infty} \int_{-\infty}^{\infty} \int_0^{2\pi} p(r, \dot{r}, \varphi, \dot{\varphi})\, dr\, d\dot{r}\, d\varphi$$

Hence

$$p(\dot{\varphi}) = \frac{\sigma}{2\dot{\sigma}} \left[1 + \frac{\sigma^2}{\dot{\sigma}^2}\, \dot{\varphi}^2 \right]^{-3/2} \tag{4.68}$$

The corresponding distribution is

$$P(\dot{\Phi}) = \text{prob}(\dot{\varphi} \le \dot{\Phi}) = \int_{-\infty}^{\dot{\Phi}} p(\dot{\varphi}) d\dot{\varphi}$$

Then

$$P(\dot{\Phi}) = \frac{1}{2} + \frac{\sigma}{2\dot{\sigma}}\,\dot{\Phi}\left[1 + \frac{\sigma^2}{\dot{\sigma}^2}\,\dot{\Phi}^2\right]^{-1/2} \tag{4.69}$$

From (4.57), $\sigma/\dot{\sigma} = \sqrt{2}/\beta v$. Thus

$$p(\dot{\varphi}) = \frac{1}{\sqrt{2}\,\beta v}\left[1 + \frac{2}{(\beta v)^2}\,\dot{\varphi}^2\right]^{-3/2} \tag{4.70}$$

and

$$P(\dot{\Phi}) = -\frac{1}{2} + \frac{1}{\sqrt{2}\,\beta v}\,\dot{\Phi}\left[1 + \frac{2}{(\beta v)^2}\,\dot{\Phi}^2\right]^{-3/2} \tag{4.71}$$

Both functions are plotted in Figure 4.7

4.8.2 Power Spectrum

The power spectrum of a power signal is defined as the Fourier transform of its autocorrelation function (refer to Appendix 9A). Let $R_{\dot{\varphi}}(\tau)$ be the autocorrelation function of $\dot{\varphi}$. Then

$$R_{\dot{\varphi}}(\tau) = E\left[\dot{\varphi}(t)\,\dot{\varphi}(t-\tau)\right]$$

Rice [8] showed that

$$R_{\dot{\varphi}}(\tau) = -\frac{1}{2}\left\{\left[\frac{R_X'(\tau)}{R_X(\tau)}\right]^2 - \left[\frac{R_X''(\tau)}{R_X(\tau)}\right]^2\right\}\ln\left\{1 - \left[\frac{R_X(\tau)}{R_X(0)}\right]^2\right\} \tag{4.72}$$

where $R_X(\tau)$ is the autocorrelation function of X. The random variable X is given by (4.19b).

We have already determined the correlation $E\left[X_1X_2\right]$ of the signals X_1 and X_2 as given by (4.28). Note that, if the frequency separation $\Delta\omega$ between X_1 and X_2 is nil, then (4.28) is the autocorrelation function of $X_1(=X)$. Accordingly,

$$R_X(\tau) = \sigma^2 J_0(\omega_m \tau)$$

Then

$$\frac{R_X(\tau)}{R_X(0)} = J_0(\omega_m \tau)$$

$$\frac{R_X'(\tau)}{R_X(\tau)} = \frac{1}{R_X(\tau)} \frac{dR_X(\tau)}{d\tau} = -\omega_m \frac{J_1(\omega_m \tau)}{J_0(\omega_m \tau)}$$

$$\frac{R_X''(\tau)}{R_X(\tau)} = \frac{1}{R_X(\tau)} \frac{d^2R_X(\tau)}{d\tau^2} = \omega_m^2 \left[\frac{J_1(\omega_m \tau)}{\omega_m \tau \, J_0(\omega_m \tau)} - 1 \right] \qquad (4.73)$$

Therefore, the power spectrum $S_\varphi^{\cdot}(f)$ is

$$S_\varphi^{\cdot}(f) = \int_{-\infty}^{\infty} R_\varphi^{\cdot}(\tau) \exp(-j\omega\tau) \, d\tau = 2\int_0^{\infty} R_\varphi^{\cdot}(\tau) \cos(\omega\tau) \, d\tau \qquad (4.74)$$

The above integral has been evaluated by numerical methods [7] and the result is shown in Figure 4.8.

Within the audio frequency (300–3400 Hz), an asymptotic form, as that given by (4.75) [7], can be used with fairly accurate results, for mobiles travelling with a speed not exceeding 96 km/h (60 mi/h). Then

$$\lim_{f \to \infty} S_\varphi^{\cdot}(f) = \left[(\dot{\sigma}/\sigma)^2 - (\dot{\sigma}_{xy}/\sigma)^4 \right] f^{-1} \qquad (4.75)$$

where

$$\dot{\sigma}_{xy} = E\left[X_1 \dot{Y}_2\right] = -E\left[X_2 \dot{Y}_1\right] = 0 \qquad \text{(refer to equation (4.57)).}$$

Then, from (4.57) and (4.75)

$$\frac{1}{\beta v} S_\varphi^{\cdot}(f) \approx \frac{\beta v}{2f} \qquad (4.76)$$

Consequently, the noise power N within the audio frequency (ω_1, ω_2), due to random FM, is

$$N = \int_{\omega_1}^{\omega_2} S_\varphi^{\cdot}(f) \, df = \frac{(\beta v)^2}{2} \ln\left(\frac{\omega_2}{\omega_1}\right) \qquad (4.77)$$

It can be seen that the noise power is a quadratic function of the vehicle's speed. Therefore, a mobile, initially running at a speed v and then at 2v ($2v \leq 98$ km/h), experiences an increase of the noise power due to the random FM of 6 dB. That is

$$\frac{N_2}{N_1} = \left(\frac{2v}{v}\right)^2 = 4 = 6 \text{ dB}$$

where N_1 is the noise power at the speed v and N_2 is this power at the speed 2v.

4.9 POWER SPECTRA OF THE RECEIVED SIGNAL

Let θ be the incidence angle of a radio wave received by the mobile, and $\omega(\theta)$ the instantaneous angular frequency of such received wave. If the vehicle moves at a constant speed v, then there will be a Doppler frequency shift equal to $\beta v\cos\theta$. Therefore,

$$\omega(\theta) = \omega_c + \omega_m \cos\theta \tag{4.78}$$

where ω_c is the carrier frequency and $\omega_m = \beta v$ is the maximum Doppler shift. Note that, from (4.78), the effective bandwidth of the received wave is equal to twice the maximum Doppler shift.

Consider a mobile station with directional antenna* in the horizontal plane, having a gain equal to $G(\theta)$. If the power distribution is $p(\theta)$, then within a differential angle $d\theta$, the total power is $W_0 G(\theta)p(\theta)d\theta$, where W_0 is the power radiated by an isotropic source. This obviously equals the differential variation of the received power with frequency, $S(f)df$. Noting that $\omega(\theta) = \omega(-\theta)$, then

$$S(\omega)|d\omega| = \frac{W_0}{2\pi}\left[G(\theta)\ p(\theta) + G(-\theta)\ p(-\theta)\right]\ |d\theta| \tag{4.79}$$

where $\omega = 2\pi f$. From (4.78)

---

* Refer to section 3.1

$$|d\omega| = |-\beta v \sin\theta|\,|d\theta| = \left[(\beta v)^2 - (\omega - \omega_c)^2\right]^{1/2} |d\theta| \tag{4.80}$$

where, for simplicity, we have used $\omega(\theta) \triangleq \omega$. Assume that the received power is uniformly distributed in the range $-\pi \le \theta \le \pi$. Hence

$$p(\theta) = \begin{cases} 1/2\,\pi & , -\pi \le \theta \le \pi \\ 0 & , \text{otherwise} \end{cases} \tag{4.81}$$

With (4.80) and (4.79) we obtain

$$S(\omega) = \frac{W_0\left[G(\theta) + G(-\theta)\right]}{\omega_m \sqrt{1 - \left(\dfrac{\omega - \omega_c}{\omega_m}\right)^2}} \tag{4.82}$$

Suppose that the transmitted signal is vertically polarized. Then the electric field E_z will be in the z-direction and can be sensed by a vertical monopole (whip) antenna. In the same way, small loop antennas along the x-axis or along the y-axis can be used to sense the magnetic H_y or H_x, respectively. The corresponding power spectra are determined as follows:

1. *Power spectrum of the electric field* E_z: vertical monopole (whip) antenna, $G(\theta) = G(-\theta) = 3/2$

$$S(\omega) = \frac{3W_0}{\omega_m}\left[1 - \left(\frac{\omega - \omega_c}{\omega_m}\right)^2\right]^{-1/2} \tag{4.83a}$$

2. *Power spectrum of the magnetic field* H_x: small loop antenna along the y-axis, $G(\theta) = G(-\theta) = (3/2)\sin^2\theta$

$$S(\omega) = \frac{3W_0}{\omega_m}\left[1 - \left(\frac{\omega - \omega_c}{\omega_m}\right)^2\right]^{1/2} \tag{4.83b}$$

3. *Power spectrum of the magnetic field* H_y: small loop antenna along the x-axis, $G(\theta) = G(-\theta) = (3/2)\cos^2\theta$

$$S(\omega) = \frac{3W_0}{\omega_m}\left[\frac{\omega - \omega_c}{\omega_m}\right]^2\left[1 - \left[\frac{\omega - \omega_c}{\omega_m}\right]^2\right]^{-1/2} \qquad (4.83c)$$

These three power spectra are plotted in Figure 4.9.

4.10 FIELD MEASUREMENT

Having described the main mobile radio propagation phenomena and the received signal's characteristics, it is now appropriate to address the main topics to be looked at when field measurements are to be carried out. In general, we are interested in characterizing the radio path between a stationary transmitter (base station) and a mobile vehicle (mobile station). The parameters to be known prior to the measurements include the power of the transmitter, the types of transmitting and receiving antennas, their gains and heights and the carrier frequency. The mobile receiver must be equipped with data recording facilities to collect and store the equally spaced signal's samples. A transducer, set up at the vehicle's wheel, can be used to interrupt a processor dedicated to the data acquisition task. In case the vehicle is stationary, a clock generator can be used with the same purpose.

We now describe the relevant points in the field strength measurement process.

1. *Sampling Interval*

As shown in Figure 4.9, for a vehicle moving at speed v, the bandwidth of the received carrier is equal to $2\omega_m$, where $\omega_m = \beta v$ is the maximum Doppler shift. If the samples are taken at regular intervals of distance d, the corresponding sampling frequency ω_s will be

$$\omega_s = 2\pi\ v/d \qquad \text{rad/s}$$

The sampling theorem requires that the sampling frequency must be at least twice the signal's bandwidth. Then

$$\omega_s = 2\pi\ v/d \geq 2(\text{Bandwidth}) = 2(2\beta v)$$

Hence

$$d \leq \lambda/4 \tag{4.84}$$

If, for instance, f_c = 900 MHz (λ = 1/3 m), then the samples must be taken at intervals less than or equal to 8.3 cm.

2. *Separation of Slow and Fast Fading*

The received signal in a mobile radio environment experiences two types of fading: slow fading, due to topographical changes and fast fading, due to multipath propagation. Therefore, the signal $s(t)$ has an area mean $m(t)$ (slow fading) and a local mean $r(t)$ (fast fading) modifying the area mean in a multiplicative way. Then $s(t) = m(t)\, r(t)$. If the variables $s(t)$, $m(t)$ and $r(t)$ expressed in dB, are denoted by $S(t)$, $M(t)$ and $R(t)$, respectively,then

$$S(t) = M(t) + R(t) \tag{4.85}$$

From the field measurement we obtain $S(t)$. We may wish to separate (filter out) $M(t)$ from $R(t)$ to determine, for instance, their distributions. The mean signal $M(t)$ is expected to vary slowly if compared with $R(t)$. Accordingly, by conveniently low pass filtering $S(t)$ we may be able to obtain $M(t)$ and then extract $R(t)$ by performing $R(t) = S(t) - M(t)$. The filtering process can be carried out by averaging the samples over a range of $2k + 1$ samples (k integer) where the mean signal is considered to be sensibly constant. Let S_i be the $i^{\underline{th}}$ sample. Hence, the $i^{\underline{th}}$ estimated area mean $\hat{M}_i$ is

$$\hat{M}_i = \frac{1}{2k + 1} \sum_{j=-k}^{k} S_{i+j} \tag{4.86}$$

Note that the signal is continuously averaged over $2k + 1$ samples, symmetrically distributed about the time index i. It is shown in Appendix 4B that (4.86) performs the function of a digital low pass filter. The estimated fast fading signal is then

$$\hat{R}_i = S_i - \hat{M}_i \tag{4.87}$$

The main concern now is with the determination of the filter length $2k + 1$ to perform an appropriate filtering. If the averaging is carried out over a sufficiently small number of neighbouring samples, then the estimated mean will contain a large number of high frequency components. In this case the filter is considered to have a large bandwidth. On the other hand, if the averaging is over a sufficiently large number of neighbouring samples, the mean signal may not remain "constant" within such interval so that the slow variation of the signal can be lost. In this case the filter is considered to have a small bandwidth and the estimated signal will be mostly constituted of low frequency components. It is demonstrated in Appendix 4B that the cut-off frequency f_{co} of the digital filter shown in (4.86) is

$$f_{co} = \frac{f_s}{2k + 1} \tag{4.88}$$

where $f_s = \omega_s/2\pi$ is the sampling frequency. From (4.84) we see that $f_s \geq 4 \frac{\beta v}{2\pi} = 4 f_m$. Consider that

$$f_s = 4\gamma f_m = 4\gamma v/\lambda \tag{4.89}$$

where $\gamma \geq 1$.

The averaging interval may be chosen so as to have the filter's cut-off frequency equal to

$$f_{co} = \alpha f_m \tag{4.90}$$

where $0 \leq \alpha \leq 1$.

From (4.88), (4.89) and (4.90) we obtain

$$2k + 1 = 4 \gamma/\alpha \tag{4.91}$$

The $2k + 1$ samples are collected within a time interval equal to $(2k + 1)/f_s$. If the vehicle moves at a speed v then the distance L, where the signal is considered to be "sensibly constant", is

$$L = \frac{2k + 1}{f_s} v \tag{4.92}$$

With (4.89) and (4.91) in (4.92) we obtain

$$L = \lambda/\alpha \tag{4.93}$$

As an example, consider a carrier f_c at 900 MHz. Assume that $\gamma = 2$, corresponding to a sampling frequency equal to four times the bandwidth (or eight times the maximum Doppler shift = twice the minimum required sampling rate). Moreover, let $\alpha = 0.04$ corresponding to a cut off frequency equal to 4% of the maximum Doppler shift. Hence, the number of samples $2k + 1$ in the filtering process (filter's length) is equal to 200. This corresponds to a distance of $L = 25\ \lambda = 8.33$ m. If the car is moving at $v = 72$ km/h then the sampling rate will be 480 samples/s with each sample being taken at 4cm interval.

3. *Validation of the Measurements*

One set of measurements may not be necessarily enough to consider the collected data as representative of the signal strength in that geographical region. It may be necessary several runs at different conditions (time of the day, weather, etc) before we can validate our results. Even if we keep the "same" measuring conditions, another set of measurement cannot be expected to coincide with the previous one. From (4.46) we understand that two same-frequency signals ($\Delta\omega = 0$) are considered to be uncorrelated if $J_0^2(2\pi\ l/\lambda) = 0$, occurring for $2\pi\ l/\lambda = 2.404$. Accordingly, $l = 0.38\lambda \approx 0.5\lambda$. For a 900 MHz carrier, this implies a distance of 13 cm. Thus, it is very unlikely that any other set of runs will be taken within this distance. Moreover, the surrounding objects may not be exactly the same any more.

Having collected the data we need to assess the accuracy of our results. Let $p = \text{prob}(R \le V)$ be the true cumulative distribution of the Rayleigh signal R(t). We estimate p by $\hat{p}$, where $\hat{p}$ is the number of occurrences of the event $R_i \le V$, averaged over the total number N of samples. Then

$$\hat{p} = \frac{1}{N} \sum_{j=1}^{N} P_i \tag{4.94}$$

where

$$p_i = \begin{cases} 1 & , R_i \le V \\ 0 & \text{otherwise*} \end{cases}$$

The expected value of $\hat{p}$ and its variance $\hat{\sigma}^2$ are (see Appendix 4C).

$$E\left[\hat{p}\right] = p \tag{4.95}$$

$$\hat{\sigma}^2 = \frac{1}{N}\, p\,(1-p) \tag{4.96}$$

Note that, from (4.96) the larger the number of samples, the less the estimated probability will deviate from the true probability. In (4.96) we are assuming the samples to be uncorrelated. However, as we have seen, uncorrelated samples occur at distances l equal to or greater than 0.38λ.

The N samples are taken within a distance of $L_T = N(1/f_s)\,v$. With (4.89) in (4.92), where we replace L by L_T and $2k+1$ by N, we obtain

$$L_T \triangleq \text{total distance} = N\lambda/4\gamma$$

Hence, the number of uncorrelated samples within N is $L_T/l = 0.65\,N/\gamma$. We now modify (4.96) by introducing this perturbation factor. Then

$$\hat{\sigma}^2 \simeq \frac{\gamma}{0.65N}\, p(1-p) \tag{4.97}$$

If the distribution of $\hat{R}$ is plotted on Rayleigh-scaled axes, the resulting curve will be a straight line. A straight line is also obtained if the distribution of $\hat{M}$ is plotted on Gaussian-scaled axes.

4. *Final Considerations*

Many other parameters, such as street orientation, tunnels, etc, may affect the area mean, but not the multipath statistics.

---

* This can be written as $p_i = 1 - \frac{1}{2}\left[\text{sgn}(R_i - V) + \left|\text{sgn}(R_i - V)\right|\right]$, where $\text{sgn}(x) = 1, 0, -1$ for $x > 0$, $x = 0$, $x < 0$, respectively.

Observations at stationary conditions also constitute an interesting investigation. Ideally, in this condition, we would not expect the received signal to experience a time varying fading. However, although in a reduced way, multipath effects will still be present due to motion of the scatterers.

4.11 RADIO CHANNEL SIMULATION

The testing of equipments or techniques using the mobile radio channel can be carried out on the field over real HF circuits or by means of simulation. The first approach is usually time consuming, costly and inexhaustive since the parameters influencing the radio channel are, in general, out of control. The second approach is more attractive, but requires the development of both a proper theoretical model and an apparatus to meet certain specifications.

In this section we shall examine two solutions to the simulation problem: one using analog techniques and another using digital signal processing (DSP) techniques. The theory behind these simulators have already been developed in section 4.5. Accordingly, a fading signal can be written as in (4.19). Not that, in section 4.5, we considered the transmission of an unmodulated carrier represented by $\cos\omega t$ and $\sin\omega t$ in (4.19). For a generic signal, say $x(t)$, the fading signal is given by

$$s(t) = Xx(t) - \hat{Y}x(t) \tag{4.99}$$

where

$$X = E_0 \sum_{i=1}^{M} a_i \cos(\omega_i t + \psi_i)$$

$$Y = E_0 \sum_{i=1}^{M} a_i \sin(\omega_i t + \psi_i)$$

$$a_i^2 = p(\theta_i)d\theta p(\psi_i)d\psi$$

$$\omega_i = \beta v \cos\theta_i$$

$$\hat{x}(t) = \frac{1}{\pi} \int_{-\infty}^{\infty} \frac{x(\tau)}{t - \tau} \, d\tau$$ is the Hilbert transform* of x(t)

Note that X and Y are independent zero-mean Gaussian random processes

4.11.1 Analog Solution

The random processes X and Y can be generated by Waves Sum or Gaussian Noise Filtering as follows.

1. *Waves Sum Solution*

Since θ_i is assumed to be uniformly distributed in the range 0–2π rad., then $p(\theta_i) = 1/2\pi$, $d\theta = 2\pi/n$ and $\theta_i = 2\pi i/n$, $i = 1, \ldots, n$. The same reasoning applies to the phase ψ_i. By using some simple trigonometric identities it is straightforward to show that Figure 4.10 implements such simulator. Some works [9,10] have shown that good results can be obtained with $n \geq 6$.

Jakes [7] has shown that the simulator is greatly simplified if the signal is represented in "terms of waves whose frequencies do not overlap". Then [7]

$$X = \frac{2E_0}{\sqrt{n}} \left[\sqrt{2} \sum_{i=1}^{n_0} \cos\psi_i \cos\omega_i t + \cos\psi_n \cos\beta vt \right]$$

$$Y = \frac{2E_0}{\sqrt{n}} \left[\sqrt{2} \sum_{i=1}^{n_0} \sin\psi_i \cos\omega_i t + \sin\psi_n \cos\beta vt \right]$$

where $n_0 = (n/2 - 1)/2$. This approach substantially reduces the number of required amplifiers.

Since the resultant signal is the sum of several cosine waves this approach yields a discrete output power spectrum.

2. *Gaussian Noise Filtering Solution*

Instead of summing shifted waves to obtain the Gaussian processes X and Y, a

---

* The Hilbert transform imposes a phase shift of 90° to all of the frequency components of x(t).

Gaussian noise generator (e.g., a zener diode) can be used. The Doppler shift can be introduced if the output of the noise generator is conveniently filtered so as to produce an output power spectrum with a shape similar to that shown in Figure 4.9 for the electric field (monopole antenna). The block diagram showing this solution is depicted in Figure 4.11.

Note that in this case the Doppler shift is directly dependent on the shaping filter's cut off frequency (refer to Figure 4.9). Since we have used a Gaussian noise generator to obtain the random processes X and Y, this approach yields a continuous output power spectrum.

4.11.2 DSP Solution

A fading simulator implemented with digital signal processing (DSP) techniques has the usual advantages of the computer (processor) supported equipments: adaptability, modularity, wider variety of features, compactability, reliability, etc. The functioning principles are exactly the same as seen before, but in this case digital techniques are used.

Basically, the mobile radio channel is modelled as tapped delay line. Each delayed signal is modulated in amplitude and phase by an independent complex-Gaussian process with variable centre frequency and bandwidth [12]. Figure 4.12 shows a fading simulator using DSP techniques [11].

The Input Interface block performs the A/D conversion of the input x(t). The N^{th} sample of x(t) is x(NT) and its Hilbert transform is $\hat{x}(NT)$, where T is the sampling period. Both in-phase x(NT) and quadrature components $\hat{x}(NT)$ are delayed by integer steps of T in the Complex Tapped Delay Line block to simulate the radio paths . The in-phase and quadrature components in each path i have their amplitudes modulated by the low-pass complex Gaussian processes W_i and $\hat{W}_i$, respectively. The amplitude modulation simulates the Rayleigh fading. Moreover, these amplitude-modulated signals are then frequency-modulated by the complex exponentials $e^{j\theta i}$ and $e^{j\hat{\theta} i}$ imposing a Doppler shift to these signals.

The real part of these signals are then added up to give the resultant digital signal. Gaussian and impulsive noise are also added to this signal. The Output Interface block performs the D/A conversion. Three paths (n = 3) as used in [11] seemed to be enough to yield very good results.

4.11.3 Some Results

In this section we show some results [21] of a fading simulator using the approach as sketched in Figure 4.11. The simulated transmission frequency and the vehicle's speed are 880 MHz and 86 km/h, respectively, corresponding to a Doppler shift of 70 Hz. The output power spectrum and the detected envelope are shown in Figure 4.13 and 4.14 respectively.

4.12 SUMMARY AND CONCLUSIONS

In this chapter we have analyzed the main phenomena concerning the multipath propagation in a mobile radio environment. The first main topic was related with the frequency shift experienced by the radio signal when the vehicle is in motion: the Doppler effect. We conjectured on a fairly simple manner of estimating the Doppler shift, but we also showed that this matter is rather complex having a precise solution given by the Relativity Theory. However, the precise solution reduces to the approximate one in case the ratio v/c (speed of the vehicle/speed of light) is small. And this is obviously our case.

Due to multipath, one single transmitted wave is received at the mobile as a sum of multiple waves each of which having its own time delay. One of the best accepted models establishes that the time delay follows a negative exponential distribution. Field measurements confirm this model and show that the delay spread (corresponding to the standard deviation of such distribution) varies from fractions of microseconds (in rural areas) to several microseconds (in urban areas).

Time delay imposes a phase shift to the received signal while the Doppler effect provokes a frequency shift. Moreover, the multiple paths produce waves with different amplitudes. The resultant signal is then given by the sum of waves having different amplitudes, phases and frequencies. Accordingly, one matter of interest is the determination of the correlation between two signals arriving at different time instants and having two different frequencies. We showed that signals with no frequency separation between them but received at antennas distant 0.5λ from one another are considered to be uncorrelated. In the same way, if the frequency separation is such that the signals' correlation is equal to 0.5, these signals are uncorrelated. This frequency separation defines the coherence bandwidth. Systems having channel bandwidth smaller than the coherence bandwidth are known as narrowband systems. In the wideband systems the channel bandwidth exceeds the coherence bandwidth. In the first case the signal experiences non-selective fading whereas in the second case we have selective fading.

The fading signal was then characterized by the level crossing rate and the average duration of fades. It was clear that, if the crossing (threshold) level is set to be sufficiently low or sufficiently high, the crossing rate will be small. The maximum rate occurs at 3 dB below the signal's rms value and the mean distance between crossings was proved to be approximately equal to 0.5λ. It was shown that the average duration of fades increases exponentially with the threshold level and is at the order of some milliseconds at the maximum crossing rate.

It was seen that an unmodulated carrier transmitted by the base station arrives at the mobile station as a Frequency Modulated wave due to the time variation of the signal's phase. Since this variation is random, the phenomenon is known as random FM. Within the voice frequency-band, the noise introduced by the random FM is a quadratic function of the mobile's speed. The power spectrum of the received signal is confined within a frequency band equal to twice the maximum Doppler shift. The shape of the spectrum is different for each one of the electromagnetic field components.

As far as field measurements are concerned, the usual procedure is to have the

transmitter at the base station and a receiving set-up at the mobile station. This receiving set-up includes, among others, data recording facilities to store the signal's samples. Slow fading is separated from fast fading by averaging the received signal over a distance of tens of wavelengths. The area mean is considered to be representative of that geographical area after several runs under the "same" conditions.

Field measurements are important for a better characterization of the service area. However, if equipments or techniques are to be tested for mobile radio applications, a wise strategy is to use a laboratory simulation apparatus. The advantage of using a mobile radio simulator is that it provides means of controlling the relevant parameters which, in a field testing, are usually out of our reach. The functioning principles of these simulators are very simple and the latest implementations use the digital signal processing approach.

APPENDIX 4A

Mean Distances Between Fadings

Let r be the envelope of the Rayleigh fading signal. Assume that each maximum of r is followed by a minimum of r such that, on average, the maxima occurrence rate, R_M, equals that of the minima occurrence, R_m.

Let $p(r,\dot{r},\ddot{r})$, be the joint probability density function of $r,\dot{r}$ and $\ddot{r}$, where the dots denote differentiation with respect to time, t. Following Rice [22] the mean maxima (or minima) occurrence rate is

$$R_m = R_M = E\left[\ddot{r} \mid \dot{r} = 0\right] = -\int_0^{\infty} dr \int_{-\infty}^{0} \ddot{r}\, p\,(r,\dot{r}=0,\ddot{r})\, d\ddot{r} \qquad (4A.1)$$

Assuming that R_m is known, the mean distance, d, between minima is

$$d = v/R_m \qquad (4A.2)$$

where v is the vehicle's speed.

4A.1 Joint Density $p(r,\dot{r},\ddot{r})$ of $r,\dot{r}$ and $\ddot{r}$

In order to find the joint distribution $p(r,\dot{r},\ddot{r})$ of r, $\dot{r}$ and $\ddot{r}$, we follow the same procedure as that described in section 4.6, as appropriate.

First we find the joint density $p(x,\dot{x},\ddot{x},y,\dot{y},\ddot{y})$ of x, $\dot{x}$, $\ddot{x}$, y, $\dot{y}$ and $\ddot{y}$ where x and y are given by (4.19b) and the dots denote differentiation with respect to t. Then we change variables to find $p(r,\dot{r},\ddot{r},\varphi,\dot{\varphi},\ddot{\varphi})$ where $r^2 = x^2 + y^2$ and $\varphi = \tan^{-1}y/x$. The expression for $p(r,0,\ddot{r})$ is obtained by setting $\dot{r} = 0$ and integrating $p(r,\dot{r}=0,\ddot{r},\varphi,\dot{\varphi},\ddot{\varphi})$ over the ranges of $0 \le \varphi \le 2\pi$, $-\infty \le \dot{\varphi} \le \infty$ and $-\infty \le \ddot{\varphi} \le \infty$.

4A.2 Minima Occurrence Rate

Following the (tedious) procedure described in the previous section, it is found that [22]

$$R_m = \frac{(a^2 - 1)^2}{(2a)^{5/2}} \left(\frac{b_2}{\pi b_0} \right)^{1/2} \sum_{n=0}^{\infty} \frac{\Gamma\left(\frac{n}{2} + \frac{5}{4} \right)}{\Gamma\left(\frac{n}{2} + \frac{7}{4} \right)} \frac{A_n}{a^n} \tag{4A.3}$$

where

$$b_n = (2\pi)^n \int_0^{\infty} S(f)(f - f_c)^n df \tag{4A.4}$$

$S(f)$ is power spectrum of the envelope r

f_c is the mid-band frequency

$$a^2 = \frac{b_0 b_4}{b_2^2} \tag{4A.5}$$

$$A_n = \sum_{i=0}^{n} \frac{\left(\frac{1}{2}\right)\left(\frac{3}{2}\right) \cdots \left(i - \frac{1}{2}\right)}{i!} (n - i + 1)\, b^i \tag{4A.6}$$

$$b = \frac{1}{2} (3 - a^2) \tag{4A.7}$$

and

$$\Gamma(z) = \int_0^{\infty} t^{z-1} e^{-t} dt \tag{4A.8}$$

is the Gamma (factorial) function.

4A.3 Mean Distance Between Fadings

Using (4.83a) for the power spectrum of the electric field in (A.4) it is found that

$$b_n = \frac{3}{2} W_0 (\omega_m)^n \frac{1.3.5 \ldots (n-1)}{2.4.6 \ldots n} \tag{4A.9}$$

where $\omega_m = 2\pi f_m$.

Using (A.9) as required in (A.5), (A.6) and (A.7) and the results in (A.3) it is found that

$$R_m \propto 2.6\, f_m \qquad (4A.10)$$

Finally with (A.10) in (A.2)

$$d \propto 0.383\lambda \propto 0.5\lambda \qquad \text{Q.E.D}$$

APPENDIX 4B

Digital Low Pass Filter

Let $x(n)$ be the n^{th} sample of a discrete signal. We want to prove that the n^{th} sample of the low pass filtered signal may be estimated as

$$y(n) = \frac{1}{2k + 1} \sum_{j=-k}^{k} x(n + j) \qquad (4B,1)$$

We introduce the delay operator z^{-1} to represent a delay of j sampling periods. Consequently, the expression (4B.1) may be rewritten as

$$H(z) = \frac{Y(z)}{X(z)} = \frac{1}{2k + 1} \sum_{j=-k}^{k} z^{-j} \qquad (4B.2)$$

Hence, using the summation properties of a geometric series

$$H(z) = \frac{z^{-k}}{2k + 1} \left(\frac{1 - z^{2k+1}}{1 - z} \right) \qquad (4B.3)$$

Frequency Response

The transfer function $H(z)$ describes a filter having an unique pole located at $z = 1$, for $\omega = 0$ and $2k + 1$ zeros, located at $z = 1$, equally spaced at $2\pi/2k+1$. Moreover, this filter has k zeros at $z = 0$. The frequency response of the filter

can be determined by using $z = e^{j\omega}$ in (4B.3). Then

$$H(e^{j\omega}) = \frac{e^{-jk\omega}}{2k+1}\left(\frac{1 - e^{j(2k+1)\omega}}{1 - e^{j\omega}}\right) \tag{4B.4}$$

or equivalently,

$$H(e^{j\omega}) = \frac{e^{-jk\omega}\; e^{j\frac{2k+1}{2}\omega}}{(2k+1)\; e^{j\omega/2}}\left(\frac{e^{j\frac{2k+1}{2}\omega} - e^{-j\frac{2k+1}{2}\omega}}{e^{j\omega/2} - e^{-j\omega/2}}\right)$$

Then

$$H(e^{j\omega}) = \frac{\sin[(2k+1)\omega/2]}{(2k+1)\sin(\omega/2)} \tag{4B.5}$$

The modulus $|H(e^{j\omega})|$ is plotted in Figure 4B.1, for $2k + 1 = 5$

Note that, from (4B.5) the phase is constant and equal to zero. Note also that the frequency is normalized, i.e., π corresponds to half of the sampling frequency ($f_s/2$). In other words in the figure 4B.1 the first null occurs for $f_s/(2k + 1)$, the second for $2f_s/(2k + 1)$ and so on (nulls will occur for $(2k + 1)\omega/2 = n\pi$, n integer. Hence $\omega = nf_s/(2k + 1)$).

Cut-Off Frequency

Let us estimate the value of the second peak of $|H(e^{j\omega})|$ (the first one occurs for $\omega = 0$ as we can see). Such peak lies within the range $2\pi/(2k + 1) < \omega < 4\pi/(2k + 1)$. Assume, for simplicity, that the second peak occurs at $\omega \approx 3\pi/(2k + 1)$. (see Figure 4B.1). In this case

$$\left|H(e^{j\frac{3\pi}{2k+1}\omega})\right| = \frac{1}{(2k+1)\sin\left(\frac{3\pi/2}{2k+1}\right)} \tag{4B.6}$$

Using the 3 dB criterion for the cut-off frequency we have

$$\left|H(e^{j\frac{3\pi}{2k+1}\omega})\right| \leq 1/\sqrt{2} \tag{4B.7}$$

With (4B.6) in (4B.7) we see that the inequality is always true for $2k + 1 \geq 2$.

For larger values of $2k + 1$ the second peak will be even smaller and we may consider that the effective cut-off will occur at the first null $(2\pi/(2k + 1))$. Then, the cut-off frequency is

$$f_{co} = \frac{f_s}{2k + 1} \tag{4B.8}$$

APPENDIX 4C

Sampling Distributions

Let X be a random variable having a probability distribution $P(X) = \text{prob}(x \leq X)$, with a mean μ and variance σ^2. Let $X_1, X_2, \ldots, X_N$ be the observed samples of such distribution. Then the sample mean $\overline{X}$ is

$$\overline{X} = \frac{1}{N} \sum_{i=1}^{N} X_i$$

The expected value of $\overline{X}$ is

$$E\left[\overline{X}\right] = E\left[\frac{1}{N} \sum_{i=1}^{N} X_i\right] = \frac{1}{N} \sum_{i=1}^{N} E\left[X_i\right] = E\left[X_i\right] = \mu$$

The variance of $\overline{X}$ is

$$\hat{\sigma}^2 = E\left[(\overline{X} - \mu)^2\right] = E\left[\left(\frac{1}{N} \sum_{i=1}^{N} X_i - \mu\right)^2\right] = E\left[\left(\frac{1}{N} \sum_{i=1}^{N} (X_i - \mu)\right)^2\right] =$$

$$= \frac{1}{N^2} E\left[\sum_{i=1}^{N} (X_i - \mu)^2 + 2 \sum_{i=1}^{N-1} \sum_{j=i+1}^{N} (X_i - \mu)\,(X_j - \mu)\right] =$$

$$= \frac{1}{N^2} \left\{\sum_{i=1}^{N} E\left[(X_i - \mu)^2\right] + 2 \sum_{i=1}^{N-1} \sum_{j=i+1}^{N} E\left[(X_i - \mu)\,(X_j - \mu)\right]\right\} =$$

$$= \frac{1}{N^2} \left\{N\, E\left[(X_i - \mu)^2\right] + N(N - 1)\, E\left[(X_i - \mu)\,(X_j - \mu)\right]\right\}$$

If the samples are independent, then the cross product will have zero expectation. Hence

$$\hat{\sigma}^2 = \frac{1}{N} E\left[(X_i - \mu)^2\right] = \frac{\sigma^2}{N}$$

Now consider the following distribution

$$X_i = \begin{cases} 0 & \text{with probability } P\left[X_i = 0\right] = 1 - p = \text{prob}(R_i > V) \\ 1 & \text{with probability } P\left[X_i = 1\right] = p = \text{prob}(R_i > V) \end{cases}$$

Then

$$E\left[X\right] = \sum_{i=0}^{\infty} X_i P\left[X = X_i\right] = 0(1 - p) + 1p = p$$

$$E\left[X^2\right] = \sum_{i=0}^{\infty} X_i^2 P\left[X = X_i\right] = 0^2(1 - p) + 1^2 p = p$$

$$E^2\left[X_i\right] = p^2$$

Hence

$$\sigma^2 = E\left[X^2\right] - E^2\left[X\right] = p(1 - p)$$

Then

$$\hat{\sigma} = \frac{p(1 - p)}{\sqrt{N}}$$

REFERENCES

[1] B.R. Davis, R.E. Bogner, "Propagation at 500 MHz for Mobile Radio", *IEEE Proceedings*, Vol. 132, part F, No. 5, August 1985.

[2] D. Halliday, R. Resnik, *Physics* – part II, John Wiley & Sons, Inc., 2nd Edition, New York.

[3] S. Ramo. J.R. Whinnery, T.V. Duzer, *Fields and Waves in Communication Electronics*, John Wiley & Sons, Inc., 1965.

[4] W.B. Davenport Jr., *Probability and Random Processes*, McGraw Hill KogaKusha, LTD, International Student Edition, 1970.

[5] I.S. Gradshteyn and I.W. Ryahik, *Table of Integrals, Series and Products*, Academic, New York 1965.

[6] M. Abramowitz and I.A. Stegun (ed.), *Handbook of Mathematical Functions with Formulas, Graphs and Mathematical Tables*, National Bureau of Standards, Applied Mathematical Series 55, June 1964.

[7] W.C. Jakes, *Microwave Mobile Communications*, John Wiley & Sons, 1974.

[8] S.O. Rice, "Statistical Properties of a Sine Wave plus Random Noise", *Bell System Technical Journal*, Vol. 27, pp. 109–157, January 1948.

[9] W.R. Bennet, "Distribution of the Sum of Randomly Pased Components", Quart. Appl. Math., pp. 385–393, 5 January 1948.

[10] M. Slack, "The probability of Sinusoidal Oscillations Combined in Random Phase", *J. IEEE*, 93, part III, pp. 76–86, 1946.

[11] L. Ehrman, L.B. Bates, J.M. Kates, "Real Time Software Simulation of the H.F. Radio Channel", *IEEE Transactions on Communications*, Vol. COM–30, No. 8, pp. August 1982.

[12] B. Goldberg, "Communication Channels, Characterization and Behaviour", *IEEE Press*, New York, 1975.

[13] G.L. Turin, "Simulation of Urban Radio Propagation and of Urban Radio Communication System", *Proceedings of International Symposium on Antennas and Propagation*, pp. 543-546, Sendai, Japan.

[14] H. Hashemi, "Simulation of the Urban Radio Propagation Channel" *IEEE Transactions Vehicular Technology*, Vol. VT-28, pp. 213-225, August 1979.

[15] E.L. Caples, K.E. Massad. T.R. Minor, "A UHF Channel Simulator for Digital Mobile Radio", *IEEE Transactions Vehicular Technology*, Vol VT-29, pp. 281-289, May 1980.

[16] T. Aulin, "Modified Model for the Fading Signal at a Mobile Radio Channel" *IEEE Transactions Vehicular Technology*, Vol. VT-28, pp. , August 1979.

[17] G.A.Arredondo, W.H. Chriss, E.H. Walker, "A Multipath Fading Simulator for Mobile Radio" *IEEE Transactions Vehicular Technology*, Vol. VT-22, pp. , November 1973.

[18] H.W.Arnold, W.F. Bodtman, "A Hybrid Multi-Channel Hardware Simulator for Frequency-Selective Mobile Radio Paths", *IEEE GTC 82*, p. A.3.1, November-December 1982.

[19] J.D.Ralphs, F.M.E. Sladen, An HF Channel Simulator Using a New Rayleigh Fading Method, The Radio and Electronic Engineer, Vol. 46, p. 579, December 1976.

[20] A.V. Oppenheim, R.W. Schafer, Digital Signal Processing, Prentice-Hall, Inc., 1975.

[21] O.C. Branquinho and M.D. Yacoub, "Multipath Effects Simulator" (in Portuguese), 9^{th} *Brazilian Telecommunications Symposium*, São Paulo, S.P., Brazil, 2-5 September 1991.

[22] S.O. Rice, "Statistical Properties of Random Noise Currents", in *Selected Papers on Noise and Stochastic Processes*, edited by Nelson Wax, Dover Publications, Inc., New York, 1954.

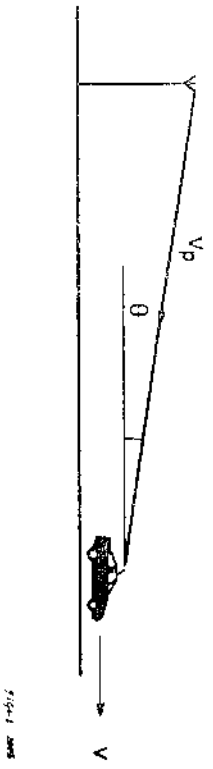

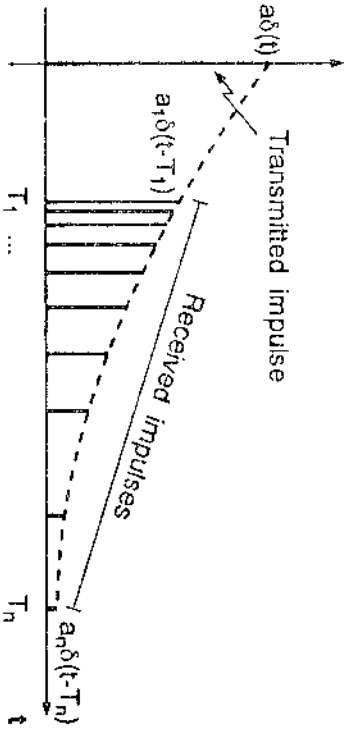

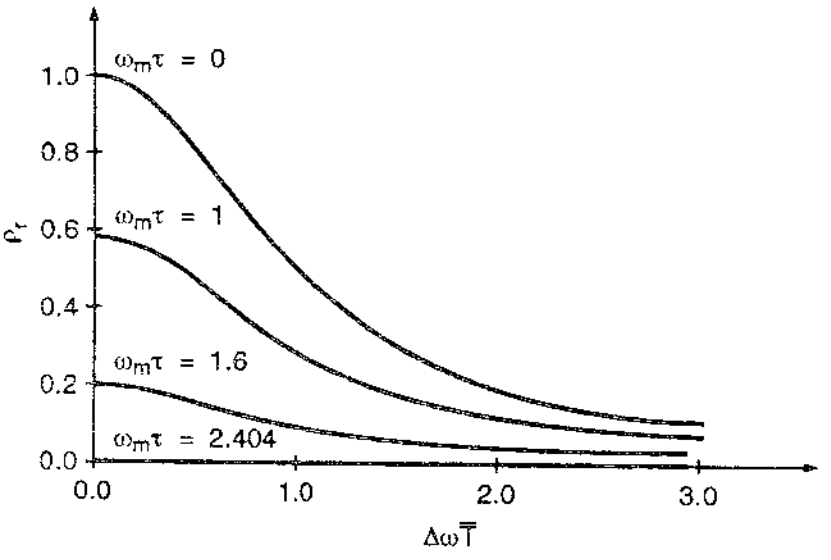

(a)

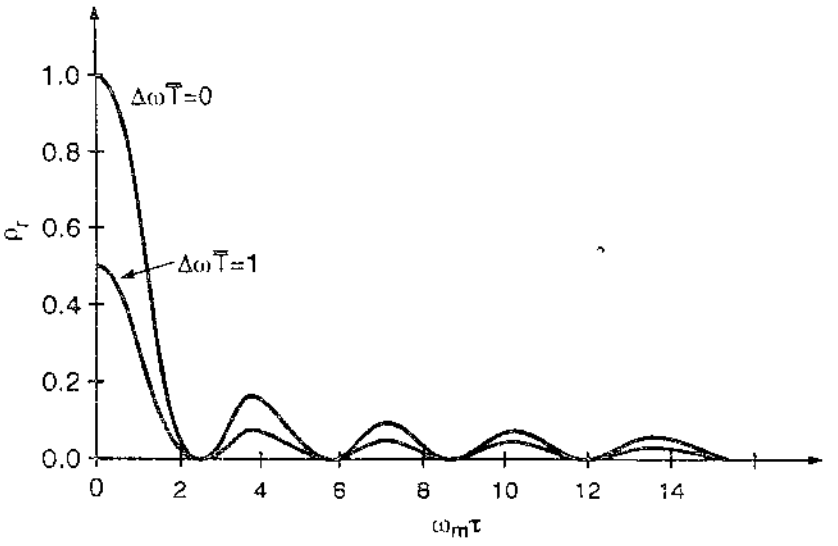

(b)

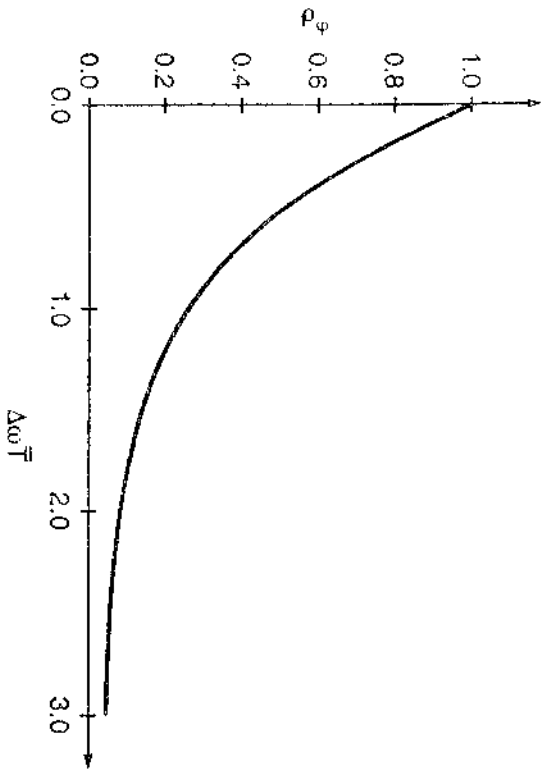

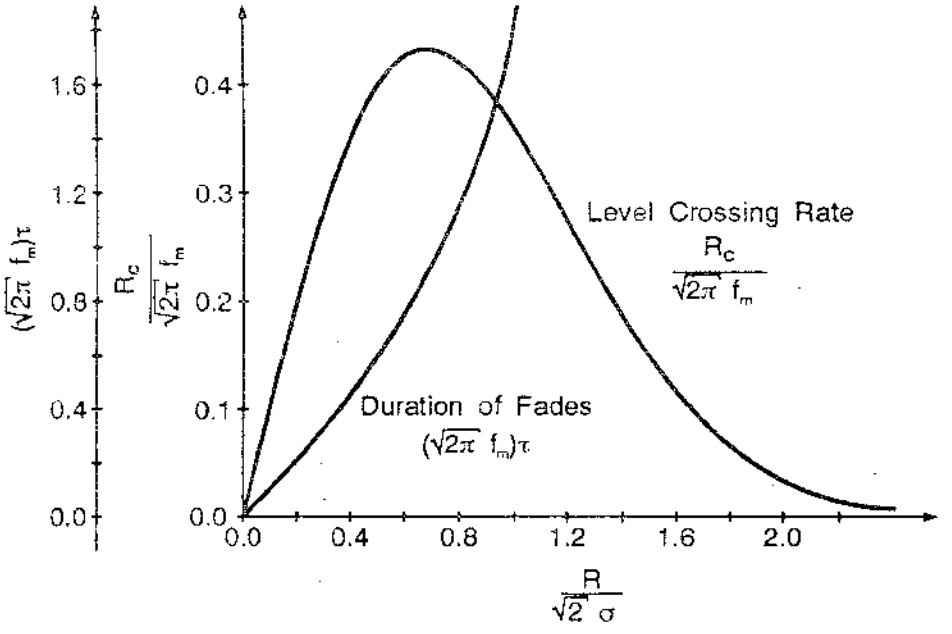

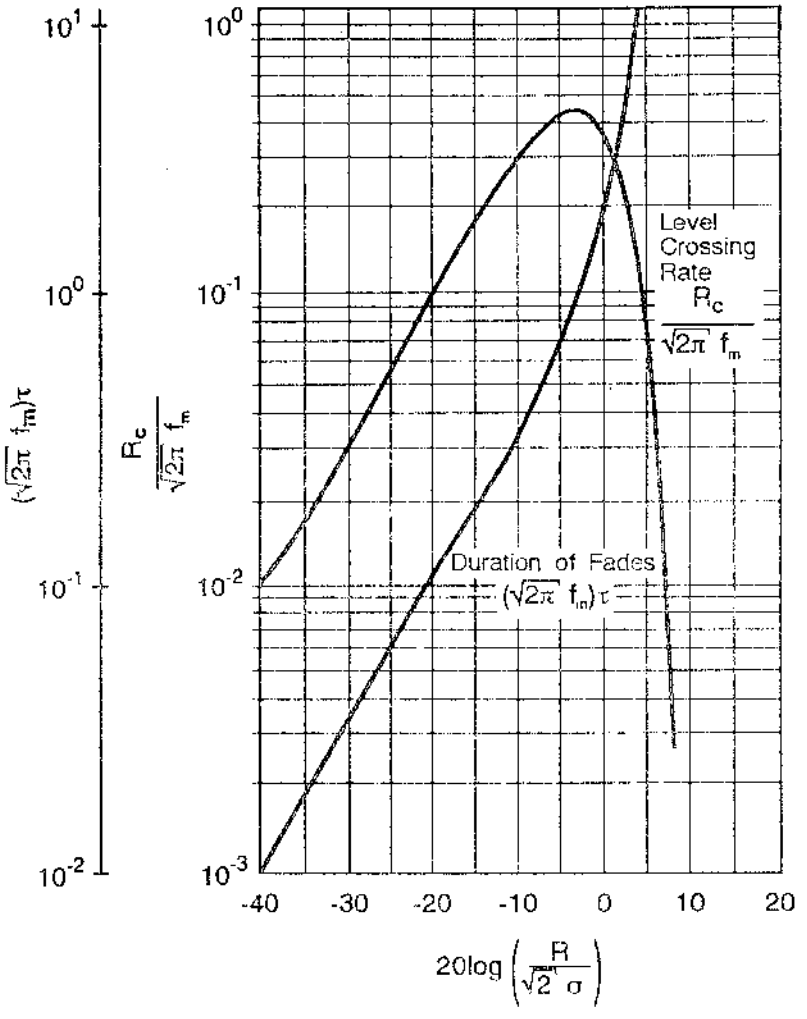
10^1
10^0
10^{-1}
10^{-2}
$(\sqrt{2\pi}\ f_m)\tau$
$\frac{R_c}{\sqrt{2\pi}\ f_m}$
10^0
10^{-1}
10^{-2}
10^{-3}
Level Crossing Rate $\frac{R_c}{\sqrt{2\pi}\ f_m}$
Duration of Fades $(\sqrt{2\pi}\ f_m)\tau$
-40
-30
-20
-10
0
10
20
$20\log\left(\frac{R}{\sqrt{2}\ \sigma}\right)$

Fig 4-6 1986

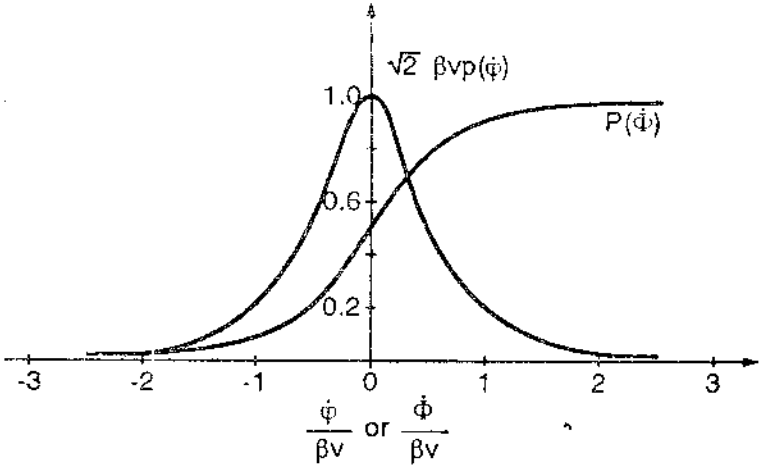

fig4-7

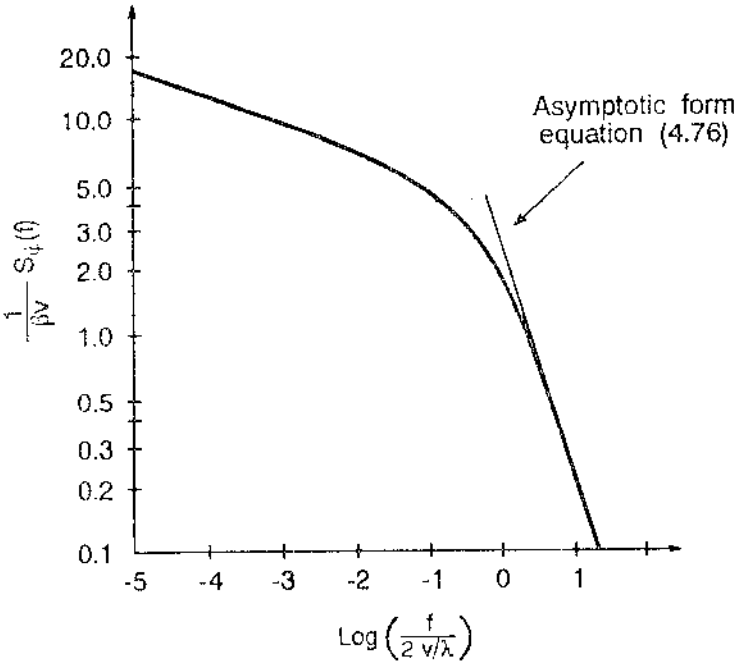
20.0
10.0
5.0
3.0
2.0
1.0
0.5
0.3
0.2
0.1
$\frac{1}{\beta^2} S_\psi(f)$
-5
-4
-3
-2
-1
0
1
$\text{Log}\left(\frac{f}{2\ v/\lambda}\right)$
Asymptotic form
equation (4.76)

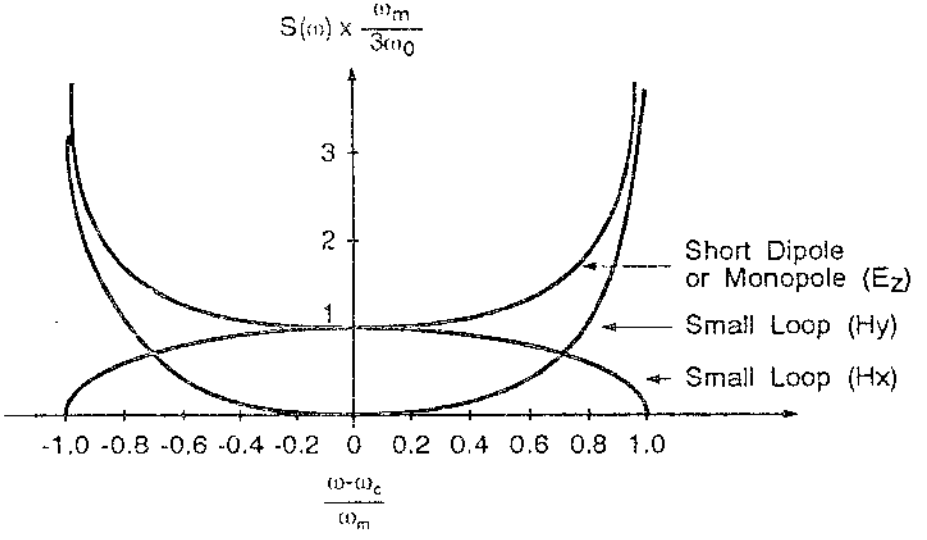

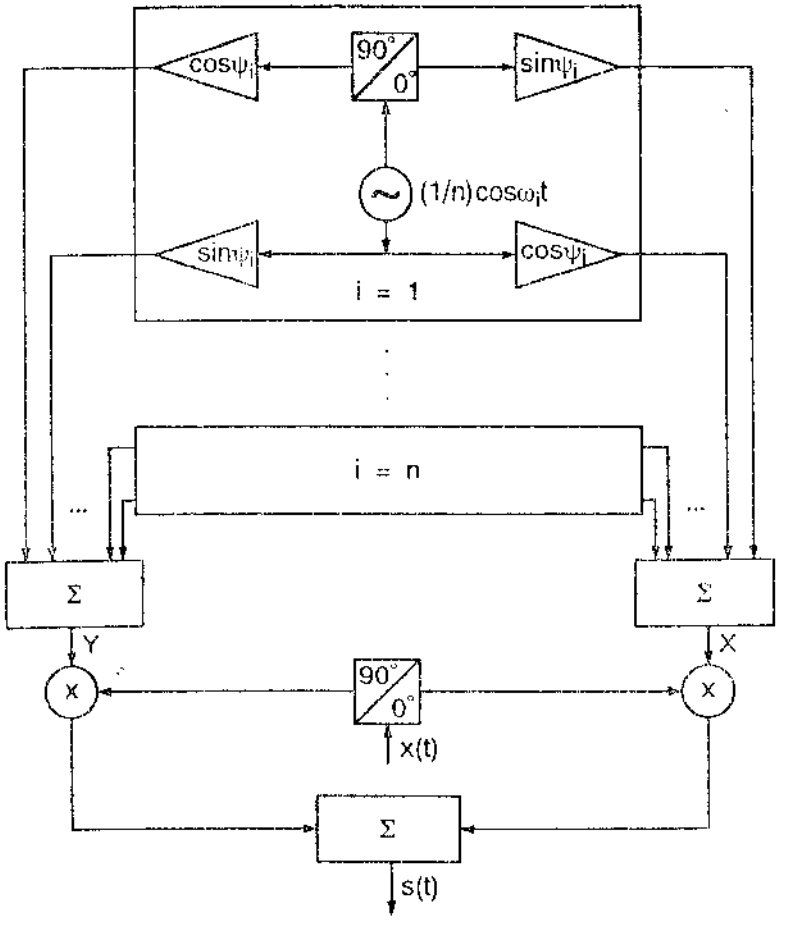
cosψi
90°
0°
sinψi
(1/n)cosωit
sinψi
cosψi
i = 1
i = n
Σ
Σ
Y
X
X
90°
0°
X
x(t)
Σ
s(t)

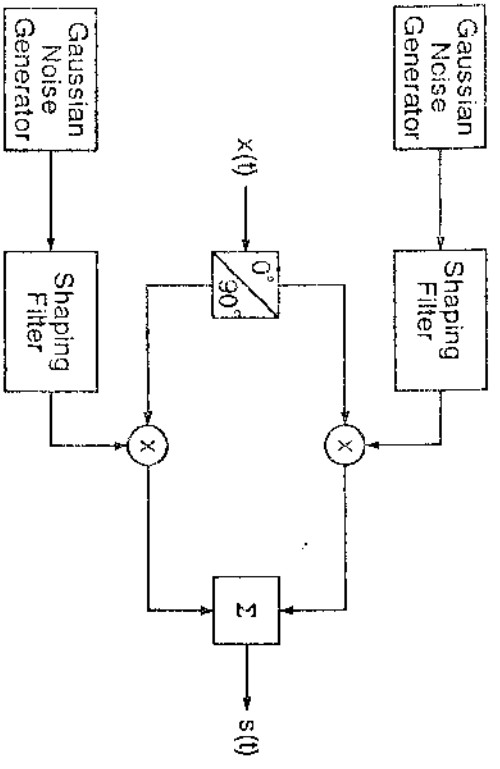

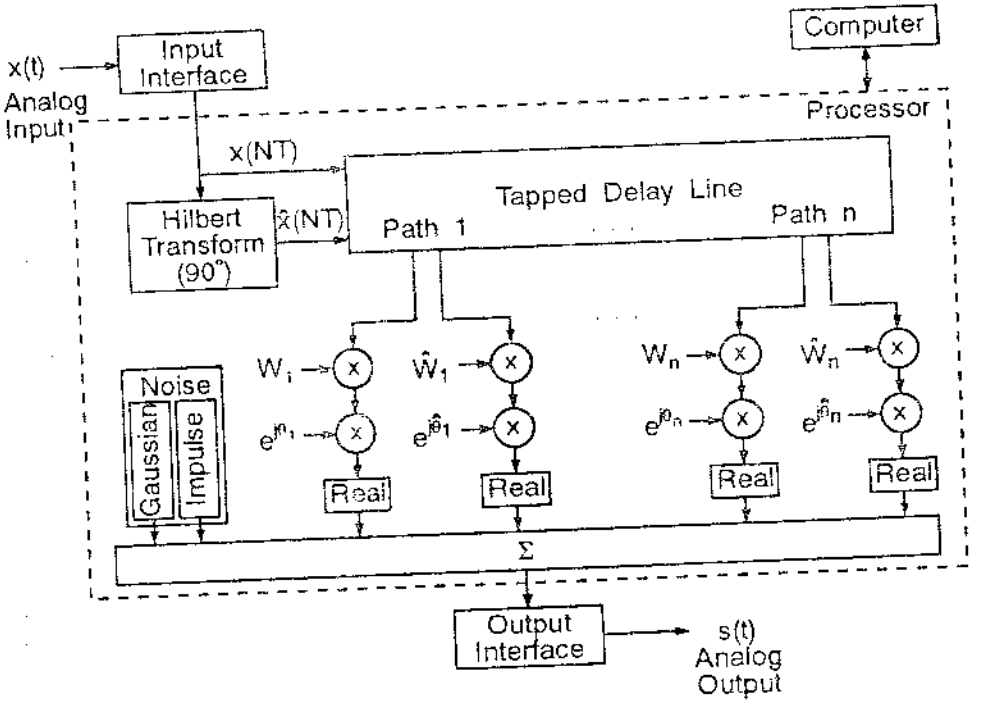

fig4-12 2006

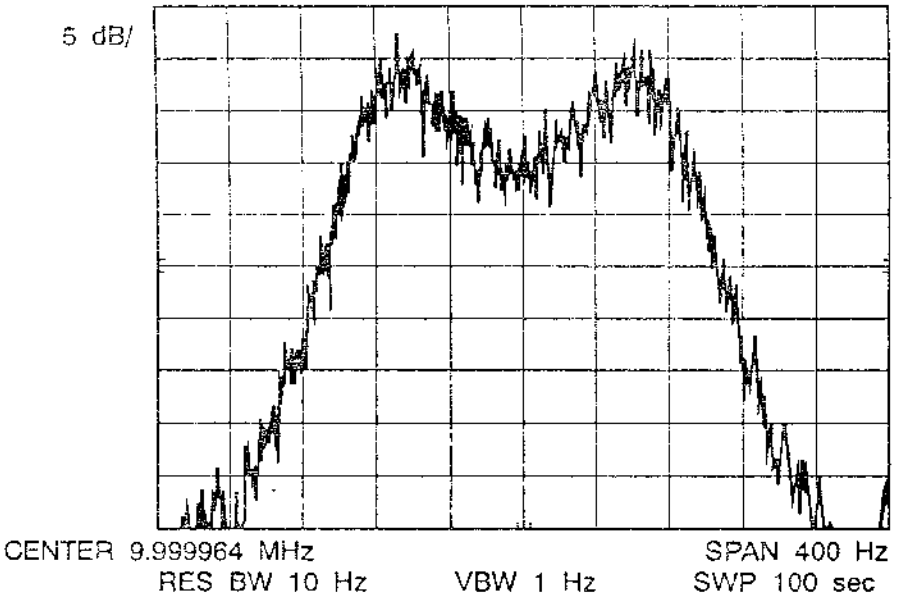

FILE: fig4-13.cdr COLOR: Composite SCREEN: Device's default TIME: Wed Nov 20 15:02:11 1991

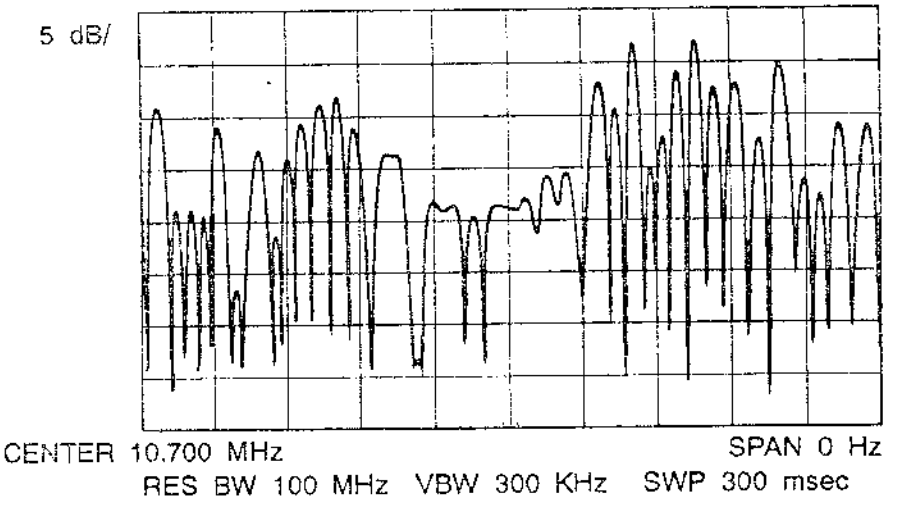

FILE: fig4-14.cdr COLOR: Composite SCREEN: Device's default TIME: Wed Nov 20 15:02:55 1991

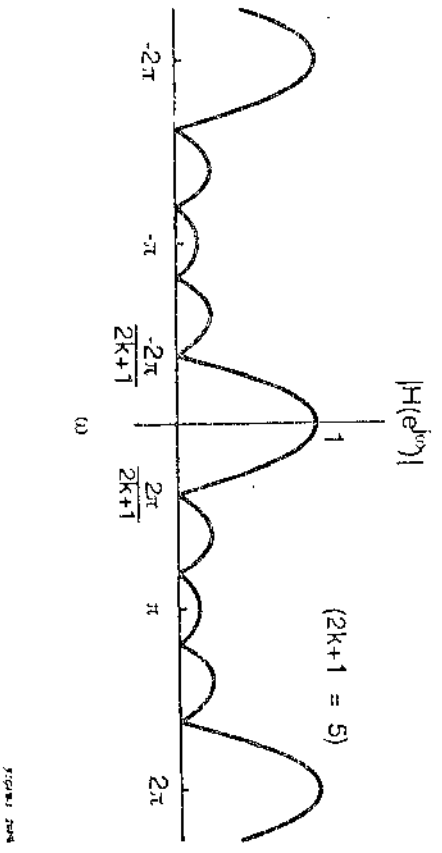

ANEXO A

VOLUME II

FOUNDATIONS OF MOBILE RADIO ENGINEERING

MICHEL DAOUD YACOUB

PART III

DIVERSITY-COMBINING METHODS

CHAPTER 5

FADING COUNTERACTIONS

PREAMBLE

Fading is considered to be one of the main causes of performance degradation in a mobile radio system. Not only can it be annoying but also disastrously harmful if we consider, for instance, its effects on data transmission. Fortunately , this is not an undefeatable enemy and, in fact, many techniques can be used to counteract its effects. This chapter aims at describing the principles, functioning, effectiveness, advantages and disadvantages of these techniques. The problem is first approached by the macroscopic side where it will be seen that only one method is effective to combat slow (lognormal) fading, namely space diversity. On the microscopic side, six techniques to combat fast (Rayleigh) fading, namely space, polarization, angle, frequency, time and hopping diversities are described. Adaptive equalization and coding also constitute effective means of counteracting fading. However, since these techniques are essentially applicable to digital communications, they will be explored in Chapter 6.

Four combining methods such as pure selection, threshold selection, maximal ratio and equal gain are then investigated. The performance of each combining technique is assessed by a measure of the signal-to-noise ratio (SNR) obtained at the output of the combiner. Accordingly, the probability distributions of the various SNRs as functions of the number of diversity branches are determined and analyzed.

It is shown that, taking into account the cost-effectiveness factor, the 2-branch diversity scheme constitutes the best option to combat fading.

5.1 INTRODUCTION

The increasing demand for mobile radio services impels the system designers and operators to find means of not only satisfying such demand but also of improving the performance of the system. One of main causes of performance degradation in the mobile radio systems is the occurrence of fading. A vehicle moving in a typical urban environment may experience extreme variations in the signal levels, and 40 dB below the mean signal strength is not quite uncommon. The envelope of the signal fades according to a Rayleigh distribution with successive minima occurring about every half wavelength of the carrier frequency.

As far as voice transmission is concerned, the effects of the multipath propagation, although annoying, may not be essentially critical. The main concern is when data or signalling are involved: a loss of communication at certain crucial instants may be extremely harmful (imagine, for instance, the system loosing control of a long duration international call at the billing instant...). It is obvious that the general consensus is towards providing a high performance system where both voice and data transmissions meet the established standards of the grade of service.

However, overcoming the effects of the multipath propagation (the fading) is not an easy task and in fact this is considered to be one of the difficult problems to be engineered in the mobile radio system design.

Fading counteractions are usually carried out by means of diversity methods. Diversity principles are based on the fact that the fadings occurring on independent channels constitute independent events. Therefore, if a certain information is redundantly available on two or more channels (known as "diversity branches"), the probability that this information is affected by a deep fade, occurring simultaneously on all of the branches, is very low. Accordingly, with a convenient algorithm (known as "combining method") it is possible to obtain a resultant signal where the effects of fading are minimized.

The use of some diversity techniques in communication systems dates back to the

1920's [5]. Since then several diversity schemes have emerged. Although not widely known as such, the handoff from one base station to another also constitutes a form of diversity. In this chapter we shall concentrate on the alternative methods, other than the handoff. Initially we describe the methods used to obtain the independent branches, i.e., how the information can be repeated over independent paths. Then we examine the methods of combining (processing) the received signals in order to obtain the best output signal.

There are basically two types of fading in a mobile radio environment: long-term and fast fadings. The methods of counteracting their effects are different and will be considered separately, as follows.

5.2 LONG TERM FADING COUNTERACTION

The methods of counteracting the lognormal fading use MACROSCOPIC diversity. The shadowing of a transmitted signal is provoked by large obstructions such as hills, mountains, and others, positioned between the base station and the mobile. A vehicle in this scenario may experience a significantly bad communication, sometimes with a complete loss of the signal.

The basic method used to combat this type of fading is by avoiding the obstruction. A straightforward way of achieving this is by providing more than one base station strategically positioned so that the mobiles always have a clear radio path to at least one base station. The mobile unit establishes communication with all of the base stations. The selection procedure is a dynamic process so that the mobile station always has the best communication.

Note that this type of diversity involves geographical separation between the base stations. Therefore, it is considered as a kind of space diversity. Moreover, since the distances involved are usually long, then it is classified as macroscopic diversity. Jakes [9] proposes corner-excited cells for the mobile radio system as shown in Figure 5.1.

In Figure 5.1 the circles represent the base stations using 120° directional antennas. At first sight it looks as if the number of base stations has been triplicated. In fact, the number of them is exactly the same since each site serves three cells. Note that the mobiles will always have a clear radio path for communication. This is a very interesting configuration because it also minimizes the cochannel interference problem, as will be seen in Chapter 7.

Shadowing appears not only in cellular systems but also in different mobile services. Portable communications integrated into the local networks as described by Cox et al [17,18] constitute one of these services. In this system "high-quality voice and data service via radio must be provided to areas with varying subscriber densities, while making efficient use of the radio spectrum" [5]. In order to achieve this, a fixed grid of radio access ports (base stations) is used. The lay-out of these ports in the grid greatly influences the system performance. The selection of the best quality radio link between a given user and the closest group of ports is supposed to be very rapid, carried out in tens of milliseconds. Figure 5.2 shows one possible configuration of a macroscopic diversity for portable communication systems.

In the example of Figure 5.2 a 3-branch diversity is depicted. The three ports numbered 1,2,3 compose a group serving the mobile users within and near the corresponding equilateral triangle. The selected signal is the best among those received from the ports 1,2,3. It can be seen that each port serves six different diversity groups. Other configurations using square or hexagonal grids with the ports located at different points of the grid are proposed and analyzed by Bernhardt [5].

5.3 SHORT TERM (FAST) FADING COUNTERACTION

The methods of counteracting fast fading use MICROSCOPIC diversity. The name microscopic is related to the distances involved in order to obtain independent radio paths, corresponding to fractions of to some wavelengths. Microscopic diversity relies on the fact that independent signals have a low probability of experiencing deep fades

at the same time instant. Consequently, the basic idea is to repeat the information through independent radio paths and then associate them in a convenient way so that the information is recovered with the effects of the fading greatly attenuated. The next section describes the various methods used to obtain the independent radio paths and the following section examines the schemes used to combine these radio paths.

5.4 DIVERSITY SCHEMES

In this section we describe the space, polarization, angle, frequency, time and hopping diversity techniques.

5.4.1 Space Diversity

The space diversity is the precursor of all of the other diversity techniques and was first applied in 1929 by the use of spaced receiving antennas for HF sky-wave reception. Due to its simple and economical implementation, in connection with the fact that no extra frequency spectrum is required, this diversity scheme is widely used.

When space diversity is mentioned it is usually implicit that the spacing is between receiving antennas. Although spaced transmitting antennas also provide diversity, the ease of its implementation is not quite the same. The transmitting antennas cannot use the same frequency and same polarization since the signals would not be separable into independent receivers [15]. If different frequencies or polarization are used then we recognize this as another technique, as described later. Consequently, our analysis here refers to receiving antennas, spaced and located at the base station and/or at the mobile. In this analysis we assume that the information is redundantly transmitted over independent branches. We recall that, although the signal is transmitted by one single antenna, due to the scattering effects of the obstructions in the environment, it arrives at the receiver in the form of various

(infinite) signals (multipath propagation). Among the "infinitude" of received signals we must discriminate those experiencing independent fadings. In other words, a correlation function between signals should be determined.

Spaced Antennas at the Base Station

One would intuitively expect that there should be reciprocity between signals received at the mobile unit and those received at the base station. As a consequence, the conclusions drawn for one case could be immediately applied to the other case. As far as signal correlation factor is concerned this is not quite true. The explanation for this is a follows. Refer to Figure 5.3. Scatterers are assumed to be randomly distributed around a circle of radius R surrounding the mobile. This radius is usually very small compared to the distance D between base station and mobile. Consequently, the beamwidth $\Delta\varphi = 2R/D$ incident on the base station is also very small. Hence, the base station antennas should be placed far away from one another so that each antenna receives a radio signal propagated through independent paths. On the other hand, the mobile unit receives the scattered signals from all of the angles. Therefore, uncorrelated signals can be received at very close distances from each other.

Our aim now is to determine the distance between the antennas at the base station receiving independent radio signals from a given mobile. This can be directly extracted from the cross-correlation expression of the envelope of two signals r_1, r_2 received at the base station by two antennas horizontally spaced by a distance d, as shown in Figure 5.4. Lee [8,19] has demonstrated that this correlation factor ρ_r is given by (see Appendix 5A)

$$\rho_r = E^2\left\{\cos\left[2\pi \frac{d}{\lambda}\cos(\theta_i - \alpha)\right]\right\} + E^2\left\{\sin\left[2\pi \frac{d}{\lambda}\cos(\theta_i - \alpha\right]\right\} \qquad (5.1)$$

where $d = v\tau$

v is the speed of the vehicle

τ is the time separation between the signals

λ is the wavelength

θ_i is the incident angle of the i^{th} wave, $\alpha - \pi/2 \le \theta_i \le \alpha + \pi/2$

α is the mean incident angle

and E[x] is the expectation of x

The expectation $E\left[f(\theta_i)\right]$ shown in equation (5.1) is calculated as

$$E\left[f(\theta_i)\right] = \int_{\alpha-\pi/2}^{\alpha+\pi/2} f(\theta_i)\, p(\theta_i)\, d\theta_i \tag{5.2}$$

where the probability density $p(\theta_i)$ is given by

$$p(\theta_i) \simeq \frac{Q}{\pi} \cos^n (\theta_i - \alpha) \tag{5.3}$$

In equation (5.3) Q is a normalization factor, obtained as follows

$$\int_{\alpha-\pi/2}^{\alpha+\pi/2} p(\theta_i) d\theta_i = 1 \tag{5.4}$$

As an example, consider an electric field pattern E_r given by

$$E_r = \cos^n(\Delta\varphi/2) \tag{5.5}$$

The 3 dB beamwidth is the value of $\Delta\varphi$ for which $E_r = 1/\sqrt{2}$. If n = 1 then the 3 dB beamwidth is $\Delta\varphi = 90^\circ$. Conversely, if the 3 dB beamwidth is $\Delta\varphi = 2^\circ$, then $n \simeq 2275$. For a given α, the value of Q can be found by using (5.3) in (5.4). Finally, the correlation factor ρ_r in (5.1) can be estimated as a function of λ and d.

Using this procedure Lee [8,19] determined, by means of numerical computation, various curves for the correlation factor. A set of such theoretical curves is shown here together with some empirical curves. Figure 5.5a shows the correlation factor for an incident angle $\alpha = 90^\circ$ (broadside propagation), having the beamwidth as a parameter. Figure 5.5b shows some empirical curves of the signal correlation as a function of the ratio h/d, where h is the antenna height and d is the distance between

antennas. The empirical curves were obtained for a frequency of 850 MHz. For a different frequency, say f, Lee [8,19] suggests the following correction factor

$$d' = \left(\frac{850}{f} \right) d \tag{5.6}$$

where d' is the new distance separation obtained at the frequency f MHz.

It is intuitively expected that the correlation between antennas 1 and 2 increases as the incidence angle α decreases. Note that for the in-line case ($\alpha = 0^o$) the correlation factor is larger than that for $\alpha \neq 0^o$ since the signals will have travelled along almost the same path.

The receiving antennas can also be vertically spaced. This configuration is easy to be implemented since the same pole can be used for the antennas. Height diversity is mainly used to provide protection against destructive interference due to ground reflections, a characteristic of the microwave line-of-sight links. Moreover this has application in the high capacity digital radios, to provide protection against the refractive ray splitting multipath.

Horizontal space diversity, gives better performance than that of the vertical separation, since the decorrelation of the received signals increases faster with the horizontal rather than with the vertical separation of the antennas. This is because the vertical beamwidth $\Delta\Omega$ is much smaller than the horizontal beamwidth $\Delta\varphi$ [20], as shown below. Refer to Figure 5.6 the vertical beamwidth $\Delta\Omega$ is approximately given by $\Delta\Omega \propto 2Rh/D^2$. Since $\Delta\varphi \propto 2R/D$, then $\Delta\Omega/\Delta\varphi \propto h/D$. Usually the antenna height h is much smaller than the distance D from the mobile to the base station. Therefore, $\Delta\varphi >> \Delta\Omega$. The great advantage of the vertical diversity is that the incidence angle of the radio wave does not affect the correlation factor.

Spaced Antennas at the Mobile

The separation distance between the antennas at the mobile can be found from the correlation factor ρ_r of the two signals r_1 and r_2 arriving at these antennas. This correlation factor has already been determined in Chapter 4 and is given by equation (4.46). Since we are interested in the correlation between the same signal arriving

through two distinct paths, we set their frequency separation $\Delta\omega$ in equation (4.46) to be equal to zero. Therefore

$$\rho_r = J_o^2(\omega_m \tau) \tag{5.7}$$

where $\omega_m = \beta v = \frac{2\pi}{\lambda} v$ is the maximum Doppler shift and τ is the time delay between the arrival of the first and the second signals. The argument $\omega_m \tau$ of the Bessel function in (5.7) can be expressed as

$$\omega_m \tau = 2\pi \frac{v\tau}{\lambda} = 2\pi \frac{d}{\lambda} \tag{5.8}$$

where $d = v\tau$ is separation distance between the two signals. Since we require these signals to be uncorrelated, we must set ρ_r to be equal to zero.

The first null of the Bessel function $J_o(\omega_m \tau)$ occurs for $\omega_m \tau = 2.404$, corresponding to a ratio $d/\lambda \simeq 0{,}38$. Consequently, a separation distance $d \simeq 0{,}38\lambda$ between the receiving antennas guarantees independence between the received signals. However, from Figure 4.3b we notice that, after this first null, the correlation factor starts increasing and reaches a maximum value of 0.16, obtained for $d \simeq 0.6\lambda$. Nevertheless, a correlation less than 0.2 can be neglected, and, in practice, a separation distance $d = 0{,}5\lambda$ has been found to be quite reasonable. As an example, with a carrier frequency of 900 MHz ($\lambda = 1/3$m) the distance between the receiving antennas would be $d \simeq 17$cm. Compare this result with that from Figure 5.5a where the distances are usually of the order of tens of wavelengths.

5.4.2 Polarization Diversity

The polarization diversity takes advantage of the orthogonality of the polarized wave components of the travelling radio wave. Although the two components of the polarized wave travel through similar paths, the obstacles encountered by these waves scatter each one of them differently. This implies that they reach their destination in the form of a large number of scattered waves with amplitudes and phases varying randomly. The orthogonality between the waves plus the randomness of amplitudes and

phases greatly contribute to strengthen the uncorrelation between the two components of the polarized wave.

Polarization diversity can be realized by means of antennas reacting individually to the E-field and to the H-field. This is achieved by the vertical electric dipole (whip antenna) and the vertical magnetic dipole (loop antenna) respectively. It is interesting to mention that the electric field produced by a loop antenna is exactly the same as the magnetic field developed by a whip antenna.

There are two great disadvantages of using this technique: (I) only two diversity branches can be used; (II) 3 dB (half of the power) is effectively lost since the signal is divided into two transmitting antennas.

5.4.3 Angle Diversity

A fading signal is the resultant of the sum of an "infinite" number of scattered signals arriving at the antenna through multiple paths. If the antenna's beamwidth is restricted to a small angle, only a few of these waves would be detected and this would improve the fading characteristics of the received signal. Consequently, a directional antenna can be used to improve the fading characteristics of the radio signal. However, it is essential to keep the received signal above an acceptable threshold. This can be accomplished by providing a number of directional antennas constantly monitoring the signal. Another method is to use an adaptive antenna keeping track of the best signal by adaptively positioning itself to point to the correct angle.

5.4.4 Frequency Diversity

Another way of providing uncorrelation between two (or more) signals carrying the same information is by transmitting the signals on two (or more) different carriers. The independence between the diversity branches is achieved if the frequencies of the carriers are sufficiently separated from one another so that fadings occurring in

these signals are uncorrelated.

One possible measure of frequency separation is the coherence bandwidth, studied in section 4.5. The signals are considered to fade independently if the frequency separation between them exceeds the coherence bandwidth by several times [9]. As defined in section 4.5, the coherence bandwidth B_c is the frequency separation for which the correlation between the signals is equal to 0.5. Accordingly, $B_c = 1/2\pi\overline{T}$ for the envelope and $B_c = 1/4\pi\overline{T}$ for the phase correlations, respectively, where $\overline{T}$ is the delay spread. In suburban areas, $\overline{T} \simeq 0.5\ \mu s$, corresponding to a coherence bandwidth of $B_c = 320$ kHz or $B_c = 160$ kHz for the envelope or phase correlations, respectively. Therefore, two fading signals are considered to be independent if the frequency separation between them is $k.B_c$, where k is a constant*. In the given example, if we consider $k = 6$, then this separation would be around 2 MHz ($\simeq 6 \times 320$ kHz).

This obviously requires a wider frequency spectrum, not usually available. A way of saving spectrum is to employ the "1:N protection switching" [15]. In this technique one spare frequency is used as a means of providing diversity to N other carriers. These N frequencies carry N independent traffic, and, when diversity is needed for a given specific carrier, its traffic is switched to the spare carrier. Another way of saving spectrum is described later in the item "Diversity by Hopping".

5.4.5 Time Diversity

As well as frequency, time separation can also provide diversity. As far as data transmission is concerned this technique is widely used and consists in repeating the message (or part of it) according to some criterion. If the intertransmission time is conveniently determined, the received signals may experience independent fadings.

Similarly to the data transmission, speech signals can be sampled and appropriately delayed to be used as a diversity branch. At the reception, the samples (or the data) are stored for a period of time equal to the required time delay. Then, the correct (or the best) information can be selected.

---

* The constant k is usually assumed to be greater than 5.

The time interval between the samples (messages) must exceed the coherence time of the channel. This can be determined from the expression of the envelope correlation between two fading signal given by equation (5.7). From (5.7) the first null of the Bessel function occurs for $\omega_m \tau = 2.404$, or $d \approx 0.38\ \lambda$. Dividing both terms by v (the vehicle's speed) we have $\tau \approx 0.38\ \lambda/v = 0.38/f_m$, where f_m is the maximum Doppler frequency and τ is the time interval between independent signals. Using the same approximation as in the case of space diversity we can assume that, if

$$\tau \geq 1/(2\ f_m) \tag{5.8}$$

the signals arriving with a time delay equal to τ fade independently. For a mobile at 72 km/h, operating at 900 MHz, the delay between the signals must exceed 8.3 ms.

If an M-branch diversity is used then a minimum time delay of $M/2f_m$ is obviously required. In the case of voice transmission the sampling rate must be greater than 8 x M kHz.

5.4.6 Diversity by Hopping

Frequency hopping and time (slot) hopping constitute efficient ways of using frequency or time diversities, respectively. The aim is to hop the information from one frequency or from one time slot to another so that the information experiences independent fadings. If only the resources (in time or frequency) of each base station are used, there is no need for synchronization between base stations. This subject is more deeply explored in Chapter 10.

5.5 COMBINING SCHEMES

There are basically four combining methods divided in two groups, namely, (i) Switched Combining and (ii) Gain Combining.

In the Switched Combining group the aim is to pick (choose) one out of the M received signals according to some criteria. In other words

$$r = \text{One out of } \left\{ r_1, r_2, \ldots, r_n \right\} \tag{5.9}$$

where r is the resultant envelope and r_i, i = 1, ..., M are the received envelopes of the signals. There are two techniques in this group, namely Pure Selection Combining and Threshold Selection Combining.

In the Gain Combining the resultant signal is a linear combination of the received signals, i.e.,

$$r = \sum_{i=1}^{M} a_i r_i \tag{5.10}$$

where a_i are the gains at each branch. The two techniques here are the Maximal-Ratio Combining and Equal-Gain Combining.

Switched Combining: Pure Selection

In the Pure Selection Combining the received signals are continuously monitored so that the best signal can be selected. In theory, the selection criterion should be based on the best signal-to-noise ratio. In practice, however, since this is difficult to obtain, the strongest signal+noise is selected. This technique requires each branch to have its own receiver. Moreover, the signals must be monitored at a rate faster than that of the fading occurrence. A block diagram showing the principles of this techniques is sketched in Figure 5.7a.

Switched Combining: Threshold Selection

One of the major problems of the Pure Selection Combining is the amount of receivers required, one for each branch. Another constraint is the high monitoring rate to select the best signal. This obviously increases both the cost of the equipment and its complexity.

A clever alternative to this approach is the Threshold Selection Combining. In this case the received signals are scanned in a sequential order, and the first signal with a power level above a certain threshold is selected. While above the threshold, the selected signal remains at the combiner's output, otherwise a scanning process is

reinitiated.

The threshold may be either fixed or variable. Setting its level is a task involving the knowledge of the mean signal strength in the geographical area. Consequently, the fixed approach may work well within the region for which the fixed threshold was found to be appropriate. On the other hand, if the conditions change, this approach can give bad results. For instance, if the mobile moves into another area where the mean signal level is lower than its fixed threshold, instability and unnecessary switchings may occur. Accordingly, a variable threshold is preferred, giving better results at the expenses of the inclusion of a circuit to estimate the mean signal level. The block diagram of both approaches are sketched in Figure 5.7b and 5.7c.

In the case of two branches, when the signal falls below the threshold, two strategies can be used to select the signal: (i) switch and stay or (ii) switch and examine. In the first strategy the other signal is always selected regardless of its power level. In the second strategy the other signal is not selected unless its power exceeds the threshold.

The switch and stay approach has the disadvantages that the output signal can stay longer below the threshold. On the other hand, the switch and examine approach has the inconvenience of the noise bursts provoked by the rapid switchings between the two signals when both are below the threshold. As a consequence, the switch and stay technique is preferable. These two techniques are illustrated in Figure 5.8.

Gain Combining: Maximal Ratio

In this technique each one of the M signals has a gain proportional to its own signal-to-noise ratio. Moreover, since the resultant signal is an overall sum of the M signals, cophasing circuitry is required. The block diagram of the Maximal Ratio Combining is shown in Figure 5.9a.

Gain Combining: Equal Gain

This technique differs from the previous one in the sense that all of the signals

have a gain equal to one. In other words, the variable gain amplifiers are eliminated as shown in Figure 5.9b

5.6 STATISTICAL PROPERTIES AND PERFORMANCE MEASURE

Due to the random characteristic of the mobile radio signal, the performance of the diversity combining techniques is assessed in a statistical basis. The performance measure of most interest is the Signal-to-Noise Ratio (SNR), γ_i, defined for each branch i as

$$\gamma_i \triangleq \frac{\text{local mean signal power}}{\text{mean noise power}}$$

For a Rayleigh fading signal having an envelope r_i, the local mean power is equal to $r_i^2/2$, corresponding to the signal power averaged over one RF cycle. In the presence of Gaussian noise with mean power equal to N_i, the SNR is then

$$\gamma_i = \frac{r_i^2}{2N_i} = \frac{r_i^2}{2N} \tag{5.11}$$

where assume that the mean noise power is equal to N in all of the branches.

Let $p(r_i)$ be the probability density function of r_i. The density $p(\gamma_i)$ can be easily found as follows

$$p(\gamma_i)\ |d\gamma_i| = p(r_i)\ |dr_i| \tag{5.12}$$

We recall from section 3.4.2 that the Rayleigh distribution is

$$p(r_i) = \frac{r_i}{\sigma^2} \exp\left(-\frac{r_i^2}{2\sigma^2}\right) \tag{5.13}$$

From (5.11), $d\gamma_i = (r_i/N)\ dr_i$. Therefore, using this result with (5.13) in (5.12), we obtain

$$p(\gamma_i) = \frac{N}{\sigma^2} \exp\left(-\frac{r_i^2}{2\sigma^2}\right) \tag{5.14}$$

Define γ_0 as the ratio of the mean signal power and the mean noise power, i.e.,

$$\gamma_0 = \frac{E_0^2/2}{N} \tag{5.15}$$

where E_0 is the amplitude of the radio wave. From (4.57) $\sigma^2 = E_0^2/2$. Then

$$\gamma_0 = \frac{\sigma^2}{N} \tag{5.16}$$

Consequently, the probability density function of γ_i is

$$p(\gamma_i) = \frac{1}{\gamma_0} \exp\left(-\frac{\gamma_i}{\gamma_0}\right) \tag{5.17}$$

The probability that γ_i is less than or equal to a given SNR, Γ, is the probability distribution function $P(\Gamma)$. Hence

$$P(\Gamma) = \text{prob}(\gamma_i \le \Gamma) = \int_0^{\Gamma} p(\gamma_i)\, d\gamma_i = 1 - \exp\left(-\frac{\Gamma}{\gamma_0}\right) \tag{5.18}$$

In the analyses that follow we shall assume that the signals in all of the diversity branches are uncorrelated and distributed as in (5.18). Our aim now is to determine the performance of each diversity technique. This is achieved by obtaining and assessing the corresponding probability distribution function of the SNR available at each combiner's output.

Switched Combining: Pure Selection

We assume that the selector is ideal and that the best signal is always present at the output. Using (5.18) the probability that the SNR's in all of the M branches are simultaneously less than or equal to a given SNR Γ_s is

$$P_{SEL}(\Gamma_s) = \text{prob}(\gamma_1, \ldots, \gamma_M \le \Gamma_s) = \left[1 - \exp\left(-\frac{\Gamma_s}{\gamma_0}\right)\right]^M \tag{5.19}$$

The probability that at least one branch has a SNR exceeding Γ_s is $1 - P_{SEL}(\Gamma_s)$, known as reliability. The corresponding curves for M = 1, 2, 3, 4, 6, 8, and 10 branches are shown in Figure 5.10.

These curves are plotted in a Rayleigh paper where the Rayleigh distribution

(curve for M = 1) appears as a straight line. It can be readily seen that there is a substantial improvement when diversity is used. The larger the number of branches the better the SNR performance. However, although increasing the number of diversity branches will always improve the SNR, the advantages of implementing more branches are not quite obvious, since the relative amelioration tends to be smaller. For example, a 99.9% reliability is achieved for a SNR equal to −30 dB for M = 1 (no diversity) or −15 dB for M = 2 or −9.8 dB for M = 3 or −7.1 dB for M = 4. The gains attained when changing from M = 1 to M = 2 or from M = 2 to M = 3 to M = 4 are respectively 50%, 35% and 28%.

Another statistics of interest is the average SNR at the output of the selector. Let Γ_s be this average. Then

$$\bar{\Gamma}_s = \int_0^\infty \Gamma_s \, p_{SEL}(\Gamma_s) \, d\Gamma_s$$

where

$$p_{SEL}(\Gamma_s) = \frac{dP_{SEL}(\Gamma_s)}{d\Gamma_s} = \frac{M}{\gamma_0}\left[1 - \exp\left(-\frac{\Gamma_s}{\gamma_0}\right)\right]^{M-1} \exp\left(-\frac{\Gamma_s}{\gamma_0}\right)$$

is the probability density function of Γ_s.

Hence

$$\bar{\Gamma}_s = \gamma_0 \sum_{I=1}^{M} 1/I \qquad (5.20)$$

Switched Combining: Threshold Selection

We assume that the system uses the switch and stay strategy and that the switching occurs at a SNR threshold level Γ_T. Let the SNR at the output of the combining circuit be γ. We want to determine the probability that γ is less than or equal to a given SNR level Γ_s, i.e.,

$$P_{SCN}(\Gamma_s) = \text{prob}(\gamma \leq \Gamma_s)$$

Since the Rayleigh signals r_1 and r_2 (refer to Figure 5.8) are statistically

indistinguishable we may write

$$P_{SCN}(\Gamma_s) = \text{prob}(\gamma \le \Gamma_s) = \text{prob}(\gamma \le \Gamma_s \mid \gamma = \gamma_1) = \text{prob}(\gamma \le \Gamma_s \mid \gamma = \gamma_2)$$

where γ_1 and γ_2 are the SNR's at branch 1 (signal r_1) and 2 (signal r_2), respectively. Let γ_x and γ_y be the portion of γ above and below the threshold Γ_T respectively, i.e., $\gamma = \gamma_x + \gamma_y$. The condition $\gamma = \gamma_i$ ($i = 1$ or $i = 2$) will occur either when $\gamma > \Gamma_T$ or $\gamma \le \Gamma_T$ given that $\gamma = \gamma_x + \gamma_y$. Consequently, the overall distribution is the sum of the corresponding weighed conditional distributions as follows

$$\text{prob}(\gamma \le \Gamma_s) = \text{prob}(\gamma \le \Gamma_s \mid \gamma = \gamma_i) = \text{prob}(\gamma \le \Gamma_s \mid \gamma > \Gamma_T)\text{prob}(\gamma > \Gamma_T \mid \gamma = \gamma_x + \gamma_y)$$
$$+ \text{prob}(\gamma \le \Gamma_s \mid \gamma \le \Gamma_T)\text{prob}(\gamma \le \Gamma_T \mid \gamma = \gamma_x + \gamma_y) \qquad (5.21)$$

The probabilities $\text{prob}(\gamma > \Gamma_T \mid \gamma = \gamma_x + \gamma_y)$ and $\text{prob}(\gamma \le \Gamma_T \mid \gamma = \gamma_x + \gamma_y)$ correspond to the proportion of the time that $\gamma > \Gamma_T$ and $\gamma \le \Gamma_T$, respectively.

Define successful transition as that occurring when the resultant SNR γ is above the threshold Γ_T, and unsuccessful transition otherwise. Given that a transition has occurred, it will be unsuccessful with probability q such that

$$q = P(\Gamma_T) = \text{prob}(\gamma \le \Gamma_T) = 1 - \exp\left(-\frac{\Gamma_T}{\gamma_0}\right) \qquad (5.22)$$

A successful transition occurs with probability p, where

$$p = 1 - q = \exp\left(-\frac{\Gamma_T}{\gamma_0}\right) \qquad (5.23)$$

Let τ_a be the average time that the SNR γ_i is above the threshold. Similarly, τ_b is defined for γ_i below the threshold. Since the switching instants occur at random, the average time that γ exceeds Γ_T, given that a successful transition has occurred, is $\tau_a/2$. In the same way, $\tau_b/2$ is the average time that γ is below Γ_T given that an unsuccessful switching has occurred. Following an unsuccessful transition, the next

transition will only occur after γ has exceeded Γ_T and fallen below it again. Therefore, the average time between the occurrence of an unsuccessful transition and the next transition is $\tau_b/2 + \tau_a$. On the other hand, the time span between a successful transition and the next transition is $\tau_a/2$. We notice that the condition $\gamma > \Gamma_T$ occurs in the successful transitions with probability $(1 - q)$ and in the unsuccessful transitions with probability q. In the first case γ exceeds Γ_T $(\gamma > \Gamma_T)$ for an average time of $\tau_a/2$ whereas in the second case the average time is τ_a. Accordingly, the average time that the SNR γ exceeds the threshold SNR Γ_T is τ_x such that

$$\tau_x = (1 - q)\,\frac{\tau_a}{2} + q\tau_a = (1 + q)\,\frac{\tau_a}{2} \tag{5.24}$$

The same reasoning applies to τ_y (the average time that $\gamma \le \Gamma_T$). Hence

$$\tau_y = q\,\frac{\tau_b}{2} \tag{5.25}$$

The ratio τ_a/τ_b is obviously equal to the ratio between the occurrence of a successful and an unsuccessful transition, i.e.,

$$\frac{\tau_a}{\tau_b} = \frac{p}{q} = \frac{1 - q}{q} \tag{5.26}$$

Similarly, the ratio between the probabilities $\text{prob}(\gamma > \Gamma_T | \gamma = \gamma_x + \gamma_y)$ and $\text{prob}(\gamma \le \Gamma_T | \gamma = \gamma_x + \gamma_y)$ is equal to the ratio between τ_x and τ_y. Hence, using equations (5.24), (5.25) and (5.26)

$$\frac{\text{prob}(\gamma > \Gamma_T | \gamma = \gamma_x + \gamma_y)}{\text{prob}(\gamma \le \Gamma_T | \gamma = \gamma_x + \gamma_y)} = \frac{\tau_x}{\tau_y} = \frac{1 - q^2}{q^2} \tag{5.27}$$

The two remaining probabilities in equation (5.21), namely $\text{prob}(\gamma \le \Gamma_S | \gamma > \Gamma_T)$ and $\text{prob}(\gamma \le \Gamma_S | \gamma \le \Gamma_T)$, are determined as follows

$$\text{prob}(\gamma \le \Gamma_S | \gamma > \Gamma_T) = \frac{\text{prob}(\Gamma_T < \gamma \le \Gamma_S)}{\text{prob}(\gamma > \Gamma_T)} = \frac{\int_{\Gamma_T}^{\Gamma_S} p(\gamma)d\gamma}{\int_{\Gamma_T}^{\infty} p(\gamma)d\gamma}$$

$$= \begin{cases} \dfrac{P(\Gamma_S) - P(\Gamma_T)}{1 - P(\Gamma_T)} = \dfrac{P(\Gamma_S) - q}{1 - q}, & \Gamma_S \ge \Gamma_T \\ 0, & \Gamma_S < \Gamma_T \end{cases} \tag{5.28}$$

In the same way

$$\text{prob}(\gamma \le \Gamma_S | \gamma \le \Gamma_T) = \frac{\text{prob}(\gamma \le \Gamma_S \text{ and } \gamma \le \Gamma_T)}{\text{prob}(\gamma \le \Gamma_T)}$$

$$= \begin{cases} \dfrac{P(\Gamma_T)}{P(\Gamma_T)} = 1, & \Gamma_S \ge \Gamma_T \\ \dfrac{P(\Gamma_S)}{P(\Gamma_T)} = \dfrac{P(\Gamma_S)}{1 - q}, & \Gamma_S < \Gamma_T \end{cases} \tag{5.29}$$

By combining equations (5.27), (5.28) and (5.29) into (5.21) we obtain the overall distribution function

$$P_{SCN}(\Gamma_S) = \begin{cases} (1 + q)\, P(\Gamma_S) - q, & \Gamma_S \ge \Gamma_T \\ qP(\Gamma_S), & \Gamma_S < \Gamma_T \end{cases} \tag{5.30}$$

The probability density function is

$$p_{SCN}(\Gamma_S) = \frac{dP_{SCN}(\Gamma_S)}{d\Gamma_S} = \begin{cases} (1 + q)\, p(\Gamma_S), & \Gamma_S \ge \Gamma_T \\ qp(\Gamma_S), & \Gamma_S < \Gamma_T \end{cases} \tag{5.31}$$

The average SNR at the output of the selector is $\bar{\Gamma}_S$

$$\bar{\Gamma}_S = \int_0^{\infty} \Gamma_S p_{SCN}(\Gamma_S)\, d\Gamma_S = \int_0^{\Gamma_T} \Gamma_S p_{SCN}(\Gamma_S)\, d\Gamma_S + \int_{\Gamma_T}^{\infty} \Gamma_S p_{SCN}(\Gamma_S)\, d\Gamma_S$$

$$\bar{\Gamma}_S = \gamma_0 + \Gamma_T \exp\left(-\frac{\Gamma_T}{\gamma_0}\right) \tag{5.32}$$

Figure 5.11 shows the distribution of Γ_S given by (5.30) for some values of threshold Γ_T. We also plot, for comparison, the distribution of Γ_S for an ideal selector, corresponding to the distribution of Γ_s for M = 2 in the pure selection combining. Also shown is the Rayleigh distribution (M = 1). Note that the curves for the threshold selection are confined between the curves for M = 1 (no diversity) and M = 2 (pure selection). For values of SNR below the threshold the curves have approximately a Rayleigh slope. Above the threshold they merge very quickly with the Rayleigh curve (M = 1). For a SNR equal to the threshold the curves touch that of the ideal selection (M = 2). This is expected since the ideal selector works as a scanning circuit having the threshold dynamically switched to be the input signal currently in use. It can be seen that the largest gains are obtainable at lower levels (below the threshold). At higher levels (above the threshold) the gains are negligible. Accordingly, the threshold level must be set to the lowest acceptable SNR. As an example, suppose that in a certain geographical area a signal of 6 dB below its mean value is considered to be acceptable. Then the reliability goes from 77,8% (no diversity) to 95% if a threshold of −6 dB is used.

Gain Combining: Maximal Ratio

Refer to Figure 9a for the block diagram of the maximal ratio combiner. The envelope of the combined signal is

$$r = \sum_{i=1}^{M} a_i r_i \tag{5.33}$$

where a_i is the gain at branch i. Assuming a mean noise power equal to N for each branch, then the total noise power N at the combiner's output is

$$\mathcal{N} = N \sum_{I=1}^{M} a_I^2 \tag{5.34}$$

Consequently, the resultant SNR γ is

$$\gamma = \frac{r^2/2}{\mathcal{N}} = \frac{1}{2} \frac{\left(\sum_{I=1}^{M} a_I r_I \right)^2}{N \sum_{I=1}^{M} a_I^2} \tag{5.35}$$

It is shown in Appendix 5B that the SNR γ is maximized if the gains a_I are chosen to be equal to the ratio of the signal-voltage to noise power of the respective branch. Thus

$$a_I = r_I/N \tag{5.36}$$

Consequently, using (5.36) in (5.35) we obtain

$$\gamma = \frac{1}{2} \frac{\left(\sum_{I=1}^{M} r_I^2/N \right)^2}{N \sum_{I=1}^{M} (r_I/N)^2} = \sum_{I=1}^{M} \frac{r_I^2}{2N} = \sum_{I=1}^{M} \gamma_I \tag{5.37}$$

Equation (5.37) shows that the resultant SNR at the output of the combiners is the sum of the SNRs of the M branches. It was shown in section 3.4.2 that the envelope r_I is a function of two independent Gaussian variates, namely x_I and y_I, having means equal to zero and variances σ^2 equal to $E_0^2/2$. Recalling that $r_I^2 = x_I^2 + y_I^2$, then

$$\gamma = \sum_{I=1}^{M} \gamma_I = \sum_{I=1}^{M} \frac{1}{2N} r_I^2 = \sum_{I=1}^{M} \frac{x_I^2}{2N} + \sum_{I=1}^{M} \frac{y_I^2}{2N} \tag{5.38}$$

It is shown in the Appendix 5C that the sum of the squares of independent standard normal random variables has a chi-square distribution with degrees of freedom equal to the number of terms in the sum. Since in (5.38) we have two M-term sums, the degree of freedom is 2M. The variance is equal to $\sigma^2/2N = \frac{1}{2} \gamma_0$. Thus the probability density function of γ is

$$p_{MAX}(\gamma) = \frac{\gamma^{M-1}\ \exp(-\gamma/\gamma_0)}{\gamma_0^{M}\ (M-1)!} \qquad , \gamma \geq 0 \tag{5.39a}$$

For low SNR

$$p_{MAX}(\gamma) \simeq \gamma^{M-1}/\gamma_0^{M}(M-1)! \tag{5.39b}$$

The distribution function $P_{MAX}(\Gamma_S)$ is

$$P_{MAX}(\Gamma_S) = \text{prob}(\gamma \leq \Gamma_S) = \int_0^{\Gamma_S} p_{MAX}(\gamma)\ d\gamma$$

Using the density given by (5.39a)

$$P_{MAX}(\Gamma_S) = 1 - \exp\left(-\Gamma_S/\gamma_0\right) \sum_{i=1}^{M} \frac{(\Gamma_S/\gamma_0)^{i-1}}{(i-1)!} \tag{5.40a}$$

For low SNR (equation (5.39b))

$$P_{MAX}(\Gamma_S) \simeq (\Gamma_S/\gamma_0)^{M}/M! \tag{5.40b}$$

The corresponding (exact) distribution is plotted in Figure 5.12. Comparing the curves of Figure 5.10 with those of Figure 5.12 we note that the maximal ratio combining gives better results than the pure selection combining. We observe that, as the number of branches increases ($M \to \infty$), the sum in (5.40a) tends to the exponential, $\exp(\Gamma_S/\gamma_0)$. Accordingly, the distribution $P_{MAX}(\Gamma_S)$ tends to zero.

The mean SNR at the output of the combiner is

$$\bar{\Gamma}_S = <\gamma> = <\sum_{i=1}^{M} \gamma_i> = \sum_{i=1}^{M} <\gamma_i> = M\ \gamma_0 \tag{5.41}$$

Gain Combining: Equal Gain

The signal output of the combiner is the direct sum of the received signals. The resultant envelope and the corresponding SNR are directly obtained from (5.33) and (5.34) by setting the gains $a_i = 1$. Hence

$$r = \sum_{i=1}^{M} r_i \tag{5.42}$$

and

$$\gamma = \frac{r^2/2}{N} = \frac{\left(\sum_{i=1}^{M} r_i\right)^2}{2NM} = \frac{r^2}{2NM} \tag{5.43}$$

The envelope r is a random variable, resulting from the sum of M independent Rayleigh variates. Let $p(r)$ be the density of r. Therefore, the density $p_{EQU}(\gamma)$ of γ can be found as

$$p_{EQU}(\gamma)\ |d\gamma| = p(r)\ |dr|$$

Using (5.43)

$$p_{EQU}(\gamma) = NM\ \frac{p(r)}{r} = NM\ \frac{p(\sqrt{2\gamma NM})}{\sqrt{2\gamma NM}} \tag{5.44}$$

The question is how to find $p(r)$. For the case where $M = 2$ (two branches) the problem can be easily tackled. The joint distribution $p(r_1,r_2)$ of two Rayleigh signals has already been determined in Chapter 4, and is given by (4.37).

For $M = 2$, $\quad r = r_1 + r_2 \quad$ or $\quad r_2 = r - r_1$

Then

$$p(r) = \int_0^r p(r_1,r_2)\Big|_{r_2=r-r_1} dr_1 = \int_0^r p(r_1,\ r - r_1)dr_1 \tag{5.45}$$

Such integral can be solved in terms of tabulated functions and the final distribution is given by

$$P_{EQU}(\Gamma_S) = 1 - \exp(-2\Gamma_S) - \sqrt{\pi\Gamma_S}\ \exp(-\Gamma_S)\ erf(\sqrt{\Gamma_S}) \tag{5.46}$$

where $erf(\cdot)$ is the error function

For $M > 2$ branches the problem is rather complicated but can be tackled with the help of computer methods, using, for instance, simulation techniques. An approximate solution for low SNR is presented by Schwartz [31] where it is shown that

$$p_{EQU}(\gamma) = \frac{2^{M-1}\ M^M}{(2M-1)!}\ \frac{\gamma^{M-1}}{\gamma^M} \tag{5.47}$$

$$P_{EQU}(\Gamma_S) \propto \frac{(M/2)^M\sqrt{\pi}}{(M-1/2)!}\,\frac{1}{M!}\left(\frac{\Gamma_S}{\gamma_0}\right)^M \tag{5.48}$$

where $(\circ)!$ is the gamma function. In particular

$$\left(M-\frac{1}{2}\right)! = \frac{1.3.5.7\ldots(2M-1)!}{2^M}$$

Note that (5.48) differs from (5.40b) by a factor equal to $\frac{(M/2)^M\sqrt{\pi}}{(M-1/2)!}$.

The distribution of Γ_S is shown in Figure 5.13.

It can be seen that the performance of this technique is slightly poorer that of the maximal ratio.

The mean value of γ is easily obtained from (5.43) as follows

$$\bar{\Gamma}_S = <\gamma> = \frac{1}{2NM} < \left(\sum_{i=1}^{M} r_i\right)^2 > = \frac{1}{2NM} \sum_{i,j}^{M} < r_i r_j > \tag{5.49}$$

In (5.49) we notice that there are M elements equal to $< r_i^2 >$ and M(M - 1) elements equal to $< r_i r_j >$, $i \neq j$. From the Rayleigh distribution (refer to Chapter 3) $<r_i^2> = E(r_i^2) = 2\sigma^2$. Since the signals are assumed to be independent, then $<r_i r_j> = <r_i><r_j> = E(r_i)\,E(r_j)$, $i \neq j$. But $E(r_i) = E(r_j) = \sqrt{\pi/2}\,\sigma$. Therefore, $< r_i r_j> = (\pi/2)\sigma^2$. Using these results in equation (5.49) we obtain

$$\bar{\Gamma}_S = \frac{1}{2NM}\left[2M\sigma^2 + M(M-1)\,\pi\,\frac{\sigma^2}{2}\right]$$

$$\bar{\Gamma}_S = \gamma_0\left[1 + (M-1)\,\frac{\pi}{4}\right] \tag{5.50}$$

where $\gamma_0 = \sigma^2/N$ (see equation (5.16)).

5.7 COMPARATIVE PERFORMANCE OF COMBINING TECHNIQUES

A quick look at the graphs of the section 5.6 shows that the maximal ratio combining is the best technique followed by equal gain, pure selection and threshold

selection, in this order. The distributions of the SNR at the output of the various combiners using $M = 2$ branches are shown in Figure 5.14. The performance of these techniques can also be shown as functions of the number of branches for a given SNR. However, it is questionable whether the improvement achieved for a number of branches greater than 2 justify the implementation costs of the hardware required.

From the plots of Figure 5.14 it can be seen that a substantial improvement is accomplished when the combining techniques are used. As an example, in the conditions where the use of no diversity gives a 90% reliability, maximal ratio, equal gain, pure selection and threshold selection would yield 99.6%, 99.5% and 99.1% reliabilities, respectively. Note that the equal gain technique gives a slightly poorer performance than that of the maximal ratio combining, even though it is much simpler to be implemented.

The performance of these techniques can also be assessed by the average SNR at the output of the respective combiners. We rewrite (5.20), (5.32), (5.41) and (5.50) as the ratio $\bar{\Gamma}_S/\gamma_0$ between the average SNR of each technique and the average SNR for $M = 1$ branch

$$\frac{\bar{\Gamma}_S}{\gamma_0} = \sum_{i=1}^{M} 1/i \qquad \text{, for pure selection} \qquad (5.51a)$$

$$\frac{\bar{\Gamma}_S}{\gamma_0} = 1 + \frac{\Gamma_T}{\gamma_0} \exp\left(-\frac{\Gamma_T}{\gamma_0}\right) \qquad \text{, for threshold scanning} \qquad (5.51b)$$

$$\frac{\bar{\Gamma}_S}{\gamma_0} = M \qquad \text{, for maximal ratio} \qquad (5.51c)$$

$$\frac{\bar{\Gamma}_S}{\gamma_0} = 1 + (M - 1)\frac{\pi}{4} \qquad \text{, for equal gain} \qquad (5.51d)$$

Note that in our derivations we have assumed $M = 2$ for the threshold selection. Moreover, its performance depends on the threshold Γ_T. In this case the best performance (maximum of equation (5.51b)) is obtained when $\Gamma_T = \gamma_0$, for which $\bar{\Gamma}_S = 1.38\ \gamma_0$. The worst results are obtained by setting Γ_T to be either very low

($\Gamma_T << \gamma_0$) or very high ($\Gamma_T >> \gamma_0$). In these situations the distribution of Γ_S approximates the Rayleigh distribution. The curves of the mean SNR versus the number of branches are shown in Figure 5.15. It can be seen that, for M = 2 the difference between the average SNR of the best performance technique (maximal ratio) and that of the "worst" performance technique (threshold selection) does not exceed 2 dB (in case Γ_T is set to be equal to γ_0).

5.8 OTHER RELEVANT POINTS

In this section we shall comment on some diversity-related topics, exploring more the conceptual ideas and avoiding mathematical derivations.

5.8.1 Combining Correlated Signals

The performance analyses of the combining techniques have been entirely based on the assumption of independent fading signals, i.e., correlation factor equal to zero. If the signals are considered to be correlated, the performance of the techniques will be different from that we have obtained. The extreme situation occurs when the correlation factor is equal to one, corresponding to have exactly the same signal in all of the branches. In this case the resultant distribution is the well-known Rayleigh distribution (M = 1), as expected. Therefore, the corresponding curves for these extreme cases, namely correlation factor equal to 0 and equal to 1 determine the performance bounds of the diversity-combining techniques.

5.8.2 Level Crossing Rate (LCR)

The use of diversity-combining techniques smooths out the deep fades, increasing the mean level of the received signal. Accordingly, lower signal levels will be crossed at lower rates compared with the crossing rates obtained when no diversity is

used. In a similar way, higher signal levels will be crossed at higher rates. On the other hand, since the resultant signal is a combination of two or more signals, the number of ripples at high levels will increase.

As far as correlation factor is concerned, its increase also leads to an increase of the LCR at low levels and to a reduction of the LCR at high levels. This is intuitively explained by the fact that, since the correlation factor gives a degree of "similarity" between the signals, a high correlation implies that the signals can be treated as only one signal.

5.8.3 Average Duration of Fades

Since the diversity-combining techniques smooth out the fades, the average fade duration is, obviously, reduced. It can be proved that, if τ is the average fade duration for M = 1 branch and τ_M is this average for M branches, then $\tau_M = \tau/M$ [9]. With the increase of the correlation between signals the average fade duration also increases.

5.8.4 Random FM

Diversity-combining techniques, if properly used, can substantially reduce the random frequency modulation. The caphasing process is one of the factors playing a significant role in this. For instance, if the reference signal is chosen to be equal to one of the M received signals, then no improvement is achieved. In other words, the random FM of the resultant signal will be exactly the same as that of the reference signal. On the other hand, if the reference signal is chosen to be equal to the resultant signal itself (the sum of the M received signals) then the resultant random FM can be reduced. Moreover, the random FM can be eliminated (or drastically reduced) if a pilot tone, having a frequency close to the carrier frequency, is transmitted along with the signal.

5.8.5 Predetection and Postdetection

The diversity receivers performing predetection have the signals detected before combining. In the receivers using postdetection, the signals are first combined and then detected. Predetection systems are usually more complex and costly. Since coherent combining is performed at an Intermediate Frequency (IF), the use of individual down converters, amplifiers and cophasing circuitry is required. On the other hand, the combined signals produce an output with less random FM and better statistics than that produced by the postdetection systems.

There are two basic methods of cophasing the received signals as shown in Figure 5.16. In one method (switches on the positions 1) a phase-shift is imposed to each one of the received signals, while in the other method (switches on the positions 2) the phase shifts are applied to the local oscillator.

The reference signal for phase comparison can be either one of the incoming signals (r_1, r_2, ..., r_n) or the combined (sum) signal r itself. In the former case, if the signal r_1 is chosen to be the reference signal, the corresponding Phase Shifter and Phase Comparator elements can be eliminated (by-passed). Maximal ratio and equal gain combining techniques require cophasing circuitry. In Figure 5.16, the block diagram corresponds to the equal gain combining scheme. Maximal ratio can be obtained by adding a Gain Control element in each branch before the summing.

The postdetection receivers are usually very simple to be implemented. They are the precursors of all the diversity-combining systems. Initially they were manually controlled, requiring an operator to select the signal that sounded best. In the postdetection receivers, cophasing is not necessary since demodulation (detection) is performed before combining. Once demodulation is accomplished, the baseband signals are all in phase. Pure selection and threshold selection use postdetection receivers.

A great number of practical diversity systems can be found in the literature [8, 9, 11, 32], with the appropriate description and analysis.

5.9 SUMMARY AND CONCLUSIONS

One of the main causes of performance degradation in a mobile radio system is the occurrence of fading. The fading may be annoying for voice but perhaps critical for data communication. Many methods for counteracting the effects of fading have been proposed and they greatly contribute to minimize such effects, consequently improving the performance of the system. The basic principle of these methods (diversity methods) is to redundantly repeat the information on two or more independently fading paths (diversity branches) so that the probability of simultaneous occurrence of fade on all of the paths is negligible. At the reception, a convenient processing of such informations (diversity combining) can lead to a better received signal.

The precursor of all of the diversity techniques is the space diversity where transmitting and/or receiving antennas are spaced far enough from each other so that the fadings occur independently in each branch. Therefore, the probability that two or more diversity branches are simultaneously in deep fade is substantially reduced. The distances between the receiving antennas depend on several factors including the kind of fading (log-normal or Rayleigh), the location of the antennas (base station or mobile), and others. In case antennas are located at the base station, the antenna's heights, the beamwidth and wave's arrival angle also affect these distances.

Slow (log-normal) fading is usually counteracted by means of space diversity where base stations are strategically positioned so that the mobile will always have a clear path for communication. Since this involves long distances (many tens of wavelengths) the slow fading counteraction methods are classified into the macroscopic diversity group.

Fast (Rayleigh) fading is counteracted by means of microscopic diversity. Space diversity is considered to be one of the simplest and most effective means of combating fading. Its great advantage is that it does not require extra frequency spectrum. While spacing between antennas at the mobile involves distances of about half wavelength, at the base station some tens of wavelengths may be necessary (but

still the distances involved are nothing compared to those used in macroscopic diversity).

Polarization diversity may also be regarded as a special case of space diversity, since it requires the use of spaced antennas. Nevertheless, it takes advantage of the independence between the orthogonally polarized waves to obtain independent fading signals. This technique has two limitations as follows. Since there are only orthogonal polarized waves, only two diversity branches can be used. Moreover, half of the signal power is lost, because the signal is used to feed two antennas.

Angle diversity uses directional antenna(s) to restrict the detection of the signal to a small number of scattered waves. It may employ either several antennas to implement the diversity branches or an adaptive antenna to track the best signal.

Frequency diversity requires one antenna at each end of the radio path but a separate transmitter for each frequency. One of its main disadvantage is the need for extra frequency spectrum.

In an M-branch time diversity system the same information is repeated M times in order to obtain M independent signals. These signals are assumed to be independent if the intertransmission time exceeds the channel coherence time. If voice transmission is involved, an increase of the sampling rate by a factor of M is required. This implies a proportional increase of the channels bandwidth. Moreover, since the diversity branches are obtained by delaying and repeating the information, storage elements must be provided at both ends of the path. The great limitation of this technique, however, is that the intertransmission time τ is a function of the maximum Doppler shift f_m. In other words, the signals are considered to be uncorrelated if $\tau \geq 1/2\ f_m = 1/2(v/\lambda)$. Accordingly, if the vehicle is stationary ($v = 0$), time diversity does not apply ($\tau \geq \infty$).

Time-slot hopping or frequency hopping are alternative ways of achieving diversity using exactly the same available resources. On the other hand they require a complex control (see Chapter 10).

As far as combining techniques are concerned, maximal ratio yields the best

performance followed by equal gain, pure selection and threshold selection, in this order. Maximal ratio and equal gain combining give almost the same performance. Accordingly, the latter is preferred due to its simplicity. Pure selection is not feasible since all of the M signals are required to be continuously monitored, demanding a considerable amount of signal processing. An alternative to the pure selection is the threshold selection where the threshold level can be conveniently set for the best performance.

If was shown that the larger the number of branches the better the system performance. However, the percentage of improvement in the SNR for a given reliability decreases with the increase of the number of diversity branches. In practice, the use of more than two diversity branches at the mobile is not feasible due to the costs and complexity. Moreover, two diversity branches already provide a substantial improvement in the received signal. For instance, at a 99% reliability the simple threshold selection technique provides a 9 dB improvement in the SNR. This, in fact, represents the power to be saved at the transmitter if the initial grade of service is to be maintained. In the same way, we can say that the effects of fading can be reduced with the increase of the transmitter power, hence avoiding diversity. In the example given, a 9 dB increase of the transmitter power would lead to a reliability of 99% without the need for diversity. However, the effects of this in the cochannel interference can be disastrous.

APPENDIX 5A

Correlation Factor of Two Signals at the Base Station

Let r_1 and r_2 be the envelopes of two Rayleigh fading signals. It has been demonstrated in Chapter 4* that the cross-correlation of these signals is given by

$$\rho_r \approx \frac{\pi}{4(4-\pi)}\,\rho^2 \propto \rho^2 \tag{5A.1}$$

where

$$\rho^2 = \frac{\mu_1^2 + \mu_2^2}{\sigma^4} \tag{5A.2}$$

and

$$\mu_1 = E[X_1 X_2] \tag{5A.3}$$

$$\mu_2 = E[X_1 Y_2] \tag{5A.4}$$

$$\sigma^2 = E[X_1^2] \tag{5A.5}$$

If the frequency difference $\Delta\omega$ between the signals is nil, then

$$E[X_1 X_2] = \frac{E_0^2}{2} \sum_i a_i^2 \cos(\omega_i \tau) = \sigma^2 \sum_i a_i^2 \cos(\omega_i \tau) \tag{5A.6}$$

and

$$E[X_1 Y_2] = \frac{E_0^2}{2} \sum_i a_i^2 \sin(\omega_i \tau) = \sigma^2 \sum_i a_i^2 \sin(\omega_i \tau) \tag{5A.7}$$

where

$$a_i^2 = p(\theta_i)\, d\theta \tag{5A.8}$$

Let the i^{th} incoming wave arrive at an angle $\theta_i - \alpha$. Hence, when in the limit $i \to \infty$, (5A.6) and (5A.7) will assume the integral form. Thus

---

* The reader is strongly recommended to review section 4.5

$$\mu_1 = \sigma^2 \int_{-\pi/2+\alpha}^{\pi/2+\alpha} p(\theta)\cos\left[\beta v\tau\cos(\theta - \alpha)\right] d\theta \tag{5A.9}$$

$$\mu_2 = \sigma^2 \int_{-\pi/2+\alpha}^{\pi/2+\alpha} p(\theta)\sin\left[\beta v\tau\cos(\theta - \alpha)\right] d\theta \tag{5A.10}$$

where we have used the Doppler frequency $\omega_i = \beta v\cos(\theta_i - \alpha)$

With (5A.9) and (5A.10) in (5A.2) we obtain

$$\rho_r = \left[\int_{-\pi/2+\alpha}^{\pi/2+\alpha} p(\theta)\cos\left[\beta v\tau\cos(\theta - \alpha)\right] d\theta\right]^2 + \left[\int_{-\pi/2+\alpha}^{\pi/2+\alpha} p(\theta)\sin\left[\beta v\tau\cos(\theta - \alpha)\right] d\theta\right]^2 \tag{5A.11}$$

Equation (5A.11) is the correlation factor at the base station. Assume that the probability density function of the i^{th} incoming wave incident at an angle α is given by

$$p(\theta_i) = \frac{Q}{\pi}\cos^n(\theta_i - \alpha) \tag{5A.12}$$

In (5A.12) Q is a normalization factor obtained from

$$\int_{-\pi/2+\alpha}^{\pi/2+\alpha} p(\theta_i)\, d\theta_i = 1 \tag{5A.13}$$

and n is related to the beamwidth $\left(\frac{\Delta\varphi}{2}\right)$ of the incoming wave.

If the electric field pattern is given by $\cos^n\left(\frac{\Delta\varphi}{2}\right)$, then n is obtained at its half power, i.e.,

$$\cos^n\left(\frac{\Delta\varphi}{2}\right) = \frac{1}{\sqrt{2}}$$

Note that the larger the value of n the smaller the beamwidth and, consequently, the more likely the angle of arrival is closer to 0^o. Figure 5A.1 shows the function $\cos^n x$ for n = 1, 10, 50.

APPENDIX 5B

Optimum Branch Gain for Maximal-Ratio Combining

This appendix aims at determining the optimum branch gain for the maximal ratio combining. This is easily done by means of the Schwarz inequality.

Schwarz Inequality

Let $R(\omega)$ and $S(\omega)$ be two complex-valued functions having complex conjugates equal to $R^*(\omega)$ and $S^*(\omega)$ respectively. These functions are related to each other by the Schwarz inequality as follows.

$$\left| \int_{-\infty}^{\infty} R(\omega)S(\omega)\, d\omega \right|^2 \le \int_{-\infty}^{\infty} |R(\omega)|^2 d\omega \int_{-\infty}^{\infty} |S(\omega)|^2 d\omega \qquad (5B.1)$$

Such inequality also holds for real functions $f(t)$ and $g(t)$

$$\left[\int_{-\infty}^{\infty} f(t)g(t) \right]^2 \le \int_{-\infty}^{\infty} g^2(t)\, dt \int_{-\infty}^{\infty} f^2(t)\, dt \qquad (5B.2)$$

and for real random variables X and Y with finite second moments

$$E^2[XY] \le E\left[X^2\right] E\left[Y^2\right] \qquad (5B.3)$$

It can be seen that the equality in the three above respective equations is satisfied if and only if

$$R(\omega) = KS^*(\omega)$$

$$f(t) = Kg(t)$$

$$X = KY$$

where K is a real-valued number. Let us start by proving (5B.1). Consider the following integral

$$I = \int_{-\infty}^{\infty} d\omega \int_{-\infty}^{\infty} |R(\omega)S(z) - S(\omega)R(z)|^2 dz \geq 0$$

where R and S are complex-valued functions. The integral I is necessarily real and positive. Expanding the functions inside the integral, we have

$$|R(\omega)S(z) - S(\omega)R(z)|^2 = |R(\omega)|^2|S(z)|^2 + |S(\omega)|^2|R(z)|^2 - R(\omega)S(z)S^*(\omega)R^*(z) - R^*(\omega)S^*(z)S(\omega)R(z)$$

Integrating term by term and observing that the first two terms after the equality sign are identical, and so are the last two ones, we have

$$I = 2\int_{-\infty}^{\infty} |R(\omega)|^2 d\omega \int_{-\infty}^{\infty} |S(\omega)|^2 d\omega - 2\int_{-\infty}^{\infty} R^*(\omega)S(\omega)d\omega \int_{-\infty}^{\infty} R(z)S^*(z)dz$$

But

$$\left| \int_{-\infty}^{\infty} R(\omega)S(\omega)\, d\omega \right|^2 = \int_{-\infty}^{\infty} R(\omega)S(\omega)d\omega \int_{-\infty}^{\infty} R^*(z)S^*(z)dz$$

Then

$$\frac{I}{2} = \int_{-\infty}^{\infty} |R(\omega)|^2 d\omega \int_{-\infty}^{\infty} |S(\omega)|^2 d\omega - \left| \int_{-\infty}^{\infty} R(\omega)S(\omega)d\omega \right|^2 \geq 0$$

proving the inequality.

The proof of (5B.2) follows the same reasoning as that of (5B.1). For the case of (5B.3) the proof is also simple. Consider the function

$$Q(K) \triangleq E\left[(X - KY)^2\right] \tag{5B.4}$$

The right hand side of (5B.4) is always nonnegative. Then

$$Q(K) = E\left[X^2\right] - 2KE\left[XY\right] + K^2E\left[Y^2\right] \geq 0$$

Q(K) is a nonnegative quadratic function of K. Its minimum is determined by equating

dQ(K)/dK to 0. Let K_0 be such minimum. Hence,

$$K_0 = E\left[XY\right] \; / \; E\left[Y^2\right]$$

It is straightforward to show that

$$Q(K_0) > 0 \quad \text{if} \quad E^2\left[XY\right] < E\left[X^2\right]E\left[Y^2\right]$$

and

$$Q(K_0) = 0 \quad \text{if} \quad E^2\left[XY\right] = E\left[X^2\right]E\left[Y^2\right]$$

proving the inequality

Optimum Branch Gain

Now let us return to the problem of determining the branch gain of the maximal ratio combining. From the corresponding section in Chapter 5 we have that the envelope of the combined signal is

$$r = \sum_{i=1}^{M} a_i r_i \tag{5B.5}$$

The total power noise at the output of the combiner is

$$N = \sum_{i=1}^{M} a_i^2 N_i \tag{5B.6}$$

where here we are assuming that each branch i has a power noise equal N_i. The resultant SNR γ is

$$\gamma = \frac{1}{2} \; \frac{\left(\sum_{i=1}^{M} a_i r_i \right)^2}{\sum_{i=1}^{M} a_i^2 N_i} \tag{5B.7}$$

From the Schwarz inequality we can write

$$\left(\sum_{i=1}^{M} a_i r_i \right)^2 = \left(\sum_{i=1}^{M} a_i \sqrt{N_i} \; \frac{r_i}{\sqrt{N_i}} \right)^2 \le \sum_{i=1}^{M} a_i^2 N_i \sum_{i=1}^{M} \frac{r_i^2}{N_i} \tag{5B.8}$$

Consequently from (5B.7) and (5B.8)

$$\gamma = \frac{1}{2} \frac{\left(\sum_{i=1}^{M} a_i r_i \right)^2}{\sum_{i=1}^{M} a_i^2 N_i} \leq \sum_{i=1}^{M} \frac{r_i^2}{2N_i} \qquad (5B.9)$$

The maximum of (5B.9) is obtained when the "less than or equal to" sign is transformed into "equal to" sign. In this case

$$a_i \sqrt{N_i} = K \frac{r_i}{\sqrt{N_i}}$$

Thus

$$a_i = K \frac{r_i}{N_i}$$

where K is real-valued number. Hence it has been proved that the optimum gain for each branch is proportional to its respective signal-voltage to noise power ratio.

APPENDIX 5C [30]

The Chi-Square Distribution

Let X_i, $i = 1,2,\ldots,k$ be independent and normal Gaussian distributed random variables with means μ_i and variances σ_i^2. We want to prove that the random variable.

$$R = \sum_{i=1}^{k} \left(\frac{X_i - \mu_i}{\sigma_i} \right)^2 \tag{5C.1}$$

has a chi-square distribution with k degrees of freedom.

Define V_i as

$$V_i \triangleq \frac{X_i - \mu_i}{\sigma_i} \tag{5C.2}$$

Hence V_i has a standard normal distribution (zero mean value and unity standard deviation). The moment generating function denoted by $M_R(s)$ is given by

$$M_R(s) \triangleq E\left[\exp(sR)\right] = \int_{-\infty}^{\infty} \exp(sr)p(r)\, dr \tag{5C.3}$$

where p(r) is the probability density function of R to be determined. But

$$E\left[\exp(sR)\right] = E\left[\exp\left(s \sum_{i=1}^{k} V_i^2\right)\right] = E\left[\prod_{i=1}^{k} \exp(sV_i^2)\right] = \prod_{i=1}^{k} E\left[\exp(sV_i^2)\right] \tag{5C.4}$$

And

$$E\left[\exp(sV_i^2)\right] = \int_{-\infty}^{\infty} \exp(sv^2)p(v)\, dv \tag{5C.5}$$

where p(v) is the density of V. As previously shown, p(v) has a standard normal (Gaussian) distribution. Then

$$E\left[\exp(sV_1^2)\right] = \int_{-\infty}^{\infty} \exp(sv^2)\,\frac{1}{\sqrt{2\pi}}\,\exp\left(-\frac{1}{2}\,v^2\right)dv = \int_{-\infty}^{\infty}\frac{1}{\sqrt{2\pi}}\,\exp\left[-\frac{1}{2}(1-2s)\,v^2\right]dv$$

$$= \frac{1}{\sqrt{1-2s}}\int_{-\infty}^{\infty}\frac{\sqrt{1-2s}}{\sqrt{2\pi}}\,\exp\left[-\frac{1}{2}(1-2s)\,v^2\right]dv = \frac{1}{\sqrt{1-2s}}\,,\ \text{for } s < \frac{1}{2} \qquad (5C.6)$$

since the above integral is equal to unity (normal curve with variance $1/(1-2s)$). Consequently,

$$M_R(s) = \prod_{i=1}^{k}\frac{1}{\sqrt{1-2s}} = \left(\frac{1}{\sqrt{1-2s}}\right)^{k/2},\ \text{for } s < \frac{1}{2} \qquad (5C.7)$$

The above equation is the moment generating function of a chi-square distribution with k degrees of freedom. The density may be found by means of the inverse function or directly from tables. Hence the chi-square density with k degrees of freedom is given by

$$p(r) = \frac{1}{\Gamma(k/2)}\left(\frac{1}{2}\right)^{k/2} r^{k/2-1}\exp\left(-\frac{1}{2}\,r\right),\ r \geq 0 \qquad (5C.8)$$

where $\Gamma(\circ)$ is the gamma function defined by

$$\Gamma(t) = \int_0^{\infty} x^{t-1}\exp(-x)\,dx \qquad (5C.9)$$

Using the above definition and then integrating by parts we obtain

$$\Gamma(t+1) = -x^t\exp(-x)\Big|_0^{\infty} + t\int_0^{\infty} x^{t-1}\exp(-x)dx$$

Then

$$\Gamma(t+1) = t\,\Gamma(t) \qquad (5C.10)$$

If $t = n$, integer,

$$\Gamma(n+1) = n! \qquad (5C.11)$$

Now going back to the problem of determining the distribution of the SNR γ given by (5.38) we have

$$\gamma = \sum_{i=1}^{M} \gamma_i = \sum_{i=1}^{M} \frac{1}{2N} r_i^2 = \sum_{i=1}^{M} \frac{x_i^2}{2N} + \sum_{i=1}^{M} \frac{y_i^2}{2N} \tag{5C.12}$$

Assume that σ^2 is the variance of the Gaussian random variables x_i and y_i. Then the SNR γ', defined by (5C.13),

$$\gamma' = \sum_{i=1}^{M} \frac{x_i^2}{\sigma^2} + \sum_{i=1}^{M} \frac{y_i^2}{\sigma^2} \tag{5C.13}$$

has a chi-square distribution with $k = 2M$ degrees of freedom. Its density $p(\gamma')$ is given by (5C.8) with the appropriate substitution of variables. Hence

$$p(\gamma') = \frac{1}{2(M-1)!}\left(\frac{\gamma'}{2}\right)^{M-1} \exp\left(-\frac{1}{2}\gamma'\right) \tag{5C.14}$$

From (5C.12) and (5C.13) we have

$$\gamma = \frac{\sigma^2}{2N}\gamma' = \frac{1}{2}\gamma_0\gamma' \tag{5C.15}$$

Then, changing variables, we obtain the distribution $p(\gamma)$

$$p(\gamma)\,|d\gamma| = p(\gamma')\,|d\gamma'| \tag{5C.16}$$

But, from (5C.15)

$$d\gamma = \frac{1}{2}\gamma_0 d\gamma' \tag{5C.17}$$

Hence, using (5C.14), (5C.15), (5C.16) and (5C.17) we have

$$p(\gamma) = \frac{\gamma^{M-1}}{\gamma_0^M} \frac{\exp(-\gamma/\gamma_0)}{(M-1)!}, \quad \gamma \geq 0$$

as used in the corresponding section of Chapter 5 (equation (5.39).

REFERENCES

[1] Y.S. Yeh, D.O. Reudinik, "Efficient Spectrum Utilization for Mobile Radio Systems Using Space Diversity", *IEEE Transactions on Communications*, Vol. COM-30, Nº 3, March 1982.

[2] W.C.(L.) Wong, R. Steele, B. Glance, D. Horn, "Time Diversity with Adaptive Error Detection to Combat Rayleigh Fading in Digital Mobile Radio", *IEEE Transactions on Communications*, Vol. COM-31, Nº 3, March 1983.

[3] M. Darnell, "Problems of Mobile H.F. Communications and Techniques for Performance Improvement", *IEE Proceedings*, Vol. 132 Pt. F, Nº 5, August 1985.

[4] M. Frullone, G. Riva, M. Sentinelli, A.M. Serra, "Performance of Digital Mobile Systems Suitable for Pan-European Operations", *Second Nordic Seminar on Digital Land Mobile Radio Communication*, Stockholm, 14-16 October 1986.

[5] R.C. Bernhardt, "Macroscopic Diversity in Frequency Reuse Radio Systems", *IEEE Journal on Selected Areas in Communications*, Vol. SAC-5, Nº 5, June 1987.

[6] E.J. Baghdady, "Novel Techniques for Counteracting Multipath Interference Effect in Receiving Systems", *IEEE Journal on Selected Areas in Communications*, Vol. SAC-5, Nº 2, February 1987.

[7] A.M.D. Turkmani, "Performance Evaluation of M-Branch Diversity with Continuous Phase Modulation Systems in Rayleigh and Log-Normal Fading", *International Symposium on Signals, Systems and Electronics, ISSSE'89*, Erlangen, September 18-20, 1989.

[8] W.C.Y. Lee, *Mobile Communications Engineering*, McGraw-Hill, Inc., 1982.

[9] W.C. Jakes, Jr., "Microwave Mobile Communications", John Wiley & Sons, Inc., 1974.

[10] D.G. Brennan, "Linear Diversity Combining Techniques" *Proc. IRE*, Vol. 47, June 1959.

[11] A.J. Rsutako, Y.S. Yeh, R.R. Murray, "Performance (Feedback and Switch Space Diversity 900 MHz Mobile Radio Systems with Rayleigh Fading", *IEEE Transactions on Communications Technology*, Vol. COM-21, November, 1973.

[12] F.T. Adachi, K. Hirade, T. Kamata, "A Periodic Switching Diversity Technique for a Digital FM Land Mobile Radio", *IEEE Transactions Veh. Technology*, Vol. VT-27, November 1978.

[13] F. Adachi, "Selection and Scanning Diversity Effects in a Digital FM Land Mobile Radio with Discriminator and Differential Detections", *IECE of Japan*, Vol. 64-E, June 1981.

[14] F. Adachi, "Postdetection Selection Diversity Effects on Digital FM Land Mobile Radio", *IEEE Transactions Veh. Technology*, Vol. VT-31, November 1982.

[15] S. Stein, "Fading Channel Issues in System Engineering", *IEEE Journal on Selected Areas In Communications*, Vol. SAC-5, Nº 2, February 1987

[16] Z.C. Fluhr, P.T. Poster, "Control Architecture", *Bell System Technical Journal*, Vol 58, Nº 1, January 1979.

[17] D.C. Cox, "Universal Portable Communications", *N. Commun. For., NCF'84*, Chicago, Illinois, Sep. 24-26, pp. 169-174, 1984 and *IEEE Transaction Vehicular Technology*, pp. 117-121, August 1985.

[18] D.C. Cox, H.W. Arnold, P.T. Poster, "Universal Digital Portable Communications: A System Perspective", *IEEE Journal on Selected Areas in Communications*, Vol. SAC-5, Nº 5, pp. 764-773, June 1987.

[19] W.C.Y. Lee, "Effects on Correlation Between Two Mobile Radio Base Stations Antennas", *IEEE Transactions on Communications*, Vol. 21, pp. 1214-1224, November 1973.

[20] P. Camwell, "Propagation and Diversity" unpublished notes on Mobile Communications, 1988.

[21] V.F. Alisouskas, W. Tomasi, Digital and Data Communications", Prentice-Hall, Inc. 1985.

[22] S. Haykin, Adaptive Filter Theory, Prentice-Hall, 1986.

[23] S.U.H. Qureshi, "Adaptive Equalization", *Proceedings of the IEEE,* Vol. 73 Nº 9, September 1985.

[24] A.V. Oppenheim, R.W. Schafer, Digital Signal Processing, Prentice-Hall, Inc., 1975.

[25] J.C.M. Mota, J.M.T. Romano, R.F. Souza, "Blind Deconvolution in Data Transmission Systems" (In Portuguese), RT-179, FEE, UNICAMP, Brazil, November 1989.

[26] G.V. Foschini, "Equalizing Without Altering or Detecting Data" *ATT Technical Journal*, Vol. 64, Nº 8, October 1985.

[27] O. Macchi, E. Eweda, "Convergence Analysis of Self-Adaptive Equalizers", *IEEE Transactions Inf. Theory*, Vol. IT-30, Nº 2, March 1984.

[28] M. Schwartz, Information Transmission, Modulation and Noise, McGraw-Hill Inc., 1970.

[29] W.B. Davenport Jr., Probability and Random Processes", McGraw-Hill KogaKusha Ltd., 1970.

[30] A.M. Mood, F.A. Graybell, D.C. Boes, Introduction to the Theory of Statistics, McGraw-Hill Inc., 1974.

[31] M. Schwartz, W.R. Bennet, S. Seymour, Communications Systems and Techniques, McGraw-Hill, New York, 1966.

[32] J.D. Parsons, J.G. Gardiner, Mobile Communications Systems, Blackie and Son Limited, Glasgow and London, 1989.

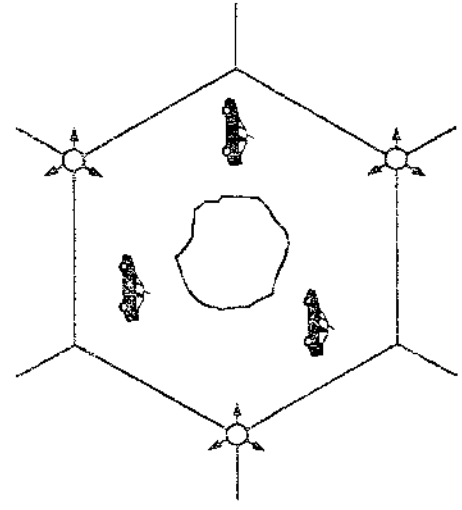

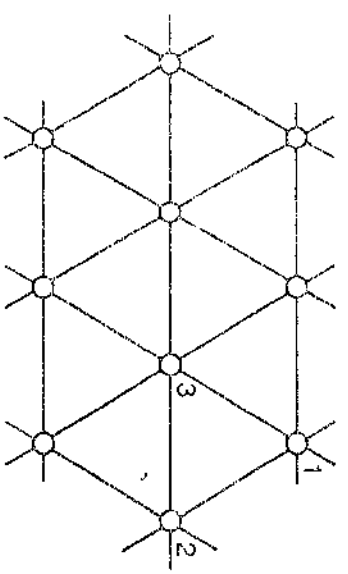

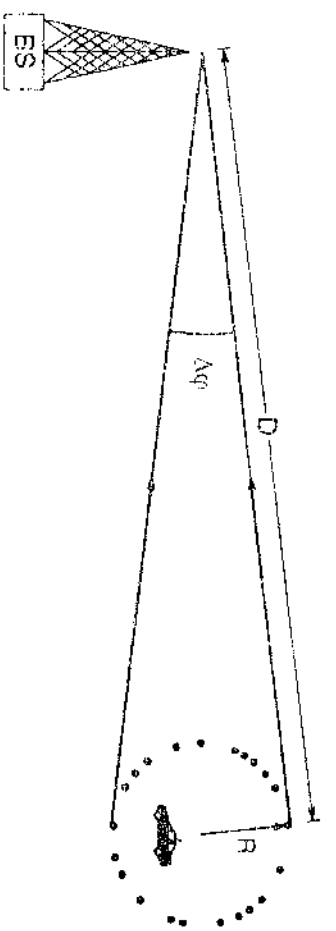

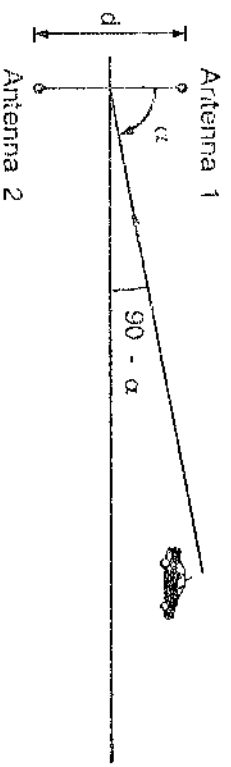

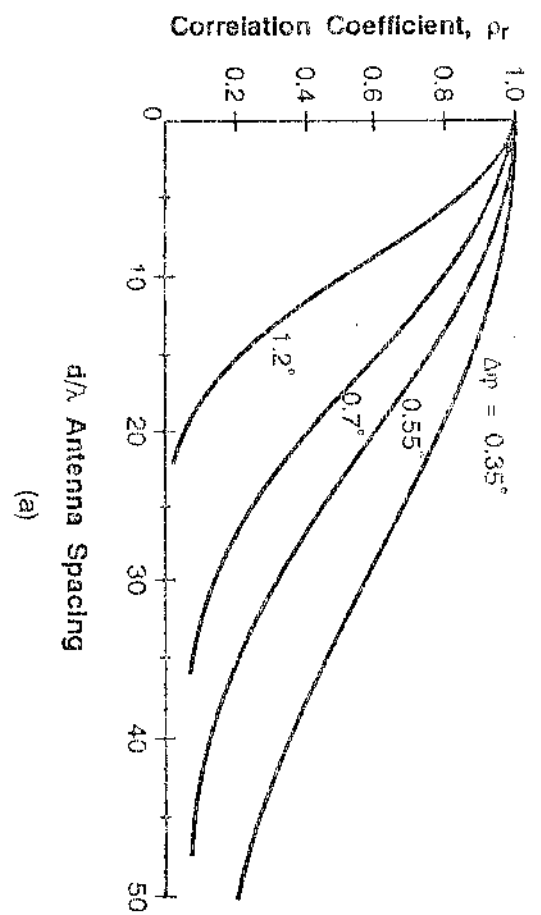

(a)

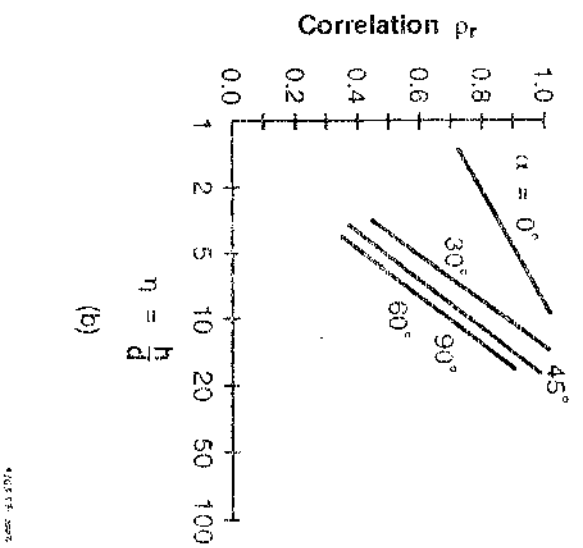

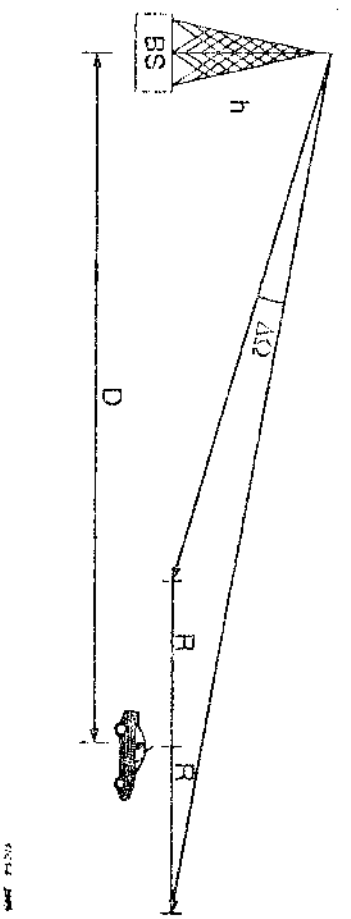

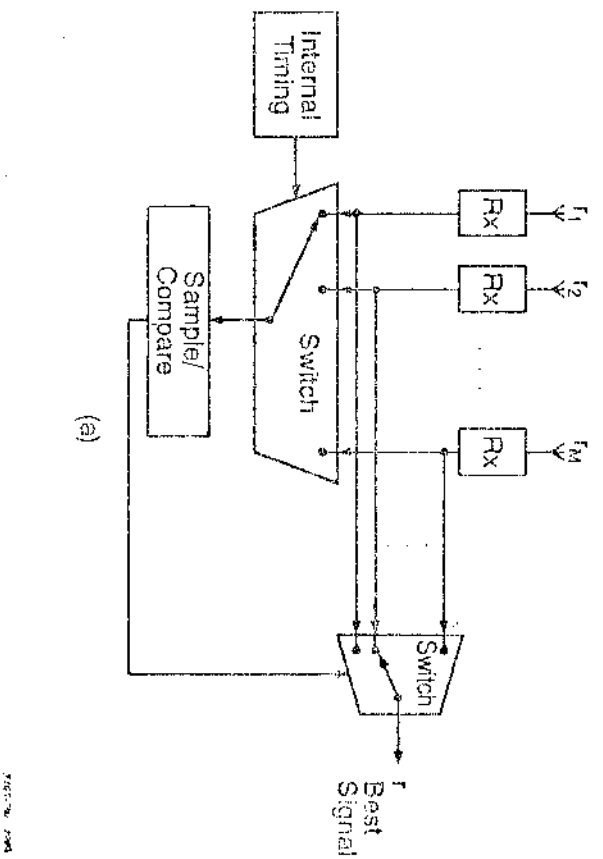

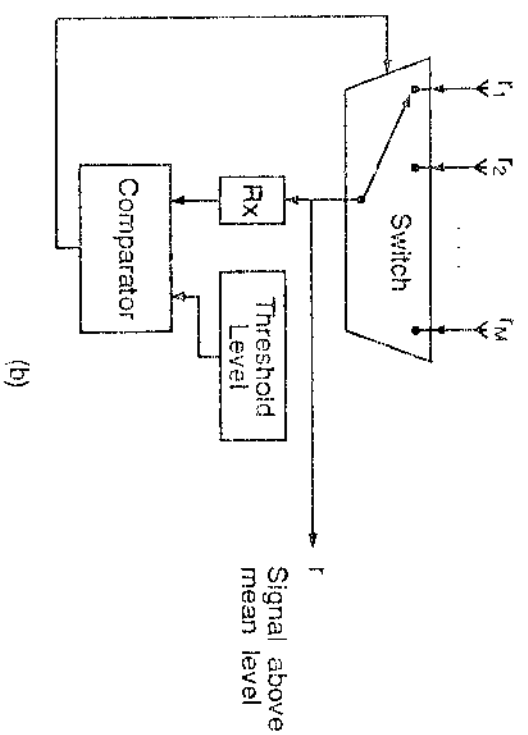

(c)

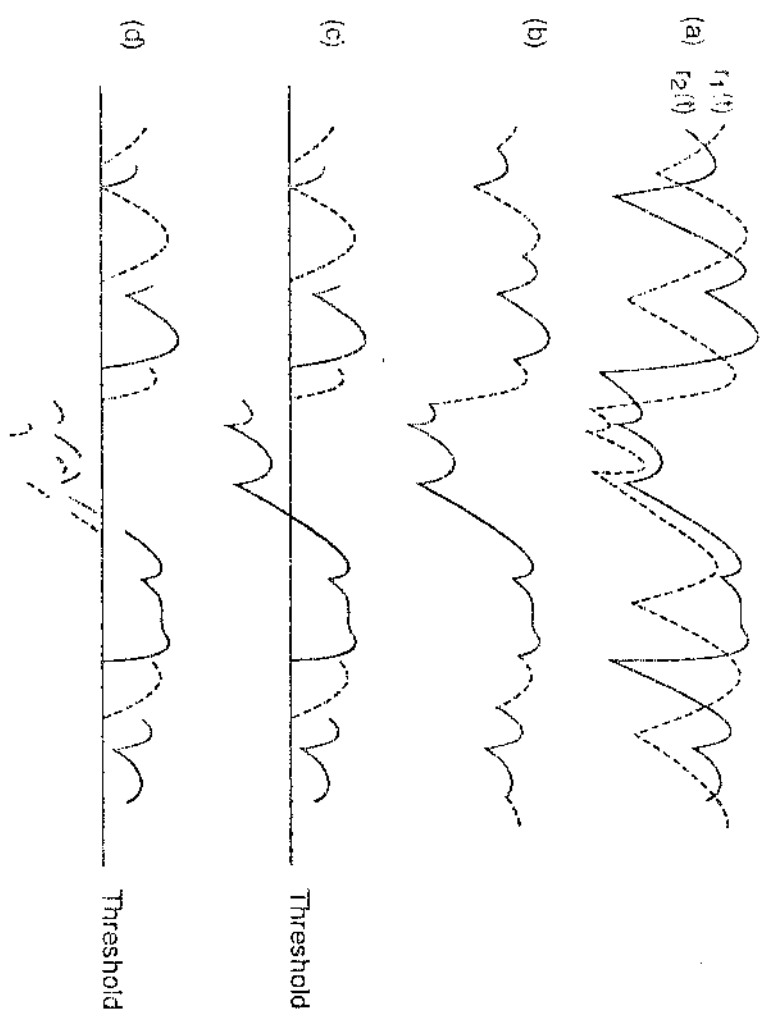

Fig. 5-8 ISM

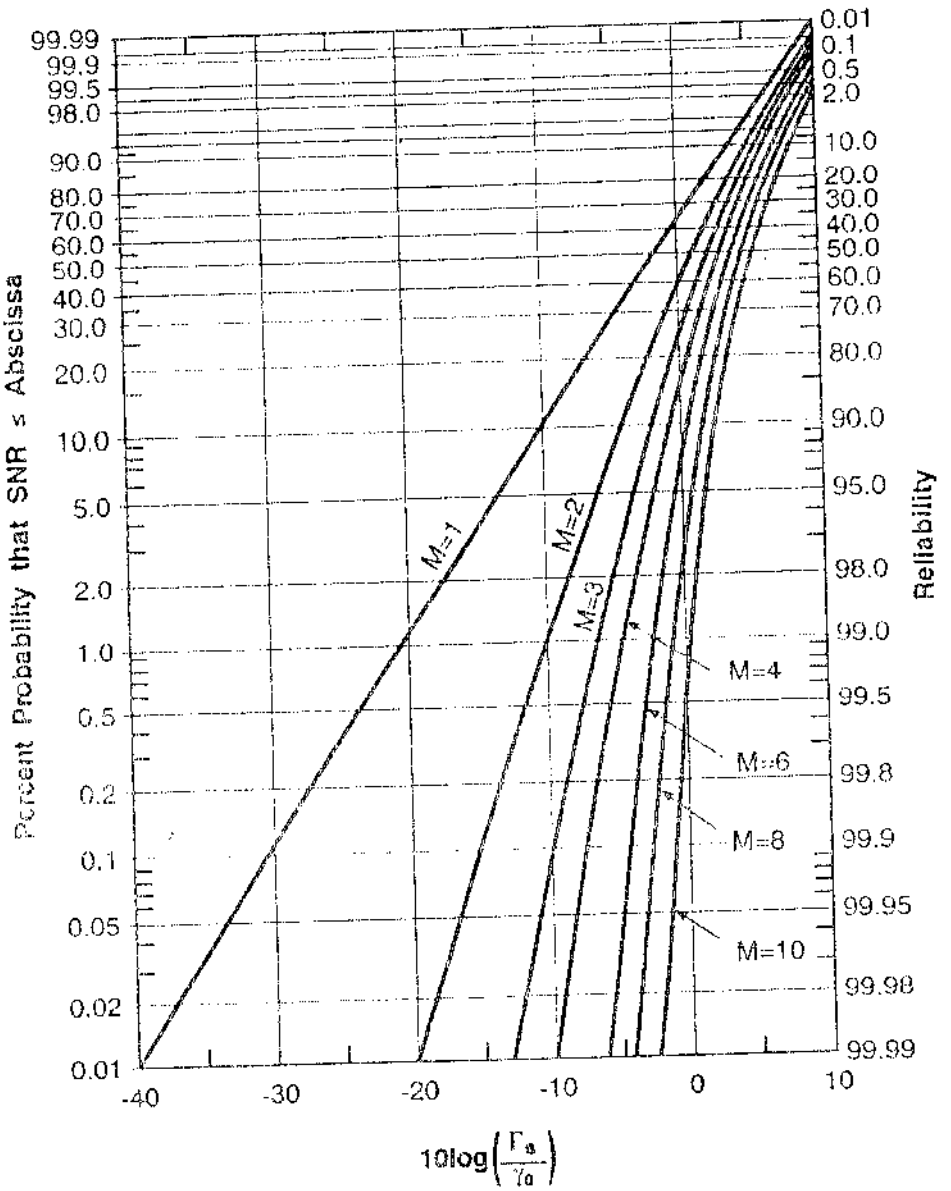
Percent Probability that SNR ≤ Abscissa
99.99
99.9
99.5
98.0
90.0
80.0
70.0
60.0
50.0
40.0
30.0
20.0
10.0
5.0
2.0
1.0
0.5
0.2
0.1
0.05
0.02
0.01
-40
-30
-20
-10
0
10
$10\log\left(\frac{\Gamma_a}{\gamma_a}\right)$
M=1
M=2
M=3
M=4
M=6
M=8
M=10
Reliability
0.01
0.1
0.5
2.0
10.0
20.0
30.0
40.0
50.0
60.0
70.0
80.0
90.0
95.0
98.0
99.0
99.5
99.8
99.9
99.95
99.98
99.99

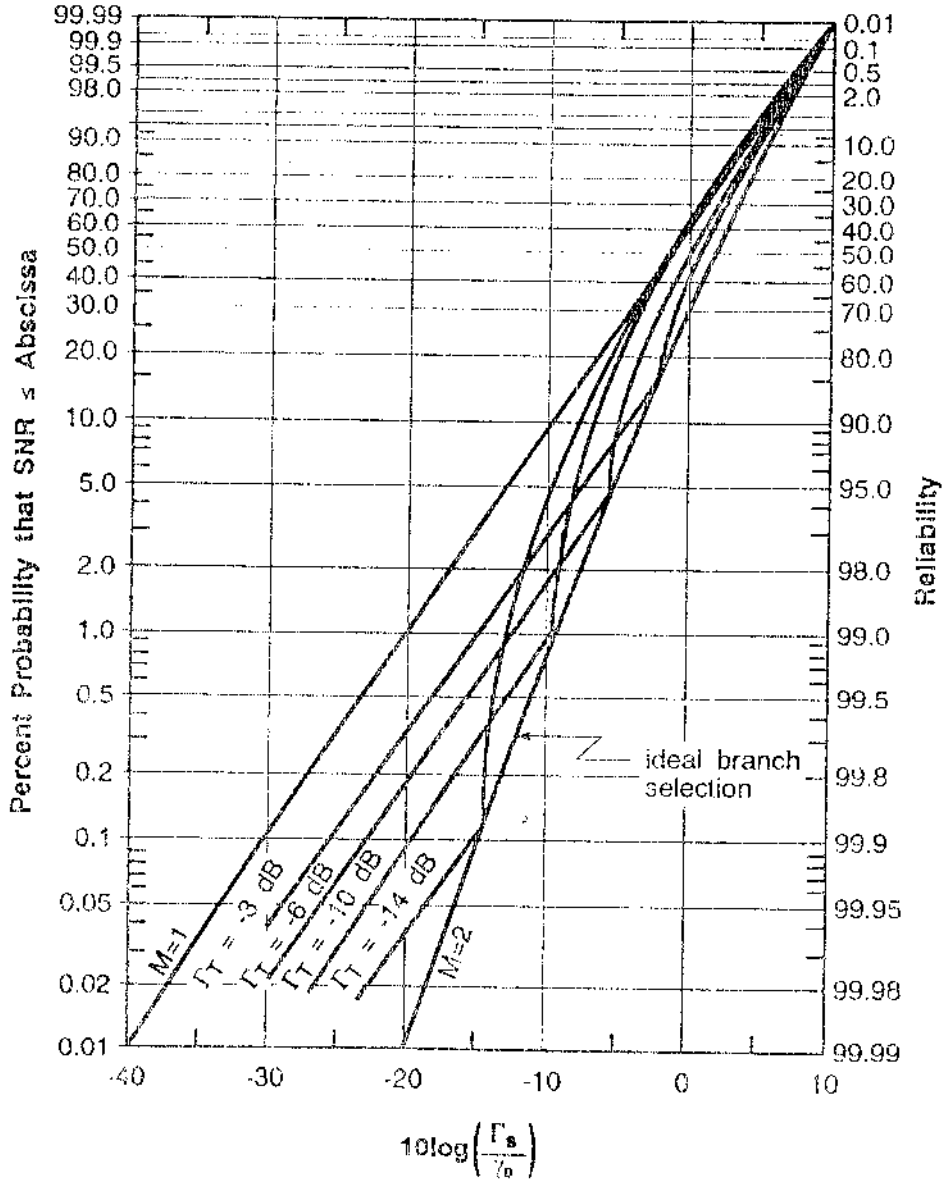
Percent Probability that SNR ≤ Abscissa
99.99
99.9
99.5
98.0
90.0
80.0
70.0
60.0
50.0
40.0
30.0
20.0
10.0
5.0
2.0
1.0
0.5
0.2
0.1
0.05
0.02
0.01
-40
-30
-20
-10
0
10
$10\log\left(\frac{\Gamma_s}{\gamma_0}\right)$
Reliability
0.01
0.1
0.5
2.0
10.0
20.0
30.0
40.0
50.0
60.0
70.0
80.0
90.0
95.0
98.0
99.0
99.5
99.8
99.9
99.95
99.98
99.99
M=1
Γ_T = -3 dB
Γ_T = -6 dB
Γ_T = -10 dB
Γ_T = -14 dB
M=2
ideal branch selection

FIGS-11 1605

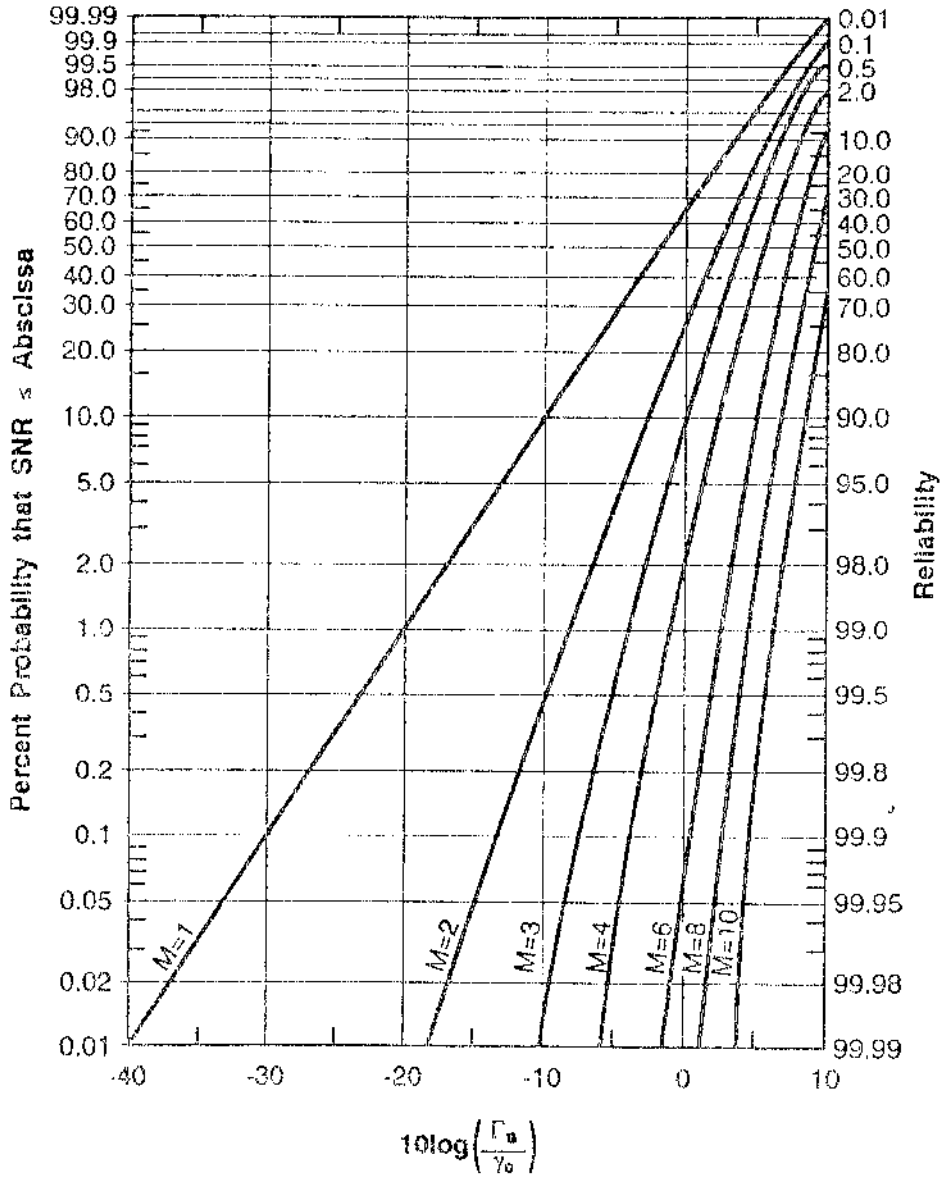
Percent Probability that SNR ≤ Abscissa
99.99
99.9
99.5
98.0
90.0
80.0
70.0
60.0
50.0
40.0
30.0
20.0
10.0
5.0
2.0
1.0
0.5
0.2
0.1
0.05
0.02
0.01
-40
-30
-20
-10
0
10
$10\log\left(\frac{\Gamma_a}{\gamma_0}\right)$
M=1
M=2
M=3
M=4
M=6
M=8
M=10
Reliability
0.01
0.1
0.5
2.0
10.0
20.0
30.0
40.0
50.0
60.0
70.0
80.0
90.0
95.0
98.0
99.0
99.5
99.8
99.9
99.95
99.98
99.99

FIGS-12 1965

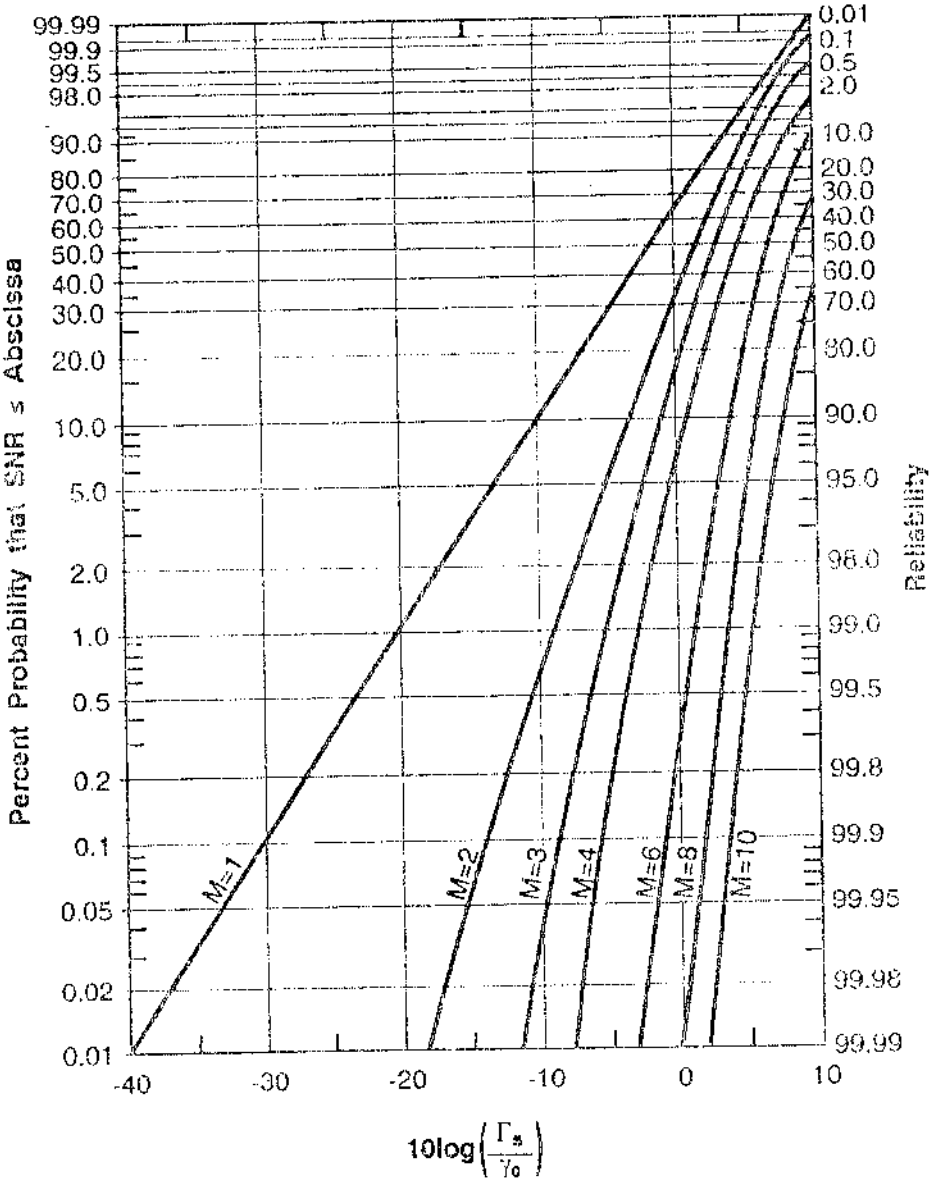
Percent Probability that SNR ≤ Abscissa
99.99
99.9
99.5
98.0
90.0
80.0
70.0
60.0
50.0
40.0
30.0
20.0
10.0
5.0
2.0
1.0
0.5
0.2
0.1
0.05
0.02
0.01
-40
-30
-20
-10
0
10
M=1
M=2
M=3
M=4
M=6
M=8
M=10
0.01
0.1
0.5
2.0
10.0
20.0
30.0
40.0
50.0
60.0
70.0
80.0
90.0
95.0
98.0
99.0
99.5
99.8
99.9
99.95
99.98
99.99
Reliability
$10\log\left(\frac{\Gamma_s}{\gamma_0}\right)$

Fig 5.13 1996

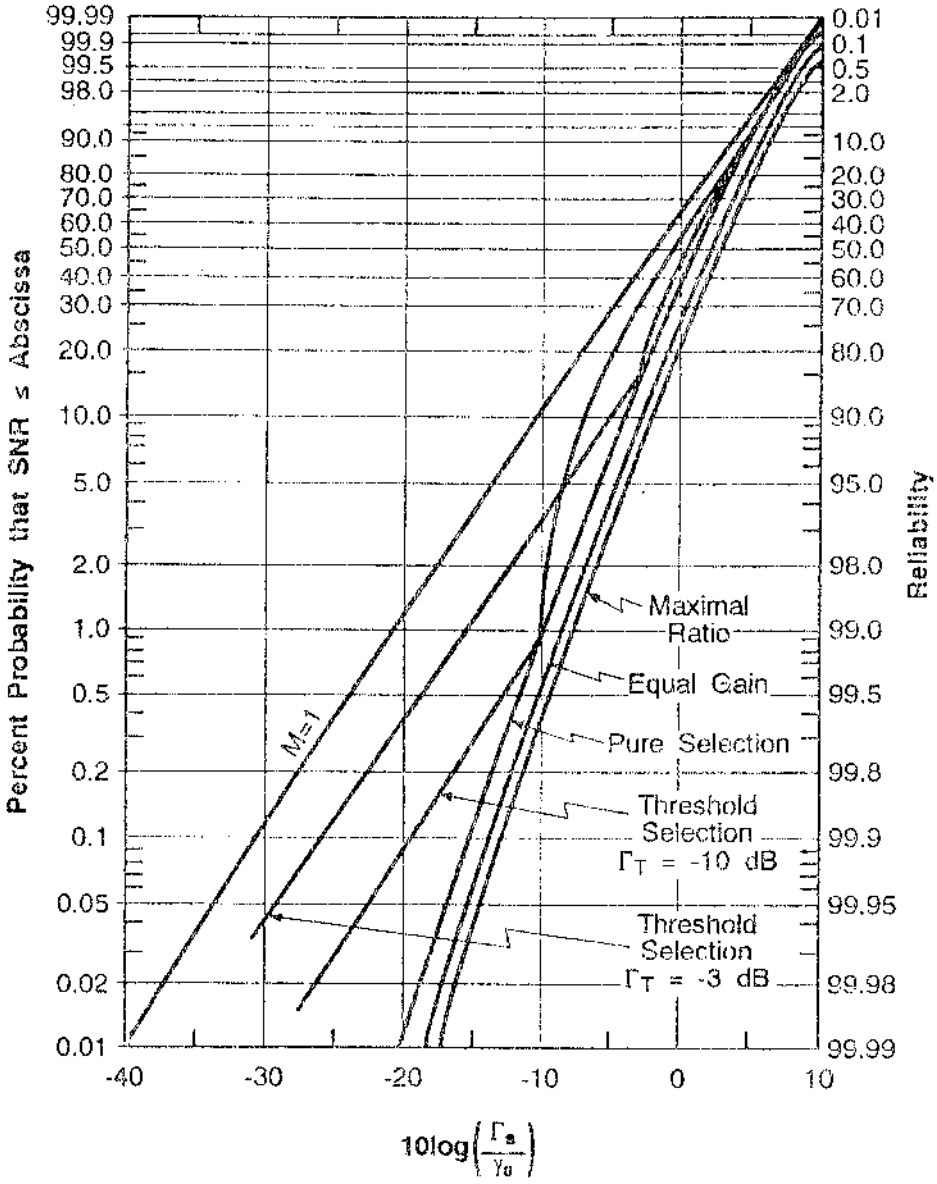
Percent Probability that SNR ≤ Abscissa
Reliability
99.99
99.9
99.5
98.0
90.0
80.0
70.0
60.0
50.0
40.0
30.0
20.0
10.0
5.0
2.0
1.0
0.5
0.2
0.1
0.05
0.02
0.01
0.01
0.1
0.5
2.0
10.0
20.0
30.0
40.0
50.0
60.0
70.0
80.0
90.0
95.0
98.0
99.0
99.5
99.8
99.9
99.95
99.98
99.99
-40
-30
-20
-10
0
10
M=1
Maximal Ratio
Equal Gain
Pure Selection
Threshold Selection
Γ_T = -10 dB
Threshold Selection
Γ_T = -3 dB
$10\log\left(\frac{\Gamma_s}{\gamma_0}\right)$

Fig. 14 - [illegible]

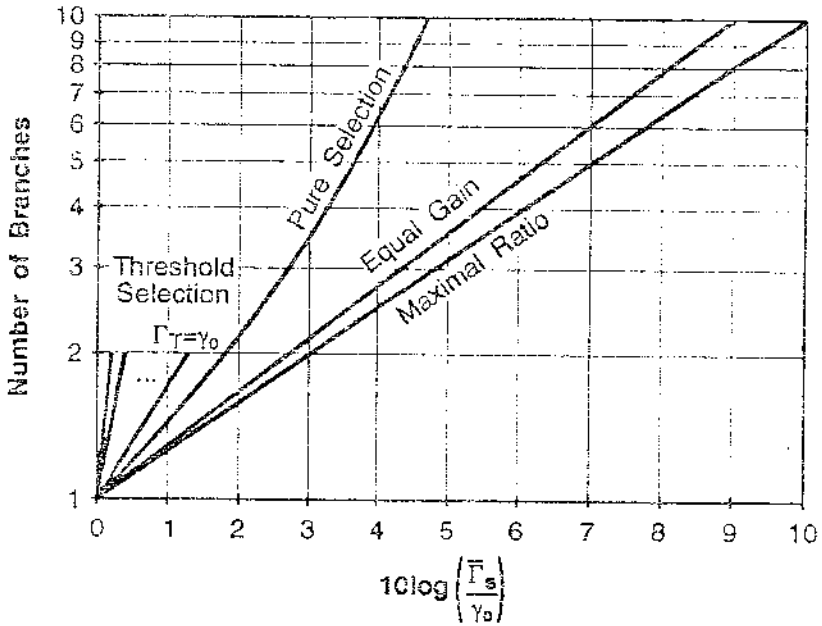

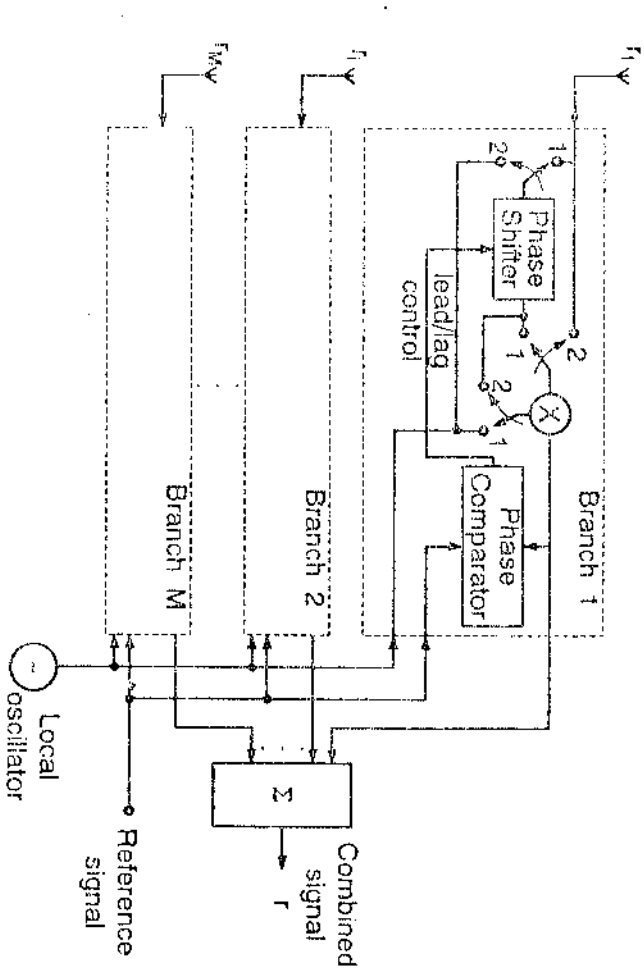

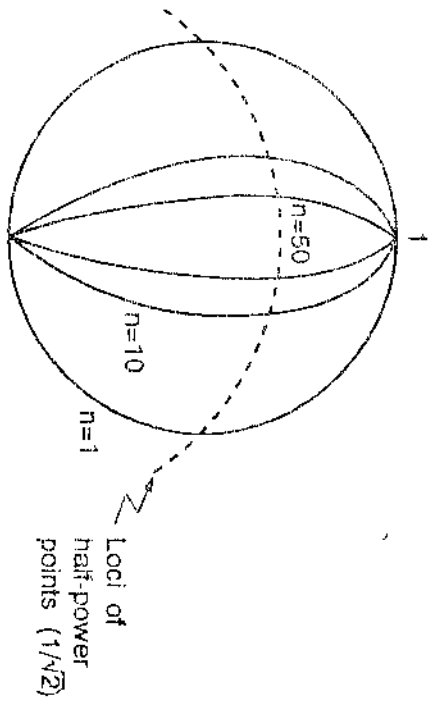

CHAPTER 6

DATA AND SIGNALLING TRANSMISSION

PREAMBLE

This chapter examines the performance of digital transmission over a fading environment. The performance measure is the bit error rate (or equivalently, the probability of bit error) for a given average signal-to-noise ratio per bit. We first review the bit error rate of some binary modulation schemes, namely FSK and PSK, to later examine how their performance can be improved. The aim is to get an insight into the qualitative improvement achieved when diversity, coding or multiple transmission are applied. Accordingly, the simple binary modulation techniques were chosen in order to ease our analysis. However, the basic principles described here can be directly applied to more elaborate modulation schemes as those studied in Chapter 9. Some other improvement techniques such as interleaving, ARQ and adaptive equalization are also briefly investigated. An appendix on channel coding is included with the objective of introducing the very basic concepts and main codes.

6.1 INTRODUCTION

In a mobile radio system, data or signalling can be transmitted over speech channels or separate signalling channels, depending on the control task to be performed. Examples of control tasks include the phases of a mobile call set up, handoff between base stations and call disconnect. Messages exchange between mobile

and base station is carried out over radio channels, whereas messages between base station and mobile switching centre usually flow through land links.

There are two types of signalling messages transmitted over the radio channels: (i) those sent as a continuous stream of bits and (ii) those sent in bursts. The former include mobile pages, systems status reports and overhead messages, and are transmitted over separate signalling channels. The latter comprise (a) call release and handoff, making use of speech channels, as well as (b) requests from mobile to base station, using separate signalling channels.

In analog systems special attention is given to problems arising from the association of voice, using analog transmission, and data, using digital transmission. In digital systems data and digitized voice can use the same digital techniques.

One very important issue in digital transmission is synchronization. Time jitter or frequency drift of the clock may provoke an increase of the bit or word error rate degrading the performance of the system. Techniques to improve bit or frame synchronization can be used to minimize the effects of both time jitter and frequency drift. A sequence of alternate 0's and 1's can be used to achieve bit synchronization. In the same way, the inclusion of one or more known word-patterns at the beginning and/or at the end of the frame can be used to achieve frame synchronization. At the reception the word-patterns are stored to be compared with the incoming sequence.*

Despite synchronization, bit or word errors can still occur due to many other factors, including fading. This chapter aims at examining the occurrence of errors in data transmission of the mobile radio system as well as investigating the usual methods employed to minimize the error occurrence. We shall restrict our attention to some binary modulation systems due to their simplicity and universal applicability. Moreover, these are the digital modulation schemes used in the analog mobile radio systems. It is understood that the digital systems use higher order modulation

---

* For more on synchronization and the definition of the TDMA structure refer to Chapter 10

schemes. Our aim in this Chapter, however, is not to compare modulation techniques but to investigate the qualitative effects of the techniques used to improve bit error rate performance. Furthermore, all of the procedures here described can be directly applied to the higher order modulation schemes.*

6.2. DIGITAL MODULATION SCHEMES

The transmission of binary data over a band pass channel requires the modulation of the data onto a carrier wave. The carrier is usually a sinusoid, conveniently keyed by the data according to one of the three basic techniques: Amplitude-Shift Keying (ASK), Frequency- Shift Keying (FSK) and Phase-Shift Keying (PSK). The PSK and FSK present a constant envelope, leading to a lower sensitivity to the amplitude nonlinearities. Consequently, these digital modulation schemes are preferably used than the ASK.

At the reception side, the detection can be carried out by either coherent or noncoherent techniques. Consequently, we may have coherent FSK or coherent PSK and noncoherent FSK or "noncoherent" PSK. In fact, it is not possible to have noncoherent PSK, since PSK requires the knowledge of the phase (contradicting the name noncoherent). A variation of PSK, based on a differential encoding of the binary data, provides the means for a noncoherent detection as required. This modulation technique is named Differential Phase-Shift Keying (DPSK).

6.3. ERROR RATES FOR BINARY SYSTEMS

As we shall see in Chapter 9, the probability of a symbol error in the presence of a stationary additive Gaussian noise depends only on the SNR associated with each

---

* For the description and analysis of the digital modulation schemes used in the digital cellular systems refer to Chapter 9.

symbol. This is true if we consider a receiver with a linear filter processing an undistorted waveform. In other words, the probability of error occurrence depends on the ratio between the energy and noise power per bit. For each one of the binary systems, given the SNR (γ_b) per bit, these probabilities are

$$\text{prob}(\text{error}|\gamma_b) = \frac{1}{2}\exp(\alpha\gamma_b), \qquad \begin{cases}\alpha = 1/2 & \text{for noncoherent FSK} \\ \alpha = 1 & \text{for "noncoherent" PSK (DPSK)}\end{cases} \tag{6.1}$$

$$\text{prob}(\text{error}|\gamma_b) = \frac{1}{2}\,\text{erfc}(\sqrt{\alpha\,\gamma_b}), \qquad \begin{cases}\alpha = 1/2 & \text{for coherent FSK} \\ \alpha = 1 & \text{for ideal PSK}\end{cases} \tag{6.2}$$

It has been shown in Chapter 5 that the distribution of γ_b in a Rayleigh fading environment is

$$p(\gamma_b) = \frac{1}{\gamma_{b0}}\exp\left(-\frac{\gamma_b}{\gamma_{b0}}\right) \tag{6.3}$$

where γ_{b0} is the average SNR/bit. Consequently, the unconditional probability of error is

$$\text{prob}(\text{error}) \triangleq p = \int_0^\infty \text{prob}(\text{error}|\gamma_b)p(\gamma_b)d\gamma_b \tag{6.4}$$

Using (6.1) and (6.3) in (6.4) we obtain

$$p = \frac{1}{2(1+\alpha\gamma_{b0})} \tag{6.5}$$

for noncoherent detection. In a similar way, with (6.2) and (6.3) in (6.4) we have

$$p = \frac{1}{2\left\{1 - \sqrt{1 + \frac{1}{\alpha\gamma_{b0}}}\right\}} \tag{6.6}$$

for coherent detection.

6.4 PROBABILITY OF ERRORS IN A DATA STREAM

Let p be the probability of bit error. The probability of having exactly m bits

in error in a message of N bits is given by the binomial expansion

$$p(N,m) = \binom{N}{m}(1-p)^{N-m}p^{m} \tag{6.7}$$

where

$$\binom{N}{m} = \frac{N!}{(N-m)!\,m!} \tag{6.8}$$

The probability of error (p_{eM}) in a message containing N bits is

$$p_{eM} = 1 - p(N,0) = 1 - (1-p)^{N} \tag{6.9}$$

We can also calculate the probability of receiving a falsely recognizable word. This corresponds to the event that the receiver recognizes a signal as one message, given that the transmitter had sent another message. If the two messages differ from each other by d bits, then the probability of this event is

$$p_{f} = (1-p)^{N-d}p^{d} \tag{6.10}$$

6.5 IMPROVING THE PERFORMANCE OF DIGITAL TRANSMISSION

Several techniques can be applied to improve the performance of digital transmission. The fading of the channels has an important effect on the bit error rate, degrading the performance of any modulation scheme as shown in Chapters 8 and 9. In other to counteract fading and, consequently, diminish the bit error rate, the following techniques can be used (individually or combined):

- Diversity
- Error Detecting and Correcting Codes
- Multiple Transmission
- Interleaving
- Automatic Repeat Request
- Adaptive Equalization

Bit error rate performance enhancement is accomplished at the expenses of increasing system complexity and cost. Some techniques can yield better results than others, but can also be more costly. Therefore, the decision for one or another technique depends on the cost versus effectiveness analysis. In the next sections we shall investigate these techniques.

6.6 DIVERSITY AND DIGITAL TRANSMISSION

The use of diversity technique for analog transmission has proved to be very effective. In this case we use the signal-to-noise ratio as the effectiveness criterion (refer to Chapter 5). The effectiveness of diversity on data (digital) transmission can be assessed by the reduction in the error rate, achieved when these techniques are used. The probability of bit error can be evaluated by averaging the conditional probability $\text{prob}(\text{error}|\gamma_b)$ over the distribution $p(\gamma_b)$ of γ_b as shown in (6.4). The distribution of γ_b depends on the diversity-combining technique as described in Chapter 5. For convenience, we shall reproduce these distributions and then estimate the probability of error, p.

1) Switched Combining: Pure Selection

The distribution of γ_b is

$$p(\gamma_b) = \frac{M}{\gamma_{b0}} \left[1 - \exp\left(-\frac{\gamma_b}{\gamma_{b0}}\right)\right]^{M} \exp\left(-\frac{\gamma_b}{\gamma_{b0}}\right) \tag{6.11}$$

1a) *Noncoherent Detection*

With (6.1) and (6.11) in (6.4) we obtain

$$\text{prob}(\text{error}) \triangleq p = \frac{M!}{2 \prod_{i=1}^{M} (i + \alpha\gamma_{b0})} \tag{6.12}$$

1b) *Coherent Detection*

Switched Combining does not require any coherent phase reference for detection.

Consequently, this kind of technique is of no use for coherent detection.

2) Switched Combining: Threshold Selection

The distribution of γ_b is

$$p(\gamma_b) = \begin{cases} (1+q)\left[1 - \exp(-\gamma_b/\gamma_{b0})\right] & , \gamma_b \geq \gamma_T \quad (6.13a) \\ q\left[1 - \exp(-\gamma_b/\gamma_{b0})\right] & , \gamma_b < \gamma_T \quad (6.13b) \end{cases}$$

where $q = 1 - \exp(-\gamma_T/\gamma_{b0})$ and γ_T is SNR threshold level.

2a) *Noncherent Detection*

The probability of error is determined as follows

$$\text{prob(error)} \triangleq p = \int_0^{\gamma_T} \text{prob(error}|\gamma_b)p(\gamma_b)d\gamma_b + \int_{\gamma_T}^{\infty} \text{prob(error}|\gamma_b)p(\gamma_b)d\gamma_b$$

In the first integral we use (6.13a) for $p(\gamma_b)$, whereas in the second integral we use (6.13b). In both of them the conditional probability $\text{prob(error}|\gamma_b)$ is given by (6.1). Hence

$$p = \frac{q + (1-q)\exp(-\alpha\gamma_T)}{2(1+\gamma_{b0})} \quad (6.14)$$

2b) *Coherent Detection*

Not applicable (see item 1b).

3) Gain Combining: Maximal Ratio

The distribution of γ_b is

$$p(\gamma_b) = \frac{\gamma_b^{M-1} \exp(-\gamma_b/\gamma_{b0})}{\gamma_{b0}^{M}(M-1)!} \quad (6.15)$$

3a) *Noncoherent Detection*

With (6.1) and (6.15) in (6.4) we have

$$\text{prob(error)} \triangleq p = \frac{1}{2(1+\alpha\gamma_{b0})^M} \quad (6.16)$$

3b) *Coherent Detection*

In a similar way, (6.2) and (6.15) in (6.4) gives the probability of error for maximal ratio coherent combining. However, no convenient closed-form solution seems to be available. We can approximate (6.15) by using the leading term of its series expansion, or equivalently, we may consider a low SNR. Both approximations correspond to the case of low bit error rates. Hence, the approximate distribution of γ_b is

$$p(\gamma_b) \approx \frac{\gamma^{M-1}}{\gamma_{b0}^{M}(M-1)!} \tag{6.17}$$

With (6.2) and (6.17) in (6.4) we obtain

$$\text{prob(error)} \triangleq p = \frac{(M-1/2)!}{2\sqrt{\pi}\ (\alpha\gamma_{b0})^{M}\ M!} \tag{6.18}$$

where $(\cdot)!$ is the gamma function . In this particular case

$$\left(M-\frac{1}{2}\right)! = \frac{1.3.5.7...(2M-1)}{2^{M}}\sqrt{\pi}$$

4) Gain Combining: Equal Gain

A closed-form solution for the equal gain combining can only be given by an approximate expression. Moreover, as shown in Chapter 5, this approximate solution differs from that of the maximal ratio by a factor of $(M/2)^{M}\sqrt{\pi}\ /\ (M-1/2)!$. Therefore, we may use this same factor, modifying the probability of error of the maximal ratio, to obtain the probability of error of the equal gain case.

4a) *Noncoherent Detection*

$$\text{prob(error)} \triangleq p = \frac{(M/2)^{M}\sqrt{\pi}}{2(M-1/2)!}\ \frac{1}{(1+\alpha\gamma_{b0})^{M}} \tag{6.19}$$

4b) *Coherent Detection*

$$\text{prob(error)} \triangleq p = \frac{(M/2)^{M}}{2(\alpha\gamma_{b0})^{M}\ M!} \tag{6.20}$$

A plot of the error rates with maximal ratio combining for both coherent and noncoherent detections is shown in Figure 6.1. We also show the probability of error in a Gaussian (non-fading) environment, for comparison. Note that the curves for PSK (α = 1) are obtained from the corresponding ones for FSK (α = 1/2), at 3 dB lower SNR.

6.7 ERROR DETECTING AND CORRECTING CODES

The signal energy per bit-to-noise power density ratio ($E_b/N_0 = \gamma_b$) is intimately related to the bit error rate. Practical implementation of a digital transmission system imposes limits on the power ratio γ_b. This, in connection with the chosen modulation scheme, dictates the system performance. The bit error rate performance can be substantially improved by means of coding. Coding is a rather extensive subject covered in many text books (e.g., [3-6]). For a summary on the subject refer to Appendix 6A.

This section is essentially concerned with the Forward Error Correction (FEC) technique as a means of error control. As far as mobile radio application is concerned, the codes were initially developed to efficiently correct burst errors, a situation likely to occur on a fading channel. However, it was verified that the bursts usually occur during an extremely long period of time, forcing the codes to have proportionally long constraint length*. A new class of codes, able to correct random errors, was then developed to be more efficiently used for mobile radio applications.

There are several types of error correcting codes available: Hamming , Golay, Reed-Muller, BCH, Reed- Solomon, etc. A linear block code A having k information bits and n-k redundancy bits is described as A(n,k). Moreover, if its minimum distance is d, this code is able to correct up to t = (d - 1)/2 bits in n bits. The

* Refer to section 6A.4 for the definition of constraint length

ratio $r = k/n$ is called code rate. As an example, the Golay (23,12) has a total length of 23 bits with 12 information bits (11 redundancy bits). Its minimum distance is known to be equal to 7. Therefore, this code is able to correct up to 3 in 23 bits. Its code rate is $12/23 \approx 1/2$.

It is easy to see that, for a code that can correct up to t bits, the probability of message error is

$$p_{eM} = 1 - \sum_{m=0}^{t} p(N.m) \tag{6.21}$$

where p(N.m), given by (6.7), is the probability of having exactly m bits in error in an N-bit message. It is important to note that, in order to keep the same transmitted power, the SNR/bit in the encoded message is multiplied by the code rate, r. In other words the average SNR/bit of the encoded message is $(k/n)\ \gamma_{b0}$.

In order to get an insight into the improvement achieved when coding is used, we shall use a 12-bit message and two codes, namely shortened Hamming (17,12) and Golay (23,12). The aim is to estimate the probability of error in the encoded message, given by (6.21). For the Hamming (17,12) we have N = 17 and t = 1, whereas for the Golay (23,12) we have N = 23 and t = 3. As for the uncoded message N = 12 and t = 0 (no error can be corrected). The bit error probability p used in (6.7) varies according to the modulation technique. It is given by (6.5) for noncoherent detection or by (6.6) for coherent detection. The resultant curves for these cases are shown in Figure 6.2.

In Figure 6.2 only the curves for the noncoherent FSK are shown. Those for coherent FSK can be obtained at approximately 2 dB lower SNR. Furthermore, as seen in Figure 6.1, the curves for PSK can be obtained at approximately 3 dB lower SNR. Bearing this in mind, hereinafter, for simplicity, only the curves for noncoherent FSK will be shown. Note that the improvement is really substantial and this is even more noticeable at higher SNR.

6.8 MULTIPLE TRANSMISSION

In this technique each message is sent an odd number of times and, at the reception, a bit-by-bit majority decision is applied. If s is the number of repeats, a $(s + 1)/2$ - out of - s majority voting process is used to determine each valid bit in the message.

The probability of bit error, p', after a $(s + 1)/2$ - out of - s majority voting is the probability of occurring at least $(s + 1)/2$ errors, i.e.,

$$p' = \sum_{i = \frac{s+1}{2}}^{s} \binom{s}{i} p^i (1 - p)^{s-i} \tag{6.22}$$

where p is the bit error probability of a single transmission. The probability of having exactly m corrupted bits in an N-bit message is, as in (6.7)

$$p(N,m) = \binom{N}{m} (1 - p')^{N-m} p'^{m} \tag{6.23}$$

The probability that more than t bits are in error is, as in (6.21)

$$p_{eM} = 1 - \sum_{m=0}^{t} p(N,m) \tag{6.24}$$

where p(N,m) is given by (6.23).

Multiple transmission is also a type of code, known as repetition code. The repetition code is represented as (s,1), having a minimum distance equal to s. Therefore, it is able to correct up to $(s - 1)/2$ errors in a s-bit message, having a rate $r = 1/s$.

As an example, consider the transmission of a 12-bit message, using the repetition code (3,1), corresponding to a 2 - out of - 3 majority voting . Then consider this same message, using the repetition code (5,1), corresponding to a 3 - out of - 5 majority voting. We shall determine the probability of occurring at least one error in the message. This can be done by setting $t = 0$ in (6.24) and using the appropriate equations as required. Note that, in this case, $N = 12$ and $s = 3$ or

s = 5, depending on the repetition code. The resultant curves are shown in Figure 6.3.

6.9 INTERLEAVING

Interleaving is a simple and efficient way of using coding to combat error bursts occurring on a fading channel. Its basic principle is to spread the code word, conveniently positioning the bits one away from another, so that they experience independent fading. In this case the error bursts affect several clustered bits belonging to several code words. Therefore, the effect of the error burst is spread over the message so that it may be possible to recover the data with the non affected bits.

Interleaving is easily implemented with the use of memories where the code words are written row by row and read out column by column.

6.10 AUTOMATIC REPEAT REQUEST

Automatic Repeat Request (ARQ) systems require error detecting code only. If an error is detected at the receiver end, a request for repeat is sent over the return channel. ARQ systems can be very efficient with a relatively small amount of added redundancy. However, the message throughput* tends to reduce due to the obvious reasons. It can be emphasized that even when a message is repeated, the repetition may still fail. Note that the ARQ message may also fail (be in error). This can be overcome by considering any incoming message in error as an ARQ message. Hence the most recent outgoing message is repeated. It is obvious that interleaving and ARQ are not effective if combined. Let p_{eM} be the probability of error in message. Then the time to transmit a set of messages is increased by $1/(1 - p_{eM})$, whereas the

* Refer to Chapter 11 for the concept of throughput.

throughput is reduced by $(1 - p_{eM})$.

6.11 ADAPTIVE EQUALIZATION

Equalization is the compensation for phase and amplitude distortions of the signals using the telephone channel. This term is now widely spread and used for any type of channel. The use of equalizers as a fading technique is a rather challenging problem. If the channel characteristics are considered to be known, the equalizers can be easily (sometimes manually) adjusted to obtain the best performance. If, however, the channel characteristics are time varying, the equalizers are led to have adaptive properties. Adaptive equalizers are also used in a stationary environment where their internal settings remain unchanged after the steady state condition is achieved. In a non stationary condition , as in the mobile radio environment, the adaptive equalizers should adjust their coefficients in real time so as to track the changes on the channel. Therefore, a conveniently designed adaptive equalizer can be used to combat fading. It may also be effective against intersymbol interference (ISI)*.

A simplified model of a digital system using adaptive equalizer is sketched in Figure 6.4. The transmitted digital sequence x(n) arrives at the receiver as the sequence x"(n), a distorted form of x(n). The aim of the adaptive equalizer is to restore the signal as close as possible to its original form. An adaptive equalizer is a transversal filter having as an output the weighed sum of the input x"(n) delayed by a set of delaying elements (Δ)**. The estimate of x(n) is x'(n), obtained by

---

* Due to the time dispersive characteristics of the channel the transmitted symbol, ideally occupying a certain time interval, is distorted and extends to the next interval used by another symbol. This type of interference is known as intersymbol interference.

** Refer to Appendix 4B for a quick look at digital filter. This subject is fully explored in [21].

conveniently sampling the equalizer's output $\hat{x}(n)$. The sampling is carried out by the Decision Device block. After a training period the estimate x'(n) closely approximates x(n) and the adaptive equalizer starts its "tracking mode". In this mode the difference x'(n) - $\hat{x}(n)$ (the error) is used to continuously adjust the filters coefficients, h_i. If the variations of the received signal are slow enough, these perturbations can be tracked and corrected.

Note that we have assumed that there is an initial training period, or equivalently, a training sequence can be interleaved with the data packets to update the equalizer's settings. If the changes in the channel characteristics are slow, these assumptions are quite reasonable. However, in digital radio systems the conditions are exactly the opposite, and this approach cannot be used.

Instead, a new class of adaptive equalizers, using "blind" strategies to adjust the filter's coefficients, are preferred. "Blind equalization" or "self adaptive equalization" does not require training sequence. Therefore, the equalizer operates only on the tracking mode with a convergence rate slower than the conventional adaptive equalizers. Many blind equalization strategies have been proposed but this is still a subject of investigation [16,17,18].

An alternative adaptive equalizer, known as decision feedback equalizer, uses a feedback configuration. In this case, from the detected symbols the ISI is determined and used to be subtracted out from the new coming symbols [19,20].

6.12 COMPARATIVE PERFORMANCE AND COMBINED TECHNIQUES

The curves obtained in Figures 6.1 and 6.3 are now combined in Figure 6.5 for comparison.

Note that the use of coding substantially improves the bit error rate performance. Moreover, the Golay (23,12) code performs remarkably better than the 3 - out of - 5 majority voting. In a similar way, the Hamming (17,12) gives better results than the 2 - out of - 3 majority voting. The use of coding implies an increase of the

transmission rate, corresponding to a proportional increase of the necessary bandwidth. In this sense both Golay (23,12) and Hamming (17,12) codes require less bandwidth than the 3 - out of - 5 and 2 - out of - 3 majority voting, respectively.

If, however, transmission rate or (equivalently) bandwidth are critical, the use of diversity can be an excellent option. Nevertheless, it can be seen that although a 2-branch diversity and a 1/2-rate code present the same degree of redundancy, the latter gives better results. In particular, the Golay (23,12) has a minimum distance of 7, roughly corresponding to a fourth-order diversity if hard-decision decoding is used.

Diversity, coding and majority voting can be combined to improve even further the bit error rate performance. Since a great deal of combination is possible, as far as diversity is concerned, we shall restrict to the maximal ratio combining technique.

1) *Diversity and Coding*

The procedure to estimate the bit error rate is the same as that described in section 6.7. We notice, however, that instead of using (6.5) or (6.6) for p we use (6.16) or (6.18), respectively.

2) *Diversity and Majority Voting*

The procedure is the same as that described in section 6.8. In a similar way we use (6.16) or (6.18) for p instead of (6.5) or (6.6), respectively.

3) *Coding and Majority Voting*

The procedure is similar to that described in section 6.8. However, in (6.5) and (6.6) the average SNR/bit is reduced to $(k/sn)\gamma_{b0}$. Furthermore, in (6.24), the parameter t is set to be equal to the number of correctable bits of the used code.

4) *Diversity and Coding and Majority Voting*

The procedure is similar to that used for the combination of coding and majority voting. The difference is that instead of using (6.5) or (6.6), we use (6.16) or (6.18) respectively.

In the examples shown here we have assumed a 12-bit message, 2-branch diversity Golay (23,12) code and the 3 - out of - 5 majority voting. The results are depicted

in Figure 6.6. Note that the combination diversity plus coding is an excellent and simple option for a substantial increase in bit error rate performance.

6.13 CHOICE OF CODE

Consider a mobile receiver working with a capture effect such that it detects only the signals found to be above the rms value by a certain threshold. Let R be the received signal, $\sqrt{2}\,\sigma$ the rms value and T the threshold. Capture occurs if

$$20\log(R/\sqrt{2}\,\sigma) \geq T \tag{6.25}$$

Due to the occurrence of fading, a data stream transmitted over a mobile radio channel will carry a proportion of corrupted bits, erroneously detected at the receiver. We want to determine the appropriate code, able to minimize the effects of the fades. In other words we want to correct the corrupted bits. The first step is to determine the mean proportion of corrupted bits in the message and then apply an appropriate code able to correct this proportion. Constraints on power and bandwidth are not considered here. Moreover a perfect interleaving is assumed so as to minimize error bursts effects. Given the threshold as in (6.25), it is possible to estimate the average duration of fades τ and the level crossing rate R_c in a straightforward manner (refer to section 4.6 and 4.7)

$$R_c = \sqrt{2\pi}\, f_m (R/\sqrt{2}\,\sigma) \exp\left[-(R/\sqrt{2}\,\sigma)^2\right] \tag{6.26}$$

$$\tau = \frac{1}{\sqrt{2\pi}\, f_m (R/\sqrt{2}\,\sigma)} \left\{ \exp\left[(R/\sqrt{2}\,\sigma)^2\right] - 1 \right\} \tag{6.27}$$

Consider a transmission rate of z bits/s. With R_c crossings/second, the mean time between crossings is equal to $1/R_c$ and the corresponding mean number of bits within this time interval is z/R_c. In a similar way, if the mean duration of the fades is τ, the mean number of faded (corrupted) bits is $z\tau$.

Therefore, the mean proportion of corrupted bits is $z\tau/(z/R_c) = \tau R_c$ in the fading interval. The proportion τR_c is the mean proportion of bits in the message to be corrected. Using (6.26) and (6.27) we obtain

$$\tau R_c = 1 - \exp\left[-(R/\sqrt{2}\,\sigma)^2\right] \tag{6.28}$$

Consider a code able to correct t out of n bits. Accordingly, the ratio t/n must exceed τR_c so as to achieve the minimum error correction requirement. Thus

$$t/n \geq 1 - \exp\left[-(R/\sqrt{2}\,\sigma)^2\right] = \tau R_c \tag{6.29}$$

Since (6.25) gives the minimum requirement for the receiver to capture on the signal, we may use an equality sign to obtain $R/\sqrt{2}\,\sigma$ as a function of T and replace it in (6.29). Hence

$$t/n \geq 1 - \exp(-10^{T/10}) \tag{6.30}$$

As an example, let capture occur for T = −9 dB. Then using (6.30) we obtain $t/n \geq 0.118$. The Golay (23,12) corrects up to t = 3 bits in an n = 23 bit-message, corresponding to a proportion of 3/23 ≈ 0.13. Therefore, this code satisfies the minimum bit error correction requirement.

6.14 SUMMARY AND CONCLUSIONS

Digital transmission over mobile radio channels is greatly impaired by the fading effects. Many techniques, if used either individually or in a combined manner, can substantially improve the performance of bit error rate. The improvement is also dependent on the digital modulation scheme, with the coherent detection giving approximately 2 dB gain on the SNR with respect to noncoherent detection.

Branch diversity by itself is a powerful technique able to improve the SNR substantially (a 12 dB improvement in the SNR for a bit error probability of 10^{-3}).

Error detecting and correcting codes are only effective if combined with interleaving. Multiple transmission is also effective but usually requires larger bandwidth.

Data and control signalling involve digital transmission but with different requirements. Data transmission, generally, can tolerate delays and bit errors, whereas signalling usually requires quick response and a very low error rate. Generally speaking, data are transmitted as long message blocks and signalling uses short messages.

Accordingly, coding is an appropriate technique to be used with data and signalling transmission. Multiple transmission is more suitable for signalling whereas ARQ is more convenient for data.

APPENDIX 6A

Channel Coding: A Basic Introduction

The aim of this appendix is to give a quick look at a special branch of the digital signal processing, the channel coding, in order to supply its basic concepts to the reader who is not familiar with this subject. It should be emphasized that the approach used here is the simplest possible and a more rigorous treatment will be left for the appropriate literature (e.g., [2,4,5,6]).

6A.1 Coding Jargons

As far as error control is concerned coding can be used in two different approaches, namely, for ERROR DETECTION and ERROR CORRECTION. The codes used in the former case are very simple and usually appear combined with an Automatic Repeat Request (ARQ) scheme. The latter approach requires more elaborate codes so that up to a certain number of bit errors can be corrected at the reception. This scheme is known as Forward Error Correction (FEC).

The redundancies are added to the message by the channel encoder at the transmission end to produce the encoded data at higher bit rate. At the reception the channel decoder conveniently treats the whole received data in order to restore the initial message.

The codes have been classified into two basic groups, namely block codes and convolutional codes. They are distinguished from one another by the absence or presence of memory, respectively. Codes can also be classified as linear or nonlinear. In linear codes two code words can be added in modulo-2 arithmetic to generate a third code word.

6A.2 Linear Block Codes

In an (n,k) linear block code a k-bit message is encoded into an n-bit code word. Accordingly, the number of redundant bits is n-k. Given that an uncoded message is transmitted at a rate z, the transmission rate of the encoded message is increased to (n/k)z so that the total transmission time can be kept unaltered. The dimensionless ratio r = k/n is known as code rate and ranges from 0 to 1.

Let u be a k-dimensional row vector containing the uncoded message and c an n-dimensional row vector containing the encoded message. Define G as a k x n Generator Matrix, such that

$$c = uG \tag{6A.1}$$

Since c contains the uncoded message plus the redundant bits, the generator matrix should be composed of a k x k identity matrix and a k x (n - k) coefficient matrix. We denote the identity matrix by I_k and the coefficient matrix by P. Assuming that the k right-most bits of the code word correspond to the uncoded message we have

$$G = \left[P \;\vdots\; I_k \right] \tag{6A.2}$$

A block code with such representation is called Linear Systematic Block Code.

Another important definition is the parity-check matrix, with dimension (n - k) x n, written as

$$H = \left[I_{n-k} \;\vdots\; P^T \right] \tag{6A.3}$$

where I_{n-k} is an (n - k) x (n - k) identity matrix and P^T is an (n - k) x k matrix, the transpose of P. Hence

$$HG^T = \left[I_{n-k} \;\vdots\; P^T \right] \left[\begin{array}{c} P^T \\ \hdashline I_k \end{array} \right] = P^T + P^T = 0$$

since we use modulo-2 arithmetic.

The matrices G and H are used in the coding and decoding operations, respectively.

1) *Error Detection: Syndrome*

When transmitting a code word c, it arrives at the reception as r = c + e, where e is an error vector containing ones at the error positions and zeros elsewhere. At the reception the decoder performs the following operation

$$s = rH^T \tag{6A.4}$$

known as syndrome of r. It is easy to show that if $s \neq 0$ then errors have been detected. If $s = 0$ then errors have not been detected (although they could still have occurred). Since r = c + e and c = uG, then

$$s = \cancel{uGH^T}^{\,0} + eH^T$$

$$s = eH^T \tag{6A.5}$$

The above equation shows that the syndrome depends only on the error pattern and not on the transmitted code word. Note that, since e is an n-dimensional row vector and H^T is an n x (n - k) matrix, then s is an (n - k)-dimensional row vector. In other words there are 2^{n-k} possible syndromes.

2) *Minimum Distance*

The Hamming distance d(x,y) between two code words x and y is defined as the number of ones obtained after the bit-by-bit exclusive-or operation between the two code words. Hence the distance between 1001 and 0111 is 3. The Hamming weight $\omega(x)$ of a code word x is defined as the number of nonzero elements of such code. In the examples given above the respective weights are 2 and 3. From the definition of Hamming distance it follows that

$$d(x,y) = \omega(x + y) \tag{6A.6}$$

The minimum distance d_{min} of a linear block code is the smallest Hamming distance between any pair of code vectors in the code, i.e.,

$$d_{min} = \min\left\{d(x,y) : x,y \in c,\ x \neq y\right\}$$

Therefore

$$d_{min} = \min\left\{\omega(x + y) : x,y \in c,\ x \neq y\right\}$$

Since $z = x + y$ is another code vector in c it follows that

$$d_{min} = \min\left\{\omega(z) : z \in c,\ z \neq 0\right\}$$

or

$$d_{min} = \omega_{min} \tag{6A.7}$$

In other words, the minimum distance is the smallest Hamming weight of the nonzero code vectors in the code.

3) *Error Correction*

An (n,k) code admits 2^n code vectors containing 2^k code words. The best decoding strategy is such that, upon receiving any code vector, the decoder associates it with the nearest code word. Define non overlapping spheres with radius t around each code word so that within each sphere all the code vectors are decoded correctly. Since (i) the spheres do no overlap and do not touch each other and (ii) the distance between two neighbouring code words is the minimum distance, then it is straightforward to show that (see Figure 6A.1).

$$d_{min} \geq 2t + 1 \tag{6A.8}$$

Consequently, we can say that an (n,k) linear block code can correct up to t errors such that

$$t \leq \left\lfloor \frac{d_{min} - 1}{2} \right\rfloor^{*} \tag{6A.8b}$$

4) *Hamming Bound*

Let i be the number of error locations in an n-bit word. Accordingly, there are $\binom{n}{i}$ possible error patterns. If t is the maximum number of error locations, the total number of all possible error patterns is $\sum_{i=0}^{t} \binom{n}{i}$. Consequently, an (n,k)

---

* $\lfloor x \rfloor$ denotes the largest integer less than on equal to x.

linear block code, able to correct up to t errors, admits 2^{n-k} syndromes (as seen before). It is obvious that the number of syndromes cannot be less than the total number of possible error patterns, i.e.,

$$2^{n-k} \geq \sum_{i=1}^{t} \binom{n}{i} \tag{6A.9}$$

Equation (6A.9) is known as the Hamming bound. Any binary code satisfying the equality condition

$$2^{n-k} = \sum_{i=0}^{t} \binom{n}{i} \tag{6A.10}$$

is known as "perfect code".

5) *An Example: Hamming Codes*

The Hamming codes have the following parameters, for any positive integer $m \geq 3$

Block length : $n = 2^m - 1$

Number of message bits : $k = 2^m - m - 1$

Number of redundant bits: $n - k = m$

Minimum distance : $d = 3$

For m = 3 we have the (7,4) Hamming code correcting up to (3 - 1)/2 = 1 bit in a 7-bit word. The corresponding generator and parity check matrices are

$$G = \left[\begin{array}{ccc:cccc} 1 & 1 & 0 & 1 & 0 & 0 & 0 \\ 0 & 1 & 1 & 0 & 1 & 0 & 0 \\ 1 & 1 & 1 & 0 & 0 & 1 & 0 \\ 1 & 0 & 1 & 0 & 0 & 0 & 1 \end{array}\right] = \left[\begin{array}{c:c} P & I_k \end{array}\right]$$

$$H = \left[\begin{array}{ccc:cccc} 1 & 0 & 0 & 1 & 0 & 1 & 1 \\ 0 & 1 & 0 & 1 & 1 & 1 & 0 \\ 0 & 0 & 1 & 0 & 1 & 1 & 1 \end{array}\right] = \left[\begin{array}{c:c} I_{n-k} & P^T \end{array}\right]$$

As an example, the code word corresponding to the message 1011 is 1001011. In a similar way, the message 1110 has 0101110 as its code word.

The syndrome is obtained by multiplying the error pattern by H^T. There are 7 possible single patterns that can be corrected. As an illustration, for an error at

the left-most bit, the error pattern is 1000000 and the corresponding syndrome is 100. For the error pattern 0000010 the syndrome is 111. For no error (0000000) the syndrome is 000, and so on.

6A.3 Cyclic Codes

Cyclic codes comprise a special class of linear block codes. Their algebraic structure is such that encoding, syndrome computation and decoding are very simple to be implemented and can be done by means of shift registers with some feedback connections. One fundamental property of this code is that any cyclic shift of a code vector in c is also a code vector in c.

This suggests that the elements of a code word of length n can be treated as the coefficients of a polynomial of degree (n - 1). Let c_i, i = 0,1,...,n-1 be the elements of a code word c. The corresponding code polynomial can be written as

$$c(D) = c_0 + c_1 D + c_2 D^2 + \ldots + c_{n-1} D^{n-1} \qquad (6A.11)$$

where D is an arbitrary real variable. If we impose that $D^n = 1$, then the multiplication of c(D) by D corresponds to a shift (rotation) of the elements of c(D) to the right. It is easy to show that if we multiply c(D) by D i times we get

$$D^i c(D) = c_{n-i} + c_{n-i+1} D + c_{n-i+2} D^2 + \ldots + c_0 D^i + c_1 D^{i+1} + c_2 D^{i+2} + \ldots + c_{n-i-1} D^{n-i} \qquad (6A.12)$$

The main theorems of the cyclic codes are presented next.

Theorem 6A.3.1

An (n,k) cyclic code admits one and only one nonzero code polynomial g(D) of minimum degree (n - k) given by

$$g(D) = 1 + g_1 D + g_2 D^2 + \ldots + g_{n-k-1} D^{n-k-1} + D^{n-k} \qquad (6A.13)$$

This is easily shown as follows.

Using the linearity property we can add g(D) and g'(D) to obtain another polynomial. The degree of the resultant polynomial is less than $n - k$, since $D^{n-k} + D^{n-k} = 0$

Note that in (6A.13) g_0 is necessarily equal to 1. In case $g_0 = 0$ and g(D) is right-shifted $n - 1$ times, a code polynomial of degree less than $n - k$ is obtained.

The polynomial g(D) is called Generator Polynomial.

Theorem 6A.3.2

Let g(D) be the code polynomial as described in Theorem 6A.3.1. A binary polynomial with degree of $n - 1$ or less is a code polynomial if and only if it is a multiple of g(D).

Let a(D) be a polynomial such that

$$a(D) = a_0 + a_1 D + \ldots + a_{k-1} D^{k-1} \qquad (6A.14)$$

Then $c(D) = a(D)g(D) = a_0 g(D) + a_1 Dg(D) + \ldots + a_{k-1} D^{k-1} g(D)$ corresponding to a linear combination of the code polynomial $g(D), Dg(D), \ldots, D^{k-1}g(D)$. This implies that c(D) is a code polynomial, given that a(D) is a multiple of g(D).

Now suppose we divide c(D) by g(D). The result is

$$c(D) = a(D)g(D) + b(D) \qquad (6A.15a)$$

where the remainder b(D) is either zero or a polynomial with degree less than that of g(D). We can rewrite (6A.15a) as

$$b(D) = c(D) + a(D)g(D) \qquad (6A.15b)$$

since $b(D) = -b(D)$ in modulo-2 arithmetic. Given that both c(D) and a(D)g(D) are code polynomials, b(D) should also be a code polynomial. However, as b(D) has a degree less than g(D), it follows that b(D) should be equal to zero, since g(D) is the nonzero code polynomial of minimum degree.

Theorem 6A.3.3

The generator polynomial g(D) is a factor of $1 + D^n$.

It can be seen that

$$D^k g(D) = 1 + D^n + g'(D) \tag{6A.16a}$$

where g'(D) is g(D) right shifted k times. This implies g'(D) being a multiple o g(D). Hence, consider that g'(D) = a(D)g(D). Rearranging (6A.16a) in modulo- arithmetic we have

$$1 + D^n = g(D)h(D) \tag{6A.16b}$$

where $h(D) = D^k + a(D)$. It can also be shown [6] that h(D) is the parity check polynomial of the (n,k) code.

1) *Encoding a Message*

Let $u = (u_0, u_1, ..., u_{k-1})$ be an uncoded message. Consider that g(D) is a generator polynomial such that an (n,k) systematic cyclic code is obtained. The message polynomial can be written as

$$u(D) = u_0 + u_1 D + ... + u_{k-1} D^{k-1} \tag{6A.17}$$

In the systematic representation we want the k bits of the message to occupy the k right-most bits of the n-bit code word. This is achieved by multiplying u(D) by D^{n-k}

$$D^{n-k} u(D) = u_0 D^{n-k} + u_1 D^{n-k+1} + ... + u_{k-1} D^{n-1} \tag{6A.18}$$

Dividing $D^{n-k}u(D)$ by the generator polynomial g(D) we obtain a quotient a(D) and a remainder b(D), i.e.,

$$D^{n-k} u(D) = a(D)g(D) + b(D) \tag{6A.19a}$$

In modulo-2 arithmetic (6A.19a) can be rewritten as

$$a(D)g(D) = b(D) + D^{n-k} u(D) \tag{6A.19b}$$

Since, according to Theorem 6A.3.2, a(D)g(D) = c(D) is a code word, we can use this in (6A.19b) and obtain

$$c(D) = b(D) + D^{n-k}u(D) \qquad (6A.20)$$

Equation (6A.20) represents a code word polynomial of the (n,k) cyclic code generated by g(D). Therefore, the steps involved in the encoding process for an (n,k) cyclic code according to a systematic representation are:

- Premultiply the message polynomial u(D) by D^{n-k}
- Divide $D^{n-k}u(D)$ by the generator polynomial g(D) in order to obtain the remainder b(D).
- Add b(D) to $D^{n-k}u(D)$ to obtain the code word polynomial c(D).

2) *Error Detection*

Upon receiving a code word, the first step in the decoding process is to calculate the syndrome. If the syndrome is nil, no errors are detected. If the syndrome is nonzero, errors are detected.

As far as cyclic codes are concerned, the syndrome calculation is carried out dividing the received encoded message by the generator polynomial. Since $c(D) = a(D)g(D) + b(D) + b(D) = a(D)g(D)$, when dividing c(D) by g(D) no remainder is obtained, in case no errors are introduced in the transmitted code word. Consequently, the remainder of the division of the received code word by the generator polynomial is the syndrome polynomial itself. Let r(D) be the received code polynomial. Then

$$r(D) = a(D)g(D) + s(D) \qquad (6A.21)$$

where s(D) is the syndrome polynomial.

3) *An Example: Hamming Codes*

Let us illustrate the coding and decoding process of a cyclic code using the (7,4) Hamming code. Since n = 7, according to Theorem 6A.3.3, the generator polynomial is a factor of $1 + D^7$. Therefore, if $1 + D^7$ is factored into irreducible polynomials* we obtain

* Irreducible polynomials are polynomials which cannot be factored out using only coefficients from the binary field.

$$1 + D^7 = (1 + D)(1 + D^2 + D^3)(1 + D + D^3)$$

Suppose we take the generating polynomial as being

$$g(D) = 1 + D + D^3$$

From (6A.16b) we have

$$h(D) = (1 + D)(1 + D^2 + D^3)$$
$$= 1 + D + D^2 + D^4$$

Let (0101) be the uncoded message. Its corresponding polynomial is $u(D) = D + D^3$. In order to obtain the uncoded message we follow the steps as previously described.

- Multiply the message by D^{n-k}

$$D^{n-k}u(D) = D^{7-4}(D + D^3) = D^4 + D^6$$

- Divide $D^{n-k}u(D)$ by $g(D)$

$$\begin{array}{r|l} D^6 + D^4 & D^3 + D + 1 \\ \hline D^6 + D^4 + D^3 & D^3 + 1 \text{ (quotient)} \\ \hline D^3 & \\ D^3 + D + 1 & \\ \hline D + 1 \text{ (remainder)} & \end{array}$$

- Obtain c(D)

$$c(D) = \underbrace{1 + D}_{b(D)} + \underbrace{D^4 + D^6}_{D^{n-k}u(D)}$$

The polynomial c(D) corresponds to the code word (1100101). Note that the four right-most bits constitute the uncoded message and the three left-most bits, the redundant bits. It can be verified that the remainder of the division c(D)/g(D) is nil. Any code word different from that produces a nonzero syndrome. As an example consider that the received code word is (1100111) represented by the polynomial $1 + D + D^4 + D^5 + D^6$. The division of such polynomial by g(D) results in a remainder equal to $1 + D + D^2$ corresponding to the syndrome of this particular error.

6A.4 Convolutional Codes

In block coding the code words are generated on a block-by-block basis. Moreover, the redundant bits at any time instant are function only of the message at that instant. In convolutional coding the encoder is a finite-state machine accepting the message bits in a serial manner. The generated code word at a certain time instant is a function of both the input at that instant and the state of the machine.

An (n,k,m) convolutional encoder accepts k serial inputs, yields n outputs and has a state machine with 2^m states. It is composed of an m-stage shift register with the output of each stage conveniently combined with the k inputs through n adders. The adders' outputs are then multiplexed so as to have one serialized encoded output. Consequently, if an information sequence of length kL is convolutionally encoded, the corresponding code word has a length n(L + m) and the code rate is given by

$$r = \frac{kL}{n(L + m)} \tag{6A.22a}$$

This reduces to

$$r \approx \frac{k}{n}, \qquad \text{if } L >> m \tag{6A.22b}$$

The constraint length is defined as the maximum number of encoder outputs that can be influenced by a single information bit. Hence the constraint length is given by n(m + 1).

As an example we show in Figure 6A.2 a (2,1,3) convolutional encoder.

1) *Encoding a Message*

Let $\mathbf{u} = (u_0, u_1, u_2, \ldots)$ be the message to be encoded using the encoder of Figure 6A.2. Since there are two adders, two corresponding sequences $c^{(1)} = (c_0^{(1)}, c_1^{(1)}, c_2^{(1)}, \ldots)$ and $c^{(2)} = (c_0^{(2)}, c_1^{(2)}, c_2^{(2)}, \ldots)$ are generated and finally combined to yield the encoded word $c = (c_0^{(1)}c_0^{(2)}, c_1^{(1)}c_1^{(2)}, c_2^{(1)}c_2^{(2)}, \ldots)$. The sequences $c^{(1)}$ and $c^{(2)}$ can be easily obtained by following the connections of the encoder

circuitry*. The corresponding expressions are shown in (6A.23a) and (6A.23b) where we have considered $c^{(1)}$ and $c^{(2)}$ to be the outputs of the top adder and the bottom adder, respectively.

$$c_l^{(1)} = u_l^{(1)} + u_{l-1}^{(1)} + u_{l-3}^{(1)} \qquad (6A.23a)$$

$$c_l^{(2)} = u_l^{(2)} + u_{l-1}^{(2)} + u_{l-2}^{(2)} + u_{l-3}^{(2)} \qquad (6A.23b)$$

We assume $u_{l-j} \triangleq 0$ for all $l < j$. Note that the above equations perform the convolution of the input sequence u with the respective response of each adder to the sequence (1,0,0...). The sequence (1,0,0...) is known as "impulse" and the output of the adder after this sequence is its "impulse response". Let $g^{(i)} = (g_0^{(i)}, g_1^{(i)}, g_2^{(i)}, \ldots)$ be the impulse response of the adder i. For the example of Figure 6A.2 we have

$$g^{(1)} = (1101)$$

$$g^{(2)} = (1111)$$

Accordingly, the response of the adder i to the sequence $u = (u_0, u_1, \ldots)$ is the following discrete convolution

$$c_l^{(i)} = \sum_{j=0}^{m} g_j^{(i)} u_{l-j}, \qquad \begin{matrix} i = 1,2,\ldots,n \\ l = 0,1,\ldots,L+m \end{matrix} \qquad (6A.24)$$

and $u_{l-j} = 0$ for all $l < j$.

Suppose, as an example, that the information sequence $u = (11001)$ is fed into the encoder of Figure 6A.2. Then

$$c^{(1)} = (10110101)$$

$$c^{(2)} = (10000111)$$

and $$c = (11,00,10,10,00,11,01,11)$$

The computations of (6A.24) can be greatly simplified if we use an appropriate

---

* The initial state of the machine should be zero (0,0,...) before any message feeds the input.

transform property by which the convolution in time domain is equivalent to multiplication in frequency domain. The frequency domain representation of a sequence is its polynomial form. Accordingly, if the impulse response $g^{(i)}$ and the message sequence **u** are expressed in their respective polynomial forms $g^{(i)}(D)$ and $u(D)$, the resultant convolution is the product of $g^{(i)}(D)$ by $u(D)$.

Hence,

$$g^{(i)}(D) = g_0^{(i)} + g_1^{(i)}D + \ldots + g_m^{(i)}D^m \qquad ,i = 1,2,\ldots,n$$

and

$$u(D) = u_0 + u_1D + \ldots + u_{l-1}D^{l-1}$$

Therefore, the convolution represented by (6A.24) can be written as

$$c^{(i)}(D) = g^{(i)}(D)u(D) \tag{6A.25}$$

For our particular example

$$g^{(1)}(D) = 1 + D + D^3$$

$$g^{(2)}(D) = 1 + D + D^2 + D^3$$

and

$$u(D) = 1 + D + D^4$$

Then

$$c^{(1)}(D) = g^{(1)}(D)u(D) = 1 + D^2 + D^3 + D^5 + D^7$$

$$c^{(2)}(D) = g^{(2)}(D)u(D) = 1 + D^5 + D^6 + D^7$$

This agrees with our previous calculations

2) *Decoding a Message*

Decoding algorithms play an essential role in the performance of a convolutional code. In this section we shall introduce the Viterbi algorithm initially implemented in a software form using a computer, and now, more recently, implemented in VLSI chips. Such algorithm is better understood if we make use of the trellis diagram. This is the expanded form of the encoder's state diagram represented in time.

2a) *State and Trellis Diagrams*

Let us first use the state diagram (SD) representation and then the trellis diagram (TD) one. For the encoder of Figure 6A.2 the SD is shown in Figure 6A.3.

In this SD each branch is labelled with input/output$^{(1)}$output$^{(2)}$ where the outputs correspond to the respective outputs represented in Figure 6A.2. Any information (message) sequence can be encoded using the SD. We assume that the encoder is initially at state (000) and that after the last non-zero message block, it returns to the state (000) by means of an m-all zero block appended to the message. Hence, the information sequence u = (11001) is encoded as (11,00,10,10,00,11,01,11).

Now, let us transform the SD of Figure 6A.3 into its corresponding trellis diagram. We start at a time instant, say j = 0, with the decoder at state (000) and at each discrete increment of time, j = 1,2,...., we trace the evolution of the encoder's state. For instance, at j = 0 we are at state (000). At j = 1 we may either move to state (100) or remain at (000), depending on whether the input is 1 or 0, respectively. The resultant trellis diagram is shown in Figure 6A.4, where the dots represent the states and each branch is labelled with the corresponding outputs. This diagram is drawn so as to have (i) the "downward transitions" (e.g., branch connecting states (000) and (100)) occurring for an input equal to 1, and (ii) the "upward transitions" (e.g., branch connecting states (100) and (010)) occurring for an input equal to 0. The "horizontal transitions", corresponding to the remaining at the same state, occur for an input equal to 0 for the state (000) and 1 for the state (111). The trellis diagram of Figure 6A.4 describes all the possible transitions for a word of length L. As an illustration for the sequence u = (11001), the corresponding code word is obtained straight from the trellis diagram, departing from state (000) and appending the m-all zero sequence (000) to u.

2b) *Maximum - Likelihood Decoder*

Let u be a message and c its corresponding N-element code word, transmitted through a noisy channel. Let c' be the received N-element code word. Consider a binary symmetric (BSC) channel where each element c'_i of c' differs from the respective element c_i of c with probability p. Then, the probability of receiving c', given that c has been transmitted, with c' differing from c by exactly d elements is

$$p(c'/c) = p^{d}(1 - p)^{N-d} \tag{6A.26}$$

The corresponding log-likelihood function is given by

$$\ln\left[p(c'/c)\right] = d\ln\left(\frac{p}{1 - p}\right) + N\ln(1 - p) \tag{6A.27}$$

The probability of an error occurrence is usually low so that it is reasonable to assume $p < 1/2$. In this case $\ln\left[p/(1 - p)\right] < 0$. Since $N\ln(1 - p)$ is a constant for all c, the decoder (maximum likelihood decoder) must choose $\hat{c}$ as an estimate of c so that the Hamming distance d between c' and c is minimized.

For a Q-ary discrete memoryless channel the log-likelihood function is obviously,

$$\ln\left[p(c'/c)\right] = \ln \prod_{i=0}^{N-1} p(c'_i/c_i) = \sum_{i=0}^{N-1} \ln\left[p(c'_i/c_i)\right] \tag{6A.28}$$

The maximum likelihood decoder chooses the estimate $\hat{c}$ if $\ln p(c'/c)$ is maximum.

2c) *The Viterbi Algorithm*

The Viterbi algorithm operates on a maximum likelihood rule basis. The general principle is to choose the path in the trellis diagram yielding the minimum accumulated Hamming distance between the received code word and the output of the decoder given at each branch of the trellis. The Hamming distance between the received code word and the sequence obtained by following a certain path in the trellis is defined as a "metric", for that particular path. The Viterbi algorithm comprises the following sequential steps:

1. Starting at time j = m compute the metric for each single path entering each state. Store the path (survivor) and its metric for each state.

2. Increment j by 1. Compute the metric for all the paths entering each state by accumulating the branch metric entering that state and the metric of the connecting survivor from the previous time unit. For each state, store the path with the lowest metric and eliminate all the other paths.

3. If $j < L + m$, repeat step 2. Otherwise, stop.

As an example, consider the message a = (110101). The corresponding transmitted

encoded word for the encoder of Figure 6A.2 is **c** = (11,00,10,01,00,10,00,01,11). Suppose that the received code word is **c'** = (11,01,10,01,00,10,00,01,01). After applying the Viterbi, algorithm the final survivor (11,00,10,01,00,10,00,01,11) is shown highlighted in Figure 6A.5, where the circled numbers are the metrics for each state and the dotted lines are the eliminated paths. The decoded message is then (110101) as wanted.

3) *Free Distance*

In connection with the decoding algorithm, the distance properties also have a great influence in the performance of a convolutional code. As we have already mentioned, the distance of a code is directly related to the capacity of computing errors in a code word. As far as convolutional code is concerned, the most important distance measure is the minimum free distance, d_{free}. The free distance is defined as the minimum Hamming distance between any two code words in the code.

Equivalently, we may say that d_{free} is the minimum weight code word of any length produced by a nonzero information sequence. Likewise, "it is the minimum weight of all paths in the state diagram that diverge from and remerge with the all-zero state"[6]. Hence the free distance of the encoder shown in Figure 6A.2 is 6, obtained as we determine the weight of the code word (11,00,10,10,11) produced by the sequence (11000) (see state diagram of Figure 6A.3). The capacity of error correction is given by $t \leq (d_{free} - 1)/2$ in a total of bits equal to the number of branches necessary to obtain the d_{free}. Therefore, in our example, $t \leq (6 - 1)/2 = 2$ in a total of 5 bits (the code is capable to correct 2 out of 5 bits).

6A.5 Trellis Code

Trellis code for band limited channels combine convolutional coding and modulation. Accordingly, channel coding and modulation are no longer performed separately as they are in the other coding schemes. This Appendix does not aim at covering this subject which is fully explored in [8-15]. An introduction to Trellis Coded Modulation (TCM) can be found in Chapter 9.

6A.6 Some Important Codes

In this section we introduce some well-known codes and their main characteristics.

1) *Hamming Codes*

These have been mainly used for error detection/correction in digital communications and data storage systems.

Parameters

Code length	$n = 2^m - 1$
Number of message bits	$k = 2^m - m - 1$
Number of redundancy bits	$m = n - k \geq 3$
Minimum distance	$d = 3$
Error correction capability	$t = 1$

Some generator polynomials for the Hamming code can be found in Table 6A.1

TABLE 6A.1 – GENERATOR POLYNOMIALS FOR HAMMING CODES.

m	g(D)	m	g(D)
3	$1 + D + D^3$	9	$1 + D^4 + D^9$
4	$1 + D + D^4$	10	$1 + D^3 + D^{10}$
5	$1 + D^2 + D^5$	11	$1 + D^2 + D^{11}$
6	$1 + D + D^6$	12	$1 + D + D^4 + D^6 + D^{12}$
7	$1 + D^3 + D^7$	13	$1 + D + D^3 + D^4 + D^{13}$
8	$1 + D^2 + D^3 + D^4 + D^8$	14	$1 + D + D^6 + D^{10} + D^{14}$

2) *Cyclic Redundancy Check Codes*

The Cyclic Redundancy Check (CRC) codes are mainly used for error detection purposes. The CRC can detect the following error patterns.

a) Error bursts of length $\leq n - k$

b) Error bursts of length $= \left[1 - 2^{-(n-k-1)}\right](n - k + 1)$

c) Error bursts of length $\geq \left[1 - 2^{-(n-k)}\right](n - k + 1)$

d) Number of error bits $\leq d - 1$

e) Any error pattern given that the number of errors is odd and the code generator polynomial presents an even number of nonzero coefficients.

Some generator polynomials for the CRC codes can be found in Table 6A.2.

TABLE 6A.2 - GENERATOR POLYNOMIALS FOR SOME CRC CODES.

Main CRC Codes	g(D)	Character Length	Prime Factor
CRC - 12	$1 + D + D^2 + D^3 + D^{11} + D^{12}$	6	$1 + D$
CRC - 16	$1 + D^2 + D^{15} + D^{16}$	8	$1 + D$
CRC - CCITT	$1 + D^5 + D^{12} + D^{16}$	8	$1 + D$

3) *Golay Code*

The (23,12) Golay code is a multiple-error correcting binary code used in several communication systems.

Parameters

Code Length $n = 23$

Number of message bits $k = 12$

Number of redundancy bits $m = 11$

Minimum distance $d = 7$

Error correction capability $t = 3$

Generator polynomials

$$g_1(D) = 1 + D^2 + D^4 + D^5 + D^6 + D^{10} + D^{11}$$

or

$$g_2(D) = 1 + D + D^5 + D^6 + D^7 + D^9 + D^{11}$$

In fact

$$1 + D^{23} = (1 + D)g_1(D)g_2(D)$$

4) *Bose, Chaudhuri and Hocquenghem Codes*

The Bose, Chaudhuri and Hocquenghem (BCH) codes are a generalization of the Hamming codes for multiple-error correction.

Parameters

Code Length	$n = 2^m - 1$
Number of message bits	$k \geq n - mt$
Number of redundancy bits	$m \leq 3$
Minimum distance	$d \geq 2t + 1$
Error correction capability	$t < 2^{m-1}$

Some generator polynomials for the BCH codes can be found in Table 6A.3.

TABLE 6A.3 - GENERATOR POLYNOMIALS FOR BCH CODES.

n	k	t	g(D) (octal)
7	4	1	13
15	11	1	23
15	7	2	721
15	5	3	2467
31	26	1	45
31	21	2	3551
31	16	3	107657
31	11	5	5423325
31	6	7	313365047

As an example, the generator polynomial of the (31,21) BCH code is $D^{10} + D^9 + D^8 + D^6 + D^5 + D^3 + 1$ (from Table 6A.3, the corresponding octal representation is 3551 having the equivalent binary representation 011 101 101 001).

5) *Reed-Solomon Codes*

The Reed-Solomon (RS) codes comprise a special and the most important subclass of q-ary BCH codes.

Parameters

Code Length	$n = q - 1 = 2^m - 1$
Number of message symbols	k

Number of redundancy symbols $n - k = 2t$

Minimum distance $d = 2t + 1$

6) *Repetition Codes*

Repetition Codes are the simplest form of linear block codes. A single message bit ($k = 1$) can be encoded into a block of n identical bits. Consequently, there are only two code words in the code, namely, an all-zero code word and an all-one code word, producing an $(n,1)$ code. Accordingly, the minimum distance is equal to n. The decoding process makes use of majority voting. The number of correctable bits is $(n - 1)/2$.

7) *Burst-Error - Correcting Codes*

The codes mentioned before are generally used for correcting random errors. As far as error bursts are concerned, special codes have been constructed both for block codes and convolutional codes. Before introducing some of them, let us define the length of a burst. A burst of length l is a vector having their nonzero components confined to i consecutive digit positions, the first and the last of which are nonzero. For example, the error vector $e = (001011000)$ is a burst of length 4.

7a) *Block Codes*

7a1) Fire Codes

These are a class of cyclic codes. The generator polynomial for the Fire Codes is constructed as follows

$$g(D) = (D^{2l-1} + 1)p(D)$$

where $p(D)$ is an irreducible polynomial of degree m

l is the burst length, such that $l \leq m$ and $2l-1$ is not divisible by ρ (see definition of ρ below).

The code length n is given by

$$n = \text{LCM}(2l - 1, \rho)$$

where LCM(X,Y) is the least common multiple of X and Y

ρ is the period of $p(D)$, given by $2^m - 1$.

The number of parity-check digits is given by $n - k = 2l - 1 + m$ constituting the higher-order exponent of the generater polynomial.

As an example, consider the irreducible primitive polynomial

$$p(D) = 1 + D + D^6$$

Then $\rho = 2^6 - 1 = 63$

For $l = 6$ we have $2l - 1 = 11$ (Note that 63 does not divide 11).

Hence $g(D) = (D^{11} + 1)(1 + D + D^6) = 1 + D + D^6 + D^{11} + D^{12} + D^{17}$

and $n = LCM(11,63) = 693.$

Therefore the (693,676) cyclic code is capable of correcting any burst error of length 6 or less.

7a2) Some Other Codes

Next we list a few computer generated cyclic and shortened cyclic codes for correcting single bursts. In Table 6A.4 the generator polynomial appears in octal notation. Hence, as an example, for the code (27,17), g(D) = 2671 and the corresponding binary notation is 010 110 111 001 yielding

$$g(D) = D^{10} + D^8 + D^7 + D^5 + D^4 + D^3 + 1$$

TABLE 6A.4 - COMPUTER GENERATED CYCLIC AND SHORTENED CYCLIC CODES.

n - k - 2l	Code (n,k)	Burst-correcting Capability l	Generator Polynomial G(D)
0	(7,3)	2	35
0	(15,9)	3	171
0	(27,17)	5	2671
0	(34,22)	6	15173
0	(50,34)	8	224531
1	(67,54)	6	36365
1	(103,88)	7	114361
2	(63,55)	3	711
2	(85,75)	4	2651
2	(131,119)	5	15163
2	(169,155)	6	55725

7b) Convolutional Codes

The burst-correcting convolutional codes are capable of correcting a given burst length, provided it is followed and preceded by an appropriate number of correct digits known as guard space. This guard space is, in fact, a function of the decoding algorithm [5].

Many convolutional codes are available for error-burst correction purposes (e.g., Berlekamp-Preparata, Iwadare-Massey, etc.). The central idea of all of such codes is that the bits involved in the decoding process of a given bit are spread in time so as to allow the smallest possible number of bits to be affected by an error. One well known technique accomplishing this is interleaving: the data stream is broken into smaller independent streams according to the desired interleaving degree.

REFERENCES

[1] G.A. Arredondo, J.C. Feggler and J.I. Smith, "Advanced Mobile Phone Service: Voice and Data Transmission", *B.S.T.J.*, Vol. 58, No. 1, January 1979.

[2] Simon S. Haykin, *Digital Communications*, John Wiley & Sons, 1988.

[3] M. Schwartz, W.R. Bennet and S. Stein, *Communications Systems and Techniques*, McGraw-Hill, 1966.

[4] S. Lin, *An Introduction to Error-Correcting Codes*, Prentice-Hall, N. J., Englewood Cliffs, 1970.

[5] W.W. Peterson and E.J. Weldon Jr., *Error-Correcting Codes*, MIT Press, Cambridge, Mass., 1972.

[6] S. Lin , D.J. Costello Jr., *Error Control Coding: Fundamentals and Applications*, Prentice-Hall, 1983.

[7] S.Stein, "Fading Channel Issues in System Engineering", *IEEE Journal on Selected Areas in Communications*, Vol SAC-5, No. 2, February 1987.

[8] G. Ungerboeck, "Channel Coding with Multilevel / Phase Signals" *IEEE Trans. Informations Theory*, IT-28, pp. 55-67, January 1982.

[9] G. Ungerboeck, "Trellis-coded Modulation with Redundant Signal Sets, Part I: Introduction", *IEEE Communications Magazine*, Vol. 25, pp. 5-11, February 1987.

[10] G. Ungerboeck, "Trellis-coded Modulation with Redundant Signal Sets, Part II: State of the Art", *IEEE Communications Magazine*, Vol. 25, pp. 12-21, February 1987.

[11] J.B. Anderson and R. de Buda, "Better Phase-Modulation Error Performance Using Trellis Phase Codes", *Electronics Letters*, Vol. 12, pp. 587-588, October 1976.

[12] J.B. Anderson and D.P. Taylor, "A Bandwidth Efficient Class of Signal-space Codes", *IEEE on Information Theory*, Vol. IT-24, pp. 703-712, November 1978.

[13] J.B. Anderson, T. Aulin and C.E. Sundberg, *Digital Phase Modulation*, Plenum, 1986.

[14] A.R. Calderbank and J.E. Majo, "A New Description of Trellis Codes", *IEEE Trans. on Information Theory*, Vol. IT-30, pp. 784-791, November 1984.

[15] A.R. Calderbank and N.J.A. Sloame, "New Trellis Codes Based on Lattices and Cosets", *IEEE Trans. Information Theory*, Vol. IT-33, pp. 177-195, March 1987.

[16] J.C.M. Mota, J.M.T. Romano and R.F. Souza, "Blind Equalization in Data Transmission Systems" (in Portuguese), RT-179, FEE, UNICAMP, Campinas, SP., Brazil, 1989.

[17] G.V. Foschini, "Equalizing Without Altering or Detecting Data", *ATT Technical Journal*, Vol. 64, No. 8, October 1985.

[18] O. Macchi and E. Eweda, "Convergence Analysis of Self-Adaptive Equalizers", *IEEE Trans. Inf. Theory*, Vol. IT-30, No. 2, March 1984.

[19] S. Haykin, *Adaptive Filter Theory*, Prentice-Hall, 1986.

[20] S.V.H. Quareshi, "Adaptive Equalization", *Proceedings of the IEEE*, Vol. 73, No. 9, September 1985.

[21] A.V. Oppenheim and R.W. Schafer, *Digital Signal Processing*, Prentice-Hall, Inc., 1975.

[22] J.G. Proakis, "Adaptive Equalization for TDMA Digital Mobile Radio", *IEEE Transactions on Vehicular Technology*, Vol. 40, Nº 2, May 1991.

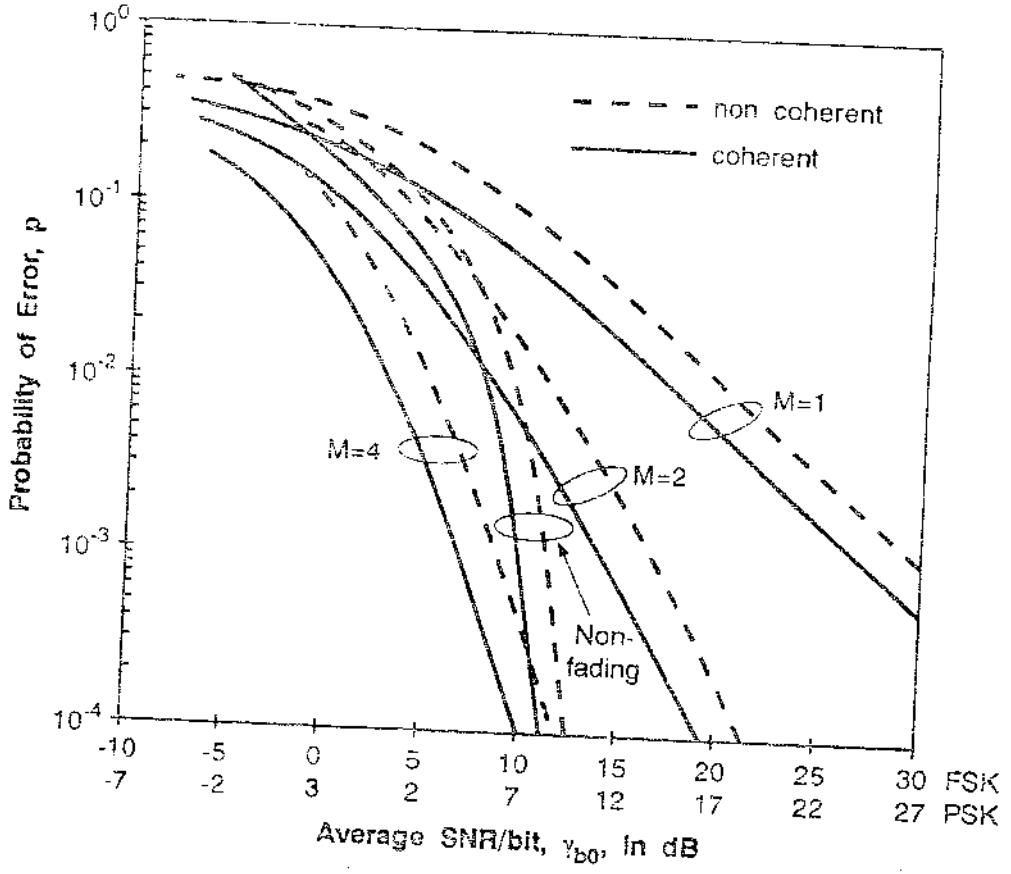

FIGURE 1596

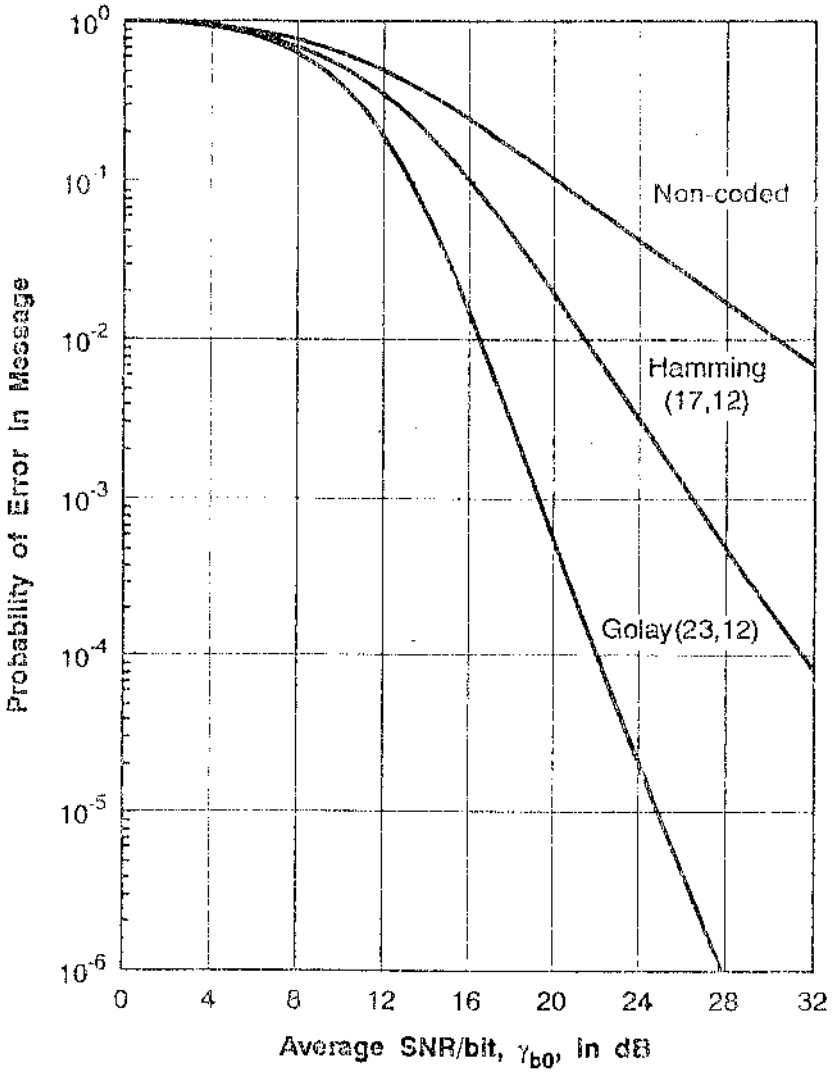
Probability of Error In Message
10^0
10^{-1}
10^{-2}
10^{-3}
10^{-4}
10^{-5}
10^{-6}
0
4
8
12
16
20
24
28
32
Non-coded
Hamming
(17,12)
Golay(23,12)
Average SNR/bit, γ_{b0}, in dB

Figure 1986

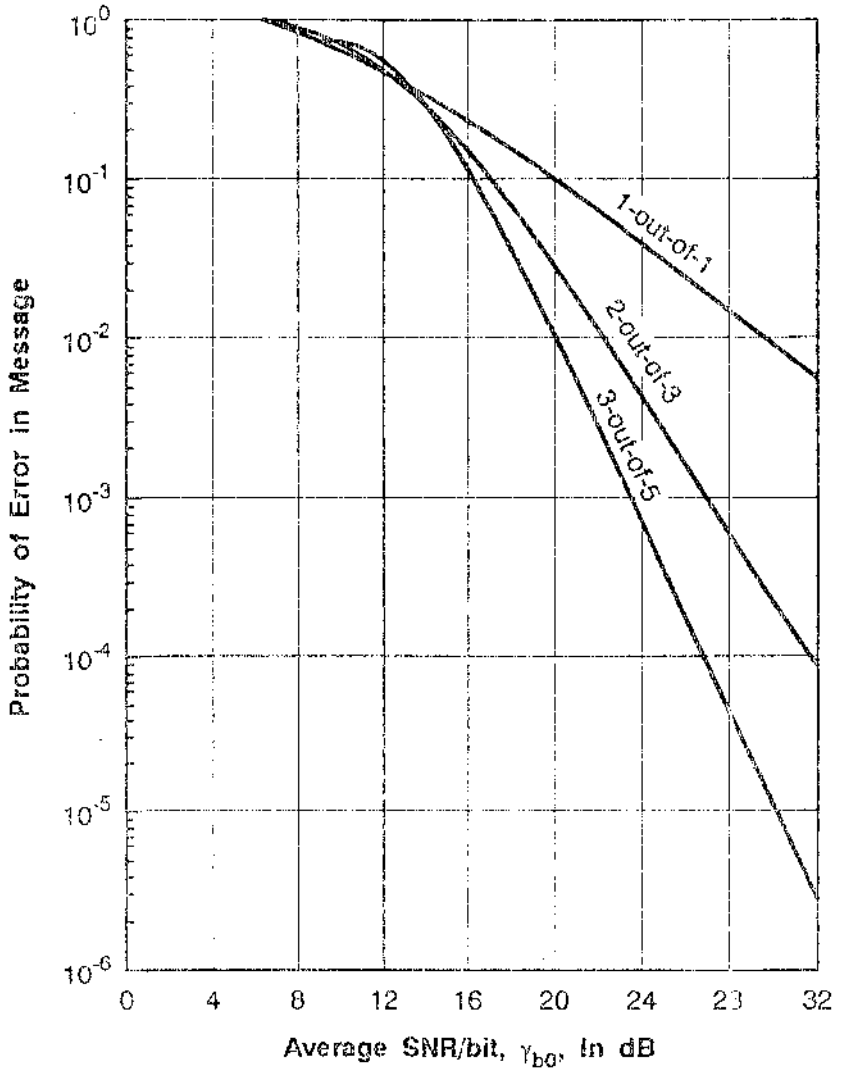

FIG. 3 (PRIOR ART)

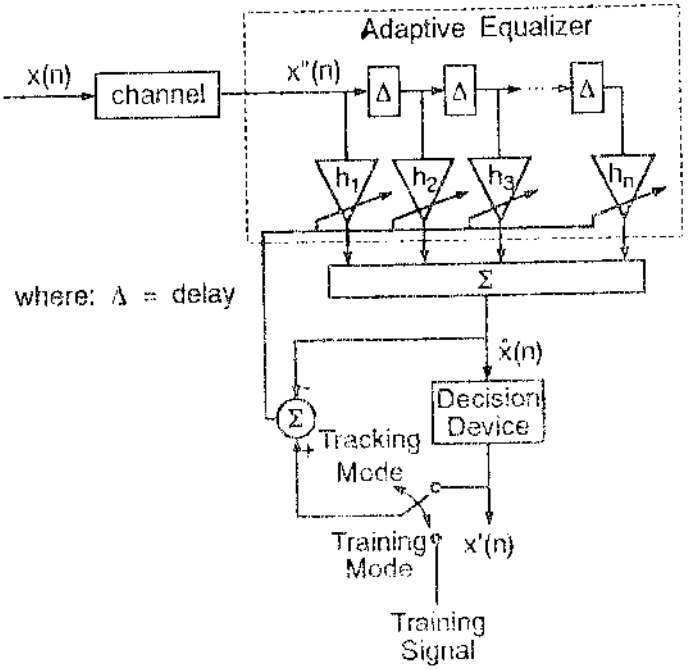
Adaptive Equalizer
x(n)
channel
x''(n)
Δ
Δ
Δ
h1
h2
h3
hn
where: Δ = delay
Σ
x̂(n)
Decision Device
Σ
Tracking Mode
Training Mode
x'(n)
Training Signal

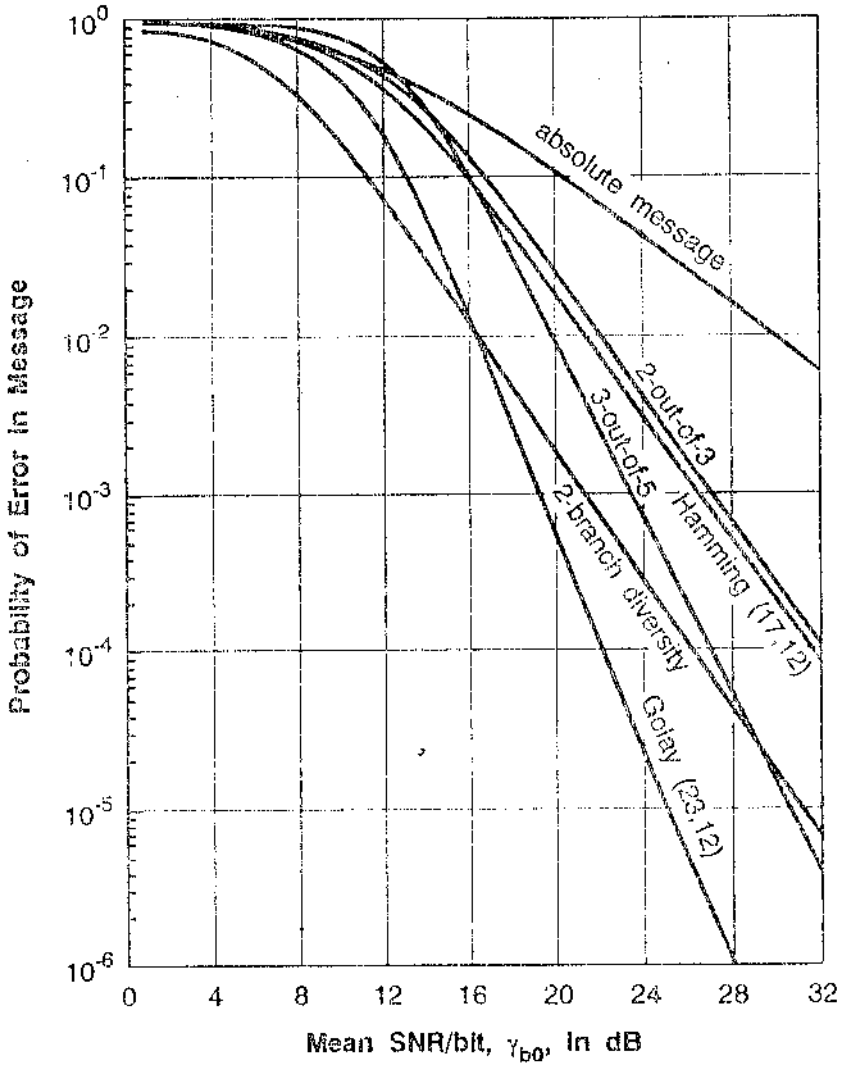
Probability of Error in Message
10^0
10^{-1}
10^{-2}
10^{-3}
10^{-4}
10^{-5}
10^{-6}
0
4
8
12
16
20
24
28
32
Mean SNR/bit, γ_{b0}, in dB
absolute message
2-out-of-3
3-out-of-5
Hamming (17,12)
2-branch diversity
Golay (23,12)

Figure 6.3

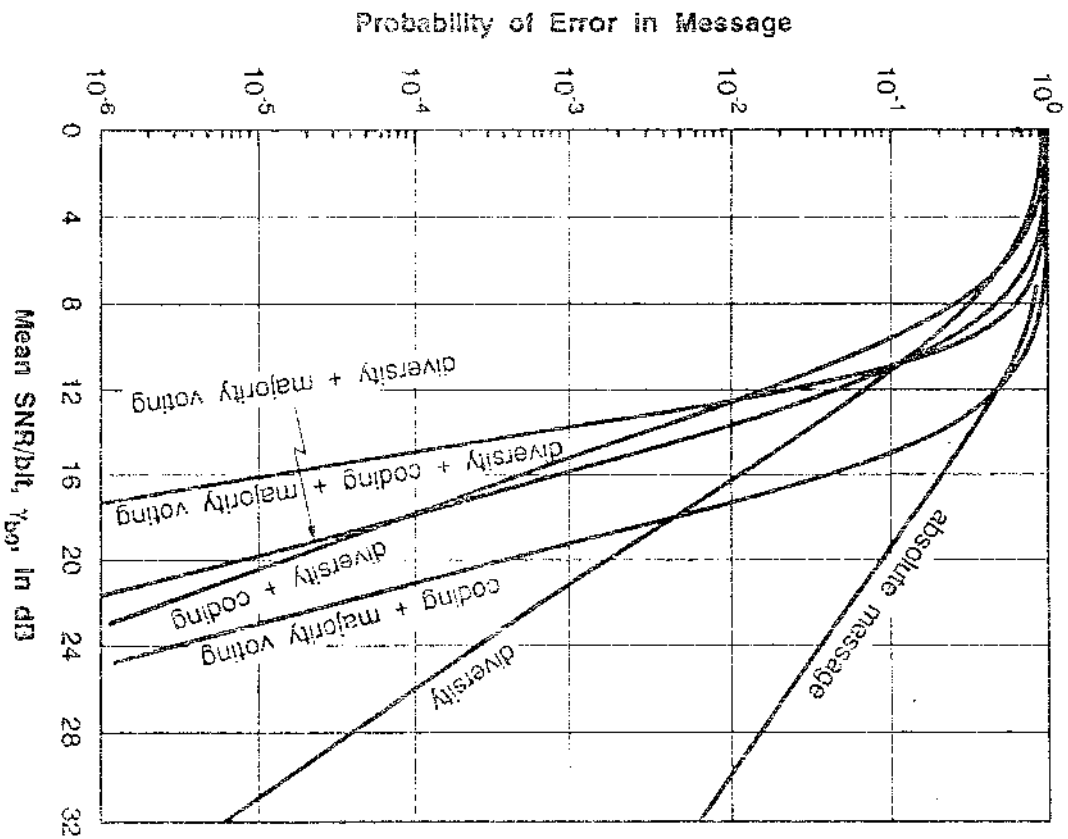

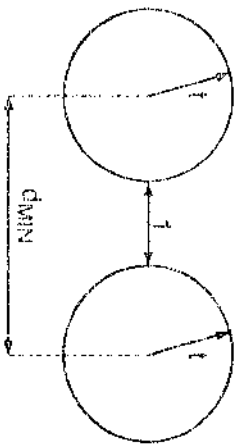

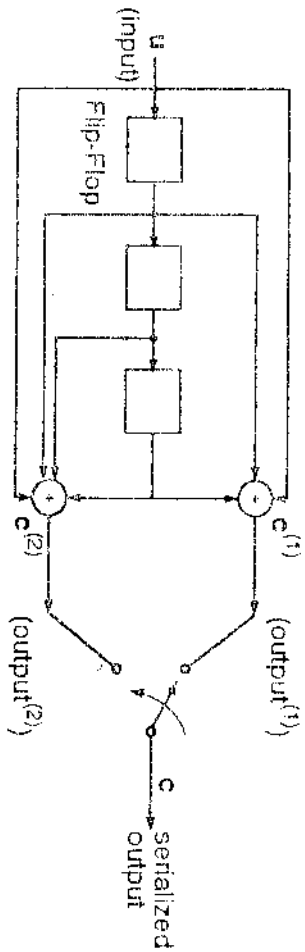

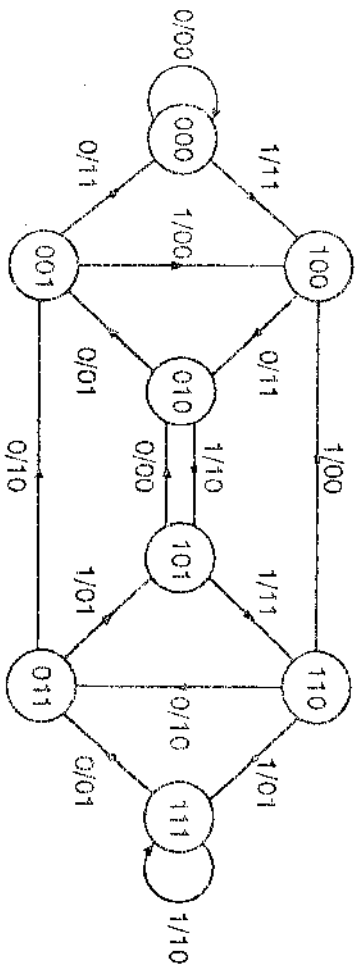

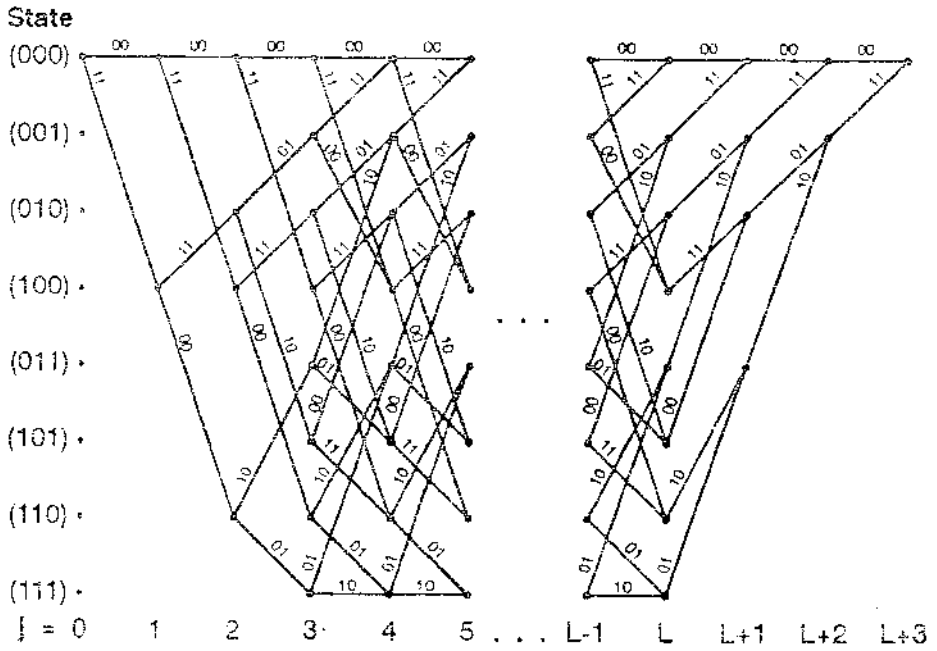

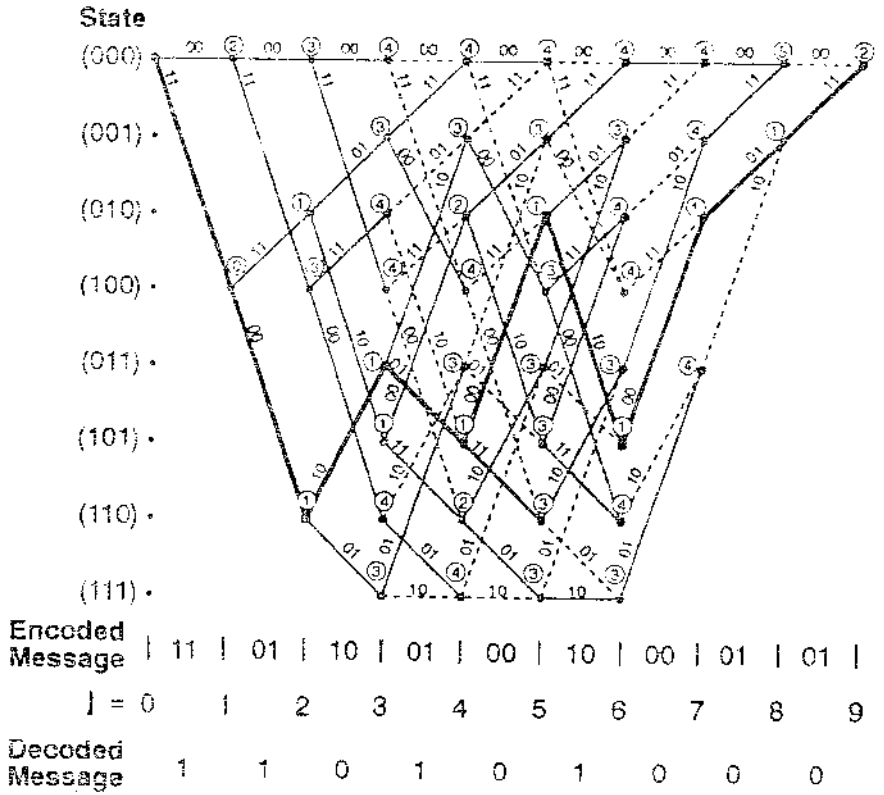

FIGURE 5 1994

PART IV

NOISE, INTERFERENCE AND MODULATION

CHAPTER 7

NOISE AND INTERFERENCE

PREAMBLE

This chapter addresses the problem of Noise and Interference. Since noise is a well known subject of any communication system, the treatment given here is rather brief and descriptive. The two types of noise, namely additive and multiplicative, are studied but special attention is paid to the former since the latter is basically the fading which has already been extensively explored in the previous chapters. The main objective of this chapter is, therefore, the interference problem which may be classified into four main categories: intermodulation, intersymbol, adjacent channel and cochannel. The intermodulation and intersymbol problems are examined, but the main focus will be on adjacent and cochannel interferences. Adjacent channel interference is treated in a different manner from that usually done by other authors. Here we emphasize the influence of the traffic load on the probability of adjacent channel interference occurrence. More specifically, we study how this probability is affected by the presence of mobiles at the boundaries between cells. Cochannel interference problems are then tackled with an initial objective of obtaining an analytical solution. This is achieved for the case of a pure Rayleigh environment, although more complex cases are treated by means of a numerical analysis. These cases include those with multiple interferers and with a fading having a log-normal or a Rayleigh combined with a log-normal distribution. An alternative approach is the use of Monte Carlo simulation, described at the end of the chapter. It is shown that this approach offers a great deal of flexibility and that the problem can be treated in a more realistic manner. The use of directional antennas as a means of counteracting cochannel interference is also discussed and the discovery of novel cellular patterns is facilitated by using simulation.

7.1. INTRODUCTION

Noise and interference are two phenomena which limit the operating range of all radio equipment [1]. Noise is an unwanted disturbance within an useful frequency band, arising from various sources and exhibiting different characteristics. Radio frequency interferences originate from the communication systems themselves. This has increasingly become one of the biggest problems to be tackled, since the growth of such systems is being accomplished very rapidly and in a chaotic manner. It is, therefore, essential to characterize the different types of noise and interference so that the system can be designed to ensure a signal level well above noise or interference. The characterization of these limiting factors is important since it helps in the development of prediction methods for communication systems performance. As a result, systems designed to operate adequately under unfavourable conditions may be achieved.

Different types and sources of noise and also their statistics will be described. An important performance measure is the carrier-to-noise ratio which will be examined for the mobile radio system case. The performance measure concerned with interference is the carrier-to-interference ratio, calculated differently for the adjacent channel and cochannel cases, since their characteristics are very distinct from each other. It will be seen that the performance with a given carrier-to-noise ratio is dependent on the modulation technique used, while the performance with a given carrier-to-interference ratio depends on the cell pattern. We will discuss the different methods of improving the system performance and introduce the novel cellular patterns which may arise when an appropriate use of directional antennas is accomplished.

7.2. NOISE

Noise disturbance is said to be of the additive or multiplicative type depending on whether the modification introduced to the signal is of additive or multiplicative

nature, respectively. The additive noise is just superimposed to the signal whereas the multiplicative noise can be viewed as an amplitude modulation of the signal by the noise.

There are many types of additive noise such as ambient, background, static, radio, etc. We are mainly interested in the radio type noise of which the most important are the atmospheric noise, galactic noise, man-made noise and receiver noise. The multiplicative noise is a peculiarity of the mobile radio system, which causes fading. The two types of fading that are commonly observed are the long term and short term fadings, and will be briefly reviewed for convenience.

7.3. ADDITIVE NOISE

The objective of this section is to examine the frequency band within which there is significant noise power of some relevant radio noise sources. As mentioned before, the main sources to be considered, are the radio receiver, the atmospheric, the galactic and the man-made. We shall start by examining the radio receiver noise.

7.3.1. Types of Additive Noise

1) *Receiver Noise*

There are two types of noise in this category: thermal noise and shot noise. They are discussed as follows.

Thermal Noise

The physical origin of this noise is the thermal agitation of the electric charge carriers in resistive materials. The thermal agitation is reduced if the resistive component is cooled down. The thermal noise is a rather common phenomenon which has already been noted by most of us: when listening to a steady hiss from a loudspeaker of a sensitive amplifier if turned on without an input signal.

J.B. Johnson [3] and H. Nyquist [4] investigated this phenomenon, the former

experimentally and the latter theoretically. They have shown that a resistor R (ohm) at a temperature T (Kelvin) will deliver a power kTB* watts within a bandwidth B (Hz) into a matched load. Classical thermodynamic considerations were used to arrive at this result and will not be reproduced here for brevity. It is possible to show that the power density spectrum of the current, due to the random motion of the electrons in a resistor R, is $S_i(\omega)$ [5]

$$S_i(\omega) = \frac{2kT/R}{1 + (\omega/\alpha)^2} \tag{7.1}$$

where α is the average number of collisions per second of an electron with the lattice structure. Usually $\alpha \simeq 10^{14}$/s, which leads us to conclude that, for angular frequencies up to $\omega = 10^{13}$ rd/s (10^{12} Hz = 1000 GHz), the power density spectrum is approximately constant ($(\omega/\alpha)^2 = 0.01 << 1$) and equal to

$$S_i(\omega) \simeq 2kT/R \tag{7.2}$$

The resistor R can be represented by a noiseless resistance in series with a voltage source v of uniform power density spectrum 2kTR, since

$$v = Ri$$

and

$$S_v(\omega) = R^2 S_i(\omega) = 2kTR \tag{7.3}$$

The mean square noise voltage is given by (see appendix 7A)

$$\overline{v^2} = 4kTRB \tag{7.4}$$

Therefore, for T = 20°C (293K), R = 10 KΩ and B = 1 GHz, the mean square noise voltage is $\overline{v^2} = 1.6\ 10^{-7}\ V^2$, corresponding to an r.m.s. fluctuation of $\sqrt{\overline{v^2}} = 0.4$ mV on the voltage of any signal present at the resistor.

Shot Noise

The shot noise appears in both thermionic diodes (triodes) and semiconductor

* $k = 1.38.10^{-23}$ Joule/Kelvin is the Boltzmann's constant.

devices. In the former the shot noise is due to the anode current, consisting of the superposition of pulses of currents disposed randomly in time. Such pulses are electrons overcoming the surface potential barrier and reaching the anode. In the semiconductor devices, similar phenomenon occurs with the electrons and holes at the tail of the energy distribution overcoming a potential barrier. As shown in Figure 7.1 the net current $i(t)$ of the device fluctuates randomly about a mean value I_o such that $i(t) = I_o + i_n(t)$, where the fluctuation current $i_n(t)$ is named "shot noise".

The mean value of $i_n(t)$ is zero. As shown in Appendix 7B the power density spectrum of the shot noise is

$$S_i(\omega) = \frac{4I_o q}{(\omega\tau)^4}\left[(\omega\tau)^2 + 2(1 - \cos\omega\tau - \omega\tau\sin\omega\tau)\right] \qquad (7.5)$$

where q is the electronic charge $= 1.6\ 10^{-19}$ C

τ is the transit time of the electron between cathode and anode (second)

$I_o = nq$, where n is the mean number of electrons in motion.

This power density is plotted in Figure 7.2. Note that for $\omega\tau \leq 0.5$ the spectrum is approximately flat and equals qI_o. If we consider the typical value of 10^{-10} second for τ we obtain $\omega \simeq 5.10^9$ rd/s $\simeq$ 800 MHz.

It is shown in Appendix 7B that the noise voltage $\overline{v^2}$ is

$$\overline{v^2} \simeq 2qI_o R^2 B \qquad (7.6)$$

Therefore, for $I_o = 1$ mA, $R = 10$ KΩ and $B = 800$ MHz, we obtain $\overline{v^2} = 25.6\ \mu V$, corresponding to an r.m.s. fluctuation of $\sqrt{\overline{v^2}} = 5$ mV (compare this result with that for thermal noise).

2) *Atmospheric Noise*

Lightning discharges in thunderstorms are the main sources of this type of noise and its level varies with the frequency, geographical region, season of the year, weather, time of the day, etc.. It has been observed that the noise level decreases

with the increasing latitude and that it has a significant value below 20 MHz, in quiet locations.

3) *Galactic Noise*

All sorts of noise originated outside the earth and its surrounding atmosphere are classified as galactic noise. The main sources are the sun, the celestial radio-sky background radiation along the galactic plane and other cosmic sources. The galactic noise has significant values within the frequency range of 15 MHz – 100 GHz. The ionosphere provides the high pass filtering, while the atmosphere provides the low pass filtering for this type of noise.

4) *Man-Made Noise*

Noise produced by man is mainly caused by electric motors, neon signs, power lines and certain medical appliances. This type of noise is certainly more significant in urban areas than in suburban areas. The difference in power in these two areas may exceed 16 dB. In urban areas ignition noise predominates and it is the dominant factor of performance degradation in mobile communications. Man-made noise is more noticeable when the sources are only less than a few kilometers away from the receiver. However, it can propagate through power lines and be noted at much further distances [2].

A comparison between the levels of different types of noise is shown in Figure 7.3 where the received noise power, F_a, is given in dB above the thermal noise kTB ($T = 290K$). Note that the receiver noise has a more significant value than the atmospheric noise for frequencies above 30 MHz. In addition, the receiver noise has a more significant value than the galactic noise for frequencies above 250 MHz. On the other hand, Galactic noise has a higher value than the atmospheric noise for frequencies above 20 MHz. However, man-made noise usually predominates over all other sorts of noise, being negligible (relative to receiver front-end noise) for frequencies above 4 GHz.

7.3.2. Characterization of Additive Noise

The noise is a random signal having amplitudes following a certain distribution. Both thermal noise and shot noise result from a relatively large ("infinite") number of statistically independent disturbances. From the central limit theorem of the probability theory, the noise amplitude r follows a normal (Gaussian) distribution p(r), with a zero mean value and an r.m.s value of σ^2, such that

$$p(r) = \frac{1}{\sqrt{2\pi}\,\sigma}\exp\left(-\frac{r^2}{2\sigma^2}\right) \qquad (7.7)$$

The major difference between the Gaussian noise and the other types of additive noise is the impulsive characteristics of the latter. Gaussian noise is simple to deal and with, usually, only the knowledge of its mean power is relevant. The strong time and location dependence of impulsive noise, makes its characterization difficult. The Gaussian noise causes a "hiss" on voice channels while the impulsive noise produces a "tick".

There is a variety of measurements that can be done to evaluate the impulsive noise characteristics, such as mean voltage, r.m.s. voltage, peak voltage, impulsiveness ratio, level crossing rate and several distributions, such as amplitude probability, pulse height, pulse duration, etc.. These measures may be useful in different situations, since the impulsive noise is greatly dependent on both time and geographical region.

Among the distributions, the amplitude probability distribution (APD) is of particular interest. It gives the proportion of time that the noise detected at the output of a receiver is above a certain level. This distribution is usually plotted on a Rayleigh paper, where the probability density function of the signal-to-(Gaussian) noise ratio is a straight line (section 5.6). When measured at the output of a receiver having a noise figure f* (f ≥ 1), the probability distribution function of

---

* In dB the noise figure is F = 10log f.

the signal-to-noise ratio (SNR), Γ, is given by (see Appendix 7C)

$$P(\Gamma) = 1 - \exp\left(-\frac{\Gamma}{f\gamma_o}\right) \tag{7.8}$$

where γ_o is the mean SNR. It is readily seen that any noise introduced by the receiver ($f > 1$) will cause a deterioration of the output SNR. A plot of this distribution for different noise figures is shown in Figure 7.4. Also shown is a typical amplitude probability distribution for a noise figure of 5 dB. Note that there are two different regions for the APD curve: one at low signal levels, corresponding to the background noise, and the other at high signal levels, corresponding to the impulsive noise.

Finally, we conclude this section by determining the output signal-to-noise ratio, SNR_o, for a given transmitter power W_t, transmitter antenna gain G_t, path loss L, receiver antenna gain G_r, thermal noise N_i and receiver noise figure F. This can be accomplished with the help of the diagram of Figure 7.5.

If all the parameters are expressed in dB, then

$$SNR_o = W_t + G_t - L + G_r - N_i - F$$

7.4. MULTIPLICATIVE NOISE

A carrier frequency, when transmitted in a mobile radio environment, has its amplitude modulated by a random noise caused by both the obstructions encountered by the signal and the multipath propagation effect as illustrated in Figure 7.6. Such random amplitude modulation is known as fading which has already been extensively studied in previous chapters, but will be briefly reviewed here. There are basically two types of fading in a mobile radio system: long-term fading and short term fading.

7.4.1. Types of Multiplicative Noise

Let us start with the long term fading.

1) *Long Term Fading*

A radio wave propagating in a dispersive medium will be attenuated by several obstructions with varying thickness and electromagnetic characteristics (electric permittivity, magnetic permeability, conductivity). A vehicle moving at a constant distance from the transmitter will receive a signal with an amplitude experiencing random attenuations due to the different properties of the attenuation constants of the random obstructions.

2) *Short Term Fading*

This type of fading is a direct consequence of the multipath propagation effect. The resultant received signal is a sum of signals reaching the mobile through an "infinite" number of paths. These signals have random amplitudes and phases that may reinforce the signal at some instants and may destruct the signal at other instants.

7.4.2. Characterization of Multiplicative Noise

Due to their random behaviour, both the long term and short term fades cannot be treated in a deterministic way but, fortunately, they can be described in a statistical basis. The corresponding probability distributions are well known and will be presented here.

1) *Long-Term Fading*

The probability density function of the received fading signal envelope follows a normal distribution,

$$p(R) = \frac{1}{\sqrt{2\pi}\,\sigma} \exp\left[-\frac{1}{2}\left(\frac{R - M}{\sigma}\right)^2\right] \tag{7.9}$$

where the envelope R, its mean value M and variance σ are given in decibels. The corresponding distribution function for an envelope R_o is thus given by

$$p(R \leq R_o) = P(R_o) = \int_{-\infty}^{R_o} p(R)dR \tag{7.10}$$

2) *Short-Term Fading*

Here we identify two situations: (i) in one of them the resultant signal is the sum of signals reaching the receiver through indirect paths only; (ii) in the other the resultant signal contains both the signal received through the direct path and also the signals from indirect paths. In the first case one has a Rayleigh density function while a Ricean density function is associated with the second case. The Rayleigh density function is given by

$$p(r) = \begin{cases} \dfrac{r}{\sigma^2}\exp\left(-\dfrac{r^2}{2\sigma^2}\right), & r \geq 0 \\ 0, & \text{otherwise} \end{cases} \tag{7.11}$$

and the Ricean density function is given by:

$$p(r) = \begin{cases} \dfrac{r}{\sigma^2}\exp\left(-\dfrac{r^2 + a^2}{2\sigma^2}\right) I_o\left(\dfrac{ar}{\sigma^2}\right), & r \geq 0 \\ 0, & \text{otherwise} \end{cases} \tag{7.12}$$

where r and σ^2 are the envelope and variance respectively; a is the amplitude of the direct wave and $I_o(\cdot)$ is the modified Bessel function of the zero$^{\text{th}}$ order. The distribution function for the Rayleigh case is given by

$$p(r \leq r_o) = \int_0^{r_o} p(r)dr = 1 - \exp\left(-\frac{r_o^2}{2\sigma^2}\right) \tag{7.13}$$

7.5. INTERFERENCE

Radio frequency interference is one of the most important problems to be considered in the design, operation and maintenance of mobile communication systems. Due to the fast growth of communication systems, it is almost impossible to maintain in operation an interference-free system, since the performance improvements of the

equipment has not been able to keep pace with the increasing demand for services.

The two major interference problems in the mobile radio systems are adjacent channel and cochannel interferences. Other types of interferences include intermodulation and intersymbol. We shall concentrate our attention on these problems but the main focus will be on the adjacent and cochannel problems in the cellular architecture. Intermodulation interference is generated in any non linear circuit when the product of two or more signals result into another signal, having a frequency that is equal or almost equal to the wanted signal. In the transmitter, the intermodulation interference usually occurs in the power amplifier, whereas in the receiver it is produced in the first converter (refer to Chapter 10).

Intersymbol interference is intrinsic to digital networks and it is a direct consequence of the limited bandwidth of the transmission medium. An ideal system should have an infinite bandwidth with a distortionless transmission, such that a sequence of pulses can be sent at a rate as high as desired. In other words, the pulse width could be made as short as desired. In practice, however, every system presents a limited bandwidth with unavoidable distortions, such that the shape of the transmitted pulses (symbols) is not kept the same. In fact, the symbols tend to spread out with a consequent overlap among them. This is known as intersymbol interference (ISI). Equalization and coding can be used to minimize the effects of ISI. This has already been briefly studied in Chapter 6.

Intermodulation and intersymbol interferences are well known phenomena which have already been extensively explored in the literature, and the treatment given is also applicable to a mobile radio environment. We shall then dedicate the rest of this chapter to the problem of adjacent channel and cochannel interference and the techniques used to counteract their effects in the cellular mobile radio system.

One of the most difficult problems is to determine whether a particular type of interference is due to adjacent channel or cochannel. Both of them present the same type of undesired output from a receiver. However, it may be possible to distinguish between them if specific identification tests are performed.

7.6. ADJACENT CHANNEL INTERFERENCE

Adjacent channel interference occurrence is basically due to equipment limitations such as frequency instability, receiver bandwidth, filtering etc. Although the equipments are designed for maximum interference performance of the system, a combination of factors, such as the cellular architecture and the random signal fluctuation, usually causes a deterioration of the received signal, primarily due to interference of adjacent channels. This is because channels are kept very near each other in the frequency spectrum for obtaining maximum spectrum efficiency.

Intra-Cell Adjacent Channel Interference

If adjacent channels are used in the same cell site, we may have a situation where a mobile station, transmitting from a short distance to the base station, will strongly interfere with the signal of another mobile, transmitting from a long distance to the same base station, on an adjacent channel. This is known as Intra-cell adjacent channel interference. One possible solution to this problem is to avoid the use of adjacent channels within the same cell.

Inter-Cell Adjacent Channel Interference

Even in the situation where adjacent channels are not used in the same cell but in adjacent cells, interference may still occur. For instance, consider two mobiles near the cell border, and each one transmitting to its "own" base station through adjacent channels. Each base station receives the wanted signal plus a certain interference level of the unwanted signal. Adjacent channel interference may occur because of two main factors: (i) both signals experience attenuation and fading; (ii) their fadings are uncorrelated (the signals travel through different trajectories) so that the interfering signal may become larger than the wanted signal. This is known as Inter-cell adjacent channel interference or Adjacent channel near use. One "possible" solution to this problem is to avoid the use of adjacent channels in adjacent cells. However, if, for example, a 7-cell cluster (refer to section 2.6) is to be implemented, adjacent channels are inevitably assigned to adjacent cells.

In this section we will investigate the statistics of the proportion of mobiles in a situation of having their adjacent channel interference problems increased due to their geographical location within the cell. In other words, if receivers are considered to be ideal, we will be estimating the probability of inter-cell adjacent channel interference. If receivers are not ideal then this probability corresponds to the incremental percentage of the signal-to-adjacent channel interference ratio (in absolute values). This probability should be a function of the propagation parameters and traffic distribution of the system. The following investigation is based on the work by Sánchez [10] complemented and enhanced by some results obtained in [11].

There are two situations to be considered: (I) interference at the mobile and (II) interference at the base station. Adjacent channel interference is more likely to occur if the vehicles are near the boundaries of the cells, because communications can be provided by the channels of more than one cell. In order to investigate the possible cases of interference, let us define some parameters. Let channel i be the reference channel, and p_1, p_2, γ, δ and μ' be probability densities, such that

p_1 = probability of occurrence of only one adjacency, i.e., only one adjacent channel (say i + 1) is active and the other adjacent channel (i − 1) is not being used;

p_2 = probability of occurrence of two adjacencies, i.e., the two possible adjacent channels (i − 1 and i + 1) are both active;

γ = proportion of mobiles with adequate communication with more than one base station, i.e., probability that a mobile can communicate through channels of two or more cells;

δ = proportion of mobiles with adequate communication with more than two base stations, i.e., probability that a mobile can communicate through channels of three or more cells;

μ' = proportion of mobiles within a cell with the signal level below a given threshold, i.e., the probability of a mobile receiving a signal level below a given value.

The probabilities p_1 and p_2 are dependent on both the channel assignment algorithm and the traffic load of the system. The probabilities γ, δ and μ', on the other hand, depend on the mean signal strength. Note that μ' and γ, δ have been defined and extensively explored in Chapter 3 (sections 3.5 and 3.6, respectively). Note also that μ' is a function of μ such that $\mu' = 1 - \mu$, where μ (the probability that the received signal is above a given threshold) is given by (3.108) or (3.111), as required. In the examples to be given here we shall assume a path loss coefficient $\alpha = 3.5$ and a standard deviation $\sigma_w = 5$ dB. As we have seen in Chapter 3, for these parameters the probability μ calculated by either (3.108) or (3.111) gives similar results. From the above definitions we can say that $\gamma - \delta$ is the proportion of mobiles with access to two base stations only.

In order to simplify our reasoning, it is convenient to relate the probabilities μ', $(\gamma - \delta)$ and δ with the geographical distribution of the mobiles within a cell. In a hexagonal cell array, δ is the probability that a mobile is at the vicinity of the border of three mutually adjacent cells (the joint corner of three adjacent cells). Therefore, $\delta/6$ is the probability that this mobile is at one out of the six possible "corners". The difference $\gamma - \delta$ gives the probability that a mobile is at the vicinity of the borders of two adjacent cells. Hence, $(\gamma - \delta)/6$ gives the probability that this mobile is at one out of the six possible joint borders. The probability that the mobile lies within the weak signal area of the cell is μ'. Now we analyze the two possible cases.

1) *Adjacent Channel Interference at the Mobile*

The conditions causing inter-cell adjacent channel interference at the mobile are depicted in Figure 7.7.

The mobile using channel i may suffer interference from channel $i + 1$ and/or channel $i - 1$ if both/either one are/is active in the adjacent cells. It is shown in Appendix 7D that the probability of adjacent channel interference at the mobile (p_M) is

$$p_M = \left[\frac{\gamma + \delta}{3}\right]_A \qquad (7.14)$$

where

$$I_A = \frac{p_1 + 2p_2}{2} \tag{7.15}$$

The parameter I_A gives the incidence of adjacency, i.e., the proportion of occurrence of adjacency.

2) *Adjacent Channel Interference at the Base Station*

The conditions causing inter-cell adjacent channel interference at the base station are depicted in Figure 7.8.

The base station B_1 receives the wanted signal from mobile unit M_1 and the interfering signal(s) from mobiles M_2 and/or M_3 transmitting in adjacent channels to base stations B_2 and B_3, respectively. Note that besides the strategic location of M_2 and/or M_3, near the cell borders, the mobile M_1 has to be located in the weak signal area of cell 1. Appendix 7D shows that the probability of inter-cell adjacent channel interference at the base station (p_B) is

$$p_B = \frac{\gamma + \delta}{3} \mu' I_A \tag{7.16}$$

where I_A is given by (7.15). We should note that γ and δ are not independent variables. It has been shown (section 3.6) that δ is a function of γ and the relation between them can be reasonably approximated by

$$\begin{aligned} \delta &\simeq 1.25\gamma^2 \quad , \qquad 0 \le \gamma \le 0.8 \\ \delta &\simeq \gamma \quad , \qquad 0.8 \le \gamma \le 1.0 \end{aligned} \tag{7.17}$$

The probabilities γ and δ are intimately related with the geographical locations from which the path losses are within some stated tolerance. They can, therefore, be written as functions of such tolerance (dB). The probability μ' also depends on the geographical location from which the signal is considered to be below a certain threshold. It can, therefore, be written as a function of such threshold (dB). The probability μ', however, is independent of γ (and consequently of δ). The probabilities p_1 and p_2 are not independent of each other, so that the parameter I_A

(incidence of adjacency) assumes values in the range from 0 to 1.

Consider, as an example, a 7-cell cluster system with all the cells having neighbours and all the channels having adjacent channels. If the traffic level is so high that all the channels are constantly active, then $p_2 = 1$ and obviously $p_1 = 0$, and $I_A = 1$. If there is no active channel then $p_1 = p_2 = 0$ and $I_A = 0$. As another example, consider the situation of Figure 7.9 with the dotted lines showing adjacent channels in use. There are 9 active channels, 6 of which (channels 1, 3, 4, 5, 15 and 16) having just one active adjacent channel and 1 (channel 2) having two active adjacent channels. Therefore $p_1 = 6/9$ and $p_2 = 1/9$ and

$$I_A = \frac{6/9 + 2 \times 1/9}{2} = \frac{4}{9}$$

Adjacent Channel Interference and Propagation Parameters

The probability μ' as a function of the threshold level (dB) may be extracted directly from Figure 3.22 by doing $\mu' = 1 - \mu$. The probabilities γ and δ as functions of the tolerance (A dB) between the radio signal strength to two and three base stations are given by Figures 3.28 and 3.33, respectively.

We can now plot the probabilities of adjacent channel interference p_M and p_B as functions of these tolerances and signal threshold (Figure 7.10). We chose as abscissa the path tolerance (A dB) to at least two base stations and as ordinate the normalized interference probabilities p_M/I_A and p_B/I_A. The probability of adjacent channel interference at the mobile is given by the upper curve only. The probability of adjacent channel interference at the base station is given as a function of the tolerance (A dB) having μ' (or equivalently the threshold T) as a parameter. Note that $p_M = p_B$ for $\mu' = 1$ (or $T \rightarrow \infty$).

As an example suppose we consider that paths within A = 6 dB of each other are valid alternatives. Then, if the mobile is in a region where the received signal is below a threshold T = 9 dB (event with μ' = 64% probability), then the normalized probability of adjacent channel interference at the base station is $p_B/I_A \approx 0.4/3 \approx 13.3\%$. At the same condition, the normalized probability of adjacent

channel interference at the mobile is $p_M/I_A \approx 0.6/3 = 20\%$ (in the latter case the value of μ' is irrelevant since the used curve is always that for $\mu' = 1$). Note that these are the maximum probabilities, since they are obtained from p_B/I_A and p_M/I_A where I_A (the incidence of adjacency) is a parameter with positive values less than or equal to 1. The parameter I_A depends on the traffic load and also on the channel assignment technique of the system.

Referring to equations (7.14) and (7.16) for the values of p_M and p_B respectively, we can see that their maxima are 2/3, obtained for $I_A = 1$, $\mu' = 1$ and $\gamma = 1$ (this latter implying $\delta = 1$). Consequently, in the extreme situation, the channels at the mobile, or at the base station, may have a 66.7% chance of adjacent channel interference. If we consider: (i) tolerance of $A = 8$ dB, (ii) threshold of $T = 12$ dB and (iii) incidence of adjacency of $I_A = 70\%$ as acceptable (reasonable) figures, then $p_M \approx 19.6\%$ and $p_B \approx 15.4\%$.

Adjacent Channel Interference and Traffic Distribution

Let us now estimate the distribution of the number of active adjacent channels. Let p(n) be the probability of n active adjacent channels (n = 0, 1, 2). The state of the channels on use or not can be expressed by the Bernoulli distribution

$$p(\omega) = p^{\omega}(1 - p)^{1-\omega} \quad , \qquad \omega = 0,1 \tag{7.18}$$

where p is the probability of finding the channel active, and ω represents the channel state: 1 for active or 0 for idle. Assume that the channels are independent and uniformly distributed. Then

$$n = \omega_1 + \omega_2 \tag{7.19}$$

The probability p(n) has a binomial probability density function

$$p(n) = \begin{pmatrix} 2 \\ n \end{pmatrix} p^n(1 - p)^{2-n} \quad , \qquad n = 0,1,2 \tag{7.20}$$

Assuming that the cells have an equal capacity (i.e., same number N of channels

per cell) and that the traffic has an even distribution (i.e., same blocking probability B in each cell), then $p = B^{1/N}$ and

$$p(n) = \binom{2}{n} B^{n/N}(1 - B^{1/N})^{2-n} \tag{7.21}$$

Consequently, the probabilities p_1 and p_2 are given by:

$$p_1 = p(1) = 2B^{1/N}(1 - B^{1/N}) \tag{7.22}$$

$$p_2 = p(2) = B^{2/N} \tag{7.23}$$

Then, the incidence of adjacency is

$$I_A = B^{1/N} = p \tag{7.24}$$

Note, as stated before, that p_1 and p_2 are dependent probabilities and can be written as

$$p_1 = 2\sqrt{p_2}\left(1 - \sqrt{p_2}\right) \tag{7.25}$$

The probability p_1 has its maximum at $B = 0.5^N$ with p_1 assuming the value 0.5. It can be noticed that the larger the number of channels per cell the greater the incidence of adjacency (even for a low blocking probability). For instance, in a 40-channel per cell system the incidence of adjacency reaches quickly the figure of 90% even for a blocking probability near 0%. The curves of p_1, p_2 and I_A as functions of B (where N is the parameter) are shown in Figure 7.11a-b-c.

7.7. COCHANNEL INTERFERENCE

Cochannel interference is a complication which arises in mobile systems using cellular architecture, because channels are used simultaneously in as many cells as possible, with the minimum acceptable separation, in order to increase the reuse efficiency. A base station receiving the wanted signal from a mobile station within

its cell may also receive unwanted signals (interferers) from mobiles within other cell clusters using the same channel. The determination of the frequency reuse distance, and hence the cell repeat pattern, has a direct influence on the cochannel interference levels: a bigger reuse distance implies a smaller cochannel interference. However, this also implies a bigger number of cells per cluster, resulting in a smaller reuse efficiency. Consequently, a trade-off between interference and efficiency must be found since they work in opposite directions.

The performance parameter of special interest is the Carrier-to-Interference ratio C/I. The ultimate objective of estimating C/I is to determine the reuse distance, and thence, the repeat cell pattern. The C/I ratio is a random variable, affected by the random phenomena such as (i) location of mobile, (ii) Rayleigh fading, (iii) log-normal shadowing, (iv) antenna characteristics and (v) cell site location.

In this section we will tackle the problem of determining C/I by using two methods, analytical and simulation. In the analytical approach the effects of Rayleigh and log-normal fading will initially be considered independently. Later they are taken into account simultaneously. The problem is firstly examined without any traffic distribution consideration, but later this is included for the completeness of the investigation. In the simulation approach a method using a Monte Carlo simulation will be described.

The C/I ratio will be determined in a statistical basis. One measure of interest is the "Outage Probability", i.e., the probability of failing to achieve adequate reception of a signal. This probability will be indicated by p(CI).

A mobile radio in a given cell receives a signal with an envelope s from its base station, but it also receives interferers (unwanted signals) having envelopes I_j, $j = 1,2,\ldots,n$ (n is the number of active cochannels from its cocells). Cochannel interference will occur whenever the wanted signal does not simultaneously exceed the minimum required signal level s_o and the interfering signals $I = \sum_{j=1}^{n} I_j$ by some protection ratio r. Consequently, the conditional outage probability, given n as the number of interferers, is

$$p(CI|n) = 1 - \int_{s_o}^{\infty} p(s) \int_{0}^{s/r} p(i)di\,ds \tag{7.26}$$

The difficulty of this method is to find the probability density function of the equivalent interfering signal I. An alternative to equation (7.26) is to consider each interfering signal I_j individually, as follows

$$p(CI|n) = 1 - \int_{s_o}^{\infty} p(s) \int_{0}^{s/r} p(i_1) \int_{0}^{(s/r)-i_1} p(i_2) \cdots \int_{0}^{(s/r)-i_1 \cdots -i_{n-1}} p(i_n)di_n \cdots di_2\, di_1\, ds \tag{7.27}$$

The difficulty now is to perform multiple integrals.

The total probability of cochannel interference can then be evaluated by

$$p(CI) = \sum_{n} p(CI|n)p(n) \tag{7.28}$$

where p(n) is the probability density function of the number of active interfering signals.

7.7.1. Cochannel Interference with Only One Type of Fading

In an interference-free system the outage probability given by (7.26) reduces to $1 - \int_{s_o}^{\infty} p(s)ds$ which is the coverage requirement for an adequate reception. This has already been fully explored in the section 3.5. In an interference environment the probability densities of both the signal and interferers have to be known and the treatment is obviously more complicated. In a mobile radio environment Rayleigh and log-normal fadings occur simultaneously and again this is another complicating factor. However, it is possible to simplify the calculations by considering only one of these fadings and by allowing some tolerances due to the other fading as described by Hughes and Appleby [12]. The use of only one type of fading can be regarded as a valid approximation whenever either Rayleigh or log-normal fading is dominant when compared with the other. For example, shadowing effect is dominant in the case where an

efficient diversity technique minimizes the Rayleigh fading. On the other hand, Rayleigh fading effect is dominant in the case where the standard deviation of the shadowing is very small.

The probability density function of SNR for the wanted signal and one interferer are the same, and in a Rayleigh environment this is given by (7.29) (reproduced from equation (5.17)).

$$p(x) = \frac{1}{x_m} \exp\left(-\frac{x}{x_m}\right) \tag{7.29}$$

where $x = s$ for the wanted signal-to-noise ratio or $x = I$ for the interferer-to-noise ratio, $x_m = s_m$ for the local mean signal-to-noise ratio and $x_m = I_m$ for the local mean interference-to-noise ratio. In the case of shadowing-only this probability is given by (7.30), as demonstrated in Appendix 7E

$$p(x) = \frac{1}{\sqrt{2\pi}\,\sigma\, x} \exp\left\{-\frac{\ln^2\left(\frac{x}{x_m}\right)}{2\sigma^2}\right\} \tag{7.30}$$

Using $p(s)$ and $p(i_j)$ (given by (7.29)) in (7.27), the outage probability in a Rayleigh environment can be estimated. In the same way, with $p(s)$ and $p(i_j)$ (given by (7.30)) in (7.27), the outage probability, in a log-normal environment, can be estimated. However, performing multiple integrals is a rather difficult task where the degree of difficulty increases with the increasing number of interferers. Let us analyze the two cases separately.

a) *Multiple Interferers in a Rayleigh Fading Environment*

The following description is based on a treatment given by Sowerby and Williamson [14], where the outage probability for multiple interferers is calculated by following an analytical method using a recursive process.

We start by defining the following notations

1) $p(C|J) \triangleq p_J^{out} \triangleq$ outage probability given J interferers

2) $\Delta p_j \triangleq p_j^{out} - p_{j-1}^{out}$

Using (7.29) in (7.27) it is straightforward to show that

$$p_o^{out} = 1 - \exp\left(-\frac{s_o}{s_m}\right) \tag{7.31}$$

and

$$p_1^{out} = 1 - \exp\left(-\frac{s}{s_m}\right) + \frac{1}{1 + \frac{\Lambda_1}{r}} \exp\left[-\frac{s}{s_m}\left(1 + \frac{\Lambda_1}{r}\right)\right] \tag{7.32}$$

where $\Lambda_1 = \frac{s_m}{I_m}$ is the local wanted-signal/interfering signal.

It can be seen that

$$\Delta p_1 = p_1^{out} - p_o^{out} = \frac{1}{1 + \frac{\Lambda_1}{r}} \exp\left[-\frac{s_o}{s_m}\left(1 + \frac{\Lambda_1}{r}\right)\right] \tag{7.33}$$

By carrying out the calculations, for increasing number of Rayleigh interferers, a pattern emerges [14] and a generalization of (7.33) is attainable. For n interferers, we have

$$\Delta p_n = p_n^{out} - p_{n-1}^{out} \tag{7.34}$$

where

$$\Delta p_n = \frac{1}{1 - \frac{\Lambda_n}{\Lambda_{n-1}}}\left(\frac{1}{1 - \frac{\Lambda_n}{\Lambda_{n-2}}}\left(\cdots\left(\frac{1}{1 - \frac{\Lambda_n}{\Lambda_1}}\left(\frac{1}{1 + \frac{\Lambda_n}{r}} \exp\left(-\frac{s_o}{s_m}\left(1 + \frac{\Lambda_n}{r}\right)\right)\right)\right.\right.\right.$$

$$\left.\left.\left. - \Delta p_1\right) - \Delta p_2\right) \cdots\right) - \Delta p_{n-1}\Bigg) \tag{7.35}$$

With the recursive use of (34) and (35) the outage probability, conditional on the number of interferers, can be obtained. Note in (7.35) that an indetermination occurs if Λ_n is equal to $\Lambda_1, \Lambda_2, \ldots, \Lambda_{n-2}$ or Λ_{n-1}. This can be avoided by using "slightly perturbed values of Λ in place of those which have the same values" [14].

For an "interference-only" environment, i.e., if the minimum signal requirement is ignored ($s_o = 0$), it is shown in Appendix 7F that

$$p_n^{out} = \sum_{j=1}^{n} \prod_{k=1}^{j} \frac{\Lambda_{k-1}/r}{1 + \Lambda_k/r} \tag{7.36}$$

where $\Lambda_o \triangleq 1$.

If all the interferers are equal, then

$$p_n^{out} = 1 - \left(\frac{\Lambda/r}{1 + \Lambda/r} \right)^n \tag{7.37}$$

The numerical examples given here will consider this situation.

b) *Multiple Interferers in a Log-Normal Fading Environment*

In the case where only log-normal fading is considered, the probability density function of the equivalent interfering signal p(I) can be approximated by a log-normal distribution [15, 16] (see next section) and used in (7.26).

7.7.2. Cochannel Interference with the Two Types of Fading

In this section we will consider the case where the received radio signal experiences both Rayleigh and log-normal fadings simultaneously. The first step in this direction is to determine the resultant probability density function. It is shown in section 3.4.4 that the combined probability of the received envelope is given by*

---

* Note that, differently from (7.29) and (7.30), this is the distribution of the envelope and not of the signal power.

$$p(s) = \sqrt{\frac{\pi}{8\sigma^2}} \int_{-\infty}^{\infty} \frac{s}{10^{S/10}} \exp\left(-\frac{\pi s^2}{4.10^{S/10}}\right) \exp\left(-\frac{(S - S_m)^2}{2\sigma^2}\right) dS, \quad s > 0, \tag{7.38}$$

where S is the local mean in dB

S_m is the area mean in dB (mean of the log-normal fading)

σ is the standard deviation in dB (typically between 5 and 12 dB in urban location).

The difficulty of dealing with multiple integrals in this case is really great due to the complexity of the joint density function itself. However, it can be shown [17] that the sum of these distributions is another distribution that can be approximated by a normal distribution, for $\sigma = 0$, and by a log-normal distribution, for $\sigma = 6$ dB and 12 dB. Consequently, the distribution of the equivalent interfering signal for $\sigma = 0$ is

$$p(i) = \frac{1}{\sqrt{2\pi}\,\sigma_i} \exp\left(-\frac{(i - \bar{I})^2}{2\sigma_i^2}\right), \quad \text{for } \sigma = 0 \tag{7.39}$$

where

$$\bar{I} = n \exp\left(\frac{I_{m/2}}{10/\ln 10}\right) \triangleq \text{mean of } i \triangleq E[i]$$

$$\sigma_i^2 = \frac{\bar{I}^2}{n} (4/\pi - 1) \triangleq \text{variance of } i \triangleq E[i^2] - E^2[i]$$

$\bar{I}$ and σ_i^2 are obtained from (7.38) with the application of the appropriate definition of moments.

For $\sigma > 0$, the distribution given in (7.38) can be approximated by a log-normal distribution. Therefore the probability density of $I = \sum_{n} I_j$ (sum of log-normal distributions) is approximately another log-normal distribution [16] given by

$$p(i) = \frac{20/\ln 10}{i\sqrt{2\pi}\,\sigma_I} \exp\left(-\frac{1}{2\sigma_I}(20\log i - I_I)^2\right), \quad \text{for } \sigma > 0 \tag{7.40}$$

where

$$\sigma_I^2 = \left(\frac{20}{\ln 10}\right)^2 \left\{ \ln\left[\exp\left(\frac{\sigma^2 + (20/\ln 10)^2 \ln(4/\pi)}{(20/\ln 10)^2} \right) + n - 1 \right] - \ln n \right\} \qquad (7.41)$$

and

$$I_I = I_m - \left(\frac{10}{\ln 10}\right) \ln\left(\frac{4}{\pi}\right) + \frac{20}{\ln 10} \ln n + \frac{\sigma^2 + (20/\ln 10)^2 \ln(4/\pi) - \sigma_I^2}{40/\ln 10} \qquad (7.42)$$

σ_I^2 and I_I are respectively the variance and mean value of I, both given in dB.

If $\sigma = 0$ (Rayleigh fading case) the density of s in (7.38) reduces to

$$p(s) = \sqrt{2\pi} \sqrt{\frac{\pi}{8\sigma^2}} \frac{s}{10^{S_m/10}} \exp\left(- \frac{\pi s^2}{4.10^{S_m/10}} \right) \qquad (7.43)$$

since in (7.38) $S = S_m$, and the integration in dS equals $\sqrt{2\pi}$. Equation (7.43) is the Rayleigh distribution.

The conditional probability of cochannel interference can then be evaluated by using (7.43) and (7.39) in (7.26) for $\sigma = 0$ or (7.38) and (7.40) in (7.26) for $\sigma > 0$.

7.7.3. Some Outage Probability Results

The outage probabilities will be determined for the "interference-only" case (i.e., a minimum signal level is not required, $s_o = 0$). It is convenient to analyze the outage probability in terms of a parameter Z defined as the margin, in dB, by which the mean value of the wanted signal, S_m, exceeds the mean value of the interfering signal, I_m, by a protection ratio R_r (all in dB), i.e.,

$$Z = S_m - (I_m + R_r) \qquad (7.44)$$

Note that Z can be used directly in the equations where both types of fading are considered (section 7.7.2). For the Rayleigh-fading-only case (section 7.7.1) the following transformation must be accomplished in order to convert linear into

logarithmic units

$$\frac{s_m}{r\,i_m} = \frac{A}{r} = 10^{Z/10} \quad \text{or} \quad \frac{s_m}{i_m} = 10^{(Z + R_r)/10} \tag{7.45}$$

In order to estimate the probability of cochannel interference p(CI), the probability density p(n) of the number of active interfering signals must be determined. The status of the channels, in use or not in use, is described by the Bernoulli distribution

$$p(\omega) = p^{\omega}(1 - p)^{1-\omega} \quad , \qquad \omega = 0,1 \tag{7.46}$$

where p is the probability of finding the channel active, and ω represents the channel state: 1 for active and 0 for idle. Assuming independent and uniformly distributed channels and considering only the six surrounding interferers

$$n = \sum_{i=1}^{6} \omega_i \tag{7.47}$$

Then p(n) has a binomial probability density function

$$p(n) = \binom{6}{n} p^n(1 - p)^{6-n} \quad , \qquad n = 0,1,\ldots,6 \tag{7.48}$$

For equal capacity cells and an evenly distributed traffic system

$$p = B^{1/N} \tag{7.49}$$

where B is the blocking probability of the cell with N channels. The distribution p(n) is shown in Figure 7.12.

Consequently, with p(n) given by (7.48) and p(CI/n) calculated as explained in the previous section, we can evaluate p(CI) as in (7.28). Figure 7.13 shows the conditional and unconditional cochannel interference probabilities, p(CI/n) and p(CI) respectively. In this figure we have considered the cases of $n = 1$ and $n = 6$ interferers and $\sigma = 0$ dB (pure Rayleigh environment) and $\sigma = 6$ dB (Rayleigh and log-normal environment).

Note that the probability of interference increases both with the number of interferers and with the standard deviation. Note also that the influence of traffic load is not significant in a mature system where the number of cells is relatively large. This can be seen in Figure 7.13 where the unconditional probability p(CI) is almost always reasonably close to the conditional probability p(CI/6). We can explain this by reasoning that, since in a mature system the number N of channels per cell tends to be large, the occupancy p of the channels approaches 100% even for a low mean blocking probability ($\lim_{N\to\infty} p = \lim_{N\to\infty} B^{1/N} = 1$). Consequently, referring to Figure 7.12, we can see that $p(n) \simeq 1$ for $n = 6$ and $p(n) \simeq 0$ for $n \neq 6$. Hence

$$p(CI) = \sum_{n} p(CI|n)p(n) \simeq p(CI/6)$$

In the case where the traffic is really low ($p \simeq 0$), the distribution of active cochannels will be predominantly given by p(1)*. Hence the final p(CI) will be a small percentage of p(CI/1). Consequently, we can assume that the upper bound for p(CI) is p(CI/6) and the lower bound is theoretically zero.

It is obvious that in a small system the traffic may have a great influence and we may expect that the curve for p(CI) will lie between those for p(CI/1) and p(CI/6).

7.7.4. Reuse Distance and Cluster Size

Let W_w and W_i be the received power of the wanted and interfering signals at the mobile located at distances d_w and d_i from the wanted and interfering base stations, respectively. It has been demonstrated in Chapter 3 (equation (3.60)) that the following relation holds

$$\frac{W_w}{W_i} = \left(\frac{d_w}{d_i}\right)^{-\alpha} \qquad (7.50)$$

* p(0), although larger than p(1), does not influence the result, since p(CI/0) = 0.

where α is an attenuation constant varying within the range from 2 to 4. It is obvious that

$$\frac{s_m}{i_m} = \frac{10^{S_m/10}}{10^{I_m/10}} = \frac{W_w}{W_i} = \left(\frac{d_w}{d_i}\right)^{-\alpha} \tag{7.51}$$

Now, let: (I) D be the distance between the wanted and interfering base stations and (II) R be the cell radius. The cochannel interference worst case occurs when the mobile is positioned at the boundary of the cell, i.e., $d_w = R$ and $d_i = D - R$. In this case

$$\frac{d_i}{d_w} = \frac{D - R}{R} = \frac{D}{R} - 1 \tag{7.52}$$

where D/R is the well known "reuse distance", and is intimately related to the cell pattern of the system. This relation is given by (refer to Chapter 2, equation (2.8))

$$\frac{D}{R} = \sqrt{3N} \tag{7.53}$$

where N is the number of cells per cluster.

Using (7.45) or (7.44), (7.51), (7.52) and (7.53) we obtain

$$\frac{D}{R} = 1 + 10^{(Z+R_r)/10\alpha} = \sqrt{3N} \tag{7.54}$$

or $$Z + R_r = 10\alpha\log(\sqrt{3N} - 1)$$

It has also been shown in Chapter 2 (equation (2.7) that N will only assume specific values, such as 1, 3, 4, 7, 9, 12, 13, ..., given by the relation

$$N = i^2 + ij + j^2 \tag{7.55}$$

where i and j are integers.

Now let us compare the outage probability for some different cluster sizes. This can be done by means of (7.54) and the curves of the Figure 7.13. The results are

shown in Table 7.1 where we are assuming a protection ratio $R_r = 0$ dB. The protection ratio depends on the modulation scheme and varies typically from 8 dB (FM with 25 kHz spacing) to 20 dB (SSB modulation). Consequently, the results of Table 7.1 are in fact an underestimate of the true values of the outage probabilities. However, these true values can be easily determined, again with the use of both equation (7.54), for a given protection ratio, and Figure 7.13.

Note that the influence of the traffic load in the outage probability is more significant for smaller clusters. Nevertheless, the smaller clusters are not feasible due to the unacceptable level of cochannel interference. For the larger clusters the traffic load is not as critical, but attention must be given to the effect of shadowing. Note that there is a remarkable difference between the outage probabilities when shadowing is not considered ($\sigma = 0$ dB) or when it is considered ($\sigma \neq 0$ dB). The increase of the standard deviation increases the cochannel interference probability. This shows that some kind of macroscopic diversity technique may be necessary to minimize the effect of shadowing.

TABLE 7.1:PROBABILITY OF COCHANNEL INTERFERENCE IN DIFFERENT CELL CLUSTERS.

		Outage Probability %			
		Channel Occupancy p = 75%		Channel Occupancy p = 100%	
N	$Z + R_r$ (dB)	σ=0 dB	σ=6 dB	σ=0 dB	σ=6 dB
1	-4.74	100	100	100	100
3	10.54	31	70	40	86
4	13.71	19	58	26	74
7	19.40	4.7	29	7	42
12	24.46	1	11	2.1	24
13	25.19	0.9	9	1.9	22

7.7.5. Cochannel Interference and Simulation

The following section is based on the work by S. Heeralall [18].

As we have seen, the outage probability calculations are not simple at all, and they become even more complex when multiple interferers are involved. However, an approximate estimation can be accomplished with the use of an extended version of equation (7.50). Since the effect of multiple interference is additive, it follows that, for n interferers

$$\frac{s_m}{i_m} = \frac{W_w}{W_I} = \frac{d_w^{-\alpha}}{\sum_{I=1}^{n} d_I^{-\alpha}} \tag{7.56}$$

The ratio s_m/i_m is calculated for fixed mobiles, usually positioned for worst case performance (i.e., $d_w = R$ and $d_I = D - R$) and ignoring fading effects. In order to get an insight into how the distribution of the cochannel-to-interference ratio can be obtained by means of simulation, consider an elementary system with a single interferer as shown in Figure 7.14. Here only one degree of freedom, namely the mobility of the interferer, is allowed.

The wanted mobile is fixed at the perimeter of the cell for minimum wanted signal. The probability that the interfering mobile is at a distance less than or equal to d_I is equal to the proportion of the shaded area $S(d_I)$, i.e.,

$$p\left[CI \le \left(\frac{R}{d_I}\right)^{-\alpha}\right] = \frac{1}{4\pi R^2}\int_{D-R}^{d_I} dS(d_I) = \frac{S(d_I)}{4\pi R^2} \tag{7.57}$$

since $S(D - R) = 0$, with $D - R \le d_I \le D + R$. The area $S(d_I)$ can be easily calculated as a function of d_I, D and R. This cumulative distribution is obtained from a set of values of $s_m/i_m = (R/d_I)^{-\alpha}$ corresponding to different positions of the interfering mobile and the probability that the mobile is at that position. If another degree of freedom is allowed, say, the mobility of the wanted mobile, then a double

integration is needed, i.e.

$$p\left[CI \le \left(\frac{d_w}{d_i}\right)^{-\alpha}\right] = \frac{1}{(4\pi R^2)^2}\int_0^{d_w} dS(d_w)\int_0^{d_i} dS(d_i)$$

$$= \frac{S(d_w)\ S(d_i)}{(4\pi R^2)^2} = \frac{4\pi\ d_w^2\ S(d_i)}{(4\pi R^2)^2} \qquad (7.58)$$

with $0 \le d_w \le R$ and $D - R \le d_i \le D + R$.

If more degrees of freedom, namely Rayleigh fading, shadowing and channel occupation are allowed, the computations as well as the analysis of the results become extremely difficult. The difficulty is obviously increased with the increasing number of interferers. The analysis in this case may be eased with the use of Monte Carlo simulation in a computer. The simulation consists of a large number of snapshots of the system layout where both the position of the mobiles (consequently, the respective mean signal strengths) and the status of the corresponding signal (active or inactive) vary according to a given distribution. The basic steps used in [18] are:

"1. The wanted signal is always active. Each interfering signal is set as active or inactive by sampling from a probability distribution which is derived from the channel occupation.

2. Step 2 is the determination of area mean signal power in dB. It is different for the two directions of transmission between mobile and base. The two scenarios are described separately below:

a) mobile-to-base case

For each active signal, the mobile must first be positioned randomly within its cell. Then the area mean signal strength from each mobile to the wanted base station must be calculated.

b) base-to-mobile case

The wanted mobile is positioned. Then mean signal strength from each base

station to the wanted mobile is calculated.

3. Log-normal shadowing is simulated by sampling from a normal distribution (of standard deviation as set at the start of the simulation) and mean equal to the area mean signal strength in dB. This gives a local mean strength in dB.

4. Rayleigh fading is simulated in a similar manner. The local mean signal strength is converted to linear units (watts) and then equated to the mean of a negative exponential distribution from which the actual signal strength (in watts) is sampled (refer to Appendix 7F).

5. Cochannel-to-interference ratios are calculated as power ratios and then converted to dB;

6. Histograms are updated."

Special simulation programs (e.g., SIMSCRIPT, SIMULA, etc.) can be used to facilitate the task of dealing with samples of probability distributions.

7.8. NOISE AND INTERFERENCE COUNTERACTIONS

The problem of additive noise is not confined to mobile radio systems. It is present in any communication network and the measures to counteract its effect are well known in the literature. Basically, the strategy is to improve the equipment performance by designing better filters and by adjusting signal power levels. The multiplicative noise, on the other hand, constitutes a big problem in the cellular mobile radio systems and the way to combat its effect is by means of macroscopic and microscopic diversity as described in Chapter 5.

Adjacent channel interference (as well as the additive noise) is a well known problem of communication systems. However, its importance in cellular systems has been accentuated due to the spectrum efficiency improvement "neurosis". Adjacent channel interference can be minimized by (i) improving the modulation techniques, (ii) improving the filtering quality of the equipment and (iii) allowing some guard channels between channels allocated to each cell. By far, the biggest problem of all

is cochannel interference, an intrinsic issue of the cellular network. We will dedicate the rest of this section to describe the method of combating this kind of interference.

There is a general consensus that the use of directional antennas substantially improves the signal-to-cochannel interference ratio. S. Heeralall [18] sums up the fundamental operation of directional antennas as follows:

"By restricting the reception of signals to directions where they are really needed, directional antennas cut down the number of significant cochannel interferers without affecting the level of carrier received. By restricting radiation of signals to directions where they are really needed, directional antennas minimize the total level of cochannel interference reaching a receiver. The result is a higher carrier-to-cochannel interference ratio".

Consequently, if the signal-to-cochannel interference ratio is improved, a lower D/R ratio becomes feasible and the implementation of a system with less hexagons per cluster can be attainable.

The performance of a cellular system with directional antennas may be evaluated in the same way as before, but (7.50) must be modified to include the gain of the antennas in each direction as follows

$$\frac{W_w}{W_i} = \frac{G_{Tw}(\theta_{Tw})G_{Rw}(\theta_{Rw})}{G_{Ti}(\theta_{Ti})G_R(\theta_{Ri})}\left(\frac{d_w}{d_i}\right)^{-\alpha} \tag{7.59}$$

where θ_{XY} is the direction of the ray at antenna X with respect to the direction of its maximum gain

$G_{XY}(\theta_{XY})$ is the gain of antenna X at the angle θ_{XY}

and X = T for transmitting antenna or X = R for receiving antenna

Y = w for the wanted antenna and Y = I for the interfering antenna.

A diagram illustrating the arrangement for the cochannel interference calculations in a 2-sector cell system is shown in Figure 7.15.

In such a simplified model, the wanted mobile is positioned at the edge of the

sector and at a distance R from the base station; φ_1 and φ_2 are the (independent) orientations of the wanted antenna and interfering antenna, respectively. The interfering mobile can move within its sector and for each position, the ratio s_m/I_m can be calculated. This can be done by varying the vector d_I from D - R to D + R in steps of Δd_I (defined as desired) and the angle θ_I from $-TAN^{-1}(R/D)$ to $TAN^{-1}(R/D)$ in steps of $\Delta\theta_I$ (defined as desired). We may suppose that, if the mobile is within the sector, then there is interference; otherwise the interference is nil. The corresponding distribution can be obtained by averaging the respective area within the sector over $4\pi R^2$. This distribution is a function of R, D, φ_1, φ_2 and the antenna radiation pattern (beamwidth β).

When multiple interferers are involved, the problem becomes much more complex and a computer simulation is preferred.

Table 7.2 shows the results for some selected cellular patterns [18, 19].

TABLE 7.2: PERFORMANCE OF SOME SELECTED CELLULAR PATTERNS.

Cellular Pattern	Carrier-to-Cochannel Interference (dB)	
cells/cluster x channel sets/cell	1st decile	median
12 x 1	12.0	23.2
7 x 3	14.5	27.0
7 x 1	8.0	19.2
4 x 6	13.5	26.3
3 x 6	12.0	24.2

The sectorized patterns described in the literature are derived from the basic cell site lattice as (N x s), where N is the number of cell sites per cluster and s is the number of sectors per cell site. The most common ones are (7 x 3), (4 x 6) and (3 x 6) sectors, where the cluster is still composed of a contiguous group of hexagons. Some novel cell configurations based on noncontiguous clusters have been proposed by S. Heeralall [18, 19] and they are briefly described here. The general idea to generate these patterns is:

"Place interfering sectors around a wanted sector such that there is a maximum spatial packing. Then each interferer is positioned and oriented to achieve the stated objective. Adjust that arrangement of cosectors until it looks like part of an infinite pattern".

An example of a new cell configuration is given in Figure 16a. This pattern has been set up as follows:

- The first interferer was placed as near as possible to the wanted sector (for minimum spatial packing). It was positioned outside the major lobe, pointing into the opposite direction with respect to the wanted sector (for minimum interference).

- To build a regular pattern, a grid of 60° sectors was used and the sectors were placed only in positions that coincided with the grid and that allowed for an infinite regular structure;

- Another interferer was placed symmetrically with respect to the wanted sector. Then a row pattern with three channel sets per row emerged (i.e., x-direction expansion);

- To move in the y-direction and obtain a two dimensional pattern, a distance of four rows was tentatively found to meet the interference levels requirements. Consequently, a pattern of 12 channels sets (4 rows of 3 sets each) was set up.

Similarly, another pattern was tried, now allowing for coverage areas to overlap, (Figure 7.16b). The difference between these two patterns is that each set now serves four grid sectors instead of one, but each grid sector is also served by three other channel sets.

Note that in this new approach:

- Reuse distance varies in different directions from any given sector;
- Cosectors do not necessarily point into the same direction;
- Clusters with cosectors in different directions have different shapes and may have different internal arrangements;
- Each 60° sector is 1/6 of a hexagon, but the number of hexagons per cluster can

vary as from 1 and can have noninteger values as well, because different sets of cosectors are allowed to overlap;

- Each cell site serves only two sectors that are 180° apart.

It is possible to obtain other patterns by visual inspection: in general, these patterns have less than 3 hexagons/cluster and less than 18 channel sets/cluster. It means that there is an improvement in both the spatial and time efficiency (trunking efficiency is improved). In the example given in Figure 7.16a there are 2 hexagons/cluster and 12 channel groups/cluster. This obviously contrasts with the widely accepted formula $I^2 + IJ + J^2 = N$, where this configuration is not allowed.

Note that each cell site serves only $2\text{-}60^{\circ}$ sectors that are 180° apart, so only 1/3 of the cell site angular range is being used. The reuse pattern is nonisotropic and, therefore, to maintain the cluster, all orientations are constrained to two possibilities only, leading to 6 cell sites per cluster.

This constraint can be removed if clusters are allowed to have non contiguous cells. Rather than filling up a service area by building up around one set of cosectors, we can replicate the basic reuse pattern as many times as necessary and rotate it each time around one cell site. Then, this procedure can be repeated around other cell sites with vacant positions. The resultant cellular pattern will have less cell sites as illustrated in Figure 7.17.

These patterns have been developed heuristically and they lead to a substantial theoretical improvement in traffic carrying capacity. The first decile of carrier-to-cochannel interference has been determined to be 11 dB and the median 22.5 dB for a channel occupation of 68.8% (Figure 7.16a). The carrier-to-cochannel cumulative distribution of the pattern of Figure 7.17 is shown in Figure 7.18.

7.9. SUMMARY AND CONCLUSIONS

Noise and interference are limiting factors of good performance of any communication system. Their effects are usually very similar, but in mobile radio,

noise and interference can be treated completely apart from each other.

Noise can modify the signal in a additive way or in a multiplicative way. The most significant type of additive noise is that caused by man, e.g., electric motors, neon lights, power lines, medical appliances, etc. It is possible to minimize its effect by designing better filters and adjusting the signal power levels. Fading can be considered as another type of noise which degrades the signal in a multiplicative manner. The ways of counteracting the fading have already been extensively studied in Chapters 5 and 6.

Interference in mobile radio system is a more complex problem to be investigated. Adjacent channel interference is usually minimized by avoiding the use of adjacent channels within the same cell. Adjacent channels in adjacent cells, however, are sometimes inevitably used because of the adopted cell pattern. In this case the presence of active mobiles near the cell borders substantially increases the probability of interference. Consequently, the probability of adjacent channel interference depends not only on the geographical distribution of the mobiles but also on the traffic profile of the system. A heavy loaded system is more likely to have problems of adjacent channel interference.

The biggest problem of all is cochannel interference, and this is an intrinsic issue of the cellular architecture. The determination of the cochannel interference must be carry out in a statistical basis due to the random factors involved in the process. Several studies have been made in this field, but they usually treat the problem in a simplified way, allowing very few degrees of freedom (mobiles positioned for the worst case, wanted and interfering mobiles fixed on a given position, etc.). Even in its simplified form, the problem is still extremely complicated to deal with, since it involves either multiple integrals (for multiple interferers) or the determination of the equivalent distribution of multiple interferers.

An alternative to the numerical analysis necessary to solve the multiple integrals is the use of Monte Carlo simulation on a computer. S. Heeralall [18, 19] has extensively used this approach, with the flexibility of allowing all the degrees

of freedom in an extremely easy manner, using the facility of an appropriate simulation program. The result was that not only cochannel-to-interference problem was investigated, but also novel cellular patterns were discovered with a much better performance than that of the traditional patterns.

APPENDIX 7A

Thermal Noise

Let $\overline{v_1^2}$ and $\overline{v_2^2}$ be the mean square noise voltages of two resistors R_1 and R_2 respectively, connected as shown in Figure 7A.1. If the resistors are at the same temperature, then in a given time interval, each must, on average, receive as much energy as it delivers to its partner [20]. Hence

$$\frac{\overline{v_1^2}}{R_1} = \frac{\overline{v_2^2}}{R_2} \tag{7A.1}$$

From (7A.1) we conclude that for the thermal noise $\overline{v^2} \propto R$. Moreover, in the equilibrium, the balance of power must hold for any frequency band. Hence, the mean power exchange per unit bandwidth is a function only of the frequency band B, resistance R and temperature T. Nyquist [4] determined that the power delivered by the resistor to a matched load is equal to kTB, where k is the Boltzmann's constant ($k = 1.38\ 10^{-23}\ JK^{-1}$). Maximum noise power transfer will occur when $R_1 = R_2 = R$. In this case, the total power dissipated in R is $\overline{RI^2}$. From Figure 7A.1

$$\overline{RI^2} = R\overline{\left(\frac{v_1 - v_2}{2R}\right)^2} = \frac{\overline{v_1^2}}{4R} + \frac{\overline{v_2^2}}{4R} \tag{7A.2}$$

since $\overline{v_1 v_2} = \overline{v_1}\ \overline{v_2} = 0$

The term $\overline{v_1^2}/4R$ corresponds to the mean power received by R due to v_1. The same reasoning applies to the term $\overline{v_2^2}/4R$. Therefore, the power delivered by one resistor is $\overline{v^2}/4R$, where $\overline{v^2}$ is its mean square noise voltage. This power, obviously, equals that estimated by Nyquist. Hence

$$\frac{\overline{v^2}}{4R} = kTB$$

or, equivalently,

$$\overline{v^2} = 4kTBR \tag{7A.3}$$

The power spectral density of v is $S_v(\omega)$ such that

$$S_v(\omega) = \overline{v^2}/2B$$

Therefore,

$$S_v(\omega) = 2kTR \tag{7A.4}$$

The power spectral density of the current i is

$$S_i(\omega) = \frac{S_v(\omega)}{R^2} = \frac{2kT}{R} \tag{7A.5}$$

APPENDIX 7B

Shot Noise [6]

Let d be the distance between the anode and cathode of a vacuum tube and V the supply voltage. An electron q with mass m will travel with speed v within a time t such that

$$m\frac{v}{t} = qE = q\frac{V}{d}$$

where E is the electric field intensity. Then

$$v = \frac{qV}{md}t \tag{7B.1}$$

If the induced electric charge in the anode is Q, then using the balance of energy

$$\frac{1}{2}mv^2 = QV \tag{7B.2}$$

Therefore, with (7B.1) in (7B.2) we have

$$Q = \frac{1}{2}\frac{q^2V}{md^2}t^2 \tag{7B.3}$$

The resultant current is

$$i_e(t) = -\frac{dQ}{dt} = \frac{q^2V}{md^2}t = \frac{2qt}{\tau^2} \tag{7B.4}$$

where $\tau = \left(\frac{2m}{qV}\right)^{1/2} d$ is the time taken by the electron to reach the anode.

Note that the current increases linearly with t, but falls abruptly to zero when the electron reaches the anode as shown in Figure 7B.1.

The triangular function of Figure 7B.1 can be written as

$$i_e = \frac{2q}{\tau^2}\left[tu(t) - \tau u(t-\tau) - (t-\tau)u(t-\tau)\right] \tag{7B.5}$$

where $u(t) = 1$ for $t > 0$ and $u(t) = 0$, otherwise.

The Fourier transform of $i_e(t)$ is $I_e(\omega)$ such that

$$I_e(\omega) = \frac{2q}{-(\omega\tau)^2}\left[1 - \exp(-j\omega\tau) - j\omega\tau\exp(-j\omega\tau)\right] \tag{7B.6}$$

Since the total current consists of the superposition of the n* individual currents $i_e(t)$, then

$$S_i(\omega) = n\left|I_e(\omega)\right|^2$$

Accordingly,

$$S_i(\omega) = \frac{4I_0q}{(\omega\tau)^4}\left[(\omega\tau)^2 + 2(1 - \cos\omega\tau - \omega\tau\sin\omega\tau)\right] \tag{7B.7}$$

where $I_0 = nq$ is the mean current.

For $\omega\tau \leq 0.5$ the spectrum is approximately flat and equal to I_0q. Therefore,

$$\overline{v^2} = 2BS_v(\omega) = 2BR^2S_i(\omega) = 2qI_0R^2B \tag{7B.8}$$

---

* n is the mean number of electrons/second.

APPENDIX 7C

Signal-to-Noise Ratio at the Output of a Receiver

The aim of this appendix is to determine the probability distribution of the SNR at the output of a receiver having a noise figure equal to f. The same distribution at the input of the receiver has already been determined in Chapter 5 (section 5.6) and is given by

$$p(\gamma_I \leq \Gamma_I) = P(\Gamma_I) = 1 - \exp\left(-\frac{\Gamma_I}{\gamma_m}\right) \tag{7C.1}$$

where γ_m is the mean SNR, γ_I is the SNR and Γ_I is a given SNR level at the receiver's input.

At the output of the receiver, however, there is an additional noise introduced by the amplifier. The grade of deterioration is given by the noise figure f defined as

$$f = \frac{\text{SNR at the Input}}{\text{SNR at the output}} = \frac{S_I/N_I}{S_0/N_0} \triangleq \frac{\gamma_I}{\gamma_0} \tag{7C.2}$$

where S_i and N_i are respectively the signal and noise powers at the input of the amplifier. Similarly, S_0 and N_0 are respectively the signal and noise powers at the output of the amplifier. If the power gain of the amplifier is G, then $S_I/S_0 = 1/G$ and

$$f = N_0/GN_I \tag{7C.3}$$

But $N_0 = G(N_I + N_a)$ where N_a is the noise power introduced by the amplifier. Thus,

$$f = 1 + N_a/N_I \tag{7C.4}$$

From (7C.2)

$$\gamma_0 = \gamma_I/f \tag{7C.6}$$

The probability density of γ_1 is (refer to (5.17))

$$p(\gamma_1) = \frac{1}{\gamma_m}\exp\left(-\frac{\gamma_1}{\gamma_m}\right) \tag{7C.7}$$

Then, by changing variables,

$$p(\gamma_0)|d\gamma_0| = p(\gamma_1)|d\gamma_1| \tag{7C.8}$$

Using (7C.6) and (7C.7) in (7C.8) we obtain

$$p(\gamma_0) = \frac{f}{\gamma_m}\exp\left(-f\frac{\gamma_0}{\gamma_m}\right) \tag{7C.9}$$

The corresponding probability distribution is

$$\text{prob}(\gamma_0 \le \Gamma_0) = P(\Gamma_0) = \int_0^{\Gamma_0} p(\gamma_0)d\gamma_0 = 1 - \exp\left(-f\frac{\gamma_0}{\gamma_m}\right) \tag{7C.10}$$

Note from (7C.10) that there is a deterioration of the SNR for any value of the noise figure different from the unit ($f \ge 1$).

APPENDIX 7D

Probability of Adjacent Channel Interference

The aim of this appendix is to determine the probability of occurrence of adjacent channel interference as a function of the following parameters

(i) proportion of active channels with only one adjacent channel in use (p_1),

(ii) proportion of active channels with two adjacent channels in use (p_2),

(iii) proportion of mobiles within the cell's weak signal area (μ'),

(iv) proportion of mobiles with access to two or more base stations (γ),

(v) proportion of mobiles with access to three or more base stations (δ).

Note that the parameters p_1, p_2, μ', γ and δ constitute probability distributions. The probabilities p_1 and p_2 are functions of the traffic load and the channel assignment algorithms, while μ', γ and δ are strictly related with the mean signal strength (the reader is referred to section 7.6 for a better understanding of these probabilities). In our analysis we assume that adjacent channels are assigned to adjacent cells.

Adjacent channel interference is more likely to occur when the mobile is near the cells' borders. Consider three neighbouring cells as shown in Figure 7D.1 and Figure 7D.2 where the dotted circular lines delimit the base stations' service areas. Note that the regions 2 and 4 represent overlapping areas where the mobiles are served by two base stations. In the same way, the regions 1, 3 and 5 represent overlapping areas where the mobiles are served by three base stations.

The probability that a mobile is served by two base stations only is $\gamma - \delta$ for all of the 6 borders of the cell. If we consider only one border then this probability is $(\gamma - \delta)/6$. Similarly, the probability that a mobile is served by three base stations is δ, while this is $\delta/6$ if we consider only one border of the cell.

7D.1 Adjacent Channel Interference at the Mobile Station

Consider the situation as depicted in Figure 7D.1. We shall examine two cases as follows

1) *One Active Adjacent Channel*

Let channel i be an active channel in a given cell. Let one of its adjacent channels (i + 1 or i - 1) be active in one of the adjacent cells (event with probability p_1). For ease of understanding assume that the mobile M_1 uses channel i whereas either M_2 uses channel i + 1 or M_3 uses channel i - 1. Interference is likely to occur if

a) M_1 lies in region 1 (event with probability $\delta/6$), or

b) M_1 lies in region 2 (event with probability $(\gamma - \delta)/6$), or

c) M_1 lies in region 3 (event with probability $\delta/6$)

Hence the probability of the event (1) is

$$p_1\left(\frac{\gamma - \delta}{6} + 2\frac{\delta}{6}\right)$$

2) *Two Active Adjacent Channels*

We assume the same channel assignment as before with the difference that all of the three channels are active (event with probability p_2). Interference is likely to occur if

a) M_1 lies in region 1 (event with probability $\delta/6$), or

b) M_1 lies in region 2 (event with probability $(\gamma - \delta)/6$), or

c) M_1 lies in region 3 (event with probability $\delta/6$. However, since the two adjacent channels may simultaneously interfere, then this event contributes with $2\delta/6$ to the total probability), or

d) M_1 lies in region 4 (event with probability $(\gamma - \delta)/6$), or

e) M_1 lies in region 5 (event with probability $\delta/6$).

Then, the probability of the event (2) is

$$p_2\left(2\frac{\gamma - \delta}{6} + 4\frac{\delta}{6}\right)$$

Adjacent channel interference at the mobile will occur with probability p_M such that

$$p_M = p_1\left(\frac{\gamma - \delta}{6} + 2\frac{\delta}{6}\right) + p_2\left(2\frac{\gamma - \delta}{6} + 4\frac{\delta}{6}\right)$$

or, equivalently

$$p_M = \left(\frac{\gamma + \delta}{3}\right)\left(\frac{p_1 + 2p_2}{2}\right) \qquad (7D.1)$$

7D.2 Adjacent Channel Interference at the Base Station

Adjacent channel interference at the base station is likely to occur when the home mobile is transmitting from a weak signal area and one or two "away" mobiles are

transmitting in adjacent channels from the overlapping areas as shown in Figure 7D.2. As in the previous case, we shall consider one and two active adjacent channels. Moreover, the home mobile is always considered to be in the weak signal area (event with probability μ') and use channel 1.

1) *One Active Adjacent Channel*

The analysis in this case is very similar to that given in section 7D.1 item (1). Hence, the probability of this event is

$$\mu' p_1 \left(\frac{\gamma - \delta}{6} + 2\frac{\delta}{6} \right)$$

2) *Two Active Adjacent Channels*

There are various situations to be analyzed in this case. The analysis is a bit more intricate and the possible situations are summarized in Table 7D.1. The probability of this event is

$$\mu' p_2 \sum \text{(probabilities given in table 7D.1)} = \mu' p_2 \left(\frac{2\gamma + 2\delta}{6} \right) \text{ (believe or not!...)}$$

Adjacent channel interference at the base station will occur with probability p_B such that

$$p_B = \mu' p_1 \left(\frac{\gamma - \delta}{6} + 2\frac{\delta}{6} \right) + \mu' p_2 \left(\frac{2\gamma + 2\delta}{6} \right)$$

or, equivalently

$$p_B = \mu' \left(\frac{\gamma + \delta}{3} \right) \left(\frac{p_1 + 2p_2}{2} \right) \qquad (7D.2)$$

TABLE 7D.1 - POSSIBLE SITUATIONS WITH 2 ADJACENT CHANNELS IN USE.

M_2 Is In region	M_3 Is In region	Number of Interferers	Probability of the Event
1	3	2	$2(\delta/6)^2$
1	4	2	$2(\delta/6)(\gamma - \delta)/6$
1	5	2	$2(\delta/6)^2$
1	Elsewhere	1	$(\delta/6)\left(1 - \frac{\delta + \gamma}{6}\right)$
2	3	2	$2(\delta/6)\left(\frac{\gamma - \delta}{6}\right)$
2	4	2	$2\left(\frac{\gamma - \delta}{6}\right)^2$
2	5	2	$2(\delta/6)\left(\frac{\gamma - \delta}{6}\right)$
2	Elsewhere	1	$\left(\frac{\gamma - \delta}{6}\right)\left(1 - \frac{\delta + \gamma}{6}\right)$
3	3	2	$2(\delta/6)^2$
3	4	2	$2(\delta/6)\left(\frac{\gamma - \delta}{6}\right)$
3	5	2	$2(\delta/6)^2$
3	Elsewhere	1	$(\delta/6)\left(1 - \frac{\delta + \gamma}{6}\right)$
Elsewhere	3	1	$(\delta/6)\left(1 - \frac{\delta + \gamma}{6}\right)$
Elsewhere	4	1	$\left(\frac{\gamma - \delta}{6}\right)\left(1 - \frac{\delta + \gamma}{6}\right)$
Elsewhere	5	1	$(\delta/6)\left(1 - \frac{\delta + \gamma}{6}\right)$

APPENDIX 7E

Distribution of the SNR in a Log-Normal Fading Environment

A log normal fading with envelope r has the following distribution, as given by (3.78)

$$p(r) = \frac{1}{\sqrt{2\pi}\, r\sigma_r} \exp\left[- \frac{\ln^2(r/m)}{2\sigma_r^2} \right] \tag{7E.1}$$

Define γ as the ratio of the local mean signal power and the mean noise power. In the presence of Gaussian noise having a mean power equal to N the SNR is then

$$\gamma = \frac{r^2/2}{N} \tag{7E.2}$$

The distribution of γ can be easily obtained by a simple change of variables as follows

$$p(\gamma)\,|d\gamma| = p(r)\,|dr| \tag{7E.3}$$

Using equations (7E.3), (7E.2) and (7E.1) we obtain

$$p(\gamma) = \frac{N}{\sqrt{2\pi}\, r^2\sigma_r} \exp\left[- \frac{\ln^2\left(\frac{2\gamma N}{m^2} \right)^{1/2}}{2\sigma_r^2} \right] \tag{7E.4}$$

Defining

$$\gamma_m \triangleq \frac{m^2/2}{N} \tag{7E.5}$$

it is straightforward to show that with (7E.5) in (7E.4) we obtain

$$p(\gamma) = \frac{1}{\sqrt{2\pi}\, \sigma_\gamma \gamma} \exp\left[- \frac{\ln^2(\gamma/\gamma_m)}{2\sigma_\gamma^2} \right] \tag{7E.6}$$

where $\sigma_\gamma = 2\sigma_r$

APPENDIX 7F

Outage Probability for the "Interference Only" Case

If no minimum signal is required ($s_0 = 0$), then from (7.34)

$$\Delta p_1 = p_1 - p_0 = p_1$$

$$\Delta p_2 = p_2 - p_1$$

$$\Delta p_3 = p_3 - p_2$$

$$\vdots$$

$$\Delta p_n = p_n - p_{n-1}$$

By adding all of the above equations we have

$$p_n = \sum_{j=1}^{n} \Delta p_j$$

Now from (7.35)

$$\Delta p_1 = \frac{1}{1 + A_1/r}$$

$$\Delta p_2 = \frac{A_1/r}{(1 + A_1/r)(1 + A_2/r)}$$

$$\vdots$$

$$\Delta p_n = \frac{(A_1/r)(A_2/r)\ldots(A_{n-1}/r)}{(1 + A_1/r)(1 + A_2/r)\ldots(1 + A_n/r)}$$

Then

$$p_n = \sum_{j=1}^{n} \prod_{k=1}^{j} \frac{A_{k-1}/r}{1 + A_k/r} \quad , \qquad \text{with } A_0 \triangleq 1$$

If all of the interferers are assumed to equally interfere the wanted signal, then $A_1 = A_2 = \ldots = A_k = A$.

Therefore,

$$p_n = \frac{1}{A/r} \sum_{j=1}^{n} \left(\frac{A/r}{1 + A/r} \right)^j$$

The above sum represents a sum of a geometric progression having a ratio equal to $\frac{\lambda/r}{1 + \lambda/r}$ which is less than one. Then

$$P_n = 1 - \left(\frac{\lambda/r}{1 + \lambda/r}\right)^n$$

REFERENCES

[1] A.D. Watt, R.M. Coom, E.L. Maxwell and R.W. Plush, "Performance of Some Radio Systems in the Presence of Thermal and Atmospheric Noise", *Proceedings of the IRE*, Vol. 46, pp. 1914-1923, December 1958.

[2] *Reference Data for Radio Engineers*, Howard W. Sams & Co., Indianapolis, Indiana, 6th edition, 19.....

[3] J.B. Johnson, "Thermal Agitation of Electricity in Conductors", *Phys. Rev.*, 32, 97-109, July 1928.

[4] H. Nyquist, "Thermal Agitation of Electric Charge in Conductors", *Phys. Rev.*, 32, 110-113, July 1928.

[5] B.P. Lathi, *Random Signal and Communication Theory*, International Textbook Co., Scranton, Pa., 1968.

[6] B.P. Lathi, *Communication Systems*, John Wiley & Sons, Inc., 1968.

[7] J.D. Parsons, J.G. Gardiner, *Mobile Communication Systems*, Blackie and Son Limited. 1989.

[8] R.A. Shepherd et al., "Measurement Parameters for Automobile Ignition Noise", Stanford Research Institute, NTIS PB 247766, June 1975.

[9] R.T. Diney and A.D. Spaulding, "Amplitude and Time-Statistics of Atmospheric and Man-Made Radio Noise", Environment Science Services Administration Technical Report ERL ISO-ITS 98, February 1970.

[10] J.H.Sánchez V., "Traffic Performance of Cellular Mobile Radio Systems", *Ph.D. Thesis*, University of Essex, England, June 1988.

[11] M.D. Yacoub, "Mobile Radio with Fuzzy Cell Boundaries", *Ph.D. Thesis*, University of Essex, England, May 1988.

[12] C.J. Hughes and M.S. Appleby, "Definition of a Cellular Mobile Radio System", *IEE Proceedings*, Vol. 132, Pt.F, Nº 5, August 1985.

[13] M. Hata, K. Kunoshita and K. Hirade, "Radio Link Design of Cellular Mobile Systems", *IEEE Trans.*, VT-31, 1982.

[14] K.W. Sowerby and A.G. Williamson, "Outage Probability Calculation for Multiple Cochannel Interferers in Cellular Mobile Radio", *IEE Proceedings*, Vol. 135, Pt.F, Nº 3, June 1988.

[15] Y.S. Yeh and S.C. Schwartz, "Outage Probability in Mobile Telephony Due to Multiple Log-Normal Interferers", *IEEE Transactions*, COM-32, pp. 380-384, 1984.

[16] L.F. Fenton, "The Sum of Log-Normal Probability Distributions in Scatter Transmission Systems", *IRE Trans. Commun. Syst.*, Vol. CS-8, pp. 57-67, March 1960.

[17] R. Muammar and S.C. Gupta, "Cochannel Interference in High Capacity Mobile Radio Systems", *IEEE Transactions on Communications*, Vol. COM-30, Nº 8, August 1982.

[18] S. Heeralall, "The Applications of Direction Antennas in Cellular Mobile Radio Systems", *Ph.D. Thesis*, University of Essex, July 1988.

[19] S. Heeralall and C.J. Hughes, "High Capacity Cellular Patterns Land Mobile Radio Systems Using Directional Antennas", *IEE Proceedings*, Vol. 136, Pt.1, Nº 1, February 1989.

[20] C.C. Goodyear, *Signals and Informations*, Butterworth & Co. Ltd., London, 1971.

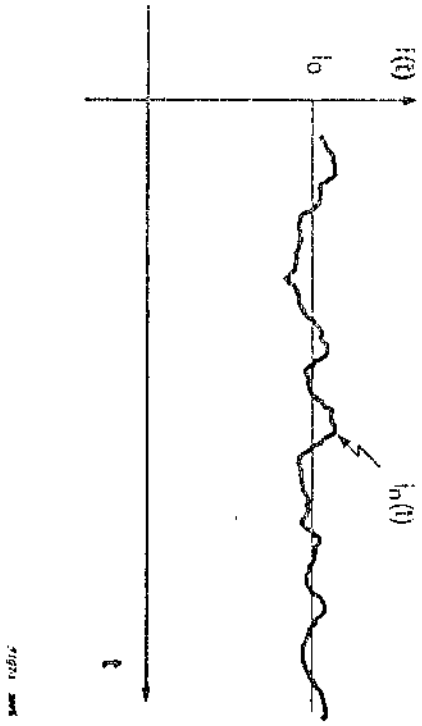

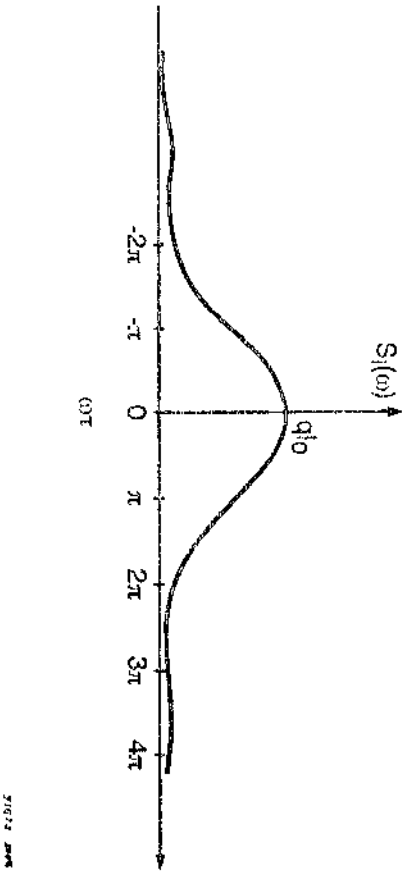

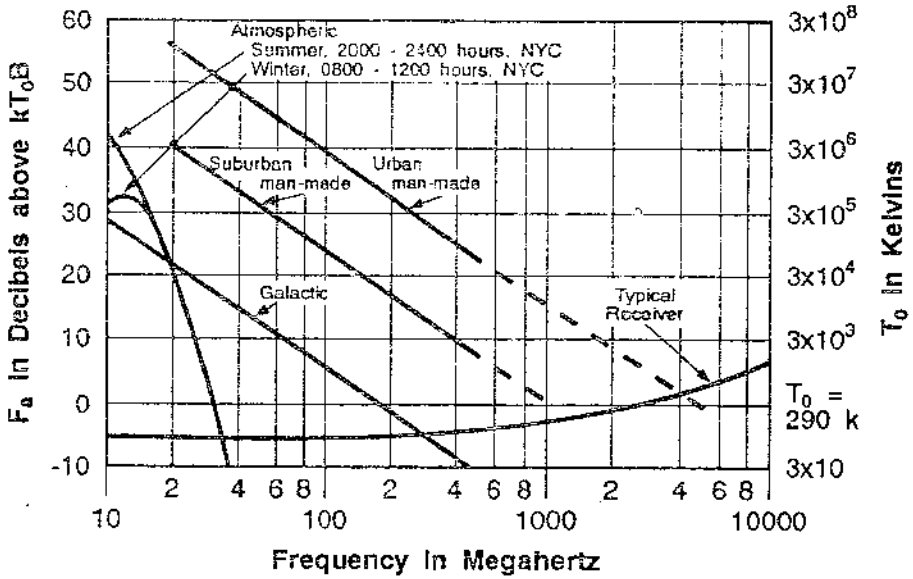

51673 2005

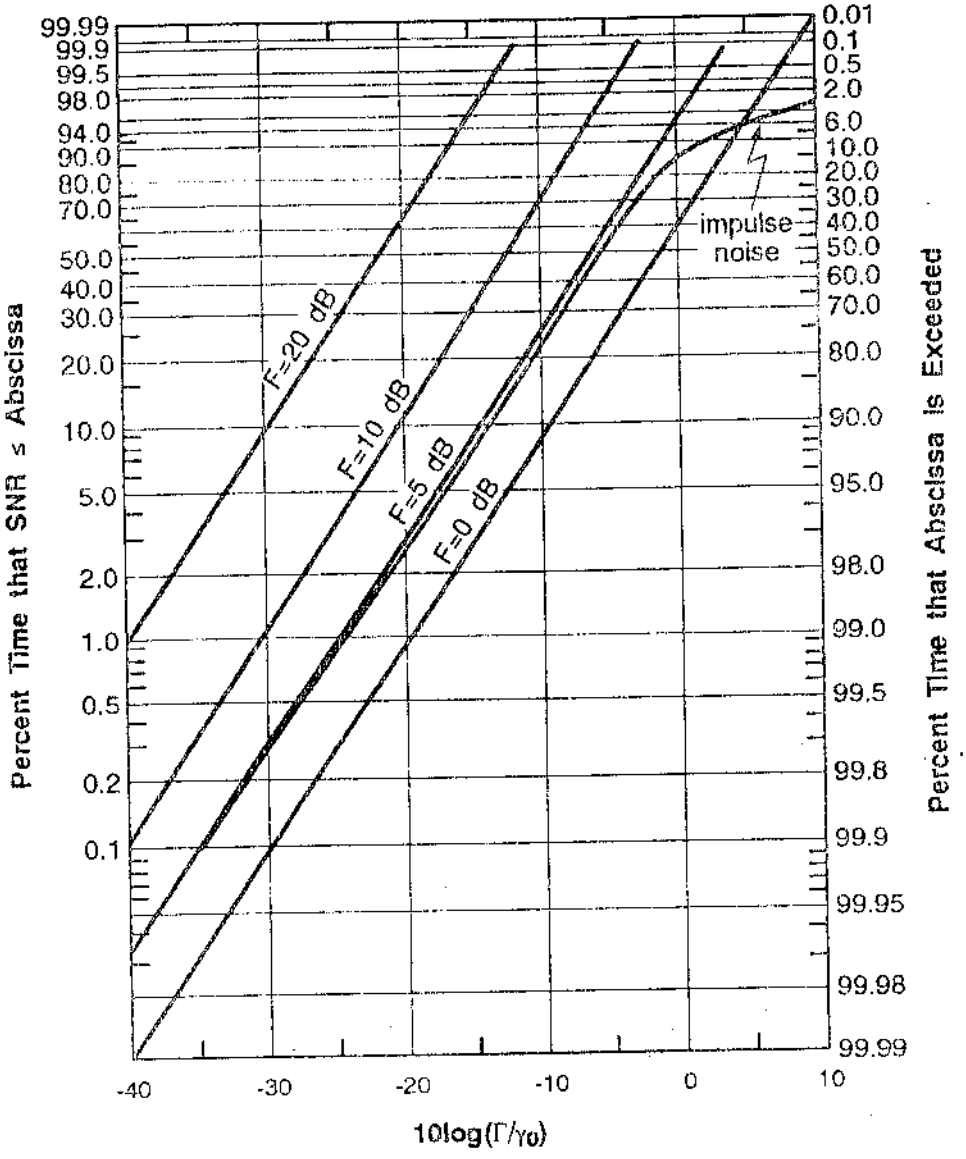
99.99
99.9
99.5
98.0
94.0
90.0
80.0
70.0
50.0
40.0
30.0
20.0
10.0
5.0
2.0
1.0
0.5
0.2
0.1
0.01
0.1
0.5
2.0
6.0
10.0
20.0
30.0
40.0
50.0
60.0
70.0
80.0
90.0
95.0
98.0
99.0
99.5
99.8
99.9
99.95
99.98
99.99
F=20 dB
F=10 dB
F=5 dB
F=0 dB
impulse
noise
-40
-30
-20
-10
0
10
Percent Time that SNR ≤ Abscissa
Percent Time that Abscissa is Exceeded
10log(Γ/γ0)

FIG7-4 1983

where:

W_t = transmitter power
G_t = transmitter antenna gain
L = path loss
G_r = receiver antenna gain
N_i = thermal noise
F = noise figure

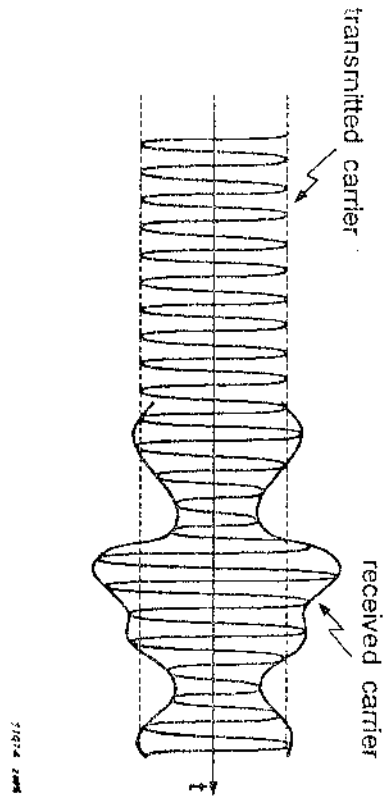

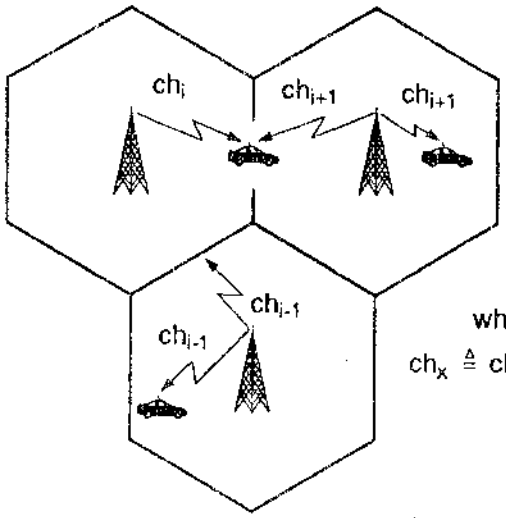
ch_i
ch_{i+1}
ch_{i+1}
ch_{i-1}
ch_{i-1}
where
$ch_x \triangleq$ channel x

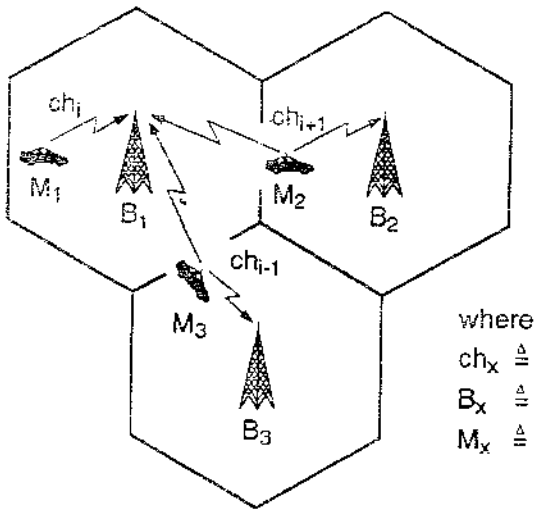

where
$ch_x \triangleq$ channel x
$B_x \triangleq$ base station x
$M_x \triangleq$ mobile x

Fig 7-8

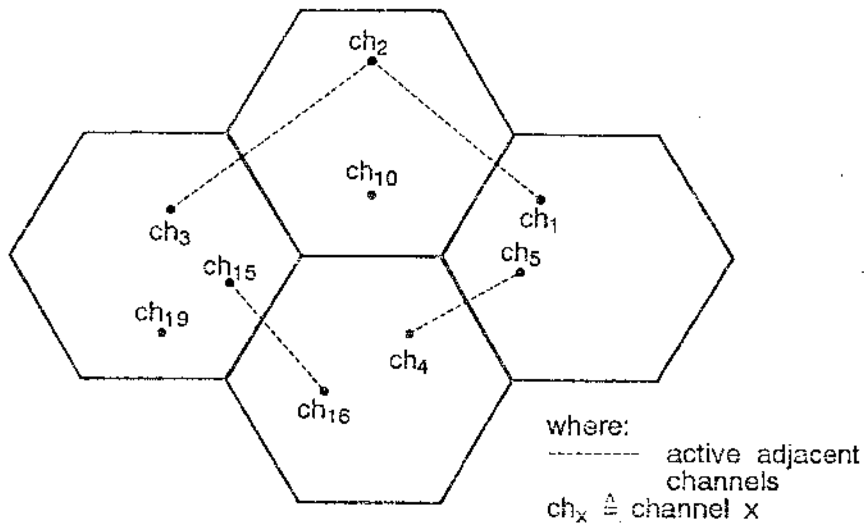

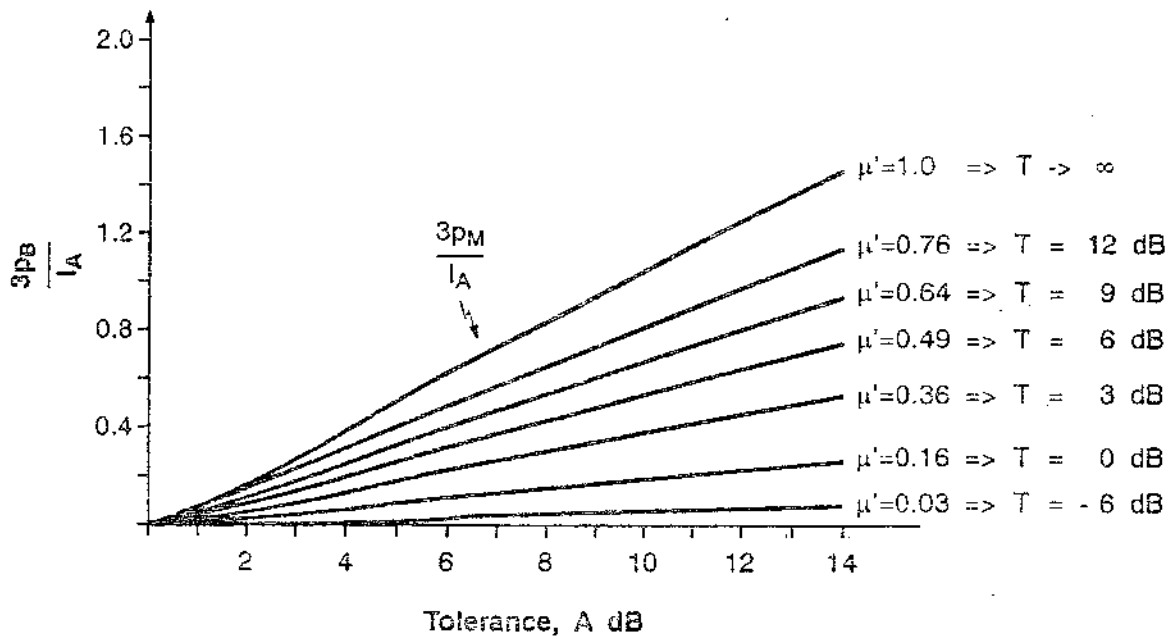

FIG7-10 150%

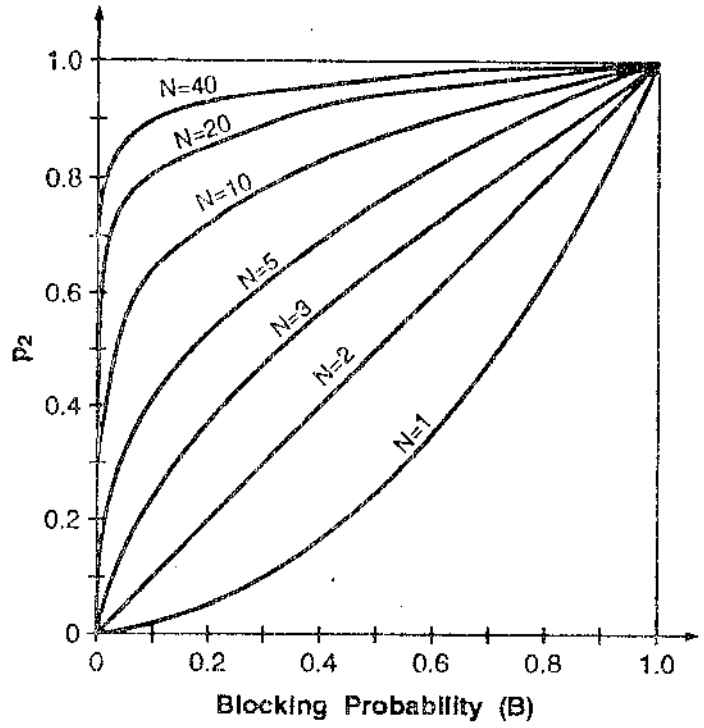
1.0
0.8
0.6
0.4
0.2
0
p_2
N=40
N=20
N=10
N=5
N=3
N=2
N=1
0
0.2
0.4
0.6
0.8
1.0
Blocking Probability (B)

(a)

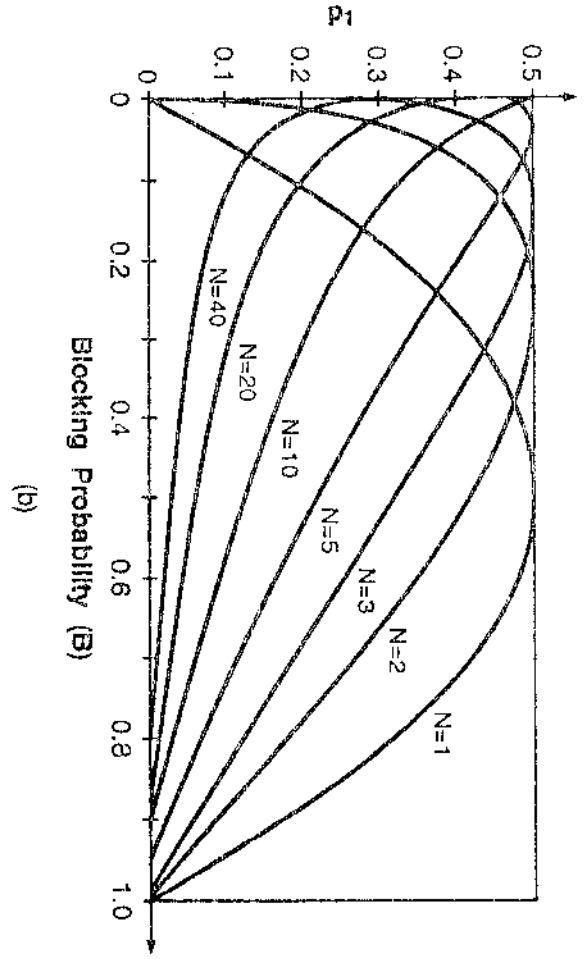

(b)

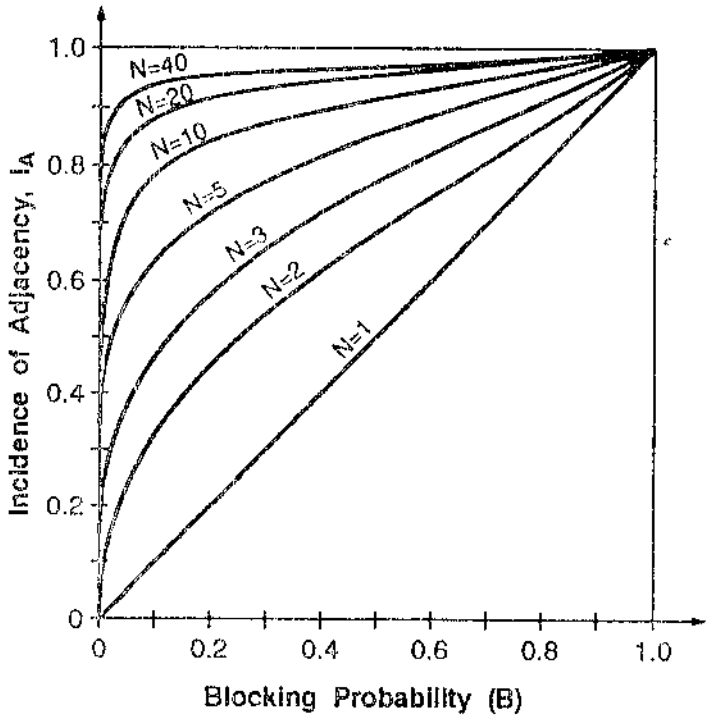
1.0
0.8
0.6
0.4
0.2
0
Incidence of Adjacency, I_A
N=40
N=20
N=10
N=5
N=3
N=2
N=1
0
0.2
0.4
0.6
0.8
1.0
Blocking Probability (B)

(c)

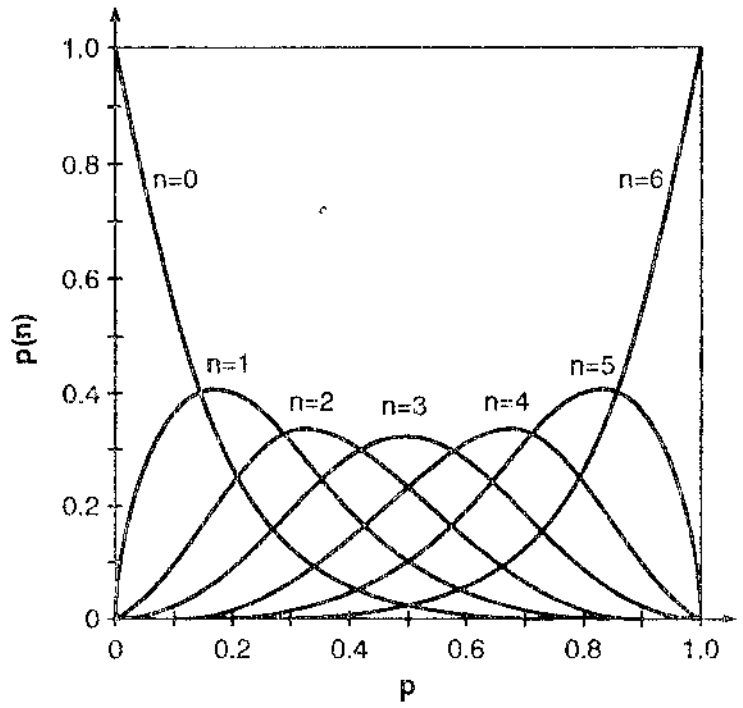
1.0
0.8
0.6
0.4
0.2
0
p(n)
n=0
n=1
n=2
n=3
n=4
n=5
n=6
0
0.2
0.4
0.6
0.8
1.0
p

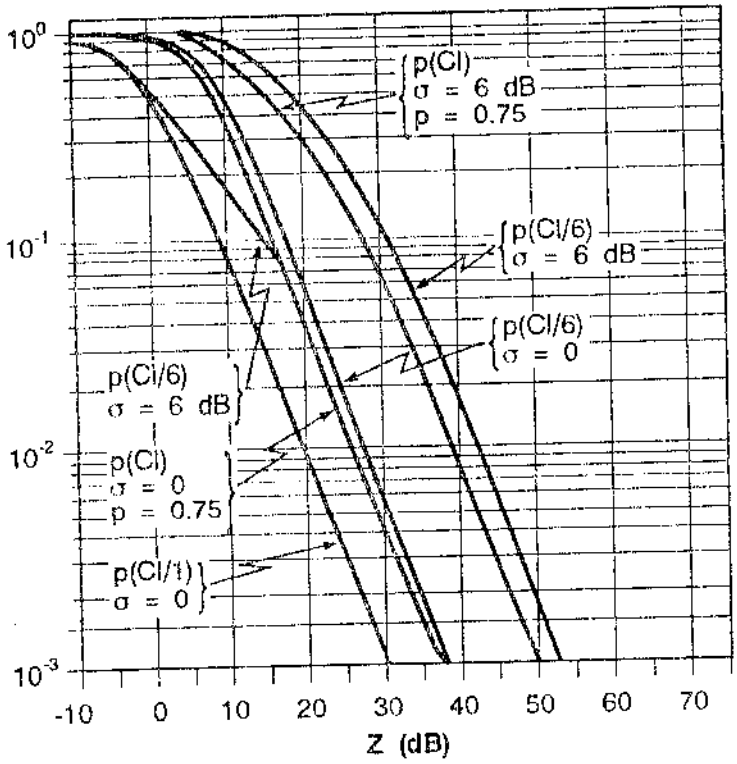
10^0
10^{-1}
10^{-2}
10^{-3}
p(Cl)
σ = 6 dB
p = 0.75
p(Cl/6)
σ = 6 dB
p(Cl/6)
σ = 0
p(Cl/6)
σ = 6 dB
p(Cl)
σ = 0
p = 0.75
p(Cl/1)
σ = 0
-10
0
10
20
30
40
50
60
70
Z (dB)

FIG 7-13 3005

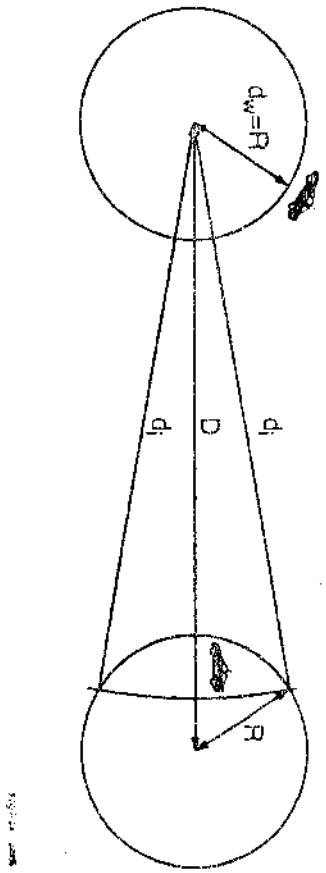

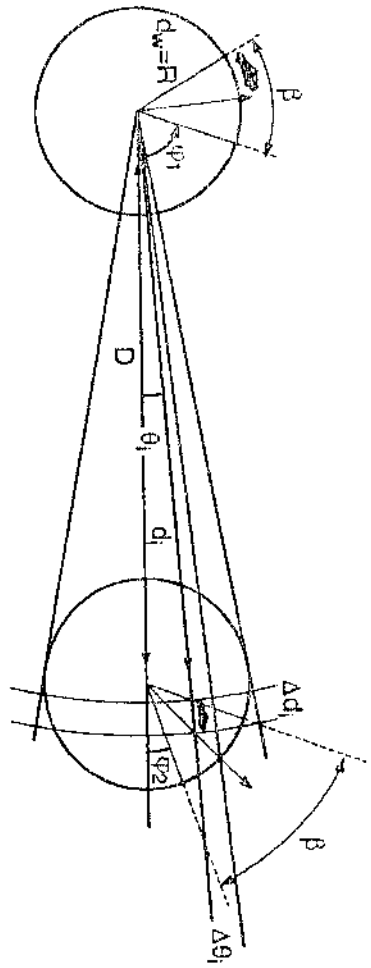

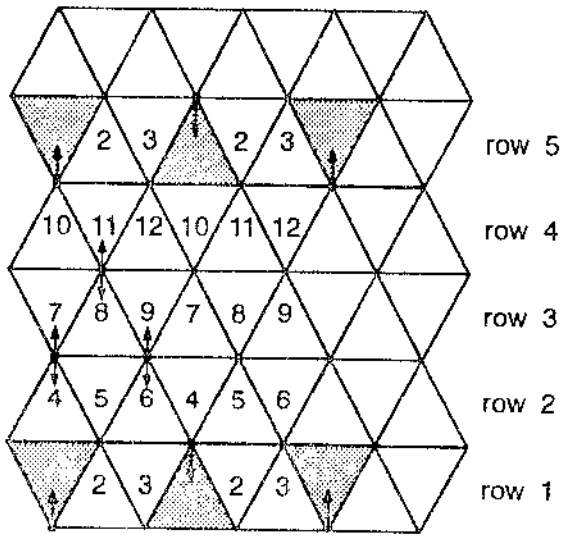

(a)

where: ▽ Channel set 1
● Base station
/ Cluster boundary
↑ Antenna orientation

FIG7-16(a) 150k

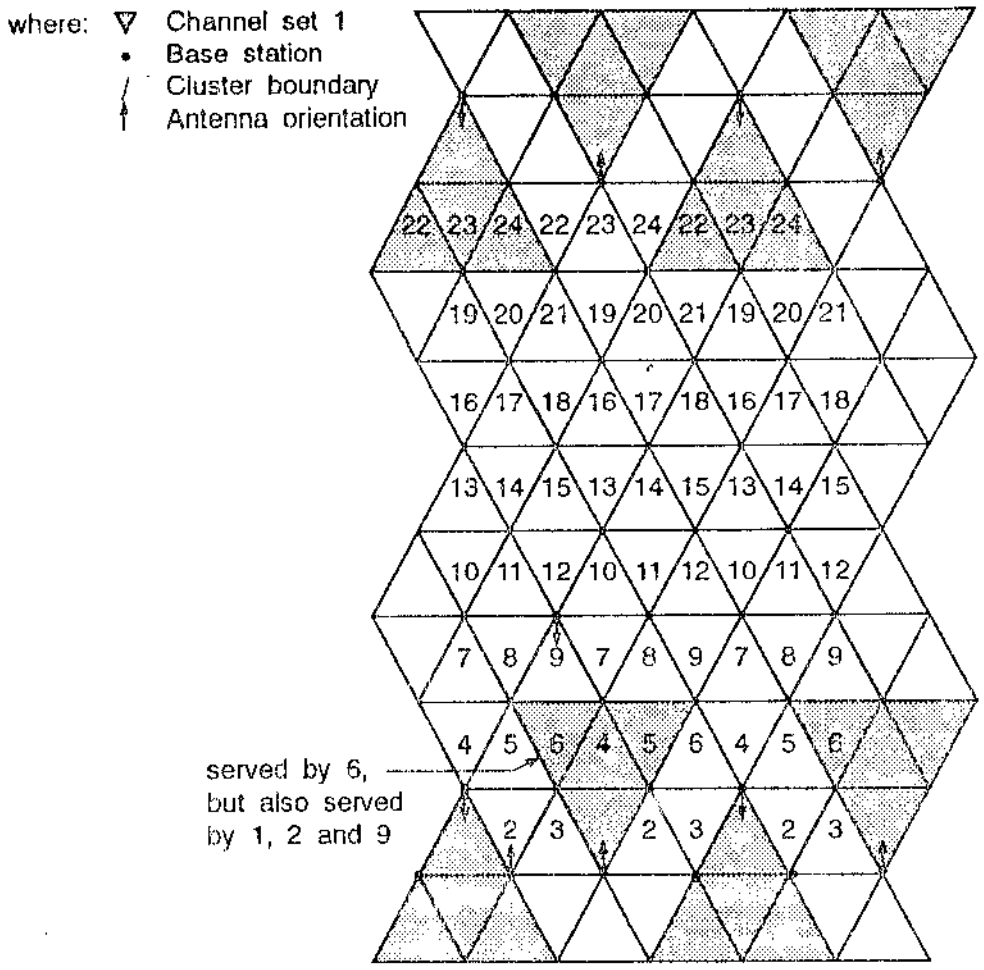

(b)

FIG7-16(b) 1503

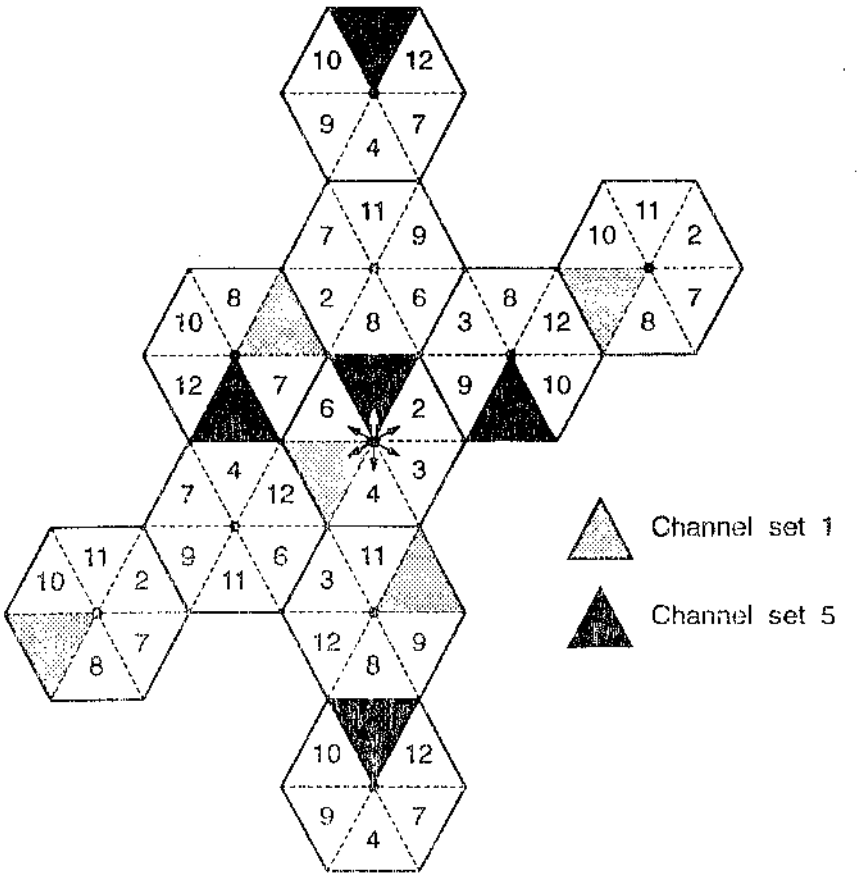
10
12
9
4
7
11
7
9
10
11
2
8
10
8
2
8
6
3
8
12
8
7
12
7
6
2
9
10
4
7
12
4
3
11
10
2
9
11
6
3
11
7
8
12
8
9
10
12
9
4
7
Channel set 1
Channel set 5

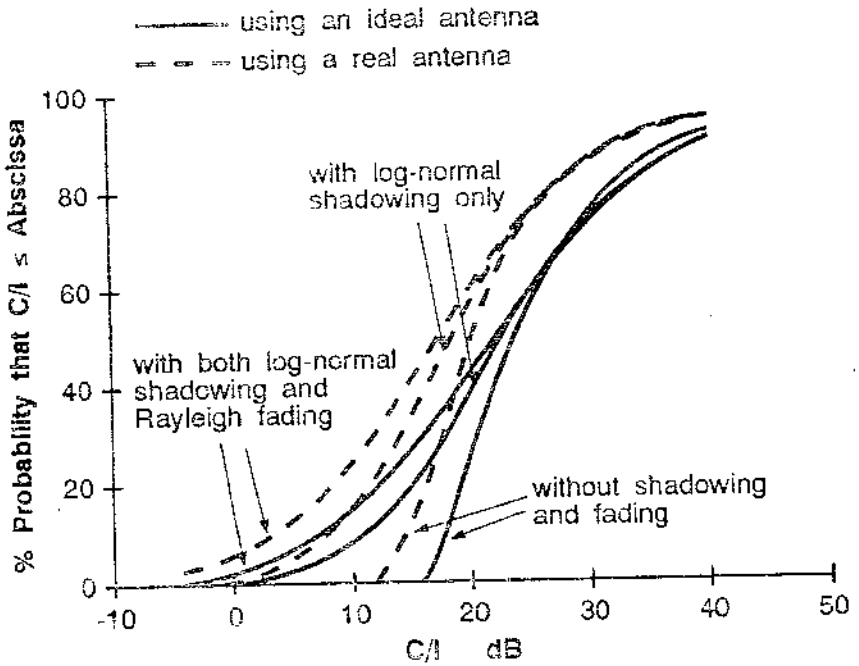

$\frac{V_1}{2}$
R_1
I
$\frac{V_2}{2}$
R_2

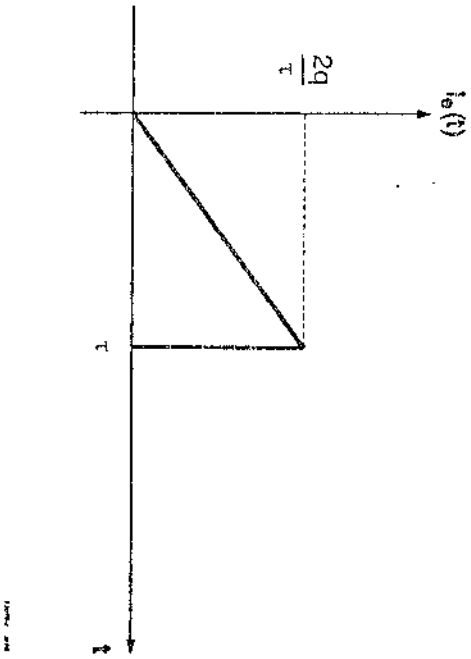

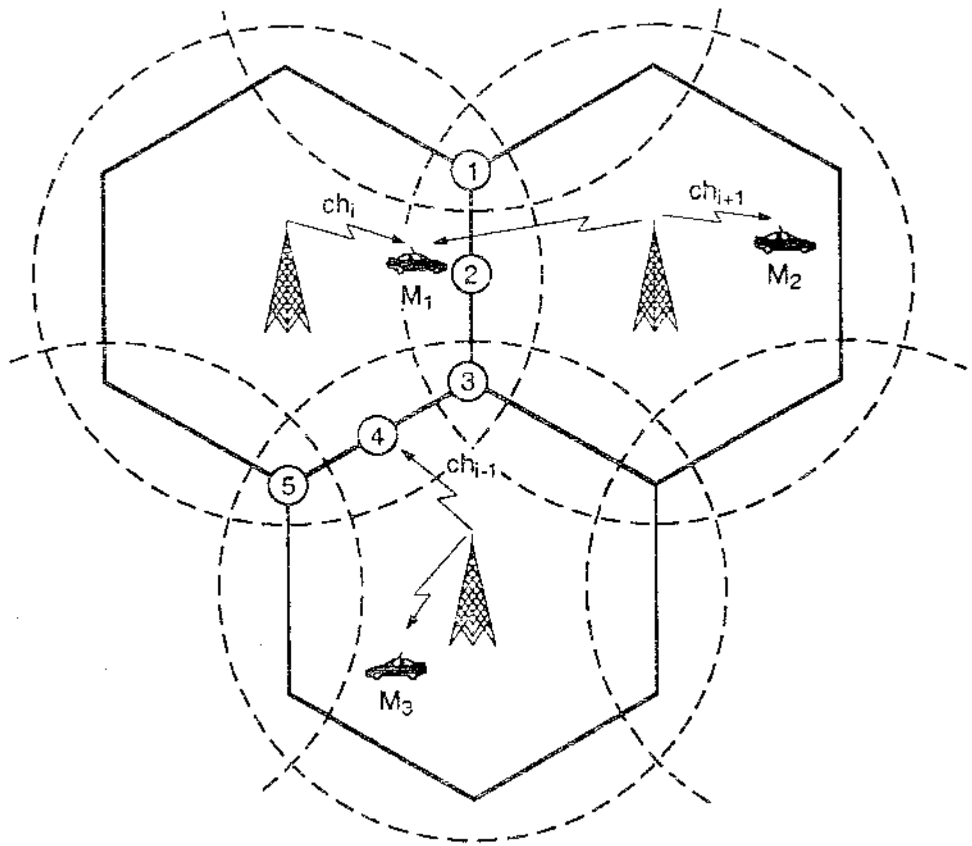

FIG 7D-1 1503

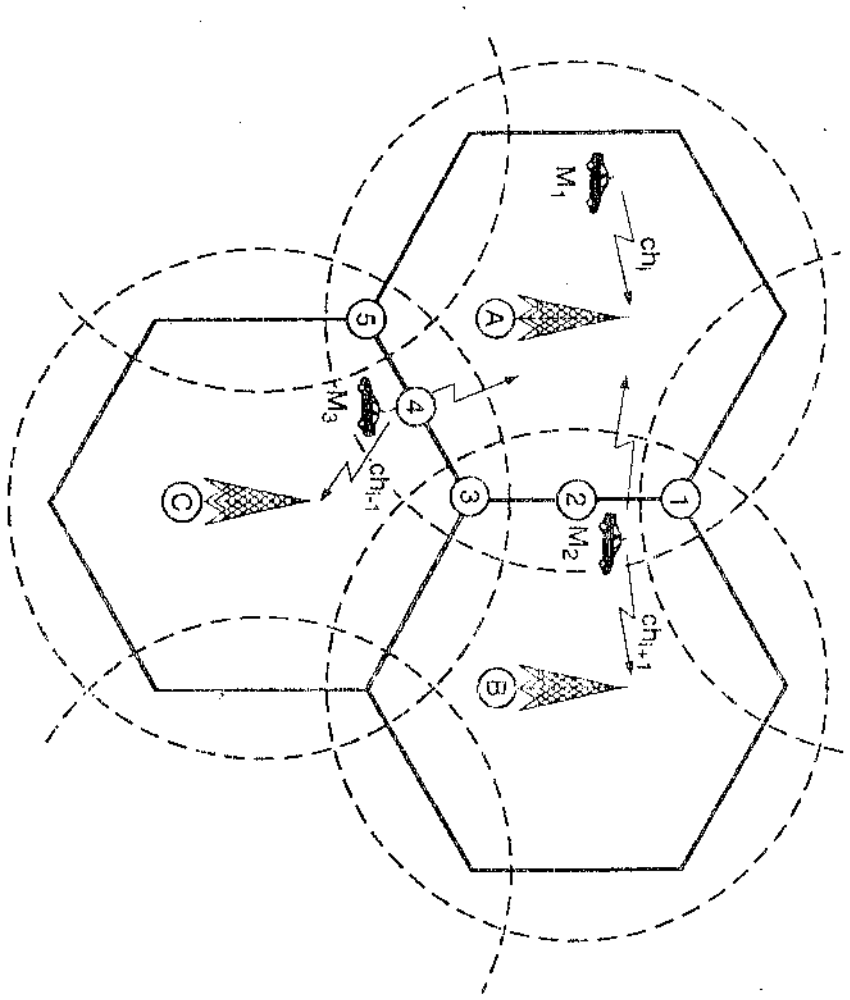

FIG 7d-2

CHAPTER 8

ANALOG MODULATION FOR MOBILE RADIO

PREAMBLE

This chapter is concerned with the performance of some analog modulation techniques, namely AM, SSB and FM in a mobile radio environment. We start the chapter by defining the performance measure parameters, consisting basically of the signal-to-noise ratio and its variations. Thereafter, we analyze each technique separately reviewing its basic principles, the required transmission bandwidth and ways of generating and detecting the modulated signals. We then formulate a general model for the received signal and analyze the performance of the modulation technique in the presence of additive and multiplicative noises. We show that multiplicative noise (fading) has a disastrous effect on AM and SSB systems and that the capture effect of the FM systems is not so prominent in the presence of fading. We also consider some emerging alternatives that may enhance the performance of the SSB systems, making them suitable for mobile radio applications.

8.1 INTRODUCTION

Modulation is a process by which one or more parameters of a carrier (amplitude or angle) are varied in accordance with a message signal (modulating wave). As a result of the modulation process, the frequency band of the message signal is shifted to a suitable region within the spectrum so that transmission over a communication channel becomes feasible. At the reception side the receiver carries out the inverse of the modulation process, named demodulation or detection, so that the message signal can be recovered.

First generation mobile radio systems used analog modulation for voice transmission. The early systems started with standard Amplitude Modulation (AM), since this was the only feasible technique available at that time, but moved quickly into Frequency Modulation (FM) as soon as it was demonstrated that its practical implementation was viable. The Single Sideband (SSB) technique was also experimented in some mobile radio services. However FM ended up predominating and today all the analog cellular systems have adopted this scheme of modulation for voice transmission. Some enhanced forms of SSB such as Transparent Tone In Band (TTIB), Feed Forward Signal Regeneration (FFSR) and Amplitude Companded Single Sideband (ACSSB), have been proposed and intensively investigated, with a good chance of being used by some mobile radio services.

In this chapter we will introduce the basics of the main analog modulation techniques and analyze their performance in the presence of both additive and multiplicative noise, having in mind that the multiplicative is what mainly characterizes the mobile radio channel.

8.2 PERFORMANCE MEASURES OF MODULATION TECHNIQUES

Any communication channel of electrical systems is subject to random fluctuations of power known as noise. Noise is a limiting factor on the power required to transport information-bearing signals and may affect the demodulation process in different manners, according to the used modulation technique.

The performance of the modulation techniques can be evaluated by some measures, including (i) Output Signal-to-Noise Ratio (SNR_O), (ii) Channel-Signal-to-Noise Ratio (SNR_C), (iii) Signal Suppression Noise Ratio (SSN), (iv) Carrier-to-Noise Ratio (γ) and (v) Figure of Merit (F) defined as follows

$$SNR_O = \frac{\text{average power of message signal at the receiver output}}{\text{average power of noise at the receiver output}} \tag{8.1}$$

$$SNR_C = \frac{\text{average power of the modulated message signal}}{\text{average power of noise measured in the message bandwidth}} \quad (8.2)$$

$$SSN = \frac{\text{average power of message signal at the receiver output}}{\text{average power of the signal suppression noise at the receiver output}} \quad (8.3)$$

$$\gamma = \frac{\text{average carrier power}}{\text{average noise power in badwidth of the modulated signal at the receiver input}} \quad (8.4)$$

$$F = \frac{SNR_O}{SNR_C} \quad (8.5)$$

The SSN is relevant in the case where the signal is affected by multiplicative noise, when it is not possible to distinguish signal from noise. Accordingly, the noise $n_s(t)$ (named signal suppression noise) is taken as the difference between the output signal y(t) (signal affected by noise) and the mean signal $\bar{y}(t)$, i.e.,

$$n_s(t) = y(t) - \bar{y}(t) \quad (8.6)$$

and

$$SSN = \frac{< \bar{y}(t)^2 >}{< (y(t) - \bar{y}(t))^2 >} \quad (8.7)$$

where $< \circ >$ denotes the time average

In the analysis carried out in this chapter we shall use the notation $\tilde{x}$ to represent the signal x in its complex form, such that $x = Re[\tilde{x}]$.

8.3 AMPLITUDE MODULATION

In this section we shall review the basic principles of the Amplitude Modulation technique and then investigate its performance in the presence of noise, first considering only the Gaussian noise and later the Rayleigh fading.

8.3.1 Basic Principles

Amplitude Modulation is defined as a process in which the amplitude of the carrier wave is varied linearly with the message signal [1]. The standard form of the AM signal s(t) is given by

$$s(t) = A[1 + k_a m(t)]\cos(2\pi f_c t) \tag{8.8}$$

where f_c is the carrier frequency, A is the carrier amplitude and k_a is the amplitude sensitivity of the modulator.

Note that the modulated wave s(t) is a modified sinusoid having a constant frequency f_c and a time varying amplitude $A[1 + k_a m(t)]$. The modulus of this amplitude is known as the envelope of the modulated wave. The factor $|k_a m(t)|_{MAX}$ is referred to as the modulation factor or the percentage modulation, if expressed as percentage.

In the case where the modulation factor $|k_a m(t)|_{MAX}$ is less than or equal to one, the term $1 + k_a m(t)$ is always nonnegative and the envelope of the wave equals $A[1 + k_a m(t)]$. If, however, the factor $|k_a m(t)|$ exceeds the unity for any t, the envelope of the wave is $A|1 + k_a m(t)|$ and there may occur overmodulation. The two cases are depicted in Figure 8.1 for a general message signal m(t).

It is noteworthy mentioning that when $|k_a m(t)|_{MAX} \leq 1$, the envelope of the modulated wave, apart from its dc component, corresponds to the message signal m(t). If, however, overmodulation occurs ($|k_a m(t)| > 1$ for some t) this one-to-one correspondence between envelope and message does not hold any longer and the wave is said to have envelope distortion.

8.3.2 Transmission Bandwidth

Equation (8.8) is the time-domain description of the standard AM wave. In order to determine the transmission bandwidth of this modulation scheme it is convenient to find the corresponding frequency-domain description of the modulated wave. This is accomplished by simply taking the Fourier transform of both sides of equation (8.8).

Let S(f) and M(f) be the Fourier transforms of s(t) and m(t), respectively. Therefore

$$S(f) = \frac{A}{2}\left[\delta(f-f_c) + \delta(f+f_c)\right] + \frac{k_a A}{2}\left[M(f-f_c) + M(f+f_c)\right] \qquad (8.9)$$

where $\delta(\cdot)$ is the Dirac delta (impulse) function.

Consider that the message signal is band-limited to the interval $-W \le f \le W$ and that the carrier frequency f_c is greater than the bandwidth W to avoid spectral overlap (frequency distortion). For a generic message signal m(t) and an AM wave s(t) the corresponding frequency spectra are shown in Figure 8.2.

Taking only the positive portion of the spectrum for the modulated wave, it can be seen that the difference between its highest frequency component $f_c + W$ and its lowest frequency component $f_c - W$ defines the transmission bandwidth B. Therefore, for an AM wave this is exactly twice the message bandwidth, i.e.,

$$B = 2W \qquad (8.10)$$

8.3.3 Generation of AM Signals

Many and efficient ways of generating AM waves are available in the literature. We will only describe some of the basic methods (without going into too much detail) just for the sake of a global overview of the subject.

High power AM signal can be generated by means of a class C RF amplifier. The modulating signal is used to vary the supply voltage to the amplifier between zero and twice the nominal supply voltage. The modulator acts as a multiplier and a dc voltage is added to the modulating signal to provide the carrier component. Low power AM signal can be generated by means of modulators using nonlinear devices (such as diodes or transistors) conveniently biased to operate in a restricted portion of their characteristic curves. Let us describe two of such circuits.

Switching Modulator: The switching modulator can be implemented as shown in Figure 8.3. The nonlinear device can be a diode working as an ideal switch, i.e., having a zero impedance when forward biased and an infinite impedance when reverse

biased. If the message signal m(t) is such that $|m(t)| << A$ then the switching of the diode will be controlled by the carrier itself. In other words, $v_2(t)$ equals $v_1(t)$ when the carrier is positive and it equals zero when the carrier is negative. This corresponds to multiply $v_1(t)$ by a non-negative square wave having a period equal to $1/f_c$. Since such wave comprises a dc voltage plus an infinite number of odd harmonic components, it means that $v_2(t)$ will contain the AM signal plus unwanted terms. The unwanted terms can be filtered out by means of a Band Pass Filter (BPF). This is shown in the equations below.

$$v_1(t) = m(t) + A\cos(2\pi f_c t) \tag{8.11}$$

and

$$v_2(t) = v_1(t) \times \text{Square wave} \tag{8.12}$$

where

$$\text{Square wave} = a_1 + a_2\cos(2\pi f_c t) + \text{other odd harmonic components} \tag{8.13}$$

(a_1 and a_2 are constants)

Then

$$v_2(t) = a_1 A\left[1 + \frac{a_2}{a_1 A}m(t)\right]\cos(2\pi f_c t) + \text{unwanted terms} \tag{8.14}$$

and

$$s(t) = a_1 A\left[1 + k_a m(t)\right]\cos(2\pi f_c t) \tag{8.15}$$

where $k_a = a_2/a_1 A$

Square-Law Modulator: The square-law modulator can also be implemented as shown in Figure 8.3, by using a convenient non-linear device. Let the non-linear device be modelled as follows

$$v_2(t) = a_1 v_1(t) + a_2 v_1^2(t) \tag{8.16}$$

where a_1 and a_2 are constants

Then, with $v_1(t)$ given by (8.11) we have

$$v_2(t) = a_1 A\left[1 + \frac{2a_2}{a_1} m(t)\right]\cos(2\pi f_c t) + \text{unwanted terms} \qquad (8.17)$$

and

$$s(t) = a_1 A\left[1 + k_a m(t)\right]\cos(2\pi f_c t) \qquad (8.18)$$

where $k_a = 2a_2/a_1$

8.3.4 Detection of AM Signals

There are two basic ways of detecting AM signals: coherently (synchronously) and noncoherently (asynchronously). The coherent techniques use a replica of the carrier wave to reverse the modulation process. Noncoherent detection uses an extra information about the carrier, transmitted in the modulated wave.

Coherent Detection: The basic block diagram for a coherent detection is shown in Figure 8.4. Consider that s(t) is the AM wave as described by (8.8) and that the local carrier differs from the transmitter carrier by a phase ϕ. After performing the multiplication and filtering out the high frequency components it is straightforward to show that

$$v_0(t) = \frac{1}{2} A\left[1 + k_a m(t)\right]\cos\phi \qquad (8.19)$$

The dc component can be extracted by means of a capacitor and the message will be left with an attenuation constant $\cos\phi$ depending on the locally generated carrier.

Another way of performing coherent detection is by using the square-law modulator of Figure 8.3. It can be seen that if $v_1(t)$ is the AM wave as described by equation (8.8) then

$$v_2(t) = a_2 k_a A^2 m(t) + \frac{1}{2} a_2 k_a^2 m^2(t) + \text{other unwanted terms} \qquad (8.20)$$

The "other unwanted terms" in (8.20) include a dc component plus higher frequency terms $(f_c, 2f_c)$, eliminated by appropriate filters. Note, however, that $m^2(t)$ in (8.20) also contains unwanted frequency components. They can be made harmless if we choose $|k_a m(t)|$ to be conveniently small.

Noncoherent Detection: Asynchronous detection can be provided by an envelope detector as shown in Figure 8.5. The circuit is based on the fact that the signal envelope follows the same shape as that of the modulating waveform m(t). Consequently, a simple rectifier followed by a low pass filter (LPF) can be used to recover the transmitted message signal. The time constant $R_\ell C$ should be chosen so that the discharging time of the capacitor through the load can be (i) slow enough to smooth out the positive peaks of the carrier wave and (ii) fast enough to follow the maximum rate of change of the modulating wave. Therefore

$$1/f_c \ll R_\ell C \ll 1/W \tag{8.21}$$

As far as charging time is concerned, if we consider that the AM wave applied to the envelope detector is supplied by a voltage source having internal impedance R_i, then it is required that

$$R_i C \ll 1/f_c \tag{8.22}$$

8.3.5 A General Model For the Received AM Signal

Consider an AM signal transmitted from the Base Station in a mobile radio environment. Due to the multipath effect this signal is deteriorated by fading. Moreover, additive noise (such as receiver noise and others) deteriorate even more the already corrupted signal. The additive noise $n_c(t)$ is modelled as a sample function of a white noise process having mean value equal to zero and a constant power spectral density equal to $\eta/2$. The parameter η is the average noise power/bandwidth (watts/Hz) measured at the front end of the receiver. The objective of our study is to determine the effects of the fading and Gaussian noise on the received wave.

Receiver Model

In order to carry out this investigation let us assume a simplified AM receiver model as shown in Figure 8.6a. The receiver signal consists of a fading AM signal component e(t) plus the channel noise $n_c(t)$. The compound wave reaches the Radio Frequency (RF) section (not shown in the figure) of the AM receiver, where the signal is down converted to an Intermediate Frequency (IF). The converted signal then feeds the IF section where most of the amplification and selectivity are provided.

The IF filter is tuned so that its midband frequency coincides with the carrier frequency. Its bandwidth B is wide enough just to accommodate the AM signal, i.e., B = 2W. An ideal IF filter has band-pass characteristics as shown in Figure 8.6b. In our model we shall use asynchronous detection, as that provided by the envelope detector.

Received Signal

A carrier $\tilde{c}(t)$ having an amplitude A and a frequency $\omega_c = 2\pi f_c$ is expressed in its exponential form as

$$\tilde{c}(t) = A\exp(j\omega_c t) \tag{8.23}$$

The carrier $\tilde{c}(t)$ transmitted by the base station arrives at the mobile's antenna through multiple paths. Accordingly, the received signal $\tilde{c}'(t)$ is composed of a number of "carriers" having amplitudes and phases varying randomly. In section 4.5 we showed that $\tilde{c}'(t)$ is described by equation (4.18a), reproduced here for convenience

$$\tilde{c}'(t) = A\sum_{i=1}^{n} a_i \exp\left[j(\omega_c t + \omega_i t - \omega_c T_i)\right] \tag{8.24}$$

We may rewrite (8.24) as

$$\tilde{c}'(t) = \tilde{R}(t)\ A\exp(j\omega_c t) = \tilde{R}(t)\ \tilde{c}(t) \tag{8.25}$$

where

$$\tilde{R}(t) = \sum_{i=1}^{n} a_i \exp\left[j(\omega_i t - \omega_c T_i)\right] = a_r(t)\exp\left[j\phi_r(t)\right] \tag{8.26}$$

Note that the transmitted carrier $\tilde{c}(t)$ is affected by a multiplicative noise $\tilde{R}(t)$ having its amplitude $a_r(t)$ Rayleigh distributed and its phase $\phi_r(t)$ uniformly distributed in the range 0–2π rad.. Since, for voice transmission in amplitude modulation the phase is not relevant, we may neglect $\phi_r(t)$ for the moment and take the real part of $\tilde{c}'(t)$ to have

$$c(t) = R_c\left[\tilde{c}'(t)\right] = a_r(t)A\cos(2\pi f_c t) \tag{8.27}$$

Now consider that the carrier c(t) is amplitude-modulated by a message signal m(t). The resultant signal is, as we have seen previously, $A[1+k_a m(t)]\cos(2\pi f_c t)$. If we assume that the modulation bandwidth is much smaller than the coherence bandwidth, then the fading will affect all the frequency components of the signal in the same manner ("flat fading") (see section 4.5), and the resultant signal e(t) at the mobile's antenna is (refer to figure 8.6a)

$$e(t) = a_r(t)A\left[1 + k_a m(t)\right]\cos(2\pi f_c t) \tag{8.28}$$

As shown in Figure 8.6a the signal e(t) is added to the Gaussian white noise $n_c(t)$. The noise signal $n_c(t)$ becomes a narrow-band noise signal n(t) after the IF filter since the filter bandwidth is small compared to its midband frequency f_c. The band limited noise can be expressed as

$$\tilde{n}(t) = \left[n_I(t) + n_Q(t)\right]\exp(j2\pi f_c t) \tag{8.29}$$

where

$$n(t) = Re\left[\tilde{n}(t)\right]$$

$n_I(t)$ is the in-phase component

and $n_Q(t)$ is the quadrature component

Hence

$$n(t) = n_I(t)\cos(2\pi f_c t) - n_Q(t)\sin(2\pi f_c t) \tag{8.30}$$

Its power spectral density follows the shape $H_{IF}(f)$ of the IF filter and is given by $\frac{\eta}{2}H_{IF}(f)$. Accordingly, the compound signal x(t) after the IF filter is

$$\begin{aligned} x(t) &= e(t) + n(t) \\ &= \left\{a_r(t)A\left[1 + k_a m(t)\right] + n_I(t)\right\}\cos(2\pi f_c t) - n_Q(t)\sin(2\pi f_c t) \end{aligned} \tag{8.31}$$

It is convenient to represent the components of x(t) by means of phasors as in Figure 8.7. The output y(t) of the envelope detector is the envelope of x(t), easily extracted from the phasor diagram of Figure 8.7

$$y(t) = \left\{\left[a_r(t)A\left[1 + k_a m(t)\right] + n_I(t)\right]^2 + n_Q^2(t)\right\}^{1/2} \tag{8.32}$$

8.3.6 The Effect of Additive Noise on AM Systems

Consider the case where the effect of Rayleigh fading is negligible (e.g., in an open area propagation case or when some diversity technique is used). Then $a_r(t) \simeq 1$ and this constitutes the standard analysis carried out in many text books (e.g.[1]). From (8.28) we see that the average power of the modulated message signal is equal to $A^2(1 + P_m)/2$ where $P_m = k_a^2 < m^2(t) >$ is the message power. The average noise power within the message bandwidth is ηW so that

$$SNR_c = \frac{A^2(1 + P_m)}{2\eta W} \tag{8.33}$$

If the average carrier power is large compared with the average noise power, then the signal term $A\left[1 + k_a m(t)\right]$ will be large compared with the noise terms $n_I(t)$ and $n_Q(t)$. In this case the receiver operates adequately. Accordingly, we may approximate (8.32) by

$$y(t) \simeq A\left[1 + k_a m(t)\right] + n_I(t) \tag{8.34}$$

Filtering out the dc component A, the receiver output will be given by $Ak_a m(t) + n_i(t)$, where $Ak_a m(t)$ constitutes the signal itself and $n_i(t)$ is the unwanted noise. The average noise power in the message bandwidth can be obtained by multiplying the noise power spectral density (η) by the message bandwidth (2W), resulting in an average power of $2\eta W$ (see Appendix 8A). The signal power is $A^2 P_m$ where $P_m = k_a^2 < m^2(t) >$ is the message power. Therefore

$$SNR_O = \frac{A^2 P_m}{2\eta W} \tag{8.35}$$

In a like manner, the carrier-to-noise ratio is given by

$$\gamma = \frac{A^2/2}{2\eta W} \tag{8.36}$$

The figure of merit is, therefore

$$F = \frac{SNR_O}{SNR_c} = \frac{P_m}{1 + P_m} \tag{8.37a}$$

In the special case of having a sinusoidal wave of frequency W and amplitude A_m as the modulating wave, we obtain $P_m = k_a^2 A_m^2/2 \triangleq \mu^2/2$ so that

$$F = \frac{\mu^2}{2 + \mu^2} \tag{8.37b}$$

If the carrier-to-noise ratio at the receiver input is very low, the message signal becomes unintelligible and the noise term dominates. The detected envelope y(t) is mainly constituted by the narrowband noise having a Rayleigh distribution*. Therefore

$$p(y) = \frac{y}{\sigma^2} \exp\left(\frac{y^2}{2\sigma^2}\right) \tag{8.38}$$

where σ^2 is the variance of the noise n(t) being equal to $2\eta W$ in AM systems.

---

* Refer to equation (8.29) for the exponential representation of the narrowband noise and compare this with equation (3.82a) of section 3.4.2 where the Rayleigh distribution is obtained.

The probability that the envelope exceeds the carrier amplitude is

$$\text{prob}(y \geq A) = \int_{A}^{\infty} p(y)\, dy = \exp\left[-\frac{A^2}{4\eta W}\right] = \exp(-\gamma) \tag{8.39}$$

We may assume that, if this event occurs with 1% probability, i.e., prob(y ≥ A) = exp(−γ) = 0.01, then the envelope detector is expected to operate satisfactorily. For this case γ = 4.6 = 6.6 dB. If such an event occurs with a 50% probability, i.e., prob(y≥A) = exp(−γ) = 0.5, then the message at the output of detector can be assumed to be lost. For this case γ = 0.69 = −1.6 dB.

8.3.7 The Effect of Multipath on AM Systems

Now consider the case where only multiplicative noise corrupts the received signal. Using (8.32), the envelope y(t) is given by

$$y(t) = a_r(t)A\left[1 + k_a m(t)\right] \tag{8.40}$$

Just for convenience let $r \triangleq a_r(t)$, so that

$$y(t) = rA\left[1 + k_a m(t)\right] \tag{8.41}$$

Note that r is a random variable having a Rayleigh distribution given by (8.38). Since this represents a multiplicative noise, the true signal output is taken as being the average of the output. Then

$$\bar{y}(t) = A\left[1 + k_a m(t)\right] \int_{0}^{\infty} r p(r)\, dr$$

$$= A\left[1 + k_a m(t)\right]\sqrt{\pi/2}\,\sigma \tag{8.42}$$

The message signal at the envelope detector output is $Ak_a m(t)\sqrt{\pi/2}\sigma$* and the

* The dc component does not contribute to the useful signal power.

corresponding signal power is $(\pi/2)(A\sigma)^2 k_a^2 \langle m^2(t)\rangle = (\pi/2)(A\sigma)^2 P_m$. The signal suppression noise is

$$n_s(t) = y(t) - \bar{y}(t) = A(r - \sqrt{\pi/2}\,\sigma)\left[1 + k_a m(t)\right] \tag{8.43}$$

It is shown in Appendix 8B that the signal-to-signal suppression noise ratio SSN is

$$SSN = \frac{P_m}{1 + P_m} \frac{\pi/2}{(2 - \pi/2)} \tag{8.44}$$

The message power P_m is usually assumed to be at the order of 0.1 to avoid overmodulation. Therefore, the SSN is approximately 0.333, corresponding to a signal suppression noise power three times as large as the signal power. This shows that Rayleigh fading by itself has a disastrous effect on AM systems.

8.4 SINGLE-SIDEBAND MODULATION

In this section the Single-Sideband (SSB) modulation is briefly described and special attention is given to its advantages with respect to the standard AM system.

8.4.1 Basic Principles

From the standard AM studies we learned that the upper and lower sidebands are symmetrical about the carrier frequency. This implies that, given either sideband, the other sideband can be determined. Therefore, it is understood that if both the carrier and one sideband are suppressed we can recover the complete signal at the receiver end.

8.4.2 Transmission Bandwidth

One of the biggest advantages of SSB modulation over the standard AM system is that it requires half of the bandwidth of that required by the AM systems. In other

words it uses exactly the message bandwidth, i.e.,

$$B = W \tag{8.45}$$

This is accomplished by band-pass filters used to suppress either the upper sideband or the lower sideband. The filter's characteristic suppressing the upper sideband is shown in Figure 8.8a. Its corresponding low pass characteristic is depicted in Figure 8.8b.

If the message m(t) has a Fourier transform M(f), then the Fourier transform of the complex envelope of the SSB signal S(f) is

$$S(f) = H_L'(f)M(f) \tag{8.46}$$

The transfer function $H_L'(f)$ of the filter can be expressed as

$$H_L'(f) = \frac{1}{2}\Big[1 - \mathrm{sgn}(f)\Big] - u(f + W) \tag{8.47}$$

where sgn(∘) is the signum function and u(∘) is the step function. Since M(f) has its spectrum within the range $-W \le f \le W$, the product u(f + W) M(f) is nil and

$$S'(f) = \frac{1}{2}\Big[1 - \mathrm{sgn}(f)\Big]\ M(f) \tag{8.48}$$

The inverse Fourier transform of (8.48) is $\tilde{s}(t)$

$$\tilde{s}(t) = \frac{1}{2}\Big[m(t) - j\hat{m}(t)\Big] \tag{8.49}$$

where $\hat{m}(t)$ is the Hilbert transform* of m(t). The SSB signal s(t) is then

$$s(t) = \mathrm{Re}\Big[\tilde{s}(t)A\exp(j2\pi f_c t)\Big] \tag{8.50}$$

yielding

---

* A Hilbert transform of a function produces a phase shift of -90° for all positive frequencies and a phase shift of $+90^{\circ}$ for all negative frequencies. The amplitudes remain the same. For a function x(t) its Hilbert transform $\hat{x}(t)$ is

$$\hat{x}(t) = \frac{1}{\pi}\int_{-\infty}^{\infty}\frac{x(\tau)}{t-\tau}\,d\tau$$

$$s(t) = \frac{A}{2}\left[m(t)\cos(2\pi f_c t) + \hat{m}(t)\sin(2\pi f_c t)\right] \qquad (8.51)$$

It is easy to show that for lower sideband suppression, instead of the plus (+) sign we obtain a minus (−) sign in (8.51).

8.4.3 Generation of SSB Signal

There are basically two methods of implementing SSB modulation, namely Filter Method and Outphasing Method.

Filter Method: This method uses a mixer (multiplier) to generate a double sideband suppressed carrier (as in Figure 8.2a without the carrier) and a filter to further suppress one of the sidebands. The difficulty in this case is to implement filters with very sharp cut-off characteristics. This becomes more critical with the increasing frequency.

Phase Discrimination Method: The modulator using this method is known as Hartley modulator. It implements the functions as expressed in (8.51). The difficulty in this case is to design a phase shifter able to maintain the 90° phase-shift over the full bandwidth of the baseband signal. This can be achieved by using two stages of quadrature modulation [4].

8.4.4 Detection of SSB signal

The baseband signal $m(t)$ can be recovered by means of coherent detection as mentioned before (refer to Figure 8.4). If the locally generated carrier has a phase shift of ϕ, the detected wave $v_0(t)$ is

$$v_0(t) = \frac{1}{4}Am(t)\cos\phi - \frac{1}{4}A\hat{m}(t)\sin\phi \qquad (8.52)$$

Note that if the phase error is nil, the received signal contains the full message (scaled by an amplitude factor). For any $\phi \neq 0$, the recovered message suffers from phase distortion, having negligible effects as far as speech is concerned, but disastrous ones on data communication.

8.4.5 A General Model For the Received SSB Signal

Following the same reasoning as for the AM case, the resultant signal e(t) at the mobile's antenna, after the multipath propagation, is

$$e(t) = a_r(t)\frac{A}{2}\left[m(t)\cos(2\pi f_c t) - \hat{m}(t)\sin(2\pi f_c t)\right] \tag{8.53}$$

where $a_r(t)$ is Rayleigh distributed.

The narrow-band noise n(t) has its midband frequency differing from the carrier frequency by $W/2$ and can be expressed as

$$n(t) = n_I(t)\cos\left[2\pi(f_c - W/2)t\right] - n_Q(t)\sin\left[2\pi(f_c - W/2)t\right] \tag{8.54}$$

The compound signal after the IF filter is $x(t) = e(t) + n(t)$. The coherent detection carries out the operations $x(t)\cos(2\pi f_c t)$ in connection with low pass filtering, so that

$$y(t) = a_r(t)\frac{A}{4}m(t) + \frac{1}{2}n_I(t)\cos(\pi W t) + \frac{1}{2}n_Q(t)\sin(\pi W t) \tag{8.55}$$

provided that no phase error is encountered in the carrier.

8.4.6 The Effect of Additive Noise on SSB Systems

If the fading is negligible, then $a_r(t) \simeq 1$. From (8.53) we observe that the in-phase and quadrature components of the SSB wave contribute with an average power of $A^2P_m/8$ each, constituting a total of $A^2P_m/4$. The average noise power is ηW. Thus

$$SNR_c = \frac{A^2 P_m}{4\eta W} \tag{8.56}$$

The carrier-to-noise ratio is

$$\gamma = \frac{A^2/2}{\eta W} \tag{8.57}$$

and the figure of merit is given by

$$F = \frac{SNR_O}{SNR_c} = 1 \tag{8.58}$$

From (8.55) we note that the average power of the recovered message, Am(t)/4, is $A^2P_m/16$. The noise component is $\left[n_I(t)\cos(\pi Wt) + n_Q(t)\sin(\pi Wt)\right]/2$. The in-phase noise component has a power spectral density equal to η in the message bandwidth W. Therefore, the corresponding average power is ηW. In the case of the modulated noise $n_I(t)\cos(\pi Wt)$ the average power is $\eta W/2$, the same applying to $n_Q(t)\sin(\pi Wt)$. Accordingly, the total power of the noise component is $(1/4)(2\eta W/2) = \eta W/4$. And the signal-to-noise ratio is

$$SNR_0 = \frac{A^2 P_m}{4\eta W} \tag{8.59}$$

8.4.7 The Effect of Multipath on SSB Systems

In the case where only multiplicative noise affects the received signal, the output of the receiver is (from (8.55))

$$y(t) = a_r(t)\frac{A}{4}m(t) \tag{8.60}$$

As in the AM case, we rewrite (8.60) as

$$y(t) = r\frac{A}{4}m(t) \tag{8.61}$$

Thus, following the same steps as before we find that the mean signal $\bar{y}(t)$ is

$$\bar{y}(t) = \frac{A}{4}m(t)\sqrt{\pi/2}\,\sigma \tag{8.62}$$

The signal suppression noise is

$$y(t) - \bar{y}(t) = \frac{A}{4}\left(r - \sqrt{\pi/2}\,\sigma\right)m(t) \tag{8.63}$$

And the signal-to-signal suppression noise ratio SSN is

$$SSN = \frac{\pi/2}{2-\pi/2} \approx 3.66 \qquad (8.64)$$

If we compare this result with that given by the standard AM case we can see that there is an improvement of 10.4 dB. The same improvement can be achieved for the case of the standard AM if an appropriate high-pass filter is used after the detector, as we explain next.

The effect of multipath propagation is to broaden each spectral line of the signal until it occupies a spectral width of $2f_m = 2v/\lambda$, where f_m is the maximum Doppler shift, v is the vehicle's speed and λ is the wavelength (refer to section 4.9). In (8.43) we see that there is a component of noise r due to the carrier fading. This can be suppressed by a high-pass filter if the spectrum of r lies below the lowest baseband frequency usually considered to be 150 Hz. In other words, we must have $f_m \leq 150$ Hz. Therefore, by filtering out the noise component due to the carrier fading the improvement achieved is quite substantial as calculated above. The modulation of the sidebands, however, cannot be removed by filtering, and remains as motion induced noise.

8.4.8 Enhanced SSB Modulation Techniques

As far as spectrum efficiency is concerned, single sideband modulation is indeed attractive. However, its performance in the presence of fading, when compared with FM, is very poor, perhaps disastrous. Accordingly, many efforts have been made towards enhancing the SSB performance for mobile radio purposes, and a number of techniques has emerged. These techniques individually or combined seem to yield very good (or at least promising) results.

McGeeham and Bateman [8,9] have proposed a scheme in which a gap within the speech band is created and a pilot tone is inserted in it prior to transmission. This technique named "Transparent Tone In Band" (TTIB) has proved to be very effective, mainly if combined with a strategy termed "Feed Forward Signal Regeneration" (FFSR). The basic principle of TTIB plus FFSR is that, at the receiver end the pilot tone is

extracted and used for three purposes:

(i) to obtain a frequency reference for demodulation;

(ii) to obtain a signal reference for the Automatic Gain Control (AGC) circuit;

(iii) to help in re-establishing the phase and amplitude of the transmitted signal, this constituting a powerful tool to combat the effects of Rayleigh (fast) fading. The basic idea of this is that the receiver, having the pilot tone as reference, corrects the phase and amplitude characteristics of the received sidebands so as to maintain constant the phase and amplitude of the pilot tone.

It is important to mention that this scheme will work well if there is high correlation between the pilot tone and the message frequencies. The envelope correlation producing an output signal-to-signal suppression noise ratio of 20 dB is 0.9998 (page 206 of ref. [2]) . The correlation factor between two signals arriving at the same time instant is given by (4.46) with $\tau = 0$ (time delay nil) and is written as

$$\rho_r = \frac{1}{1 + (\Delta\omega\overline{T})^2} \tag{8.65}$$

where $\Delta\omega$ is the frequency separation (rd/s) between the signals, and $\overline{T}$ is the delay spread. Let $\overline{T} = 1$ μs (in an urban area $\overline{T} \simeq 3\mu s$, in a suburban area $\overline{T} \simeq 0.5\mu s$). Therefore, the required frequency separation Δf must be no greater than 2.25 kHz, which for a 3kHz voice channel impels the pilot tone to be placed within the voice frequency band, preferably in the middle of the band.

Another enhanced SSB technique is the "Amplitude-Companded Single Sideband (ACSSB) using a process of (i) COMPressing the signal prior to modulation and transmission and (ii) expANDING the compressed signal to restore its dynamic range at the reception. This companding technique seems to strengthen the SSB against the effects of multipath.

8.5 FREQUENCY MODULATION

Frequency modulation is well known for its outstanding performance as far as

audio output signal-to-noise ratio is concerned. The analysis of the FM communication scheme is considerably more complicated than that of the amplitude modulation techniques but can be simplified if some approximations are carried out. In this section we shall review some of the FM fundamentals in connection with some detailed analysis based on the work by Rice [5,6].

8.5.1 Basic Principles

Frequency modulation is a nonlinear process in which the frequency of the carrier is varied according to the message signal. Let $\theta(t)$ be the angular argument of a carrier $\tilde{s}(t)$ such that, expressed in its exponential form*

$$\tilde{s}(t) = A\exp\left[j\theta(t)\right] \tag{8.66}$$

Define the instantaneous frequency $f_i(t)$ as

$$f_i(t) = \frac{1}{2\pi}\frac{d\theta(t)}{dt} \tag{8.67}$$

In frequency modulation it is assumed that the instantaneous frequency is centred at f_c but varies linearly with the message signal $m(t)$, i.e.,

$$f_i(t) = f_c + k_f m(t) \tag{8.68}$$

where k_f is the frequency sensitivity. Integrating (8.68) and multiplying by 2π we obtain the angular argument $\theta(t)$. Then using $\theta(t)$ in (8.66) we obtain the modulated wave $\tilde{s}(t)$

$$\tilde{s}(t) = A\exp\left[j(2\pi f_c t + \phi_s(t))\right] \tag{8.69}$$

where

$$\phi_s(t) = 2\pi k_f \int_0^t m(t)dt + \phi_s(0) \tag{8.70}$$

---

* In FM we shall use the exponential representation of the sine wave due to its convenience. We note, however, that $\mathrm{Re}[\tilde{s}(t)]$ is what really matters.

In our analysis we shall assume $\phi_s(0) = 0$. Note from (8.69) that the envelope o the FM wave is constant. Moreover, its average power is independent of the message an is given by $A^2/2$.

Single-Tone FM

Let the message signal m(t) be a sinusoidal wave given by

$$m(t) = A_m \cos(2\pi Wt) \tag{8.71}$$

In this case the FM wave is given by

$$\tilde{s}(t) = A\exp\left[j\left(2\pi f_c t + \beta\sin(2\pi Wt)\right)\right] \tag{8.72}$$

where $\beta \triangleq k_f A_m/W \triangleq \Delta f/W$ is the modulation index and Δf is the frequency deviation.

The complex envelope $A\exp\left[j\beta\sin(2\pi Wt)\right]$ in (8.72) is a periodic function having a fundamental frequency equal to W. Therefore, it can be expanded in the form of a complex Fourier series as

$$A\exp\left[j\beta\sin(2\pi Wt)\right] = A\sum_{n=-\infty}^{\infty} J_n(\beta)\exp(j2\pi nWt) \tag{8.73}$$

where the complex Fourier coefficients $J_n(\beta)$ are given by

$$J_n(\beta) = \frac{1}{2\pi}\int_{-\pi}^{\pi}\exp\left[j(\beta\sin x - nx)\right]dx \tag{8.74}$$

and $x = 2\pi Wt$

The coefficients $J_n(\beta)$ are known as the n^{th} order Bessel function of the first kind. Hence the FM wave in (8.72) can be written in terms of the Bessel function as

$$\tilde{s}(t) = A\sum_{n=-\infty}^{\infty} J_n(\beta)\exp\left[j2\pi(f_c + nW)t\right] \tag{8.75}$$

8.5.2 Transmission Bandwidth

Referring to (8.75) we understand that the FM wave contains 2n side frequencies

centred at f_c. In other words the transmission bandwidth is B = 2nW. Since n varie from $-\infty$ to $+\infty$ the theoretical required bandwidth is infinite. However, i practice, it is possible to specify an effective bandwidth within which the distortic is considered to be under tolerable limits.

Consider, initially, the case of the single-tone modulation. If we examine th tables of the Bessel function, it can be seen that $J_n(\beta)$ diminishes very rapidly fo $n > \beta$ and more specifically for large β. In fact, for large β the ratio n/β tends t unity. In this case, since $n = \beta$ and $B = 2nW$, we have $B = 2\beta W = 2\Delta f$. For small β, onl $J_0(\beta)$ and $J_1(\beta)$ are relevant. Therefore $B = 2W$. With these two limiting case J.R. Carson [10] suggested that an approximate rule for transmission bandwidth of a FM wave generated by a single-tone modulating wave is

$$B = 2\Delta f + 2W = 2W(1 + \beta) \tag{8.76}$$

This is known as Carson's rule. In practice, this rule is applied even for non-sinusoidal modulation where W is assumed to be the highest frequency in th modulating waveform.

Narrowband FM (NBFM)

Narrowband FM is of great interest in mobile radio communications where spectrum efficiency is critical. It is commonly used when the channel spacing is fairly smal (12.5 kHz or 25 kHz). This is achieved when the modulation index is small ($\beta << 1$). In this case $J_0(\beta) \approx 1$, $J_1(\beta) \approx \beta/2$ and $J_n(\beta) \approx 0$ for $n > 1$. With these values we obtain from (8.75) the expression for the single tone NBFM.

$$s(t) = \mathrm{Re}\left[\tilde{s}(t)\right]$$

$$= A\cos(2\pi f_c(t) + \frac{\beta A}{2}\cos\left[2\pi(f_c + W)t\right] - \frac{\beta A}{2}\cos\left[2\pi(f_c + W)t\right] \tag{8.77}$$

For a general case of modulating wave m(t), when β is very small then $\phi_s(t)$ is also very small and we may approximate $\cos\left[\phi_s(t)\right] \approx 1$ and $\sin\left[\phi_s(t)\right] \approx \phi_s(t)$. Therefore, from (8.69) the NBFM equals

$$s(t) = Re\left[\tilde{s}(t)\right] \simeq A\cos(2\pi f_c t) - \phi_n(t)A\sin(2\pi f_c t) \qquad (8.78)$$

which closely resembles an AM wave. In this case, however, the side bands are symmetrically placed about a line at 90° to the carrier and this generates a signal with a varying frequency and a quasi-constant amplitude. In other words, the NBFM contains a residual amplitude modulation. The bandwidth is B = 2W as we determined previously.

Wideband FM (WBFM)

This is the case where $\beta >> 1$. The FM wave contains an "infinite" number of side-frequency components symmetrically placed around the carrier.

8.5.3 Generation of FM Signals

Two basic methods are available to generate FM waves: Indirect FM and Direct FM as described below.

Indirect FM: In this method, first a narrow-band FM wave is generated and then, by means of frequency multiplication the increased frequency deviation is obtained, producing a wideband FM. A multiplier consists of a non-linear device having an input-output relation given in a polynomial form. Let this relation be given by (8.79)

$$u = a_1 v + a_2 v^2 + \ldots + a_n v^n \qquad (8.79)$$

where a_1, a_2, ..., a_n are constants, u is the output and v is the input. Suppose that v is a NBFM wave (equation (8.78)) with frequency deviation Δf. The signal u (equation (8.79)), therefore, contains a dc component plus n frequency-modulated waves at f_c, $2f_c$, ..., nf_c with frequency deviation Δf, $2\Delta f$, ...,$n\Delta f$, respectively. A bandpass filter can be used to select the appropriate WBFM. Figure 8.9 depicts a block diagram of an indirect FM modulator.

Instead of frequency multipliers, this function can be accomplished by phase-locked-loops which are now readily available in integrated-circuit form.

Direct FM: This can be accomplished by means of LC circuits where the capacitance

is provided by a fixed capacitor shunted by a voltage-variable capacitor (varactor or varicap). The varicaps are diodes which, when reverse biased, present a capacitance varying linearly with the voltage. As an example of this type of modulator we present the Hartley oscillator shown in Figure 8.10.

If the capacitance is such that $C = C_0 - km(t)$, then

$$f_i(t) = \frac{1}{2\pi\sqrt{(L_1 + L_2)C}} = f_i(t) = f_0\left[1 - \frac{k}{C_0}\, m(t)\right]^{-1/2} \simeq f_0 + k_f m(t) \qquad (8.80)$$

where

$$f_0 = \frac{1}{2\pi\sqrt{C_0(L_1 + L_2)}} \qquad \text{and} \qquad k_f = f_0 k/2C_0$$

for $km(t)/C_0 << 1$

Equation (8.80) shows that the instantaneous frequency of the oscillator varies linearly with the message signal. Direct FM at microwave frequencies can be generated by Gunn semiconductor diodes typically operating at 10 GHz. It is able to provide deviation of about 30 MHz/V [4]

8.5.4 Detection of FM Signals

There are many ways of recovering the modulating signal from an FM wave. The basic idea of the FM demodulators is the frequency-to-voltage conversion. Let us describe some of the more popular techniques.

Balanced Frequency Discriminator: Let an FM wave $\tilde{s}(t)$, as expressed by (8.69), be the input of a differentiator having a gain a. Its output $v_1(t)$ is therefore

$$v_1(t) = \mathrm{Re}\left[a\frac{d\tilde{s}(t)}{dt}\right] = 2\pi a A f_c\left[1 + \frac{k_f}{f_c}\, m(t)\right]\cos\left[2\pi f_c t + \phi_s(t) + \pi/2\right] \qquad (8.81)$$

Provided that $|k_f m(t)/f_c| < 1$, an envelope detector may be used to recover the amplitude variations of this signal. The output of the detector is $|v_1(t)| = 2\pi a A f_c\left[1 + k_f m(t)/f_c\right]$. Note that the envelope of the wave contains the

message m(t) plus a dc component. The bias term (dc component) can be removed by means of a capacitor. Another way of removing this dc component is to use a symmetrical configuration of the envelope detector combined with the differentiator. If this symmetrical configuration is such that its output $|v_2(t)|$ equals $2\pi aAf_c\left[1 - k_f m(t)/f_c\right]$ then the baseband output $v_0(t)$ can be obtained by performing $v_0(t) = |v_1(t)| - |v_2(t)|$. A close realization of such a scheme is shown in Figure 8.11 where the upper and lower resonant filters are tuned to frequencies above and below the unmodulated carrier frequency f_c respectively.

Instantaneous Frequency Detector: Consider a time interval T such that $f_c^{-1} << T << W^{-1}$. Hence within T (i) the message signal may be assumed as essentially constant and (ii) a considerable number of zero crossings of the FM wave occurs. If the number of zero crossings of the FM wave is counted within T, then, effectively an estimate of the instantaneous frequency of the wave is obtained. That is, let n_0 be the number of zero crossings within T. The instantaneous frequency f_i is therefore approximately $n_0/2T$. Since the instantaneous frequency is proportional to the message signal (see equation (8.68)) we conclude that m(t) can be recovered from a knowledge of f_i. A block diagram of this kind of demodulator is shown in Figure 8.12. The output of the limiter is a square wave version of its FM wave. These pulses are shaped (shortened up) by the pulse generator and averaged over T by the low pass filter (integrator) to produce m(t).

Phase-Locked Loop: A block diagram of a Phase-Locked Loop (PLL) is depicted in Figure 8.13. The voltage-controlled oscillator (VCO) is a circuit producing sine wave whose frequency is varied according to its input voltage. In fact, the VCO is a frequency modulator (FM) with central frequency equal to the unmodulated carrier. Its output has a phase-shift of 90^0 with respect to the unmodulated carrier when its input voltage is nil.

Let us analyze the PLL functioning. Refer to Figure 8.13. Consider that the FM signal $s_1(t)$ at the PLL input is

$$s_1(t) = A_1 \cos\left[2\pi f_c t + \phi_1(t)\right] \tag{8.22}$$

where

$$\phi_1(t) = 2\pi k_1 \int_0^t m(t)\, dt \tag{8.83}$$

Suppose that the VCO output $s_2(t)$ (output of an FM modulator) is expressed as

$$s_2(t) = A_2 \cos\left[2\pi f_c t + \phi_2(t)\right] \tag{8.84}$$

where

$$\phi_2(t) = 2\pi k_2 \int_0^t v_c(t)\, dt \tag{8.85}$$

The product wave $e(t) = s_1(t) \times s_2(t)$ would contain a high-frequency component $k_m A_1 A_2 \sin\left[4\pi f_c t + \phi_1(t) + \phi_2(t)\right]$ (eliminated by the filter and the VCO) and a low-frequency component $k_m A_1 A_2 \sin\left[\phi_1(t) - \phi_2(t)\right]$, where k_m is the multiplier gain. If the phase error $\phi_1(t) - \phi_2(t)$ is zero, the PLL is said to be in phase-lock. When this error is very small we may approximate the sine function by its argument, i.e.,

$$e(t) = k_m A_1 A_2 \sin\left[\phi_1(t) - \phi_2(t)\right] \approx k_m A_1 A_2 \left[\phi_1(t) - \phi_2(t)\right] \tag{8.86}$$

Differentiating both sides of (8.86) we obtain

$$\frac{de(t)}{dt} \approx k_m A_1 A_2 \left[\frac{d\phi_1(t)}{dt} - 2\pi k_2\, v_0(t)\right] \tag{8.87}$$

Let $V_0(f)$, $E(f)$ and $\Phi_1(f)$ be the frequency domain representation of $v_0(t)$, $e(t)$ and $\phi_1(t)$, respectively. Taking the Fourier transform of (8.87) and using the relation $V_0(f) = H(f)E(f)$ we have

$$V_0(f) = -\frac{(jf/k_2)}{1 + 1/L(f)}\, \Phi_1(f) \tag{8.88}$$

where

$$L(f) = k_m k_2 A_1 A_2 \frac{H(f)}{jf} \tag{8.89}$$

is known as the open-loop transfer function of the PLL. When L(f) >> 1 we obtain $V_0(f) \propto (jf/k_2)\Phi_1(f)$. Its time-domain representation (inverse Fourier transform) is

$$v_0(t) \propto \frac{1}{2\pi k_2} \frac{d\Phi_1(t)}{dt} = \frac{k_1}{k_2} m(t) \tag{8.90}$$

In other words, the output $v_0(t)$ of the PLL is proportional to the original message signal m(t).

8.5.5 A General Model For the Received FM Signal

Assume an FM receiver model as shown in Figure 8.14. The received FM signal e(t) has a carrier frequency f_c and a bandwidth B such that its frequency band lies in the range $f_c - B/2 \leq |f| f_c + B/2$. It is considered that only a negligible amount of power is encountered outside this band. The IF filter operates with a midband frequency f_c and bandwidth B. An ideal IF filter has a bandpass characteristic as shown in Figure 8.6b. In practice, however, the filter may present a "bell shape" characteristic as depicted in Figure 8.15. Consider that this "bell-shaped filter" can be approximated by a Gaussian shape such that

$$H_{IF}(f) = \exp\left[-\pi(f - f_c)^2/B^2\right] + \exp\left[-\pi(f + f_c)^2/B^2\right] \tag{8.91}$$

Since the noise spectral density $S_n(f)$ follows the shape of the IF filter, we have

$$S_n(f) = \frac{\eta}{2} H_{IF}(f) \tag{8.92}$$

Following the same steps as those for the AM and SSB cases (refer to sections 8.3.5 and 8.4.5) it is straightforward to determine the compound signal x(t) at the FM detector's input. It is appropriate, in the FM case, to represent the narrow-band additive noise in its exponential form $\left[n_I(t) + jn_Q(t)\right]\exp(j2\pi f_c t)$. Accordingly,

$$x(t) = e(t) + n(t)$$

$$= \left\{a_r(t)A\exp\left[j(\phi_s(t) + \phi_r(t))\right] + n_I(t) + jn_Q(t)\right\}\exp(j2\pi f_c t) \tag{8.93}$$

where $\phi_s(t)$, given by (8.70), is the phase due to the message itself and $\phi_r(t)$ is the random phase due to the multipath effect. Using the phasor representation as depicted in Figure 8.16 we obtain

$$x(t) = y(t)\exp\left[j\phi_y(t)\right]\exp(j2\pi f_c t) \tag{8.94}$$

where

$$y^2(t) = \left\{a_r(t)A\cos\left[\phi_s(t) + \phi_r(t)\right] + n_I(t)\right\}^2$$

$$+ \left\{a_r(t)A\sin\left[\phi_s(t) + \phi_r(t)\right] + n_Q(t)\right\}^2 \tag{8.95}$$

and

$$\phi_y(t) = \phi_s(t) + \phi_r(t) + \phi_n(t) \tag{8.96}$$

8.5.6 Effect of Additive Noise on FM Systems

In a non-Rayleigh environment the multipath propagation effect is irrelevant so that the multiplicative noise can be neglected, i.e., $a_r(t) = 1$ and $\phi_r(t) = 0$. The FM signal power is $A^2/2$ and the noise power is given by the integral of the noise power spectral density. Therefore, using (8.91) in (8.92) the IF signal-to-noise ratio, γ, of x(t) is

$$\gamma = \frac{A^2/2}{\int_{-\infty}^{\infty} S_n(f)\,df} = \frac{A^2}{2\eta B} \tag{8.97}$$

The channel signal-to-noise ratio is easily obtained as

$$SNR_c = \frac{A^2}{2\eta W} \tag{8.98}$$

Output Signal Power

Equating (8.93) and (8.94) for the non-Rayleigh case we obtain

$$y(t)\exp\left[j\phi_y(t)\right] = A\exp\left[j\phi_s(t)\right] + n_I(t) + jn_Q(t) \tag{8.99}$$

As studied before, the output of the FM detector is proportional to the derivative of the IF output signal's phase $\phi_y(t)$. Hence, by first taking the natural logarithm of (8.99) and then differentiating both sides with respect to time, we obtain

$$\frac{\dot{y}(t)}{y(t)} + j\dot{\phi}_y(t) = \frac{j\dot{\phi}_s(t)A\exp\left[j\phi_s(t)\right] + \dot{n}_I(t) + j\dot{n}_Q(t)}{A\exp\left[j\phi_s(t)\right] + n_I(t) + n_Q(t)}$$

$$\triangleq f(\phi,\dot{\phi},n_I,\dot{n}_I,n_Q,\dot{n}_Q) \tag{8.100}$$

Since $\dot{\phi}_y(t)$ involves random variables, the mean signal output $v_0(t)$ must be estimated by the expectation (mean value) of the random variable $\dot{\phi}_y(t)$, i.e., $v_0(t) = E\left[\dot{\phi}_y(t)\right]$. The four random variables, namely $n_I(t)$, $n_Q(t)$, $\dot{n}_I(t)$, $\dot{n}_Q(t)$ are independent and Gaussian distributed. Rice [5] has shown that

$$E\left[\frac{\dot{y}(t)}{y(t)} + j\dot{\phi}_y(t)\right] = \int_{-\infty}^{\infty}\int_{-\infty}^{\infty}\int_{-\infty}^{\infty}\int_{-\infty}^{\infty} f(\phi,\dot{\phi},n_I,\dot{n}_I,n_Q,\dot{n}_Q)p(n_I,\dot{n}_I,n_Q,\dot{n}_Q)dn_I d\dot{n}_I dn_Q d\dot{n}_Q$$

$$= j\dot{\phi}(t)\left[1 - \exp(-\gamma)\right] \tag{8.101}$$

Given that $\dot{y}(t)/y(t)$ and $\dot{\phi}_y(t)$ are independent random variables,

$$E\left[\dot{y}(t)/y(t) + j\dot{\phi}_y(t)\right] = E\left[\dot{y}(t)/y(t)\right] + j\,E\left[\dot{\phi}_y(t)\right] \tag{8.102}$$

Comparing this expression with that of (8.101) we notice that $E\left[\dot{y}(t)/y(t)\right] = 0$ and

$$E\left[\dot{\phi}_y(t)\right] = \dot{\phi}_s(t)\left[1 - \exp(-\gamma)\right] \tag{8.103}$$

Note that $\dot{\phi}_s(t)$ is proportional to the message $m(t)$.

Assuming a proportionality constant equal to one, the output $v_0(t)$ of th demodulator is the message m(t) attenuated by a factor $\left[1 - \exp(-\gamma)\right]$ due to th presence of noise. That is

$$v_0(t) = E\left[\dot{\phi}_y(t)\right] = m(t)\left[1 - \exp(-\gamma)\right] \tag{8.104}$$

The output baseband signal S_0 is

$$S_0 = E\left[v_0^2(t)\right] = \left[1 - \exp(-\gamma)\right]^2 E\left[\dot{\phi}^2(t)\right]$$

$$= \left[1 - \exp(-\gamma)\right]^2 P_m \tag{8.105}$$

where P_m is the input modulation signal power. For a single-tone modulation it i shown in Appendix 8C that

$$P_m = \alpha(2\pi\Delta f)^2 \tag{8.106}$$

where α is a constant. With the use of (8.76) in (8.106) we obtain

$$P_m = \alpha\pi^2(B - 2W)^2 \tag{8.107}$$

Using (8.107) in (8.105) we obtain

$$S_0 = \alpha\pi^2(B - 2W)^2\left[1 - \exp(-\gamma)\right]^2 \tag{8.108}$$

The normalized baseband signal $10\log(S_0/W^2)$ is plotted versus the IF SNR, γ, for different values of the baseband bandwidth ratios B/2W in Figure 8.17. In these plots we have assumed P_m = 10 dB below $(2\pi\Delta f)^2$, i.e., α = 0.1. This probably prevents the signal deviation peaks from exceeding the IF bandwidth.

Output Noise Power

The output noise is given by $\dot{\phi}_n(t)$. The noise spectral density $S_{\dot{\phi}_n}(f)$ is the Fourier transform of its autocorrelation function $R_{\dot{\phi}_n}(\tau)$, i.e.,

$$S_{\dot{\phi}_n}(f) = \int_{-\infty}^{\infty} R_{\dot{\phi}_n}(\tau)\exp(j2\pi f\tau)d\tau \tag{8.109}$$

with the autocorrelation function expressed as (refer to Appendix 9A)

$$R_{\dot{\phi}_n}(\tau) = E\left[\dot{\phi}_n(t)\,\dot{\phi}_n(t+\tau)\right] \tag{8.110}$$

Rice [5] has shown that, the baseband noise with modulation closely approximates that without modulation. Therefore, from Figure 8.16 with $\phi_s(t) = 0$ (note that $\phi_r(t) = 0$ and $a_r(t) = 1$ since no Rayleigh fading is being considered)

$$\phi_n(t) = \tan^{-1}\frac{n_Q(t)}{A + n_I(t)} \tag{8.111}$$

Differentiating both sides of (8.111)

$$\dot{\phi}_n(t) = \frac{\left[A + n_I(t)\right]\dot{n}_Q(t) - n_Q(t)\dot{n}_I(t)}{\sec^2\phi_n(t)\left[A + n_I(t)\right]^2} = \frac{\left[A + n_I(t)\right]\dot{n}_Q(t) - n_Q(t)\dot{n}_I(t)}{\left[A + n_I(t)\right]^2 + n_Q^2(t)} \tag{8.112}$$

With (8.112) in (8.110) the autocorrelation function can be evaluated, provided that the corresponding probability density function is known. Since there are four random variables involved, namely $n_I(t)$, $n_Q(t)$, $\dot{n}_I(t)$ and $\dot{n}_Q(t)$ the autocorrelation turns out to be an eight-fold integral which requires the evaluation of the joint distribution of these variables in t and in $t + \tau$. This is obviously extremely difficult to carry out, but an approximation can be used. Rice [5] divided the noise spectrum $S_n(f)$ into three parts, such that

$$S_n(f) = S_1(f) + S_2(f) + S_3(f) \tag{8.113}$$

$S_1(f)$ equals the output noise spectrum when the carrier is very large; $S_2(f)$ equals the output noise spectrum when the carrier is absent; $S_3(f)$ is a correction factor vanishing for both a very small and a very large carrier. It predominates in the threshold region of γ.

Accordingly, $S_1(f)$ relates to $S_{\dot{\phi}_n}(f)$ in the same way as the output baseband signal power S_0 relates to $S_{\dot{\phi}_s}(f)$ (equation (8.105))

$$S_1(f) = \left[1 - \exp(-\gamma)\right]^2 S_{\dot{\phi}_n}(f) \tag{8.114}$$

Since differentiation in the time domain is equivalent to multiplication by $j2\pi f$ in the frequency domain, then the following relation holds

$$S_{\dot{\phi}_n}(f) = (2\pi f)^2 S_{\phi_n}(f) \tag{8.115}$$

But, from (8.111), if the carrier is very large

$$\phi_n(t) \simeq \frac{n_Q(t)}{A} \tag{8.116}$$

and

$$\dot{\phi}_n(t) \simeq \frac{\dot{n}_Q(t)}{A} \tag{8.117}$$

Therefore, from (8.115)

$$S_{\dot{\phi}_n}(f) = \left(\frac{2\pi f}{A}\right)^2 S_{n_Q}(f) \tag{8.118}$$

It is shown in Appendix 8A that the spectrum of the in-phase component $n_I(t)$ and the quadrature component $n_Q(t)$ of a narrowband process $n(t)$ is

$$S_{n_I}(f) = S_{n_Q}(f) = S_n(f - f_c) + S_n(f + f_c) \tag{8.119}$$

Hence, using (8.91), (8.92), (8.97), (8.119), (8.118) and (8.114) we obtain

$$S_1(f) = \frac{\left\{2\pi f\left[1 - \exp(-\gamma)\right]\right\}^2 \exp(-\pi f^2/B^2)}{2B\gamma} \tag{8.120}$$

As far as $S_2(f)$ and $S_3(f)$ are concerned, Rice [5] has shown that their sum equals $2\pi B\sqrt{2\pi}(1 - \mathrm{erf}\sqrt{\gamma})$ for each side of the spectrum. Davis [7] has found an empirical approximation given by

$$S_2(f) + S_3(f) \simeq \frac{4\pi B \exp(-\gamma)}{\sqrt{2(\gamma + 2.35)}} \tag{8.121}$$

The total output noise power N_{GA} of the baseband filter due to a Gaussian noise is

$$N_{GA} = \int_{-W}^{W} \left[S_1(f) + S_2(f) + S_3(f) \right] df$$

$$= \frac{a\left[1 - \exp(-\gamma)\right]^2}{\gamma} + \frac{8\pi BW \exp(-\gamma)}{\sqrt{2(\gamma + 2.35)}} \qquad (8.122)$$

where

$$a \triangleq \frac{(2\pi)^2}{2B} \int_{-W}^{W} f^2 \exp(-\pi f^2/B^2) df \qquad (8.123)$$

Using the MacLaurin expansion

$$a = \frac{(2\pi)^2}{2B} \int_{-W}^{W} f^2 \sum_{i=0}^{\infty} \frac{(-\pi f^2/B^2)^i}{i!} df$$

$$= \frac{4\pi W^3}{3B} \left\{ 1 - \frac{6\pi}{10}\left(\frac{W}{B}\right)^2 + \frac{12\pi^2}{56}\left(\frac{W}{B}\right)^4 + \ldots \right\} \qquad (8.124)$$

The normalized baseband noise power $10\log(N_{GA}/W^2)$ is plotted versus γ in Figure 8.17. The SNR_o is therefore

$$SNR_o = \frac{S_o}{N_{GA}} = \frac{\alpha\pi^2 (B - 2W)^2 \left[1 - \exp(-\gamma)\right]^2}{\frac{a\left[1 - \exp(-\gamma)\right]^2}{\gamma} + \frac{8\pi BW \exp(-\gamma)}{\sqrt{2(\gamma + 2.35)}}} \qquad (8.125)$$

which is plotted in Figure 8.17.

If $\gamma >> 1$, then, from (8.105) and (8.122) respectively,

$$S_o \simeq P_m \qquad (8.126)$$

and

$$N_{GA} \simeq \frac{a}{\gamma} \simeq \frac{4\pi W^3}{3B\gamma} = \frac{2}{3}\left(\frac{2\pi}{A}\right)^2 \eta W^3 \qquad (8.127)$$

With $P_m = \alpha(2\pi\Delta f)^2$ the SNR_o becomes

$$SNR_o = S_o/N_{GA} \propto 3\alpha\beta^2(B/W)\gamma \tag{8.128}$$

where $\beta = \Delta f/W$. This shows that SNR_o and bandwidth are interchangeable in FM systems. The figure of merit in this case is

$$F = \frac{SNR_o}{SNR_c} = 3\alpha\beta^2 \tag{8.129}$$

Note from Figure 8.17 that the threshold and capture effects are quite evident: when γ is large the FM receiver captures on the signal and suppresses the noise. When γ is small the opposite effect occurs.

8.5.7 The Effect of Multipath on FM Systems

The capture effect of the FM receivers, so prominent in a non-fading environment, tends to vanish in multipath conditions due to the rapid fading. When the signal fades in such a way that the receiver looses capture, the baseband output signal is suppressed. The rapid random suppression of the signal constitutes a noise component, known as signal suppression noise. Additionally, the deep fades are accompanied by rapid phase changes producing another noise component: the random FM noise (refer to section 4.8). The total baseband output noise N_o is, therefore, composed of the following elements: (i) Signal suppression noise (N_{SS}); (ii) Random FM noise (N_{RF}) and (iii) Gaussian additive noise (N_{GA}). The statistical properties of the three noise components are different so that an absolute measure of the quality of the mobile radio channel is not possible. In particular, the random FM noise is independent of the carrier-to-noise ratio γ. As for the measure of quality, subjective tests seemed to indicate that the average signal-to-average noise ratio gives a good measure [2]. Consider initially an output noise N_o constituted by the signal suppression noise and the Gaussian noise, i.e., $N_o \triangleq N_{SS} + N_{GA}$. The average signal-to-average noise ratio is, in this case, $\overline{S}_o/\overline{N}_{SA}$. For the random FM situation this is $\overline{S}_o/\overline{N}_{RF} = \overline{S}_o/N_{RF}$, since $\overline{N}_{RF} = N_{RF}$.

If the fading rate is small compared to the IF bandwidth (this is usually the case for the microwave carrier frequencies where we have 50–1000 fades/second) then a quasistatic approximation can be used. In this approximation the signal and the noise can be expressed as functions only of the instantaneous IF SNR, γ. Accordingly, the averages can be taken over the statistics of γ having a negative exponential distribution (refer to section 5.6) written as

$$p(\gamma) = \frac{1}{\gamma_0} \exp\left(-\frac{\gamma}{\gamma_0}\right) \tag{8.130}$$

where γ_0 is the average IF SNR

Therefore, the mean signal output voltage averaged over γ is

$$\overline{v}_0(t) = E\left[v_0(t)\right] = \int_0^\infty v_0(t)p(\gamma)\, d\gamma \tag{8.131}$$

With (8.104) and (8.130) in (8.131) we obtain

$$\overline{v}_0(t) = m(t)\frac{\gamma_0}{1 + \gamma_0} \tag{8.132}$$

Hence, the mean signal output power is

$$S_o = \frac{\gamma_0^2}{(1 + \gamma_0)^2} P_m \tag{8.133}$$

where $P_m = < m^2(t) >$ is the message power given by (8.107)

The signal suppression noise is $n_s(t) = v_0(t) - \overline{v}_0(t)$ and the corresponding power is

$$N_{SS} = < \left[v_0(t) - \overline{v}_0(t)\right]^2 > = \left[\frac{1}{1 + \gamma_0} - \exp(-\gamma)\right]^2 P_m \tag{8.134}$$

The average output noise power N_{SA} is

$$\overline{N}_{SA} = \int_0^\infty (N_{SS} + N_{GA})p(\gamma)d\gamma \tag{8.135}$$

With (8.134), (8.122) and (8.130) in (8.135) we get

$$\bar{N}_{SA} = \left[\frac{1}{1+2\gamma_0} - \frac{1}{(1+\gamma_0)^2}\right] P_m + \frac{a}{\gamma_0} \log\frac{(1+\gamma_0)^2}{1+2\gamma_0} + 8BW\sqrt{\frac{\pi}{2\gamma_0(1+\gamma_0)}}$$

$$x \exp\left[2.35\,\frac{1+\gamma_0}{\gamma_0}\right] \operatorname{erfc}\sqrt{2.35\,\frac{1+\gamma_0}{\gamma_0}} \qquad (8.136)$$

where a is given by (8.123) and $\operatorname{erfc}(x) \triangleq 1 - \operatorname{erf}(x)$.

The average signal-to-average noise is $\bar{S}_0/\bar{N}_{SA}$ which can be obtained straight from the ratio between (8.133) and (8.136). As for the random FM it is shown in section 4.8 that the corresponding output noise N_{RF} within the frequency range ω_1 to ω_2 is given by (4.77) reproduced here for convenience

$$N_{RF} = \frac{(\Gamma v)^2}{2} \ln\left(\frac{\omega_2}{\omega_1}\right) \qquad (8.137)$$

where $\Gamma = 2\pi/\lambda$ and v is the mobile's speed. Assuming an audio band of $\omega_1 = 300$ Hz and $\omega_2 = 3000$ kHz, the average signal-to-average noise is given by

$$\frac{S_o}{N_{RF}} = \frac{(B-2W)^2}{20(v/\lambda)^2 \ln 10} \frac{\gamma_0^2}{(1+\gamma_0)^2} \qquad (8.138)$$

where α has been assumed to be 0.1.

Both ratios $\bar{S}_o/\bar{N}_{SA}$ and $\bar{S}_o/N_{RF}$ are plotted in Figure 8.18 [7] as functions of the average carrier to noise ratio γ_0, where we are assuming a mobile's speed of 96 km/h (60 mi/h) and a carrier frequency of 900 MHz (λ = 1/3 m) corresponding to a Doppler shift of v/λ = 80 Hz.

The interpretation of Figure 8.18 is eased if we carry out the following reasoning. The overall signal-to-noise ratio SNR_o must include all the noise components as follows

$$SNR_o = \frac{\bar{S}_o}{\bar{N}_{SA} + \bar{N}_{RF}} = \frac{(\bar{S}_o/\bar{N}_{SA})\,(\bar{S}_o/N_{RF})}{(\bar{S}_o/\bar{N}_{SA}) + (\bar{S}_o/N_{RF})} \qquad (8.139)$$

We can rewrite (8.139) as $SNR_o = XY/(X+Y)$ where X and Y may assume the values of either ratio, indistinctly. Expressing SNR_o in dB we have

$$10\log SNR_o = 10\log X + 10\log Y - 10\log(X+Y)$$

If $X >> Y$ then $10\log SNR_o \approx 10\log Y$.

When $X \approx Y$ then $10\log SNR_o \approx 10\log X - 10\log 2$

$$\approx 10\log Y - 10\log 2$$

Using the same reasoning, we may interpret the curves of Figure 8.18 as follows. For small values of γ_0, $\overline{S}_o/\overline{N}_{SA} << \overline{S}_o/N_{RF}$, so that $\overline{S}_o/\overline{N}_{SA}$ predominates. Therefore $SNR_o \approx \overline{S}_o/\overline{N}_{SA}$. For large values of γ_0 the opposite situation occurs so that $SNR_o \approx \overline{S}_o/N_{RF}$. For intermediate values of γ_0, the maximum difference between SNR_o and $\overline{S}_o/\overline{N}_{SA}$ or $\overline{S}_o/\overline{N}_{RF}$ is -3 dB ($= -10\log 2$) attained when $\overline{S}_o/\overline{N}_{SA} = \overline{S}_o/N_{RF}$. Finally, we may use the following interpretation for the overall SNR_o curves. They coincide with those of $\overline{S}_o/\overline{N}_{SA}$ for small γ_0 and with those of $\overline{S}_o/N_{RF}$ for large γ_0. For intermediate values of γ_0 the overall SNR_0 curves perform a smooth transition from the $\overline{S}_o/\overline{N}_{SA}$ curves to the $\overline{S}_o/N_{RF}$ ones with a difference between them not exceeding than 3 dB.

Note that the pronounced threshold due to capture observed in the non-Rayleigh case (Figere 8.17) is not present any longer. As the transmitter power is increased (γ_0 is increased) the output signal-to-noise ratio increases approximately linearly with γ_0. Threshold crossings are, therefore, less frequent but the random FM noise remains unchanged (it does not depend on γ_0) and becomes the dominant noise component. Hence, the limiting output signal-to-noise ratio is given by (8.138) for large γ_0, i.e.,

$$SNR_{\text{limiting}} = \lim_{\gamma_0 \to \infty} \frac{S_o}{N_{RF}} = \frac{(B - 2W)^2}{20\, f_m^2 \ln 10} \qquad (8.140)$$

where $f_m = v/\lambda$.

8.6 SUMMARY AND CONCLUSIONS

The standard AM scheme has in its favour the ease of implementation and spectrum saving: demodulation can be carried out by means of envelope detector or square-law detector and the transmission bandwidth is only twice the message bandwidth. On the

other hand, additional power is required to transmit the carrier. The SSB modulatic requires the minimum transmitter power and minimum transmission bandwidth but th receivers are more complex. The FM scheme usually necessitates more frequenc spectrum but yields a better performance in the presence of noise.

As far as additive noise is concerned the FM systems operating above a minimu carrier-to-noise ratio (FM threshold) usually gives a better performance than that c the SSB and AM systems. Since this performance depends on the transmission bandwidt we may say that for FM, bandwidth and signal-to-noise ratio are interchangeable. A comparative performance of these systems is shown in Figure 8.19.

When fading (multiplicative noise) is taken into account standard AM an conventional SSB experience a disastrous performance. The SSB scheme still give better results than AM with a signal-to-signal suppression noise ratio 10.4 dB abov that of the AM. The FM technique is also substantially affected by the effects o fading, but has a noticeable better performance.

Generally speaking, the fading spectrum lies below the information spectrum. Thi suggests that the use of a convenient filter can improve the noise performance of AM systems. However, since the fading depends on the speed of the vehicle, fading and information spectra may overlap with a consequent degradation on the signal quality This can be minimized by the transmission of a pilot tone that can be used fo frequency or gain control. In narrowband systems, both the pilot tone and the modulated signal are equally affected by the fading (flat fading). For slow fading the automatic gain control (AGC) circuit may be able to compensate for the variations of the amplitude of the signal "cancelling out" the fading. However, this requires a minimum 30 dB carrier-to-noise ratio in order to have the AGC of the receiver working satisfactorily. For high fading rates, occurring in urban areas, the AGC is substantially less effective.

Some new SSB modulation schemes using an in-band pilot tone and companded amplitude have been proposed and are likely to be used in some mobile radio services such as satellite mobile communications.

APPENDIX 8A

Power Spectral Density of a Narrow-Band Noise

A narrow-band noise n(t) centred at a frequency f_c, can be written as a function of its in-phase component $n_I(t)$ and quadrature component $n_Q(t)$ as follows

$$n(t) = n_I(t)\cos(2\pi f_c t) - n_Q(t)\sin(2\pi f_c t) \tag{8A.1}$$

Given n(t) we can obtain the in-phase component $n_I(t)$ by performing the multiplication $2n(t)\cos(2\pi f_c t)$ followed by a low-pass filtering of the resultant signal. In the same way, the quadrature component can be obtained by performing $2n(t)\sin(2\pi f_c t)$ and low-pass filtering the resultant signal. Therefore, we may write these components as

$$n_I(t) = 2n(t)\cos(2\pi f_c t) \tag{8A.2}$$

$$n_Q(t) = 2n(t)\sin(2\pi f_c t) \tag{8A.3}$$

The power spectral density $S_{n_I}(f)$ of the random process $n_I(t)$ is the Fourier transform of its auto-correlation function $R_{n_I}(\tau)$. This autocorrelation function is given by

$$\begin{aligned} R_{n_I}(\tau) &= E\left[n_I(t+\tau)n_I(t)\right] \\ &= E\left[4n(t+\tau)n(t)\cos(2\pi f_c t + 2\pi f_c \tau)\cos(2\pi f_c t)\right] \\ &= 4E\left[n(t+\tau)n(t)\right]\ \frac{1}{2}\ E\left[\cos(2\pi f_c \tau) + \cos(4\pi f_c t + 2\pi f_c \tau)\right] \\ &= 2R_n(\tau)\cos(2\pi f_c \tau) \end{aligned} \tag{8A.4}$$

The Fourier transform of $R_n(\tau)$ is $S_n(f)$. The Fourier transform of the modulated process $R_n(\tau)\cos(2\pi f_c \tau)$ is $\frac{1}{2} S_n(f+f_c) + \frac{1}{2} S_n(f-f_c)$, such that

$$S_n(f) = S_n(f-f_c) + S_n(f+f_c) \tag{8A.5}$$

The same reasoning can be applied to obtain an equal relation for $S_{n_Q}(f)$, i.e,

$$S_{n_Q}(f) = S_n(f-f_c) + S_n(f+f_c) \qquad (8A.$$

APPENDIX 8B

Signal-to-Signal Suppression Noise Ratio of AM System

The section 8.3.7 has shown that the message signal power at the envelo detector's output is $(\pi/2)(A\sigma)^2P_m$. Using (8.42) and (8.43) it follows that the sign suppression noise power is

$$< \left[y(t) - \bar{y}(t)\right]^2 > = A^2 < (r - \sqrt{\pi/2}\,\sigma)^2 > < \left[1 + k_a m(t)\right]^2 > \qquad (8B.1$$

Expanding the first term of the product we have

$$< (r - \sqrt{\pi/2}\,\sigma)^2 > = < r^2 - 2r\sqrt{\pi/2}\,\sigma + \pi/2\,\sigma^2 >$$

$$= < r^2 > - 2 < r > \sqrt{\pi/2}\,\sigma + < \pi/2\,\sigma^2 > \qquad (8B.2$$

But

$$< r^2 > = \int_0^\infty r^2 p(r)dr = 2\sigma^2 \qquad (8B.3$$

where p(r) is given by (8.38).

And

$$< r > = \int_0^\infty r p(r)dr = \sqrt{\pi/2}\,\sigma \qquad (8B.4$$

Therefore, with (8B.4) and (8B.3) in (8B.2), we have

$$< (r - \sqrt{\pi/2}\,\sigma)^2 > = (2 - \pi/2)\sigma^2 \qquad (8B.5)$$

Expanding the second term of the product (equation (8B.1) and assuming that th message m(t) has a zero mean value we obtain

$$< \left[1 + k_a m(t)\right]^2 > = 1 + P_m \qquad (8B.6)$$

where

$$P_m = k_a^2 < m^2(t) >$$

Accordingly, with (8B.6) and (8B.5) in (8B.1), the signal-to-signal suppression noise ratio SSN is

$$SSN = \frac{(\pi/2)\ \sigma^2\ P_m}{< (y(t) - \overline{y(t)})^2 >} = \frac{P_m}{1 + P_m}\ \frac{\pi/2}{(2 - \pi/2)} \qquad (8B.7)$$

APPENDIX 8C

Single-Tone Modulation

Consider a sinusoidal wave of frequency W as the modulating wave, and assume a frequency deviation of Δf. Hence the modulated signal is

$$\tilde{s}(t) = A \exp\left[j2\pi f_c t + \frac{\Delta f}{W} \sin(2\pi W t)\right]$$

where we have used

$$2\pi k_f \int_0^t m(t)\ dt = \frac{\Delta f}{W} \sin(2\pi W t)$$

Differentiating both sides of the above equation we obtain

$$m(t) = \frac{\Delta f}{k_f} \cos(2\pi W t)$$

Therefore, the average power P_m is

$$P_m = (\Delta f/k_f)^2/2$$

$$= \alpha(2\pi\Delta f)^2$$

where $\alpha = \dfrac{1}{2(2\pi k_f)^2}$, with k_f in Hz/Volts.

REFERENCES

[1] Simon Haykin, *An Introduction to Analog and Digital Communications*, John Wiley & Sons. Inc., Singapore, 1989.

[2] William C. Jakes Jr., *Microwave Communications Engineering*, John Wiley & Sons. Inc., 1974.

[3] William C. Y. Lee, *Mobile Communications Engineering*, McGraw Hill Inc., 1982

[4] J.D. Parsons and J.G. Gardiner, *Mobile Communication Systems*, Blackie and Son Ltd., 1989.

[5] S.O. Rice, "Noise in FM Receivers", In *Proceedings, Symposium of Time Series Analysis*, M Rosnblatt (ed.), Chapter 25 Wiky, New York, 1963.

[6] S.O. Rice, "Statistical Properties of a Sine Wave Plus Random Noise", *Bell System Technical Journal*, Vol. 27, pp. 109-157, January 1948.

[7] B.R. Davis, "FM Noise with Fading Channels and Diversity", *IEEE Transactions on Communications Tech.*, Vol. COM-19, Nº 6, December 1971.

[8] J.P. McGeeham and A.J. Bateman, "Phase-Locked Transparent Tone-in-Band (CTTIB): a New Spectrum Configuration Particularly Suited to the Transmission of Data Over SSB Mobile Radio Networks", *IEEE Transactions on Communications*, Vol COM-32(I), pp. 81-87, 1984.

[9] J.P. McGeeham and A.J.Bateman, "Theoretical and Experimental Investigation of Feed Forward Signal Regeneration as a Means of Combating Multipath Propagation Effects in Pilot-Base SSB Mobile Radio Systems", *IEEE Transactions on Vehicular Technology*, Vol VT-32, pp. 106-120, February 1983.

[10] J.R. Carson and T.C. Fry, "Variable Frequency Electric Circuit Theory with Applications to the Theory of Frequency Modulation", *BSTJ*, Vol. 16, pp. 513-540, October 1937.

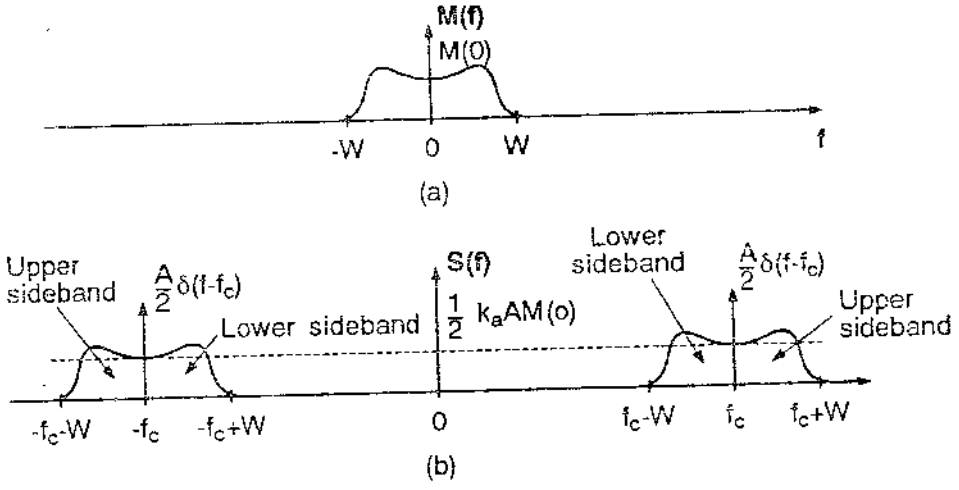

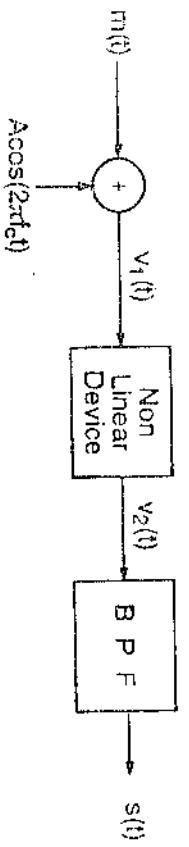

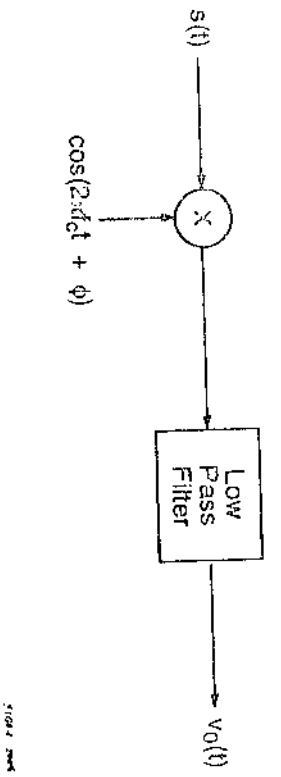

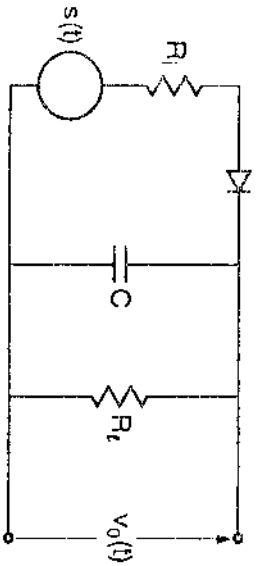

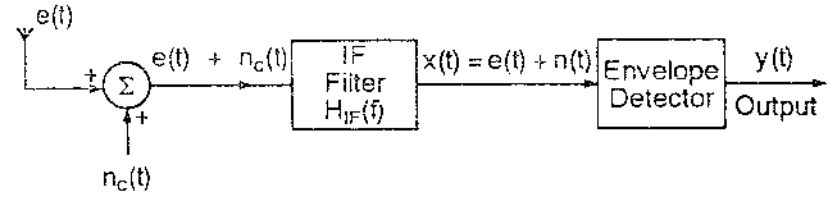

(a)

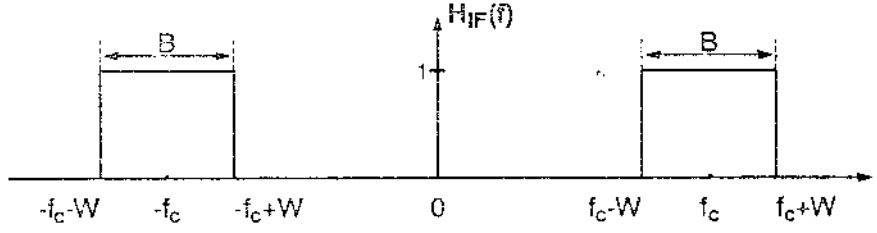

(b)

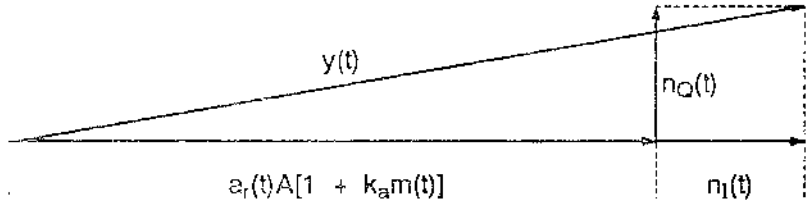

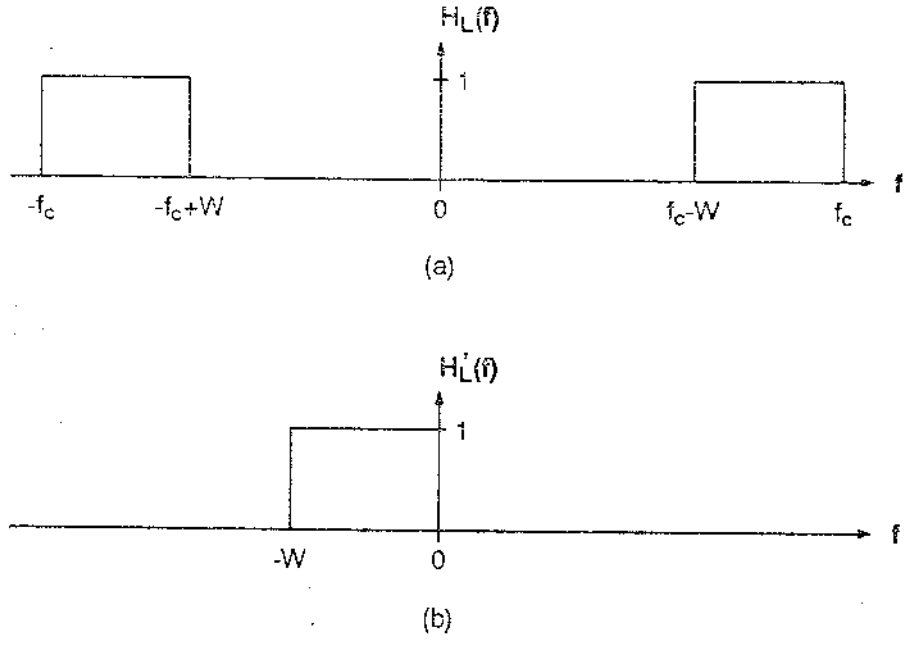

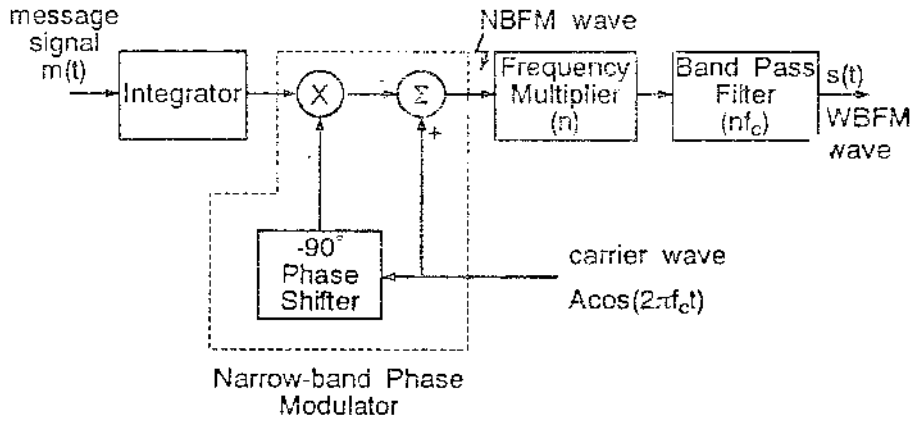

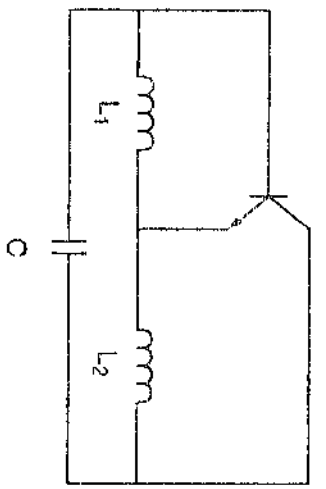

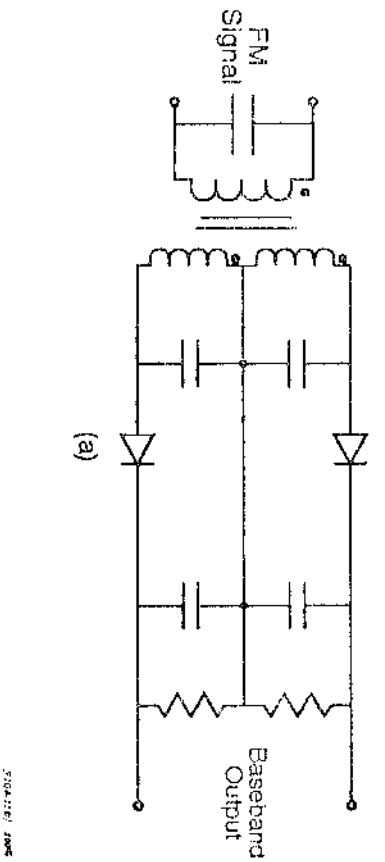

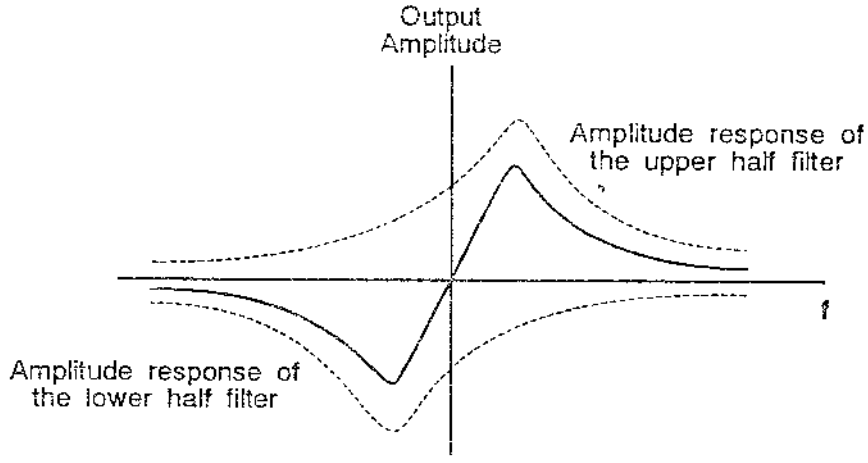

(b)

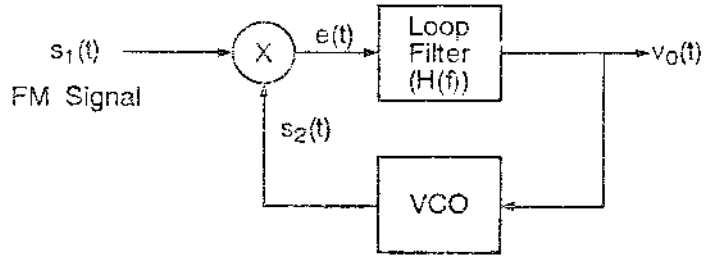

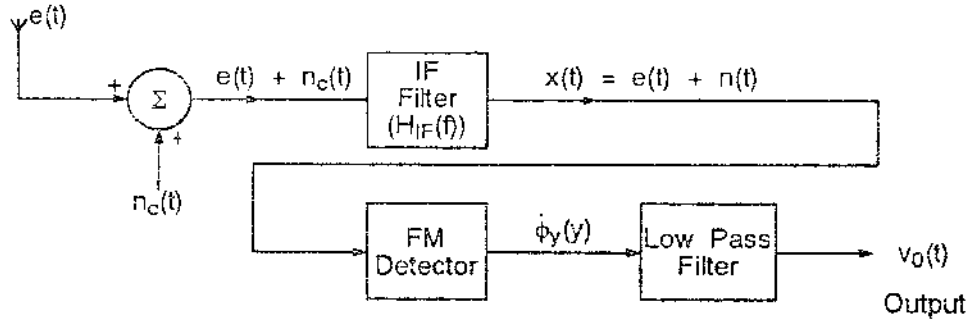

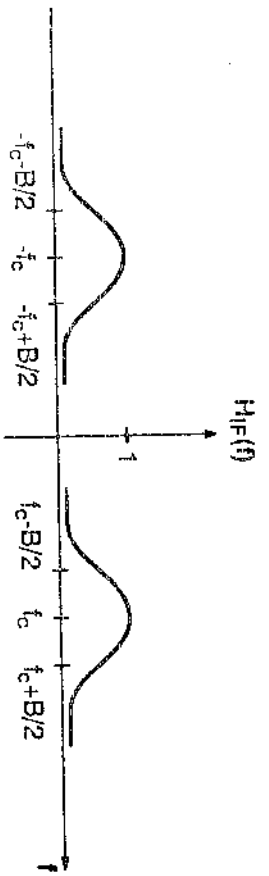

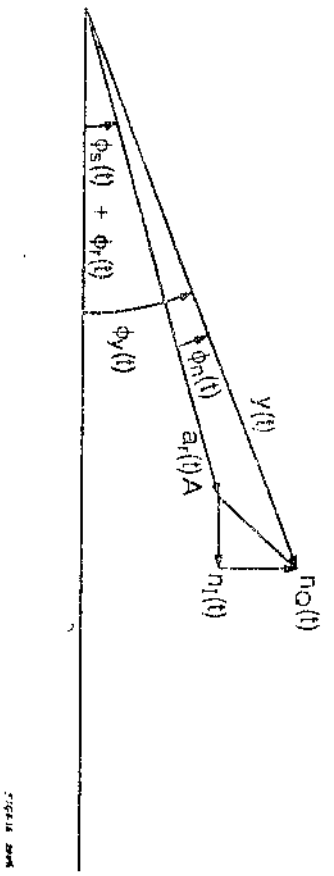

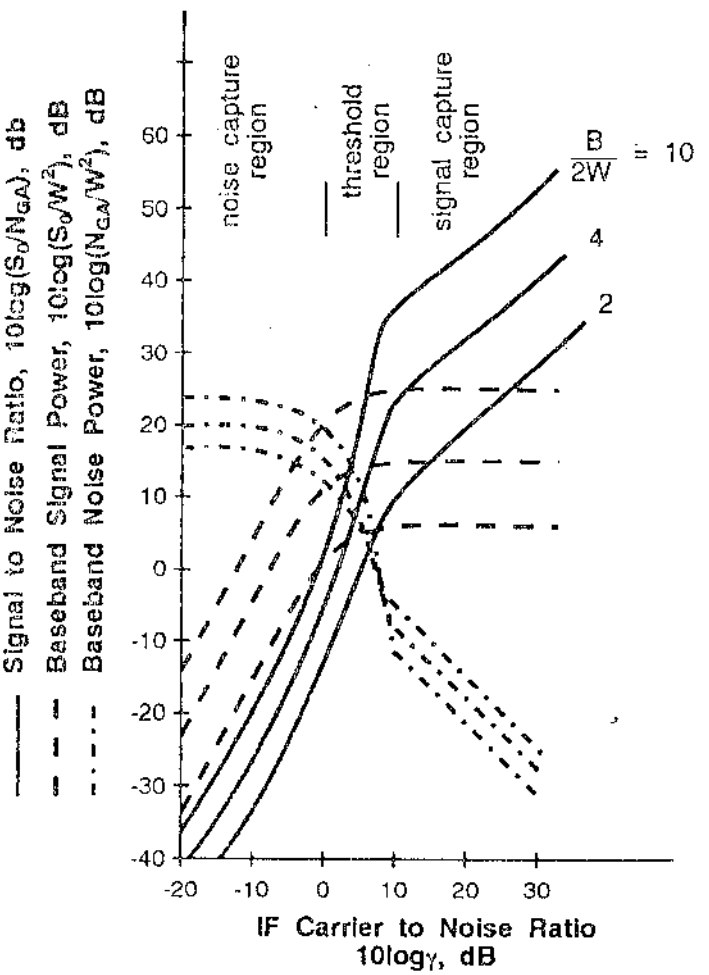
Signal to Noise Ratio, 10log(S0/NGA), db
Baseband Signal Power, 10log(S0/W2), dB
Baseband Noise Power, 10log(NGA/W2), dB
noise capture region
threshold region
signal capture region
B/2W = 10
4
2
60
50
40
30
20
10
0
-10
-20
-30
-40
-20
-10
0
10
20
30
IF Carrier to Noise Ratio
10logγ, dB

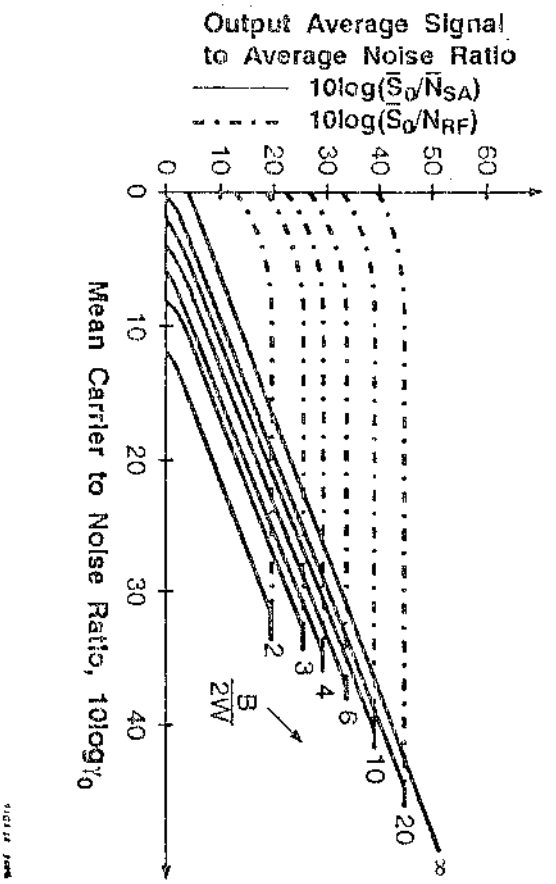

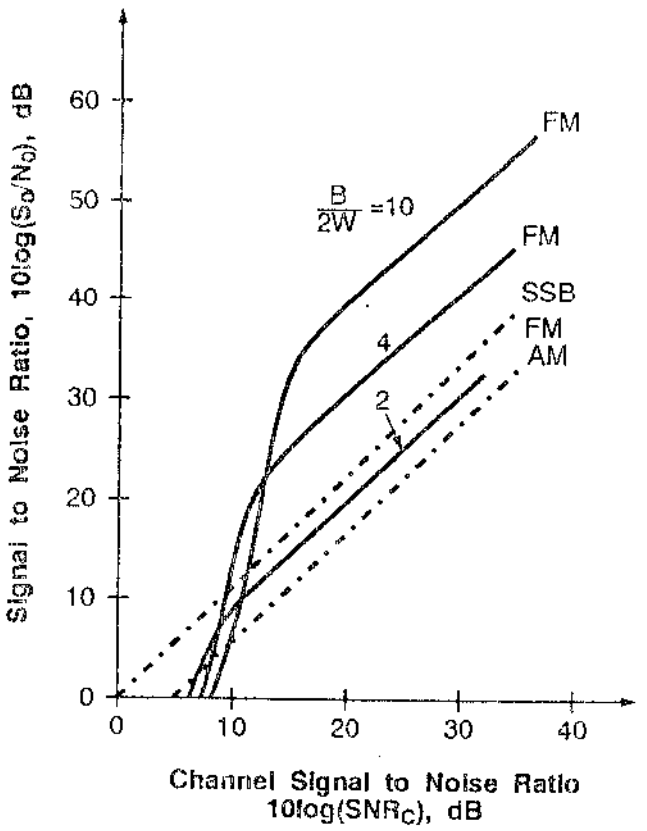
Signal to Noise Ratio, 10log(So/No), dB
60
50
40
30
20
10
0
0
10
20
30
40
FM
B/2W =10
FM
SSB
FM
AM
4
2
Channel Signal to Noise Ratio
10log(SNRC), dB

CHAPTER 9

DIGITAL TECHNIQUES FOR MOBILE RADIO

PREAMBLE

This chapter examines two basic techniques used in the digital mobile radio systems, namely speech coding and modulation. Since there is a "countless" number of speech coding and modulation schemes, we chose to analyze those selected to be used in the European and American digital cellular radio systems, in connection with their closely related techniques. Initially we introduce the basic principles of Linear Prediction Coding and Vector Quantization. In Linear Prediction Coding the Linear Prediction basics are briefly examined. Thence we describe some LPC techniques such as RELP, RPE-LPC, MPE-LPC, RPE-LTP, MPE-LTP, CELP and VSELP. Since the speech coding techniques RPE-LTP and VSELP have been selected to be used in the European and the American systems respectively, they are better explored. We then examine some higher order modulation schemes such as QPSK, DQPSK, MSK and GMSK. Their basic principles are studied and generation, detection, power spectra and bit error rate performance of the respective signals are explored. In the bit error rate studies the technique performance is examined taking into account a Gaussian channel and a Rayleigh fading channel. In the latter we consider the slow fading case for all the modulation schemes and the fast fading case for DQPSK and GMSK only, since these are the techniques selected to be used in the European and American systems.

9.1 INTRODUCTION

An analog signal using a digital communication system experiences two processes prior to transmission: A/D Conversion and Modulation. The Analog-to-Digital (A/D) Conversion reduces the complex analog waveform to a convenient digital configuration. The Modulation then processes the obtained digital waveform to make it suitable for transmission.

A/D Conversion

The A/D Conversion comprises three basic steps, namely, Sampling, Quantizing and Coding. Sampling is a process of detecting the instantaneous value of a waveform, usually carried out at regular time intervals. The sampling theorem requires that a signal should be sampled at a frequency at least twice as high as the highest frequency present in the waveform. For telephony signals the speech is bandlimited to 3.4 kHz. Allowing for the guard band, we approximate this to 4 kHz, leading to a sampling rate of 8 kHz (corresponding to an interval of 125 μs between samples). After sampling, a sequence of pulses is obtained. These pulses have their amplitudes equal (or proportional) to the amplitude of the analog input signal at the sampling instant. The resultant waveform is known as Pulse Amplitude Modulation (PAM) signal.

The next step in the digitization process is Quantization. Quantization consists in assigning a new value of amplitude to each pulse, corresponding to the nearest level available in the specially created finite discrete set of amplitude - levels. This step introduces noise in the process, the Quantization Noise, due to the difference between the true amplitude and the assigned one. The larger the number of quantization levels the smaller the quantization noise. It has been found that a signal-to-quantization noise of 30 to 40 dB is required for telephony signals, achieved with a minimum of 256 quantization levels [20].

Coding is the next step in the digitization process. The oldest and conceptually simplest coding technique used in speech and video signals is PCM [1]. In PCM the PAM signal is converted into a binary stream and multiplexed for serial transmission. The

256 ($=2^8$) quantization levels can be represented (encoded) by a minimum of 8 bits, resulting in a transmission rate of 8000 samples/second x 8 bits/sample = 64 kbits/s. Accordingly, a 3.4 kHz analog speech signal using PCM requires a 32 kHz bandwidth for baseband transmission, almost ten times as large as that of the analog transmission. This constitutes one of the main constraints of using PCM-encoded signals for digital mobile radio, where the frequency spectrum has to be carefully administered. There are some spectrally efficient modulation techniques that can be used to minimize this problem. The implications of using such techniques will be explored later in this section. Another solution to this problem is the use of modern speech coding algorithms.

In conventional 64-kbits/s PCM each sample is quantized and encoded independently, regardless of the redundancy present in the speech. It is reported that successive samples present a correlation coefficient of not less than 0.85 [20]. If the correlation between samples is taken into account, fewer bits can be used to represent the speech. Modern speech coding algorithms explore the redundancy of speech signals to reduce the transmission bit rate. There is a "countless" number of speech coding techniques already developed and also under investigation. A complete study of these techniques is well beyond the scope of this book. We shall restrict ourselves to the fundamentals of the speech coding techniques, exploring both the algorithms chosen to be used in the European and American digital cellular systems and the related algorithms.

Modulation

Modulation can be considered as a second coding stage [21]. Many aspects have to be considered in a choice of a modulation technique, including (i) required bandwidth, (ii) intersymbol interference, (iii) adjacent channel interference and (iv) bit error rate performance (BER)

Binary modulations, such as ASK, FSK and PSK, are rather simple and robust but spectrally inefficient. In this sense, multilevel modulation techniques are preferred, despite their inferior BER performance. In order to get an insight into

these problems, consider a B-kHz bandwidth channel. Roughly speaking, a binary modulator can transmit B kbits/s through this channel. Suppose now that each pair of binary symbol is encoded as one symbol. For instance, in ASK this could be achieved by assigning the symbols 0, 1, 2 and 3 to the pairs 00, 01, 10 and 11, respectively. Accordingly, the symbol rate is divided by 2 with a corresponding decrease by a factor of 2 of the occupied bandwidth. On the other hand, the error rate performance is degraded due to the increase of the number of levels that must be distinguished from one another at the reception.

In a way similar to speech coding, there is a myriad of digital modulation techniques. Therefore, a full investigation on these techniques is well beyond the scope of this book. We shall concentrate on the techniques chosen to be used in the European and American digital cellular systems and on those more closely related to them.

9.2 SPEECH CODING FOR MOBILE RADIO

The ultimate objective of the speech-coding algorithms is to transmit, store or synthesize speech at a given quality using fewer bits [1]. Bit rate reduction is accomplished by taking advantage of both the redundancies in the speech signal and the perceptual limitations of the ear. Speech redundancies are related to the following human tract characteristics:

- Speech spectrum changes relatively slowly compared to the sampling rate.
- Vibration rate of the vocal cords also changes relatively slowly.
- Speech energy is concentrated at the lower frequencies.
- Speech sounds can be modelled as periodic or noisy excitations passing through the vocal tract (filter), as shall be detailed later.

One limitation of the human audition, that can be explored by the speech coding algorithms, is its relatively low sensitivity to the signal's phase. Moreover, the hearing is more strongly sensitive to a small portion of the audible frequency

spectrum.

Bit rate is directly related to transmission bandwidth. Accordingly, bit rate reduction implies bandwidth reduction, accomplished at the expenses of degrading speech quality. At a given bit rate, speech quality can be improved by increasing the complexity of the algorithm. Therefore in assessing the overall speech-coding algorithm performance, the three parameters, namely Rate, Quality and Complexity must be taken into consideration.

The parameter Quality presents different requirements varying according to the service. There are basically four Quality classes to be considered, as follows:

- Broadcast Quality, referring to wideband transmission with high quality speech.
- Toll Quality, referring to the speech as heard over a switched telephone network.
- Communication Quality, referring to the highly intelligible speech but with more distortion than the toll one.
- Synthetic Quality, referring to the "machinelike" speech.

The speech quality can be evaluated by means of objective measures (e.g., SNR) or subjective measures (e.g., the mean opinion score - MOS).

The Complexity parameter is related to the processing required to implement the coding algorithm. This is usually measured in Mega Operations Per Second - MOPS.

Speech coders are usually grouped into two categories: waveform coders and voice coders (vocoders). Waveform coders are further divided into Time-domain (TW) and Spectral-domain waveform (SW) coders. The former takes advantage of the periodicity and slowly varying intensity of the signal, whereas the latter explores the speech redundancies across frequencies. Vocoders assume speech production model to reproduce the speech. Waveform coders usually yields superior speech quality but operates at higher bit rates. Examples of TW coders include PCM, DPCM, ADPCM, etc. As SW coders we have Subband Coding (SBC), Adaptive Transform Coding (ATC) and others. The Linear Predictive Coding (LPC) techniques such as Residual Excited Linear Prediction (RELP), etc., are examples of vocoders. In this chapter we shall concentrate our attention on

the vocoders.

Vocoders

The basic speech production model of the vocoders assumes a clear separation between excitation and vocal tract filter information. The excitation is the sound-production mechanism, while the vocal tract is the "device" used to modulate the sound. With this assumption the information is encoded separately, with a substantial decrease in the bit rate.

The excitation may be either voiced or unvoiced. Voiced sounds are quasi-periodic, occurring in the larynx where air flow can be periodically interrupted by the vocal folds. Unvoiced sounds are noisy and aperiodic, generated at a narrow constriction of the vocal tract (usually toward the mouth end). The voiced sound production can be modelled as a response of the vocal tract filter excited with a periodic sequence of impulses spaced by a fundamental period equal to the *pitch* period. Unvoiced sound corresponds to the response of the vocal tract when excited with a white noise sequence [11]. The vocal tract is modelled as a filter having its parameters varying with time. Therefore, in theory, if (i) the filter's coefficients, (ii) a voiced/unvoiced parameter and (iii) the pitch period are available, the corresponding speech signal may be reproduced in its entirety, except for the quantization error and noise. A block diagram illustrating a typical model of speech production is depicted in Figure 9.1.

A considerable number of low-bit-rate speech coding techniques is available and analyzed in the literature [1,12]. The most popular technique is the Linear Predictive Coding (LPC), comprising a series of other algorithms using the LPC basic principles. In this chapter we shall examine the LPC fundamentals and the techniques chosen to be used in the European and American digital cellular mobile radio systems. With the same objective, we shall describe Vector Quantization, a way of further reducing the bit rate.

9.3 LINEAR PREDICTIVE CODING

Linear Predictive Coding (LPC) owes its popularity to its simplicity, compactness and precise representation of the speech. Simplicity and compactness are accomplished at the expenses of some approximations sacrificing the nasal and unvoiced sounds. Before proceeding our studies, we shall examine some of the Linear Prediction fundamentals aiming at the speech coding applications.

Linear Prediction

Linear prediction is a form of estimation using a linear combination of present and past samples of a stationary process to predict a sample of the process in the future. Let S_{n-k}, $k = 1,...,M$, be random samples from a stationary process $S(t)$, and S_n the sample to be predicted. The estimation of S_n is $\hat{S}_n$ such that

$$\hat{S}_n = \sum_{k=1}^{M} h_k S_{n-k} \tag{9.1}$$

where h_k, $k = 1,...,M$ are constants and M is the number of delay elements. The filter designed to implement the estimation $\hat{S}_n$ is called Linear Predictor. Accordingly, h_k are the filter coefficients and M is referred to as the filter order. The difference between the true sample S_n and its estimation $\hat{S}_n$ is called prediction error, ε_n, i.e.,

$$\begin{aligned} \varepsilon_n &= S_n - \hat{S}_n \\ &= S_n - \sum_{k=1}^{M} h_k S_{n-k} \end{aligned} \tag{9.2}$$

The structure implementing (9.2) is known as Analysis Filter or Inverse Filter. We may invert (9.2) to obtain S_n given (i) the error, (ii) the past samples and (iii) the filter coefficients.

Therefore

$$S_n = \varepsilon_n + \sum_{k=1}^{M} h_k S_{n-k} \tag{9.3}$$

The structure implementing (9.3) is called Synthesis Filter. Three of such filters are shown in Figure 9.2.

Linear Predictive Coding

The standard LPC vocoder provides two basic functions for speech production: analysis, carried out at the transmissi . side and synthesis, carried out at the reception end. The analysis consists of three basic functions: (i) deciding whether the speech is voiced or unvoiced, (ii) determining the pitch period in case of voiced sounds and (iii) calculating the filter coefficients. The synthesis consists in choosing either a periodic or white noise waveform to excite its filter and modelling the vocal tract. The determination of the optimum filter coefficients at the transmission end may either involve the calculation and minimization of the prediction error over the relevant past samples or some specially designed algorithms.

The number of samples used in the analysis-synthesis process is such that the duration of the segment formed by these samples is 10-30 ms. During this period the speech production process may be considered as essentially stationary. The resultant of this simplistic process is a synthetic ("machinelike") quality speech with a typical transmission rate of 2.4 kbits/s. Moreover, the intelligibility of the produced speech is poor for breathy or nasal sounds.

9.4 VECTOR QUANTIZATION

Vector Quantization (VQ) is not a speech-coding technique on its own. On the contrary, it is a general coding principle used in connection with the speech-coding techniques to further reduce the number of required coding bits. In general, the speech coders assume each instantaneous speech sample S_n independently, having most of its redundancy removed in the analysis process. However, consecutive samples are far from random, keeping some correlation between them. Vector quantization considers consecutive samples of S_n as a block (or vector) and encode them appropriately to remove further redundancy. Consider, for example, 10 5-bit speech samples (a total of

50 bits). It may be possible to use 10 bits in a VQ scheme in order to encode the information contained in these 50 bits, since "the number of distinct sounds in speech is not sufficiently large to warrant 50 bits" [12].

Let k be the number of consecutive samples (the frame). After the normal analysis (without VQ) a set of k scalar parameters is generated. A codebook containing p k-dimensional vector is created so that, instead of the k scalar parameters, a $\log_2 p$-bit code word is sent. The index $\log_2 p$ identifies the vector most closely representing the initial set of k scalar parameters. Accordingly, the complexity of the encoder is increased by the additional task of searching for the appropriate vector among the p possible ones in the codebook to be encoded and sent. On the other hand, the complexity of the decoder remains unchanged, although more memory is required to accommodate a replica of the codebook.

The two key problems of VQ is the creation of and searching the codebook. Codebook creation may involve iterative procedures by the use of large training sequence of speech containing a representative amount of phonemas. An initial codebook is assumed, but the optimum codewords are obtained by averaging all of the vectors of the training sequence that can be mapped onto the initial codeword. As for the searching problems, many suboptimal algorithms can be used in order to avoid the substantially time consuming process, represented by the full codebook search.

9.5 SOME LPC TECHNIQUES

In this section we shall examine some of the main techniques using the LPC principles. The aim is to present the speech codec algorithms that have been adopted by the European as well as by the American digital cellular systems.

Waveform speech coders produce toll-quality speech at rates above 16 kbits/s, whereas standard LPC vocoders provide synthetic-quality speech at rates below 2.4 kbits/s. The higher quality speech achieved by the former is due to the transmission of the residual error, ε_n, (see (9.2)) in its entirety. Standard LPC vocoders, on the

other hand, provide information about voicing, pitch period and gain. Both of them yield the filter coefficients. It is possible to combine some of the characteristics of the waveform coders with those of the LPC vocoder in order to improve speech quality of the latter at the expenses of a little increase of its bit rate. These "hybrid" (vo)coders are still able to produce toll-quality speech at rate ranging from 4.8 to 13 kbits/s. Some of these techniques are described below.

Residual-Excited Linear Prediction (RELP)

The Residual-Excited Linear Prediction algorithm uses the same parameters as those of standard LPC in addition to the low-pass filtered residual error. The low-pass filtering ranges from 0 to typically 900 Hz, where the frequencies are supposed to carry the highest perceptual importance. This contributes to the naturalness of the speech as well as to a better reproduction of the voiced sounds (the weak points of the standard LPC vocoders). Since the filtered baseband retains the waveshape, pitch and gain parameters need not be sent. This greatly simplifies the RELP analyzer and improves the LPC synthesis.

Regular-Pulse Excited LPC (RPE-LPC)

Instead of using spectral information to improve speech quality as in the RELP case, Regular-Pulse Excited LPC operates in the time domain. In the RPE-LPC the residual (error) signal is represented by a given number of impulses per frame of speech data. A reduction (decimation) factor of 8:1 is quite common. For example, a frame containing 64 residual samples is reduced to 8 equally spaced samples. Like RELP, in RPE-LPC pitch and gain parameters are not sent.

Multi-Pulse Excited LPC (MPE-LPC)

This technique operates in a way similar to RPE-LPC. The difference, however, consists in that the impulses chosen to represent the residual signal are not necessarily equally spaced. On the contrary, their positions and amplitudes are selected to yield the best representation of the error signal. In a sense, multipulse residual "resembles a skeleton of the actual residual signal" [12].

Both RPE-LPC and MPE-LPC may include a Long-Term Prediction (LTP) to provide

information about the pitch period. In the former case we have the RPE-LTP and in the latter the MPE-LTP.

The GSM Codec

More than 20 different codec proposals were considered for evaluation by the European Digital Cellular Radio, the GSM system. Out of them, 4 were selected for test, namely, RPE-LPC, MPE-LTP, SBC-Adaptive PCM in 14 subbands and SBC-Adaptive Differential PCM in 6 subbands. The results of the test are summarized in Table 9.1 [13].

TABLE 9.1 - COMPARISON BETWEEN CODEC PROPOSALS FOR THE GSM SYSTEM

Source: P. Vary, K. Hellwig, R. Hofmann, R.J. Sluyter, C. Galand and M. Rosso, "Speech Code for the European Mobile Radio System". Proceedings Int. Conf. on Acoustics Speech and Signal Processing, ICASSP-1988, pp. 227-230. Reprinted with permission.

Codec	Speech Quality MOS (out-of-5)	Net Bit Rate Kbits/s	Complexity MOPS
RPE-LPC	3.54	14.77	1.5
MPE-LTP	3.27	13.20	4.9
SBC-APCM	3.14	13.00	1.5
SBC-ADPCM	2.92	15.00	1.9
FM	1.95		

Note that all of the codecs exceeded the speech quality of that given by a companded FM with CNR of 18 dB and 26 dB moving at 36 Km/h. Note also that the RPE-LPC codec has the highest average quality score. Finally, the chosen codec was a combination of RPE-LPC and MPE-LTP resulting in the RPE-LTP with a net bit rate of 13 kbits/s.

A simplified block diagram of RPE-LTP GSM codec is shown in Figure 9.3 [14]. The speech signal, sampled at 8 kHz, is subdivided into 20 ms-segments (160 samples per segment). During each segment interval the coefficients $r_n(k)$ of the LPC Inverse Filter are calculated by the LPC Analysis block, so that the residual ϵ'_n is minimized.

The pitch is predicted by the LTP Analysis Filter (Pitch Predictor) and subtracted from ε'_n to generate the "Gaussian noise like" error ε_n. The LTP Filter is characterized by the pitch period, p_n, and a gain factor g_n. The residual signal ε_n is low-pass filtered (LPF) at 4/3 kHz and only every third sample of the resultant signal is selected for transmission. The coefficients $r_n(k)$, in number of 8, and the parameters p_n and g_n are encoded with 3.6 kbits/s, while the samples of the filtered residual is encoded with 9.6 kbits/s.

At the decoder the parameters X_n, p_n, g_n and $r_n(k)$ are used in the Grid Position and Synthesis Filter to synthesize the speech.

Code-Excited Linear Prediction (CELP)

The Code-Excited Linear Prediction algorithm uses LPC techniques in connection with vector quantization through an analysis-by-synthesis procedure. Figure 9.4 shows the basic structure of the CELP codec. The basic analysis procedure consists in finding an optimum codeword (vector) c_k in the codebook according to some subjective error criterion. Each codeword is scaled by a gain factor g_k and processed through the LTP and LPC Synthesis Filters to Synthesize the predicted speech term $\hat{S}_n$. The residual $\varepsilon_n = S_n - \hat{S}_n$ is processed through the Perceptual Weighting Filter (PWF) and used in a full search procedure to find the best codeword that minimizes the energy of ε_n. The codebook index k, the gain g_k, and the filters parameters are sent and used at the decoder to synthesize the speech.

The American Codec [18]

The speech coding algorithm used in the American digital mobile radio system is a variation on CELP, called Vector-Sum Excited Linear Prediction (VSELP). It uses codebooks with predefined structure so that full search is avoided, significantly reducing the time required for the optimum codeword search. A block diagram of the VSELP codec is shown in Figure 9.5. The long term predictor lag l is determined from the past output of the LTP filter and the current input speech using a closed loop approach. This VSELP utilizes two codebooks, each of which with their own gains. The long term prediction lag is determined first, assuming no input from these two

codebooks. Once the prediction lag is established, the first codebook is searched, assuming no input from the other codebook. Having determined the optimum codeword, the other codebook is then searched in order to minimize the energy of the prediction error e_n even further. The signal p_n is the weighted input speech for the subframe minus the zero input response of the weighted LPC Synthesis filter. The sampling rate is 8 kHz and 160 samples are grouped to form a 20 ms-frame. A subframe is composed of 40 samples (5 ms) and the order of the short term predictor is 10. The basic data rate of the speech coder is 7950 bits/s.

9.6 DIGITAL MODULATION FOR MOBILE RADIO

The process of conversion of a digital baseband signal into an IF or an RF signal for transmission is called *digital modulation*. The inverse process, the digital demodulation, is carried out at the reception, being done by means of coherent, differentially coherent or noncoherent detection. In coherent detection both transmitter and receiver work synchronously. Consequently, a carrier and timing recovery circuitry are required at the receiver. Since this is not necessary in either differentially coherent or noncoherent detections, the corresponding receivers are less complex. On the other hand, coherent detection yields a better bit-error-rate performance than that of noncoherent and differentially coherent detection for a given carrier-to-noise ratio.

The choice of the modulation technique must take into account two factors, namely power and spectral efficiencies. Power efficient techniques are those having low error probability (10^{-4} or 10^{-8}) in a relatively low carrier-to-noise ratio environment (8.4 dB or 12 dB respectively). Spectrally efficient techniques are those capable of transmitting high bit rate per bandwidth (2 bits/s/Hz or more).

As far as mobile radio is concerned, due to the scarcity of bandwidth, spectral efficiency is what we would usually have to consider in a choice of modulation scheme. However, we must not forget that the mobile radio environment is rather "unkind", so

that a spectrally efficient technique may give an untolerably poor performance. The 64-QAM modulation scheme, with 4.5-bit/s/Hz, and the 256-QAM, with 6.6-bit/s/Hz, are examples of such techniques [1]. On the other hand, QPSK with 2-bit/s/Hz and also MSK are good examples of power efficient techniques. Since DQPSK and GMSK are the techniques chosen to be used in the American and European digital cellular radio systems, respectively, and QPSK and MSK are closely related to them, we shall concentrate our attention on them.

9.7 QPSK AND λ SHIFTED DQPSK MODULATION SCHEMES

QuadriPhase-Shift Keying (QPSK) and λ Shifted Differentially Encoded QuadriPhase-Shift Keying (λ Shifted DQPSK) are special cases of multiphase (M-ary PSK) modulation where the information is contained in the phase of the carrier. In particular, for a quadriphase modulation, the phase of the carrier takes on one of four equally spaced values such as λ, $\lambda + \pi/2$, $\lambda + \pi$ and $\lambda + 3\pi/2$, where λ is the initial phase.

QPSK Modulation

According to the above definition, the general representation for a set of quadriphase signalling waveform is

$$s_i(t) = A\cos\left[2\pi f_c t + (i-1)\frac{\pi}{2} + \lambda\right] \qquad (9.4)$$

where $i = 1,2,3,4$, $0 \le t \le T$, T is the symbol duration, A is the carrier amplitude and f_c is the carrier frequency.

Each one of the 4 possible phases corresponds to a unique pair of information bits. The assignment of 2 information bits to the 4 possible phases is usually done so that the code words representing the adjacent phases differ by one bit. This is known as Gray encoding. For example, we may assign the phases λ, $\pi/2 + \lambda$, $\pi + \lambda$ and $3\pi/2 + \lambda$ to the pairs 00, 01, 11 and 10, respectively.

Define ϕ_i as the instantaneous phase of the modulated signal (i.e., the signal

phase at the current symbol interval)

$$\phi_I \triangleq (I - 1)\pi/2 + \lambda \tag{9.5}$$

Then, from (9.4)

$$s_I(t) = A\cos\left(2\pi f_c t + \phi_I\right) \tag{9.6}$$

Expanding the cosine function in (9.6) we have

$$s_I(t) = I_I A\cos(2\pi f_c t) - Q_I A\sin(2\pi f_c t) \tag{9.7}$$

where

$$I_I \triangleq \cos\phi_I \qquad , \qquad Q_I \triangleq \sin\phi_I \tag{9.8}$$

The signal described by (9.7) can be viewed as two quadrature carriers with amplitudes $A\cos\phi_I$ and $A\sin\phi_I$ varying according to the transmitted phases in each signalling interval. In particular, when $\lambda = \pi/4$ we have $\phi_I = (2I - 1)\pi/4$. In this case the amplitudes of the quadrature carriers take on two possible values $\pm A\sqrt{2}$ at each symbol interval.

λ Shifted DQPSK Modulation

In DQPSK the information is differentially encoded. Accordingly, symbols are transmitted as changes in phase rather than absolute phases. The DQPSK modulation can be viewed as the noncoherent version of the QPSK. In order to understand how it operates we start by explaining the binary Differentially encoded PSK (DPSK). In binary DPSK a bit 1 is sent by shifting the current phase of the carrier by π rad. A bit 0 is transmitted by leaving the current phase of the carrier unchanged. In effect, in a more general binary DPSK the current carrier phase is shifted by λ rad. when a 0 is transmitted and by $\lambda + \pi$ rad when a 1 is transmitted. If λ is chosen to be equal to 0, an information containing a long string of zeros is transmitted with no phase shift in the carrier. Consequently, the spectrum of the

transmitted signal can be very narrow in such interval. However, if λ is chosen to be different from zero, the carrier phase is shifted in every signalling interval. In this case the width of the signal spectrum is approximately equal to 1/T, where T is symbol duration.

In a λ shifted DQPSK the relative phase shifts between successive intervals are λ, $\lambda + \pi/2$, $\lambda + \pi$ and $\lambda + 3\pi/2$, where λ takes on the usual values of 0 or $\pi/4$. Since in DQPSK modulation the information is transmitted as changes of phases, the current carrier phase, ϕ_i, is written as the difference between the previous carrier phase, ϕ_{i-1}, and the phase change, $\Delta\phi_i$, to be introduced. Note that $\Delta\phi_i$ is a function of the current symbol. Therefore

$$\phi_i = \phi_{i-1} - \Delta\phi_i \tag{9.9}$$

Using the definitions of (9.8) applied to (9.9) we have

$$\begin{aligned} I_i &= I_{i-1}\cos\Delta\phi_i - Q_{i-1}\sin\Delta\phi_i \\ Q_i &= I_{i-1}\sin\Delta\phi_i - Q_{i-1}\cos\Delta\phi_i \end{aligned} \tag{9.10}$$

where $I_{i-1} = \cos\phi_{i-1}$ and $Q_{i-1} = \sin\phi_{i-1}$ are the amplitudes at the previous symbol interval. The DQPSK signal can be written in the same way as in (9.7). If λ is chosen to be equal to $\pi/4$, then the amplitudes of the quadrature carriers can take on one of five possible values, 0, $\pm A$, $\pm A/\sqrt{2}$.

9.7.1 Generation and Detection of QPSK and DQPSK signals

A quadriphase PSK signal can be viewed as two binary PSK signals impressed on the quadrature carriers. This approach can be used to simplify the generation and detection of quadriphase PSK signals. Without loss of generality we shall assume $\lambda = \pi/4$.

Modulation

Consider a binary data stream, b(t), entering the modulator. The first step in

the modulation process is to split this binary sequence into two separate binary streams, namely O and E, by a serial-to-parallel converter. All of the odd numbered bits form a stream O and all of the even numbered bits form a stream E. At a given symbol instant i the pair (O_iE_i) represents a symbol and the corresponding carrier phase change. Accordingly, the next step is to encode the two data streams so that the binary-data to carrier-phase correspondence can be achieved.

Let the sequences I and Q be the encoded data. As far as QPSK modulation scheme is concerned these sequences assume only two possible values, $\pm 1/\sqrt{2}$, as stated in the previous section. Moreover, these values correspond to absolute phases of the carrier and they are functions only of the current symbol. Hence, an absolute phase encoder can be implemented by means of a simple combinatorial logic. As for the DQPSK, the phase change is a function of both the previous phase and the current symbol. Therefore, a sequential state machine may be used to implement a differential phase encoder.

The data-phase correspondence for QPSK and the data-phase change correspondence for DQPSK are shown in Table 9.2. Note that I_i and Q_i are equal to $\cos\phi_i$ and $\sin\phi_i$ respectively, at any signalling interval. Therefore, the final step in the modulation process is to implement the functions as described by (9.7). The resultant block diagram is shown in Figure 9.6

TABLE 9.2 - DATA-PHASE AND DATA-PHASE CHANGE CORRESPONDENCES FOR QPSK AND DQPSK.

			QPSK			DEQPSK		
i	O_i	E_i	ϕ_i	I_i	ϕ_i	$\Delta\phi_i$	I_i	Q_i
1	0	0	$\pi/4$	$1/\sqrt{2}$	$1/\sqrt{2}$	$\pi/4$	Depend	on
2	0	1	$3\pi/4$	$-1/\sqrt{2}$	$1/\sqrt{2}$	$3\pi/4$	previous	data
3	1	1	$-3\pi/4$	$-1/\sqrt{2}$	$-1/\sqrt{2}$	$-3\pi/4$	according	to
4	1	0	$-\pi/4$	$1/\sqrt{2}$	$-1/\sqrt{2}$	$-\pi/4$	(9.10).	

Demodulation

Demodulation of QPSK signals is carried out by means of a coherent detection with

the carrier required to be recovered at the receiver. Multiplication of the received signal by the in-phase and quadrature carriers, followed by integration (low-pass filtering) of the products, yields signal components proportional to $\cos\phi_i$ and $\sin\phi_i$ respectively. Since these components assume values $\pm 1/\sqrt{2}$, the information is extracted from the sign of the decision variable.

Demodulation of DQPSK signals is carried out by means of differentially coherent detection. This detection scheme differs from the coherent detection in that the recovered carrier (used in the latter) is replaced by the received signal being delayed by one symbol interval. Consider a received signal $s_i(t)$ as given by (9.6) and its delayed version $s_{i-1}(t) = A\cos(2\pi f_c + \phi_{i-1})$. By performing the multiplication $s_i(t)s_{i-1}(t)$ followed by integration (low-pass filtering) a signal component proportional to $\cos(\phi_i - \phi_{i-1})$ is obtained. Since, from (9.9) $\phi_i - \phi_{i-1} = -\Delta\phi_i$, and the phase change $\Delta\phi_i$ assumes values as given by Table 9.2 (i.e., $\Delta\phi_i = \pm \pi/4, \pm 3\pi/4$), then $\cos\Delta\phi_i = \pm 1/\sqrt{2}$. Therefore, the in-phase component of the information is extracted from the sign of the decision variable. Likewise, the quadrature component can be obtained by multiplying $s_i(t)$ and the delayed signal $s_{i-1}(t)$, the latter with a phase shift of $\pi/2$ rad.. The resultant signal (after the low-pass filtering) is proportional to $\sin(\phi_i - \phi_{i-1})$, assuming values of $\pm 1/\sqrt{2}$. Figure 9.7 shows a block diagram of the demodulator.

9.7.2 Power Spectra of QPSK and DQPSK Signals

Consider initially the QPSK modulation scheme. It is assumed that the information data at the modulator input is random, with both symbols (1 and 0) considered to be statistically independent and equally likely. During the signalling interval $0 \le t \le T$, the amplitudes of the quadrature carriers may assume the values $+g(t)$ or $-g(t)$, where $g(t)$ is the symbol shaping function. In particular, as seen before, $g(t) = A/\sqrt{2}$. Therefore, the in-phase and quadrature components can be viewed as random binary waves, each of which having a power spectral density, $S_g(f)$, equal to $(A^2T/2)\text{sinc}^2(Tf)$, where T is the symbol duration and $\text{sinc}(x) = \dfrac{\sin(\pi x)}{(\pi x)}$ (see

Appendix 9A). The power spectral densities $S_Q(f)$ and $S_I(f)$ of the respective modulated components $\pm g(t)\cos(2\pi f_c t)$ and $\pm g(t)\sin(2\pi f_c t)$, generating $s_l(t)$, are given by (see Appendix 9A).

$$S_Q(f) = S_I(f) = \frac{1}{4}\left[S_g(f - f_c) + S_g(f + f_c)\right] \tag{9.11}$$

Since these components are statistically independent, the resultant power spectral density, $S_s(f)$, of the band-pass signal $s_l(t)$ is the sum of their individual power spectral densities, i.e., $S_s(f) = 2S_Q(f) = 2S_I(f)$. However, for convenience, we shall use the one-sided (positive-frequency) representation, S(f), of the spectrum, so that $S(f) = 2S_s(f)$. Therefore

$$\begin{aligned} S(f) &= (A^2/2)T\text{sinc}^2\left[T(f - f_c)\right] \\ &= 2(A^2/2)T_b\text{sinc}^2\left[2T_b(f - f_c)\right] \end{aligned} \tag{9.12}$$

where T_b is the bit duration ($T = 2T_b$). The power spectral density of the QPSK signal is plotted in Figure 9.11, normalized with respect to T and the carrier power $A^2/2$.

The differential encoding does not modify the power spectral density, so that (9.12) also applies to DQPSK signals [1].

9.7.3 BER Performance Over a Gaussian Channel

QPSK Signal

The QPSK signal, $s_l(t)$, arrives at the receiver as $s_l(t)$ + Noise. The demodulator estimates the mean value of each bit composing the symbol and decides for level 1 if the detected bit is positive and for level 0 otherwise. An error occurs if at least one bit is erroneously detected.

Probability of Erroneous Decision

Since the demodulator presents two symmetrical detection branches, we shall concentrate our analysis on only one of them. Consider, for instance, the in-phase

detection branch and a locally generated carrier of $\sqrt{2}\cos(2\pi f_c t)$*. The estimated mean value of the received signal is (see Figure 9.7).

$$\bar{I} = \frac{1}{T}\int_0^T \left[s_i(t) + \text{Noise}\right]\sqrt{2}\cos(2\pi f_c t)dt$$

$$= \frac{A}{\sqrt{2}}\cos\left[(2I - 1)\frac{\pi}{4}\right] + n(t) \qquad (9.13)$$

where n(t) is a Gaussian noise with a mean value equal to zero and a variance equal to $N_0/2$. Without loss of generality we may assume $I = 1$, corresponding to bit 1 being transmitted. Accordingly, the estimated value $\bar{I}$ is $A/2 + n(t)$. If the noise exceeds $A/2$, an erroneous decision is made. Define a decision variable $v(t)$ such that

$$v(t) = n(t) - A/2 \qquad (9.14)$$

Since n(t) is a Gaussian variable with distribution p(n), v(t) is also a Gaussian variable with a distribution p(v), such that $p(n)|dn| = p(v)|dv|$.

Therefore

$$p(v) = \frac{1}{\sqrt{\pi N_0}}\exp\left[-\left(\frac{v + A/2}{\sqrt{N_0}}\right)^2\right] \qquad (9.15)$$

An erroneous decision is taken if $v(t) = n(t) - A/2 > 0$, occurring with a probability P_W, such that

$$P_W = \text{prob}(v > 0) = \int_0^\infty p(v)dv \qquad (9.16)$$

Using the transformation of the variables $z(t) = (v(t) + A/2)/\sqrt{N_0}$ and the relation $p(z)|dz| = p(v)|dv|$ we obtain

$$P_W = \frac{1}{\sqrt{\pi}}\int_{A/2\sqrt{N_0}}^\infty \exp(-z^2)dz = \frac{1}{2}\text{erfc}(A/2\sqrt{N_0}) \qquad (9.17)$$

where erfc(∘) is the complementary error function.

---

* The signal $\sqrt{2}\cos(2\pi f_c t)$ is chosen for the optimum detection criterion.

We may express (9.17) in terms of the carrier-to-noise ratio, γ_c, and the signal-to-noise ratio per bit, γ_b, using the following relations

$$\gamma_c = A^2/2N_0 \qquad \text{and} \qquad \gamma_c = 2\gamma_b \tag{9.18}$$

Therefore

$$P_W = \frac{1}{2}\text{erfc}\left(\sqrt{\gamma_c/2}\right) = \frac{1}{2}\text{erfc}\left(\sqrt{\gamma_b}\right) \tag{9.19}$$

Probability of Symbol Error

A symbol is correctly detected if both bits composing that symbol are correctly detected. The probability of this event is $(1 - P_W)^2$. Therefore, the probability of symbol error, P_e, is

$$P_e = 1 - (1 - P_w)^2 \tag{9.20}$$

Probability of Bit Error

The derivation of the bit error probability, P_b, as a function of the symbol error probability is rather tedious because of its dependence on the particular mapping of symbols onto signal phases. When Gray code is used and the symbol error is acceptably small, the following approximation works reasonably well.

The most probable errors correspond to an erroneous selection of an adjacent phase to the wanted phase. Since adjacent phases are encoded with the minimum distance criteria (1 bit difference between adjacent code words), most 2-bit symbol errors contain only a single bit error. Therefore, we may use the following approximation

$$P_b \approx \frac{1}{2} P_e \tag{9.21}$$

Hence from (9.21), (9.20) and (9.19) we obtain

$$P_b = \frac{1}{2} P_e = \frac{1}{2}\left[\text{erfc}\left(\sqrt{\gamma_b}\right) - \frac{1}{4}\text{erfc}^2\left(\sqrt{\gamma_b}\right)\right] \tag{9.22}$$

Equation (9.22) is plotted in Figure 9.8

DQPSK Signal

The derivation of the probability of a binary digit error for four-phase DPSK with Gray coding is rather cumbersome. We shall only state the final result and refer the interested readers to Proakis [4].

$$P_b = \int_b^\infty x\exp\left(-\frac{a^2 + x^2}{2}\right) I_0(ab)dx - \frac{1}{2}\exp\left[-\frac{1}{2}(a^2 + b^2)\right] I_0(ab) \qquad (9.23)$$

where $I_0(\circ)$ is the modified Bessel function of order zero and

$$a = \sqrt{\frac{\gamma_b}{2}}\sqrt{2 + \sqrt{2}} - \sqrt{2 - \sqrt{2}}$$

$$b = \sqrt{\frac{\gamma_b}{2}}\sqrt{2 + \sqrt{2}} + \sqrt{2 - \sqrt{2}} \qquad (9.24)$$

Equation (9.23) is plotted in Figure 9.8.

9.7.4 BER Performance Over a Fading Channel

In studying the BER performance over a fading channel we may discern between two situations, namely, slow and fast Rayleigh fading environments. In the former case we use the quasi-static approximation in which the non-selective fading phenomenon occurs (narrowband transmission). In the latter case, due to wideband transmission (high bit rate), the Doppler shift cannot be neglected, and the signal is affected by selective fading.

Probability of Bit Error

For a small number of diversity branches*, errors are usually assumed to occur in bursts in a fading environment. Therefore, we may consider that, for any symbol, all of the 3 possible symbol errors are equally likely and occur with probability $P_e/3$, where P_e is the average symbol error probability. Moreover, there are $\binom{k}{2}$ ways in which k bits out of 2 may be in error. Consequently, the average number of

* In our analysis we shall consider only one diversity branch.

bit error per 2-bit symbol is

$$\frac{P_e}{3}\sum_{k=1}^{2} k\binom{k}{2} = \frac{4}{3}P_e$$

The average bit error probability is obtained by dividing the above result by 2, the number of bits per symbol. Hence

$$P_b = \frac{2}{3}P_e = \frac{2}{3}\left[1 - (1 - P_W)^2\right] \tag{9.25}$$

QPSK Signal (Non Selective Fading)

The probability of an erroneous decision is obtained by averaging (9.19) over the probability density function of γ_b (or γ_c). We shall explore the SNR/bit (γ_b) case, knowing that the calculations for γ_c follow exactly the same procedure. In a Rayleigh environment the distribution of γ_b is

$$p(\gamma_b) = \frac{1}{\gamma_{b0}}\exp\left(-\frac{\gamma_b}{\gamma_{b0}}\right) \tag{9.26}$$

where γ_{b0} is the average SNR/bit. Accordingly

$$P_W = \int_0^\infty \frac{1}{2}\,\mathrm{erfc}(\gamma_b)p(\gamma_b)d\gamma_b \tag{9.27}$$

With (9.26) in (9.27) we obtain

$$P_W = \frac{1}{2}(1 - F) \tag{9.28}$$

where

$$F = \sqrt{\frac{\gamma_{b0}}{1 + \gamma_{b0}}} \tag{9.29}$$

Therefore, with equations (9.29), (9.28) and (9.25) the bit error probability of a QPSK fading signal can be calculated. The corresponding curve is plotted in Figure 9.8. It is straightforward to show that, for large γ_{b0} ($\gamma_{b0} >> 1$), the BER can be well approximated by

$$P_b \approx \frac{1}{3\gamma_{b0}} = \frac{2}{3\gamma_{c0}} \tag{9.30}$$

where γ_{c0} is the average carrier-to-noise ratio.

DQPSK Signal (Non-Selective Fading)

The bit error probability for a DQPSK fading signal can be estimated by averaging (9.23) over the distribution of γ_b, given by (9.26). Equivalently, the corresponding probability of an erroneous decision can be averaged over the distribution of γ_b and used in the appropriate equations. Again in this case we shall simply state the result [5]. It has been found that

$$F = \frac{\gamma_{b0}}{\sqrt{(\gamma_{b0} + 1)^2 - 1/2}} \tag{9.31}$$

With (9.31), (9.28) and (9.25) the bit error probability of DQPSK fading can be calculated. This is plotted in Figure 9.8. For $\gamma_{b0} >> 1$ a good approximation for BER is easily found to be

$$P_b \approx \frac{2}{3\gamma_{b0}} = \frac{4}{3\gamma_{c0}} \tag{9.32}$$

DQPSK Signal (Selective Fading)

In a fast Rayleigh fading environment the envelope correlation of the signal is different from unity. It is shown that [5], in this case,

$$F = \frac{J_0(2\pi f_D T)}{\sqrt{2(1 + 1/\gamma_{b0})^2 - J_0^2(2\pi f_D T)}} \tag{9.33}$$

where $J_0(2\pi f_D T)$, the normalized envelope correlation, is the zeroth order Bessel function of the first kind, and f_D is the maximum Doppler frequency.

With equations (9.33), (9.28) and (9.25) the BER of the DQPSK signal in a fast fading environment can be estimated. This is plotted in Figure 9.8 for several values of the parameter $f_D T$. Note that when $f_D T = 0$ we have $J_0(0) = 1$ and (9.33) equals (9.29).

9.8 MSK AND GMSK MODULATION SCHEMES

Minimum Shift Keying (MSK) and Gaussian Minimum Shift Keying (GMSK) are specia cases of binary Frequency Shift Keying (FSK) modulation in which the phase informatio of the received signal is fully explored so that noise performance can b significantly improved. In particular, GMSK is an improved version of MSK as w shall see in this section. In all of the cases each binary symbol is identified b one carrier frequency. Moreover, the changes of frequencies of the modulated carrier keyed by the binary input, do not affect the carrier phase. This type of FSI modulation is known as Continuous-Phase Frequency-Shift Keying (CPFSK).

MSK Modulation

Let s(t) be a CPFSK signal defined within the time interval $0 \le t \le T_b$ so that

$$s(t) = A\cos\left[2\pi f_c t + \theta(t)\right] \tag{9.34}$$

where T_b is the bit interval, $\theta(t)$ is the phase of s(t), f_c is the nominal carrie frequency and A is the carrier amplitude.

The carrier frequency is chosen as

$$f_c = \frac{1}{2}(f_0 + f_1) \tag{9.35}$$

where f_0 and f_1 are frequencies used to transmit symbols 0 and 1, respectively. Th phase $\theta(t)$ is a linear function of time as given by (9.36).

$$\theta(t) = \theta(0) \pm \pi\Delta f t \quad , \quad 0 \le t \le T_b \tag{9.36}$$

where $\Delta f = f_0 - f_1$ is the frequency deviation, and $\theta(0)$ is the carrier initia phase. The initial phase, $\theta(0)$, assumes the values 0 or π depending on the pas history of the modulation process. Note from (9.36) that the plus and minus sign correspond to the transmission of symbols 0 and 1, respectively.

When the frequency deviation Δf is chosen to be half of the input bit rate, i.e., $\Delta f = 1/2T_b$, the phase of the signal s(t) can take on only* the values $+\pi/2$ or $-\pi/2$

* Note that the phase shifts are modulo-2π.

at odd multiples of T_b, and the values 0 or π at even multiples of T_b. Because $\Delta f = 1/2T_b$ is the minimum frequency spacing that enables the symbols 0 and 1 to be detected without mutual interference, this special case of a CPFSK modulation is referred to as Minimum Shift Keying (MSK). Note that MSK is a binary digital FM with a modulation index of 0.5.

Considering $\Delta f = 1/2T_b$ and using (9.36) and (9.35) in (9.34), we conclude that

$$s(t) = \pm A\cos(2\pi f_0 t) \qquad \text{for symbol 0}$$

and

$$s(t) = \pm A\cos(2\pi f_1 t) \qquad \text{for symbol 1} \tag{9.37}$$

where the plus sign corresponds to $\theta(0) = 0$ and the minus sign corresponds to $\theta(0) = \pi$. We may condition $\theta(0)$ to be 0 if the previous symbol was 0 and to be π if the previous symbol was 1. Therefore, with this assumption, the generated signals for each combination of symbols are as given by Table 9.3.

TABLE 9.3 – GENERATED SIGNALS IN THE MSK MODULATION.

Previous Symbols	Present Symbol	S(t)
0	0	$A\cos(2\pi f_0 t)$
0	1	$A\cos(2\pi f_1 t)$
1	0	$-A\cos(2\pi f_0 t)$
1	1	$-A\cos(2\pi f_1 t)$

With the above considerations and using standard trigonometric identities (9.34) may be rewritten as

$$s(t) = g(t)\cos(2\pi f_c t) + g(t - T_b)\sin(2\pi f_c t) \tag{9.38}$$

where

$$g(t) = A\cos\left[\theta(0)\right]\cos\left(\frac{\pi}{2T_b}t\right) \quad , \quad -T_b \le t \le T_b \tag{9.39}$$

is the symbol shaping function.

GMSK Modulation

From the above discussion we understand that the MSK modulation yields a constant envelope and has coherent detection capability. Moreover, as we shall see, the bandwidth of the modulated wave is relatively narrow. On the other hand, its out-of-

band radiation cannot be neglected, constituting a serious constraint for mobile rad applications.

The output power spectrum of MSK can be controlled by low-pass filtering th binary input data prior to modulation. This guarantees the constant envelop property, an essential feature that renders the mobile signal robust against fading However, in order to accomplish this, the Low Pass Filter (LPF) must present th following properties [6]:

- narrow bandwidth and sharp cutoff, to suppress high-frequency components;
- low overshoot impulse response, to protect against excessive instantaneou frequency deviation;
- preservation of the filter output pulse area, corresponding to a phase shift of $\pi/2$, for simple coherent detection.

The above conditions are satisfied by a Gaussian LPF and the modified MSK modulation is referred to as Gaussian MSK or GMSK.

9.8.1 Generation and Detection of MSK and GMSK Signals

Modulation

An orthogonal modulator, as described by (9.38), can be designed to implement the MSK function. Since the spectral density of an orthogonal FSK signal depends on its symbol shaping functions, the latter can be manipulated to yield the desired output power spectrum. Consequently, several related modulation techniques can be derived by simply using an appropriate symbol shaping function. Tamed Frequency Modulation (TFM) and Minimum Shift Keying are some of the many existing techniques that use an orthogonal modulator, as shown in Figure 9.9a.

However, the simplest way of generating an MSK signal or a GMSK signal is by means of an FM modulator. In the case of MSK, the information bit stream is used to modulate the frequency of a VCO. As for GMSK, the information bit stream is first low pass filtered through a Gaussian filter and then used to modulate the frequency of a VCO. This scheme is shown in Figure 9.9b. The weak point of this solution is the

difficulty of keeping the centre frequency within a range where the linearity and sensitivity of the FM modulator are still kept. More elaborate solutions, such as, the orthogonal modulator or the use of PLL circuitry, can be used to minimize this problem.

Demodulation

Like the QPSK systems, MSK and also GMSK can be coherently demodulated in quadrature channels, as shown in Figure 9.10a. Note that the integration interval is $2T_b$ and that the quadrature channel is delayed by one bit interval (T_b) with respect to the in-phase channel. After the threshold detection (decision device) the bits are combined to restore the original information.

Noncoherent detection can be accomplished by the use of a limiter and frequency discriminator as shown in Figure 9.10b. This is an easy and economical way of performing demodulation at the expenses of a system performance degradation. The Limiter supplies the Discriminator with a constant envelope signal. The Discriminator has an output proportional to the derivative of the instantaneous phase of the input signal, corresponding to the signal frequency. The Decision Device samples the detected frequency and compares it with a set of thresholds to decide the transmitted frequency.

9.8.2 Power Spectra of MSK and GMSK Signals

The power spectral density is determined on the assumption that the input binary wave is random, with symbols 1 and 0 equally likely and transmitted during statistically independent time slots. The power spectral density of the band-pass signal is basically dependent on its symbol-shaping functions g(t), given by (9.39), and $g(t - T_b)$. These functions have the same energy spectral densities $\psi_g(f)$ given by $|G(f)|^2$, where G(f) is the Fourier transform of g(t). Therefore

$$\psi_g(f) = 16\frac{AT_b^2}{\pi^2}\left[\frac{\cos 2\pi T_b f}{1 - (4T_b f)^2}\right]^2 \qquad (9.40)$$

The power spectral densities of the in-phase and quadrature components are given by $\psi_g(f)$ averaged over the symbol-shaping function duration $2T_b$, i.e., $S_Q(f) = S_I(f) = \psi_g(f)/2T_b$ (see Appendix 9A). Since these components are statistically independent, by following the same reasoning as in the QPSK case (section 9.7.2) we find that the one-sided power spectral density, S(f), of the MSK signal s(t) is,

$$S(f) = \frac{16(A^2/2)}{\pi^2} T_b \left\{ \frac{\cos\left[2\pi T_b (f - f_c)\right]}{1 - \left[4T_b (f - f_c)\right]^2} \right\}^2 \qquad (9.41)$$

The spectral density of an MSK signal given by (9.41) can be seen in Figure 9.11 normalized with respect to T_b and the carrier power $A^2/2$. Note that the MSK spectrum falls off at a higher rate than that of QPSK. On the other hand, the main lobe of the MSK spectrum is wider than that of QPSK, having their respective first nulls occurring for $T_b(f - f_c) = 0.75$ and 0.5.

As for the GMSK signal, its power spectrum corresponds to that of the MSK signal but modified by the effects of the premodulation Gaussian low-pass filtering. This is shown in Figure 9.11 (from [6]) where the normalized 3 dB down bandwidth, B_bT_b, of the Gaussian LPF is a parameter. Note that, when B_bT_b tends to infinity, the power spectrum of GMSK coincides with that of MSK. As B_bT_b increases, so does the rate at which the power spectrum falls. The parameter B_bT_b has a great influence on the spectrum efficiency and must be carefully selected by the system designer. Murota [6] has shown that an optimum condition for maximizing the spectral efficiency of GMSK cellular radio system is obtained when $B_bT_b = 0.25$. For this situation, (i) with a channel spacing of 25 kHz, (ii) with a bit rate of $1/T_b = 16$ kbits/s and (iii) with a predetection rectangular band-pass $B_iT_b = 1$, the out-of-band radiation power-to-total power ratio is less than -60 dB, as specified by CCIR [7].

9.8.3 BER Performance Over a Gaussian Channel

In this section we shall consider the bit error rate performance of MSK and GMSK

modulations in the presence of additive white Gaussian noise using coherent detection.

MSK Signal

The detection of an MSK signal s(t) is carried out in a way similar to that of QPSK. The mean value of the received signal is evaluated at each branch of the demodulation as indicated in Figure 9.10a. These estimated values are

$$\bar{I} = \frac{1}{2T_b}\int_{-T_b}^{T_b}\left[s(t) + \text{Noise}\right]\sqrt{2}\cos\left(\frac{\pi}{2T_b}\right)\cos(2\pi f_c t)dt$$

$$= \bar{Q} = \frac{1}{2T_b}\int_{0}^{2T_b}\left[s(t) + \text{Noise}\right]\sqrt{2}\sin\left(\frac{\pi}{2T_b}\right)\sin(2\pi f_c t)dt$$

$$= A/2 + n(t) \qquad (9.42)$$

Following the same procedure as for the QPSK, we find that both techniques present the same bit error probability P_b

$$P_b = \frac{1}{2}\left[\text{erfc}\left(\sqrt{\gamma_b}\right) - \frac{1}{4}\text{erfc}^2\left(\sqrt{\gamma_b}\right)\right] \qquad (9.43)$$

Equation (9.43) is plotted in Figure 9.12.

GMSK Signal

The GMSK modulation may be viewed as a modified version of MSK, both MSK and GMSK constituting binary digital modulations. As such, their BER performance, for high signal-to-noise ratio, γ_b, may be approximated by

$$P_b \approx \frac{1}{2}\text{erfc}\left(\sqrt{\alpha\gamma_b}\right) \qquad (9.44)$$

where the parameter α depends on the premodulation Gaussian low pass filter. In other words, α is a function of the parameter B_bT_b. For $B_bT_b = \infty$, α is found to be equal to 1, corresponding to the case of the MSK modulation. For the optimum condition $B_bT_b = 0.25$, the parameter α is found to be approximately equal to 0.68 [6]. The probability of the bit error for this condition is plotted in Figure 9.12.

9.8.4 BER Performance Over a Fading Channel

MSK Signal (Non-Selective Fading)

As we remarked before, the BER performance of the MSK modulation equals that of QPSK. Therefore, its bit error probability can be estimated by using (9.29) in (9.28) and the resultant equation in (9.25). The corresponding curve is reproduced in Figure 9.12.

A thorough study on the performance of MSK system in fast Rayleigh fading environment (selective fading) with differential and discriminator detection can be found in the publications by Hirade et al. [8,9] and in the book edited by Feher [1].

GMSK Signal (Non-Selective Fading)

An approximate BER performance can be estimated by averaging (9.43) over the distribution of γ_b given by (9.26). The resultant bit error probability, neglecting the quadratic term $\text{erfc}^2(\circ)$, is

$$P_b \propto \int_0^{\infty} \frac{1}{2}\text{erfc}\left(\sqrt{\alpha\gamma_b}\right) p(\gamma_b)d\gamma_b$$

$$\propto \frac{1}{2}\left(1 - \sqrt{\frac{\alpha\gamma_{b0}}{1 + 2\gamma_{b0}}}\right) \qquad (9.45)$$

where the parameter α depends on the premodulation Gaussian LPF bandwidth. This BER is plotted in Figure 9.12 for $\alpha = 0.68$ ($B_bT_b = 0.25$).

GMSK Signal (Selective Fading)

The BER performance of the GMSK modulator in a fast Rayleigh fading environment has been evaluated experimentally by means of a Rayleigh fading simulator [6]. The corresponding curves for various values of the maximum Doppler frequency, f_D, is shown in Figure 9.12 [6].

9.9 COMBINED TECHNIQUES

In the introduction section of this chapter we remarked that the main processes

composing a digital communication system are A/D Conversion and Modulation. In fact this is a simplified model of a digital system, adopted as such for convenience. A more complete model would include a Channel Coding block in between A/D Conversion and Modulation. The Channel Coding is responsible for introducing redundancy in the speech signal after the A/D Conversion process. It may sound curious (or rather senseless) reintroducing redundancy into a signal from which most of it had been extracted in a previous step. The interesting point is that the extracted redundancy has an unpredictable characteristic, while the reintroduced one is totally controllable. The signal without the "unpredictable" redundancy is very susceptible to a disastrous (abrupt) degradation with the noise increase in the system. With the inclusion of the controllable redundancy the signal may suffer a graceful degradation, instead.

The use of controllable redundancy (error-correcting codes) improves the error rate performance of the system at the expenses of extra bits included in the data stream. Accordingly, the modulator must operate at higher bit rate, requiring extra channel bandwidth. Higher order modulation schemes can be used to save bandwidth , but larger signal power is required in order to maintain the same error probability. Some alternative solutions have recently been proposed and they are briefly described next.

TCM - Combined Modulation and Coding

In Trellis Coded Modulation (TCM) modulation and coding are treated not as individual entities, but rather as a unique process. In TCM a higher order modulation is combined with convolutional code to improve the error rate performance while keeping the bandwidth unaltered. At the receiver end, instead of performing demodulation and then decoding, both processes are carried out in one single step. The performance of the system is dictated by the free Euclidean distance between the transmitted signal sequences, instead of the free Hamming distance of the convolutional code. Therefore, the choice of code and signal constellation must be performed jointly. The detection process should involve soft decision rather than hard

decision, improving the performance.

This combined scheme was first explored by Ungerboeck [22], using a modulator constellation twice as large as that necessary for uncoded transmission. Although the bandwidth was kept the same, a power gain was accomplished. The asymptotic coding gain of Ungerboeck codes is given by

$$G = 10\log\left(\frac{d_{free}}{d_{ref}}\right)^2$$

where d_{free} is the free Euclidean distance of the code, and d_{ref} is the minimum Euclidean distance of an uncoded modulation scheme operating with the same energy per bit.

Unequal Error Protection

Redundancy can be more efficiently utilized if the bits with more relevant information of the speech signal are better protected. This technique is known as Unequal Error Protection.

9.10 SUMMARY AND CONCLUSIONS

The main appeal for digital communication is that it renders the system more flexible to accommodate the technological evolution. Following the worldwide trend of network digitization, the second generation of mobile radio has adopted the full digital approach. The digital technology is rather attractive but requires a special attention when radio transmission is involved. The problems become more challenging in the mobile radio case.

One of the greatest challenges of using digital radio communication is the reduction of the required bandwidth. As we know, digital transmission requires a far greater bandwidth than that of the analog transmission. As far as digital transmission is concerned, bandwidth reduction is directly related to bit rate reduction.

The use of appropriate speech coding algorithms can drastically reduce the number of bits required to encode the speech. These algorithms are based on the fact that the human speech contains a great deal of redundancy. If the redundancies are appropriately extracted, the resultant speech will still present acceptable quality and can be represented with fewer bits. From the conventional 64-kbits/s PCM, the speech coding algorithms have evolved to a bit rate of less than 8 kbits/s still keeping toll-quality.

Higher order modulation schemes can also be used to reduce bandwidth. Given that a high order modulation is used, the other requirement is that it should present an almost constant envelope for robustness against fading. Moreover, "insensitivity" to non linear amplification is also a requisite. The great challenge, however, is to conciliate power efficiency and spectral efficiency. Power efficient techniques present low bit error rate, obtained at the expenses of a wider spectrum. Spectrally efficient modulation techniques, on the other hand, offer a poor BER performance.

A promising approach is to combine modulation and coding to be treated as an unique entity. In the combined approach it is possible to introduce redundancy (error-correcting code) to render the transmission robust while keeping the same bandwidth. The usual approach is known a Trellis Coded Modulation (TCM). It is also possible to extract the redundancy of the speech by means of a Trellis Coded Quantization (TCQ) [23] and then combine TCQ/TCM in order to make large mean-square error in the source coding very unlikely [24].

APPENDIX 9A

Power Spectral Density

9A.1 Power Spectral Density

Let g(t) be a power signal* and $g_T(t)$ its truncated version, so that $g_T(t) = g(t)$ for $-T \le t \le T$ and $g_T(t) = 0$, otherwise. Therefore, the average signal power is

$$P = \lim_{T\to\infty}\frac{1}{2T}\int_{-T}^{T} g^2(t)dt = \lim_{T\to\infty}\frac{1}{2T}\int_{-\infty}^{\infty} g_T^2(t)dt \qquad (9A.1)$$

Let $G_T(f)$ be the Fourier transform of $g_T(t)$,i.e., $G_T(f) = \mathfrak{F}\left[g_T(t)\right]$. Using the convolution property we note that

$$\mathfrak{F}\left[g_T^2(t)\right] = G_T(f) * G_T(f) = \int_{-\infty}^{\infty} G_T(\lambda)G_T(f-\lambda)d\lambda \qquad (9A.2)$$

Using the definition of the Fourier transform we have

$$\mathfrak{F}\left[g_T^2(t)\right] = \int_{-\infty}^{\infty} g_T^2(t)\exp(-2\pi ft)dt \qquad (9A.3)$$

Equating (9.2) and (9A.3) for $f = 0$ we obtain

$$\int_{-\infty}^{\infty} g_T^2(t)dt = \int_{-\infty}^{\infty} G_T(\lambda)G_T(-\lambda)d\lambda = \int_{-\infty}^{\infty} |G_T(\lambda)|^2 d\lambda \qquad (9A.4)$$

Replacing (9A.4) into (9A.1) with a convenient change of variables we obtain

$$P = \int_{-\infty}^{\infty} S_g(f)df$$

---

* Power signal has infinite energy

where

$$S_g(f) = \lim_{T\to\infty} \frac{1}{2T} |G_T(f)|^2 \tag{9A.5}$$

is called the power spectral density or power spectrum of g(t).

9A.2 Correlation Function

We can rewrite (9A.5) in terms of $\overline{G}_T(f)$, the complex conjugate of $G_T(f)$. Hence

$$S_g(f) = \lim_{T\to\infty} \frac{1}{2T} G_T(f)\overline{G}_T(f) \tag{9A.6}$$

Using the convolution property we find that

$$\begin{aligned} \mathfrak{F}\left[g_T^2(t)\right] &= \lim_{T\to\infty} \frac{1}{2T} g_T(\tau) * g_T(-\tau) \\ &= \lim_{T\to\infty} \frac{1}{2T} \int_{-\infty}^{\infty} g_T(t)g_T(t-\tau)dt \triangleq R_g(\tau) \end{aligned} \tag{9A.7}$$

The function on the right hand side, $R_g(\tau)$, is called autocorrelation function of the power signal. This function can be redefined in terms of the power signal as

$$R_g(\tau) = \lim_{T\to\infty} \frac{1}{2T} \int_{-\infty}^{\infty} g_T(t)g_T(t-\tau)dt \tag{9A.8}$$

From (9A.7) we conclude that the power spectral density is the Fourier transform of the autocorrelation function, i.e.,

$$S_g(f) = \int_{-\infty}^{\infty} R_g(\tau)\exp(-2\pi\tau f)d\tau \tag{9A.9}$$

Now consider a stationary process X(t). Its autocorrelation function is defined as

$$R_x(\tau) = E\left[X(t)X(t-\tau)\right] \tag{9A.10}$$

9A.3 Modulated Wave

Let y(t) be a modulated wave

$$y(t) = g(t)\cos(2\pi f_c t) \tag{9A.11}$$

Using (9A.5)

$$S_y(f) = \lim_{T\to\infty} \frac{1}{2T} |Y_T(f)|^2 \tag{9A.12}$$

where $Y_T(f) = \mathfrak{F}\left[y_T(t)\right]$ and

$$y_T(t) = g_T(t)\cos(2\pi f_c t) \tag{9A.13}$$

Hence

$$Y_T(f) = \frac{1}{2}\left[G_T(f - f_c) + G_T(f + f_c)\right] \tag{9A.14}$$

With (9A.14) in (9A.12) we find

$$S_y(f) = \lim_{T\to\infty} \frac{1}{4}\left[|G_T(f - f_c)|^2 + |G_T(f + f_c)|^2\right]$$

$$\frac{1}{4}\left[S_g(f - f_c) + S_g(f + f_c)\right] \tag{9A.15}$$

since $G_T(f - f_c)$ and $G_T(f + f_c)$ are non overlapping spectra (their cross-product is nil).

The same result is obtained for a modulated stationary process Y(t) such that

$$Y(t) = X(t)\cos(2\pi f_c t + \theta) \tag{9A.16}$$

where X(t) is a stationary process and θ is a random variable uniformly distributed over 0 and 2π. In this case

$$R_y(\tau) = E\left[Y(t + \tau)Y(t)\right]$$

$$= \frac{1}{2}E\left[X(t + \tau)X(t)\right]E\left[\cos(2\pi f_c \tau) + \cos(4\pi f_c t + 2\pi f_c t + 2\theta)\right]$$

$$= \frac{1}{2}R_x(\tau)\cos(2\pi f_c \tau) \tag{9A.17}$$

Taking the Fourier transform of (9A.17) we find

$$S_y(f) = \frac{1}{4}\left[S_x(f - f_c) + S_x(f + f_c)\right] \tag{9A.18}$$

9A.4 Random Binary Wave [11]

Let x(t) be a sample function of a random binary process X(t) assuming amplitude levels of -A and +A with equal probability . Let T be the duration of each pulse. Consider t_d, the sample value of a uniformly distributed variable T_d, as the starting time of the first pulse. Hence the distribution of T_d is

$$p_{Td}(t_d) = \frac{1}{T} \qquad 0 \le t_d \le T \tag{9A.19}$$

We want to find the autocorrelation function $R_x(t_i,t_j)$ where t_i and t_j are the times of observations of X(t).

If $|t_i - t_j| > T$, then $X(t_i)$ and $X(t_j)$ occur in different-pulse intervals. Therefore, they are independent and

$$E\left[X(t_i)X(t_j)\right] = E\left[X(t_i)\right]E\left[X(t_j)\right] = 0$$

since $$E\left[X(t)\right] = 0 \quad \forall\ t$$

Let $|t_i - t_j| < T$, with $t_i = 0$ and $t_j < t_i$. In this case $X(t_i)$ and $X(t_j)$ occur in the same pulse interval if $t_d < T - |t_j - t_j|$. Therefore

$$E\left[X(t_i)X(t_j)/t_d\right] = A^2 \qquad , \qquad t_d < T - |t_i - t_j|$$

Then

$$R_x(\tau) = E\left[X(t_i)X(t_j)\right] = \int_0^{T-|\tau|} A^2 P_{Td}(t_d)dt_d$$

$$= A^2\left(1 - \frac{|\tau|}{T}\right) \qquad |\tau| < T \tag{9A.20}$$

where $\tau = |t_i - t_j|$.

Taking the Fourier transform of $R_x(\tau)$ we obtain

$$S_x(f) = A^2 T \text{sinc}^2(fT) \tag{9A.21}$$

where $\text{sinc}(x) = \sin(\pi x)/(\pi x)$.

If we estimate the energy spectral density $\psi_g(t)$ of a rectangular pulse g(t) of amplitude A and duration T we obtain

$$\psi_g(f) = |G(f)|^2 = A^2 T^2 \text{sinc}^2(fT) \tag{9A.22}$$

Therefore we may state that the power spectral density $S_x(f)$ of a random binary wave assuming values +g(t) and -g(t) is given by

$$S_x(f) = \frac{\psi_g(f)}{T} \tag{9A.23}$$

where T is symbol duration and g(t) is the symbol shaping function.

REFERENCES

[1] K. Feher, ed., *Advanced Digital Communications - Systems and Signal Processing Techniques*, Prentice-Hall , N. Jersey, 1987.

[2] Simon Haykin, *Digital Communications*, John Wiley & Sons, 1988.

[3] K. Feher, *Digital Communications, Satellite/Earth Station Engineering*, Prentice-Hall, N.J., 1981.

[4] J.G. Proakis, *Digital Communications*, McGraw-Hill, 1983.

[5] H. Suzuki, "Canonic Receiver Analysis for M-ary Angle Modulations in Rayleigh Fading Environment", *IEEE Transactions Vehicular Technology*, Vol. VT-31, No. 1, February 1982.

[6] K. Murota and K. Hirade, "GMSK Modulation for Digital Mobile Radio Telephony", *IEEE Transactions Communications*, Vol COM-29, No. 7, July 1981.

[7] CCIR Rec. 478-3, *Technical Characteristics of Equipment and Principles Governing the Allocation of Frequency Channels Between 25 and 1000 MHz for the Land Mobile Service*, p. 13, 1982.

[8] K. Hirade, M. Ishizuka and F. Adachi, "Error-Rate Performance of Digital FM with Discriminator-Detection in the Presence of Cochannel Interference Under Fast-Rayleig Environment", *Trans. IECE of Japan*, Vol. 61-E, p.704, September 1978.

[9] K. Hirade, M. Ishizuka, F. Adachi and K. Ohtani, "Error-Rate Performance of Digital FM with Differential Detection in Land Mobile Radio Channel, *IEEE Transaction Vehicular Technology*, Vol. VT-28, p. 204, August 1979.

[10] F. Adachi and K. Ohno, "Performance Analysis of GMSK Frequency Detection with Decision Feedback Equalization in Digital Land Mobile Radio, *IEE Proceedings*, Vol. 135, Pt. F, No. 3, June 1988.

[11] S. Haykin, *Digital Communications*, John Wiley & Sons, 1988.

[12] D. O'Shaughnessy, *Speech Communication - Human and Machine*, Addison-Wesley Publishing Company, 1987.

[13] P. Vary, K. Hellwig, R. Hofmann, R.J. Sluyter, C. Galand and M. Rosso, "Speech Codec for the European Mobile Radio System", *Proceedings Int. Conf. on Acoustics Speech and Signal Processing, ICASSP-1988*, pp. 227-230

[14] P. Vary, "GSM Speech Codec", *Proceedings of the Digital Cellular Radio Conference*, Hagen FRG, October 1988.

[15] B.S. Atal and M.R. Schroeder, "Stochastic Coding of Speech Signals at Very Low Bit Rates", *Proc IEEE Int Conf. Communications*, p. 48.1, May 1984.

[16] M.R. Schroeder and B.S. Atal, "Code-Excited Linear Prediction (CELP): High Quality Speech at Very Low Bit Rates", *Proc IEEE Int. Conf. Acoust, Speech, Signal Processing*, pp. 937-940, March 1985.

[17] EIA/TIA, Project Number 2215, Cellular System-Dual-Mode Mobile Station - Base Station Compatibility Standard, IS-54, December 1989.

[18] J.P. Adoul, P. Mabilleau, M. Delprat and S. Morissette, "Fast CELP Coding Based on Algebraic Codes", *Proc IEEE Int. Conf. Acoust, Speech, Signal Processing*, pp. 1957-1960, 1987.

[19] J.P. Adoul and C. Lamblin, "A Comparison of Some Algebraic Structures for CELP Coding of Speech, *Proc IEEE Int. Conf. Acoust, Speech, Signal Processing*, pp. 1953-1956, 1987.

[20] J.C. Bellamy, *Digital Telephony*, John Wiley & Sons, N.Y., 1982.

[21] G. Calhoun, *Digital Cellular Radio*, Artech House, 1988.

[22] G. Ungerboeck, "Channel Coding with Multilevel/Phase Signals", *IEEE Transaction Information Theory*, VT IT-28, pp. 55-67, January 1982.

[23] M.W. Marcellin and T.R. Fischer, "Trellis Coded Quantization of Memoryless and Gauss-Markov Sources", *IEEE Transaction Communication*, Vol. 38, pp. 82-93, January 1990.

[24] T.R. Fischer and M.W. Marcellin, "Joint Trellis Coded Quantization/Modulation", *IEEE Transaction Communication*, Vol. 39, No. 2, pp. 172-176, February 1991.

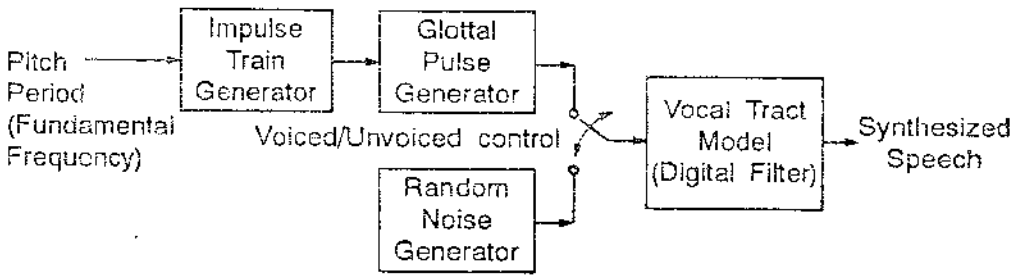

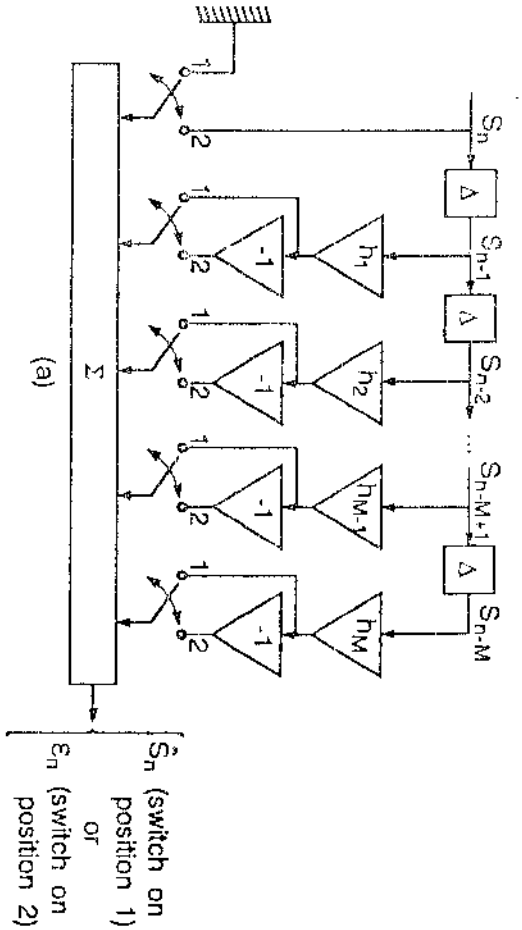

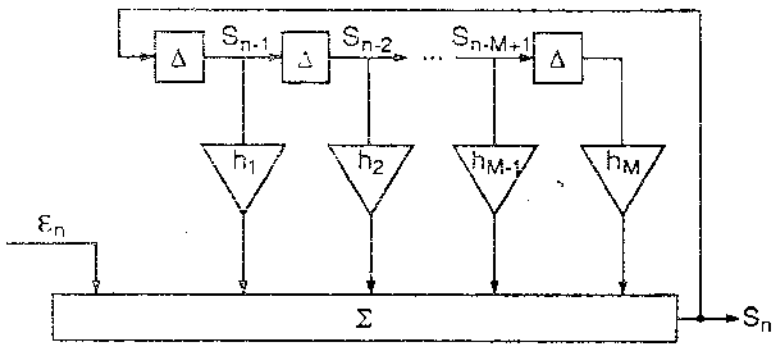

(b)

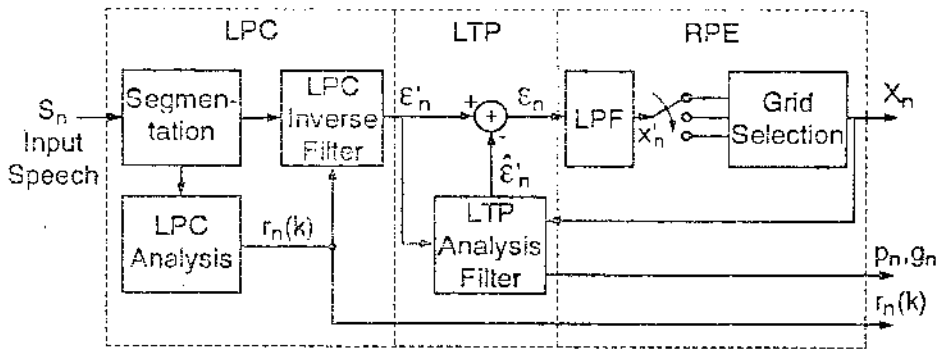

(a)

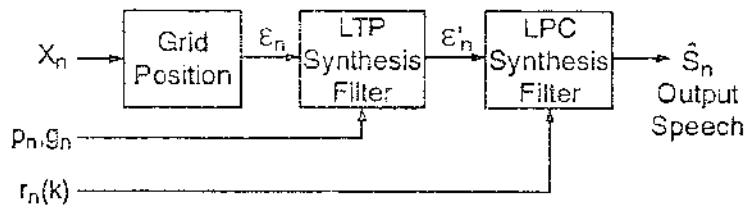
X_n
Grid Position
ε_n
LTP Synthesis Filter
ε'_n
LPC Synthesis Filter
$\hat{S}_n$ Output Speech
P_n, g_n
$r_n(k)$

(b)

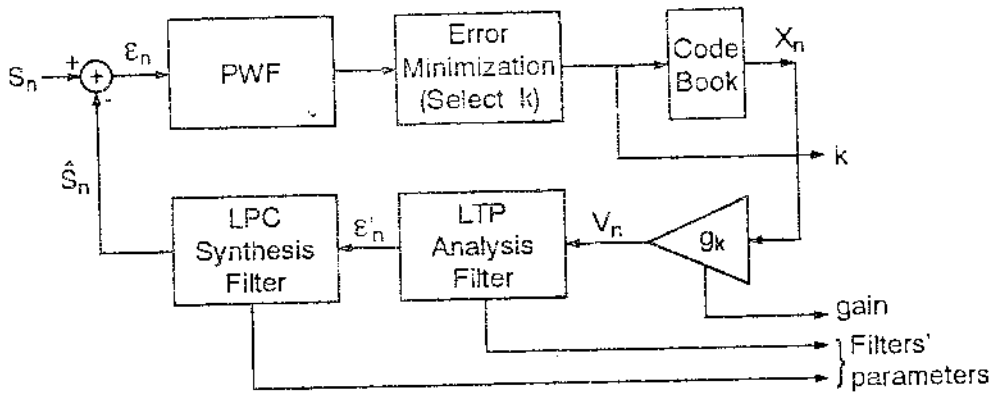
S_n
+
-
ε_n
PWF
Error Minimization (Select k)
Code Book
X_n
k
$\hat{S}_n$
LPC Synthesis Filter
ε'_n
LTP Analysis Filter
V_n
g_k
gain
Filters' parameters

(a)

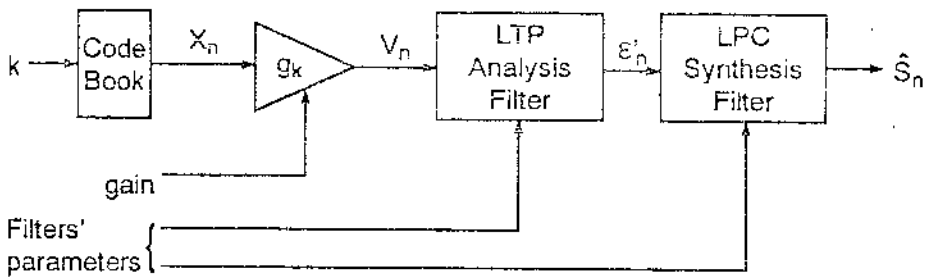

(b)

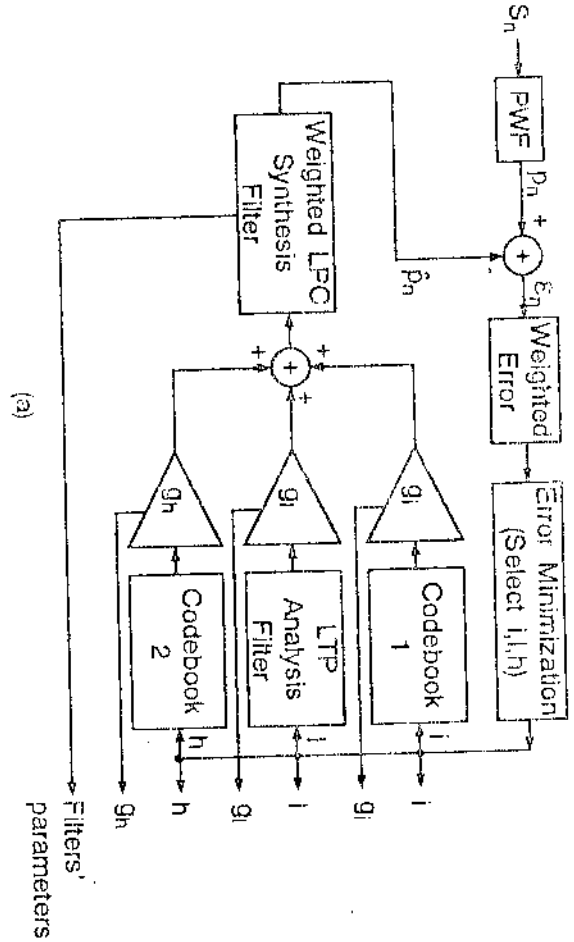

(a)

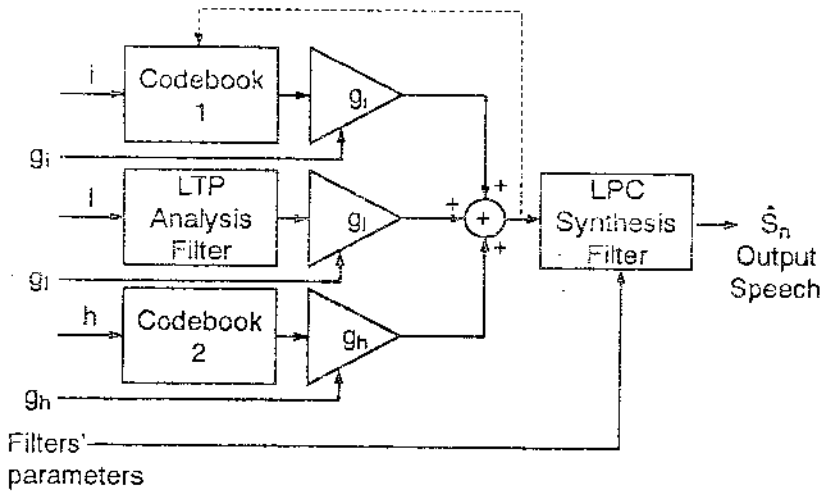

(b)

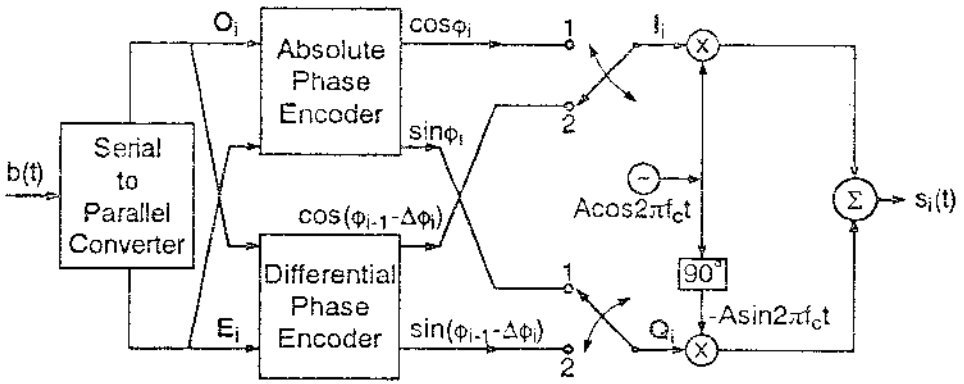
b(t)
Serial to Parallel Converter
O_i
E_i
Absolute Phase Encoder
Differential Phase Encoder
$\cos\varphi_i$
$\sin\varphi_i$
$\cos(\varphi_{i-1}-\Delta\varphi_i)$
$\sin(\varphi_{i-1}-\Delta\varphi_i)$
1
2
1
2
I_i
Q_i
$A\cos 2\pi f_c t$
90°
$-A\sin 2\pi f_c t$
Σ
$s_i(t)$

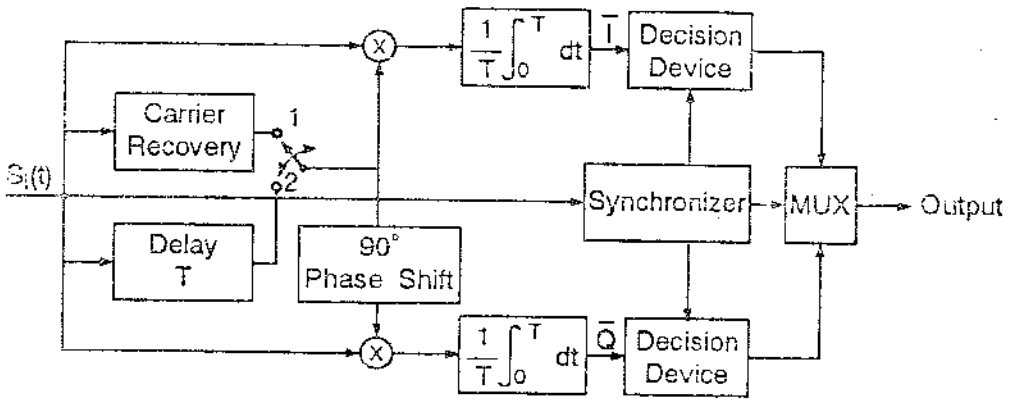

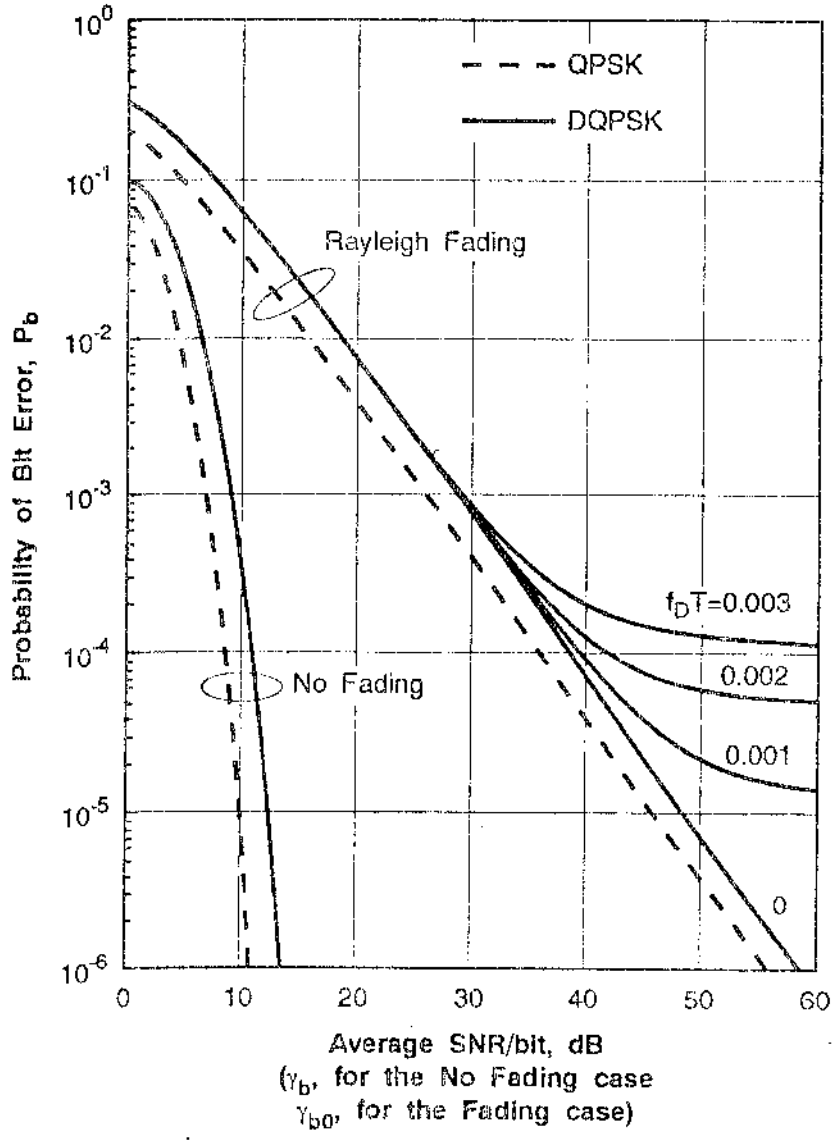
QPSK
DQPSK
Rayleigh Fading
No Fading
f_DT=0.003
0.002
0.001
0
Probability of Bit Error, P_b
10^0
10^{-1}
10^{-2}
10^{-3}
10^{-4}
10^{-5}
10^{-6}
0
10
20
30
40
50
60
Average SNR/bit, dB
(γ_b, for the No Fading case
γ_{b0}, for the Fading case)

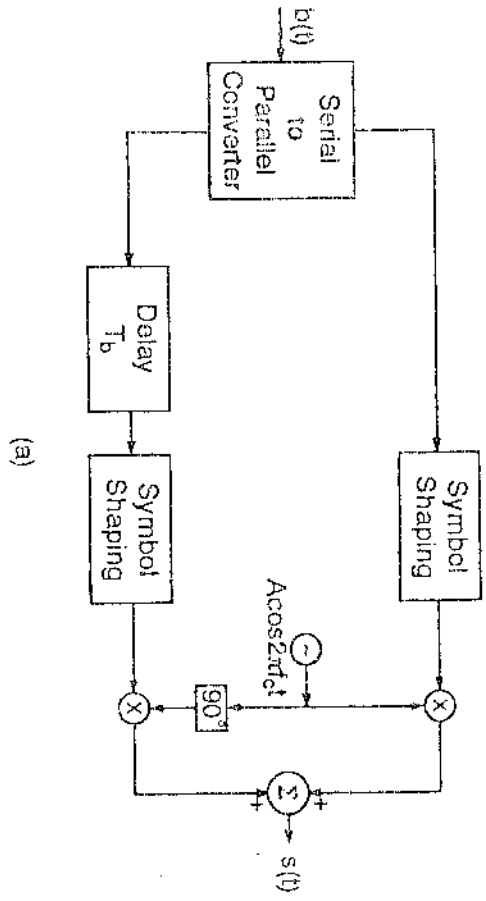

(a)

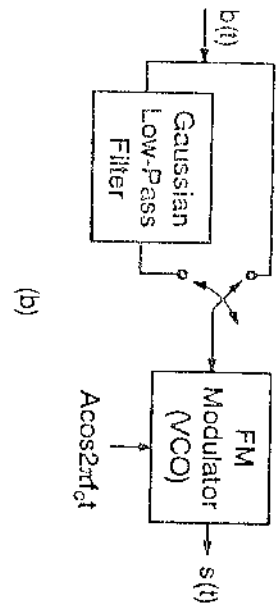

(b)

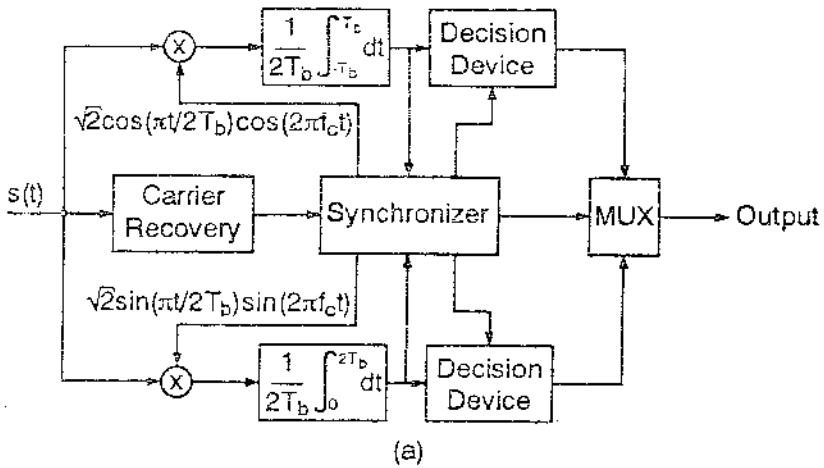

(a)

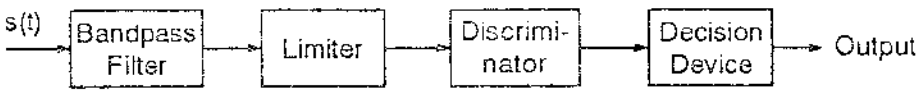

(b)

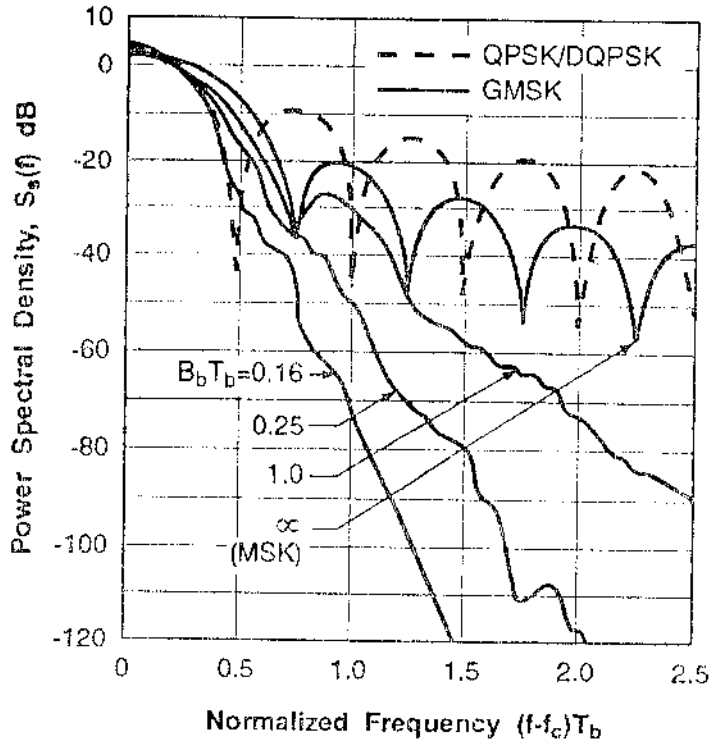
10
0
-20
-40
-60
-80
-100
-120
0
0.5
1.0
1.5
2.0
2.5
QPSK/DQPSK
GMSK
B_bT_b=0.16
0.25
1.0
∝
(MSK)
Power Spectral Density, $S_s(f)$ dB
Normalized Frequency $(f-f_c)T_b$

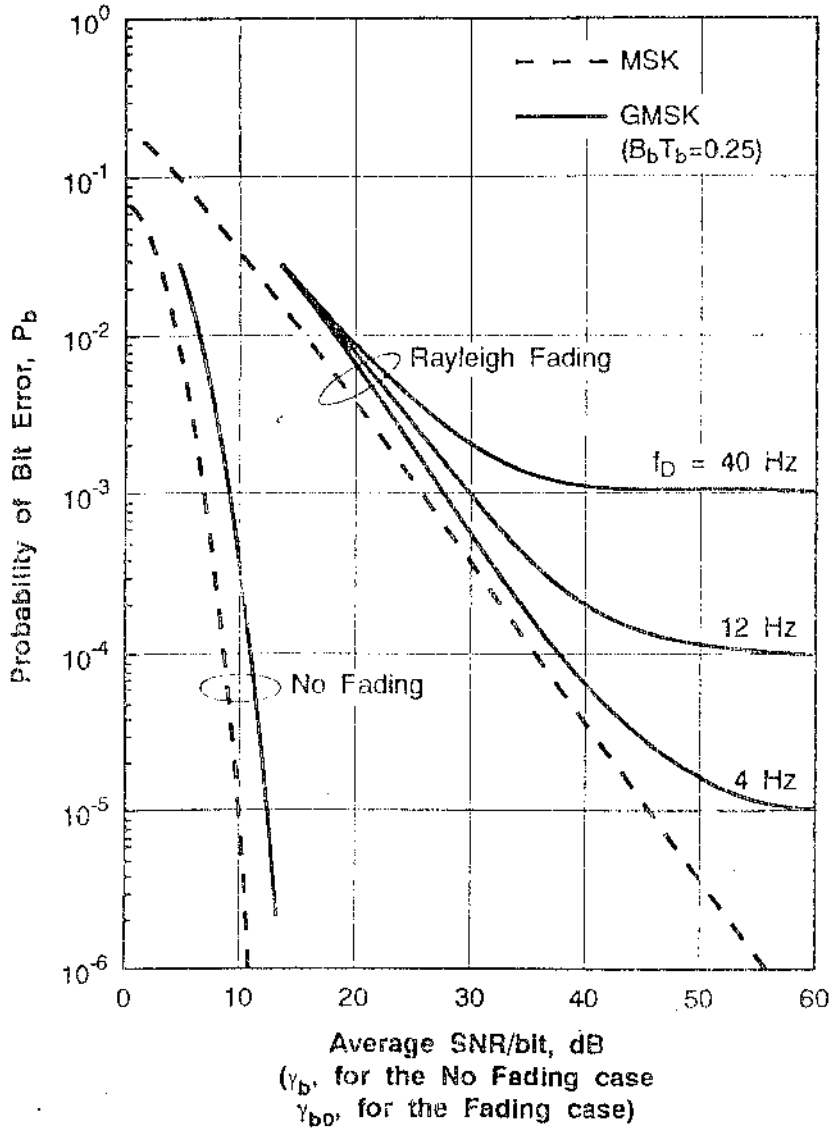
MSK
GMSK
(B_bT_b=0.25)
Rayleigh Fading
f_D = 40 Hz
12 Hz
4 Hz
No Fading
Probability of Bit Error, P_b
10^0
10^{-1}
10^{-2}
10^{-3}
10^{-4}
10^{-5}
10^{-6}
0
10
20
30
40
50
60
Average SNR/bit, dB
(γ_b, for the No Fading case
γ_{bD}, for the Fading case)

Fig 8.12 1503

ANEXO A

VOLUME III

FOUNDATIONS OF MOBILE RADIO ENGINEERING

MICHEL DAOUD YACOUB

PART V

MULTIPLE ACCESS

CHAPTER 10

MULTIPLE - ACCESS ARCHITECTURE

PREAMBLE

This chapter examines the various transmission technologies that can be used in a mobile radio system. The different approaches can be broadly grouped into two categories: narrowband and wideband transmission. Narrowband and wideband systems are then examined and their features and limitations are discussed. The bulk of the chapter is dedicated to the three multiple access schemes, namely FDMA, TDMA and CDMA. These methods are analyzed independently, according to their own characteristics. The basics of the three access schemes and their advantages/disadvantages are also considered. Particularly, for the FDMA case we discuss the effects of nonlinearities of the radio equipment circuitry. In TDMA systems the main issues are timing hierarchy, synchronization and efficiency measures. CDMA systems are then analyzed in the light of information of the spread spectrum technology. Accordingly, a great deal of the corresponding section is steered towards providing the background for spread spectrum fundamentals and techniques. Finally, we discuss the modes of providing two-way communications in a fully-trunked system. These techniques are named Frequency Division Duplex and Time Division Duplex and their main characteristics are briefly analyzed.

10.1 INTRODUCTION

Resources sharing can be a very efficient way of achieving high capacity in any communication network. As far as mobile radio systems are concerned the resources are

the channels, or more generically, the bandwidth. To be more efficient the access mode must allow any terminal (the mobiles) to be able to use the resources in a fully-trunked system. If the channels are assigned on demand, the procedure is called Demand-Assigned Multiple Access (DAMA), or simply Multiple Access.

Depending on how the available spectrum is utilized the system can be broadly classified into Narrowband or Wideband. In the narrowband architecture the total frequency band is split into several narrowband channels, whereas in the wideband architecture the whole or a significant amount of the spectrum is available to all the users.

There are basically three access methods according to the means (frequency, time, code) used to implement them:

- Frequency Division Multiple Access (FDMA)
- Time Division Multiple Access (TDMA)
- Code Division Multiple Access (CDMA)

FDMA is intrinsically a narrowband architecture while CDMA is a wideband one. TDMA, on the other hand, can be implemented either as a narrowband or as a wideband system.

When two-way communications are involved, the full-duplex connection can be provided by means of frequency or time division. In the first case we have Frequency Division Duplex (FDD) and in the second case we have Time Division Duplex (TDD).

All these issues will be examined in this chapter.

10.2 NARROWBAND AND WIDEBAND ARCHITECTURES [3]

Narrowband Architecture

Narrowband systems divide the total frequency spectrum into as many channels as the technology allows. Actually, each channel comprises a set of two carrier frequencies used for the two-way communication. Frequencies used for the uplink (mobile to base station) are named *reverse channels*, whereas frequencies of the

the channels, or more generically, the bandwidth. To be more efficient the access mode must allow any terminal (the mobiles) to be able to use the resources in a fully-trunked system. If the channels are assigned on demand, the procedure is called Demand-Assigned Multiple Access (DAMA), or simply Multiple Access.

Depending on how the available spectrum is utilized the system can be broadly classified into Narrowband or Wideband. In the narrowband architecture the total frequency band is split into several narrowband channels, whereas in the wideband architecture the whole or a significant amount of the spectrum is available to all the users.

There are basically three access methods according to the means (frequency, time, code) used to implement them:

- Frequency Division Multiple Access (FDMA)
- Time Division Multiple Access (TDMA)
- Code Division Multiple Access (CDMA)

FDMA is intrinsically a narrowband architecture while CDMA is a wideband one. TDMA, on the other hand, can be implemented either as a narrowband or as a wideband system.

When two-way communications are involved, the full-duplex connection can be provided by means of frequency or time division. In the first case we have Frequency Division Duplex (FDD) and in the second case we have Time Division Duplex (TDD).

All these issues will be examined in this chapter.

10.2 NARROWBAND AND WIDEBAND ARCHITECTURES [3]

Narrowband Architecture

Narrowband systems divide the total frequency spectrum into as many channels as the technology allows. Actually, each channel comprises a set of two carrier frequencies used for the two-way communication. Frequencies used for the uplink (mobile to base station) are named *reverse channels*, whereas frequencies of the

FDMA and narrowband TDMA are considered as narrowband architectures.

Wideband Architecture

The main feature of wideband systems is that either all the spectrum available or a considerable portion of it is used by each carrier. This is exactly the case for wideband TDMA systems, whereas CDMA systems frequently use the whole frequency spectrum.

The great advantage of wideband systems is that the transmission bandwidth always exceeds the coherence bandwidth for which the signal experiences only selective fadings. That is, only a small fraction of the frequencies composing the signal is affected by fading. While fades are quite frequent and deep (20–40 dB) in narrowband systems the spreading of the signal throughout the whole bandwidth in wideband systems works towards minimizing their effects, so that these same fades would provoke a much milder effect (2–3 dB) [14]. Likewise, both deliberate and non intentional interferences are reduced with the use of wideband techniques.

In particular, CDMA systems do not experience blocking probability of any kind. Since all the subscribers can use all the spectrum at the same time (see section 10.5), in theory, new calls are always possible. The corresponding signals will be spread throughout the spectrum in the same way as the signals of the calls already established. The only consequence is the degradation of the signal-to-interference ratio, since any information, other than that of the wanted signal, works as an interfering (unwanted) signal. Accordingly, wideband systems are claimed to have a graceful performance degradation with the increase of the number of users.

10.3 FREQUENCY-DIVISION MULTIPLE ACCESS

The most conventional method of multiple access is Frequency-Division Multiple Access - FDMA. In FDMA the signals (from the mobiles or base stations) are transmitted on carriers using different RF centre frequencies. The simplest arrangement within the FDMA architecture is the one where a separate carrier for each

channel is provided. This scheme, known as Single-Channel per Carrier (SCPC), is very efficient in that the channels can be used in a demand-assigned mode.

Within a cell all the channels are available to all the mobiles and the channel assignment is carried out on a first-come-first-served basis. The number of channels, given a frequency spectrum, depends not only on the modulation technique but also on the guard bands between the channels. These guard bands allow for imperfect filters and oscillators and can be used to minimize adjacent channel interference.

Amongst all the available channels some are dedicated for control purposes. The number of control channels varies with the size of the system, but this usually constitutes a small proportion of the total number. Note that analog as well as digital systems can use SCPC/FDMA, the only requirement being the use of only one channel per carrier. Figure 10.1 depicts the SCPC/FDMA format.

10.3.1 Main Features of the FDMA Architecture

In this section we consider some of the main features of the FDMA architecture including digital FDMA [3].

1)*SCPC/FDMA.* In a Single-Channel per Carrier (SCPC)/FDMA a separate frequency is alloted to each telephone circuit.

2)*Continuous Transmission.* The channels, once assigned, are used in a non time-sharing basis. This means that both subscriber and base station can use their corresponding allotted channels continuously and simultaneously.

3) *Narrow Bandwidth.* Since each allotted channel is used by only one subscriber, the required bandwidth is reasonably narrow. The existing analog cellular systems use 25-30 kHz channels. Digital FDMA systems can make use of low bit rate speech coding techniques to reduce even more the channel band.

4) *Low ISI.* Intersymbol interference (ISI) is an intrinsic problem of digital systems and is particularly critical in a mobile radio environment. If the delay spread is not negligible compared to the symbol duration then a great deal of digital processing (adaptive equalization) must be required in order to minimize the ISI

effects (see section 6.11). Digital FDMA systems, using constant-envelope digital modulation, may require bit rates around 1 bit/Hz [5]. Therefore, a 25-kHz channel can support a transmission rate of 25 kbits/s, corresponding to a symbol duration of 40 μs if one bit per symbol is used. Since delay spreads vary from tenth of microseconds to a few microseconds (delay spreads of 5 μs are quite unusual) ISI is likely to be very low.

5) *Low Overhead.* Speech channels carry overhead messages for control purposes. In analog FDMA these messages comprise, for instance, hand-off signalling. In digital FDMA they may also include bits for synchronization, the framing, etc. Since the allotted channels can be used continuously, fewer bits need be dedicated for control as compared to TDMA channels. Therefore, more bits can be used to improve the transmission quality (error correcting codes, etc.).

6) *Simple Hardware.* Given that (i) very little or even no digital processing to combat ISI may be required, (ii) ease of framing and synchronization can be achieved, besides other reasons, less complex hardware can be used in both mobile unit and base station.

7) *Use of Duplexer.* Since (i) the system operates on a full duplex basis, (ii) only one antenna is used for transmission and reception and (iii) both transmitter and receiver are on continuously, the use of duplexer (filters between transmitter and receiver) is mandatory in order to avoid interference. The cost of the duplexer represents as much as 10% of the total cost of the mobile unit equipment [3].

8) *High Base Station Cost.* The SCPC/FDMA architecture requires the use of one transmitter, one receiver, two codecs and two modems per channel. If more than one channel, say n, could share the same carrier as in TDMA, the number of these equipments at the base station would be divided by n. If on the one hand the use of more than one channel per carrier increases the complexity and therefore the costs of the equipments, on the other hand this renders the system more capable of accommodating more subscribers, making the equipment per subscriber less costly.

9) *Perceptible Hand-off.* The continuous transmission on the FDMA channels makes

the transition from one channel to another, when a handoff is to take place, a rather perceptible phenomenon. In fact, the interruption of transmission can be long enough to provoke a "click" or several "clicks" in case many hand-offs are necessary (e.g., in small cells systems, etc.). In TDMA systems the idle time slots can be used for this, so that the interruption of transmission can be well worked out to reduce these "clicks".

10.3.2 Effects of Nonlinearities on FDMA Systems

The N channels available in the cell can share the same antenna at the base station by two possible ways, as follows:

1) Each channel has its own Power Amplifier and the N amplifiers have their outputs connected to a Power Combiner which feeds a common antenna.

2) All the N channels share a common Power Amplifier having its output connected to the antenna.

Both the Power Combiner and the Power Amplifier present nonlinear properties, usually in the form of a saturation at high power levels. There are many effects due to these nonlinearities:

1) Spectral Spreading

2) Modulation Transfer

3) Signal Suppression

4) Intermodulation

We shall describe each one of these effects.

Spectral Spreading

The wanted signal exceeds its own bandwidth causing adjacent channel interference.

Modulation Transfer

Amplifying devices may produce AM/PM conversion where a change in the envelope of a multicarrier input causes a change in the output phase of each signal component. Let A(t) be the input envelope and $\theta(A)$ the phase modulation induced by the envelope

fluctuation. For small input drive levels the following relationship holds true [2].

$$\theta(A) \propto KA^2(t) \tag{10.1}$$

where K is a constant.

Consider that the input x(t) is a summation of N sinusoids, i.e.,

$$x(t) = \sum_{i=1}^{N} A_i \cos\left[\omega_0 t + \phi_i\right] \triangleq A(t)\cos\left[\omega_0 t + \phi(A)\right] \tag{10.2}$$

where

$$A^2(t) = \left(\sum A_i \cos\phi_i\right)^2 + \left(\sum A_i \sin\phi_i\right)^2 \tag{10.3}$$

is the squared envelope, and

$$\phi(A) = \tan^{-1}\left(-\frac{\sum A_i \sin\phi_i}{\sum A_i \cos\phi_i}\right) \tag{10.4}$$

is the resultant phase.

The AM/PM output, y(t), is also a summation of sinusoids, each shifted by $\theta(A)$, that is

$$y(t) = \sum_{i=1}^{N} A_i \cos\left[\omega_0 t + \phi_i + \theta(A)\right] \tag{10.5}$$

For $\theta(A) << 1$, $\cos\left[\theta(A)\right] \approx 1$ and $\sin\left[\theta(A)\right] \approx \theta(A)$. Therefore

$$\begin{aligned} y(t) &= \sum_{i=1}^{N} A_i \cos\left(\omega_0 t + \phi_i\right) - \theta(A) \sum_{i=1}^{N} A_i \sin\left(\omega_0 t + \phi_i\right) \\ &= A(t)\cos\left[\omega_0 t + \phi(A)\right] + d(t) \\ &= x(t) + d(t) \end{aligned} \tag{10.6}$$

Using (10.1), the distortion term d(t) can be expressed by

$$d(t) \propto - KA^2(t)A(t)\sin\left[\omega_0 t + \phi(A)\right]$$

$$\propto - KA^3(t)\sin\left[\omega_0 t + \phi(A)\right] \tag{10.7}$$

Compare the signals x(t) and d(t) (equations (10.2) and (10.7), respectively). Note that, the distortion occurs at precisely the same frequencies, has a different amplitude and is 90^0 shifted in phase.

Signal Suppression

When the amplifier operates near its linear region the output voltage g(x) is proportional to the input voltage x(t), i.e.,

$$g(x) = Gx(t) \tag{10.8}$$

where G is known as small-signal voltage gain. Outside the linear region (10.8) does not hold true and

$$g(x) < Gx(t) \tag{10.9}$$

Consider an envelope sinusoid of amplitude B received by the mobile, in the presence of a large Gaussian interference. Let the Gaussian term be a large number of other independent sinusoidal signals with a resultant envelope A. The interference A has a Rayleigh density p(A), such that

$$p(A) = \frac{A}{\sigma^2}\exp\left(\frac{-A^2}{2\sigma^2}\right) \tag{10.10}$$

It is shown by Spilker [2] that the ratio between the output signal-to-noise ratio SNR_o and the input signal-to-noise ratio SNR_i is

$$\frac{SNR_o}{SNR_i} = R \tag{10.11}$$

where

$$R = \frac{\left[\int_0^\infty A\,g(A)\,p(A)dA\right]^2}{\left[\int_0^\infty g^2(A)p(A)dA\right]\left[\int_0^\infty A^2 p(A)dA\right]} \tag{10.12}$$

and g(A) is the envelope output.

Using the Schwarz inequality (see Appendix 5B) we conclude that R, the signal-suppression ratio, is less than or equal to one ($R \leq 1$). Accordingly, there can be no signal enhancement, no matter what the nonlinearity g(A) should be.

Intermodulation

Intermodulation (IM) is the presence of unwanted signal-dependent spectral components. In this section we shall illustrate the fundamentals of IM effects and calculate the magnitude of the intermodulation products (IP) through an example.

Let g(x) be the voltage transfer function of a nonlinear device, such that

$$g(x) = k_1 x + k_2 x^2 + k_3 x^3 \tag{10.13}$$

where x is the input voltage and k_i are constants. Consider that the input x is composed by three narrowband bandpass signals.

$$x = A\cos a + B\cos b + C\cos c \tag{10.14}$$

with $a = (\omega_c - \Delta)t$, $b = \omega_c t$, $c = (\omega_c + \Delta)t$

where ω_c is the carrier frequency and Δ is the separation between adjacent carrier frequencies.

Under the conditions that (i) $\omega_c >> \Delta$ and (ii) a zonal filter is placed after the nonlinear device to remove out-of-band harmonics, with (10.14) in (10.13) we obtain*

$$g(x) = \underbrace{C_1\cos a + C_2\cos b + C_3\cos c}_{\text{wanted signal}} + \underbrace{C_4\cos(2b-a) + C_5(2b-c) + C_6\cos(a-b+c)}_{\text{intermodulation products}} \tag{10.15}$$

The values of the constants in (10.15) are shown below

$C_1 = k_1 A + \frac{3}{4}k_3 A(A^2 + 2B^2 + 2C^2)$, linear at $a = \omega_c - \Delta$

$C_2 = k_1 B + \frac{3}{4}k_3 B(2A^2 + B^2 + 2C^2)$, linear at $b = \omega_c$

* In this case the out-of-band terms are of type dc, 2a, 2b, 2c, a+b, a-b, a+c, a-c, b+c, b-c, 2a-b, 2a-c, 2c-a, 2c-b, a+b-c and -a+b+c exceeding the range $\omega_c - \Delta < \omega < \omega_c + \Delta$.

$$C_3 = k_1 C + \frac{3}{4} k_3 C(2A^2 + 2B^2 + C^2) \quad \text{, linear at} \quad c = \omega_c + \Delta$$

$$C_4 = \frac{3}{4} k_3 AB^2 \quad \text{, intermodulation at} \quad 2b - a = \omega_c + \Delta$$

$$C_5 = \frac{3}{4} k_3 B^2 C \quad \text{, intermodulation at} \quad 2b - c = \omega_c - \Delta$$

$$C_6 = \frac{3}{2} k_3 ABC \quad \text{, intermodulation at} \quad a - b + c = \omega_c$$

It is possible to completely avoid third or third and fifth order IM products by widening the bandwidth and assigning the channels appropriately. Consider that N sinusoids occupy a bandwidth of NB, where B is assigned to each signal channel. The total required bandwidth in order to avoid IM is MB where $MB \geq NB$. The relation between N and M is shown in Figure 10.2 [2]. As an example, if $N = 4$ then $M = 7$ or $M = 20$ to avoid third order or third and fifth order IM products, respectively.

The appropriate assignment of the N channels out of the M required channels was obtained by Spilker [2] and is shown in Table 10.1.

TABLE 10.1 – FREQUENCY PLANS TO AVOID THIRD–ORDER IM PRODUCTS

Source: W.C.Y. Lee, *Mobile Communications Design Fundamentals*, Howard W. Sams, Indianopolis, IN., 986, reprinted with permission.

IM product spreading	Nº of Carriers N	Nº of Required Channels M	Frequencies F_i
YES (limited to 3B	3	4	1,2,4
	4	7	1,2,5,7
	5	12	1,2,5,10,12
	6	18	1,2,5,11,13,18
	7	26	1,2,5,11,19,24,26
	8	35	1,2,5,10,16,23,33,35
	9	46	1,2,5,14,25,31,39,41,46
	10	62	1,2,8,12,27,46,48,57,60,62
NO	3	7	1,3,7
	4	15	1,3,7,15

The upper part of the table shows the frequency plan with IM products spreading limited to 3B while the lower part shows this without IM product spreading.

10.4 TIME-DIVISION MULTIPLE ACCESS

Time-Division Multiple Access (TDMA) is the primary alternative to Frequency-Division Multiple Access (FDMA). TDMA takes advantage of the sampling (Nyquist) theorem in accommodating more information within a radio frequency by increasing the bit transmission rate. Accordingly, a carrier frequency can be shared by several (say n) terminals, each of which making use of this carrier in separate non overlapping time slots. The number of time slots per carrier depends on many factors, such as modulation technique, available bandwidth, etc., characterizing the narrowband TDMA or the wideband TDMA. An illustration of the TDMA architecture is shown in Figure 10.3.

In digital cellular radio the users have access to all frequencies within the cell and to all time slots within the frequencies. Note, therefore, that such access mode is, in fact, a combination of FDMA and TDMA.

Transmission from or to a given mobile unit is carried out in a non continuous mode, characterizing the buffer-and-burst communication. Once the mobile has accessed a carrier, transmission and reception are performed in distinct time slots, separated from one another by some guard time slots which can be used by other mobiles. The use of the buffer-and-burst mode implies that the channel transmission rate must be faster than the coding (or coding plus overhead) rate by a factor equal to or greater than the number of time slots per carrier.

10.4.1 Main Features of the TDMA Architecture

In this section we shall examine the main characteristics of the TDMA architecture [3].

1) *Multiple Channels per Carrier.* The total time of a carrier is divided up into time slots so that it can be shared by more than one user. In the European system (GSM) the number of voice channels per carrier is 8 while in the American system this is 3.

2) *Burst Transmission.* The channels are used in a time-sharing basis. Therefore,

the signal transmission occurs during specific time slots.

3) *Narrow/Wide Bandwidth.* The bandwidths of the TDMA systems depends on various factors including the modulation scheme. Carrier spacing varies from tens of kHz to hundreds of kHz. The European system uses 200 kHz carrier spacing with a 271 kbits/s transmission rate. The corresponding figures for the American system are 30 kHz and 48.6 kbits/s.

4) *High ISI.* Intersymbol interference is intrinsically related to the symbol rate and not to TDMA architecture. However, TDMA systems usually take advantages of the digital transmission to increase the symbol rate, resulting in high ISI. Note that for the GSM system the symbol duration is 3.6 μs which is already comparable to the delay spread in urban areas. For the American system this is not as critical, although both systems make use of adaptive equalization to combat ISI.

5) *High Overhead.* Because of the burst transmission characteristic of the TDMA systems, synchronization can be a complicated issue. Therefore, a reasonable amount of the total transmitted bits must be dedicated to synchronization purposes. This, in connection with the guard time between time slots, can represent 20–30% of the channel bits.

6) *Complex Hardware.* The use of digital technology permits the inclusion of several facilities in the mobile unit, increasing its complexity. One example of this is the use of slow-frequency hopping to counteract multipath fading, as proposed by the GSM system.

7) *No Duplexer Used.* Because transmission and reception are carried out on different time slots, the duplexer can be completely avoided. Instead, a switching circuit can be used to turn the transmitter and receiver on or off at the convenient times.

8) *Low Base Station Cost.* The use of multiple channels per carrier provides a proportional reduction of the equipments at the base station.

9) *Efficient Hand-off.* TDMA systems can take advantage of the fact that the transmitter is switched off during idle time slots to improve the hand-off procedure.

10) *Efficient Power Utilization.* FDMA systems require a 3 to 6 dB power back-off [2] in order to minimize intermodulation effects. TDMA can achieve efficiencies of 90% or more compared to the 3 to 6 dB loss in power of FDMA. Time-division multiplex systems can operate the output amplifier at full saturation, resulting in a better power utilization.

11) *IM Minimization.* Intermodulation products can be minimized if a convenient guard time between slots is used.

10.4.2 Timing Hierarchy

Timing hierarchy is an ordered set of time duration or intervals used to control and configure a TDMA system. Figure 10.4 illustrates a typical timing hierarchy where not all levels are necessarily used. The fields shown in Figure 10.4 are described below.

1) *Superframe:* number of sequential frames organized to distribute system and network control or signalling information.

2) *Frame:* time interval over which the signal format is established and then repeated indefinitely.

3) *(Time) Slot:* a subdivision of a frame.

4) *Burst Time:* an integer number of time slots.

5) *Burst:* an accessing signal that uses a certain number of slots in the frame.

6) *Guard Time:* a time interval between bursts to assure that no overlap occurs.

7) *Preamble:* initial portion of a burst, consisting of the following elements.

   7.1) CR: carrier recovery, used in coherent demodulating systems;

   7.2) STR: symbol-timing recovery, also known as clock or bit timing recovery (BTR);

   7.3) UW: unique word or burst code word (BCW) for burst synchronization;

   7.4) HKS: house keeping symbols such as signalling bits, order wire for voice or data, command and control signalling and error-monitoring symbols.

8) *Message:* portion of a burst containing the desired data.

9) *Postamble:* end portion of a burst, used for initialization of the next burst.

10.4.3 Measures of Efficiency

There are several measures of efficiency that can be used in a TDMA system. We shall consider three types.

Frame Efficiency (η_F): is the ratio of the portion of the frame available for messages to the total frame length.

$$\eta_F = 1 - \frac{S + \sum_{i=1}^{n} \left(G_i + P_i + Q_i \right) T_S}{F} \tag{10.16}$$

where F = frame length (μs)

S = number of symbols in synchronization bursts

G_i = guard time of access i (μs)

P_i = number of symbols in preamble of access i

Q_i = number of symbols in postamble of access i

T_S = symbol length (μs)

n = number of accesses.

Burst Efficiency (η_B): is the ratio of useful message information to the total bits transmitted

$$\eta_B = \frac{rM}{P + M + Q} \tag{10.17}$$

where r = coding rate of the codec

M = message symbols per burst

P = number of symbols in preamble

Q = number of symbols in postamble

System Efficiency (η_S): is the ratio of the useful capacity (paying traffic) to the available capacity. For a Gaussian channel,

$$\eta_S = B = \log_2 \left(1 + \frac{E_S T_S}{N_0 B} \right) \tag{10.18}$$

where B = channel bandwidth

E_S = energy per symbol

T_S = symbol length

N_0 = spectral density of white Gaussian noise.

10.4.4 Time Alignment and Synchronization

The TDMA architecture requires that the mobiles using a common carrier must have their transmitted signals reaching the base station receiver at exactly the right time so that signal overlapping do not occur. If the base station provides a reference signal, those mobiles nearer the base station will respond earlier than those located further away. The non-overlap control can be done by dimensioning the guard time appropriately. For instance, if a mobile is 35 km away from the base station, the time taken for a radio signal to travel the 70 km to and back from the mobile is $70.10^3/3.10^8$ = 0.23 ms. Hence 0.23 ms is the guard period to be provided on each time slot.

A more clever solution is the use of the following time alignment process which has been adopted by both the GSM and American systems: the mobile is informed how much it must advance or retard the transmit burst in order to be correctly synchronized at the base station. By using this procedure in the above example, the GSM system [5] claims to reduce the guard time to 30 μs.

The mobile station derives timing from a common source which tracks the base station symbol rate as perceived at the mobile receiver. The frequency tracking is maintained over all specified operating conditions. The synchronization word must have good autocorrelation properties to facilitate synchronization and training.

10.5 CODE-DIVISION MULTIPLE ACCESS

Code-Division Multiple Access (CDMA) is an access method where all the users (i)

are permitted to transmit simultaneously, (ii) operate at the same nominal frequency and (iii) use the entire system bandwidth. One of the main features of CDMA is that very little dynamic coordination is required, as opposed to FDMA and TDMA where frequency and time management is critical.

Since all the users can transmit simultaneously throughout the whole system frequency spectrum, a private code must be assigned to each user so that his (or her) transmission can be identified. This privacy is achieved by the use of codes with very low cross-correlation among themselves (orthogonal codes). CDMA system works asynchronously, in that each user can initiate the transmission at any time instant. Therefore, as far as digital communication is concerned, transition times of a user's message symbols may not coincide with the other users. This simplifies the network synchronization but can complicate the design of good codes.

Note that in CDMA systems, in theory, "there is no limit" on the numbers of users. What happens is a graceful degradation of performance as the number of simultaneous users increases. Note also that multipath interference is substantially reduced because the signal is spread in the whole spectrum and usually only part of it is affected. In the same way, CDMA systems offer a high resistance to deliberate jamming because transmission is carried out in an encoded way, only known by the users involved.

To accomplish CDMA, spread spectrum (SS) techniques must be used. In this section we shall present a notion of spread spectrum and the essential characteristics of the techniques used. Although spread spectrum can be used in both analog and digital communications, we shall stress its application in the latter.

10.5.1 Spread Spectrum Fundamentals

General Considerations

Spread spectrum is defined as a communication technique in which the intended signal is spread over a bandwidth in excess of the minimum bandwidth required to transmit the signal. This is accomplished by the use of a wideband encoding signal at

the transmitter, which is required to operate in synchronism with the receiver where the encoding signal is also known. By allowing the intended signal to occupy a bandwidth far in excess of the minimum bandwidth required to transmit it, the signal will have a noise-like appearance. This works as a "disguise", rendering the spread spectrum communication able to reject interference.

A typical spread spectrum system is depicted in Figure 10.5. Note that the spectrum-spreading function is an additional block which is included in a conventional communication system, corresponding to a "second level" modulation. Therefore, generating a spread spectrum signal involves two steps, as follows. First the carrier is modulated by the baseband digital information with rate $R_b = 1/T_b$, where T_b is the baseband symbol duration. The modulated signal $s_i(t)$ is used to modulate a wideband function $c_i(t)$ with rate $R_c = 1/T_c$, where R_c is called *chip rate*. From the Fourier analysis we know that the multiplication of two functions in the time domain corresponds to their convolution in the frequency domain. Therefore, if $s_i(t)$ is narrowband and $c_i(t)$ is wideband, the product $c_i(t)s_i(t)$ will have a spectrum that is approximately the same as that of $c_i(t)$ (wideband).

The wideband signal $s_i(t)c_i(t)$ is passed through the channel where other wideband signals, interference I(t) and additive noise n(t) are superimposed to the desired signal. Assuming M instantaneous users in the CDMA system, the received signal, r(t), is given by

$$r(t) = \sum_{j=1}^{M} c_j(t)s_j(t) + I(t) + n(t) \qquad (10.19)$$

It is assumed that the same spreading function $c_i(t)$, used at the transmitter, is locally generated at the receiver. Furthermore, both transmitter and receiver are supposed to operate synchronously. The resulting "despread" signal u(t) is

$$u(t) = c_i(t)\left[\sum_{j=1}^{M} c_j(t)s_j(t) + I(t) + n(t)\right]$$

$$= c_i^2(t)s_i(t) + c_i(t)\left[\sum_{\substack{j=1 \\ (j\neq i)}}^{M} c_j(t)s_j(t) + I(t) + n(t)\right] \qquad (10.20)$$

If the set of spreading functions are chosen so that they have low cross-correlation among themselves, then only the original, modulated wave form remains after the correlation process. Other waveforms are not correlated and will be spread, appearing as noise to the modulator. That is

$$u(t) = Ks_j(t) + \text{Noise} \tag{10.21}$$

where $K \triangleq c_i^2(t) = \text{constant}$

and $c_i(t)\left[\sum_{\substack{j=1 \\ (j \neq i)}}^{M} c_j(t)s_j(t) + I(t) + n(t)\right]$ constitutes the Noise component.

Note that $Ks_j(t)$ is bandpass, whereas the Noise component is wideband. Thus by applying u(t) to the bandpass filter (BPF) with a bandwidth just large enough to accommodate the modulated signal $Ks_j(t)$, the Noise component is made bandpass, therefore with much less power. Consequently, a jammer or interference power density in the information bandwidth of the received signal will be effective only if its total power is increased by the same amount as the bandwidth expansion of the signal.

Processing Gain

Process gain (G_p) is defined as the difference in dB between output and input signal-to-noise ratios. In absolute values

$$G_p = \frac{SNR_0}{SNR_I} \tag{10.22}$$

It represents the gain achieved by processing a spread-spectrum signal over an unspread signal. Clearly, this coincides with the ratio between the corresponding bandwidths. That is

$$G_p = \frac{B_S}{B_U} \tag{10.23}$$

where B_S is the bandwidth of the spread signal and B_U is the bandwidth of the unspread one.

Jamming Margin

Jamming Margin (M_J) gives the amount of interference above the intended signal with which the system is expected to operate. The jamming margin accounts for internal losses L and is given by

$$M_J = \frac{G_p}{L\,SNR_0} \tag{10.24a}$$

or

$$M_J(dB) = G_p(dB) - \left[L + SNR_0\right](dB) \tag{10.24b}$$

10.5.2 Spread Spectrum Techniques

There are several spread spectrum techniques that can be used in the communication systems. Each one of them is usually applied to specific fields so that very little competition between them occurs [9]. We shall give an overview of the principal techniques but the main focus will be on the two most widely used technique, as follows.

Direct Sequence or Direct Spread or Pseudonoise Systems: The modulated carrier is further modulated by a digital code sequence whose bit rate is much higher than the information signal bandwidth.

Frequency Hopping or Multiple Frequency, Code-Selected, Frequency Shift Keying Systems: The carrier hops "randomly" from one frequency to another.

Time Hopping Systems: This is exactly the pulse modulation. The code sequence keys the transmitter on and off. Since the code sequence is pseudorandom the times when the transmitter is on and off are also pseudorandom.

Pulsed-FM or Chirp Systems: The carrier varies (is swept) over a wide band, according to some known way, during each pulse period. This technique does not necessarily employ coding.

Frequency Hopping/Direct Sequence Systems: The direct sequence modulated signal has its centre frequency hopping periodically.

Time/Frequency Hopping: When frequency hopping alone is not enough to combat interference, then time hopping is also recommended. This combination is mainly used to minimize the near/far problem in which the stronger signals will interfere with the weaker ones. In such case it is convenient to time all transmissions so that the wanted and unwanted signals are never transmitted at the same time.

Time Hopping/Direct Sequence: When direct sequence alone is not enough to provide high capacity to accommodate users in the CDMA systems, time hopping is an efficient way of helping in traffic control.

Having presented the main spread spectrum techniques we shall describe, in a more detailed way, the two most widely used schemes, namely, Direct Sequence and Frequency Hopping.

1) *Direct Sequence Systems*

Direct Sequence (DS) or Direct Spread (DS) or Pseudonoise (PN) Spread Spectrum (SS) uses a code sequence to modulate a carrier (or a modulated carrier). In principle, any modulation technique such as AM (pulse), FM or PM can be used. However the most widespread form is the Binary Phase-Shift-Keying (BPSK) modulation. A DS/SS system simplified model is depicted in Figure 10.6. Note that the information signal m(t) and the spreading sequence c(t) are combined before phase-modulating the carrier p(t). This is convenient for digital modulation purposes [1].

The PN code c(t) is a pseudorandom binary sequence with a chip rate R_c much larger than the information bit rate R_b. The multiplication of the PN code by the information signal results in a frequency spectrum with a bandwidth approximately equal to that of the sequence spectrum. The resultant signal is then modulated onto a carrier and transmitted. At the receiver an exact replica of the PN code is used in synchronism with the transmitter to unspread the received signal.

Note from (10.20) that if the binary sequence $c_j(t)$ is composed by digits alternating between the levels −1 and +1, then $c_j^2(t) = 1 = K$. Therefore, from (10.21) $u(t) = s_1(t)$ + Noise. Assuming a BPSK modulation in the DS/SS system of Figure 10.6, a sketch of the time domain representation of the signals can be seen in Figure 10.7

If the bandwidths of the spread and unspread signals are taken as being the main-lobe of their spectra, then $B_s = 2(1/T_c) = R_c$ and $B_U = 1/T_b = R_b$ *. Therefore, using (10.23) the processing gain of a DS/SS system is

$$G_p = \frac{2T_b}{T_c} = \frac{2R_c}{R_b} \tag{10.25}$$

Note that the larger the chip rate the larger the processing gain.

The choice of modulation as well as code rate depend basically on (I) the available bandwidth, (II) required process gain and (III) baseband information rate. Given a code rate, multilevel modulation techniques can be used to reduce the RF bandwidth. Note, however, that the process gain is a function of this bandwidth.

2) *Frequency Hopping Systems*

In Direct Sequence systems the spreading of the transmission bandwidth appears in a continuous form when the PN sequence is combined with the information to modulate the carrier. The performance of spread-spectrum systems depends on the processing gain which, by its turn, is dependent on the PN sequence chip rate. The generation of the PN code relies on the available technology to produce high chip rates. This, however, is a serious constraint, imposing practical limitations to the obtainment of a better processing gain.

Frequency Hopping (FH), an alternative to the DS systems, is a spread spectrum technique with the spreading of the transmission bandwidth appearing in a discrete form. This is achieved by allowing the carrier to hop from one frequency to another in a sequence dictated by the PN code. A basic FH/SS system is shown in Figure 10.8.

At a given time instant the output of FH transmitter is a single frequency. Over a period of time its output signal spectrum is ideally rectangular with the same

---

* We are making the usual assumption that the power spectral density of a random pulse train is given by the $[(\sin x)/x]^2$ response (refer to Appendix 9A). Specifically, for a baseband signal this is $T_b[\sin(\omega T_b/2)/(\omega T_b/2)]^2$. For a modulated signal the power spectrum is $T_c\left\{\sin[(\omega-\omega_p)T_c/2]/[(\omega-\omega_p)T_c/2]\right\}^2$, where ω_p is the carrier angular frequency. Therefore, for positive frequencies $B_s = 2/T_c$ and $B_u = 1/T_b$.

amount of power in every frequency, as depicted in Figure 10.9.

In practice, however, the hopping process generates spurious frequencies causing interchannel interference (crosstalk).

At the receiver the transmitted signal is mixed with a synchronous locally generated replica of the transmitter frequency sequence, offset by the intermediate frequency, f_{IF}. Again, any signal different from the local replica is spread by the multiplication and rejected as noise.

An usual modulation scheme for FH systems is M-ary Frequency-Shift Keying and this combination is referred to as FH/MFSK. As far as demodulation is concerned, the non coherent approach is commonly used because it is extremely difficult to maintain phase relationships between frequency steps.

There are two basic FH systems, as follows:

- Slow-Frequency Hopping (SFH) Systems, in which several symbols of information are transmitted on each frequency hop.
- Fast-Frequency Hopping (FFH) Systems, in which several hops occur during the transmission of one symbol.

In SFH systems each symbol is a chip, whereas in FFH systems the chip in characterized by a hop. An illustration of the frequency changes of SFH and FFH systems is shown in Figure 10.10.

Deliberate interference is possible if the spectral content of the transmitted signal is measured and the interfering signal is tuned to the corresponding portion of the frequency band. To combat this, the frequency hopper must hop at a sufficiently fast rate so as to skip to another frequency before the interferer can cause trouble. For mobile application purposes this implies that the carrier frequency should hop as fast as possible because distances between wanted and interfering signals vary. Therefore, the exact time required to change to another frequency also varies.

If the frequency separation between discrete frequencies is such that it equals the message bandwidth, then from (10.25)

$$G_p = N \tag{10.26}$$

where N is the number of available frequency choices (or channels used for hopping).

10.5.3 Synchronization

Synchronization is considered to be one of the most difficult parts of the CDMA architecture implementation. A rigid system timing is not required, but transmitters and receivers must work synchronously so that the despreading of the wanted information and the spreading of the unwanted signals can be accomplished.

There are basically two regions of uncertainty as far as synchronization is concerned: code phase and carrier frequency. The PN code phase uncertainty must be resolved to better than one chip duration. Ideally, once synchronization is achieved, it should continue to be so forever. There are, however, sources of errors that must be taken into account when designing a CDMA system. One of such sources is the Doppler effect which affects both the carrier frequency and the code rate. Moreover, multipath propagation also imposes phase shifts in the received signal which can be really harmful at high rate transmission. Other sources of uncertainty include the clock stability and clock rate offset.

Accordingly, the synchronization process comprises two sequential steps: initial synchronization and tracking. The initial synchronization task is the most complicated of all. The tracking process can always be based on the knowledge of the timing gained previously. An extensive list of synchronization methods can be found in the literature [9,10] and will not be reproduced here.

10.6 TWO-WAY COMMUNICATION

Two-way communication in a full-duplex fully trunked system can be implemented by means of frequency division, time division and code division methods. The latter is exactly the CDMA system, which has been described in section 10.5. Frequency division and time division will be characterized next.

Frequency Division Duplex

In Frequency Division Duplex (FDD) communications each direction of transmission (forward channel and reverse channel) has a separate frequency band. Consequently, simultaneous transmission in both directions is feasible. As explained in the FDMA case, a large interval between these frequency bands must be allowed so that interference can be minimized. In the same way, sharp filters with strong out-of-band rejection must be used in the radio equipments to reduce adjacent channel interference.

Time Division Duplex

In Time Division Duplex (TDD) communications both directions of transmission use one contiguous frequency allocation, but two separate time slots. Since transmission from mobile to base and from base to mobile alternates in time, this scheme is also known as "Ping-Pong". As a consequence of the use of the same frequency band, the communication quality in both directions is the same. A guard time between the two time slots must be allowed in order to avoid interference. Moreover, synchronization among base stations should be provided, again for interference minimization purposes.

10.7 SUMMARY AND CONCLUSIONS

The choice of an access scheme for mobile radio systems is a rather complex task that may involve several aspects other than that of system capacity. In particular, many queries are still to be solved, remaining as matters of controversies. As far as analog systems are concerned the range of options is not so vast, so that the FDMA architecture is always used. For digital systems, however, the three methods, namely FDMA, TDMA and CDMA are applicable each of which presenting advantages and disadvantages. In this section we shall discuss some of these issues [13], steering the analysis towards the digital approach.

1a) *Advantages of SCPC/FDMA*

- Channel equalization is not necessary because the channels operate within

the coherence bandwidth.

- Reduction of information bit rate can directly increase system capacity.
- Involved technology is well known.
- Ease of compatibility with existing analog systems.

1b) *Disadvantages of SCPC/FDMA*

- Growth techniques do not differ much from those used for the analog systems.
- Terminals are costly since they require narrowband filters which are not realizable in VLSI.
- Bit Transmission rate is fixed.

2a) *Advantages of TDMA*

- Channel equalization can be used to combat fast fading.
- Bit Transmission rate may be variable as multiple or submultiple of the basic single channel rate.
- Signal strength and bit error rates can be monitored on a frame-by-frame basis, facilitating and speeding up the handoff process.

2b) *Disadvantages of TDMA*

- High peak power on the uplink (mobile to base station) is required.
- Considerable amount of signal processing may be required when matched filtering and correlation detection are to be implemented.
- This increases the power consumption and imposes delay in the signal.

3a) *Advantages of CDMA*

- Spectral density is reduced.
- Protection against jamming is provided.
- Message privacy is provided.
- Multipath effects are greatly minimized.

3b) *Disadvantages of CDMA*

- Spread spectrum techniques still remain to be explored for wide spread commercial applications.

Final Remarks

Narrowband access schemes (FDMA and narrowband TDMA) are simple to implement but offer very little regarding protection against interference, noise, blocking, etc. Wideband systems are potentially more attractive, but require considerable advances in signal processing before they can be fully explored.

REFERENCES

[1] V.K. Bhargava, D. Haccoun, R. Matyas and P. Nuspl, *Digital Communications by Satellite*, John Wiley & Sons, 1976.

[2] J.J. Spilker Jr., *Digital Communications by Satellite*, Prentice-Hall, 1977.

[3] G. Calhoun, *Digital Cellular Radio*, Artech House, 1988.

[4] J. Tarallo and G.I. Zysman, "A Digital Narrowband Cellular System" *Proceedings of the 37th IEEE Vehicular Technology Conference*, pp. 279-280, Tampa, June 1-3, 1987.

[5] J. Uddenfelt and B. Persson, "A Narrowband TDMA System for a New Generation Cellular Radio", *Proceedings of the 37th IEEE Vehicular Technology Conference*, pp. 286-292, Tampa, June 1-3, 1987.

[6] V.K. Bhargava, D. Haccoun, R. Matyas and P. Nuspl, *Digital Communications by Satellite*, John Wiley & Sons, 1981.

[7] D.M. Balston, "Pan-European Cellular Radio: or 1991 and all that", *Electronics & Communication Engineering Journal*, January/February, 1989.

[8] *IS-54, EIA/TIA Project Number 2215*, "Cellular System: Dual-Mode Mobile Station - Base Station Compatibility Standard", December 1989.

[9] M.K. Simon, J.K. Omura, R.A. Scholtz and B.K. Levitt, "Spread Spectrum Communications", Vol. 1,2,3, *Computer Science Press*, 1985.

[10] R.C. Dixon, *Spread Spectrum System*, 2nd Edition, John Wiley & Sons, 1984.-

[11] R.L. Pickholtz, D.L. Schilling and L.B. Milstein, "Theory of Spread Spectrum Communications - A Tutorial", *IEEE Trans. on Communications*, Vol. COM-30, pp. 855-884, May 1982.

[12] J.K. Holmes, *Coherent Spread Spectrum Systems*, John Wiley & Sons, 1982.

[13] G.R. Cooper and C.D. McGillem, *Modern Communications and Spread Spectrum*, Mc Graw-hill, 1986.

[14] J.D. Parsons and J.G. Gardiner, *Mobile Communication Systems*, Blackie & Sons, 1989.

[15] G.R. Cooper, R.W. Nettleton and D.P. Grybos, "Cellular Land-Mobile Radio: Why Spread Spectrum?" *IEEE Communications Magazine*, March 1979.

[16] W.C.Y. Lee, "Overview of Cellular CDMA", *IEEE Trans. Veh. Tech.*, Vol. VT-40, pp. 291-302, May 1991.

[17] K.S.Gilhousen, I.M. Jacobs, R. Padovani, A.J. Viterbi, L.A. Weaver, Jr., and C.E. Wheatley III, "On Capacity of a Cellular CDMA System", *IEEE Trans. Veh.*, Vol. VT-40, pp. 303-312, May 1991.

[18] R.L. Pickholtz, L.B. Milstein and D.L. Schilling, "Spread Spectrum for Mobile Communications", *IEEE Trans. Veh.*, Vol. VT-40, pp. 313-322, May 1991.

[19] K. Raith and J. Uddenfeldt, "Capacity of Digital Cellular TDMA Systems", *IEEE Trans. Veh.*, Vol. VT-40, pp. 323-332, May 1991.

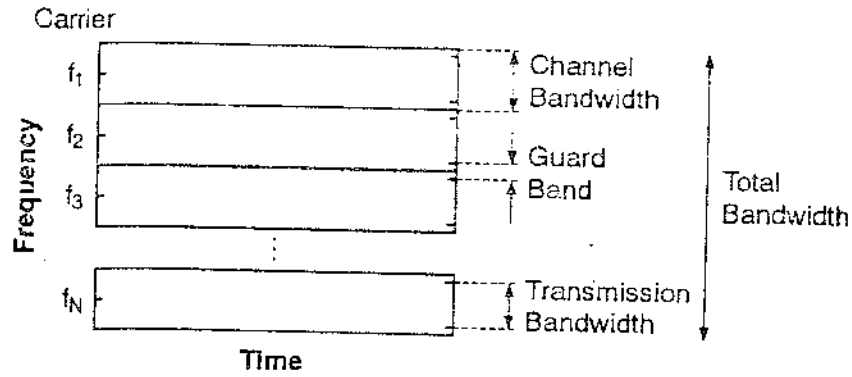

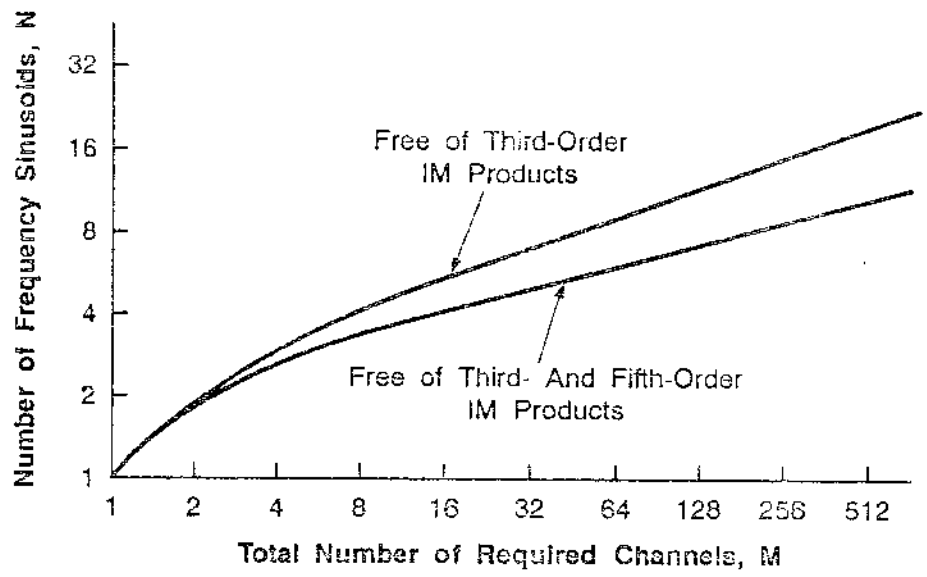

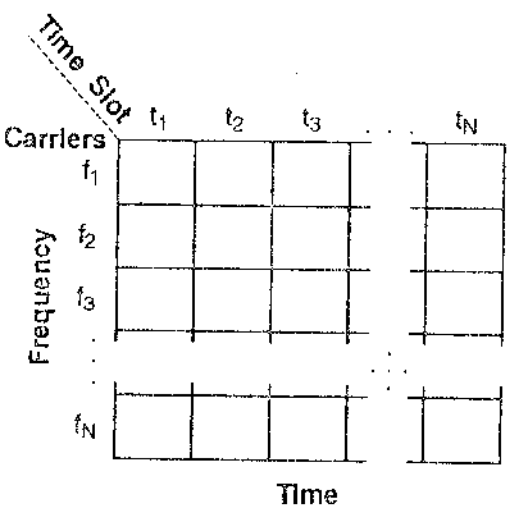
Time Slot
Carriers
t_1
t_2
t_3
t_N
f_1
f_2
f_3
f_N
Frequency
Time

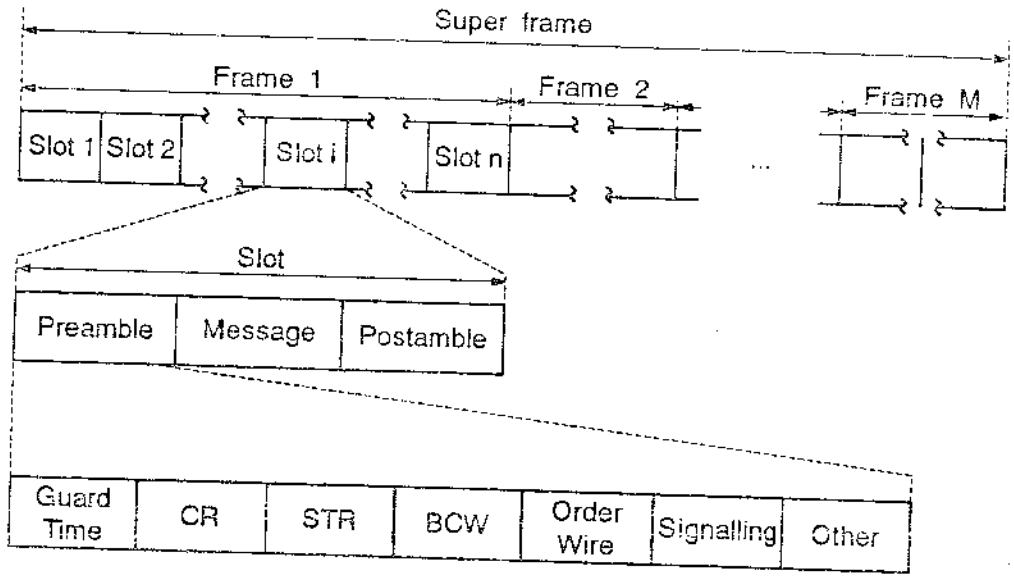

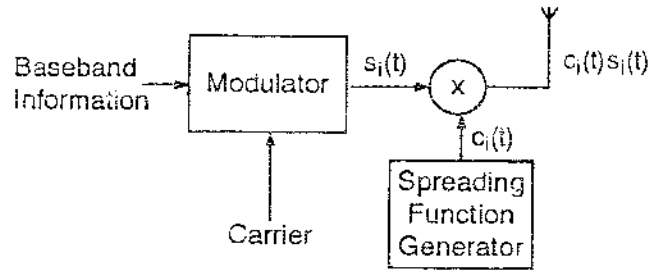
Baseband
Information
Modulator
$s_i(t)$
x
$c_i(t)s_i(t)$
$c_i(t)$
Spreading
Function
Generator
Carrier

(a)

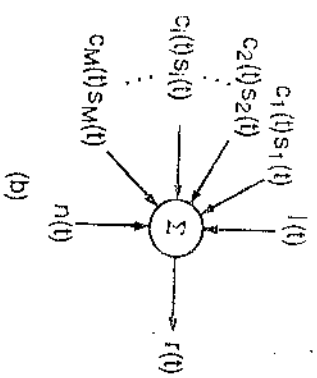

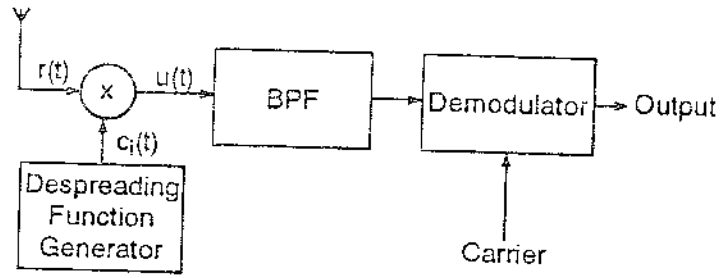

(c)

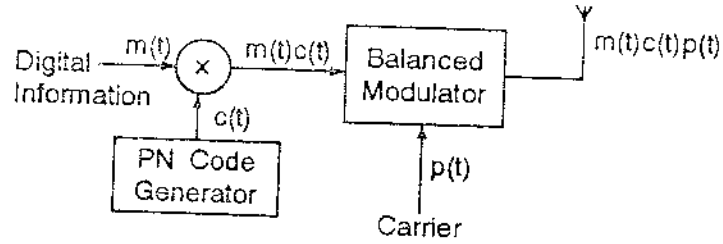

(a)

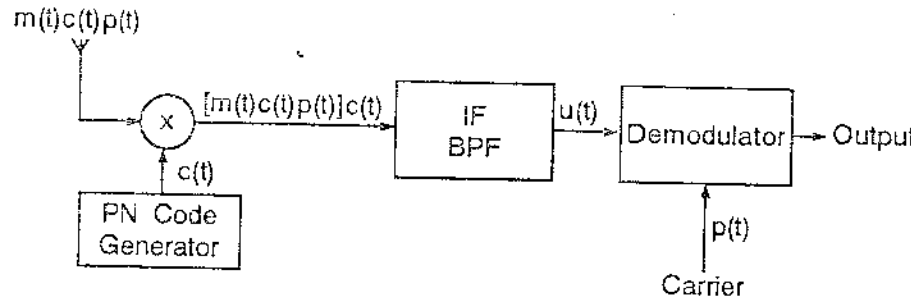
m(i)c(t)p(t)
X
[m(t)c(t)p(t)]c(t)
IF
BPF
u(t)
Demodulator
Output
c(t)
PN Code
Generator
p(t)
Carrier

(b)

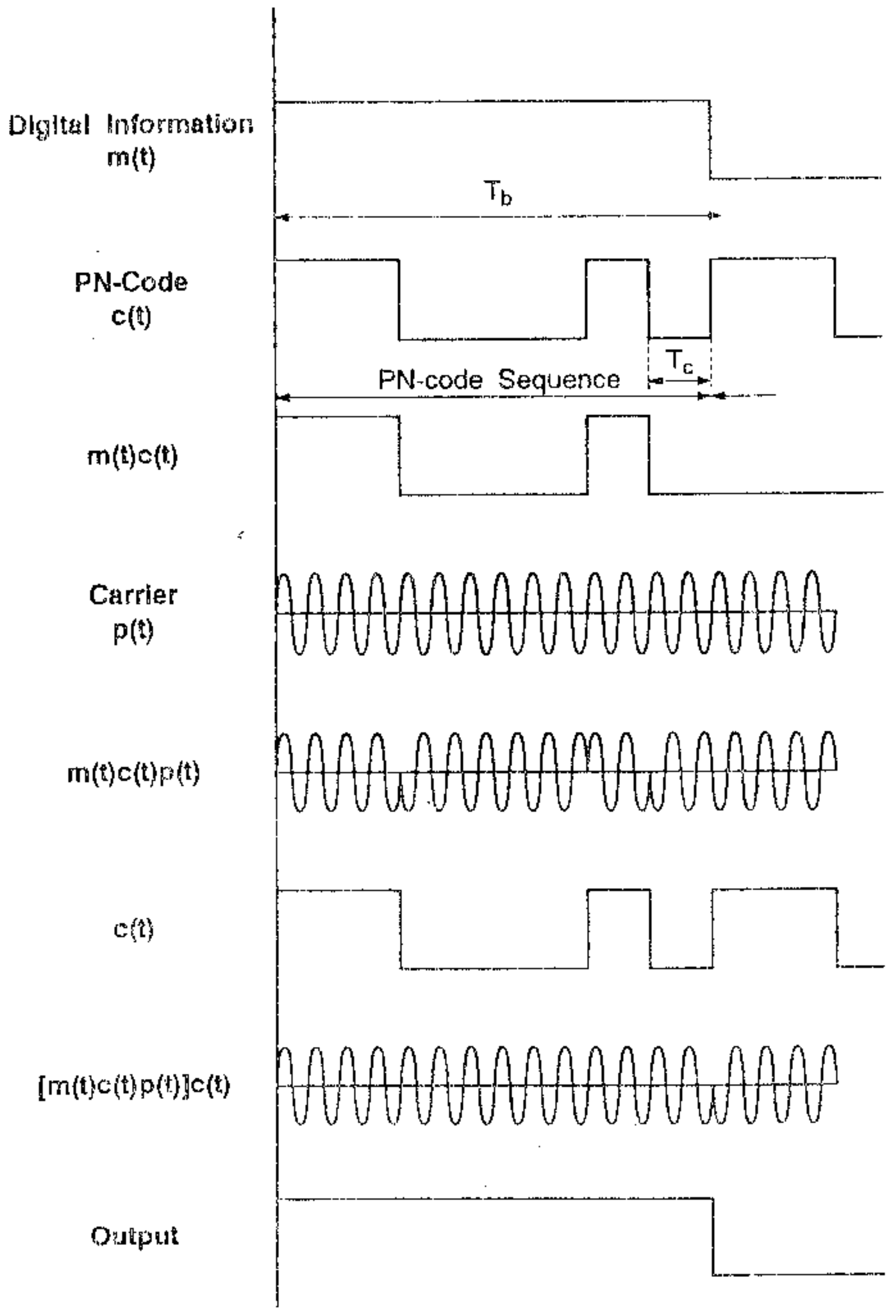
Digital Information
m(t)
T_b
PN-Code
c(t)
T_c
PN-code Sequence
m(t)c(t)
Carrier
p(t)
m(t)c(t)p(t)
c(t)
[m(t)c(t)p(t)]c(t)
Output

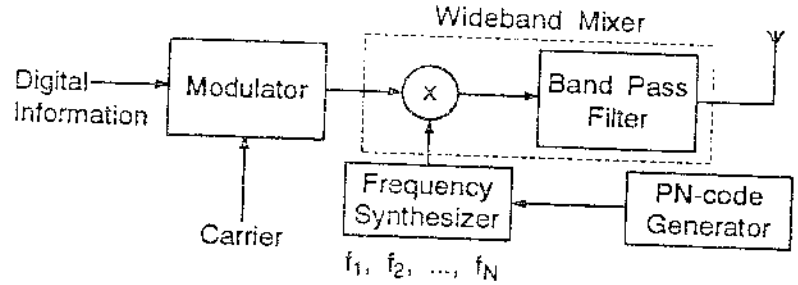

(a)

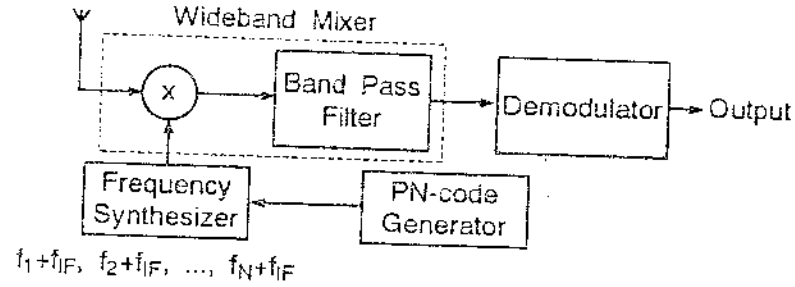
Wideband Mixer
X
Band Pass Filter
Demodulator
Output
Frequency Synthesizer
PN-code Generator
f_1+f_{IF}, f_2+f_{IF}, ..., f_N+f_{IF}

(b)

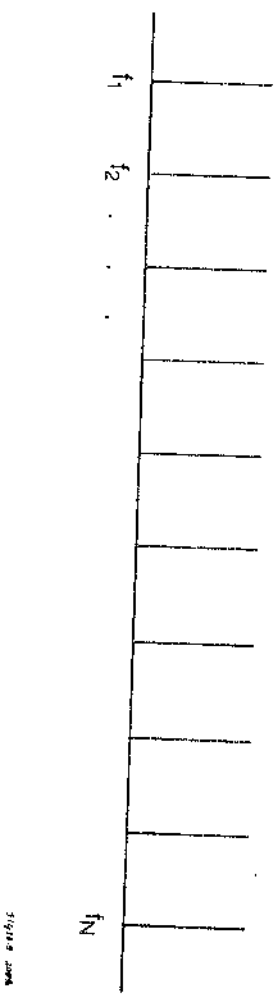

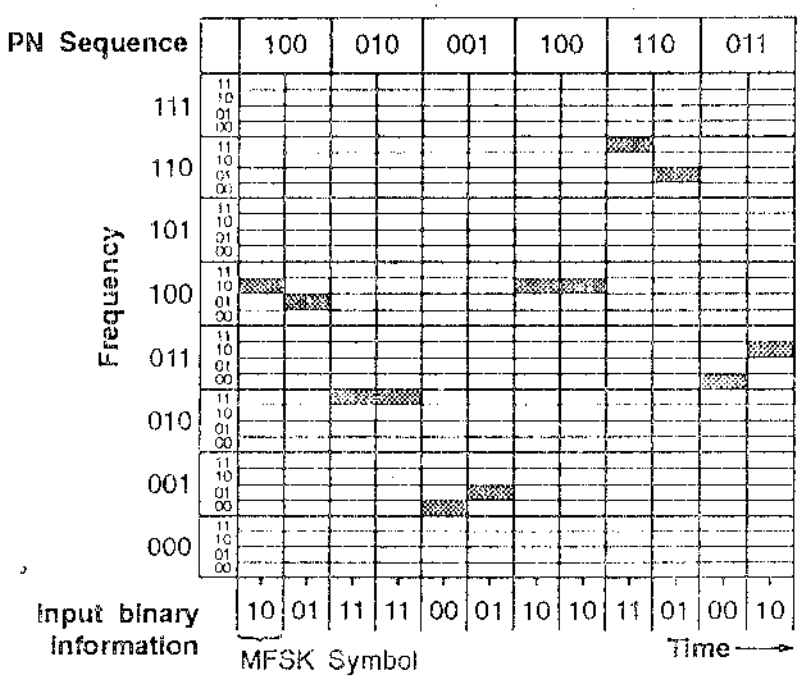
PN Sequence
100
010
001
100
110
011
Frequency
111
110
101
100
011
010
001
000
Input binary information
10 01 11 11 00 01 10 10 11 01 00 10
MFSK Symbol
Time

(a)

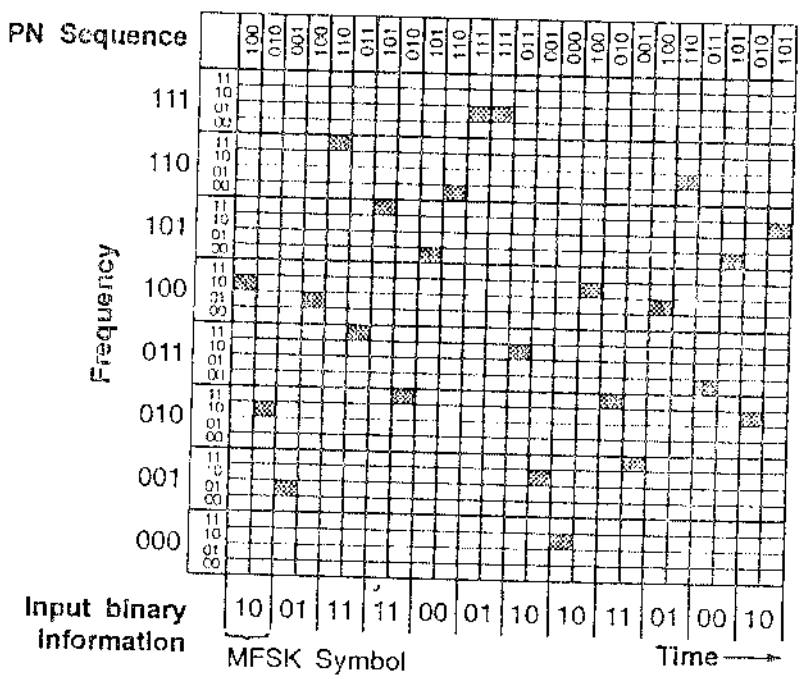
PN Sequence
Frequency
111
110
101
100
011
010
001
000
Input binary information
10 01 11 11 00 01 10 10 11 01 00 10
MFSK Symbol
Time

(b)

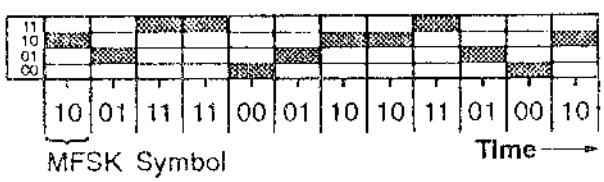

(c)

CHAPTER 11

ACCESS PROTOCOLS

PREAMBLE

This chapter gives an introduction to the multiple access protocols commonly used in multiple access communication networks. The aim is to provide the basic concepts for the analysis of one particular protocol in a mobile radio environment. The mobile radio system constitutes a typical example of a multiple access communication network where the control channels are shared by the mobile stations. The performance of the protocols is assessed by their throughput and special attention is paid to the Slotted ALOHA, chosen to be analyzed in a mobile radio environment. The radio channel is characterized by path loss (near/far effect) and Rayleigh fading. Moreover, the receiver is considered to work with capture effect. Contrary to what is initially expected, the combination of these phenomena greatly enhance the performance of the chosen protocol.

11.1 INTRODUCTION

The mobile radio system constitutes a typical example of multiple access communication network where the terminals, represented by the mobile stations, share the radio channels as common resources. The radio channels are divided into speech channels and control channels, the latter constituting the target of the present chapter.

Resources sharing is intrinsically associated with system efficiency. Accordingly, it is desirable to optimize the use of the channels, keeping them busy

with useful information as long as possible. However, due to the sharing, message collisions may occur in case more than one terminal attempts to transmit simultaneously. Therefore, a certain access discipline is mandatory, so that conflicts among terminals are kept to a minimum but with a maximum utilization of the channels.

11.2 PROTOCOLS CATEGORIES

The multiple access protocols are classified according to how much coordination is required to access the shared resources. Accordingly, there are three basic categories as follows.

a) *Random Access*

There is no coordination among the terminals. A terminal transmits a message according to its own convenience. As a consequence, message collisions are very likely to occur. The terminals are informed if they have been involved in a collision by monitoring the acknowledgement signal transmitted by the receiver over a separate channel.

b) *Scheduled Access*

There is a total coordination among the channels. A terminal only transmits a message within a slot specially allotted for it. No collisions occur, but the channels may not be efficiently used.

c) *Hybrid Access*

A certain degree of coordination is combined with the random access so that collisions are minimized.

11.3 PERFORMANCE EVALUATION

Many factors, such as (i) the ratio of the channel propagation delay to the transmission delay, (ii) the traffic arrival process and others may have a great

in the analysis of a specific access protocol when this is applied to a mobile radio system.

1) *ALOHA Protocols*

The ALOHA is the best known protocol among those belonging to the random access category. It is based on the following strategy. As soon as the message is ready for transmission the terminal accesses the channel and sends its message. In case of collision occurrence, a random time is awaited until retransmission is attempted.

Figure 11.1a illustrates the timing of packet transmission using ALOHA. It can be seen that the packet's vulnerable period is T = 2 packet times. Therefore, from (11.2), the probability that an arbitrary packet is overlapped by k packets is

$$P_k = \frac{(2G)^k}{k!} \exp(-2G) \tag{11.3}$$

The probability of a successful transmission in T packet times is the probability that no message is generated within T, i.e., $p = P_0 = \exp(-GT)$. Therefore, from (11.1), the throughput of the ALOHA protocol is

$$S = G\exp(-2G) \tag{11.4}$$

Using (11.4) we determine the maximum throughput of the ALOHA as being equal to $1/2e$ ($\approx 0{,}184$), corresponding to an offered traffic G of 0.5 packet per packet time.

2) *Slotted ALOHA*

In the Slotted ALOHA the time is divided into fixed length time slots. The terminal always awaits the next slot boundary to send its packet. Consequently, the vulnerable period is T = 1 packet time as illustrated in Figure 11.b. Accordingly, from (11.2), the probability that a packet is overlapped by k packets is

$$P_k = \frac{G^k}{k!} \exp(-G) \tag{11.5}$$

Following the same steps as in the previous analysis, the throughput of this protocols is

$$S = G\exp(-G) \tag{11.6}$$

Using (11.6) we determine the maximum throughput of the Slotted ALOHA as being equal to 1/e (≈ 0.368) corresponding to an offered load of 1 packet per packet time.

3) *Tree Algorithm*

The Tree Algorithm belongs to a class of protocols known as Splitting Algorithms. It is based on the following strategy. In the occurrence of a collision the terminals not involved in such collision go into a waiting state. Those involved are split into two groups according to a established rule, (e.g., by flipping a coin). The first group is permitted to use one time slot whereas the second group can use the next time slot, in case the first group is successful. However, if another collision occurs, a further splitting is carried out until, eventually a group with only one active terminal will be allowed to successfully transmit. The maximum throughput of this algorithm is 0.43 [7].

4) *First-Come-First-Served Algorithm*

This is another type of splitting algorithm where packets are transmitted in a First-Come-First-Served (FCFS) mode. At each time slot (say time slot k) only the packet arriving within a specified allocation time interval, (say from T(k) to T(k) + α(k)) are entitled to be transmitted. If a collision occurs the allocation interval is split into two equal subintervals (from T(k) to T(k) + α(k)/2 and from T(k) + α(k)/2 to T(k) + α(k)) and the packet arrived in the first subinterval is sent. In the case of another collision a further splitting (α(k)/4) is required and so on, until the transmission is successful. The throughput of this algorithm is 0.487 [8].

5) *Carrier Sense Multiple Access Protocols*

The basic characteristics of the Carrier Sense Multiple Access (CSMA) protocols is that each terminal monitors the status of the channel before transmission. If the channel is idle, the terminal transmits, otherwise the terminal awaits. There are several variations of this strategy.

a) 1-persistent CSMA – The terminal waits until the channel is free.

b) Nonpersistent CSMA – The terminal waits a random time to retry the transmission

c) p-persistent CSMA - This protocol is applicable to slotted channels. In the case the channel is idle the packet is sent in the first possible slot with probability p or in the next slot with probability 1-p.

d) CSMA/CD - In this protocol the terminal continuously monitors its own transmission for Collision Detection (CD) purposes. In case of collision, the transmission is aborted and a jamming signal is sent, instead. This jamming signal, sent for some units of time, is used as a "collision consensus enforcement mechanism" [1].

Although in all the CSMA protocols the channel is sensed prior to transmission, collision can still occur due to the propagation delay time. In other words a channel can be detected as idle though a remote terminal is already making use of it. Let a be the propagation delay between the furthest terminals. Hence, the throughput of the nonpersistent CSMA is [9]

$$S = \frac{G\exp(-aG)}{G(1 + 2a) + \exp(-aG)} \tag{11.7}$$

6) *Time Division Multiple Access*

In Time Division Multiple Access (TDMA) protocol, time is divided into slots and these are clustered into frames. Each slot is dedicated to a particular user.

7) *Frequency Division Multiple Access*

In Frequency Division Multiple Access (FDMA) protocol the spectrum is divided into subbands and each subband constitutes a channel also dedicated to a particular user.

8) *Code Division Multiple Access*

In Code Division Multiple Access (CDMA) protocol, different terminals transmit with different codes. Hence, a receiver tuned to the code of one specific transmission will interpret the other transmissions as noise.

9) *Packet Reservation Multiple Access*

Packet Reservation Multiple Access (PRMA) [11-13] can be viewed as a combination of TDMA and Slotted ALOHA. The channel bit stream is organized in slots and frames, as

in TDMA. Each slot within a frame can either be idle (available for contention) or busy (reserved). Terminals with new information to transmit contend for access to the idle slots, as in Slotted ALOHA. Once a terminal is successful in the contention for a time slot in one frame, this slot is reserved for its exclusive use in subsequent frames, until it has no more packets to send.

Terminals are informed about the status (available or reserved) of each time slot by a continuous signal stream broadcast by the base station. Permission to contend for any idle time slot is granted according to a given probability, representing a design parameter in the PRMA system.

Due to its time slot reservation characteristics, the PRMA protocol is equally suitable for handling both periodic and random informations. Periodic information is represented by (i) packets belonging to a long stream of data information and (ii) by the speech packets. Isolated data packets constitute the random type of information.

While data packets can experience delays in case of system congestions, conversational speech requires prompt packet delivery. Accordingly, besides throughput, PRMA require other performance parameters, represented by the *number of simultaneous conversations* that can take place for a given *packet dropping probability* (P_{drop}). The P_{drop} parameter is related to the speech quality objectives. It depends on the maximum time the speech packet can be held before being discarded by its terminal.

Experiments [12] show that for a channel rate = 720 kbits/s, a source rate = 32 kbits/s, a frame duration = 16 ms, overhead = 64 bits/frame and a maximum delay = 32 ms, the throughput is estimated as being 0.48. Moreover, for a $P_{drop} \leq 0.01$ the number of simultaneous conversation is 37. Note that in such condition, the number of channels per carrier is 720/32 = 22.5. Therefore, the number of simultaneous conversation per channel is 37/22.5 = 1.7.

11.5 SOME COMMENTS ON THE PROTOCOLS

The pure ALOHA and the Slotted ALOHA protocols are both susceptible to unstability. With the increase of the traffic load, the probability of collision increases substantially and eventually no packet is successfully transmitted. There are many ways of stabilizing these protocols by controlling the retrial process.

The splitting algorithms (e.g. Tree and FCFS) have the advantage of better stability but are more complex to be implemented. The theoretical analysis of the FCFS protocol is particularly intricate and its performance is usually obtained by means of simulation.

The CSMA protocols are not free from collision even though the channels are sensed before transmission is allowed. This is due to the propagation delay time, having a substantial influence in the protocols' performance.

The scheduled (also known as reservation-based) protocols (e.g. TDMA, FDMA, CDMA) suffer from the common disadvantage of not efficiently using the available resource. if a terminal has nothing to send, its slot is left free. This is particularly critical when messages are to be sent in bursts.

The performance of some protocols, as far as throughput is concerned, is shown in Figure 11.2. Note that the CSMA is greatly dependent on the delay parameter a. The CSMA/CD is a more elaborate protocol, giving better results than the others.

The PRMA protocol is still under investigation with the aim at being-used in the third generation mobile radio system. "The vision of the third generation is the merger of cellular and cordless technologies into a means of generalized wireless access to advanced information services" [12]. By serving densely populated areas this system must handle the most diverse types of informations such as voice, computer data, facsimile and network control messages.

We now turn our attention to the analysis of the Slotted ALOHA in a mobile radio environment. Due to its simplicity and good performance, this protocol has been chosen to be used by the Pan-European mobile communication system [10]. It is employed by the

mobile stations to provide the initial access to the base station.

11.6 SLOTTED ALOHA IN A MOBILE RADIO ENVIRONMENT

The three main propagation characteristics in a mobile radio environment are (I) shadowing, (II) multipath propagation and (III) near/far phenomenon. Shadowing occurs due to obstruction. The envelope of the signal experiencing this phenomenon has log-normal distribution. Multipath propagation occurs due to the various signal scatterers randomly distributed around the mobile. The envelope of the resultant signal has a Rayleigh distribution. The near/far phenomenon is related to the different power levels experienced at the base station by the signals transmitted from mobile stations positioned at different locations in the cell. If d is the distance between mobile and base station, the received mean signal power is given as a function of $d^{-\alpha}$ where α is a parameter in the range $2 \leq \alpha \leq 4$. The combination of these effects are usually seen as a threat to the performance of any transmission system. Accordingly, many equalization techniques are developed so as to counteract the effect of these phenomena.

However, we will show that, contrary to what is usually expected, the performance of the Slotted ALOHA is greatly enhanced when employed in this "unkind" environment. We shall analyze the Slotted ALOHA protocol in the presence of Rayleigh fading combined with the near/far phenomenon. Considerations on the effects of shadowing is carried out at the end of the chapter. The analysis that follows is based on the work by Arnbak and Blitterwijk [3].

11.6.1 Capture Effect

In the studies of standard ALOHA networks it is assumed that any collision provokes the destruction of all of the packets involved leading to the retransmission of these packets.

On the other hand, it is plausible to assume that when two or more mobiles are

competing for a time slot, the receiver at the base station will capture on the strongest signal. Let W be the power of the wanted signal and $I_k = \sum_{j=1}^{k} I_j$ the joint power of the other k interfering signals. Capture will occur when W exceeds I_k by a given threshold R_0. Therefore, the wanted packet is considered destroyed in a collision if and only if

$$W/I_k < R_0 \tag{11.8}$$

This implies that in our model the probability of collision given by (11.5) is conditional on the fact that the inequality expressed by (11.8) holds. Hence

$$\text{prob(k collisions given } W/I_k < R_0) = p_k = \frac{G^k}{k!}\exp(-G) \tag{11.9a}$$

Let r_k be the probability that $W/I_k < R_0$, i.e.,

$$r_k = \text{prob}(W/I_k < R_0) \tag{11.9b}$$

Then the unconditional probability of collisions q is

$$q = \sum_{k=1}^{\infty} p_k r_k \tag{11.10}$$

where p_k and r_k are given by (11.9a) and (11.9b), respectively.

Capture will occur with probability p where

$$p = 1 - q \tag{11.11}$$

Therefore, using (11.10) in (11.11) and then substituting (11.11) in (11.1), the channel throughput is obtained as

$$S = Gp = G\left[1 - \sum_{k=1}^{\infty} p_k r_k\right] \tag{11.12}$$

The probability distribution of the signal-to-interference ratio W/I_k can be written as a function of their respective distributions as follows. Define the random

variables R and I such that

$$W = RI \quad , \qquad 0 \le R < \infty \tag{11.13a}$$

$$I = I_k \quad , \qquad 0 \le I < \infty \tag{11.13b}$$

The joint distribution of R and I is

$$p(R,I) = |J| p(W,I_k)$$

where $|J| = \begin{vmatrix} \frac{\partial W}{\partial R} & \frac{\partial W}{\partial I} \\ \frac{\partial I_k}{\partial R} & \frac{\partial I_k}{\partial I} \end{vmatrix} = I$ is the Jacobian of the transformation, defined by (11.13). Since W and I_k are independent random variables

$$p(R,I) = Ip(W)p(I_k) \tag{11.14}$$

Hence, the density of R is

$$p(R) = \int_0^\infty p(R,I)dI$$

$$= \int_0^\infty Ip(W)p(I_k)dI$$

$$= \int_0^\infty Ip(RI)p(I)dI \tag{11.15}$$

Therefore, the corresponding distribution of R is r_k where

$$r_k = \text{prob}(R \le R_0) = \int_0^{R_0} p(R)dR \tag{11.16}$$

11.6.2 Probability Density of the Mean Power

Let $p(W|\overline{W})$ be the distribution of the signal W conditional on the mean power $\overline{W}$.

In a similar way, $p(I_k|\bar{I}_k)$ is the distribution of the interfering signal conditional on the mean interference $\bar{I}_k$. If we consider only multipath propagation, both W and I_k have a Rayleigh distribution, such that (refer to Chapter 5, equation (5.17))

$$p(X|\bar{X}) = \frac{1}{\bar{X}}\exp\left(-\frac{X}{\bar{X}}\right) \tag{11.17}$$

where $X = W$ and $\bar{X} = \bar{W}$ or $X = I_k$ and $\bar{X} = \bar{I}_k$, as required.

The unconditional probabilities $p(W)$ and $p(I_k)$ are obtained by averaging the corresponding conditional probabilities $p(W|\bar{W})$ and $p(I_k|\bar{I}_k)$ over the distributions of $\bar{W}$ and $\bar{I}_k$, respectively. Hence,

$$p(W) = \int_0^\infty \frac{1}{\bar{W}}\exp\left(-\frac{W}{\bar{W}}\right)p(\bar{W})d\bar{W} \tag{11.18}$$

and

$$p(I) = p(I_k) = \int_0^\infty \frac{1}{\bar{I}_k}\exp\left(-\frac{I_k}{\bar{I}_k}\right)p(\bar{I}_k)d\bar{I}_k \tag{11.19}$$

With (11.18) and (11.19) in (11.15) and then using (11.15) in (11.16) we obtain (refer Appendix 11A.1)

$$r_k = \int_0^\infty p(\bar{W})\left(\int_0^\infty p(\bar{I}_k)\frac{R_0\bar{I}_k}{R_0\bar{I}_k + \bar{W}}d\bar{I}_k\right)d\bar{W} \tag{11.20}$$

The mean duration of the fadings is usually at the order of some milliseconds (see section 4.7) while the duration of a time slot in a random access channel is about fractions of a millisecond*. Accordingly, we may assume that all of the received signals remain with the same mean power for the duration of a time slot so that their powers can be added directly. Therefore, the density of the mean interference signal is obtained by convolving the individual densities of the signal as many times (k times) as required, (refer to Appendix 11A.2), i.e.,

* For the GSM system this is 6.577 ms [10].

$$p(\bar{I}_k) = \left[p(\overline{W})\right]^{*k} \tag{11.21}$$

where *k signifies a k-fold convolution.

11.6.3 Rayleigh Fading and Path Loss Combined

Let $\overline{W}$ be the normalized mean power with respect to the power transmitted by the mobile from the border of the cell. Moreover, let h be the ratio between the distances d/d_{max} where d is the distance from the mobile to the base station and d_{max} is the cell radius. We have seen in Chapter 3 that

$$\overline{W} = h^{-\alpha} \tag{11.22}$$

where α is the path loss slope in the range $2 \le \alpha \le 4$.

Define G(h) as the number of packets per time slot offered per unit area at a normalized distance h. Let the mean number of packets be both Poisson distributed and a function of h only. Then, the total offered traffic is

$$G_t = 2\pi \int_0^{\infty} hG(h)dh \tag{11.23}$$

Assuming an uniform distribution for the mobiles within the cell the density of h is

$$p(h) = \frac{2\pi hG(h)}{G_t} \tag{11.24}$$

Since $\overline{W}$ is a function of h (see (11.22)) its density is obtained as

$$p(\overline{W})\left|d\overline{W}\right| = p(h)\left|dh\right| \tag{11.25}$$

From (11.22) $\left|d\overline{W}\right| = \alpha h^{-(\alpha+1)}\left|dh\right|$ and $h = \overline{W}^{-1/\alpha}$. Replacing these results and (11.24) in (11.25) we obtain

$$p(\overline{W}) = \frac{2\pi}{\alpha G_t}\overline{W}^{-(1+2/\alpha)}\, G(\overline{W}^{-1/\alpha}) \tag{11.26}$$

We now have all the necessary tools to evaluate the performance of Slotted ALOHA in a mobile radio environment. Once the traffic distribution G(h) is known, the densities $p(\overline{W})$ and $p(\bar{I}_k)$ can be calculated by means of (11.26) and (11.21), respectively. Then these densities are used in (11.20) to obtain r_k. Finally, the probability r_k is used in (11.12) to evaluate the system throughput.

As an example, consider the following quasi-uniform traffic distribution as depicted in Figure 11.3

$$G(h) = \frac{G_t}{\pi}\exp\left(-\frac{\pi}{4}h^4\right) \tag{11.27}$$

This distribution has been "chosen for its analytical convenience" [3].

Setting $\alpha = 4$ and by following the steps above described the throughput S(h) as a function of h is

$$S(h) = G(h)\left[1 - \exp(-G_t)\sum_{k=1}^{\infty}\frac{G_t^k}{k!}r_k\right] \tag{11.28}$$

where (see Appendix 11A.3)

$$r_k = \sqrt{\pi}\,\gamma_k\exp(\gamma_k^2)\operatorname{erfc}(\gamma_k) \tag{11.29}$$

and

$$\gamma_k = k\frac{\sqrt{\pi}}{2}\sqrt{R_0}\,h^2 \tag{11.30}$$

The total traffic captured by the receiver is S

$$S = 2\pi\int_0^{\infty} hS(h)dh \tag{11.31}$$

yielding

$$S = G_t\exp(-G_t)\sum_{k=1}^{\infty}\frac{G_t^k}{k!}\frac{1}{k\sqrt{R_0} + 1} \tag{11.32}$$

The curves of the normalized conditional throughput S(h)/G(h) versus the

normalized distance h with different total traffic G_t and capture threshold R_0 are shown in Figure 11.4. The overall throughput S for the various capture threshold R_0 is shown as a function of the total traffic G_t in Figure 11.5. Note from Figure 11.5 that it is substantially improved with the increasing capture threshold. For a capture threshold tending to infinity, corresponding to the case of no capture, the throughput curve coincides with that of standard Slotted ALOHA

11.7 SUMMARY AND CONCLUSIONS

This chapter introduced some of the protocols commonly employed in multiple access communications networks. The mobile radio system is an example of multiple access network where the access protocol is used by the mobile station to provide its initial contact with the base station. In particular, the Slotted ALOHA is an efficient and easy-to-be implemented protocol, chosen to be utilized by the Pan-European mobile radio system. The performance of this protocol is affected by the various propagation phenomena occurring in the mobile environment. In our analysis we included the near/far effect (path loss) and Rayleigh fading. The calculations of the throughput are rather laborious but the results are encouraging.

It has been shown that packet destruction and unstability are greatly improved in the mobile radio environment as compared to the standard Slotted ALOHA network. Contrary to what is usually expected, the performance enhancement is provided by the mobile radio propagation phenomena. Both path loss and Rayleigh fading act independently on the users, naturally splitting them into different classes of access power. This greatly improves the channel efficiency. Since the subscribers are in motion, the randomness of the signal power and the time to initiate a transmission after a collision provide the real mobile channel a natural priority. This priority is dynamically changed at each time instant.

The inclusion of shadowing in the calculations will slightly degrade the overall performance but the results are still encouraging [6].

"The third generation mobile radio system will probably convey information of several types including voice, computer data, facsimile and network control messages" [12]. In this sense, new proposals of access protocols able to handle data and speech have emerged and they have been under investigation [11-13].

APPENDIX 11A

Slotted ALOHA in Mobile Radio Environment

11A.1 Derivation of Equation (11.20)

Given that $I = I_k$ and $W = RI_k$ we use (11.18) and (11.19) in (11.15). We then use (11.15) in (11.16) to obtain r_k

$$r_k = \int_0^{R_0}\int_0^{\infty}\int_0^{\infty}\int_0^{\infty} \frac{I_k}{\bar{W}\,\bar{I}_k} \exp\left[-I_k\left(\frac{\bar{W} + R\bar{I}_k}{\bar{W}\,\bar{I}_k}\right)\right] p(\bar{W})p(\bar{I}_k)\,dR\,dI_k\,d\bar{W}\,d\bar{I}_k$$

By first integrating in I_k and then in R we have

$$r_k = \int_0^{\infty}\int_0^{\infty} \frac{R_0\bar{I}_k}{\bar{W} + R_0\bar{I}_k} p(\bar{W})p(\bar{I}_k)\,d\bar{W}\,d\bar{I}_k \qquad (11A.1)$$

11A.2 Probability Density of a Sum of Independent Random Variables

Laplace Transform

The Laplace transform of a function f(t) is F(s) defined as

$$f(t) \Leftrightarrow F(s) \triangleq \int_{-\infty}^{\infty} f(t)e^{-st}dt$$

Assuming f(t) = 0 for t < 0, the one-sided Laplace transform of f(t) is

$$F(s) = \int_0^{\infty} f(t)e^{-st}dt \qquad (11A.2)$$

Convolution

Define * as the convolution operator. The convolution of two functions of continuous time f(t) and g(t) is

$$f(t) * g(t) = \int_{-\infty}^{\infty} f(t - \tau)g(\tau)d\tau$$

If f(t) and g(t) take zero values for $t < 0$, then

$$f(t) * g(t) = \int_{0}^{t} f(t - \tau)g(\tau)d\tau \qquad (11A.3)$$

Laplace Transform of the Convolution

Equation (11A.3) can be rewritten as

$$f(t) * g(t) = \int_{0}^{t} f(t - \tau)g(\tau)d\tau + 0\int_{t}^{\infty} f(t - \tau)g(\tau)d\tau$$

$$= \int_{0}^{\infty} u(t - \tau)f(t - \tau)g(\tau)d\tau \qquad (11A.4)$$

where $u = (t - \tau) = \begin{cases} 1 & , \tau \le t \\ 0 & , \tau > t \end{cases}$

Substituting (11A.4) in (11A.2) and then interchanging the order of integration with respect to the variables t and τ we have

$$f(t) * g(t) \Leftrightarrow \int_{\tau=0}^{\infty} g(\tau)\left[\int_{t=0}^{\infty} u(t - \tau)f(t - \tau)e^{-st}dt\right]d\tau \qquad (11A.5)$$

The inner integral in (11A.5) is equal to $e^{-\tau s}F(s)$. Therefore

$$f(t) * g(t) \Leftrightarrow F(s)\int_{\tau=0}^{\infty} g(\tau)e^{-s\tau}d\tau$$

Thus

$$f(t) * g(t) \Leftrightarrow F(s)G(s) \qquad (11A.6)$$

This result applies to the convolution of any number of functions. Accordingly, if $p(x_i)$, $i = 1,...,n$ have Laplace transforms $P_i(s)$, $i = 1,...,n$ respectively, then

$$p(x_1) * p(x_2) * \ldots * p(x_n) \Leftrightarrow \prod_{i=1}^{n} P_i(s) \tag{11A.7}$$

Sum of Independent Random Variables

Let X_i, $i = 1,\ldots,n$ be independent random variables having probability densit functions equal to $p(x_i)$, $i = 1,\ldots,n$ respectively. Assume that the Laplace transforn of $p(x_i)$ is $P_i(s)$. Given that $X = \sum_{i=1}^{n} X_i$, we want to determine the density of X. Le p(x) be this density with Laplace transform P(s). Thus

$$p(x) \Leftrightarrow P(s) = \int_0^{\infty} e^{-sx} p(x)dx \tag{11A.8}$$

Using the transformation of random variables

$$p(x)dx = p(x_1,x_2,\ldots,x_n)dx_1dx_2\ldots dx_n$$

Since X_i, $i = 1,\ldots,n$ are independent random variables

$$p(x)dx = p(x_1,x_2,\ldots,x_n)dx_1dx_2\ldots dx_n = \prod_{i=1}^{n} p(x_i)dx_i \tag{11A.9}$$

Using (11A.9) in (11A.8) we obtain

$$p(x) \Leftrightarrow P(s) = \int_0^{\infty} e^{-sx_1} p(x_1)dx_1 \int_0^{\infty} e^{-sx_2} p(x_2)dx_2 \ldots \int_0^{\infty} e^{-sx_n} p(x_n)dx_n$$

Therefore

$$p(x) \Leftrightarrow P(s) = \prod_{i=1}^{n} P_i(s) \tag{11A.10}$$

With (11A.7) and (11A.10) we conclude that

$$p(x) = p(x_1) * p(x_2) * \ldots * p(x_n) \Leftrightarrow \prod_{i=1}^{n} P_i(s) = P(s) \tag{11A.11}$$

11A.3 Distribution r_k of R as a Function of the Normalized Distance h

(Equation (11.29)

Assume that at the normalized distance h the mean power $\bar{W}$ is constant and equal to $h^{-\alpha}$. Then, from (11.20)

$$r_k = \int_0^\infty p(\bar{W})d\bar{W} \int_0^\infty p(\bar{I}_k)\frac{R_0\bar{I}_k}{R_0\bar{I}_k + h^{-\alpha}}d\bar{I}_k$$

$$= \int_0^\infty p(\bar{I}_k)\frac{R_0\bar{I}_k}{R_0\bar{I}_k + h^{-\alpha}}d\bar{I}_k \qquad (11A.12)$$

With (11.27) in (11.26) we obtain

$$p(\bar{W}) = \frac{1}{2}\bar{W}^{-3/2}\exp\left(-\frac{\pi}{4\bar{W}}\right) \qquad (11A.13)$$

The Laplace transform of $p(\bar{W})$ is equal to $\exp(-\sqrt{\pi}\sqrt{s})$.

Therefore, from (11.21) in connection with (11A.11)

$$p(\bar{I}_k) = \left[p(\bar{W})\right]^{*k} \Leftrightarrow \exp(k\sqrt{\pi}\sqrt{s})$$

From the tables of Laplace transform

$$p(\bar{I}_k) = \frac{k}{2}\bar{I}_k^{-3/2}\exp\left(-\frac{\pi k^2}{4\bar{I}_k}\right) \Leftrightarrow \exp(k\sqrt{\pi}\sqrt{s}) \qquad (11A.14)$$

With (11A.14) in (11A.12) we obtain

$$r_k = k\int_0^\infty \frac{R_0h^4}{R_0h^4 + t^2}\exp\left(-\frac{\pi}{4}k^2t^2\right)dt$$

From tables of integrals

$$r_k = \sqrt{\pi}\gamma_k\exp(\gamma_k^2)\mathrm{erfc}(\gamma_k) \qquad (11A.15)$$

where

$$\gamma_k = k\frac{\sqrt{\pi}}{2}\sqrt{R_0}h^2$$

REFERENCES

[1] V.O.K. Li, "Multiple Access Communications Networks", *IEEE Communications Magazine*, Vol. 25, No. 6, June 1987.

[2] D.J.Goodman and A.A.M. Saleh, "The Near/Far Effect in Local ALOHA Radio Communications", *IEEE Transactions on Vehicular Technology*, Vol. VT-36, No. 1, February 1987.

[3] J.C. Arnbak and W. Van Blitterswijk, "Capacity of Slotted ALOHA in Rayleigh Fading Channels", *Journal on Selected Areas in Communications*, Vol. SAC-5, No. 2, pp. 261-269, February 1987.

[4] N. Abramson, "The Throughput of Packet Broadcasting Channels", *IEEE Transactions on Communications*, Vol. COM-25, pp. 117-128, January 1977.

[5] C. Namislo, "Analysis of Mobile Radio Slotted ALOHA Network" *IEEE Journal on Selected Areas in Communications*, Vol. SAC-2, pp. 583-588, July 1984.

[6] Y.K. Ling and K.W. Cattermole, "The Random-Access Control Channel of a Cellular Mobile Radio System", 5th *U.K. Teletraffic Symposium*, Birminghan, England, 1988.

[7] J.I. Capetanakis, "Tree Algorithms for Packet Broadcasting Channels", *IEEE Transactions on Information Theory*, Vol IT-25, pp.505-515, September 1979.

[8] R.G. Gallager, "Conflict Resolution in Random Access Broadcast Networks", *Proc. AFOSR Workshop on Comm. Theory and Appl.*, Provincetown, MA, September 1978.

[9] L. Kleinrock and F.A. Tobagi, "Packet Switching in Radio Channels: Part 1 - Carrier Sense Multiple Access Modes and Their Throughput Delay Characteristics", *IEEE Transactions on Communications*, Vol. COM-23, No. 12, pp. 1400-1416, December 1975.

[10] CEPT/CCH/GSM, "Physical Layer on the Radio Path: General Description," GSM recommendation 05.01, Draft 3.1.0, February 1988.

[11] S. Nanda, "Analysis of Packet Reservation Multiple Access: Voice Data Integration for Wireless Network," *IEEE Globecom Conf.*, San Diego, pp. 1984-1988, Dec. 1990.

[12] D.J. Goodman and S.X. Wei, "Efficiency of Packet Reservation Multiple Access", *IEEE Trans. on Vehicular Tech.*, Vol. 40, Nº 1, pp. 170-176, Feb. 1991.

[13] D.J. Goodman, "Trends in Cellular and Cordless Communications", *IEEE Communications Magazine*, pp. 31-40, June 1991.

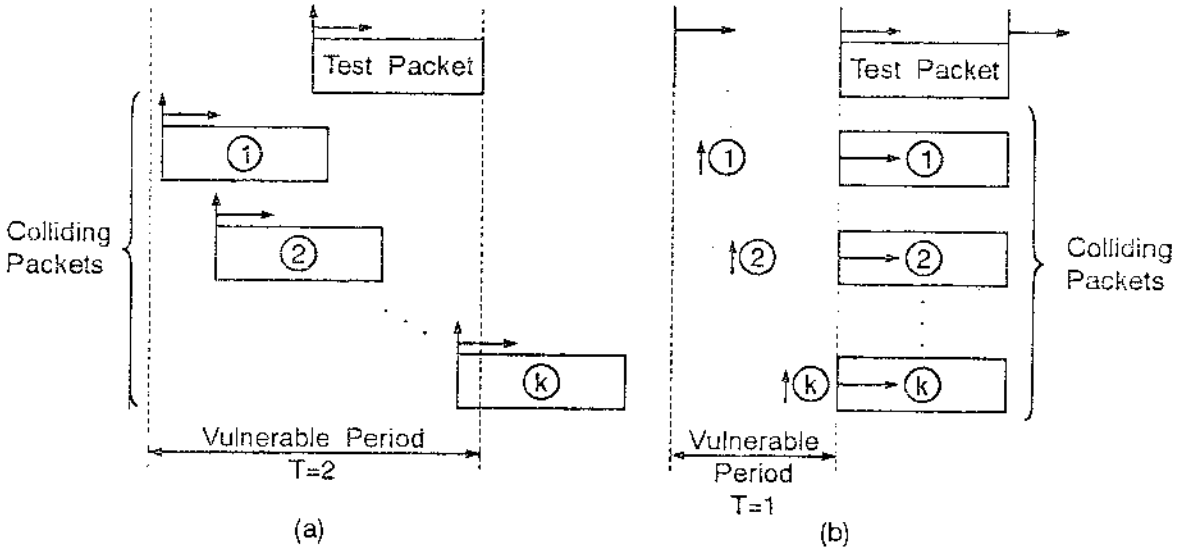

where: ↑ ≙ instant when the packet is ready
→ ≙ instant of transmission

FIG 11-1 (50%)

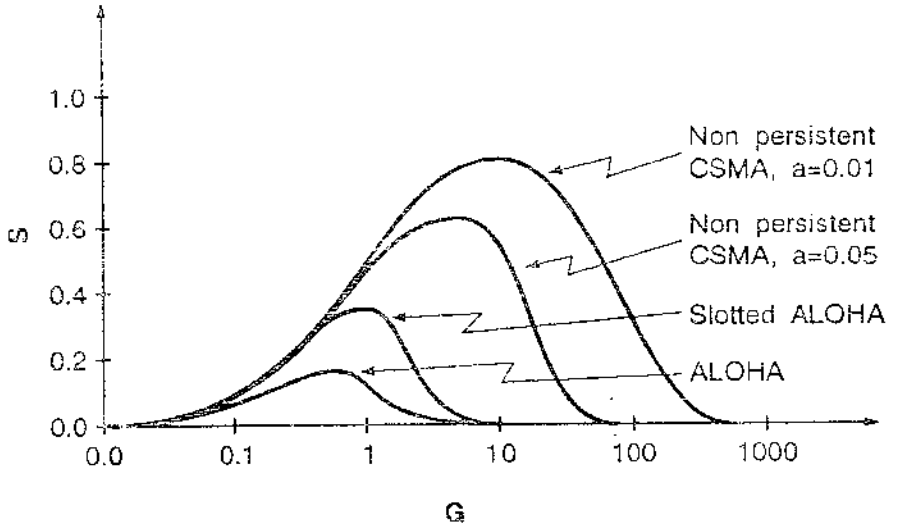

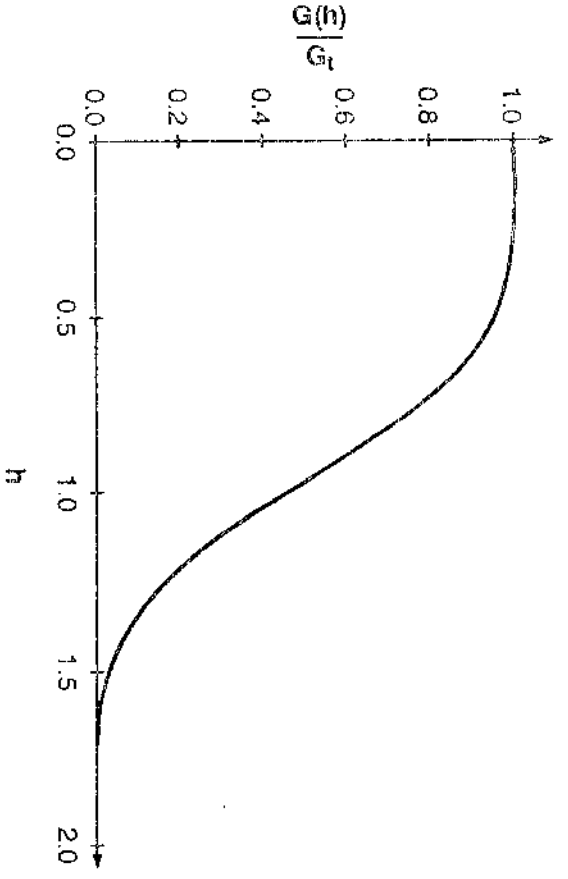

Figure xxx

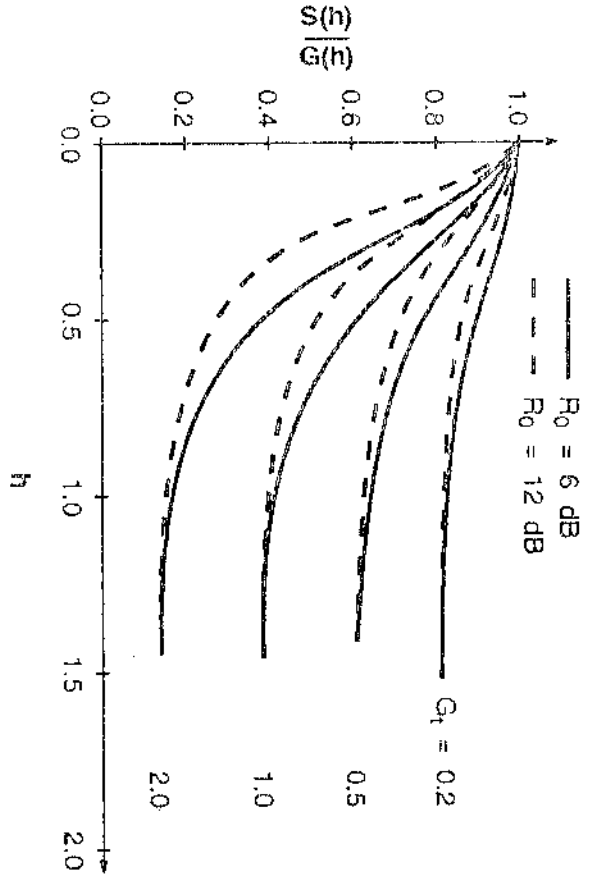

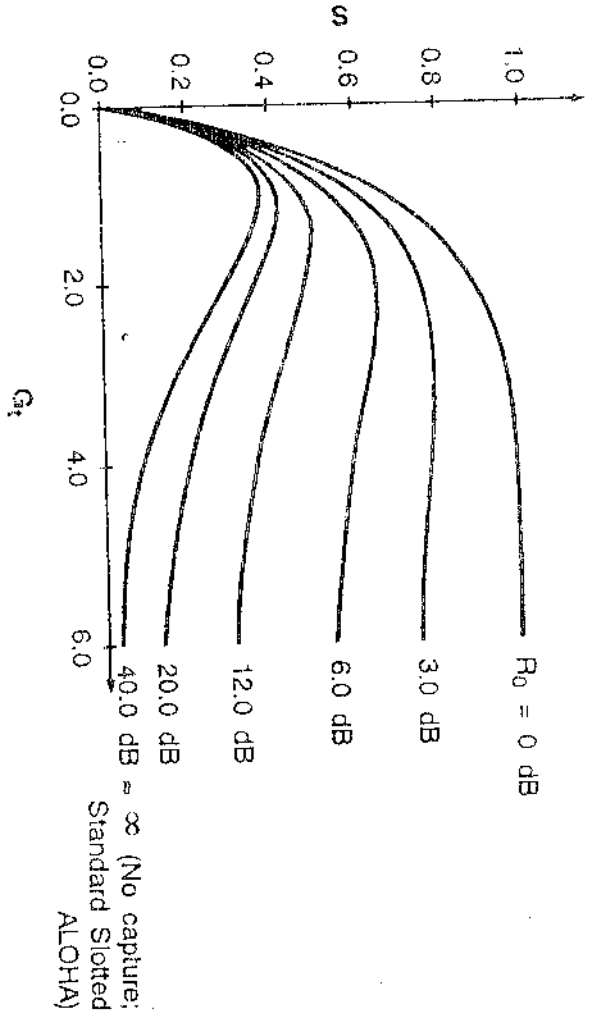

PART VI

TRAFFIC

CHAPTER 12

TRAFFIC ASPECTS IN MOBILE RADIO SYSTEMS

PREAMBLE

This chapter examines some of the main channel allocation techniques that can be used in a mobile radio system. It starts by reviewing the basic principles of queueing and traffic theory, commonly used in the teletraffic analysis. The allocation techniques are divided into two groups, namely, Global and Local. The global techniques usually imply a substantial change in the usage pattern of the channels, requiring the involvement of the central processor. In the local techniques, although some small change in the usage pattern of the channels may occur, the channels are used within or closely adjacent to their planned service area. In this case the decisions are taken locally, involving two or three neighbouring cells.

The global allocation techniques are investigated by means of simulation, where the main phenomena, such as handoff, cochannel interference, adjacent channel interference and others, are taken into account. Special attention is given to the Hybrid Channel Allocation technique where it is shown that a small proportion of dynamic channels is enough to provide a substantial gain in traffic capacity.

The local techniques are investigated by means of the Markov process in a 2-cell system. The aim is to get an insight into the main phenomena involved and not to provide a quantitative performance measure. In particular, we examine the Blocking Threshold Variation technique using numerical analysis. It is shown that even with the use of a small proportion of the channels for alternative routing, a significant gain in traffic capacity can be achieved. An approximate expression for the mean blocking probability is found to give results very close to those of the exact solution.

12.1 INTRODUCTION

Although the traffic characteristics of a mobile radio system is rather distinct from that of a fixed telephone network, the system planning and design are still carried out with the tools of the conventional traffic theory. According to the expected traffic and cochannel interference requirements, the geographical region is divided into cells. Given the traffic in each cell and the desired mean blocking probability, the Erlang-B formula is used to determine the number of channels per cell, assuming no handoff and no roaming. The design is later adjusted to take into account these factors.

All the cells can be built to have the same area but different number of channels per cell, chosen to meet the blocking probability requirements. Alternatively, the cells can present the same number of channels but their sizes must be tailored so that the traffic in each cell can experience the desired grade of service.

The traffic distribution vary in time and in space, but they are commonly bell shaped. High concentrations are found in the city centre during the rush hour, decreasing towards the outskirts. After the rush hour and towards the end of the day, this concentration changes as the users move from the town centre to their homes.

Note that, because of the mobility of the users, handoffs and roaming are always occurring, reducing the channel holding times in the cell where the calls are generated. This increases the traffic in the cell where the mobiles go to. Accordingly, the Erlang-B formula no longer applies. A full investigation on the traffic performance of a mobile radio system requires all the phenomena to be taken into account, rendering intricate any traffic model. We may, however, introduce many simplifications and obtain a qualitative rather than a quantitative result to better understand the main phenomena.

In this chapter we shall examine some channel assignment techniques, particularly analyzing the Hybrid assignment algorithm. Moreover, we shall investigate an alternative routing technique using the fuzzy traffic of the cells -- the Blocking

Threshold Variation algorithm. The chapter initiates by presenting some queueing and traffic theory fundamentals.

12.2 QUEUEING AND TRAFFIC THEORY FUNDAMENTALS

In the traffic analysis of a mobile radio system it is widely accepted that (i) calls have a Poisson arrival, (ii) holding times have a negative exponential distribution and (iii) blocked calls are lost.

In this section we shall examine the basic principles of queueing and traffic theories used to analyze the various channel assignment algorithms in a mobile radio system.

12.2.1 Call Arrival Process

Consider the call arrival as a random process. Let a time interval t be divided into n equal subintervals with length t/n each. Choose n to be sufficiently large such that:

(i) only one arrival can occur in any subinterval t/n

(ii) call arrivals are independent from each other

(iii) the probability $p_1(1)$ that an arrival occurs in one of the subintervals is proportional to the subinterval length. Hence $p_1(1) = \lambda t/n$, where $\lambda > 0$. Accordingly, the probability of no arrivals in t/n is $1 - \lambda t/n$.

The probability of exactly k arrivals in n subintervals can be evaluated using the binomial distribution. Then

$$p_k(n) = \binom{n}{k} \left(\lambda \frac{t}{n}\right)^k \left(1 - \lambda \frac{t}{n}\right)^{n-k} \qquad (12.1)$$

The sum between brackets in (12.1) can be written using the Newton's binomial expansion*. The limit of $p_k(n)$ as n tends to infinity will be the probability p_k of

* $(a+b)^N = \sum_{j=1}^{N} \binom{N}{1} a^1 b^{N-1}$

k arrivals in the time interval t. It is straightforward to show that, in this case

$$p_k = \frac{(\lambda t)^k}{k!}\exp(-\lambda t) \tag{12.2}$$

Equation (12.2) is the Poisson probability distribution. Its mean is $E[k] = \sum_{k=0}^{\infty} kp_k = \lambda t$. The parameter λ is the mean arrival rate of calls (calls/sec.). The variance is $E[k^2] - E^2[k] = \lambda t$.

Mean Interarrival Time

Let τ be a random variable denoting the time between adjacent arrivals with probability distribution and density given by A(t) and a(t), respectively. The distribution A(t) is the probability that the time between arrivals τ is less than or equal to t. Hence

$$A(t) = \text{prob}(\tau \leq t) = 1 - \text{prob}(\tau > t)$$

But prob(τ > t) is exactly the probability that no arrivals occur within t, that is, p_0. Therefore, with k = 0 in (12.2)

$$A(t) = 1 - \exp(-\lambda t) \tag{12.3}$$

The density a(t) is obtained by differentiating A(t) with respect to t. Thus

$$a(t) = \lambda\exp(-\lambda t) \tag{12.4}$$

Equation (12.4) is referred to as the negative exponential distribution. The mean interarrival time is

$$E[t] = \int_0^{\infty} ta(t)dt = 1/\lambda$$

Memoryless Property of the Negative Exponential Distribution

This property refers to the fact that the past history of an exponentially distributed random variable has no influence in predicting its future. In our particular case, consider the situation where a call has just arrived. The distribution of the time until the next call arrival is still a negative exponential,

as we shall demonstrate.

Let t_0 be a time where no arrival occurs. What is the probability that the next arrival occurs within a time t from t_0? To answer this question we require to calculate the probability $\text{prob}(\tau \leq t + t_0 \mid \tau > t_0)$. Using the conditional probability properties we have

$$\text{prob}(\tau \leq t + t_0 \mid \tau > t_0) = \frac{\text{prob}(t_0 < \tau \leq t + t_0)}{\text{prob}(\tau > t_0)}$$

$$= \frac{\text{prob}(\tau \leq t + t_0) - \text{prob}(\tau \leq t_0)}{\text{prob}(\tau > t_0)} \qquad (12.5)$$

The probability $\text{prob}(\tau \leq x)$ is given by A(x). Therefore, using (12.3) in (12.5) we obtain

$$\text{prob}(\tau \leq t + t_0 \mid \tau > t_0) = 1 - \exp(-\lambda t)$$

which is exactly the distribution A(t).

12.2.2 Call Holding Time

Let t be a time interval divided into n equal subintervals of length t/n each. Choose n to be sufficiently large such that:

(i) The probability that a call terminates within one subinterval is proportional to its length. That is, this probability equals $\mu t/n$, where $\mu > 0$

(ii) The call termination occurs independently of which subinterval is considered.

Let τ be a random variable denoting the call holding time with probability distribution and density given by H(t) and h(t), respectively. The distribution H(t) is the probability that the holding time τ is less than or equal to t. Hence

$$1 - H(t) = 1 - \text{prob}(\tau \leq t) = \text{prob}(\tau > t)$$

The probability prob(τ > t) that a call originated at time zero will not terminate before t is given by the probability that it will not terminate in any of the n subintervals of length t/n, when n tends to infinity. Then

$$1 - H(t) = \lim_{n \to \infty} \left(1 - \mu \frac{t}{n}\right)^n = \exp(-\mu t)$$

Thus

$$H(t) = 1 - \exp(-\mu t) \tag{12.6}$$

The density is obtained by differentiating (12.6) with respect to t. Hence

$$h(t) = \mu \exp(-\mu t) \tag{12.7}$$

In the same way, in the interarrival time distribution case the mean holding time is $1/\mu$.

12.2.3 Birth-Death Processes

"A Markov process with a discrete state space is referred to as a Markov chain. A set of random variables (X_n) forms a Markov chain if the probability that the next value (state) is x_{n+1} depends only upon the current value (state) x_n and not upon any previous values" [1]. In analytical form we have

$$\text{prob}\left[X(t_{n+1}) = x_{n+1} \middle| X(t_n) = x_n, \ldots, X(t_1) = x_1\right] = \text{prob}\left[X(t_{n+1}) = x_{n+1} \middle| X(t_n) = x_n\right] \tag{12.8}$$

A birth-death process constitutes a special case of Markov process where transitions are allowed to occur only between neighbouring states. Let S_k denote the state of the system at a given time when the population of the system (number of busy channels) is k. A transition from S_k to S_{k+1} implies a birth within the population, occurring with a rate λ_k. A transition from S_k to S_{k-1} implies a death with a rate μ_k. Note that λ_k and μ_k are rates and not probabilities. They can, however, be

converted into probabilities if they are multiplied by the infinitesimal time dt, leading to the probability of such a transition occurring during dt.

An one-dimensional birth-death process can be represented by means of a state transition rate diagram as depicted in Figure 12.1. Let $p_k(t)$ be the probability that the system is in state S_k at the time instant t. By simply inspecting Figure 12.1 we may write the following relation

prob. of reaching the state $S_k = \left[\lambda_{k-1}p_{k-1}(t) + \mu_{k+1}p_{k+1}(t)\right]dt$

prob. of departing from the state $S_k = (\lambda_k + \mu_k)dtp_k(t)$

The difference between the above probabilities equals the differential probability $dp_k(t)$, such that

$$\frac{dp_k(t)}{dt} = \lambda_{k-1}p_{k-1}(t) + \mu_{k+1}p_{k+1}(t) - (\lambda_k + \mu_k)p_k(t) \qquad (12.9)$$

As t tends to infinity, the system tends to an equilibrium solution where the transient behaviour vanishes. Accordingly, $dp_k(t)/dt$ tends to zero and we denote $p_k(t)$ by p_k. Therefore, from (12.9)

$$\lambda_{k-1}p_{k-1} + \mu_{k+1}p_{k+1} = (\lambda_k + \mu_k)p_k \qquad , k \geq 0 \qquad (12.10)$$

where $p_{-1} = 0$, $\mu_o = 0$ and $\lambda_{-1} = 0$. Equation (12.10) shows that, in equilibrium, the flow rate into S_k equals the flow rate out of S_k. By writing (12.10) sequentially for k = 0,1,2,3,.... and observing that the probabilities p_k must sum to unity

$$\sum_{k=0}^{\infty} p_k = 1 \qquad (12.11)$$

we may solve the set of equations to obtain

$$p_k = p_0 \prod_{i=0}^{k-1} \lambda_i/\mu_{i+1} \qquad (12.12)$$

where

$$p_0 = \left[1 + \sum_{k=1}^{\infty} \prod_{l=0}^{k-1} \lambda_l / \mu_{l+1} \right]^{-1} \qquad (12.13)$$

Blocked Calls Held

Consider a system with an infinite number of servers. Assume that the arrival (birth) rate is constant and equal to λ and that the departure (death) rate from each server is equal to μ. Thus

$$\lambda_k = \lambda \quad , \qquad k \geq 0$$

$$\mu_k = k\mu \quad , \qquad k \geq 1$$

Then, using these parameters in equations (12.12) and (12.13) we obtain

$$p_k = \left[(\lambda/\mu)^k / k! \right] \left[\sum_{l=0}^{\infty} (\lambda/\mu)^l \right]^{-1}$$

Hence

$$p_k = \frac{A^k}{k!} \exp(-A) \qquad (12.14)$$

where $A = \lambda/\mu$ is the traffic offered in Erlangs (erl.). The mean value and the variance of the above distribution have already been determined in section 12.2.1 and they are both equal to A. Assume that the system has N channels (N servers) and that arrivals, occurring when all N channels are busy, remain in the system for one holding time. If during this period a channel becomes free, a waiting customer seizes the channel for the remainder of the holding time . The blocking probability in this case is

$$B = \sum_{k=N}^{\infty} \frac{A^k}{k!} \exp(-A) \qquad (12.15)$$

The above equation is referred to as Molina's formula [2].

Blocked Calls Cleared

In this case the system is assumed to have N channels and calls arriving when all the channels are found to be busy are lost. Then, the state transition diagram of Figure 12.1 terminates at the state S_N (N channels) and

$$\lambda_k = \lambda \quad , \qquad k \leq N - 1$$

$$\mu_k = k\mu \quad , \qquad k < N$$

With the above transition rates in (12.12) and (12.13) and noticing that the upper limit of the sum in (12.13) is equal to N we obtain

$$p_k = \frac{A^k/k!}{\sum_{I=0}^{N} A^I/I!} \tag{12.15}$$

Blocking will occur when all the N channels are busy. The probability of this event is

$$E(A,N) = p_N = \frac{A^N/N!}{\sum_{I=0}^{N} A^I/I!} \tag{12.16a}$$

which is known as Erlang-B formula. Another useful way of writing the Erlang-B formula is in its recursive way. It is easy to show that

$$E(A,N) = \frac{E(A,N-1)}{N/A + E(A,N-1)} \tag{12.16b}$$

The Erlang-B formula is well established in the form of table as shown in Appendix 12C (from ref. [21]). An approximation can be obtained for large values of N, when the denominator of (12.16a) tends to exp(A) such that

$$E(A,N) \simeq \frac{A^N}{N!}\exp(-A) \tag{12.17}$$

Blocked Calls Delayed

In this model the blocked calls are allowed to queue up and wait to be served. Then

$$\lambda_k = \lambda \quad , \qquad k \geq 0$$

$$\mu_k = \begin{cases} k\mu \ , & 0 \leq k \leq N \\ N\mu \ , & k \geq N \end{cases}$$

Using the same procedure as in the previous case we obtain

$$p_k = \frac{A^k}{k!} p_0 \quad , \qquad 0 \le k \le N$$

$$p_k = \frac{A^k}{k!} N^{N-k} p_0, \qquad k \ge N$$

where
$$p_0 = \left[\sum_{k=0}^{N-1} \frac{A^k}{k!} + \frac{A^N}{N!} \frac{1}{1 - A/N} \right]^{-1} \tag{12.18}$$

The probability of delaying (no channel is available) is

$$\text{prob[queueing]} \triangleq C(N,A) = \sum_{k=N}^{\infty} p_k$$

Using p_k for $k \ge N$ we obtain

$$C(N,A) = \frac{A^N}{N!} \frac{1}{1 - A/N} p_0 \tag{12.19}$$

The above equation is known as Erlang-C formula.

Finite Population

In the previous cases we considered a Poisson traffic generated by an infinite population. If, however, the population is finite, say with M customers, the birth rate becomes dependent on the size of this population, decreasing as each customer seizes a server. Assuming a pure loss system we have

$$\lambda_k = (M - k)\lambda \quad , \qquad k \le N - 1$$

$$\mu_k = k\mu \qquad , \qquad k < N$$

Accordingly,

$$p_k = \frac{\binom{M}{k} A^k}{\sum_{i=0}^{N} \binom{M}{i} A^i} \tag{12.20}$$

This is known as the Engset distribution.

12.2.4 Alternative Routing (Wilkinson's Theory)

In standard telephone networks a stream of traffic can reach its destination through a direct path or indirect paths. The trunks in the direct path form a high

usage route constituting the first option routing. If all these trunks are busy, the overflow traffic may use an alternative path to reach its destination. While the traffic using the direct route has Poisson characteristics, the overflow traffic presents peakednesses and is not considered to be Poisson any longer. It is better described by its variance V_i such that [3]

$$V_i = F_i\left[1 - F_i + \frac{A_i}{1 + N_i + F_i - A_i}\right] \qquad (12.21)$$

where A_i is the traffic offered to route i,

F_i is the overflow traffic from route i,

N_i is the number of trunks on route i.

The overflow traffic is obtained from

$$F_i = A_i E(A_i, N_i) \qquad (12.22)$$

Since an overflow route takes traffic from n other routes, its mean total traffic A and variance V are

$$A = \sum_{i=1}^{n} A_i \qquad \text{and} \qquad V = \sum_{i=1}^{n} V_i \qquad (12.23)$$

The equivalent random (Poisson) traffic A_e, when offered to an "imaginary" full-availability group of N_e trunks, results in an overflow traffic with mean and variance equal to A. Recall from section 12.2.1 that the variance-to-mean ratio of a Poisson traffic is the unity. It is possible to show [4] that these parameters are approximately given by

$$A_e = V + \frac{3V}{A}\left(\frac{V}{A} - 1\right) \qquad (12.24)$$

$$N_e = A_e\left(1 - \frac{1}{A + V/A}\right)^{-1} - A - 1 \qquad (12.25)$$

Suppose that the stipulated blocking probability for the alternative route is B. Hence the overflow traffic from this route is AB. Consider that the alternative route

has N_a trunks. Accordingly, the overflow traffic produced by the equivalent traffic A_c when offered to a group of $N_c + N_a$ trunks should be equal to AB. Therefore

$$B = \frac{A_c}{A} E(N_c + N_a, A_c) \tag{12.26}$$

12.3 TRAFFIC PERFORMANCE ENHANCEMENT TECHNIQUES

Channel allocation plays a very important role in the traffic performance of a mobile radio system. The simplest channel assignment algorithm uses Fixed Allocation. It has the maximum spatial efficiency in channel reuse, as the channels are always assigned at the minimum reuse distance. Moreover, since each cell has a fixed set of channels, the channel assignment control for the calls can be distributed among the base stations [5]. The main problem of the Fixed Allocation is its inability to deal with the alteration of the traffic pattern. Due to the mobility of the subscribers, some cells may experience a sudden growth in the traffic offered with a consequent deterioration of the grade of service, while other cells may have free channels that cannot be used by the congested cells.

The steps to assign channels on a fixed basis are as follows:

1) The repeat pattern (cluster size) is determined according to the allowable signal-to-interference ratio.

2) The cluster with the highest traffic is chosen for the initial design. The traffic per cell in this cluster is then determined.

3) Given the traffic per cell and an allowable blocking probability, the number of channels per cell can be determined using the Erlang-B formula.

4) In case the total number of available channels is not enough to provide the required grade of service, the area covered by one cluster should be reduced in order to reduce the traffic per cell.

5) The other clusters can reuse the same channels according to the reuse pattern. However, cells with less traffic may use less channels so that not all channels need

to be provided by the base stations.

12.3.1 Global Assignment Techniques

The main channel allocation techniques such as Borrowing, Dynamic and Hybrid algorithms are briefly described in Chapter 2 (section 2.12.1). These techniques have been extensively explored in the literature [5,12]. In particular, they are thoroughly investigated by Sanchez [5] and Sanchez and Eade [12] with most of the mobile radio phenomena (cochannel interference, adjacent channel interference, handoffs, etc.) included.

The Dynamic channel allocation comprises a set of algorithms with the common characteristics that all the channels are available for all the cells. The Dynamic algorithm choosing the first dynamic channel available not exceeding the reuse constraints is of particular interest due to its simplicity. In the algorithms where there is a pool of channels to be dynamically used according to the traffic demand, spatial efficiency is not usually considered.

The results show [5] that these techniques require a substantial amount of memory and data interchange between Base Station and Mobile Switching Centres. For an even traffic distribution and low blocking probability these global techniques perform better than the Fixed Allocation algorithm. With the increase of traffic, the spatial inefficiency of dynamic channels cause both the Dynamic algorithms and the Hybrid techniques with high proportion of dynamic channels to reverse their performance with respect to the Fixed assignment. For uneven traffic distribution, where more flexibility is required, the Dynamic followed by Hybrid and Borrowing techniques perform better than the Fixed algorithm. In section 12.4 we shall examine the Hybrid technique in more detail.

12.3.2 Local Assignment Techniques

These techniques treat the traffic with access to more than one base station as

available for alternative routing. This traffic is mostly encountered at the border's region of the cells where base station's service areas overlap. While the application of these techniques implies some change in the usage pattern of the channels, the rearrangement is purely local and do not imply any complex global network management. Moreover, since the flexible channels are within or closely adjacent to their service area, there are no serious implications for frequency reuse pattern. Let us describe the main techniques [14-20].

- *Mean Adaptation (MAP):* divides the flexible traffic among the cells in a proportion controlled by the estimate of the imbalance of each cell.

- *Adaptive Response to Blocking (ARB)* (also known as "Directed Retry" [13]): diverts the blocked flexible calls to the cell presenting free channels.

- *Adaptation to Mean and Blocking:* is the combination of *MAP* and *ARB*.

- *Instantaneous Adaptation (IAP):* diverts the flexible traffic to the cell with smaller number of busy channels. When the cells present an equal number of busy channels, the flexible traffic is equally shared by these cells.

- *Instantaneous and Mean Adaptation (IMA):* is similar to IAP. However, in case the cells present an equal number of busy channels, the flexible traffic is directed to the least imbalanced cell.

- *Full IMA (FIMA):* combines the characteristics of IMA and AMB to yield an optimum strategy.

- *Blocking Threshold Variation (BTV):* to be described in section 12.5.

These strategies have been extensively analyzed in [14-20] showing that a substantial improvement in the traffic performance can be achieved. In the results to be given next we use the symbol "<" to mean "better than" (i.e., less mean blocking) and "≡" to mean "equivalent to". Hence:

a) For an even traffic distribution, IAP ≡ IMA < ARB ≡ AMB < MAP

b) For an uneven traffic distribution, IMA < IAP < ARB and AMB < ARB

b1) When traffic balance cannot be accomplished and

- For high imbalance, IMA < AMB

- For low imbalance, AMB < IMA

- For very high imbalance, AMB < MAP < IMA < IAP < ARB.

FIMA gives the best performance amongst all these strategies. However, it is substantially more complicated to be implemented, not justifying its application. Moreover, the improvement achieved is not significantly greater than that of IMA [18].

12.4 HYBRID CHANNEL ALLOCATION [5,12]

In Hybrid allocation a proportion of the channels is assigned on a fixed basis, while the remaining channels form a common pool for dynamic assignment. The dynamic channels (N_d) are requested by the cell when its fixed channels (N_f) are all being used. It can be seen that this technique may range from the Fixed ($N_d = 0$) to the totally Dynamic ($N_f = 0$) allocation. Accordingly, its performance depends on the traffic profile and on the proportion of dynamic-to-fixed (N_d/N_f) channels.

12.4.1 Initial Performance Assessment

The usefulness of the Hybrid technique can be initially assessed using an analytical approach as that described by the Wilkinson's theory (refer to section 12.2.4). The traffic blocked when all the fixed channels are busy can be treated as an overflow traffic. The dynamic channels are equivalent to the trunks available on the indirect (alternative) route. Therefore, for a given traffic per cell A_1, offered to a group of fixed channels N_1 ($N_1 = N_f$), the overflow traffic F_1 can be calculated using (12.22). The variance V_1 is then determined by (12.21) and the total traffic A with variance V on the alternative route can be estimated by (12.23), where n is equal to the number of cells using the pool of dynamic channels. Then the equivalent random traffic A_e offered to the group of N_e channels are determined by (12.24) and (12.25), respectively. The overall blocking probability is determined by (12.26) where $N_a = nN_d$.

This procedure has been used to assess the performance of a 7-cell cluster having

a total of 105 channels (15 channels/cell) and an even traffic distribution. The result is shown in Figure 12.2 (theoretical curves). Note that the curves for the proportion of dynamic-to-fixed channels equal to 00/15 and 15/00 can be obtained directly by the Erlang-B formula by performing $E(A_i,15)$ and $E(7A_i,105)$, respectively. In particular, the theoretical and the simulated curves (see section 12.4.2) for the proportion 00/15 differ by a factor smaller than 1%. Therefore, for practical purposes they are considered to be "coincident". However, this may not be true if the proportion of handoffs increases.

12.4.2 Simulation Results

The results obtained in the previous sub-section apply to an ideal situation where the traffic in each cell is considered to be independent from that of its neighbours. The handoffs of calls imply a mutual traffic dependence between cells so that these results are not accurate. Moreover, in our analysis the call using a dynamic channel is supposed to continue with this channel until the termination of the call.

It is possible, however, to rearrange the calls so that the dynamic channels can be used only if there are no fixed channels available. This means that a call, using a dynamic channel, would be transferred to a fixed channel, in case this fixed channel is rendered available during that period. Consequently, more dynamic channels can be left free, rendering the system more capable to cope with alterations in the traffic. Call rearrangement can also be carried out amongst the dynamic channels so that they can be more efficiently used. We may also allow the handoffs to be requested a certain number of times to decrease their blocking probability.

It can be seen that, if all the phenomena occurring in a real mobile radio system are to be taken into account, then an analytical solution for the channel allocation techniques is not feasible. The use of simulation can overcome the intractability of the analytical solutions, constituting an important tool for the traffic analysis in a mobile radio system.

Traffic Model

In order to simulate an infinite system with a finite number of cells, these cells can be placed on a toroidal surface so that the mobiles can roam indefinitely in any direction over the torus surface without leaving the system. A system with 7 7-cell clusters (49 cells), as shown in Figure 12.3, can be used for this purpose. Note that the cells at the edges are repeated to form a toroidal surface.

This system was simulated assuming: (i) 105 channels per cluster, (ii) one guard channel between adjacent channels within the cell, (iii) 40% of the calls being handed off, (iv) up to 10 attempts of handoffs during a time-out period of 0.5 minutes, (v) negative exponential distribution with mean value equal to 2 minutes for the call holding time and (vi) Poisson-originated traffic per cell with even distribution. The results are shown in Figure 12.2.

Compare the theoretical and the simulated curves. Note that "as the traffic level increases more channels are needed in each cell up to a point where the Fixed Allocation 15/00 outperforms the other proportions"[5]. This is a direct consequence of the spatial inefficiency in the dynamic channels, since they are not always allocated at the minimum reuse distance. Accordingly, there may be reversion points where the Hybrid technique become worse than the Fixed one.

12.5 BLOCKING THRESHOLD VARIATION [20]

The Blocking Threshold Variation (BTV) is a channel assignment strategy treating the traffic with access to more than one base station as available for alternative routing. The performance of this strategy has been thoroughly investigated by Mencia [20], where a 2-cell system is considered. It is recognized, however, that there are reservations to be made, since in a practical network larger clusters interact. The joint process of two cells gives some guide to the phenomena to be expected, but not a precise quantitative solution.

12.5.1 The BTV Strategy Routing Procedure

Consider two adjacent cells in a mobile radio system each of which with N channels. Define Flexible (or Alternative) traffic as the traffic with access to more than one base station. As far as the flexible traffic is concerned, the BTV strategy divides the cells into two categories as follows:

1) First-option cell: is the subscriber's own cell.

2) Second-option cell: is the subscriber's alternative cell.

Let T ($0 \leq T \leq N + 1$) be the blocking threshold of each cell. For convenience we shall assume the same threshold for both cells. The blocking threshold T corresponds to the starting-point from which the first-option cell with T busy channels should be avoided. In this case the second-option cell is chosen to carry this alternative traffic, if its number of busy channels is smaller than T. If the number of busy channels is greater than T in both cells, the flexible traffic is diverted to the least loaded cell.

Suppose now that the cells present the same number of busy channels, exceeding the threshold T. In this case the strategy assumes one out of three possible alternatives:

- Alt1: To keep the flexible traffic within the first-option cell.
- Alt2: To split the flexible traffic equally between the cells.
- Alt3: To divert the flexible traffic to the second-option cell.

It is interesting to note that, for $T = N + 1$, the flexible traffic is not used. For $T = N$ this strategy coincides with ARB (Directed Retry). For $T = 0$ and with Alt2, BTV is equivalent to IAP. For $T = 0$ and with Alt3, BTV is equivalent to IMA.

12.5.2 Traffic Parameters

The traffic offered is defined by three independent variables: fixed traffic of cell 1 (A_1), fixed traffic of cell 2 (A_2) and flexible traffic (A_{12}). It is convenient to analyze the system in terms of a global traffic variable A, such that

$$A = A_1 + A_2 + A_{12} \tag{12.27}$$

Define β ($-1 \leq \beta \leq 1$) as the imbalance of fixed traffic between cells and γ ($0 \leq \gamma \leq 1$) as the proportion of flexible traffic. Thus

$$\beta = (A_1 - A_2)/(A_1 + A_2) \tag{12.28}$$

and

$$\gamma = A_{12}/A \tag{12.29}$$

Assuming the subscribers to be uniformly distributed within the cell, the parameter γ may be obtained as the proportion of overlapped area, as estimated in section 3.7.4. In terms of the parameters A, β and γ we have

$$\begin{aligned} A_1 &= \frac{1}{2}A(1 + \beta)(1 - \gamma) \\ A_2 &= \frac{1}{2}A(1 - \beta)(1 - \gamma) \end{aligned} \tag{12.30}$$

The number of channels per cell (N) and the blocking threshold (T) also constitute parameters to be considered in our traffic analysis.

12.5.3 Traffic Model

The traffic process is modelled by means of a two-dimensional birth-death process. The state number is a two-component vector (I,J) where I and J are the number of busy channels in cell 2 and cell 1, respectively. There are two upward transition densities from each state (I,J), namely $\lambda 1_{IJ}$ and $\lambda 2_{IJ}$, defined by the rate of arrival in cell 1 and cell 2, respectively. Similarly, there are two downward transitions $\mu 1_{IJ}$ and $\mu 2_{IJ}$ defined by the rate of departure from cells 1 and 2. The state transition diagram is shown in Figure 12.4.

The balance equation for the state (I,J) can be written as

$$\begin{aligned} &-(\lambda 1_{IJ} + \mu 1_{IJ} + \lambda 2_{IJ} + \mu 2_{IJ})P_{IJ} + \mu 1_{IJ+1}P_{IJ+1} + \lambda 1_{IJ-1}P_{IJ-1} \\ &+ \mu 2_{I+1J}P_{I+1J} + \lambda 2_{I-1J}P_{I-1J} = 0 \end{aligned} \tag{12.31}$$

where p_{xy} is the equilibrium state probability. By writing (12.31) for all the $(N + 1)^2$ states, a system of $(N + 1)^2$ linearly dependent equations are obtained. Since p_{xy} are probability distributions, the usual constraint

$$\sum_{I=0}^{N} \sum_{J=0}^{N} p_{IJ} = 1 \tag{12.32}$$

replacing any one of the balance equations eliminates the indetermination. Hence, the equilibrium state probabilities can be calculated by solving a system of $(N + 1)^2$ equations.

In our analysis we shall assume that: (i) Traffic is Poisson, (ii) Holding time has a negative exponential distribution, (iii) Flexible calls occur with probability γ and (iv) Flexible calls may be routed to either cell as required.

Transition Probability Densities

With the negative exponential distribution assumption, the probability of a reduction in the occupancy of either cell is proportional to the number of busy channels in that cell. For simplicity, we consider the mean holding time to be equal to one. Hence

$$\begin{aligned} \mu 1_{IJ} &= I \\ \mu 2_{IJ} &= J \end{aligned} \tag{12.33}$$

Assuming that each cell takes its own fixed traffic plus some proportion of the flexible traffic we have

$$\begin{aligned} \lambda 1_{IJ} &= A_1 + \frac{1}{2}(1 + \alpha_{IJ})A_{12} \\ \lambda 2_{IJ} &= A_2 + \frac{1}{2}(1 - \alpha_{IJ})A_{12} \end{aligned} \tag{12.34}$$

where α_{IJ} are routing coefficients defining the proportion of flexible traffic to be taken by each cell. These coefficients are state-dependent and are determined according to the routing procedure. Hence

1) If the number of busy channels I and J in each cell is smaller than the blocking threshold T, then the flexible calls of a given cell will stay in their own

cell. Therefore, the ratio A_1/A_2 must equal that of $(1 + \alpha_{ij})/(1 - \alpha_{ij})$. Therefore, $\alpha_{ij} = \beta$. In the same way.

2) If $i > T$ and $j \geq i$, then $\alpha_{ij} = -1$

3) If $j > T$ and $i \geq j$, then $\alpha_{ij} = 1$

4) If $i = j \geq T$, then α_{ij} depends on the Alternative

4.1) For ALT1: $\alpha_{ij} = \beta$

4.2) For ALT2: $\alpha_{ij} = 0$

4.3) For ALT3: $\alpha_{ij} = -\text{sgn}(\beta)$

where sgn(x) = -1, 0 or 1 for $x < 0$, $x = 0$ or $x > 0$, respectively.

The routing coefficients α_{ij} can be written as functions of i, j and T, using a three-level logic, as shown in Appendix 12A.

12.5.4 Performance Measures

Define B_1, B_2 and B_{12} as the blocking probabilities of cell 1, cell 2 and cells 1-and-2, respectively. They can be obtained from the equilibrium state probabilities as follows

$$B_1 = \sum_{i=0}^{N} p_{iN} \quad , \quad B_2 = \sum_{j=0}^{N} p_{Nj} \quad , \quad B_{12} = B_1 \cap B_2 = p_{NN} \tag{12.35}$$

The principal measure used to assess the system performance is the mean blocking probability B_m over all bundles of traffic

$$B_m = (A_1B_1 + A_2B_2 + A_{12}B_{12})/A \tag{12.36}$$

12.5.5 Analytical Solutions

As we have seen, the number of states in the 2-dimensional birth-death process is a quadratic function of the number of channels per cell. In general, the 2-dimensional process does not admit the simple one-dimensional form of solution given in section 12.2.3. Accordingly, numerical analysis with the use of computer is the most common tool used to solve a set of $(N + 1)^2$ equations. Nevertheless, it is possible to

obtain analytical solutions for special cases where not all the parameters are considered or their variations are limited to some specific range. Let us consider these cases.

1) *Erlang-B Formula*

The Erlang-B formula can be used in three limiting cases as follows.

a) No Flexibility: In this case the flexible traffic is nil ($\gamma = 0$). Accordingly, the two cells are considered to be isolated from one another so that we have $B_1 = E(A_1,N)$, $B_2 = E(A_2,N)$ and $B_{12} = 0$. The mean blocking is given by (12.36).

b) Full Flexibility: In this case the fixed streams of traffic are nil and all the traffic is flexible ($\gamma = 1$). Hence, the two cells are equivalent to one cell with 2N channels. Therefore, $B_1 = B_2 = 0$ and $B_m = B_{12} = E(A,2N)$.

c) Maximum Threshold: The case when $T = N + 1$ is equivalent to that when $\gamma = 0$ (no flexibility).

2) *Approximate Formula*

It is shown in Appendix 12B that, by means of low-traffic analysis, an approximate solution is given by

$$B_m = E(A/2,N)(1 + K\beta^2)(1 - \gamma)^{N-T+1} + \gamma^{1/N}\left[1 - (1 - \gamma)^{N-T+1}\right]E(A,2N) \qquad (12.37)$$

where

$$K = \left[(N + 1)(N - A) + (A/2)^2\right]/2 \qquad (12.38)$$

In fact, this approximate solution yields satisfactory results over a wide range of the parameters as we shall see in section 12.5.8.

12.5.6 Some Results

The performance of a 2-cell system using the Blocking Threshold Variation strategy has been assessed by means of a numerical analysis, as described in the previous sub-sections. It was verified [20] that there is no significant difference between the three alternatives (Alt1, Alt2, Alt3) of the strategy. Rigorously speaking, Alt3 gives the best performance, followed by Alt2 and Alt 1, in this order.

Recall from the definition of these alternatives that in Alt3, when both cells present an equal number of busy channels, the flexible traffic is diverted to the second-option cell whereas, in Alt1, it remains in its own cell. In this condition (both cells with equal number of busy channels) the second-option cell is more likely to be less loaded than the other cell. Therefore, traffic balance can be more quickly reached with Alt3. However, we must emphasize that the performance of these strategies is fairly similar, so that, for practical purposes, they are considered to be equivalent to each other.

In the results to be given here, each cell is assumed to have 6 channels so that there are up to 7 blocking thresholds. Moreover, since the mean blocking is an even function with respect to the imbalance parameter, just half of the range of this parameter needs to be explored.

Figure 12.5 shows the mean blocking versus the imbalance parameter for 50% flexibility (γ = 0.5) and total traffic A = 6 erl.. Note that there is a substantial improvement in the mean blocking with the use of the strategy. The improvement is more significant when the threshold varies from T = 7 to T = 6. We notice that for T = 5 and T = 4 the results are even better, but below this (T ≤ 3) there is not much gain, and the curves practically coincide with each other.

Figure 12.6 shows the mean blocking versus the flexibility parameter for a traffic imbalance of 50% (β = 0.5) and total traffic A = 6 erl.. Note that for T = N + 1 the mean blocking is independent of the flexibility, as expected. For γ = 0.5 the mean blocking reduces from approximately 12% (for T = 7) to less than 3% (for T ≤ 4) with the use of the BTV strategy.

Figure 12.7 shows the mean blocking versus traffic. Note that within the range 2%-20% of the blocking probability the system has the best performance. It can be seen that, for B_m = 5% the improvement in traffic capacity is greater than 50% when BTV is used with a threshold T ≤ 4.

The approximate formula given by (12.37) was also checked against the exact solution throughout a wide range of variation of the parameters. The results are

quite encouraging not only for low traffic, where the exact and approximate curves are almost coincident, but also for high traffic as shown in Figure 12.8.

12.5.7 Extension of the Model for Larger Clusters

The model used here can be extended to deal with larger clusters where more cells interact. In this case we may also consider the flexible traffic with access to three base stations as available for alternative routing. We showed in Chapter 3 (section 3.7.5) that, if δ is the proportion of traffic with three or more alternative radio paths and γ is this proportion for two or more paths, then, $\delta \simeq 1.25\gamma^2$ is a good approximation in the range $0 \leq \gamma \leq 0.8$. Moreover, since $\gamma = 50\%$ is a fairly realistic figure in the mobile radio systems (refer to section 3.7.5), then $\delta \simeq 31\%$. It has been shown [19] that with the use of the third path option, the increase in traffic capacity may exceed the figure of 20% on the top of the improvement achieved when only two paths are used for alternative routing, for a grade of service of 5%.

When clusters including different capacity cells are considered, then the imbalance parameter must be modified to include, not only the traffic per cell, but also the number of channels per cell. Hence each cell i would be associated with an individual imbalance β_i such that

$$\beta_i = (B_i - \bar{B})/\bar{B} \tag{12.39}$$

where B_i is the blocking probability of cell i due to its fixed traffic, and $\bar{B}$ is the average blocking probability experienced by all of the fixed streams of traffic.

If cell i has N_i channels and a fixed traffic equal to A_i then

$$B_i = E(A_i, N_i) \tag{12.40}$$

The average blocking $\bar{B}$ is

$$\bar{B} = \frac{\left(\sum_{i=1}^{n} A_i B_i\right)}{\left(\sum_{i=1}^{n} A_i\right)} \tag{12.41}$$

where n is the number of cells in the system.

12.6 SUMMARY AND CONCLUSIONS

The traffic process in a mobile radio system greatly departs from that of the fixed telephone network. However, in general, design and planning have not been optimized for the practical situation in which the subscribers are mobile. In this case the classical teletraffic theory can be used just to provide an insight into the problem. A better assessment of the system performance can be achieved by means of simulation where the complex realistic situations can be taken into account without much difficulty.

Because of the reduced availability of frequency spectrum, many techniques to improve the spectrum efficiency have been proposed. One way of increasing the channel utilization, and consequently the spectrum efficiency, is by means of properly assigning the channels in the system. Channel assignment can be carried out in a global or in a local manner. In the global approach a centralized control of the allocation process must be provided. The local approach takes advantage of the fact that mobiles with access to more than one base station can be used for alternative routing. In this case the control for the channel assignment process can be local since only two or three neighbouring cells may be involved.

From the various global assignment algorithms investigated in [5,12] the Hybrid Channel Allocation with rearrangement seemed to give the best results. In particular, the Borrowing technique requires a high control complexity without much improvement. The totally Dynamic algorithm has low spatial efficiency and may have an inferior performance than that of the Fixed allocation for high traffic. On the other hand, the performance of the Hybrid allocation is very dependent on the traffic characteristics. The right proportion of dynamic-to-fixed channels can only be determined if the traffic distribution, proportion of handoffs and other factors are considered to be known. For irregular traffic distributions, more dynamic channels are necessary to

cope with the unexpected peaks of traffic. Under normal conditions, a low proportion of dynamic channels can be used with very good results in the system performance.

As for the local approach techniques, they are usually very simple to be implemented and do not require the involvement of the system central control. While there may be some change in the usage pattern of channels, all channels are used within or closely adjacent to their planned service area, so that there are no serious implications for frequency reuse pattern.

From the various available techniques we chose to analyze the "Blocking Threshold Variation" (BTV) algorithm because of its "multi-purpose" characteristics. In fact, the BTV strategy may coincide with some of the other techniques, depending on the blocking threshold T. If T is set to be equal to N + 1, where N is the number of channels per cell, then the flexible traffic is not used for alternative routing. If T = N, then BTV coincides with the Adaptive Response to Blocking (ARB) strategy (also known as Directed Retry). In case T = 0 and the alternative Alt2 is used, then BTV is equivalent to the Instantaneous Adaptation (IAP). If, however, T = 0 and Alt3 is used, then BTV coincides with the Instantaneous and Mean Adaptation (IMA).

It has been verified that the difference in performance between the three alternatives (Alt1, Alt2 and Alt3) is not significant, so that any one of them can be used to give a similar gain in traffic. Accordingly, when both cells present an equal number of busy channels, exceeding the blocking threshold T, then the flexible traffic can be directed to any cell, indistinctly.

It has also been shown that it is not necessary to set a very low blocking threshold to obtain a reasonable gain in performance. For example, in a 6-channel per cell system a threshold equal to 4 was already enough to yield a considerable gain in traffic. Below 4 the gain is even greater, but not significant for practical purposes. Accordingly, we may reserve a fixed amount of channels within each cell and use the others for alternative routing. The fixed channels can be primarily used for some services considered to be essential (e.g., handoff).

APPENDIX 12A

Three-Level Logic

12A.1 Three-level Algebra

Define:

- *Input Variable* as a variable assuming only the logic levels −1, 0 or +1.

- *Output Variable* as the value of an algebraic expression assuming any real value.

Define X_{-1}, X_0 and X_1 as *Indication Functions* assuming the value +1 only when the input variable X is equal to −1, 0 or +1 respectively, and 0 otherwise. Accordingly,

$$X_1 = -X(1 - X)/2$$
$$X_0 = 1 - |X|$$
$$X_1 = X(1 + X)/2 \qquad (12A.1)$$

Define

- *Term* as the product of Indication Functions

- *Factor* as the value of the Output Variable for a given term.

The Output Variable is then given by the sum of the Terms each of which multiplied by their respective factors. As an example, consider the following truth table where A and B are the Input and C is the output variables.

From this table the output variable can be written as

$$C = 5A_{-1}B_{-1} + 3A_{-1}B_0 - 2A_0B_0 + 0.3A_1B_{-1}$$

TABLE 12A.1 – AN EXAMPLE OF THE 3-LEVEL LOGIC ALGEBRA.

A	B	C
−1	−1	5
−1	0	3
−1	1	0
0	−1	0
0	0	−2
0	1	0
1	−1	0.3
1	0	0
1	1	0

12A.2 The Routing Coefficients for the BTV Strategy

The input variables can be written as functions of the instantaneous states (I,J) and the threshold T. Let I, J and K be these variables such that

$$I = \mathrm{sgn}(i - T)$$

$$J = \mathrm{sgn}(j - T)$$

$$K = \mathrm{sgn}(i - j) \qquad (12A.3)$$

where sgn(x) = -1, 0 or 1 for $x < 0$, $x = 0$ or $x > 0$, respectively. The routing coefficients α_{ij} can be written as functions of I, J and K. Following the routing procedures of the BTV strategy and having in mind the equations (12.34), the Table 12A.2 is set up

TABLE 12A.2 - ROUTING COEFFICIENT FOR THE BTV STRATEGY.

I	J	α_{IJ}	Routing Procedure Relative to the Flexible Traffic
-1	-1	β	To keep it in its own cell
-1	0	-1	To divert it to cell 2
-1	1	-1	To divert it to cell 2
0	-1	1	To divert it to cell 1
0	0	A	To be defined below. It depends on the alternative
0	1	-1	To divert it to cell 2
1	-1	1	To divert it to cell 1
1	0	1	To divert it to cell 1
1	1	B	To be defined. It depends on the values of I and J

The factor A is obtained according to the procedure taken by each alternative. It can be easily verified that

$$\text{For Alt1} \qquad A = \beta$$

$$\text{For Alt2} \qquad A = 0$$

$$\text{For Alt3} \qquad A = -\mathrm{sgn}(\beta) \qquad (12A.3)$$

The factor B corresponds to the case where $i > T$ and $j > T$. Following the same procedure as for Table 12A.2 we obtain

$$B = -K_{-1} + AK_0 + K_1 \qquad (12A.4)$$

Therefore, from Table 12A.2 we have

$$\alpha_{ij} = \beta I_{-1}J_{-1} - I_{-1}J_0 - I_{-1}J_1 + I_0J_{-1} + AI_0J_0 - I_0J_1 + I_1J_{-1} + I_1J_0 + BI_1J_1 \qquad (12A.5)$$

where A and B are given by (12A.3) and (12A.4), respectively.

APPENDIX 12B

Approximate Mean Blocking Probability for the BTV Strategy

12B.1 Mean Blocking Versus Imbalance

In the absence of flexibility ($\gamma = 0$) we have $B_1 = E(A_1,N)$, $B_2 = E(A_2,N)$ and $B_{12} = 0$. Hence with $\gamma = 0$ in (12.30) and then using these results in (12.36) we obtain

$$B_m(A,\beta,0) = \frac{1}{2}(1+\beta)E\left[\frac{1}{2}(1+\beta)A,N\right] + \frac{1}{2}(1-\beta)E\left[\frac{1}{2}(1-\beta)A,N\right] \qquad (12B.1)$$

Suppose that for an arbitrary f(x) expandable as a power series

$$g(x,\beta) = \frac{1}{2}(1+\beta)f(x+\beta x) + \frac{1}{2}(1-\beta)f(x-\beta x) \qquad (12B.2)$$

Define

$$f(x) = \sum_k a_k x^k$$

and

$$g(x) = x^n f(x) = \sum_k a_k x^{k+n} \qquad (12B.3)$$

with $k, n \geq 0$.

Then, differentiating both sides of (12B.3) r times

$$g^{(r)}(x) = \sum_k a_k (k+n)^{(r)} x^{k+n-r} = r! \sum_k a_k \binom{k+n}{r} x^{k+n-r}$$

where $(k+n)^{(r)} = (k+n)(k+n-1)\ldots(k+n-r+1)$

Then

$$\sum_k a_k \binom{k+n}{r} x^k = \frac{x^{r-n}}{r!} g^{(r)}(x)$$

Specifically with $n = 1$

$$\sum_k a_k \binom{k+1}{r} x^k = \frac{x^{r-1}}{r!} g^{(r)}(x)$$

Now this can be used to evaluate (12B.2).

Hence

$$g(x,\beta) = \frac{1}{2}\sum_k a_k x^k\left[(1+\beta)^{k+1} + (1-\beta)^{k+1}\right]$$

$$g(x,\beta) = \sum_k a_k x^k \sum_j \beta^{2j}\binom{k+1}{2j}$$

$$g(x,\beta) = \sum_j \beta^{2j} \sum_k a_k x^k \binom{k+1}{2j}$$

Finally

$$g(x,\beta) = \sum_j \beta^{2j}\frac{x^{2j-1}}{(2j)!}g^{(2j)}(x) \qquad \text{,where } g(x) = xf(x) \tag{12B.4}$$

As an example, consider f(x) as the one-channel Erlang blocking probability

$$f(x) = E(x,1) = \frac{x}{1+x}$$

Then

$$g(x,\beta) \frac{x}{1+x} + \beta^2\frac{x}{(1+x)^3} + O(x^3\beta^4)$$

With large value of N, the exact expression is rather complex, but there is a good approximation as that given by (12.17), i.e.,

$$f(x) = \frac{1}{N!}x^N e^{-x} \simeq E(x,N)$$

which gives

$$g(x,\beta) = f(x)\left\{1 + \beta^2\left[\frac{1}{2}N(N+1) - (N+1)x + \frac{1}{2}x^2\right]\right\} + O(\beta^4) \tag{12B.5}$$

Note that in our case x = A/2 (compare equations (12B.2) and (12B.1). Therefore, from (12B.1) and (12B.5) we obtain

$$B_m(A,\beta,0) \simeq E(A/2,N)(1 + K\beta^2) \tag{12B.6}$$

where

$$K = \left[N(N + 1) - (N + 1)A + (A^2/2)\right] / 2 \qquad (12B.7)$$

12B.2 Low Traffic Analysis

Consider a low traffic approximation where the blocking states are dominated by the states (0,N) for cell 1 and (N,0) for cell 2. As an approximation we may reduce the 2-dimensional diagram of Figure 12.4 to a one-dimensional diagram containing the states (0,0)(0,1)...(0,N) and (0,0),(1,0),...,(N,0). Hence, the mean blocking probability is

$$B_m \simeq \frac{A_1 p_{0N} + A_2 p_{N0}}{A} \qquad (12B.8)$$

where p_{0N} and p_{N0} are the equilibrium state probabilities of the states øN and Nø respectively. These probabilities can be calculated by means of the standard one-dimensional form of solution given in section 12.2.3. Up to the state (0,T) the traffic offered to cell 1 is $A(1 + \beta)/2$, obtained from (12.30) with $\gamma = 0$. From (0,T) up to (0,N) the traffic is exactly that given by (12.30). The same reasoning applies to cell 2. Therefore, from the one-dimensional solution

$$p_{0N} = \left[\frac{A}{2}(1 + \beta)\right]^T \left[\frac{A}{2}(1 + \beta)(1 - \gamma)\right]^{N-T} \frac{p_{00}}{N!}$$

and

$$p_{N0} = \left[\frac{A}{2}(1 - \beta)\right]^T \left[\frac{A}{2}(1 - \beta)(1 - \gamma)\right]^{N-T} \frac{p_{00}}{N!} \qquad (12B.9)$$

Using (12.30) and (12B.9) in (12B.8) we obtain

$$B_m = \left[p_{00}(A/2)^N/N!\right](1 + \beta^2)(1 - \gamma)^{N-T+1} + O(\beta^4) \qquad (12B.10)$$

12B.3 Approximate Formula

Observe the similarity between (12B.10) and (12B.6). As an attempt to obtain an

approximate expression for the overall mean blocking, we may combine both equations and neglect the higher order terms as follows

$$B_m \propto E(A/2,N)(1 + K\beta^2)(1 - \gamma)^{N-T+1} \qquad (12B.11)$$

Note, however, that for $\gamma = 1$ (12B.11) reduces to zero, while the true value would be E(A,2N). We may overcome this limitation by adding a new term such that

$$B_m \propto E(A/2,N)(1 + K\beta^2)(1 - \gamma)^{N-T+1} + f(\gamma,N)E(A,2N) \qquad (12B.12)$$

where the function $f(\gamma,N)$ must satisfy the following conditions

$$f(\gamma,N) = \begin{cases} 0 \text{ for } \gamma = 0 & , \text{ no matter } T \\ 0 \text{ for } T = N + 1, & \text{no matter } \gamma \\ 1 \text{ for } \gamma = 1 & , \text{ no matter } T \end{cases}$$

One function satisfying these restrictions is

$$f(\gamma,N) = \gamma^a\left[1 - (1 - \gamma)^{N-T+1}\right] \qquad (12B.13)$$

where a is a constant. It was found that satisfactory results are obtained for $a = 1/N$. Therefore, the approximate formula for the mean blocking is given by (12B.12) where $f(\gamma,N)$ is defined in (12B.13) with $a = 1/N$ and K is given by (12B.7).

APPENDIX 12C

Source: From *Telephone Traffic Theory Tables and Charts*, Siemens Aktiengesellschaft, Munich, 1970.

Blocked Calls Cleared - Erlang B

	A,Erl												
	Blocking Probability												
N	1.0%	1.2%	1.5%	2%	3%	5%	7%	10%	15%	20%	30%	40%	50%
1	.0101	.0121	.0152	.0204	.0309	.0526	.0753	.111	.176	.250	.429	.667	1.00
2	.153	.168	.190	.223	.282	.381	.470	.595	.796	1.00	1.45	2.00	2.73
3	.455	.489	.535	.602	.715	.899	1.06	1.27	1.60	1.93	2.63	3.48	4.59
4	.869	.922	.992	1.09	1.26	1.52	1.75	2.05	2.50	2.95	3.89	5.02	6.50
5	1.36	1.43	1.52	1.66	1.88	2.22	2.50	2.88	3.45	4.01	5.19	6.60	8.44
6	1.91	2.00	2.11	2.28	2.54	2.96	3.30	3.76	4.44	5.11	6.51	8.19	10.4
7	2.50	2.60	2.74	2.94	3.25	3.74	4.14	4.67	5.46	6.23	7.86	9.80	12.4
8	3.13	3.25	3.40	3.63	3.99	4.54	5.00	5.60	6.50	7.37	9.21	11.4	14.3
9	3.78	3.92	4.09	4.34	4.75	5.37	5.88	6.55	7.55	8.52	10.6	13.0	16.3
10	4.46	4.61	4.81	5.08	5.53	6.22	6.78	7.51	8.62	9.68	12.0	14.7	18.3
11	5.16	5.32	5.54	5.84	6.33	7.08	7.69	8.49	9.69	10.9	13.3	16.3	20.3
12	5.88	6.05	6.29	6.61	7.14	7.95	8.61	9.47	10.8	12.0	14.7	18.0	22.2
13	6.61	6.80	7.05	7.40	7.97	8.83	9.54	10.5	11.9	13.2	16.1	19.6	24.2
14	7.35	7.56	7.82	8.20	8.80	9.73	10.5	11.5	13.0	14.4	17.5	21.2	26.2
15	8.11	8.33	8.61	9.01	9.65	10.6	11.4	12.5	14.1	15.6	18.9	22.9	28.2
16	8.88	9.11	9.41	9.83	10.5	11.5	12.4	13.5	15.2	16.8	20.3	24.5	30.2
17	9.65	9.89	10.2	10.7	11.4	12.5	13.4	14.5	16.3	18.0	21.7	26.2	32.2
18	10.4	10.7	11.0	11.5	12.2	13.4	14.3	15.5	17.4	19.2	23.1	27.8	34.2
19	11.2	11.5	11.8	12.3	13.1	14.3	15.3	16.6	18.5	20.4	24.5	29.5	36.2
20	12.0	12.3	12.7	13.2	14.0	15.2	16.3	17.6	19.6	21.6	25.9	31.2	38.2
21	12.8	13.1	13.5	14.0	14.9	16.2	17.3	18.7	20.8	22.8	27.3	32.8	40.2
22	13.7	14.0	14.3	14.9	15.8	17.1	18.2	19.7	21.9	24.1	28.7	34.5	42.1
23	14.5	14.8	15.2	15.8	16.7	18.1	19.2	20.7	23.0	25.3	30.1	36.1	44.1
24	15.3	15.6	16.0	16.6	17.6	19.0	20.2	21.8	24.2	26.5	31.6	37.8	46.1
25	16.1	16.5	16.9	17.5	18.5	20.0	21.2	22.8	25.3	27.7	33.0	39.4	48.1

A,Erl (continued)

N	Blocking Probability												
	1.0%	1.2%	1.5%	2%	3%	5%	7%	10%	15%	20%	30%	40%	50%
26	17.0	17.3	17.8	18.4	19.4	20.9	22.2	23.9	26.4	28.9	34.4	41.1	50.1
27	17.8	18.2	18.6	19.3	20.3	21.9	23.2	24.9	27.6	30.2	35.8	42.8	52.1
28	18.6	19.0	19.5	20.2	21.2	22.9	24.2	26.0	28.7	31.4	37.2	44.4	54.1
29	19.5	19.9	20.4	21.0	22.1	23.8	25.2	27.1	29.9	32.6	38.6	46.1	56.1
30	20.3	20.7	21.2	21.9	23.1	24.8	26.2	28.1	31.0	33.8	40.0	47.7	58.1
31	21.2	21.6	22.1	22.8	24.0	25.8	27.2	29.2	32.1	35.1	41.5	49.4	60.1
32	22.0	22.5	23.0	23.7	24.9	26.7	28.2	30.2	33.3	36.3	42.9	51.1	62.1
33	22.9	23.3	23.9	24.6	25.8	27.7	29.3	31.3	34.4	37.5	44.3	52.7	64.1
34	23.8	24.2	24.8	25.5	26.8	28.7	30.3	32.4	35.6	38.8	45.7	54.4	66.1
35	24.6	25.1	25.6	26.4	27.7	29.7	31.3	33.4	36.7	40.0	47.1	56.0	68.1
36	25.5	26.0	26.5	27.3	28.6	30.7	32.3	34.5	37.9	41.2	48.6	57.7	70.1
37	26.4	26.8	27.4	28.3	29.6	31.6	33.3	35.6	39.0	42.4	50.0	59.4	72.1
38	27.3	27.7	28.3	29.2	30.5	32.6	34.4	36.6	40.2	43.7	51.4	61.0	74.1
39	28.1	28.6	29.2	30.1	31.5	33.6	35.4	37.7	41.3	44.9	52.8	62.7	76.1
40	29.0	29.5	30.1	31.0	32.4	34.6	36.4	38.8	42.5	46.1	54.2	64.4	78.1
41	29.9	30.4	31.0	31.9	33.4	35.6	37.4	39.9	43.6	47.4	55.7	66.0	80.1
42	30.8	31.3	31.9	32.8	34.3	36.6	38.4	40.9	44.8	48.6	57.1	67.7	82.1
43	31.7	32.2	32.8	33.8	35.3	37.6	39.5	42.0	45.9	49.9	58.5	69.3	84.1
44	32.5	33.1	33.7	34.7	36.2	38.6	40.5	43.1	47.1	51.1	59.9	71.0	86.1
45	33.4	34.0	34.6	35.6	37.2	39.6	41.5	44.2	48.2	52.3	61.3	72.7	88.1
46	34.3	34.9	35.6	36.5	38.1	40.5	42.6	45.2	49.4	53.6	62.8	74.3	90.1
47	35.2	35.8	36.5	37.5	39.1	41.5	43.6	46.3	50.6	54.8	64.2	76.0	92.1
48	36.1	36.7	37.4	38.4	40.0	42.5	44.6	47.4	51.7	56.0	65.6	77.7	94.1
49	37.0	37.6	38.3	39.3	41.0	43.5	45.7	48.5	52.9	57.3	67.0	79.3	96.1
50	37.9	38.5	39.2	40.3	41.9	44.5	46.7	49.6	54.0	58.5	68.5	81.0	98.1

(continued)

N	A, Erl: Blocking Probability 1.0%	1.2%	1.5%	2%	3%	5%	7%	10%	15%	20%	30%	40%	50%
51	38.8	39.4	40.1	41.2	42.9	45.5	47.7	50.6	55.2	59.7	69.9	82.7	100.1
52	39.7	40.3	41.0	42.1	43.9	46.5	48.8	51.7	56.3	61.0	71.3	84.3	102.1
53	40.6	41.2	42.0	43.1	44.8	47.5	49.8	52.8	57.5	62.2	72.7	86.0	104.1
54	41.5	42.1	42.9	44.0	45.8	48.5	50.8	53.9	58.7	63.5	74.2	87.6	106.1
55	42.4	43.0	43.8	44.9	46.7	49.5	51.9	55.0	59.8	64.7	75.6	89.3	108.1
56	43.3	43.9	44.7	45.9	47.7	50.5	52.9	56.1	61.0	65.9	77.0	91.0	110.1
57	44.2	44.8	45.7	46.8	48.7	51.5	53.9	57.1	62.1	67.2	78.4	92.6	112.1
58	45.1	45.8	46.6	47.8	49.6	52.6	55.0	58.2	63.3	68.4	79.8	94.3	114.1
59	46.0	46.7	47.5	48.7	50.6	53.6	56.0	59.3	64.5	69.7	81.3	96.0	116.1
60	46.9	47.6	48.4	49.6	51.6	54.6	57.1	60.4	65.6	70.9	82.7	97.6	118.1
61	47.9	48.5	49.4	50.6	52.5	55.6	58.1	61.5	66.8	72.1	84.1	99.3	120.1
62	48.8	49.4	50.3	51.5	53.5	56.6	59.1	62.6	68.0	73.4	85.5	101.0	122.1
63	49.7	50.4	51.2	52.5	54.5	57.6	60.2	63.7	69.1	74.6	87.0	102.6	124.1
64	50.6	51.3	52.2	53.4	55.4	58.6	61.2	64.8	70.3	75.9	88.4	104.3	126.1
65	51.5	52.2	53.1	54.4	56.4	59.6	62.3	65.8	71.4	77.1	89.8	106.0	128.1
66	52.4	53.1	54.0	55.3	57.4	60.6	63.3	66.9	72.6	78.3	91.2	107.6	130.1
67	53.4	54.1	55.0	56.3	58.4	61.6	64.4	68.0	73.8	79.6	92.7	109.3	132.1
68	54.3	55.0	55.9	57.2	59.3	62.6	65.4	69.1	74.9	80.8	94.1	111.0	134.1
69	55.2	55.9	56.9	58.2	60.3	63.7	66.4	70.2	76.1	82.1	95.5	112.6	136.1
70	56.1	56.8	57.8	59.1	61.3	64.7	67.5	71.3	77.3	83.3	96.9	114.3	138.1
71	57.0	57.8	58.7	60.1	62.3	65.7	68.5	72.4	78.4	84.6	98.4	115.9	140.1
72	58.0	58.7	59.7	61.0	63.2	66.7	69.6	73.5	79.6	85.8	99.8	117.6	142.1
73	58.9	59.6	60.6	62.0	64.2	67.7	70.6	74.6	80.8	87.0	101.2	119.3	144.1
74	59.8	60.6	61.6	62.9	65.2	68.7	71.7	75.6	81.9	88.3	102.7	120.9	146.1
75	60.7	61.5	62.5	63.9	66.2	69.7	72.7	76.7	83.1	89.5	104.1	122.6	148.0

Blocked Calls Cleared - Erlang B

(continued)

A,Erl

N	Blocking Probability												
	1.0%	1.2%	1.5%	2%	3%	5%	7%	10%	15%	20%	30%	40%	50%
76	61.7	62.4	63.4	64.9	67.2	70.8	73.8	77.8	84.2	90.8	105.5	124.3	150.0
77	62.6	63.4	64.4	65.8	68.1	71.8	74.8	78.9	85.4	92.0	106.9	125.9	152.0
78	63.5	64.3	65.3	66.8	69.1	72.8	75.9	80.0	86.6	93.3	108.4	127.6	154.0
79	64.4	65.2	66.3	67.7	70.1	73.8	76.9	81.1	87.7	94.5	109.8	129.3	156.0
80	65.4	66.2	67.2	68.7	71.1	74.8	78.0	82.2	88.9	95.7	111.2	130.9	158.0
81	66.3	67.1	68.2	69.6	72.1	75.8	79.0	83.3	90.1	97.0	112.6	132.6	160.0
82	67.2	68.0	69.1	70.6	73.0	76.9	80.1	84.4	91.2	98.2	114.1	134.3	162.0
83	68.2	69.0	70.1	71.6	74.0	77.9	81.1	85.5	92.4	99.5	115.5	135.9	164.0
84	69.1	69.9	71.0	72.5	75.0	78.9	82.2	86.6	93.6	100.7	116.9	137.6	166.0
85	70.0	70.9	71.9	73.5	76.0	79.9	83.2	87.7	94.7	102.0	118.3	139.3	168.0
86	70.9	71.8	72.9	74.5	77.0	80.9	84.3	88.8	95.9	103.2	119.8	140.9	170.0
87	71.9	72.7	73.8	75.4	78.0	82.0	85.3	89.9	97.1	104.5	121.2	142.6	172.0
88	72.8	73.7	74.8	76.4	78.9	83.0	86.4	91.0	98.2	105.7	122.6	144.6	174.0
89	73.7	74.6	75.7	77.3	79.9	84.0	87.4	92.1	99.4	106.9	124.0	145.9	176.0
90	74.7	75.6	76.7	78.3	80.9	85.0	88.5	93.1	100.6	108.2	125.5	147.6	178.0
91	75.6	76.5	77.6	79.3	81.9	86.0	89.5	94.2	101.7	109.4	126.9	149.3	180.0
92	76.6	77.4	78.6	80.2	82.9	87.1	90.6	95.3	102.9	110.7	128.3	150.9	182.0
93	77.5	78.4	79.6	81.2	83.9	88.1	91.6	96.4	104.1	111.9	129.7	152.6	184.0
94	78.4	79.3	80.5	82.2	84.9	89.1	92.7	97.5	105.3	113.2	131.2	154.3	186.0
95	79.4	80.3	81.5	83.1	85.8	90.1	93.7	98.6	106.4	114.4	132.6	155.9	188.0
96	80.3	81.2	82.4	84.1	86.8	91.1	94.8	99.7	107.6	115.7	134.0	157.6	190.0
97	81.2	82.2	83.4	85.1	87.8	92.2	95.8	100.8	108.8	116.9	135.5	159.3	192.0
98	82.2	83.1	84.3	86.0	88.8	93.2	96.9	101.9	109.9	118.2	136.9	160.9	194.0
99	83.1	84.1	85.3	87.0	89.8	94.2	97.9	103.0	111.1	119.4	138.3	162.6	196.0
100	84.1	85.0	86.2	88.0	90.8	95.2	99.0	104.1	112.3	120.6	139.7	164.3	198.0

A,Erl

(continued)

N	Blocking Probability												
	1.0%	1.2%	1.5%	2%	3%	5%	7%	10%	15%	20%	30%	40%	50%
102	85.9	86.9	88.1	89.9	92.8	97.3	101.1	106.3	114.6	123.1	142.6	167.6	202.0
104	87.8	88.8	90.1	91.9	94.8	99.3	103.2	108.5	116.9	125.6	145.4	170.9	206.0
106	89.7	90.7	92.0	93.8	96.7	101.4	105.3	110.7	119.3	128.1	148.3	174.2	210.0
108	91.6	92.6	93.9	95.7	98.7	103.4	107.4	112.9	121.6	130.6	151.1	177.6	214.0
110	93.5	94.5	95.8	97.7	100.7	105.5	109.5	115.1	124.0	133.1	154.0	180.9	218.0
112	95.4	96.4	97.7	99.6	102.7	107.5	111.7	117.3	126.3	135.6	156.9	184.2	222.0
114	97.3	98.3	99.7	101.6	104.7	109.6	113.8	119.5	128.6	138.1	159.7	187.6	226.0
116	99.2	100.2	101.6	103.5	106.7	111.7	115.9	121.7	131.0	140.6	162.6	190.9	230.0
118	101.1	102.1	103.5	105.5	108.7	113.7	118.0	123.9	133.3	143.1	165.4	194.2	234.0
120	103.0	104.0	105.4	107.4	110.7	115.8	120.1	126.1	135.7	145.6	168.3	197.6	238.0
122	104.9	105.9	107.4	109.4	112.6	117.8	122.2	128.3	138.0	148.1	171.1	200.9	242.0
124	106.8	107.9	109.3	111.3	114.6	119.9	124.4	130.5	140.3	150.6	174.0	204.2	246.0
126	108.7	109.8	111.2	113.3	116.6	121.9	126.5	132.7	142.7	153.0	176.8	207.6	250.0
128	110.6	111.7	113.2	115.2	118.6	124.0	128.6	134.9	145.0	155.5	179.7	210.9	254.0
130	112.5	113.6	115.1	117.2	120.6	126.1	130.7	137.1	147.4	158.0	182.5	214.2	258.0
132	114.4	115.5	117.0	119.1	122.6	128.1	132.8	139.3	149.7	160.5	185.4	217.6	262.0
134	116.3	117.4	119.0	121.1	124.6	130.2	134.9	141.5	152.0	163.0	188.3	220.9	266.0
136	118.2	119.4	120.9	123.1	126.6	132.3	137.1	143.7	154.4	165.5	191.1	224.2	270.0
138	120.1	121.3	122.8	125.0	128.6	134.3	139.2	145.9	156.7	168.0	194.0	227.6	274.0
140	122.0	123.2	124.8	127.0	130.6	136.4	141.3	148.1	159.1	170.5	196.8	230.9	278.0
142	123.9	125.1	126.7	128.9	132.6	138.4	143.4	150.3	161.4	173.0	199.7	234.2	282.0
144	125.8	127.0	128.6	130.9	134.6	140.5	145.6	152.5	163.8	175.5	202.5	237.6	286.0
146	127.7	129.0	130.6	132.9	136.6	142.6	147.7	154.7	166.1	178.0	205.4	240.9	290.0
148	129.7	130.9	132.5	134.8	138.6	144.6	149.8	156.9	168.5	180.5	208.2	244.2	294.0
150	131.6	132.8	134.5	136.8	140.6	146.7	151.9	159.1	170.8	183.0	211.1	247.6	298.0

Blocked Calls Cleared - Erlang B

A,Erl (continued)

N	Blocking Probability												
	1.0%	1.2%	1.5%	2%	3%	5%	7%	10%	15%	20%	30%	40%	50%
202	181.7	183.2	185.2	188.1	192.9	200.6	207.2	216.5	231.8	247.9	285.4	334.2	402.0
204	183.6	185.2	187.2	190.1	194.9	202.7	209.4	218.7	234.1	250.4	288.2	337.5	406.0
206	185.5	187.1	189.2	192.1	196.9	204.7	211.5	221.0	236.5	252.9	291.1	340.9	410.0
208	187.5	189.1	191.1	194.1	199.0	206.8	213.6	223.2	238.8	255.4	293.9	344.2	414.0
210	189.4	191.0	193.1	196.1	201.0	208.9	215.8	225.4	241.2	257.9	296.8	347.5	418.0
212	191.4	193.0	195.1	198.1	203.0	211.0	217.9	227.6	243.5	260.4	299.6	350.9	422.0
214	193.3	194.9	197.0	200.0	205.0	213.0	220.0	229.8	245.9	262.9	302.5	354.2	426.0
216	195.2	196.9	199.0	202.0	207.0	215.1	222.2	232.0	248.2	265.4	305.3	357.5	430.0
218	197.2	198.8	201.0	204.0	209.1	217.2	224.3	234.2	250.6	267.9	308.2	360.9	434.0
220	199.1	200.8	202.9	206.0	211.1	219.3	226.4	236.4	252.9	270.4	311.1	364.2	438.0
222	201.1	202.7	204.9	208.0	213.1	221.4	228.6	238.6	255.3	272.9	313.9	367.5	442.0
224	203.0	204.7	206.8	210.0	215.1	223.4	230.7	240.9	257.6	275.4	316.8	370.9	446.0
226	204.9	206.6	208.8	212.0	217.1	225.5	232.8	243.1	260.0	277.8	319.6	374.2	450.0
228	206.9	208.6	210.8	213.9	219.2	227.6	235.0	245.3	262.3	280.3	322.5	377.5	454.0
230	208.8	210.5	212.8	215.9	221.2	229.7	237.1	247.5	264.7	282.8	325.3	380.9	458.0
232	210.8	212.5	214.7	217.9	223.2	231.8	239.2	249.7	267.0	285.3	328.2	384.2	462.0
234	212.7	214.4	216.7	219.9	225.2	233.8	241.4	251.9	269.4	287.8	331.1	387.5	466.0
236	214.7	216.4	218.7	221.9	227.2	235.9	243.5	254.1	271.7	290.3	333.9	390.9	470.0
238	216.6	218.3	220.6	223.9	229.3	238.0	245.6	256.3	274.1	292.8	336.8	394.2	474.0
240	218.6	220.3	222.6	225.9	231.3	240.1	247.8	258.6	276.4	295.3	339.6	397.5	478.0
242	220.5	222.3	224.6	227.9	233.3	242.2	249.9	260.8	278.8	297.8	342.5	400.9	482.0
244	222.5	224.2	226.5	229.9	235.3	244.3	252.0	263.0	281.1	300.3	345.3	404.2	486.0
246	224.4	226.2	228.5	231.8	237.4	246.3	254.2	265.2	283.4	302.8	348.2	407.5	490.0
248	226.3	228.1	230.5	233.8	239.4	248.4	256.3	267.4	285.8	305.3	351.0	410.9	494.0
250	228.3	230.1	232.5	235.8	241.4	250.5	258.4	269.6	288.1	307.8	353.9	414.2	498.0
	.976	.982	.988	.988	1.014	1.042	1.070	1.108	1.176	1.250	1.428	1.666	2.000

A,Erl (continued)

N	Blocking Probability												
	1.0%	1.2%	1.5%	2%	3%	5%	7%	10%	15%	20%	30%	40%	50%
300	277.1	279.2	281.9	285.7	292.1	302.6	311.9	325.0	346.9	370.3	425.3	497.5	598.0
	.982	.984	.990	1.000	1.016	1.044	1.070	1.108	1.174	1.248	1.428	1.668	2.000
350	326.2	328.4	331.4	335.7	342.9	354.8	365.4	380.4	405.6	432.7	496.7	580.9	698.0
	.982	.988	.994	1.004	1.020	1.046	1.070	1.108	1.176	1.250	1.430	1.666	2.000
400	375.3	377.8	381.1	385.9	393.9	407.1	418.9	435.8	464.4	495.2	568.2	664.2	798.0
	.986	.990	.996	1.004	1.018	1.046	1.072	1.110	1.176	1.250	1.428	1.666	2.000
450	424.6	427.3	430.9	436.1	444.8	459.4	472.5	491.3	523.2	557.7	639.6	747.5	898.0
	.988	.994	.998	1.006	1.022	1.048	1.070	1.108	1.176	1.250	1.428	1.668	2.000
500	474.0	477.0	480.8	486.4	495.9	511.8	526.0	546.7	582.0	620.2	711.0	830.9	998.0
	.991	.994	1.000	1.008	1.022	1.047	1.073	1.110	1.176	1.249	1.429	1.666	2.000
600	573.1	576.4	580.8	587.2	598.1	616.5	633.3	657.7	699.6	745.1	853.9	997.5	1198.
	.993	.997	1.002	1.010	1.024	1.049	1.073	1.110	1.176	1.250	1.428	1.665	2.00
700	672.4	676.1	681.0	688.2	700.5	721.4	740.6	768.7	817.2	870.1	996.7	1164.	1398.
	.994	.998	1.004	1.011	1.025	1.050	1.073	1.110	1.176	1.250	1.433	1.67	2.00
800	771.8	775.9	781.4	789.3	803.0	826.4	847.9	879.7	934.8	995.1	1140.	1331.	1598.
	.997	1.000	1.004	1.013	1.025	1.050	1.074	1.111	1.172	1.249	1.42	1.67	2.00
900	871.5	875.9	881.8	890.6	905.5	931.4	955.3	990.8	1052.	1120.	1282.	1498.	1798.
	.997	1.001	1.006	1.013	1.025	1.046	1.077	1.112	1.18	1.25	1.43	1.66	2.00
1000	971.2	976.0	982.4	991.9	1008.	1036.	1063.	1102.	1170.	1245.	1425.	1664.	1998.
	.998	1.000	1.006	1.011	1.03	1.05	1.07	1.11	1.18	1.25	1.43	1.67	2.00
1100	1071.	1076.	1083.	1093.	1111.	1141.	1170.	1213.	1288.	1370.	1568.	1831.	2198.

REFERENCES

[1] L. Kleinrock, *Queueing Systems*, Volume I: Theory, John Wiley & Sons, N. York, 1975.

[2] E.C. Molina, "The Theory of Probabilities Applied to Telephone Trunking Problems", *BSTJ*, Vol. 6, pp. 461-494.

[3] R.I. Wilkinson, "Theories for Toll Traffic Engineering in the USA", *BSTJ*, Vol. 35, pp. 421-524.

[4] Y. Rapp, "Planning of Junction Network in a Multi-Exchange Area", *Ericsson Technics.*, Vol. 20, p. 77.

[5] J.H. Sánchez V., "Traffic Performance of Cellular Mobile Radio Systems", *Ph.D Thesis*, University of Essex, June 1988.

[6] S.M. Elnoubi, R. Singh and S.C. Gupta, "A New Frequency Channel Assignment Algorithm in High Capacity Communication Systems", *IEEE Transactions Vehicular Technology*, Vol. VT-31, No. 3, pp.125-131, August 1982

[7] H Sekiguchi, H. Ishikawa, M. Koyama and H. Sawada, "Techniques for Increasing Frequency Spectrum Utilization in Mobile Radio Communication Systems", *IEEE CH2037-0/85/0000-0026*, pp. 26-31, 1985.

[8] D.C. Cox and D.O. Reudnik, "Dynamic Channel Assignment in Two-Dimensional Large-Scale Mobile Radio Systems" *BSTJ*, Vol. 51, No. 7, pp. 1611-1629, September 1972.

[9] Y Furuya and Y. Akaiwa, "Channel Segregation, A Distributed Channel Allocation Scheme for Mobile Communication Systems", *Proc. 2nd Nordic Sem. on Digital Land Mobile Comm.*, pp. 311-315, October 1986.

[10] D. Everitt and D. Manfield, "Performance Analysis of Cellular Mobile Communication Systems with Dynamic Channel Assignment", *IEEE JSAC*, Vol. 7, No. 8, October 1989.

[11] B. Arazi, "New Channel Assignment Strategy in Cellular Mobile Radiocommunication Systems", *IEE Proc.*, Vol. 133, Part F, No. 6, pp. 569-575, October 1986.

[12] J.H. Sánchez V. and J.P. Eade, "A Simulation Study of Cellular and Sectorized Mobile Telephone Systems using a Hyb-id Channel Allocation Technique", *Proc. 5th UK Teletraffic Symposium,* Aston U.K. pp. 11/1-10, July 1988.

[13] B. Eklundh, "Channel Utilization and Blocking Probability in a Cellular Mobile Telephone System with Directed Retry", 11th *ITC*, 1985.

[14] M.D. Yacoub, K.W. Cattermole and D.M. Rodriguez, "Alternative Routing in Cellular Mobile Radio", *Third U.K. Teletraffic Symposium,* Colchester, June 1986.

[15] M.D. Yacoub and K.W. Cattermole, "Cellular Mobile Radio with Fuzzy Cell Boundaries", *Fourth U.K. Teletraffic Symposium,* Bristol, May 1987.

[16] M.D. Yacoub, "Mobile Radio with Fuzzy Cell Boundaries", *Ph.D Thesis,* University of Essex, April 1988.

[17] M.D. Yacoub and K.W. Cattermole, "Improving Traffic Capacity with the Use of the Fuzzy Cell Boundary Traffic in a Mobile Radio System", *ISSSE'89,* Erlangen, West Germany, September 1989.

[18] M.D. Yacoub and K.W. Cattermole, "Novel Technique for Efficient Channel Utilization in a Mobile Radio System", *IEEE Global Telecommunications Conference,* San Diego, CA, USA, December 2-5, 1990.

[19] M.D. Yacoub and K.W. Cattermole, "Use of the Third path Option as a Means of Improving Capacity of Mobile Radio System", 13th *ITC*, Copenhagen, Denmark, June 1991.

[20] J.C.E. Mencia, "Performance of a Mobile Radio System with the Blocking Threshold Variation" (in Portuguese), M.Sc. Dissertation, UNICAMP, Campinas, Brazil, January 1991.

[21] *Telephone Traffic Theory, Tables and Charts,* Siemens Aktiengesellschaft, Munich, 1970.

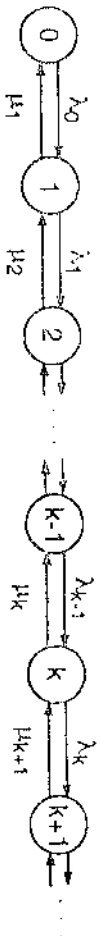

Figure

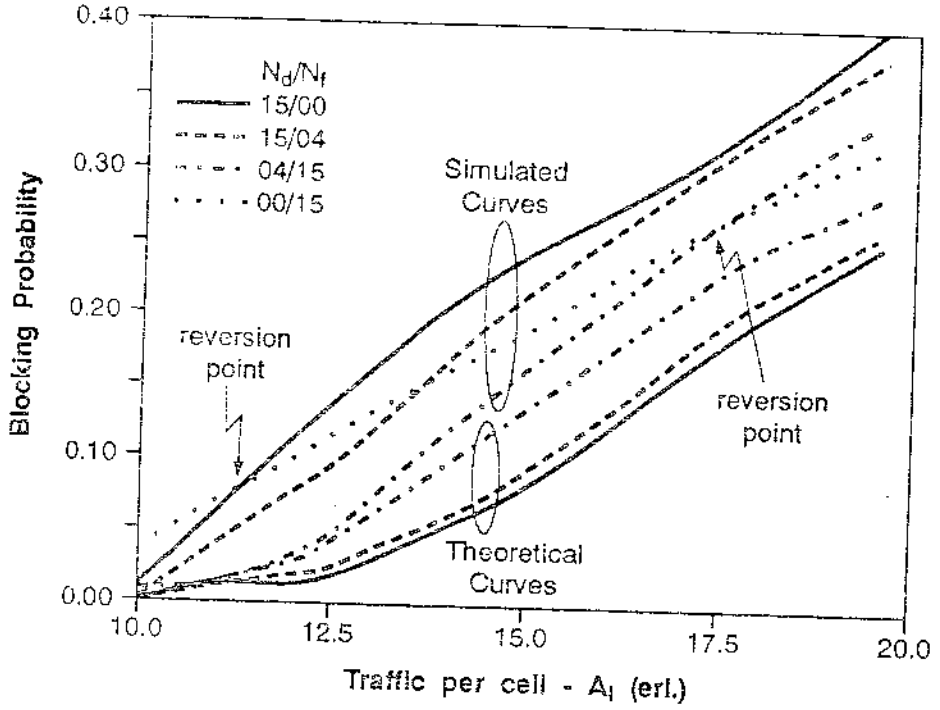

FIGURE 12-2

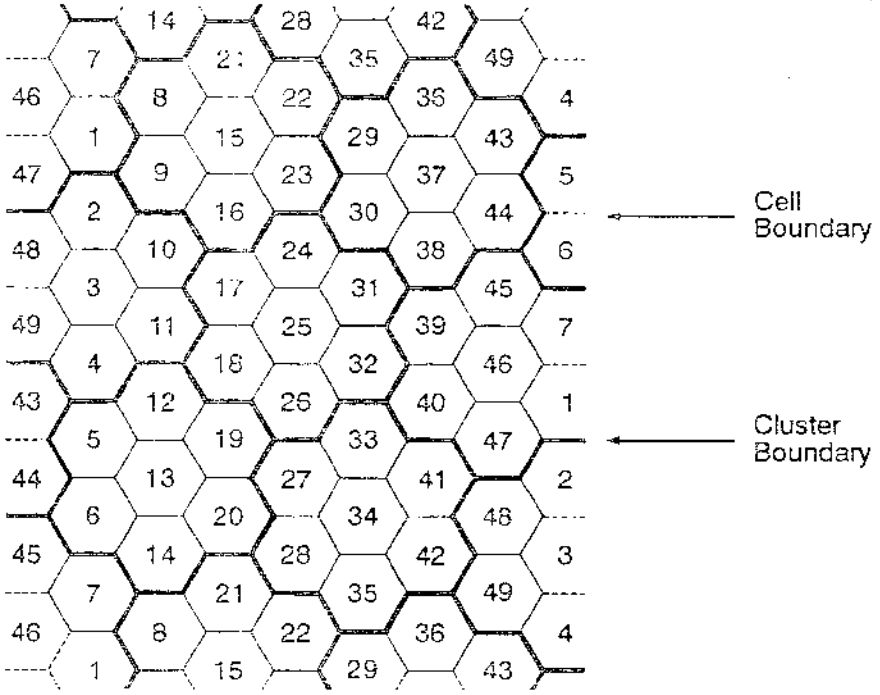

FIG12.1 1504

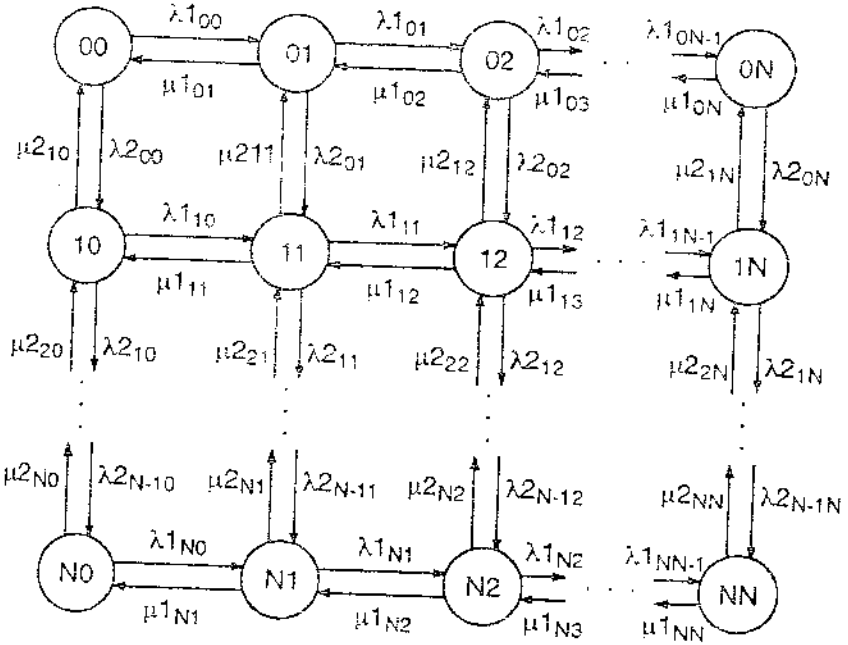

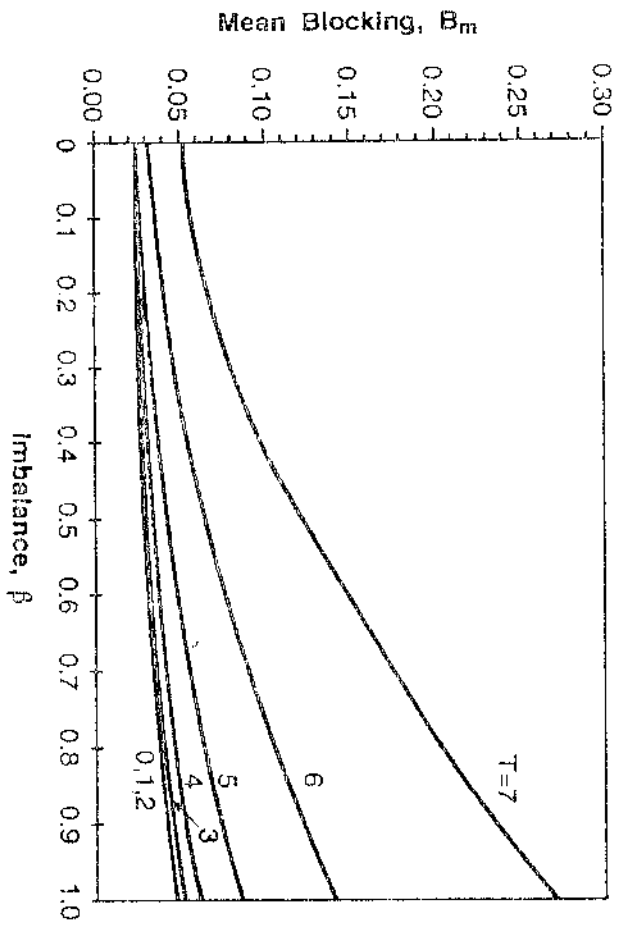

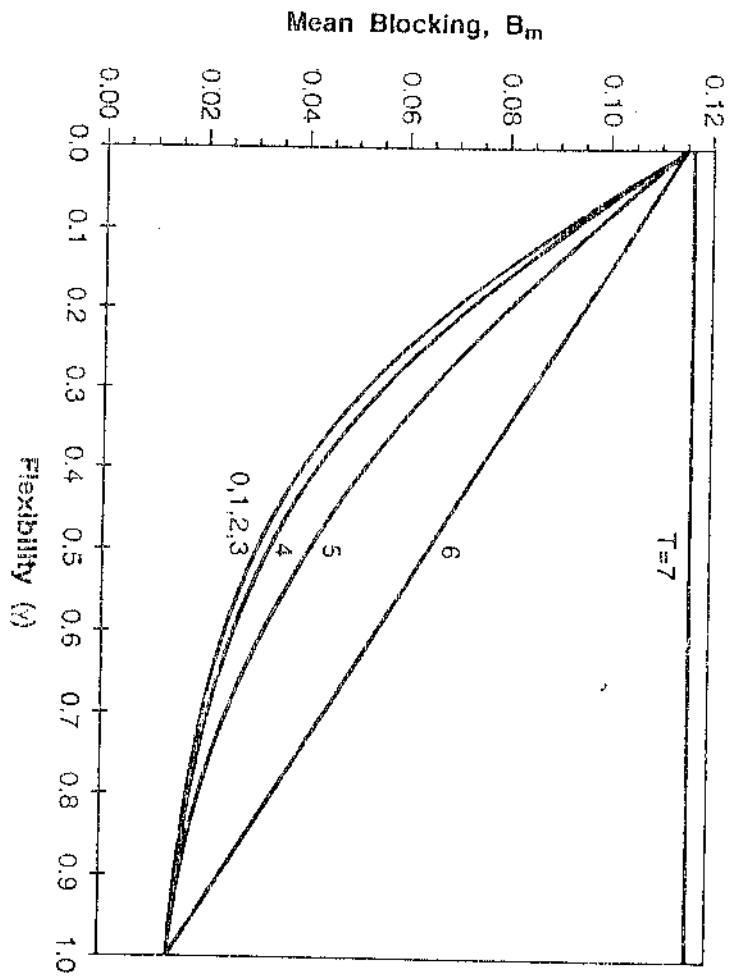

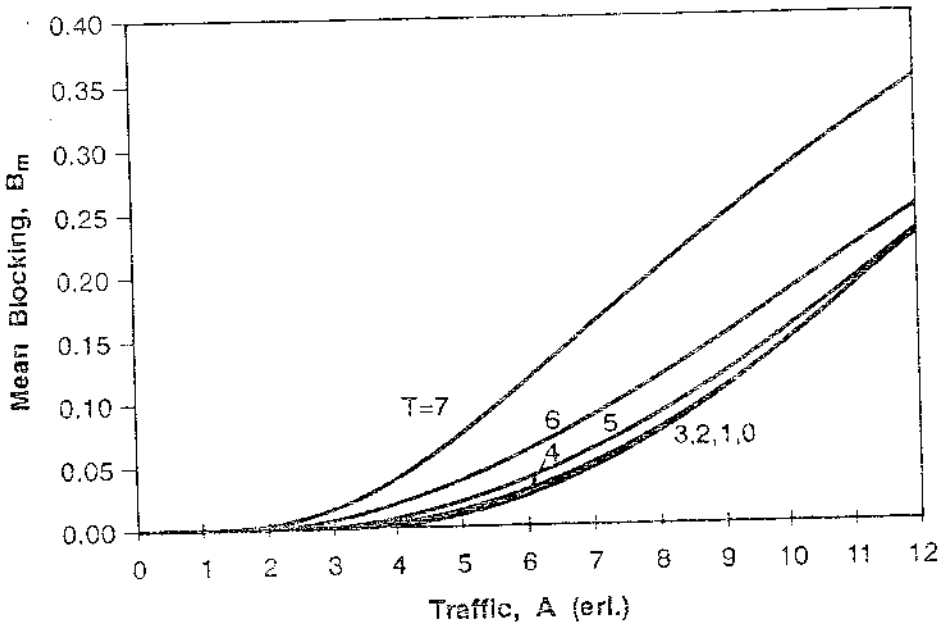

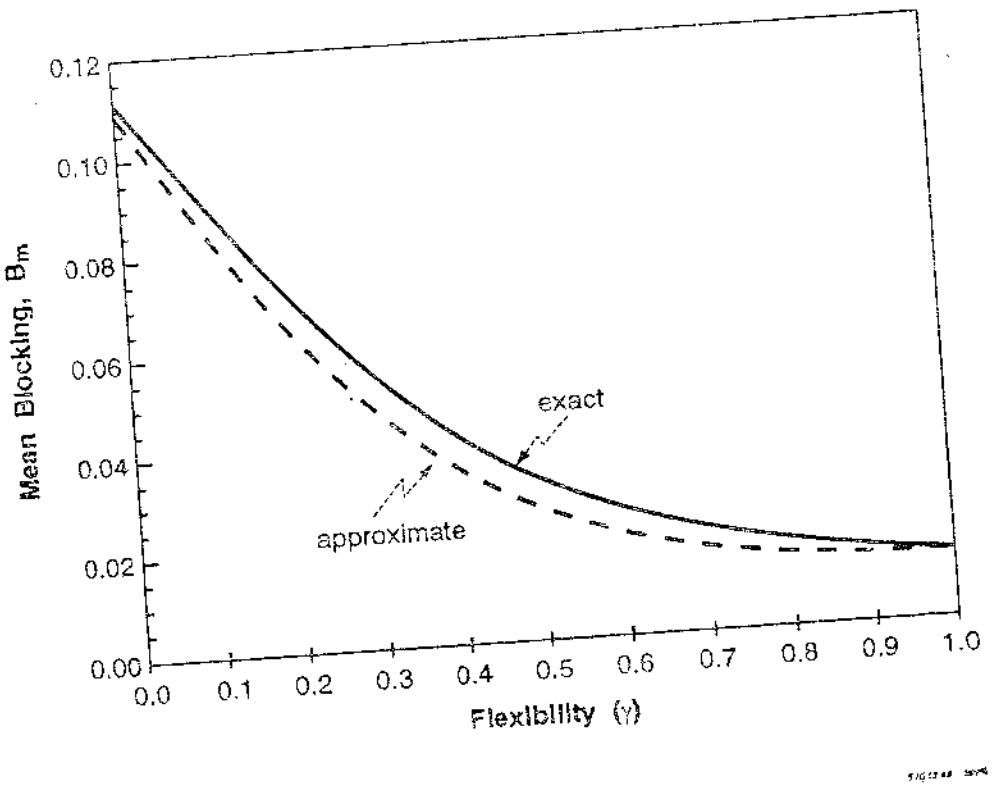
0.12
0.10
0.08
0.06
0.04
0.02
0.00
Mean Blocking, B_m
exact
approximate
0.0
0.1
0.2
0.3
0.4
0.5
0.6
0.7
0.8
0.9
1.0
Flexibility (γ)